EXPERIMENTAL STUDY OF THE STATIC AND DYNAMIC CHARACTERISTICS OF A LONG (L/D=0.65) SMOOTH ANNULAR SEAL OPERATING UNDER TWO-PHASE (LIQUID/GAS) CONDITIONS

A Dissertation

by

MIN ZHANG

Submitted to the Office of Graduate and Professional Studies of
Texas A&M University
in partial fulfillment of the requirements for the degree of

DOCTOR OF PHILOSOPHY

Chair of Committee,	Dara W. Childs
Committee Members,	Luis A. San Andrés
	Gerald L. Morrison
	W. Lynn Beason
Head of Department,	Andreas A. Polycarpou

December 2017

Major Subject: Mechanical Engineering

Copyright 2017 Min Zhang

ABSTRACT

This research documents the development of a 2-phase annular-seal stand (2PASS) in the Turbomachinery Laboratory at Texas A&M University to investigate the static and dynamic characteristics of annular seals operating under 2-phase flow conditions. The 2PASS is modified from an existing air-annular seal test stand. It uses either spargers or a specially designed mixer to make a 2-phase flow, comprised of air and silicone oil (PSF-5cSt).

Smooth annular seals with (length L=57.785 mm and length-to-diameter ratio L/D=0.65) are tested in the centered position for three radial clearances (C_r=0.140, 0.163, and 0.188 mm) with zero intentional pre-swirl. Due to the difficulties in making homogeneous mixtures over the gas-volume fraction (GVF) range from 10% to 92%, tests are performed at pure- and mainly-oil conditions (GVF≤10%) and pure- and mainly-air conditions (92%≤GVF≤100%), respectively. Under pure- and mainly-oil conditions, tests are conducted at exit pressure P_e=6.9 bars, rotor speed ω=5, 7.5, 10, and 15 krpm, pressure drop PD=31, 37.9, and 48.3 bars, and inlet GVF=0%, 2%, 4%, 6%, 8%, and 10%. At pure- and mainly-air conditions, tests are performed at inlet pressure P_i=62 bars, ω=10, 15, and 20 krpm, pressure ratio PR=0.57, 0.5, and 0.43, and inlet GVF=100%, 98%, 95%, and 92%. Leakage mass flow rate $\dot{m}$ and rotordynamic coefficients are measured, and the effects of changing inlet GVF, C_r, PD (or PR), and ω are studied.

Test results show that adding fine air bubbles into the oil flow does not significantly change $\dot{m}$, but remarkably influences the seal's rotordynamic performance. Increasing inlet GVF from zero to 10% generally decreases direct stiffness K when C_r=0.163 and 0.140 mm, but increases K when PD=31 and 37.9 bars and C_r=0.188 mm. As K drops to a large enough negative value, the seal stator's 1st natural frequency drops significantly, causing a sub-synchronous vibration (instability at the stator's 1st damped natural frequency), preventing further tests. Increasing inlet GVF from zero to 10% has little effect on effective damping C_{eff} and does not change the seal's stabilizing force when C_r=0.188 mm, but generally increases C_{eff} and makes the seal more stabilizing when C_r=0.163 and 0.140 mm.

For all three clearances under pure- and mainly-air conditions, $\dot{m}$ drops slightly (by less than 6%) as inlet GVF decreases from 100% to 98%, and then increases (by about 45%) with further decreasing inlet GVF to 92%. The oil presence in the air stream significantly impacts the seal's rotordynamic characteristics. Direct dynamic stiffness K_Ω is frequency dependent and

generally increases as Ω increases, especially after injecting oil. As inlet GVF decreases from 100% to 92%, K_Ω generally decreases except that it increases as inlet GVF decreases from 100% to 98% in the following circumstances: (1) cases with PR=0.43 and C_r=0.188 mm, and (2) the case with PR=0.43, ω=20 krpm, and C_r=0.163 mm. Decreasing the seal's K_Ω would decrease the critical speed of the rotor in a centrifugal compressor.

As Ω increases, C_{eff} changes from negative (destabilizing) to positive (stabilizing) at Ω_c (the cross-over frequency). Ω_c is of great interest to the system stability. Injecting oil into the air stream increases Ω_c, making the seal less stabilizing. Increasing C_r from 0.140 to 0.188 mm decreases Ω_c, making the seal more stabilizing. However, an immediate disadvantage is that $\dot{m}$ increases significantly (by about 58%) as C_r increases from 0.140 to 0.188 mm.

A program developed by San Andrés based on a bulk-flow model and the Moody friction model with isothermal and homogeneous-mixture assumptions produces predictions to compare with test results. For all three clearances at pure- and mainly-oil conditions, the program reasonably predicts $\dot{m}$ and C_{eff}. For most cases, K predictions are not close to test results. In a centrifugal pump, the poor agreement in K leads to prediction inaccuracy in the rotor's critical speed.

For all three clearances at pure- and mainly-air conditions, the program adequately predicts $\dot{m}$. Predicted K_Ω values are close to test results only under pure-air conditions when PR=0.5 and 0.57. For all other test conditions, K_Ω predictions are larger than measured, and the difference decreases as Ω increases due to the frequency dependence of K_Ω. In a centrifugal compressor, this discrepancy would mean that the rotor's critical speed would be lower than predicted. Ω_c predictions agree with measurements when inlet GVF=100% and 98%, but are larger than measured results (by more than 37.1%) when inlet GVF=95% and 92%. Therefore, when inlet GVF=95% and 92%, the seal is more stabilizing than predicted.

DEDICATION

This dissertation work is dedicated to my family.

ACKNOWLEDGEMENTS

First and foremost, I would like to express my sincere thanks to Dr. Childs for giving me the opportunity to work at the Turbomachinery Laboratory, and his invaluable support and guidance in my research.

I would also like to thank Dr. San Andrés, Dr. Morrison, and Dr. Beason for graciously serving on my committee.

Sincere thanks to Stephen Phillips for the technical support on the test cell, and Ray Mathews for the help in the machine shop.

Special thanks to fellow graduate research assistants James Mclean, Jan Soto, Dung Tran, Hari Shrestha, J.J. Thiele, Andrew Crandall, Stephen Arthur, and Mauricio Ramirez. Many thanks to the undergraduate assistants Keaton Hruzek and Kyle Miller.

Finally, I want to thank my parents and wife for their unfailing love and support.

CONTRIBUTORS AND FUNDING SOURCES

Contributors

This work was supervised by a dissertation committee consisting of Professor Dara W. Childs, Professor Luis A. San Andrés, and Professor Gerald L. Morrison of the Department of Mechanical Engineering and Professor W. Lynn Beason of the Department of Civil Engineering.

The test rig described in Section 3 was completed by the student, in collaboration with James E. Mclean Jr. of the Department of Mechanical Engineering. All other work conducted for the dissertation was completed by the student independently.

Funding Sources

A consortium of private corporations in the oil and gas and compressor manufacturers provided funds plus direct funding from the Turbomachinery Laboratory.

NOMENCLATURE

a_m, b_m, c_m, e_m	Coefficients in Moody's friction factor formula [-]
$\boldsymbol{A}_{ij}$	Fourier transforms of the stator acceleration in i direction due to a shake in j direction [L/T^2]
c	Cross-coupled damping [FT/L]
C	Direct damping [FT/L]
C_{eff}	Effective damping [FT/L]
C_{ij}	Damping coefficients [FT/L]
C_r	Seal radial clearance [L]
D	Seal inner diameter [L]
D_r	Rotor diameter [L]
$\boldsymbol{D}_{ij}$	Fourier transforms of the relative displacement of the stator to the rotor in i direction due to a shake in j direction [L]
ek_Ω	The uncertainty of cross-coupled dynamic stiffness k_Ω [F/L]
eK_Ω	The uncertainty of direct dynamic stiffness K_Ω [F/L]
f_r, f_s	Moody's friction factors on the rotor and stator surfaces [-]
f_{sX}, f_{sY}	Seal's reaction forces acting on the rotor in X and Y directions [F]
f_z	Axial friction factor [-]
$\boldsymbol{F}_{ij}$	Fourier transforms of the excitation force in i direction due to a shake in j direction [F]
F_r	The radial component of the seal's reaction force [F]
F_θ	The circumferential component of the seal's reaction force [F]
GVF	Gas-volume fraction, defined by Eq. (12) [-]
$\boldsymbol{H}_{ij}$	Complex dynamic stiffness coefficients introduced in Eq. (19) [F/L]
k	Cross-coupled stiffness [F/L]
$\bar{k}$	The mean of the cross-coupled dynamic stiffness k_Ω [F/L]
k_r, k_s	Turbulent shear parameters on the rotor and stator surfaces [-]
k_z	Axial flow shear parameter [-]
k_Ω	Cross-coupled dynamic stiffness [F/L]
K	Direct stiffness [F/L]

K_{ij}	Stiffness coefficients [F/L]
K_Ω	Direct dynamic stiffness [F/L]
L	Seal length [L]
m_q	Cross-coupled virtual-mass [M]
$\dot{m}$	Leakage mass flow rate [M/T]
M	Direct virtual-mass [M]
M_{ij}	Virtual-mass coefficients [M]
$[M_S]$	Stator-mass coefficient matrix [M]
M_{Sij}	Mass coefficients of the stator assembly [M]
P	Pressure [F/L^2]
PD	Pressure drop, PD=inlet pressure P_i-exit pressure P_e [F/L^2]
P_{gi}	Gas pressure at seal inlet [F/L^2]
PR	Pressure ratio, PR=P_i/P_e [-]
P_V	Liquid vapor pressure [F/L^2]
$\dot{Q}$	Volume flow rate [L^3/T]
r_r, r_s	Mean surface roughness at rotor and stator [L]
Re	Reynolds number [-]
Re_a	Axial Reynolds number [-]
Re_r, Re_s	Reynolds numbers relative to the rotor and stator surfaces [-]
Re_θ	Circumferential Reynolds number [-]
R_g	Gas constant [-]
S	Liquid surface tension per unit length [F/L]
t_e	Excitation time [T]
T	Temperature [T]
$u_0(0)$	Pre-swirl ratio [-]
V_a	Axial bulk-flow velocity [L/T]
V_θ	Circumferential bulk-flow velocity [L/T]
$V_{\theta 0}$	Circumferential velocity of the fluid at the seal inlet [L/T]
WFR	Whirl Frequency Ratio [-]
x, y	Relative displacements of the stator to the rotor in X and Y directions [L]
ε_0	Static eccentricity ratio [-]
μ	Viscosity [FT/L^2]

ξ	Empirical entrance loss coefficient [-]
ρ	Density [M/L^3]
τ_z	Axial wall shear stress function [F/L^2]
ω	Rotor speed [T^{-1}]
Ω	Excitation frequency [T^{-1}]

Subscripts

X, *Y*	*X* and *Y* directions of the coordinate system defined in Fig. 20
e	Seal exit condition
i	Seal inlet condition
l	Liquid component
g	Gas component

Acronyms

ESP	Electrical Submersible Pump
GOR	Gas/Oil Ratio
GVF	Gas-Volume Fraction
LGMR	Liquid/Gas Mass Ratio
LVF	Liquid-Volume Fraction, LVF=1-GVF
OSI	Onset Speed of Instability
P&ID	Piping and Instrumentation Diagram
2PASS	2-Phase Annular-Seal Stand

TABLE OF CONTENTS

Page

Page

LIST OF FIGURES

Page

Page

Page

Page

LIST OF TABLES

Page

Page

Page

Page

Page

Page

Page

Page

Page

Page

Page

Page

Page

Page

1. INTRODUCTION

Centrifugal pumps use smooth annular seals to minimize the leakage from high pressure areas to low pressure areas and increase efficiencies. The geometry of a smooth seal is similar to that of a plain journal bearing; however, the pressure distribution in a smooth seal is different. The axial leakage flow experiences a sudden pressure drop at the seal inlet. In combination with the pressure drop through the seal due to wall friction, this gives rise to a centering force, known as the "Lomakin effect". The "Lomakin effect" may produce large centering forces on the rotor and significantly affect the rotordynamic characteristics of a centrifugal pump. Rotor speed ω, pre-swirl ratio $u_0(0)$, and other factors also influence the seal forces.

Childs [1] gives the following reaction force model for seal forces:

$$-\begin{Bmatrix} f_{sX} \\ f_{sY} \end{Bmatrix} = \begin{bmatrix} K_{XX} & K_{XY} \\ K_{YX} & K_{YY} \end{bmatrix} \begin{Bmatrix} x \\ y \end{Bmatrix} + \begin{bmatrix} C_{XX} & C_{XY} \\ C_{YX} & C_{YY} \end{bmatrix} \begin{Bmatrix} \dot{x} \\ \dot{y} \end{Bmatrix} + \begin{bmatrix} M_{XX} & M_{XY} \\ M_{YX} & M_{YY} \end{bmatrix} \begin{Bmatrix} \ddot{x} \\ \ddot{y} \end{Bmatrix}, \tag{1}$$

where f_{sX} and f_{sY} are the seal's reaction forces in X and Y directions, K_{XX} and K_{YY} represent the direct stiffness coefficients, K_{XY} and K_{YX} are the cross-coupled stiffness coefficients, C_{XX} and C_{YY} denote the direct damping coefficients, C_{XY} and C_{YX} are the cross-coupled damping coefficients, M_{XX} and M_{YY} denote the direct virtual-mass coefficients, M_{XY} and M_{YX} are the cross-coupled virtual-mass coefficients, x and y are the relative displacements of the stator to the rotor in X and Y directions, $\dot{x}$ and $\dot{y}$ are the relative velocities of the stator to the rotor in X and Y directions, and $\ddot{x}$ and $\ddot{y}$ are the relative accelerations of the stator to the rotor in X and Y directions. Stiffness, damping, and virtual-mass coefficients are rotordynamic coefficients, and they are generally functions of static eccentricity ratio ε_0.

Since the rotordynamic coefficients of a smooth seal under two-phase conditions may be functions of the excitation frequency Ω, Eq. (1) becomes:

$$\begin{aligned} -\begin{Bmatrix} f_{sX} \\ f_{sY} \end{Bmatrix} &= \begin{bmatrix} K_{XX}(\Omega) & K_{XY}(\Omega) \\ K_{YX}(\Omega) & K_{YY}(\Omega) \end{bmatrix} \begin{Bmatrix} x \\ y \end{Bmatrix} + \\ &\begin{bmatrix} C_{XX}(\Omega) & C_{XY}(\Omega) \\ C_{YX}(\Omega) & C_{YY}(\Omega) \end{bmatrix} \begin{Bmatrix} \dot{x} \\ \dot{y} \end{Bmatrix} + \begin{bmatrix} M_{XX}(\Omega) & M_{XY}(\Omega) \\ M_{YX}(\Omega) & M_{YY}(\Omega) \end{bmatrix} \begin{Bmatrix} \ddot{x} \\ \ddot{y} \end{Bmatrix} \end{aligned} \tag{2}$$

For small motion around the concentric position, the following assumptions simplify Eq. (2):

$$
\begin{aligned}
&K_{XX}(\Omega)=K_{YY}(\Omega)=K(\Omega),\ K_{XY}(\Omega)=-K_{YX}(\Omega)=k(\Omega),\\
&C_{XX}(\Omega)=C_{YY}(\Omega)=C(\Omega),\ C_{XY}(\Omega)=-C_{YX}(\Omega)=c(\Omega),\\
&M_{XX}(\Omega)=M_{YY}(\Omega)=M(\Omega),\ M_{XY}(\Omega)=-M_{YX}(\Omega)=m_q(\Omega),
\end{aligned}
\tag{3}
$$

where K is the direct stiffness, k is the cross-coupled stiffness, C is the direct damping, c is the cross-coupled damping, M is the direct virtual-mass, m_q is the cross-coupled virtual-mass.

Equation (2) becomes:

$$
-\begin{Bmatrix} f_{sX} \\ f_{sY} \end{Bmatrix}=\begin{bmatrix} K(\Omega) & k(\Omega) \\ -k(\Omega) & K(\Omega) \end{bmatrix}\begin{Bmatrix} x \\ y \end{Bmatrix}+\begin{bmatrix} C(\Omega) & c(\Omega) \\ -c(\Omega) & C(\Omega) \end{bmatrix}\begin{Bmatrix} \dot{x} \\ \dot{y} \end{Bmatrix}+\begin{bmatrix} M(\Omega) & m_q(\Omega) \\ -m_q(\Omega) & M(\Omega) \end{bmatrix}\begin{Bmatrix} \ddot{x} \\ \ddot{y} \end{Bmatrix} \tag{4}
$$

Figure 1 shows the reaction forces generated by a seal on a forward precessing (in the direction of shaft rotation) rotor. r_0 is the radius of the small circular orbit around the concentric position. The radial force component F_r resists the radial motion of the rotor and defines the effective stiffness K_{eff} as

$$
K_{eff}=\frac{F_r}{r_0}=K(\Omega)+c(\Omega)\Omega-M(\Omega)\Omega^2 \tag{5}
$$

The circumferential force component F_θ defines the effective damping C_{eff}, which is an indicator of the seal's stabilizing capacity.

$$
C_{eff}=\frac{F_\theta}{\Omega r_0}=-\frac{k(\Omega)}{\Omega}+C(\Omega)+m_q(\Omega) \tag{6}
$$

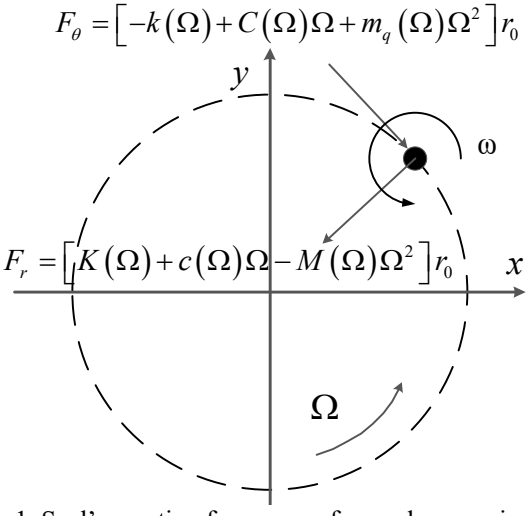

Figure 1. Seal's reaction forces on a forward precessing rotor

Experimental studies exist for smooth annular seals operating under either gas or liquid conditions. In 1997, Marquette et al. [2] tested a smooth seal (length-to-diameter ratio L/D=0.45, seal inner diameter D=50.8 mm, and radial clearance C_r=0.11 mm) at rotor speed ω=10.2, 17.4, and 24.6 krpm, pressure drop PD=41.4, 55.2, and 68.9 bars, and multiple eccentricities (from zero to 0.5). The test fluid was water, and the flow was turbulent. For the concentric position, test results showed that direct stiffness increased as PD increased but decreased as ω increased. Cross-coupled stiffness was not sensitive to changes in PD and (as expected) increased as ω increased. Direct damping increased as PD increased but was not sensitive to changes in ω. Direct virtual-mass was not sensitive to changes in either ω or PD.

In 2004, Kerr [3] tested a set of smooth gas seals (L/D=0.73, D=117.2 mm, C_r=0.1 and 0.2 mm) with inlet pressure P_i=70 bars, ω=10.2, 15.2, and 20.2 krpm, and no intentional pre-rotation of the fluid at the seal inlet. When C_r=0.1 mm, pressure ratio PR=0.17 and 0.53. When C_r=0.2 mm, PR=0.28, 0.39, and 0.48 and 0.65. Test results showed that direct stiffness generally increased as Ω increased. Direct stiffness was invariant with changes in ω, increased as PR increased, and decreased as C_r increased. The cross-over excitation frequency Ω_c, at which effective damping increased from negative to positive, had a considerably impact on the system stability. Ω_c increased as ω increased, did not change discernibly as PR increased, and increased as C_r increased.

Current knowledge and technology are enough to guide the design of a single-phase smooth annular seal; however, some compressors and pumps must function under two-phase flow conditions. For example, Ransom et al. [4] note that centrifugal compressors handling natural gas must tolerate a small amount of liquid-carryover (gas-volume fraction GVF≥95%). The two-phase flow in a smooth annular seal not only decreases the machine efficiency but may also lead to vibration issues. For example, Brenne et al. [5] report sub-synchronous vibrations in a single-stage centrifugal compressor operating under a wet-gas condition with a GVF of 97%. Therefore, the effects of two-phase flow conditions on the performance of smooth annular seals must be investigated. The increased knowledge will help in designing multiphase turbomachines and avoiding problems in field operations.

Smooth seals are widely used in pumps, but they are never used in centrifugal compressors; however, test data are sorely needed to examine the correctness of predictions [6] for annular seals with 2-phase flow, and obtaining results for a smooth seal is an appropriate starting place.

1.1 Wet-Gas Compression

In natural gas compression, there is always a small amount of liquid-carryover in the natural gas stream. Typically, scrubbers and separators purge the liquid components before the process stream enters the compressors. Natural gas applications, particularly offshore applications, do not favor systems with separation devices, because those devices are large. Wet-gas compression, one of the most important recent developments in centrifugal compressor technology, has developed to directly handle the liquid components without purging them by a separation system. Eliminating the separation system significantly reduces the size, weight, and cost of a gas compression system and makes wet-gas compressors more attractive to the oil & gas industry. However, the presence of the liquid phase in the gas stream may cause sub-synchronous vibrations and affect the mechanical vibration performance of a compressor, according to Brenne et al. [5]. The balance of this section provides an overview of the past and current research on the mechanical vibration performances of compressors operating under wet-gas conditions.

Vannini et al. [7] reported that GE conducted a field test in 1972 for a back-to-back multistage compressor under wet-gas conditions. The compressor showed a performance decrease. Inspections revealed that the performance decrease would be induced by the deterioration of labyrinth shaft-end seals, which could be caused by high vibrations. GE designed two sets of tests to verify whether the high vibrations were induced by the presence of liquid in the labyrinth shaft-end seals. In the first set of the tests, when liquid was injected into the gas stream at suction flanges, the compressor's vibrations were not affected significantly. In the second set of the tests, when liquid was injected radially through vent lines into the labyrinth shaft-end seals, a sub-synchronous lateral vibration occurred. The frequency of the sub-synchronous vibration was approximately 0.5ω. Elliptical bearings and tilting pads bearings were mounted and tested, respectively. The sub-synchronous vibration occurred irrespective of bearing types; however, it was more evident when using elliptical bearings. Vannini et al. [7] concluded that the presence of liquid in the labyrinth shaft-end seals could lead to sub-synchronous vibrations.

Vannini et al. [7] also discussed a wet-gas-compression test campaign conducted by GE in 1993 for a vertical 8-stage barrel compressor. The wet-gas flow was made by mixing nitrogen

and heavy oil before entering the compressor inlet. The GVF varied from 99.16% to 97.97%. Test data showed that there were no rotordynamic problems induced by the liquid presence.

In 2005, Brenne et al. [5] experimentally investigated the effects of liquid presence on the performance of a single-stage centrifugal compressor. The test fluid was a mixture of hydrocarbon gas and hydrocarbon condensate with GVF≥97%. The liquid was injected into the pressurized gas stream before entering the compressor inlet by two different patterns: (1) droplet injection pattern, aiming to distribute liquid droplets uniformly in gas, and (2) film injection pattern, aiming to produce a liquid film uniformly covering the wet surface of the inlet pipe. Tests were performed at suction pressures of 30 and 70 bars and rotor speeds of 9651 and 10732 rpm. The rotor speeds were less than the compressor's first critical speed, which was between 20300 and 21130 rpm. In general, the compressor's vibrations were not affected significantly by a small amount of hydrocarbon condensate (GVF≥97%). However, when suction pressure=30 bars, ω=9,651 rpm, and GVF=97%, sub-synchronous vibrations occurred, as shown in Fig. 2. Those sub-synchronous vibrations consisted of multiple frequencies around 0.5ω, and they disappeared when GVF increased above 98%. Brenne et al. [5] believed that the sub-synchronous vibrations were induced by the entrainment of liquid into impeller-eye seals or balance-piston seals.

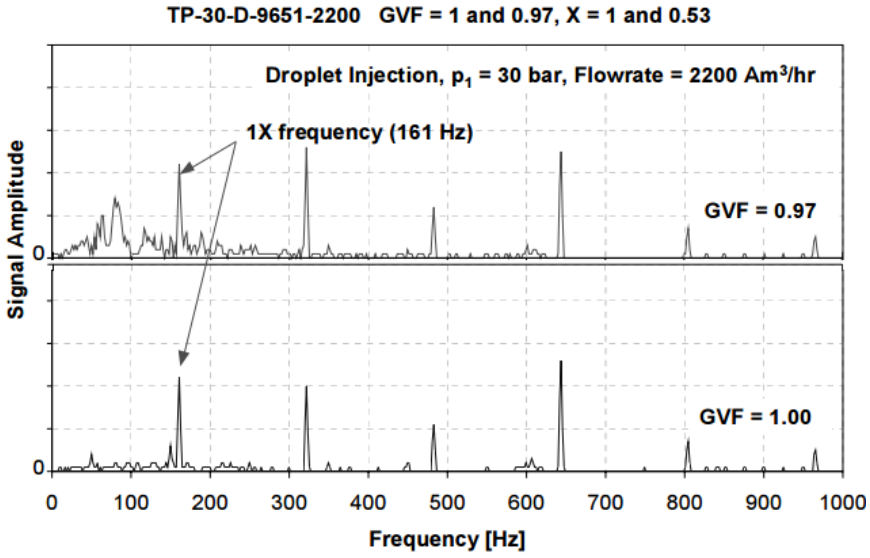

Figure 2. Effects of two-phase flow on the compressor's vibration (horizontal component), measured at the driven-end of the machine (9651 rpm and 30 bars suction pressure) [5]

In 2011, Griffin and Maier [8] experimentally evaluated the rotordynamic performance of an oil-free integrated motor-compressor machine with liquid injected at its inlet. The liquid/gas mass ratio (LGMR) at the machine inlet was up to 0.5. LGMR is the ratio of the mass of the liquid to the mass of the gas. The LGMR at the inlet of the compressor section of this integrated separator-compressor machine was not stated, but it should be much less than at the machine inlet because of the work of the separator section. The test results showed that the machine's rotordynamic performance was insensitive to the liquid injection. To assess the system stability, a magnetic bearing exciter was used to measure the logarithmic decrement. In some cases, the logarithmic decrement increased slightly with increasing liquid flow rate; i.e., adding liquid improved the system stability slightly.

Since 2010, GE Oil & Gas has collaborated with Southwest Research Institute (SwRI) on a closed-loop test stand to completely assess the mechanical vibration performances (including the vibration levels and system stabilities) of centrifugal compressors operating under wet-gas conditions. Ransom et al. [4], Bertoneri et al. [9], Vannini et al. [7], and Vannini et al. [10] presented test data from this test stand. Those references are discussed separately below.

In 2011, Ransom et al. [4] experimentally investigated the effects of wet-gas conditions on the mechanical vibration performance of a two-stage centrifugal compressor with a labyrinth balance piston seal. The compressor was tested at three rotor speeds (8, 9.5, and 11 krpm) and multiple GVFs varying from 99.5% to 95% with a suction pressure of about 20 bars. The test fluid was made by mixing air and water before the compressor inlet. Test results showed that the presence of liquid had negligible effects on lateral vibrations, which were always small and dominated by the synchronous response through all test cases.

In 2014, Bertoneri et al. [9] experimentally studied the performance of a single-stage centrifugal compressor operating under wet-gas conditions. The shaft end seals, impeller eye seal, and balance piston seal were all teeth-on-stator (TOS) labyrinth seals. The test rig was modified from the test rig of Ransom et al. [4]. The test fluid was a mixture of air and water with GVFs varying from 100% to 97%. The atomized water was injected through spiral injectors into the dry suction gas stream at suction pressure=10, 15, and 18.5 bars. The compressor was tested at ω=9, 11.5, and 13.5 krpm. Test data demonstrated that lateral, axial, and torsional vibrations were not affected significantly by a small amount of water in air (GVF$\geq$97%) in most test cases. In 2014, Vannini et al. [7] published more test results for this test rig. They further noted that critical speed was not sensitive to the liquid presence. Additionally, the measured logarithmic

decrement increased with decreasing GVF from 100% to 97%. This trend agreed well with the test results of Griffin and Maier [8].

From 2014 to 2015, Vannini et al. [7] and Vannini et al. [10] modified the test rig of Bertoneri et al. [9] by injecting liquid directly into the seals (including shaft-end seals, an impeller-eye seal, and a balance-piston seal) of the single-stage compressor to investigate the effects of seal flooding on the compressor's rotordynamic performance. All seals were teeth-on-stator (TOS) labyrinth seals. Test results showed that flooding the seals may cause synchronous vibrations, as shown in Fig. 3. Figure 3 shows the variation of GVF on the bottom part and the waterfall plot of the lateral vibrations on the top part with ω=13.5 krpm (225 Hz) and suction pressure=10 bars. As time increases, GVF increases from 97% to 100% (LVF decreases from 3% to zero). Since the 0.5XREV (0.5ω) response is always present irrespective of dry seals or flooded seals, it is not related to seal flooding. Another sub-synchronous vibration occurs at a frequency of about 0.45XREV (0.45ω), which decreases slightly (within 20%) as GVF increases. Vannini et al. [7] thought the 0.45XREV sub-synchronous vibration was induced by the flooded TOS labyrinth balance-piston seal, whose annular cavities between teeth may trap liquid, because that there was no evident time lag between the closure/opening of liquid injectors and the disappearance/occurrence of the 0.45XREV sub-synchronous vibration.

To confirm this thought, Vannini et al. [7] injected nitrogen to purge the annular cavities of the TOS labyrinth balance-piston seal and found that the amplitude of the 0.45XREV sub-synchronous vibration was reduced significantly. The amplitude of the 0.45XREV sub-synchronous vibration was further reduced by replacing the original TOS labyrinth balance-piston seal with a pocket damper seal (PDS) which had physical brakes in the circumferential direction.

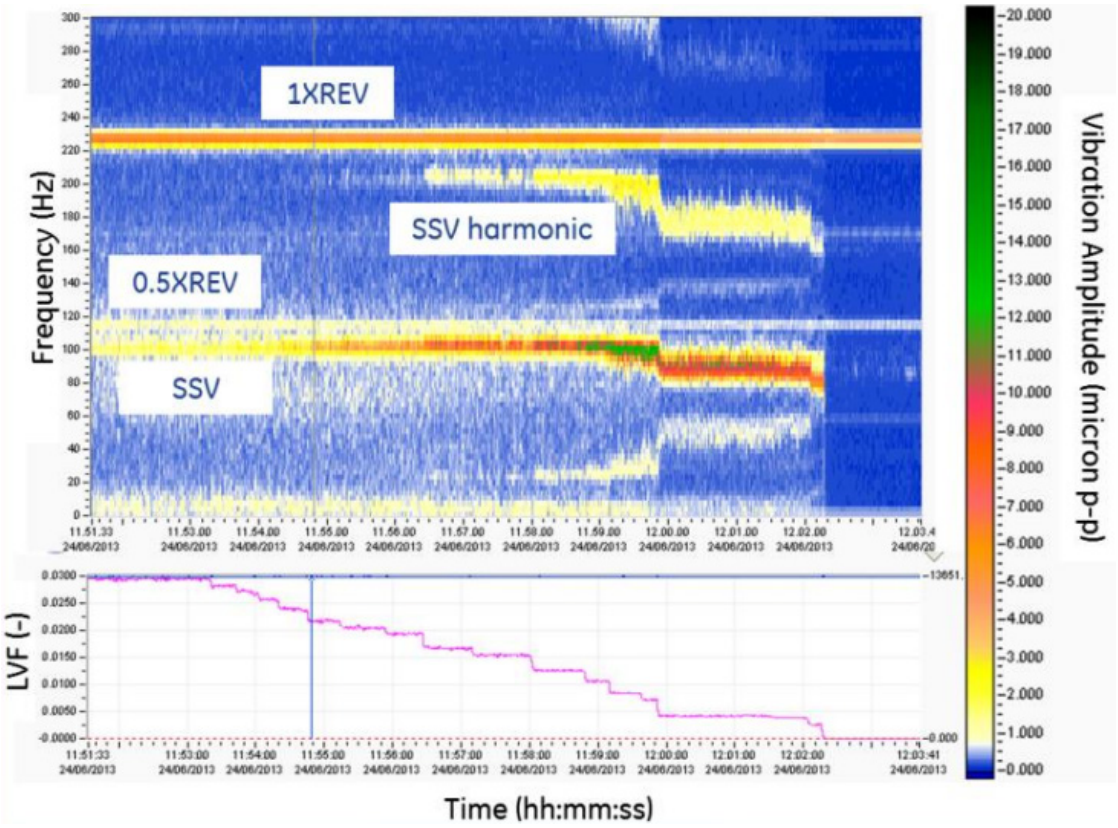

Figure 3. Typical waterfall plot of lateral vibrations at high flow region, ω=13.5 krpm, liquid-volume fraction LVF=1-GVF, GVF changes from 97% to 100% [10]

To provide a physical explanation for the experimental findings above, Vannini et al. [10], in 2015, conducted a multiphase CFD investigation of the original TOS labyrinth seal and the new PDS. Under wet-gas conditions, the cavities in the labyrinth seal showed a strong tendency to trap liquid. The trapped liquid had a high circumferential momentum, and it probably induced a sub-synchronous vibration. In a PDS cavity, some liquid was trapped; however, the liquid in a PDS cavity did not build up because it recirculated steadily in the circumferential direction, as shown in the CFD prediction of Fig. 4. The circumferential velocity of the liquid in a PDS cavity was much smaller in magnitude than in a corresponding labyrinth seal cavity and was even negative. Therefore, the PDS was less likely to prompt a sub-synchronous vibration, and it was a better option than the TOS labyrinth seal regarding the vibration performance. However, a drawback was that replacing the TOS labyrinth seal with the PDS led to an increase in leakage rate.

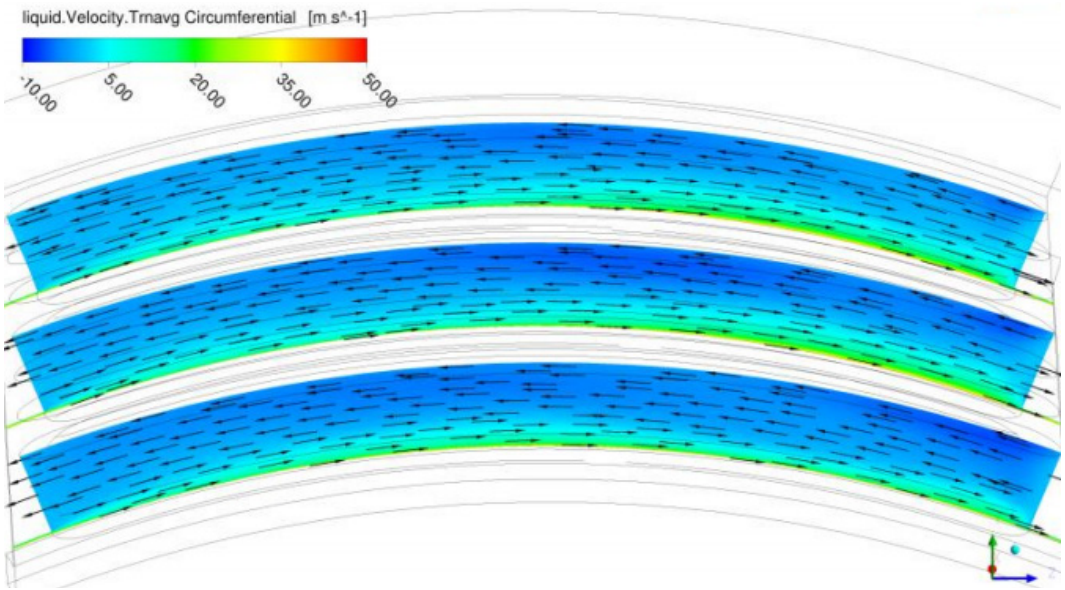

Figure 4. Time averaged circumferential velocity contour plot of the liquid in the PDS cavities, seal inlet GVF=70% (rotor rotating from left to right, and fluid flowing from bottom to top) [10]

With limited literature published on the mechanical vibration impact of wet-gas compressors, a general conclusion cannot be drawn to guide the design of annular seals in a wet-gas compressor. More experimental studies are needed to investigate the effects of wet-gas conditions on the performance of an annular seal.

1.2 Multiphase Pumps

With the increasing demand of the oil & gas industry, many pumps companies are developing multiphase pumps, which can handle liquid-gas flow directly without separating the liquid from a mixed flow. In general, there are two categories of multiphase pumps: rotordynamic pumps and positive displacement pumps. Since no annular seals are used in positive displacement pumps, this section only covers rotordynamic pumps, which have two types: centrifugal pumps and helico-axial pumps.

Many experimental studies focusing on the *performances* of multiphase centrifugal pumps have been published; however, those works were conducted to determine the operating performances of multiphase centrifugal pumps rather than the impacts of annular seals on the vibration characteristics.

Historically, helico-axial pumps did not have annular seals. However, according to Bibet et al. [11], this situation changed when the first multiphase helico-axial pump, equipped with a balance-piston seal, was introduced to the market in 2011. The balance piston seal compensated the axial thrust induced by impellers and made it possible to increase the pressure differential of a multiphase helico-axial pump. In 2013, Bibet et al. [11] presented the design process and test validation of a balance-piston seal in a full scale 1.8MW high boost helico-axial multiphase pump. The design of the balance-piston seal was chosen to be a smooth seal since textured seals, such as hole-pattern and honeycomb seals, tended to accumulate solid particles and liquid droplets in their cavities. The smooth balance-piston seal was then split into three segments by introducing two deep circumferential grooves. Swirl brakes were employed to reduce the pre-swirl ratio and enhance system stability. Test results showed that the system was stable through most cases; however, sub-synchronous vibrations occurred in some multiphase cases under low pressure differentials. In those cases, the pump was super-synchronously unstable.

To predict the rotordynamic coefficients and optimize the design of the smooth balance-piston seal, Bibet et al. [11] conducted CFD simulations. However, the simulations were only for pure-liquid conditions and did not include two-phase flow conditions. Therefore, more studies are needed to reveal the effects of gas components on a smooth annular seal in a multiphase pump.

1.3 Cryogenic Annular Seals

Besides the wet-gas compressors and multiphase pumps noted in preceding sections, two-phase flow may also occur in a cryogenic liquid annular seal. According to Beatty and Hughes [12], when a cryogenic liquid seal is operating close to saturation, the pressure drop and enthalpy rise through the seal induce the sealed fluid to be much closer or even over the saturation point. In this case, boiling occurs, and the sealed fluid changes from a single-phase liquid to a two-phase mixture of boiling liquid and vapor. Although the formation process of the liquid-gas mixture in a cryogenic liquid annular seal differs from that in multiphase pumps and wet-gas compressors, the prediction models and experimental studies of a cryogenic liquid annular seal are still relevant, because in all three types of applications, the gas presence changes the fluid compressibility significantly.

In 1981, Hughes and Beeler [13] developed the first prediction model for a cryogenic smooth annular seal with a phase change. The sealed fluid was turbulent, and it was regarded as a homogeneous liquid-gas mixture in thermodynamic equilibrium. Besides the phase change, the model also accounted for viscous dissipation, wall shear, fluid inertia, and inlet flow loss. The inlet pressure drop was simplified as an isentropic process. In 1987, Beatty and Hughes [12] made an improvement by using a new method to estimate the inlet thermodynamics state and calculated the mass flow rate of a centered smooth interstage seal (seal annular diameter D=65 mm, seal length L=26 mm, and radial clearance C_r=0.174 mm) in a Space Shuttle Main Engine High-Pressure Oxidizer Turbopump, where the sealed fluid was assumed to be turbulent, nearly adiabatic, close to the saturated point, and in thermodynamic equilibrium. The mixture properties were determined based on a homogeneous assumption. Numerical results showed that the formation of the vapor in the seal reduced the mass flow rate. Extending L, increasing ω, and reducing C_r could also reduce the mass flow rate.

In 1990, Beatty and Hughes [14] studied the effects of flow patterns on the leakage prediction of a cryogenic smooth annular seal. A stratified flow model rather than a homogeneous model was used to calculate the mixture properties. The stratified flow model assumed that the boiling liquid and vapor flowed separately at different velocities. A stratified flow could happen in some high-speed turbomachinery, such as rocket turbo-pumps, where the strong centrifugal inertia effect tended to drive the liquid phase from the vapor phase outward to the stationary surface while the vapor phase was still staying close to the shaft. For the smooth interstage seal analyzed by Beatty and Hughes [12], mass leakage rate predictions from the stratified flow model were close to predictions from the homogeneous model. Note that the effects of the flow pattern on the dynamic characteristics of a cryogenic liquid annular seal were not studied.

In 1987, Hendricks [15] measured the leakage rate and the pressure profile of a straight-smooth cryogenic-annular seal (L/D=0.51, D=84.2 mm, and C_r=0.1346 mm) at static (nonrotating) conditions. Tests were conducted at both concentric and eccentric positions over a range of temperature and inlet pressure for both liquid nitrogen and liquid hydrogen. Test data showed that a sufficiently large pressure drop through the seal could lead to a two-phase flow region in the test cryogenic-annular seal.

In 1998, Arauz and San Andrés [16, 17] employed a “continuous vaporization” bulk-flow model to analyze the mass flow rate, pressure profile, and rotordynamic coefficients of

cryogenic annular seals operating close to the saturated status. They divided the whole flow through a seal into three regimes: all-liquid, liquid-gas mixture, and all-gas. The liquid-gas mixture was assumed to be homogeneous and in thermodynamic equilibrium. The flow turbulence, friction effect, and viscous dissipation were included in governing equations. Moody's friction model was used to determine shear stress. A perturbation analysis was conducted to identify the static and dynamic characteristics of a seal. The predicted leakage rates and pressure profiles were validated using Hendricks' test data [15] for several liquid nitrogen cases with two-phase flow regions at the seal exit. The predicted leakages, torques, and exit mixture qualities correlated well with the predictions of Beatty and Hughes [12] for a cryogenic smooth seal with a phase change.

The predictions of rotordynamic characteristics were presented for cases with different supply temperatures, which controlled the flow structures (all-liquid, liquid-mixture, all-mixture, and all-gas) in a seal. The phase change significantly impacted the dynamic performance of a seal. As the sealed fluid changed from pure-liquid to a mixture of liquid and vapor within a short physical zone, the direct stiffness increased while the cross-coupled stiffness decreased. Also, the presence of a two-phase flow made damping coefficients more sensitive to Ω. For example, the direct damping decreased with increasing Ω. Additionally, when $\Omega=\omega$, whirl frequency ratio (WFR) decreased significantly as the phase change occurred, implying that the gas presence improved the system stability.

In 1999, Oike et al. [18] designed a test apparatus, which could visually display the two-phase flow in cryogenic smooth floating-ring seals. Tests were conducted under temperatures from 80 to 98 K, pressure differences up to 1.25 MPa, and rotor speeds up to 40 krpm. The observed two-phase flow was homogeneous. The two-phase flow region in the seal clearance increased with increasing ω; however, an increase of the two-phase flow region did not always lead to a decrease in the leakage mass flow rate. The effects of the two-phase flow area on the leakage flow mass rate depended on the upstream subcooling degree and the seal clearance.

In 2013, Hassini and Arghir [19] employed the same bulk-flow model as Arauz and San Andrés [16, 17] to predict the rotordynamic coefficients of a smooth cryogenic-annular seal with accommodations to handle choked flow regimes and a new method to estimate the speed of sound in both single-phase and two-phase flow regimes. Hassini and Arghir [19] covered a wider range of Ω (from 0 to 6ω) than Arauz and San Andrés [16, 17], who only presented the rotordynamic characteristics at 3 excitation frequencies (0.01ω, 0.5ω, and 1ω). For pure-liquid

cases, the complex dynamic stiffness coefficients could be curve-fitted to obtain constant stiffness, damping, and virtual-mass coefficients. For gas-dominated cases, in which the phase change occurred at the very inlet of the seal, the dynamic coefficients were sensitive to Ω, and their dependencies on Ω show some similarities with those in pure-gas cases, especially when $\Omega > 2\omega$.

1.4 Two-Phase Annular Seals

In 1992, Salhi et al. [20] measured the axial pressure gradient in a narrow annular space formed by two concentric cylinders under two-phase flow conditions. The exterior cylinder was fixed, and the interior cylinder was rotating at speeds up to 10 krpm. The interior cylinder diameter was 50 mm, and the annular space length was 312 mm. Tests were carried out at C_r=0.5 and 1 mm. The test liquid consisted of 95% water and 5% soluble oil. Nitrogen was injected through a sintered-metal element at the inlet, making a two-phase mixture at 5% gas/oil ratio (GOR). GOR is the ratio of the volume of gas to the volume of liquid at standard conditions (15.56 °C and 1 bar). Since the pressures at the seal inlet were not stated, GOR could not be converted to GVF. Photographic pictures at the outlet of the test cell showed that the diameter of nitrogen bubbles was around 30 μm. The Reynolds number of the mixture was above 4000. The measured pressure drop coefficients were consistent with the predictions from a homogeneous model. This consistency led to a hypothesis that the gas remained dispersed in liquid because the separation effect induced by the centrifugal force was limited by the turbulent flow and stopped by the coalescence time of a bubble. Therefore, the homogeneous model seemed to be validated experimentally for a two-phase flow case with a small amount of gas in liquid (GOR=5%).

In 1994, Iwatsubo and Nishino [21] experimentally investigated the dynamic characteristics of a long smooth annular seal (L/D=1, D=70 mm, and C_r=0.5 mm) operating under two-phase (water-air) conditions at low inlet pressures (up to 4 bars) and low rotor speeds (0.5 to 3.5 krpm). Test data were only valid for mean GVFs less than 70%. When mean GVF>70%, the random vibration of the rotor due to the 2-phase flow was large and produced large measurement uncertainties. The mean GVF was defined as the average value between the seal inlet and the seal exit. The measured seal forces increased as inlet pressure increased, and this tendency did not change as mean GVF changed. The measured seal forces and the identified rotordynamic (stiffness and damping) coefficients decreased as mean GVF increased from zero

to 70%. Although predictions were made to compare to the test results, the prediction model was based on an inappropriate assumption, which simplified the mixture to be an incompressible flow.

In 2011, San Andrés [6] used a modified one-control-volume bulk-flow model to analyze the static and dynamic characteristics of annular pressure seals operating under two-phase (liquid-gas) flow conditions. The two-phase mixture was assumed to be isothermal, homogeneous, and in thermostatic equilibrium. The wall stress model was based on Moody's friction formula. The static and dynamics performances of a seal were determined by a perturbation analysis.

For an example long smooth annular seal (L/D=0.75, D=116.8 mm, and C_r=0.1267 mm) operating with a mixture of nitrogen gas and light oil (ISO VG2) at P_i=71 bars, ω=10 krpm, and GVFs from zero to 100%, predictions showed that power loss and leakage mass flow rate generally decreased as GVF increased. However, when GVF≈0.1, the increased viscosity of the lubricant led to a flow laminarization and produced a dip in power loss, as shown in Fig. 5. Cross-coupled stiffness and direct damping decreased as GVF increased, except in the region where the flow became laminar; i.e., GVF≈0.1, as shown in Fig. 6. Direct stiffness increased dramatically as GVF increased from 0 to 0.1 and then dropped significantly as GVF increased to about 0.25. When GVF>0.25, direct stiffness increased with increasing GVF. Cross-coupled damping coefficients were small and inconsequential.

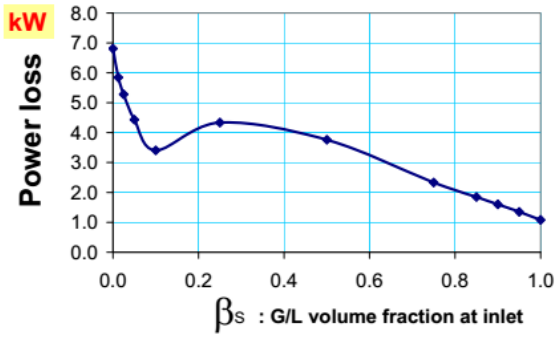

Figure 5. Predicted effects of GVF on power loss [6]

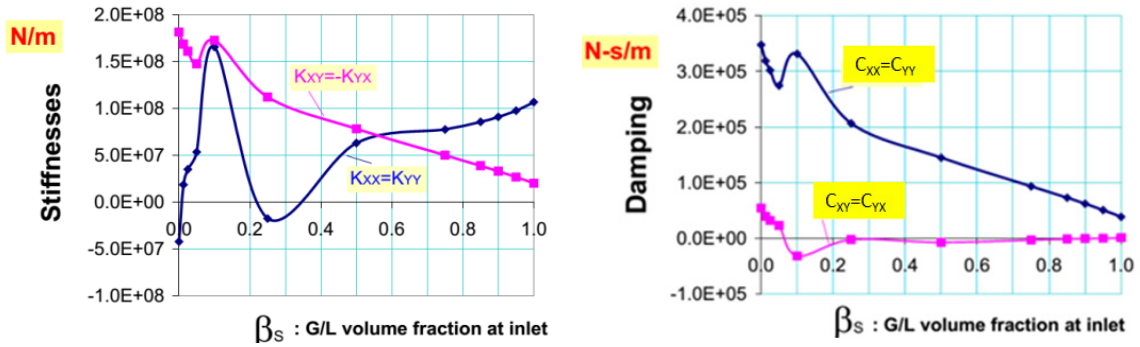

Figure 6. Predicted effects of GVF on stiffness and damping coefficients [6]

In 2011, Arghir et al. [22] employed Kleynhans and Childs's [23] two-control-volume bulk-flow model to study the rotordynamic characteristics of a centered textured-annular seal (L=35 mm, D=76.5 mm, and C_r=0.1 mm) operating under bubbly flow conditions with low GVFs, ranging from 0.1% to 10%. Benefitting from the two-control-volume method, the mass flow exchange between two control volumes and the effects of the cell depth were taken into consideration. The fluid inertia effect was also included. The model treated the textured seal as a smooth seal with equivalent friction factors on the two surfaces forming the seal clearance. The friction factors were determined by a 3-dimensional Navier-Stokes analysis. To simplify the analysis, the axial and circumferential flow were assumed to be dominated by Poiseuille effect and Couette effect, respectively. The mixture properties were determined using a homogeneous-mixture assumption.

For pure-liquid cases, all rotordynamic coefficients had no or slight dependencies on **Ω**. The presence of dissolved gas in liquid introduced compressibility to the sealed fluid, and made the rotordynamic coefficients significantly dependent on **Ω**, especially when GVF≥5%. For GVF≤1%, the effects of GVF could be ignored. In addition, cross-coupled stiffness, direct virtual-mass, and cross-coupled virtual-mass decreased as GVF increased from 0.1% to 10%. Since those predictions were made for a round-hole-pattern seal with an area ratio of 44%, they could not be assessed using San Andrés's [6] predictions or Iwatsubo and Nishino's [21] test results.

In 2015, San Andrés et al. [24] introduced a test rig to measure the leakage flow rate and rotordynamic coefficients of a short smooth annular seal (L/D=0.36, D=127 mm, and C_r=0.127 mm) operating under two-phase flow conditions. The test fluid was a mixture of ISO VG 10 oil and air. All tests were conducted at nonrotating conditions and ambient temperature. The exit

pressure was ambient. Leakage mass flow rates were measured at two inlet pressures (3 and 3.5 bars) and multiple GVFs ranging from 100% to zero (multiple LVFs ranging from zero to 100%). As shown in Fig. 7, measured leakage mass flow rate increased as GVF decreased from 100% to zero (LVF increases from zero to 100%). Predictions were given based on San Andrés's [6] bulk-flow model. Figure 7 shows that the measured leakage rates agreed well with the predictions. In Fig. 7, P_s is the seal supply pressure, and P_a denotes the ambient pressure.

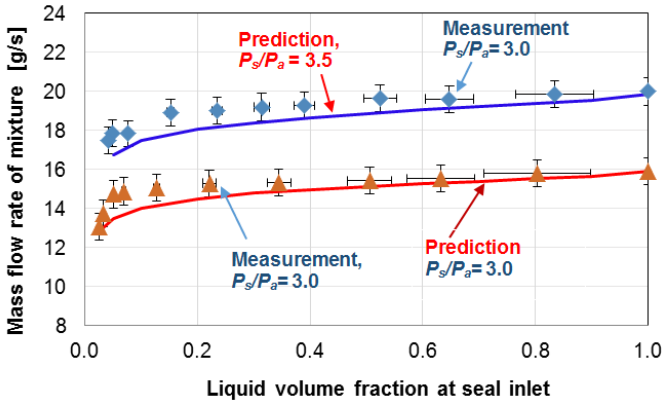

Figure 7. Measurements and predictions of mass flow rate (liquid-volume fraction=1-GVF, GVF at seal inlet decreases from 100% to zero) [24]

Rotordynamic coefficients of the seal were measured at three different GVFs (100%, 98%, and 96%) when P_i=2 bars. The seal cartridge was excited by two orthogonally mounted electromagnetic shakers with periodic loads, comprising multiple frequencies from 30 Hz to 200 Hz, in increments of 10 Hz. The real parts of the system's complex dynamic stiffness were curved-fitted to obtain frequency independent stiffness and virtual-mass coefficients. Measured direct stiffness and direct virtual-mass coefficients in the horizontal direction were different from the measured values in the vertical direction. As GVF decreased from 100% to 96%, measured direct stiffness increased by 78.6% from 1.4 to 2.5 MN/m in the horizontal direction and increased by 30% from 1 to 1.3 MN/m in the vertical direction. When GVF was dropped from 100% to 96%, measured direct virtual-mass increased from zero to about 1.2 kg in the horizontal direction and increased from zero to 0.9 kg in the vertical direction.

The imaginary parts of the system's complex dynamic stiffness could not be characterized by frequency independent damping coefficients since they were not proportional to

Ω. The liquid presence in air significantly affected the measured damping characteristics. Damping coefficients measured at GVF=96% were more than 20 times larger than at GVF=100%.

Quoting San Andrés et al. [24], "Damping force coefficients, although decreasing steadily with excitation frequency, are at about 50% of the experimental coefficients. The larger the content of liquid in the mixture, the larger the discrepancy. Predicted dynamic stiffnesses agree with the test coefficient only for the case with pure gas. Presently, the tests conducted without journal rotation and with a low supply/discharge pressure ratio (max. 3.5) show the mixture flow character is not homogeneous, in particular near the exit lane of the seal."

In 2017, San Andrés and Lu [25] presented more test data from the same test rig for the same test seal but with a rotating rotor (ω up to 3.5 krpm). The exit pressure was 1 bar, and P_i was up to 3.5 bars. The GVF varied from zero to 90%, which is a typical range for multiphase pumps. As GVF increased, the mass flow rate and drag power decreased continuously. Rotordynamic coefficients were obtained for cases with P_i=2.5 bars and ω=3.5 krpm. When GVF=0%, direct dynamic stiffness decreased as Ω increased, indicating a large positive direct virtual-mass term. However, after adding air into the oil, direct dynamic stiffness increased as Ω increased. Both direct damping and cross-coupled dynamic stiffness decreased as inlet GVF increased. Adding air into the oil significantly decreased the effective damping. Predictions from San Andrés's [6] model correlated well with measurements when GVF≤60%. For 60%<GVF≤90%, predicted force coefficients were lower than measurements in magnitude.

As noted above, existing test data are limited by some deficits, such as low supply pressures, low ω, narrow GVF ranges, etc. Thus, a comprehensive set of test data is needed to study the static and dynamic characteristics of a two-phase annular smooth seal and validate the current prediction models.

2. OBJECTIVES

Despite the potentially adverse impacts of two-phase flow conditions on the static and dynamic characteristics of a smooth annular seal and the performance of a wet-gas compressor or a multiphase pump, previous experimental studies on a two-phase smooth annular seal are scarce. This dissertation discusses a comprehensive experimental investigation into the effects of two-phase flow conditions on a smooth annular seal through completion of the following tasks:

1. Modify an existing air-annular seal test stand to 2PASS. The development of 2PASS has one limitation and four major challenges.

   Limitation: Although an ideal test stand should investigate the performance of a smooth annular seal with any GVF (zero to 100%), the GVF range is limited to mainly-oil conditions (GVF≤10%) and mainly-air conditions (92%≤GVF≤100%) due to the difficulties in making a homogeneous 2-phase mixture with GVF between 10% and 92%. Since most wet-air compressors are operating with a GVF above 95%, the test GVF range meet the needs of wet-gas compressor companies. However, it cannot completely satisfy the interests of multiphase pump companies since their multiphase rotordynamic pumps are expected to cope with any GVF (zero to 100%).

   Challenge 1: Design an oil/air mixer, aiming to make a homogeneous mainly-air mixture (92%≤GVF≤100%). Since no commercial mixers could be found to meet the requirements of this test program, the mixer is designed mainly using CFD simulations and a low-pressure mixing test. During the low-pressure test, the pressure in the mixing chamber shown in Fig. 10 is reduced from 62 bars to 5.5 bars, and the stainless-steel mixing chamber is replaced by an acrylic mixing chamber, which allows the use of a high-speed camera to take slow motion videos and photographic pictures to visually inspect the mixing quality and estimate oil droplet size.

   Challenge 2: Specify and install oil/air separation equipment, including a vertical oil/air separator, a bubble eliminator, and a coalescer. The separated oil is pumped back to oil tanks, and the purified air is discharged outside.

Challenge 3: Due to the possibility of "slugs" in the mixed flow and the possible negative direct stiffness of the test seals, 2PASS is too fragile to handle 2-phase flow under some seal configurations and/or some test conditions.

Challenge 4: 2-phase flow might introduce more fluctuations into data acquisition than air flow and then increase the uncertainties of the identified rotordynamic coefficients. The stator assembly is excited longer than under pure-air conditions, aiming to reduce the uncertainties of the identified rotordynamic coefficients by averaging more test data.

2. Experimentally investigate the effects of changes in radial clearance (C_r), GVF, pressure drop/ratio (PD/PR), and rotor speed (ω) on the mass flow leakage rate and rotordynamic coefficients of a smooth annular seal.
3. Compare test results to the predictions from a program developed by San Andrés [6] to investigate his predictive model for a smooth annular seal operating under 2-phase flow conditions.

3. TEST RIG DESCRIPTION*

The 2PASS is modified from an existing air-annular seal test stand in the Turbomachinery Laboratory at Texas A&M University to accommodate two-phase flow test conditions. Childs et al. [26] describe the existing air-annular seal test stand. The following major modifications has been completed by the author and James McLean under the supervision of Dr. Dara Childs, Professor of Mechanical Engineering, Texas A&M University, and some of these modifications will be discussed further in Sec. 3.1.

(1) To eliminate possible water/oil contamination, the supply fluid for hydrostatic bearings (that supported the test rotor) is changed from water to the test liquid (silicone oil PSF-5cSt).

(2) To increase the maximum test rotor speed under pure-liquid conditions, the test seal's inner diameter is reduced from 114.3 mm (4.5 in) to 89.306 mm (3.5160 in), and the electric motor is upgraded from 93 kW (125 hp) to 110 kW (150 hp).

(3) To reduce the minimum test rotor speed from 10 krpm to 5 krpm, an external lubrication system is added for the existing gearbox.

(4) The water-supply/return system is removed, and a new silicone-oil supply/return system is designed, built, and installed.

(5) A sparger system is designed, built, and installed, aiming to make homogeneous mainly-liquid mixtures.

(6) An oil/gas mixer is designed, built, and installed, aiming to make homogeneous mainly-air mixtures.

(7) To separate liquid components from the exhaust mixed flow and purify gas before discharging, separation equipment (including a vertical oil/gas separator, a bubble eliminator, and a coalescer) are specified and installed.

(8) The data acquisition system and programmable logic controller (PLC) control system is upgraded.

---

* Portion of this section is reprinted with permission from "Experimental Study of the Static and Dynamic Characteristics of a Long Smooth Seal with Two-Phase, Mainly-Air Mixtures," by Zhang, M., McLean, J., and Childs, D., 2017, *ASME J. Eng. Gas Turbines Power*, 139(12), p. 122504, Copyright 2017 by ASME.

3.1 Experimental Setup

Figure 8 depicts the piping and instrumentation diagram (P&ID) of the 2PASS, which consists of the following sections: air-supply section, oil-supply/return section, mainly-oil mixing section, mainly-air mixing section, and test section. Each section is discussed separately below.

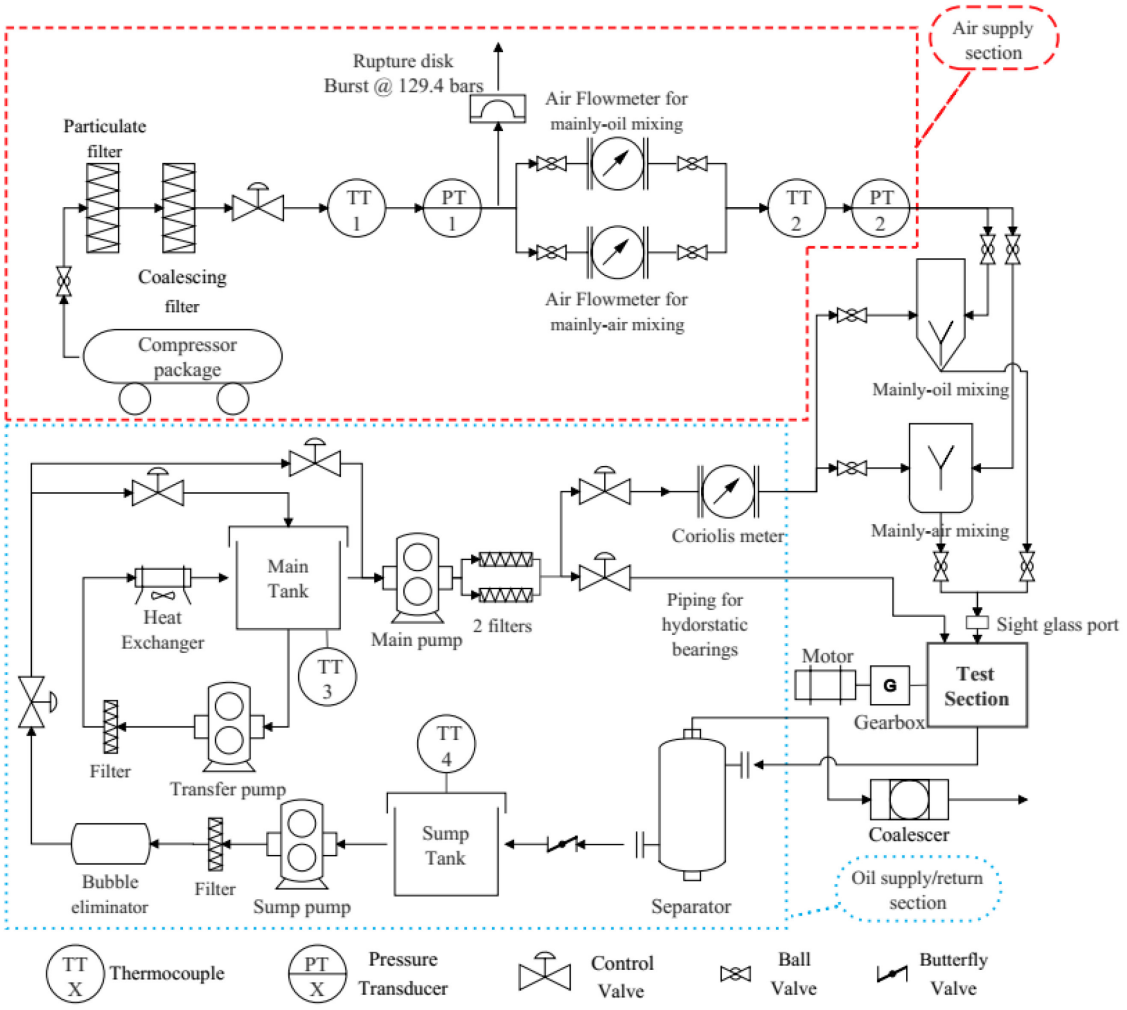

Figure 8. Piping and instrumentation diagram of the 2PASS [27]

3.1.1 Air-Supply Section

The 2PASS employs its predecessor's air-supply system. A compressor delivers air at a maximum supply pressure of 172 bars. A particulate filter removes solid particles, and a coalescing filter removes liquid droplets from the compressed-air stream. A rupture disk with a burst pressure of 129.4 bars ensures safety. A control valve adjusts the air flow, and turbine flowmeters with different ranges measure the volume flow rate. The low-range turbine flowmeter measures the flow rate of air entering the mainly-oil mixing section. The high-range turbine flowmeter measures the flow rate of air entering the mainly-air mixing section. Thermocouples and pressure transducers measure the temperatures and pressures before and after turbine flowmeters.

3.1.2 Oil-Supply/Return Section

The 2PASS renovation removed the water-supply/return system in the existing air-annular seal test stand, and a new oil-supply/return system supplies silicone oil for the mixing sections and the hydrostatic bearings (described in Sec. 3.1.5 below). Figure 8 shows that two filters immediately after the main pump ensure that the oil supply is clean. The oil flow splits into two pipes: one pipe supplies oil for the hydrostatic bearings that support the rotor, and the other pipe provides oil for the mixing sections. A Coriolis flow meter measures the mass flow rate and density of the oil.

The two-phase flow from either the mainly-oil mixing section or mainly-air mixing section is injected into the test section. After the test section, the exhaust mixture enters a vertical oil/gas separator, which separates most air components from the mixture. A coalescer removes the liquid-carryover before the separated air discharges into the environment. The separated oil flows into a sump tank by the effect of gravity. A sump pump transfers the oil to a main tank or the main pump. A bubble eliminator removes the dissolved gas components in the oil. A heat exchanger loop cools the oil in the main tank; hence, the oil from the sump tank is normally hotter than the oil from the main tank. A control valve on the line from the sump tank to the

main pump adjusts the hot-oil flow rate and controls the discharge oil temperature of the main pump.

3.1.3 Mainly-Oil Mixing Section

Spargers produce mainly-oil mixtures by injecting air bubbles into the oil stream. Figure 9 shows the PI&D of the mainly-oil mixing section. The mainly-oil mixing section uses two spargers, and Table 1 gives their properties. Each sparger mounts in a tee. As the compressed air flows through the porous surface of a sparger, the silicon oil, flowing through the annulus between the sparger and pipe, shears the bubbles, resulting in an excellent mixing performance. A pressure relief valve with a relief pressure of 75.8 bars ensures safety. Two pressure transducers measure the pressures of oil and air before mixing, respectively.

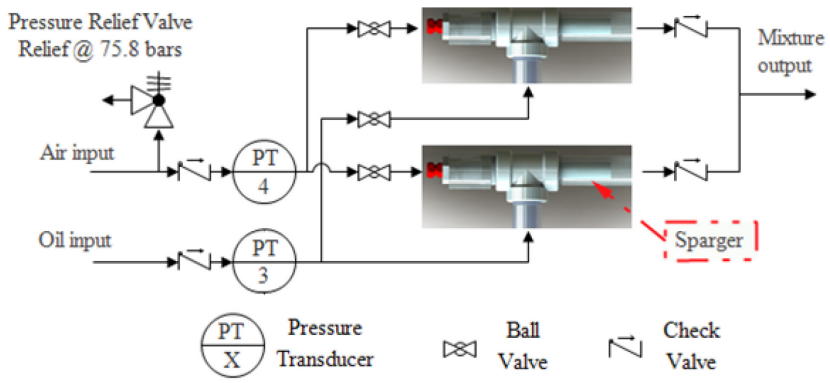

Figure 9. P&ID of mainly-oil mixing section

Name	Mott 850-Series sintered porous metal element
Porous Outer Diameter (mm)	25.4
Wall Thickness (mm)	3.2
Porous Length (mm)	215.9
Nominal Length Without Fitting (mm)	304.8
Media Grade (μm)	10
Material	316L stainless steel

Table 1. Properties of the sparger

3.1.4 Mainly-Air Mixing Section

Figure 10 depicts the oil-air mixer that produces mainly-air mixtures. The mixer consists of the following 3 chambers: oil chamber, air chamber, and mixing chamber. Silicone oil enters the oil chamber and then flows into 9 injection tubes. At the other end of each injection tube, a spray nozzle (as described in Table 2) produces fine liquid droplets spreading in the mixing chamber. The compressed air, injected into the air chamber section from another line, passes through the clearances between the plate and injection tubes, and meets the atomized liquid droplets in the mixing chamber. The liquid-air mixture flows through a converging cone which compresses the mixture back into a manageable pipe diameter.

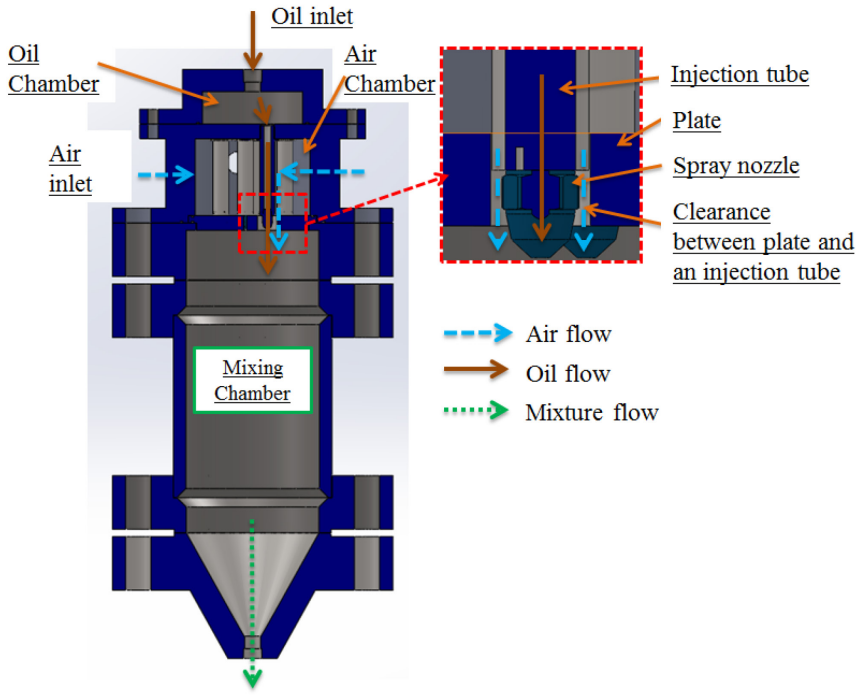

Figure 10. Section view and flow illustration of the oil-gas mixer [27]

In Fig. 11, an acrylic cylinder replaces the steel chamber shown in Fig. 10. An acrylic chamber provides visual confirmation of the mixer's performance. A high-speed camera with a sample rate of 8300 fps records the resulting mixture. The strength of the acrylic chamber limits

the mixing pressure to 5.5 bars. For a mixture of air and water with GVF=97% at 25 ºC, the water droplets distribute evenly in the acrylic mixing chamber with a diameter of about 0.25 mm.

Type	Hollow Cone Spray Nozzle
Model	1/4KKBP200S303
Standard Pressure (bar)	3
Spray Angle (º)	55±5
Spray Capacity (l/min)	2±0.1

Table 2. Properties of the spray nozzle

Figure 11. Gas-oil mixer with an acrylic mixing chamber

According to Bracco [28], the mean droplet size of liquid drops produced by a nozzle is proportional to the surface tension σ, but inversely proportional to the gas density ρ_g,

$$\bar{D} = B\frac{\sigma}{\rho_g} X_{xmax} \frac{2\pi}{v_r}, \tag{7}$$

where v_r is the relative velocity between the liquid and gas, X_{xmax} is a coefficient depending on the Weber number, and B is a constant coefficient.

Using Eq. (7) to predict the droplet size of the silicon oil injected in the compressed air at 25ºC and 62 bars,

$$D_{est} = \frac{\sigma_{oil}}{\sigma_{water}} \cdot \frac{\rho_{g,5.5}}{\rho_{g,62}} \cdot 250\ \mu\text{m} = \frac{0.0197}{0.072} \cdot \frac{6.44\ \text{kg/m}^3}{72.54\ \text{kg/m}^3} \cdot 250\ \mu\text{m} = 6.2\ \mu\text{m}, \qquad (8)$$

where D_{est} is the estimated mean droplet size of silicone oil, σ_{oil} is the surface tension of silicone oil, σ_{water} is the surface tension of water, $\rho_{g,5.5}$ is the air density at 5.5 bars and 25ºC, and $\rho_{g,62}$ is the air density at 62 bars and 25ºC. 62 bars is the supply pressure for the test seal under pure- and mainly-air conditions. Note the real mean droplet size of the silicone oil may be larger than D_{est} for the following reasons:

1. D_{est} is calculated based on the assumption that X_{xmax}, B, and v_r do not change significantly when changing from water to silicone oil and increasing the pressure in the mixing chamber from 5.5 bars to 62 bars.
2. Liquid droplets may merge when flowing in the pipes connecting the oil/air mixer and the test section.

3.1.5 Test Section

Figure 12 shows a cross-section view of the test section. Two hydrostatic bearings support the rotor, and use silicone oil at 69 bars as lubricant. The hydrostatic bearings provide high support stiffness to the rotor compared to the stiffness from test seals. A high-speed disc-type coupling connects the rotor to a Lufkin Gearbox. The gearbox increases the electric motor speed to the expected rotor speed by a ratio of 1:6.96, and a variable-speed drive controls the motor speed.

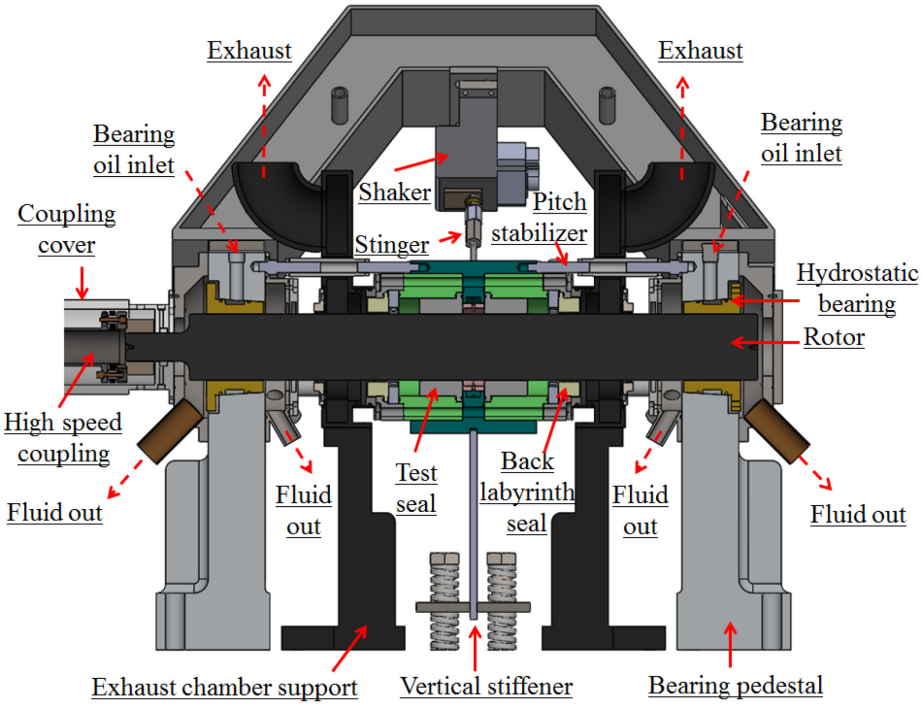

Figure 12. Cross-section view of the test section [27]

Figure 13 shows connections to the stator assembly. Two hydraulic shakers and three pairs of pitch stabilizers (shown in Fig. 12) support the stator assembly. Two orthogonally-oriented stingers connect the hydraulic shakers to the stator assembly. The hydraulic shakers not only control the static position of the stator and but also excite the stator with a pre-programed pseudo-random waveform. The pseudo-random waveform consists of 14 frequencies, ranging from 10 Hz to 140 Hz with increments of 10 Hz. The excitation force is adjusted to ensure that the peak-to-peak stator dynamic amplitude is less than 20% of the radial clearance. The pitch stabilizers, installed in an equilateral triangle pattern on each end of the stator assembly, control the stator's axial positon and enable the alignment between the stator and rotor.

Figure 14 shows additional supports (two pairs of horizontal cables and a vertical stiffener) to rotordynamically stabilize the stator. Picardo and Childs [29] used the horizontal cables to eliminate a stator dynamic instability by introducing orthotropic support stiffness for the stator. Mehta and Childs [30] added the vertical stiffener to overcome the static instability of the stator induced by negative static direct stiffness of the test seals.

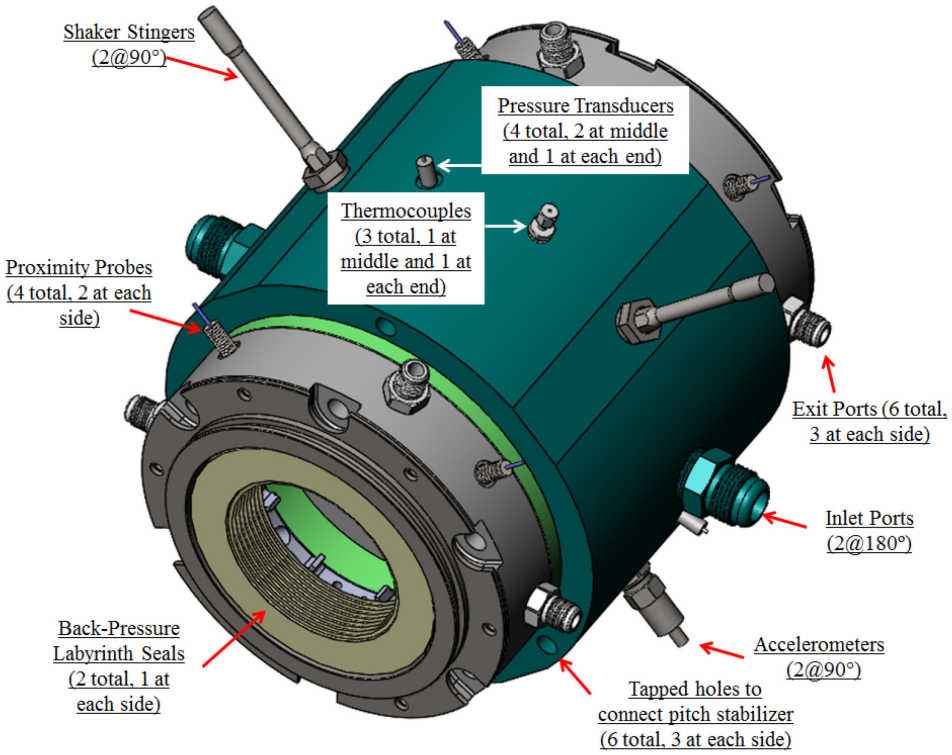

Figure 13. 3-D model of the stator assembly

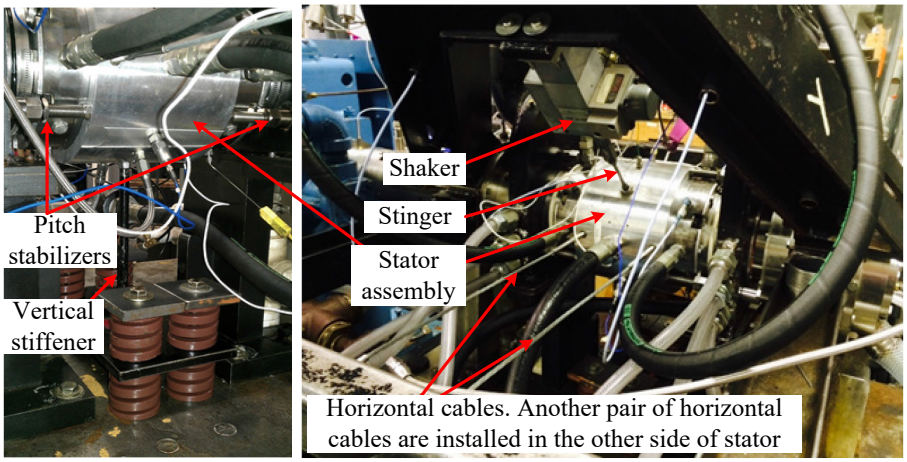

Figure 14. Photograph of the test section [27]

Figure 15 depicts the cross-section view of the stator assembly. For ease of viewing, the seal clearances are shown greatly enlarged. The stator assembly comprises two test seals, two swirl brakes, and two back-pressure labyrinth seals. The test seals and back-pressure labyrinth

seals are installed back-to-back to minimize the net-thrust force developed by the pressure drop through each seal. During tests, the test fluid enters the stator assembly through two inlet ports at the center annulus and flows through a zero pre-swirl guide insert.

Figure 16 shows the section view of the zero pre-swirl guide insert. The fluid then flows through test seals and reaches the back-pressure annuluses upstream of the back-pressure labyrinth seals. In this cavity, the fluid either exits radially through exit ports or axially through the back-pressure labyrinth seals. A bleed valve, downstream of the exit ports, adjusts the back pressures of test seals. Fully closing the bleed valve forces all fluid to discharge through the back-pressure labyrinth seals and generates the maximum back pressure for a certain supply pressure. Swirl brakes, upstream of the back-pressure labyrinth seals, reduce the circumferential velocity of the test fluid and minimizing the cross-coupled stiffness coefficients produced by the back-pressure labyrinth seals.

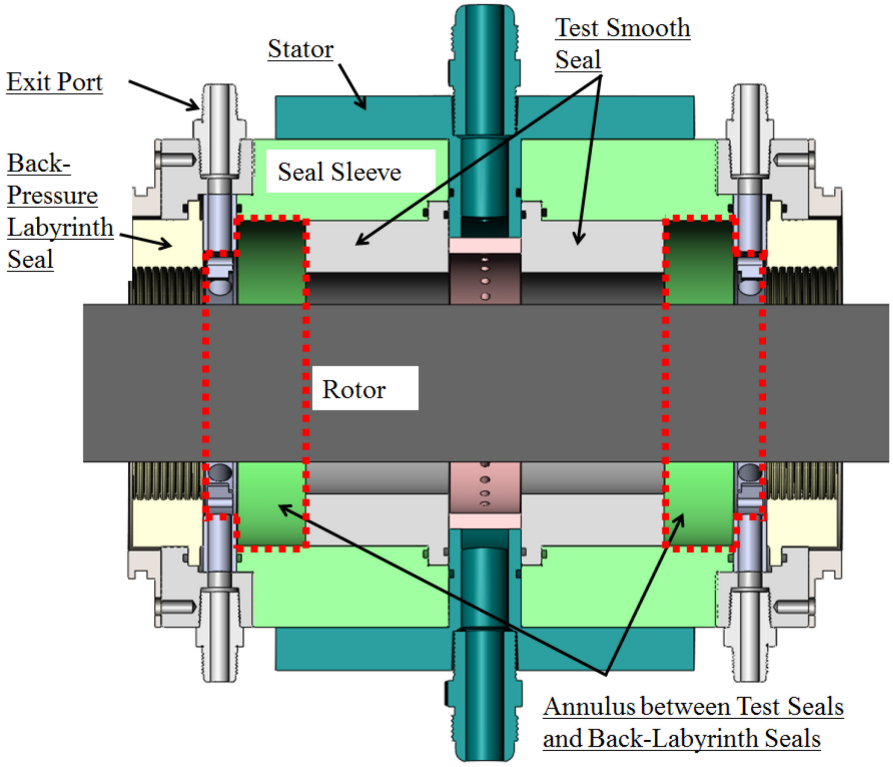

Figure 15. Section view of the stator assembly [27]

The zero pre-swirl-guide insert shown in Fig. 16 guides the test fluid radially inwards to produce a flow with minimum circumferential velocity at the seal inlet. However, the circumferential velocity of the test fluid at the seal inlet $V_{\theta 0}$ is not zero due to the rotor rotation. Figure 17 depicts a pitot tube setup (including a pitot tube and a static pressure orifice) that determines $V_{\theta 0}$. A differential pressure transmitter measures the difference between the total pressure P_t and static pressure P_s at the seal inlet. Bernoulli's equation determines

$$V_{\theta 0} = \left[2\left(P_t - P_s \right) / \rho \right]^{1/2}, \tag{9}$$

where ρ is the test fluid density defined in Eq. (13).

The pre-swirl ratio $u_0(0)$ is the ratio of $V_{\theta 0}$ to the surface speed of the rotor:

$$u_0(0) = \frac{V_{\theta 0}}{0.5 D_r \omega}, \tag{10}$$

where D_r is the rotor diameter.

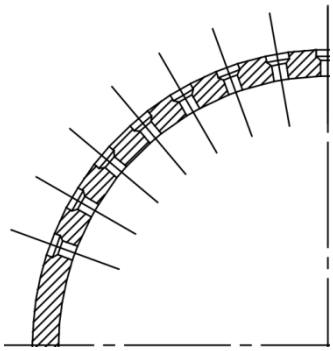

Figure 16. Cross-section of the zero pre-swirl guide insert [27]

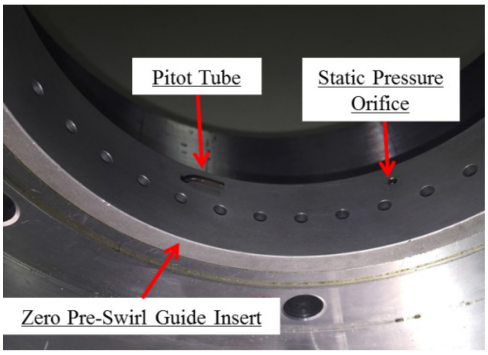

Figure 17. Pitot tube and static pressure orifice

3.2 Instrumentation

Table 3 gives the uncertainties of the instrumentations in the air-supply section and oil-supply/return section.

2PASS uses the same test-section instrumentation as its predecessor, and Kerr [3] describes the instrumentation in detail. Kurtin et al. [31] performed the uncertainty analysis for them, and Table 4 shows the results.

Parameter	Uncertainty
Air Volumetric Flow Rate for Mainly-Air Conditions	0.305 ACFM (0.52 m^3/h)
Air Volumetric Flow Rate for Mainly-Oil Conditions	0.0414 ACFM (0.0703 m^3/h)
Liquid Mass Flow	0.11 kg/min
Liquid Density	0.18 kg/m^3

Table 3. Static uncertainties for volume/mass flow rates and oil density

Parameter	Uncertainty
Pressure	0.838 psi (0.06 bars)
Temperature	5.613 °F (3.1 K)
Pitot Tube Differential Pressure	1.276 in-H_2O (0.0032 bars)

Table 4. Static uncertainties for instruments in the test section [31]

3.3 Test Fluid

The test fluid is a mixture of silicone oil (PSF-5cSt) and air. Silicone oils are non-Newtonian fluids, and their viscosities are only constant for shear rates below certain values (critical shear rates), as shown in Fig. 18. The critical shear rate increases as the nominal viscosity of the fluid decreases. Although Fig. 18 does not show the rheological behavior of the test silicone oil (PSF-5cSt), the vendor (Clearco Products Co., Inc.) [32] states that silicone oil (PSF-5cSt) shows Newtonian behavior under shear; i.e., its viscosity remains unchanged as shear rate increases.

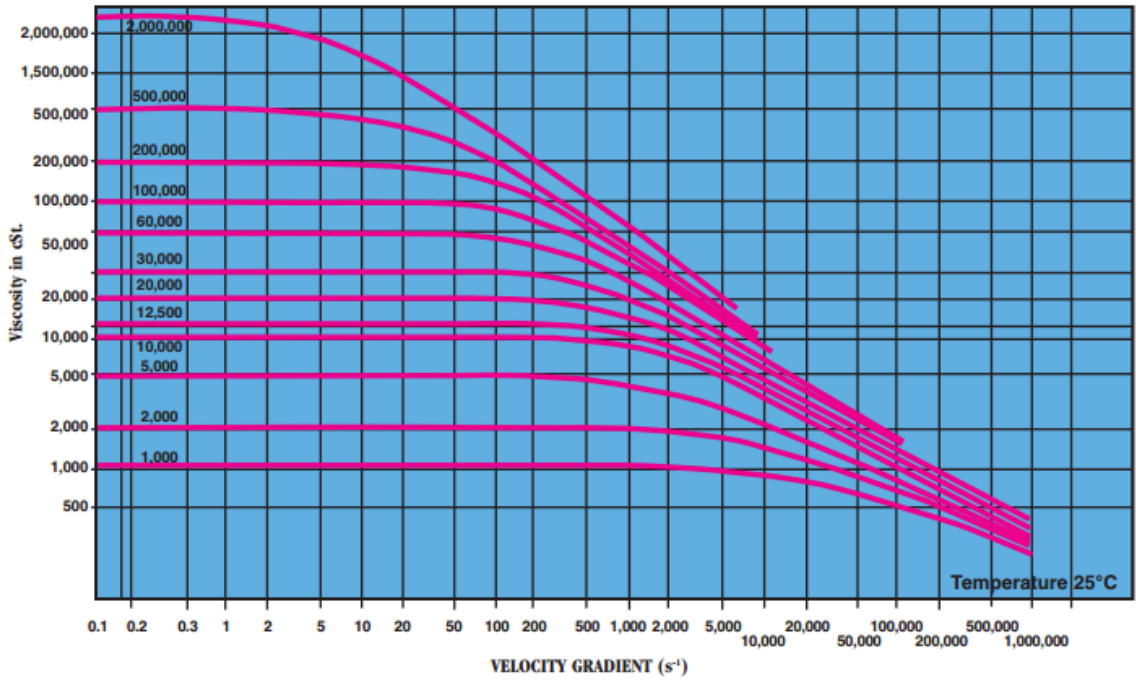

Figure 18. Silicone oils' viscosities under shear [33]

Silicon oil (PSF-5cSt) was used for the following reasons:

1. It is hydrocarbon-based, non-flammable, hydrophobic, chemically inert, and has high resistance to oxidation [34]. It mixes safely with air, and air is cheaper than other non-explosive gas sources; e.g. nitrogen.
2. The viscosity-temperature coefficient, which is the ratio of the oil viscosity at 99 ºC to the oil viscosity at 38 ºC, is as low as 0.54 [34]. Therefore, the oil viscosity is not very sensitive to temperature change. It allows a tolerance in temperature control. Under mainly-oil conditions, the seal inlet temperature was controlled between 37.8 ºC and 40.6 ºC.
3. The surface tension is only 0.0197 N/m, which is approximately 1/3 that of water [34]. A smaller surface tension leads to the formations of smaller liquid droplets, which are more likely to be distributed uniformly in an air stream than larger liquid droplets.

The measured viscosity index of silicone oil (PSF-5cSt) is 817, and Table 5 shows the other properties of silicone oil (PSF-5cSt).

Chemical Name	Polydimethylsiloxane
Appearance	Clear, colorless, odorless
Viscosity-Temperature Coefficient	0.54
Viscosity @ 25 ºC (cSt)	5
Specific Gravity	0.918
Flash Point (ºC)	135
Pour Point (ºC)	-90
Vapor Pressure @ 25°C (Pa)	133.3
Thermal Expansion (m^3/ m^3·ºC)	0.00109
Thermal Conductivity @25ºC (W/m·K)	1.172
Surface Tension (N/m)	0.0197
Boiling Point (ºC)	>200

Table 5. Silicone oil specifications and data [34]

The test fluid was visually inspected through a sight-glass view port shortly upstream of the inlet ports of the stator. In most test cases, the two-phase mixture appeared homogeneous; i.e., the air bubbles (or oil droplets) are distributed evenly in the oil (or air) flow. Thus, a homogeneous assumption is used here to determine the mixture properties.

The gas phase (air) is simplified as an ideal gas with the following state equation:

$$\rho_g = \frac{P}{ZR_gT}, \tag{11}$$

where Z is the gas compressibility factor, R_g is the gas constant, P is the pressure, and T denotes the temperature.

The gas-volume fraction GVF is:

$$\mathrm{GVF} = \frac{\dot{Q}_g}{\dot{Q}_g + \dot{Q}_l}, \tag{12}$$

where $\dot{Q}_g$ and $\dot{Q}_l$ are the local volume flow rates of gas and liquid.

From Tao et al. [35], the equivalent density of a gas-liquid mixture is:

$$\rho = \rho_g \mathrm{GVF} + (1 - \mathrm{GVF})\rho_l, \tag{13}$$

where ρ_l denotes the liquid density.

According to Diaz [36], for a homogeneous, quasi-static, and isothermal mixture of a Newtonian incompressible liquid and an ideal gas, the local pressure P defines the local GVF,

$$\mathrm{GVF} = \frac{1}{1 + \dfrac{P - \left(P_V + 2S/C_r\right)}{P_{gi}} \left(\dfrac{1}{\mathrm{GVF}_i} - 1 \right)}, \tag{14}$$

where P_V is the liquid vapor pressure, P_{gi} is the gas pressure at the seal inlet, S is the liquid surface tension per unit length, C_r is the radial clearance, GVF_i is the GVF at the seal inlet.

From San Andrés [6], Eq. (14) simplifies to

$$\mathrm{GVF} = \frac{1}{1 + \dfrac{P}{P_{gi}} \left(\dfrac{1}{\mathrm{GVF}_i} - 1 \right)}, \tag{15}$$

since the magnitude of (P_V+2S/C_r) is negligible (only a few millibars for oil).

According to Eq. (12), the GVF at the seal inlet GVF_i is determined by the volume flow rates of gas and liquid at the seal inlet. Since silicone oil is considered incompressible, the liquid volume flow rate at the seal inlet $\dot{Q}_{il}$ is:

$$\dot{Q}_{il} = \frac{\dot{m}_l}{\rho_l}, \tag{16}$$

where $\dot{m}_l$ and ρ_l are the mass flow rate and density of the oil measured by the Coriolis meter.

The gas volume flow rate at the seal inlet $\dot{Q}_{ig}$ differs from the volume flow rate measured by a turbine flowmeter $\dot{Q}_{FM}$.

$$\dot{Q}_{ig} = \dot{Q}_{FM} \frac{P_{FM} T_i}{T_{FM} P_i}, \tag{17}$$

where P_{FM} and T_{FM} are the pressure and temperature measured immediately after the turbine flowmeters, and P_i and T_i are the pressure and temperature measured at the seal inlet.

Unlike effective density, there is no widely recognized effective viscosity model for a gas-liquid mixture. Many models have been proposed; however, they differ significantly and can even be contradictory. This dissertation uses the model of Fourar and Bories [37],

$$\mu = \left(1 - \mathrm{GVF}\right)\mu_l + \mathrm{GVF}\mu_g + 2\sqrt{\mathrm{GVF}\left(1 - \mathrm{GVF}\right)\mu_l \mu_g}, \tag{18}$$

since it is used by the *XLHseal_mix* program [6], which produces predictions to compare with test data.

3.4 Test Seals

Figure 19 shows the test seal's drawing. The nominal length of the test seal is 57.785 mm (2.2750 inches), and the test seal's inner diameter is 89.306 mm (3.5160 inches).

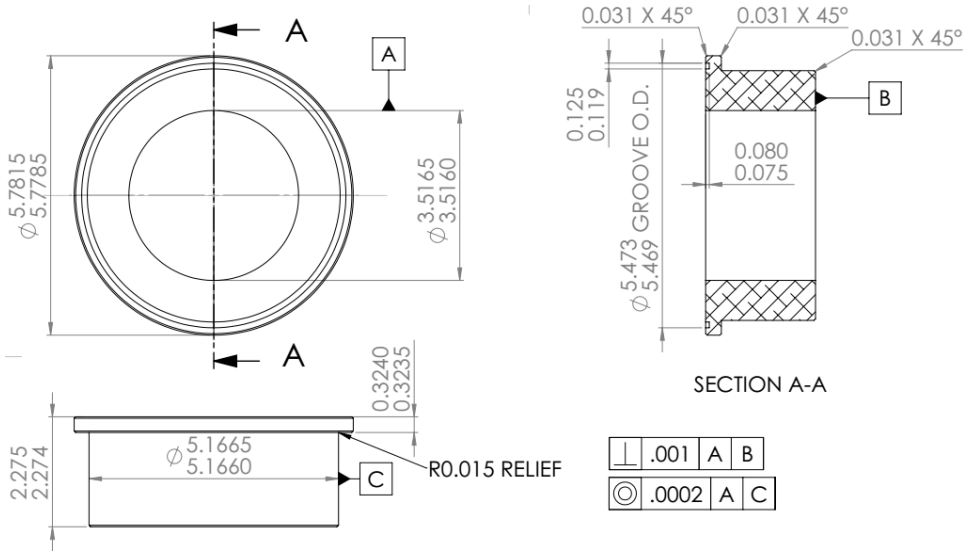

Figure 19. Test smooth seal (dimensions are in inches)

3.5 Test Rotors

Tests employ three rotors with diameters of 88.930 mm (3.5012 inches), 88.981 mm (3.5032 inches), and 89.027 mm (3.5050 inches), yielding radial clearances of 0.188 mm (7.4 mils), 0.163 mm (6.4 mils), and 0.140 mm (5.5 mils).

4. EXPERIMENTAL PROCEDURE

4.1 Parameter Identification

This dissertation uses the dynamic parameter-identification approach discussed by Mehta and Childs [30]. Figure 20 shows the shaking (X-Y) and gravity-oriented (x_1-y_1) coordinate systems. The frequency-domain equation of motion for the stator is

$$\begin{bmatrix} \boldsymbol{F}_{XX} & \boldsymbol{F}_{XY} \\ \boldsymbol{F}_{YX} & \boldsymbol{F}_{YY} \end{bmatrix} - [M_S] \begin{bmatrix} \boldsymbol{A}_{XX} & \boldsymbol{A}_{XY} \\ \boldsymbol{A}_{YX} & \boldsymbol{A}_{YY} \end{bmatrix} = \begin{bmatrix} \boldsymbol{H}_{XX} & \boldsymbol{H}_{XY} \\ \boldsymbol{H}_{YX} & \boldsymbol{H}_{YY} \end{bmatrix} \begin{bmatrix} \boldsymbol{D}_{XX} & \boldsymbol{D}_{XY} \\ \boldsymbol{D}_{YX} & \boldsymbol{D}_{YY} \end{bmatrix}, \tag{19}$$

where $\boldsymbol{F}_{ij}$ are the Fourier transforms of the excitation forces, $[M_S]$ is the stator-mass matrix, $\boldsymbol{A}_{ij}$ are the Fourier transforms of the stator accelerations, $\boldsymbol{D}_{ij}$ are the Fourier transforms of the relative displacements of the stator to the rotor, and $\boldsymbol{H}_{ij}$ are the complex dynamic stiffness coefficients. The subscript ij denotes the measured value in the i direction due to the excitation in the j direction. $\boldsymbol{H}_{ij}$ values are related to rotordynamic coefficients by:

$$\boldsymbol{H}_{ij} = \left(K_{ij} - \Omega^2 M_{ij}\right) + \boldsymbol{j}\Omega C_{ij}, \quad \boldsymbol{j} = \sqrt{-1}, \tag{20}$$

where K_{ij}, C_{ij}, and M_{ij} are the frequency-independent seal stiffness, damping, and virtual-mass coefficients, and $\boldsymbol{\Omega}$ is the excitation frequency. Note that Eq. (20) assumes that the rotordynamic coefficients are independent from $\boldsymbol{\Omega}$, but this is not required for the identification procedure.

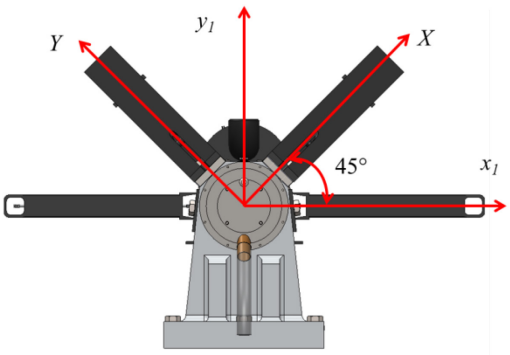

Figure 20. X-Y coordinate system [27]

$[M_S]$ is the stator-mass matrix

$$[M_S]=\begin{bmatrix} M_{SXX} & M_{SXY} \\ M_{SYX} & M_{SYY} \end{bmatrix}, \tag{21}$$

where M_{Sij} are mass coefficients of the stator assembly in the X-Y frame. Since the supports of the stator assembly are almost symmetric about y_1 axis (vertical direction), $M_{SXX}\approx M_{SYY}$, and $M_{SXY}\approx M_{SYX}\approx 0$.

A baseline test excites the stator without test fluid or rotor rotation, and identifies M_{Sij}. In the baseline case, M_{ij} values are extremly close to zero since there is only uncompressed air in the seal clearance; i.e., the real components of the complex dynamic stiffness coefficients Re($\boldsymbol{H_{ij}}$) barely depend on Ω. Therefore, M_{Sij} can be determined by minimizing the frequency dependencies of the identified Re($\boldsymbol{H_{ij}}$) in the baseline test. Figure 21 shows Re($\boldsymbol{H_{ij}}$) for a typical baseline test. With M_{SXX}=46.53 Kg, M_{SYY}=47.78 Kg, and M_{SXY}=M_{SYX}=0.69 Kg, Re($\boldsymbol{H}_{ij}$) values are almost invariant with Ω. Note that M_{Sij} may vary slightly after disassembling and reassembling the stator assembly.

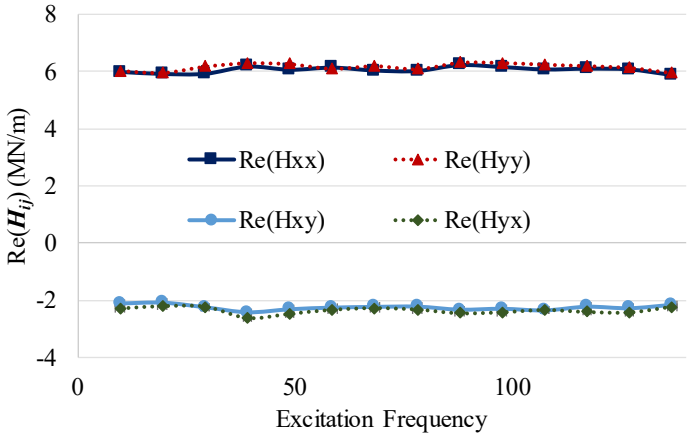

Figure 21. Real parts of complex dynamic stiffness coefficients for a baseline test

4.2 Repeatability Analysis

During tests, the hydraulic shakers, shown in Fig. 13, alternately excite the stator in the X and Y directions with a pre-programed waveform, which consists of an ensemble of pseudo-random frequencies [38], ranging from 10 Hz to 140 Hz in increments of 10 Hz. The waveform

lasts 0.1024 seconds. Along each direction, the shaker steadily repeats the waveform 640 times for cases under single-phase and mainly-oil conditions and 1280 times for cases at mainly-air conditions. Post-processing divides the force, acceleration, and displacement measurements into 10 groups in each direction. The Fourier Transforms converts data from the time-domain to the frequency domain. Further processing assembles the 10 groups from each direction into 100 complex force, acceleration, and displacement matrices. Equation (19) produces 100 complex dynamic stiffness matrices. The matrix of standard deviations of all complex dynamic stiffness matrices represents the repeatability values of measured complex dynamic stiffness coefficients, and each plot for complex dynamic stiffness coefficients presents these repeatability values using error bars.

5. EXPERIMENTAL RESULTS FOR PURE- AND MAINLY-OIL TESTING

A baseline test excites the stator at zero speed without any test fluid to characterize the baseline dynamics of the test section. The contribution of the back-pressure labyrinth seals to the system dynamics is negligible, because of their short length (28.58 mm) and large clearance (0.254 mm). Post-processing computes repeatability values for the baseline test ($\sigma_{baseline}$) using the procedure described in Sec. 4.2. Thus, the total repeatability σ_{total} of a measurement is:

$$\sigma_{total} = \sqrt{\sigma_{baseline}^2 + \sigma_{test}^2} \ , \tag{22}$$

where σ_{test} is the test-data repeatability.

Figure 22 shows the real and imaginary parts of $\boldsymbol{H}_{ij}$ for a typical mainly-oil test (after subtracting the baseline data) when PD=31 bars, C_r=0.188 mm, inlet GVF=4%, and ω=15 krpm. Dots represent measured data, and lines show the corresponding least-squares fitting curves. Figure 22(a) demonstrates that the quadratic function shown in Eq. (20) fits Re($\boldsymbol{H}_{ij}$) well, and delivers frequency-independent stiffness K_{ij} and virtual-mass M_{ij} coefficients. Figure 22(b) shows that the linear function of Ω shown in Eq. (20) fits Im($\boldsymbol{H}_{ij}$) well, and produces frequency-independent damping coefficients C_{ij}.

The magnitudes of K_{ij}, M_{ij}, and C_{ij} coefficients in Fig. 22 are (as expected) almost identical in *X* and *Y* directions. Therefore, the following discussion uses the average values for the rotordynamic coefficients:

$$K = \frac{K_{XX} + K_{YY}}{2} \tag{23}$$

$$k = \frac{K_{XY} - K_{YX}}{2} \tag{24}$$

$$C = \frac{C_{XX} + C_{YY}}{2} \tag{25}$$

$$c = \frac{C_{XY} - C_{YX}}{2} \tag{26}$$

$$M = \frac{M_{XX} + M_{YY}}{2} \tag{27}$$

$$m_q = \frac{M_{XY} - M_{YX}}{2}, \tag{28}$$

where K is the direct stiffness, k is the cross-coupled stiffness, C is the direct damping, c is the cross-coupled damping, M is the direct virtual-mass, and m_q is the cross-coupled virtual-mass.

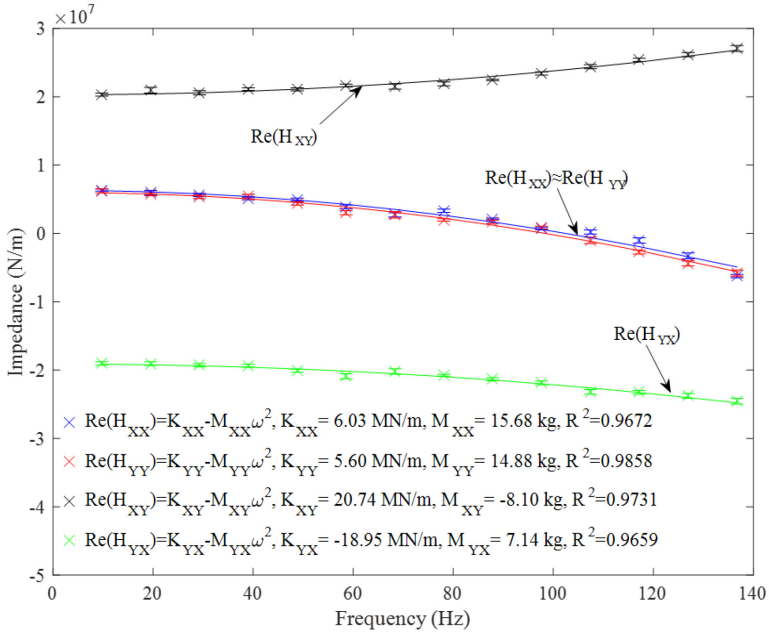

(a) Re(***H**ij*)

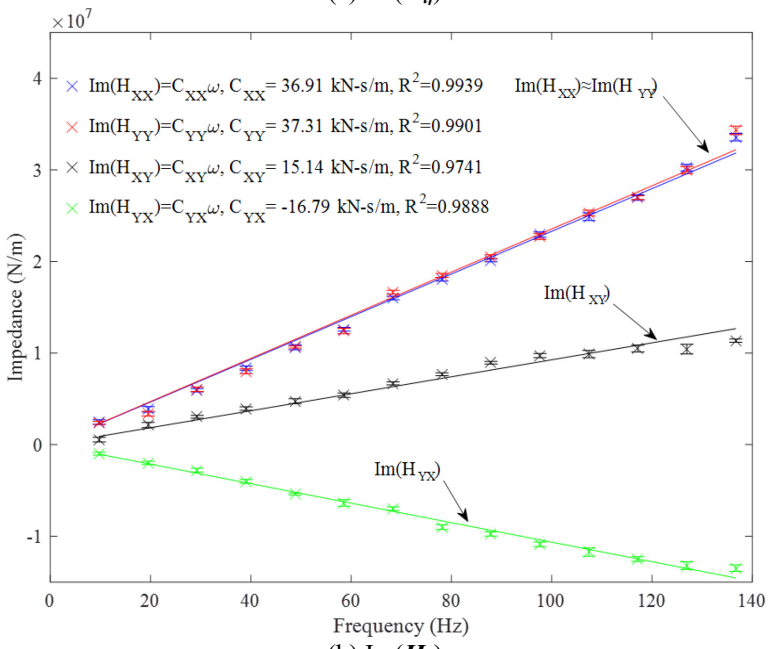

(b) Im(***H**ij*)

Figure 22. The (a) real and (b) imaginary parts of H_{ij} for a typical mainly-oil case (PD=31 bars, C_r=0.188 mm, inlet GVF=4%, and ω=15 krpm) after subtracting baseline data

5.1 Test Matrix

For tests under pure- and mainly-oil conditions, the test seal is centered, the seal exit pressure P_e is 6.9 bars, the seal inlet temperature is 39.4 °C, and there is no intentional fluid pre-rotation. The targeted test matrix covers:

a) 6 inlet GVFs: 0, 2%, 4%, 6%, 8%, and 10%,

b) 4 rotor speeds (ω): 5, 7.5, 10, and 15 krpm,

c) 3 pressure drops (PDs): 31, 37.9, and 48.3 bars,

d) 3 radial clearances (C_r): 0.188, 0.163, and 0.140 mm.

The targeted test matrix was not completed due to stator instabilities. In the omitted cases, the stator had sub-synchronous vibrations, some with significant amplitudes. Figure 23 shows the vibration spectra plots of the stator-rotor relative displacement in *Y* direction (*y*) at C_r=0.140 mm and PD=48.3 bars. Since two hydrostatic bearings support the rotor and provide high support stiffness compared to the stiffness from test seals, the displacement of the rotor is negligible, and the vibration spectra plots in Fig. 23 also describe the motion of the stator. When ω=5 krpm and inlet GVF=0% and 2%, the *y* displacement signal exhibits a small (less than 1 μm) synchronous component. Figure 23(c) shows that when the inlet GVF increases to 4%, the stator experiences a pronounced sub-synchronous vibration in the *Y* direction at 0.155ω. When inlet GVF=4%, the stator is stable without external excitations, but becomes unstable immediately when excited by hydraulic shakers. Inlet GVF cannot be increased to 6% even without external excitations.

When inlet GVF=0%, the stator exhibits sub-synchronous vibration at 0.297ω when ω increases to 10 krpm. At 10 krpm, the stator is stable without external excitations, but becomes unstable immediately when excited by hydraulic shakers.

Figure 23 shows that as inlet GVF increases from zero to 4%, the frequency of the sub-synchronous vibration decreases from 49.48 to 12.92 Hz, and the ratio of the sub-synchronous frequency to the rotor speed drops from 0.297 to 0.155. Since there is no intentional fluid pre-rotation provided, the ratio of the circumferential flow velocity within the seal annulus to the rotor surface speed should not be very different at different test conditions for a long smooth annular seal. So, the sub-synchronous vibrations are not likely to be induced by the average flow circumferential velocity.

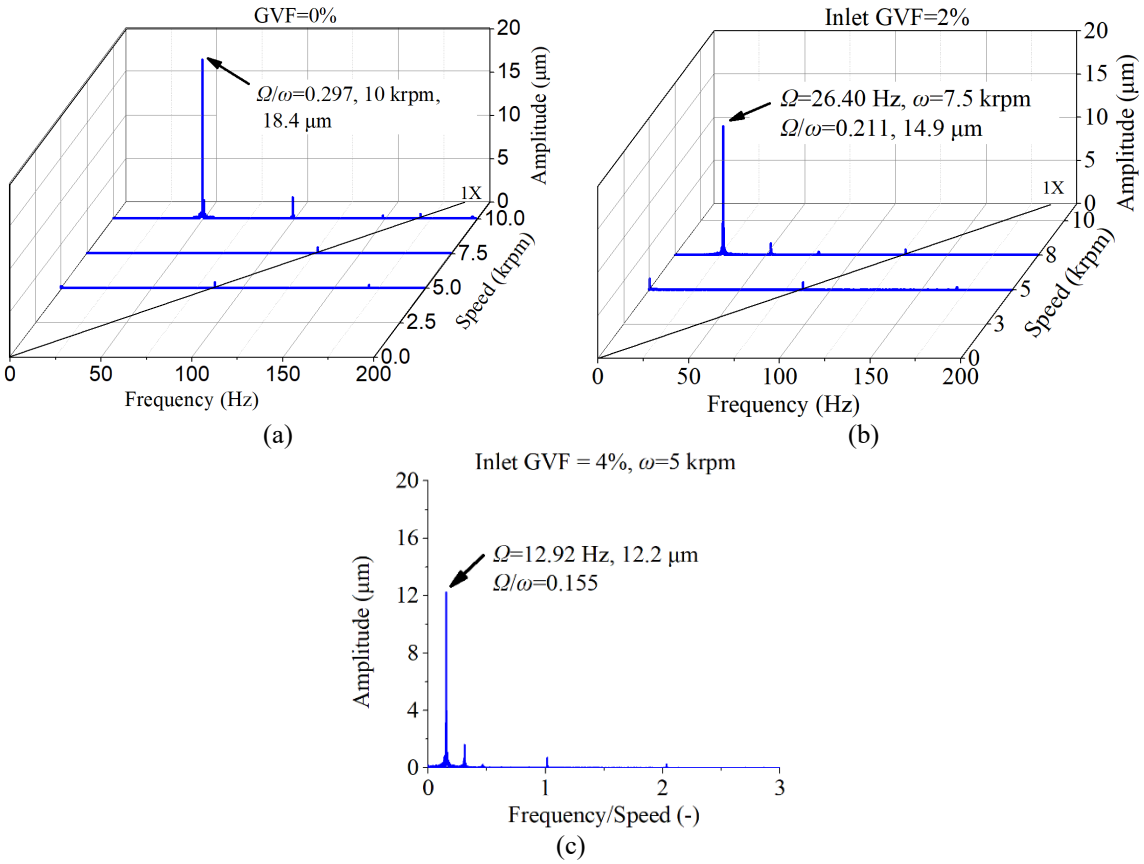

Figure 23. Vibration spectra plots of y when PD=48.3 bars and C_r=0.140 mm for (a) inlet GVF=0%, (b) inlet GVF=2%, and (c) inlet GVF=4%

Recall that hydraulic shakers and other mechanical components support the stator. For stable cases, the seal is also concentric with the rotor. When the test fluid enters the test section, the seal reaction force in the test seal clearance acts on the stator. Sec. 5.4 discusses the seal's direct stiffness K. One explanation for the sub-synchronous vibrations in Fig. 23 is that K becomes negative and lowers the stator's 1st natural frequency. This hypothesis suggests the sub-synchronous vibrations in Fig. 23 occur at the stator's 1st (rigid body) damped natural frequency. Tests cannot measure the seal's K in these (unstable) cases, so this hypothesis cannot be proved directly by measurements. The results herein omit test cases that encountered sub-synchronous vibrations.

Table 6 shows the resultant test matrix. The test campaign adds an extra PD of 24.1 bars for C_r=0.163 mm to study the effects of changing PD at this clearance. The test point at C_r=0.188 mm, PD=31 bars, ω=15 krpm, and inlet GVF=10% produced poor mixing quality, and

consequently produced large uncertainties for rotordynamic coefficients. The discussions below omit this case. The mainly-oil mixture in this case cannot be treated as homogeneous since large air bubbles are observed through the sight-glass view port shortly upstream of the inlet ports of the test section.

<table>
<tr><th rowspan="2">PD (bars)</th><th rowspan="2">Inlet GVF (%)</th><th colspan="4">C_r=0.188 mm</th><th colspan="3">C_r=0.163 mm</th><th colspan="3">C_r=0.140 mm</th></tr>
<tr><th colspan="4">ω (krpm)</th><th colspan="3">ω (krpm)</th><th colspan="3">ω (krpm)</th></tr>
<tr><td rowspan="6">48.3</td><td>0</td><td>5</td><td>7.5</td><td>10</td><td>15</td><td rowspan="6" colspan="3">Omitted due to stator instabilities</td><td>5</td><td>7.5</td><td rowspan="6">-</td></tr>
<tr><td>2</td><td>5</td><td>7.5</td><td>10</td><td>15</td><td>5</td><td rowspan="5">-</td></tr>
<tr><td>4</td><td>5</td><td>7.5</td><td>10</td><td>15</td><td rowspan="4">-</td></tr>
<tr><td>6</td><td>5</td><td>7.5</td><td>10</td><td>15</td></tr>
<tr><td>8</td><td>5</td><td>7.5</td><td>10</td><td>15</td></tr>
<tr><td>10</td><td>5</td><td>7.5</td><td>10</td><td>15</td></tr>
<tr><td rowspan="6">37.9</td><td>0</td><td rowspan="2">-</td><td>7.5</td><td>10</td><td>15</td><td>5</td><td>7.5</td><td>10</td></tr>
<tr><td>2</td><td>7.5</td><td>10</td><td>15</td><td>5</td><td>7.5</td><td rowspan="5">-</td></tr>
<tr><td>4</td><td>5</td><td>7.5</td><td>10</td><td>15</td><td>5</td><td>7.5</td></tr>
<tr><td>6</td><td>5</td><td>7.5</td><td>10</td><td>15</td><td>5</td><td>7.5</td></tr>
<tr><td>8</td><td>5</td><td>7.5</td><td>10</td><td>15</td><td>5</td><td rowspan="2">-</td></tr>
<tr><td>10</td><td>5</td><td>7.5</td><td>10</td><td>15</td><td>-</td></tr>
<tr><td rowspan="6">31</td><td>0</td><td rowspan="4">-</td><td>7.5</td><td>10</td><td>15</td><td>5</td><td>7.5</td><td rowspan="6">-</td><td>5</td><td>7.5</td><td>10</td></tr>
<tr><td>2</td><td>7.5</td><td>10</td><td>15</td><td>5</td><td>7.5</td><td>5</td><td>7.5</td><td>10</td></tr>
<tr><td>4</td><td>7.5</td><td>10</td><td>15</td><td>5</td><td rowspan="3">-</td><td>5</td><td>7.5</td><td>10</td></tr>
<tr><td>6</td><td>5</td><td>7.5</td><td>10</td><td>15</td><td>5</td><td>5</td><td>7.5</td><td rowspan="3">-</td></tr>
<tr><td>8</td><td>5</td><td>7.5</td><td>10</td><td>15</td><td rowspan="2">-</td><td>5</td><td>7.5</td></tr>
<tr><td>10</td><td>5</td><td>7.5</td><td>10</td><td>-</td><td>5</td><td>7.5</td></tr>
<tr><td rowspan="6">24.1</td><td>0</td><td rowspan="6" colspan="4">Not covered by target test matrix</td><td>5</td><td>7.5</td><td>10</td><td rowspan="6" colspan="3">Not covered by target test matrix</td></tr>
<tr><td>2</td><td>5</td><td>7.5</td><td rowspan="5">-</td></tr>
<tr><td>4</td><td>5</td><td>7.5</td></tr>
<tr><td>6</td><td>5</td><td>7.5</td></tr>
<tr><td>8</td><td>5</td><td>7.5</td></tr>
<tr><td>10</td><td>5</td><td>7.5</td></tr>
</table>

Table 6. Resultant test matrix under pure- and mainly-oil conditions

Recall from Sec. 3.1.5 that the zero pre-swirl-guide insert injects the test fluid radially inwards to produce a flow with minimum circumferential velocity at the seal inlet. However, the fluid's pre-rotation at the seal inlet is not zero due to the rotor rotation. Table 7 shows measured pre-swirl ratio $u_0(0)$ for all pure- and mainly-oil cases. The maximum $u_0(0)$ is 0.22.

As shown in Table 4, the uncertainty of the pitot tube differential pressure is 0.0032 bars. This uncertainty produces the uncertainty of $u_0(0)$. Since the effective density of the fluid

varies with inlet GVF, the uncertainty of $u_0(0)$ varies with inlet GVF. Table 8 shows the uncertainties of measured $u_0(0)$ values.

PD (bars)	Inlet GVF (%)	C_r=0.188 mm				C_r=0.163 mm			C_r=0.140 mm		
		5 krpm	7.5 krpm	10 krpm	15 krpm	5 krpm	7.5 krpm	10 krpm	5 krpm	7.5 krpm	10 krpm
48.3	0	0.04	0.10	0.12	0.16				0.11	0.13	
	2	0.04	0.10	0.12	0.16				0.09		
	4	0.04	0.10	0.12	0.16						
	6	0.03	0.10	0.12	0.16				-	-	-
	8	0.03	0.09	0.11	0.16						
	10	0.03	0.08	0.10	0.15						
37.9	0	-	0.09	0.13	0.19		-		0.11	0.14	0.19
	2		0.10	0.13	0.19				0.11	0.14	
	4	0.09	0.10	0.13	0.19				0.11	0.14	
	6	0.09	0.10	0.13	0.19				0.11	0.14	-
	8	0.09	0.10	0.13	0.19				0.10	-	
	10	0.10	0.10	0.13	0.19				-		
31	0	-	0.11	0.14	0.22	0.09	0.13	-	0.09	0.16	0.21
	2		0.11	0.14	0.22	0.09	0.13		0.10	0.17	0.22
	4		0.11	0.14	0.22	0.09	-		0.09	0.17	0.22
	6	0.07	0.11	0.14	0.22	0.09			0.09	0.18	-
	8	0.09	0.11	0.14	0.22	-			0.09	0.17	
	10	0.09	0.11	0.14	-				0.09	0.17	
24.1	0	Not covered by target test matrix				0.11	0.14	0.20	Not covered by target test matrix		
	2					0.10	0.14	-			
	4					0.10	0.14				
	6					0.10	0.14				
	8					0.10	0.14				
	10					0.10	0.14				

Table 7. Measured pre-swirl ratios under pure- and mainly-oil conditions

Inlet GVF (%)	5 krpm	7.5 krpm	10 krpm	15 krpm
0	0.04	0.02	0.02	0.01
2	0.04	0.02	0.02	0.01
4	0.04	0.02	0.02	0.01
6	0.04	0.02	0.02	0.01
8	0.04	0.03	0.02	0.01
10	0.04	0.03	0.02	0.01

Table 8. Uncertainties of measured pre-swirl ratios under pure- and mainly-oil conditions

5.2 Reynolds Number

For a bulk-flow model, the Reynolds number *Re* is

$$Re = \sqrt{Re_\theta^2 + Re_a^2} \quad , \tag{29}$$

where Re_θ is the circumferential Reynolds number, and Re_a is the axial Reynolds number.

Re_θ is

$$Re_\theta = \frac{\rho C_r D_r \omega}{4\mu}, \tag{30}$$

where ρ is the effective density defined by Eq. (13), μ is the effective viscosity defined by Eq. (18), D_r is the rotor diameter, and C_r is the radial clearance.

Re_a relates to $\dot{m}$ by

$$Re_a = \frac{\rho}{\mu} V_a C_r = \frac{\rho}{\mu} \frac{\dot{m}}{\rho C_r \pi D_r} C_r = \frac{\dot{m}}{\mu \pi D_r}, \tag{31}$$

where V_a is the axial bulk-flow velocity.

Figure 24 shows the Reynolds number at the seal inlet Re_i versus inlet GVF over a range of ω, C_r, and PD values. Re_i increases slightly (by less than 12%) as inlet GVF increases from zero to 10%, due to the decrease in μ induced by the air additions to the oil flow.

Figure 25 presents the Reynolds number at the seal exit Re_e versus inlet GVF over a range of ω, C_r, and PD values. Re_e increases with increasing inlet GVF, and the effects of changing inlet GVF on Re_e are more pronounced than on Re_i since the GVF at the seal exit is larger than inlet GVF due to the pressure drop through the seal. For example, when PD=37.9 bars and ω=7.5 krpm, as inlet GVF increases from zero to 10%, Re_e increases by 53.9%, but Re_i only increases by 9.6%.

As expected, Re_e and Re_i values increase as C_r or PD increase since $\dot{m}$ increases with increasing C_r or PD.

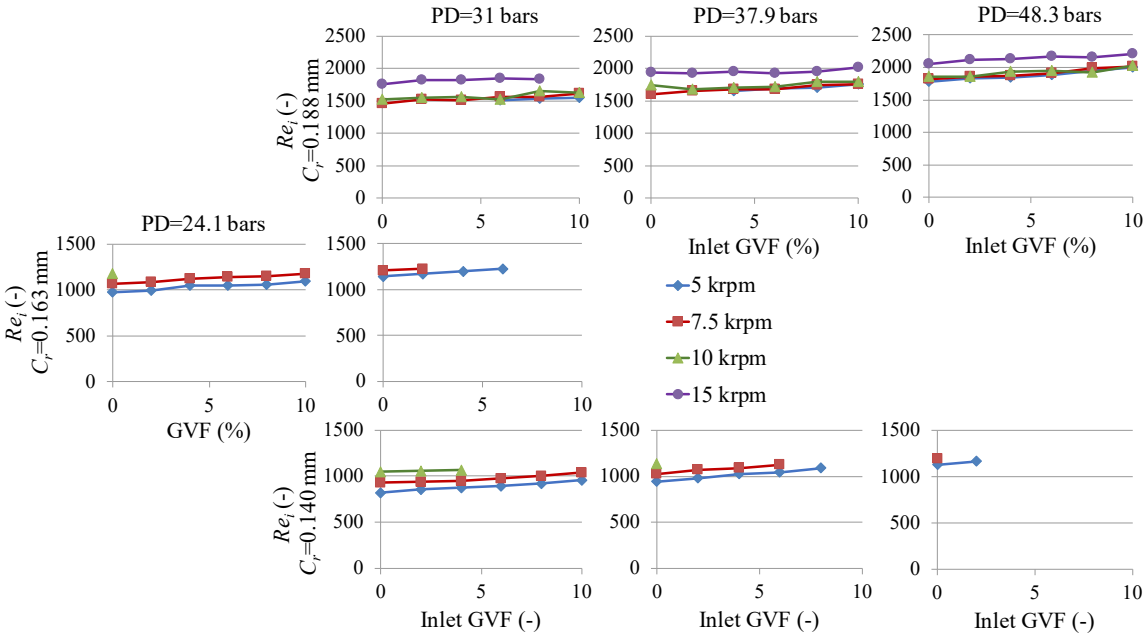

Figure 24. Calculated Re_i under pure- or mainly-oil conditions

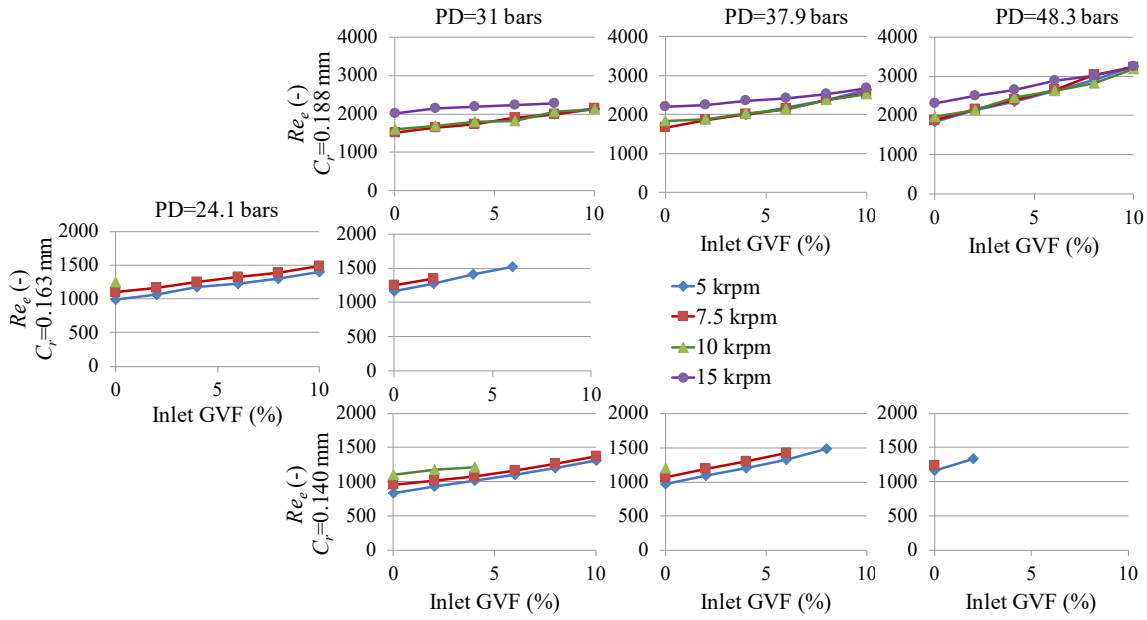

Figure 25. Calculated Re_e under pure- or mainly-oil conditions

Although $\dot{m}$ is constant throughout the seal, the calculated axial Reynolds number at the seal exit $Re_{a,e}$ is larger than the axial Reynolds number at the seal inlet $Re_{a,i}$ since μ at the seal

exit is smaller than at the seal inlet because: (1) the temperature rise through the seal decreases the oil viscosity μ_l, and (2) the pressure drop through the seal increases GVF, and μ decreases as GVF increases.

Recall from Eq. (13), ρ decreases as GVF increases. Although decreasing ρ can decrease Re_θ, the circumferential Reynolds number at the seal exit $Re_{\theta,e}$ is larger than the circumferential Reynolds number at the seal inlet $Re_{\theta,i}$ because the drop in μ has more impact on Re_θ than the drop in ρ. Therefore, the Reynolds number at the seal exit Re_e is greater than the Reynolds number at the seal inlet Re_i, as shown in Figs. 24 and 25.

From Cornish [39] and Yamada [40], the stability of a laminar flow within the seal annulus not only depends on Re_a but also depends on Re_θ. Cornish [39] gives the boundary line, at which Taylor vortices occur, for a smooth water seal with L=150 mm, D=60 mm and C_r=0.0139 mm. Figures 26(a) and (b) show this boundary by a solid line. Regarding this boundary line, the critical Taylor number $Re_{\theta,c}(2C_r/D_r)^{1/2}$ increases as Re_a increases to 600. $Re_{\theta,c}$ is the critical circumferential Reynolds number. From Yamada [40], $Re_{\theta,c}(2C_r/D_r)^{1/2}$ decreases when Re_a increases beyond 600, and the boundary line beyond 600 is almost symmetric with the solid line about the line of Re_a=600. Also, according to Yamada [40], for a smooth water annular seal with ω=0 rpm (Re_θ=0), the critical Reynolds number Re_c=the critical axial Reynolds number $Re_{a,c}\approx$1500. Figures 26(a) and (b) show the boundary line beyond Re_a=600 by a dashed line. The solid line and dashed line form the border between laminar and turbulent flow.

Figure 26(a) shows the Taylor number at the seal inlet $Re_{\theta,i}(2C_r/D_r)^{1/2}$ versus $Re_{a,i}$ for pure- and mainly-oil cases, and Fig. 26(b) depicts the Taylor number at the seal exit $Re_{\theta,e}(2C_r/D_r)^{1/2}$ versus $Re_{a,e}$. The filled symbols are for pure-oil cases, and the hollow symbols are for mainly-oil cases. From Fig. 26(a), the flow at the seal inlet is laminar when C_r=0.140 and 0.163 mm, but turbulent when C_r=0.188 mm. From Fig. 30(b), when C_r=0.188 mm, the flow at the seal exit is turbulent. When C_r=0.140 and 0.163 mm, the flow at the seal exit is laminar except for some mainly-oil cases, where hollow symbols are above but close to the dash line. This dissertation treats these exceptional cases as laminar for the following two reasons:

1. For mainly-oil conditions, the mixture's density and viscosity are calculated by Eqs. (13) and (18) rather than being measured directly, the accuracies of calculated Reynolds numbers depend on the correctness of the homogeneous mixture assumption and the models of the mixture density and viscosity. So, the calculated

Reynolds numbers at mainly-oil conditions have less credibility than at pure-oil conditions.

2. The length of the test seal is only 38.5% of Cornish's [39] test seal. This difference can push up the boundary line since the test seal has a shorter time to develop turbulence than Cornish's test seal.

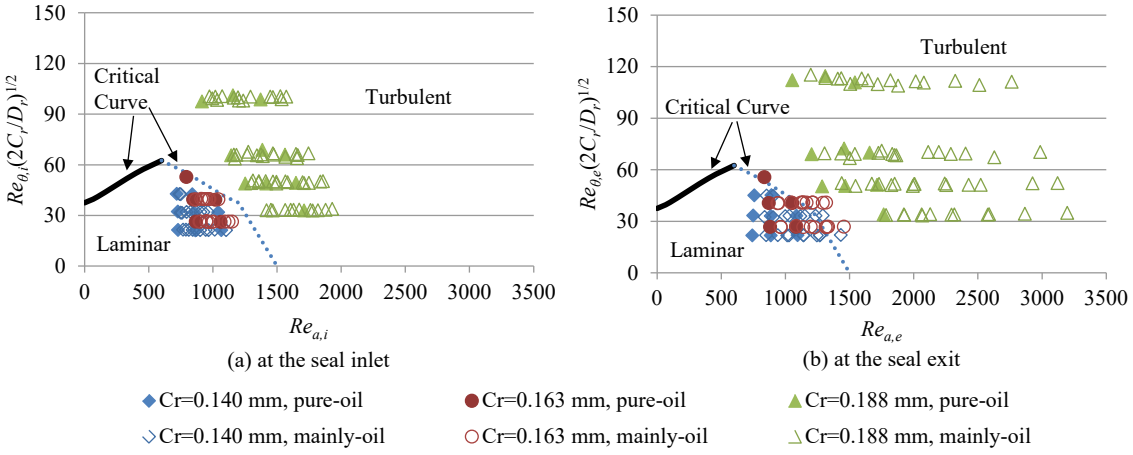

Figure 26. Axial and circumferential Reynolds numbers

In short, the flow within the seal annulus is laminar when C_r=0.140 and 0.163 mm, but turbulent when C_r=0.188 mm. Note, for some C_r=0.188 mm cases, the transitional effects may still be evident; i.e., the flow may not be fully turbulent.

5.3 Leakage Mass Flow Rate

Figure 27 shows the test seal's leakage mass flow rate $\dot{m}$ versus inlet GVF for a range of ω, C_r, and PD values. Increasing inlet GVF from zero to 10% barely changes $\dot{m}$ when C_r=0.188 mm, but increases $\dot{m}$ slightly (by less than 8%) when C_r=0.140 and 0.163 mm. Recall from Eq. (13) and Eq. (18) that both effective viscosity and effective density decrease as inlet GVF increases. Decreasing effective viscosity can increase $\dot{m}$, while decreasing effective density can decrease $\dot{m}$. For C_r=0.188 mm, test results (negligible changes in $\dot{m}$ as inlet GVF increases) indicate that the decrease in effective viscosity and the decrease in effective density have close

but opposite effects. For C_r=0.140 and 0.163 mm, test data ($\dot{m}$ increases slightly as inlet GVF increases) imply that the decrease in effective viscosity has slightly more impact than the decrease in effective density.

For pure-oil conditions at C_r=0.188 mm, $\dot{m}$ decreases by (18%~29%) as ω increases from 5 to 15 krpm. This outcome agrees with the test data of Jolly et al. [41] for a long (L/D=0.625) turbulent-water smooth seal and the test results from Marquette et al. [2] for a turbulent-water smooth (L/D=0.458) seal. This trend continues after adding air into the oil flow.

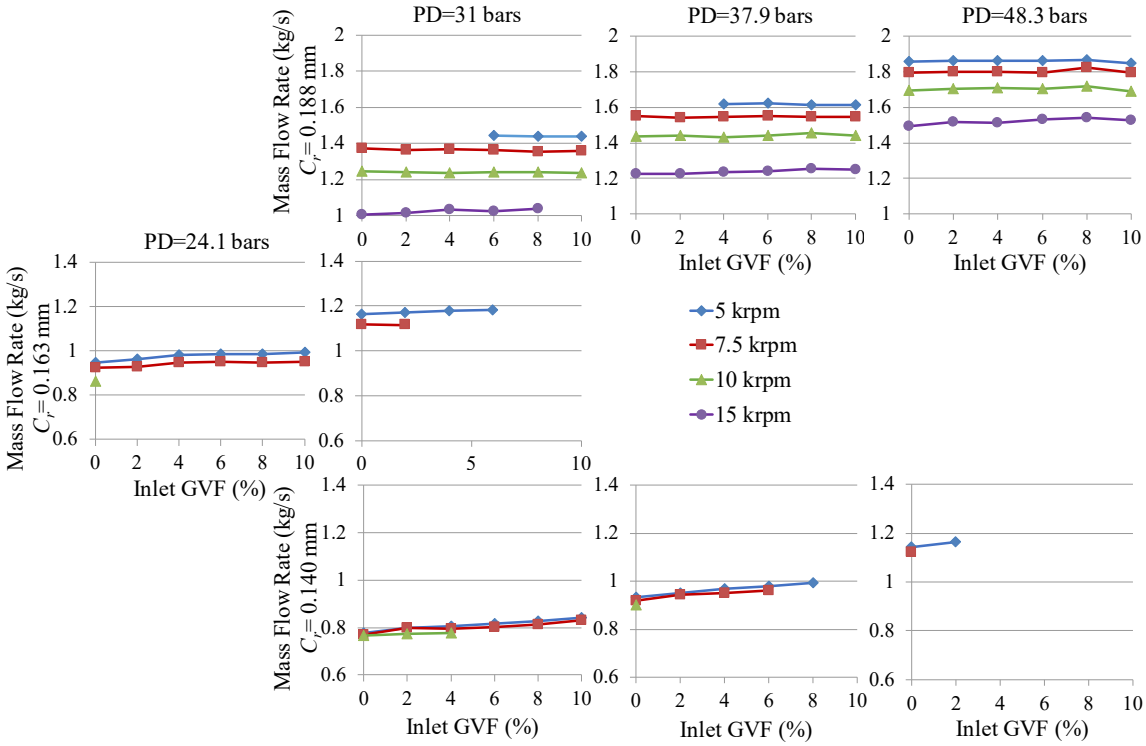

Figure 27. Measured $\dot{m}$ vs. inlet GVF under pure- or mainly-oil conditions

In Fig. 27, $\dot{m}$ decreases as ω increases for C_r=0.188 mm because the axial wall shear stress function τ_z increases as ω increases. The derivation of the relationship between τ_z and ω follows. According to Soulas and San Andrés [42], τ_z is a function of the axial flow shear parameter k_z

$$\tau_z = \frac{\mu}{C_r} k_z V_a \,, \tag{32}$$

where μ is the mixture viscosity, and V_a is the axial bulk-flow velocity

Recall from Sec. 5.2 that the flow is turbulent for C_r=0.188 mm. For turbulent flow, k_z is [42]

$$k_z = 0.5\left(k_r + k_s\right), \tag{33}$$

where k_r is the turbulent shear parameter at the rotor surface, and k_s is the turbulent shear parameter at the stator surface. k_r and k_s are:

$$k_{r,s} = f_{r,s} Re_{r,s} \tag{34}$$

$$f_{r,s} = a_m \left[1 + \left(c_m r_{r,s} / C_r + b_m / Re_{r,s}\right)^{e_m}\right] \tag{35}$$

$$Re_r = \frac{\rho}{\mu} C_r \sqrt{\left(V_\theta - 0.5 D_r \omega\right)^2 + V_a^2} \tag{36}$$

$$Re_s = \frac{\rho}{\mu} C_r \sqrt{V_\theta^2 + V_a^2}\,, \tag{37}$$

where f_r is the rotor surface friction factor, f_s is the stator surface friction factor, r_r is rotor surface mean roughness, r_s is stator surface mean roughness, Re_r is the Reynolds number relative to the rotor surface, Re_s is the Reynolds number relative to the stator surface, and V_θ is the circumferential bulk-flow velocity. A_m, b_m, c_m, and e_m are 0.001375, 5×10^5, 10^4, and 1/3, respectively. The stator and rotor surfaces are nominally smooth, and the surface roughness values from drawings are:

$$r_r = r_s = 0.4\ \mu\text{m} \tag{38}$$

Assuming V_θ is half of the rotor surface speed, $D_r\omega/4$, Re_r and Re_s become

$$Re_r = Re_s = \frac{\rho}{\mu} C_r \sqrt{\left(\frac{D_r \omega}{4}\right)^2 + V_a^2} \tag{39}$$

Because Re_r=Re_s and r_r= r_s, f_r = f_s, and k_r=k_s. Hence k_z is:

$$k_z = a_m \frac{\rho}{\mu} C_r \sqrt{\left(\frac{D_r \omega}{4}\right)^2 + V_a^2} + a_m \left[\frac{c_m r_r}{C_r}\left(\frac{\rho}{\mu} C_r \sqrt{\left(\frac{D_r \omega}{4}\right)^2 + V_a^2}\right)^{1/e_m} + b_m \left(\frac{\rho}{\mu} C_r \sqrt{\left(\frac{D_r \omega}{4}\right)^2 + V_a^2}\right)^{1/e_m - 1}\right]^{e_m} \tag{40}$$

Substituting Eq. (40) into Eq. (32) renders

$$\tau_z = a_m \rho V_a \sqrt{\left(\frac{D_r \omega}{4}\right)^2 + V_a^2} + a_m \frac{\mu V_a}{C_r}\left[\frac{c_m r_r}{C_r}\left(\frac{\rho}{\mu} C_r \sqrt{\left(\frac{D_r \omega}{4}\right)^2 + V_a^2}\right)^{1/e_m} + b_m \left(\frac{\rho}{\mu} C_r \sqrt{\left(\frac{D_r \omega}{4}\right)^2 + V_a^2}\right)^{1/e_m - 1}\right]^{e_m}. \quad (41)$$

Thus, when C_r=0.188 mm (turbulent flow), increasing ω increases τ_z and reduces $\dot{m}$.

For C_r=0.140 and 0.163 mm, the flow conditions within the seal annulus are laminar (as discussed previously in Sec. 5.2), and increasing ω barely changes $\dot{m}$ because under laminar flow conditions, k_z=12 is a constant [43], and τ_z is not related to ω.

As expected, $\dot{m}$ increases as C_r or PD increases for all clearances.

5.4 Direct Stiffness

Figure 28 shows K versus inlet GVF for a range of ω, C_r, and PD values. K can be comparable in magnitude to the direct stiffness of a hydrodynamic bearing and can strongly affect the rotordynamic characteristics of a centrifugal pump.

For C_r=0.188 mm, K generally increases as PD increases, which agrees with the test results from Marquette et al. [2] for a fully-turbulent-water smooth seal. In a centrifugal pump, this stiffness increment will increase the natural frequency of the rotor and increase the rotor's critical speed. Increasing the natural frequency of the rotor would also increase the onset speed of instability (OSI) and enhance the rotor's stability. Increasing ω also generally increases K. This outcome is contrary to Marquette et al.'s [2] test results, where K decreases with increasing ω. The predictions (presented in Appendix A.2) agree with Marquette et al.'s [2] test results but disagree with the author's measurements. A possible reason for this disagreement is that transitional effects might still be evident in many cases when C_r=0.188 mm; i.e., the flow is not fully turbulent.

In regard to the effects of changes in inlet GVF when C_r=0.188 mm, increasing inlet GVF increases K at low PDs (31 and 37.9 bars). At the highest PD (48.3 bars), K first increases as inlet GVF increases from zero to 6% and then drops with further increasing inlet GVF to 10%. The predictions in Appendix A.2 show that K always decreases with increasing inlet GVF from zero to 10% for all PDs. Hence the predicted trend only agrees with test results when PD=48.3 bars and 6%≤inlet GVF≤10%. A possible explanation is that the transitional effects disappear,

and the flow becomes fully-turbulent when PD=48.3 bars and inlet GVF=6%, and this flow status transition significantly changes the effects of changes in inlet GVF.

For C_r=0.140 and 0.163 mm, the effects of changing inlet GVF, ω, or PD on K are different and even contrary to the trends observed at C_r=0.188 mm; specifically, K generally decreases as inlet GVF, ω, or PD increase. A possible reason for this is that the flow transitions from laminar to turbulent as C_r increases from 0.163 to 0.188 mm, as previously discussed in Sec. 5.2.

Seal wear that increases C_r is a known cause for vibration issues in centrifugal pumps. The only circumstance where only C_r changes is at PD=31 bars. The flow remains laminar as C_r increases from 0.140 to 0.163 mm, but transitions to turbulent as C_r increases further to 0.188 mm. As C_r increases from 0.140 to 0.188 mm when ω=7.5 krpm, there is no clear trend of K. For the laminar flow only, as C_r increases from 0.140 to 0.163 mm, K drops significantly when ω=5 and 7.5 krpm. For example, when inlet GVF=2% and ω=7.5 krpm, K decreases from 22.8 to -4.5 MN/m.

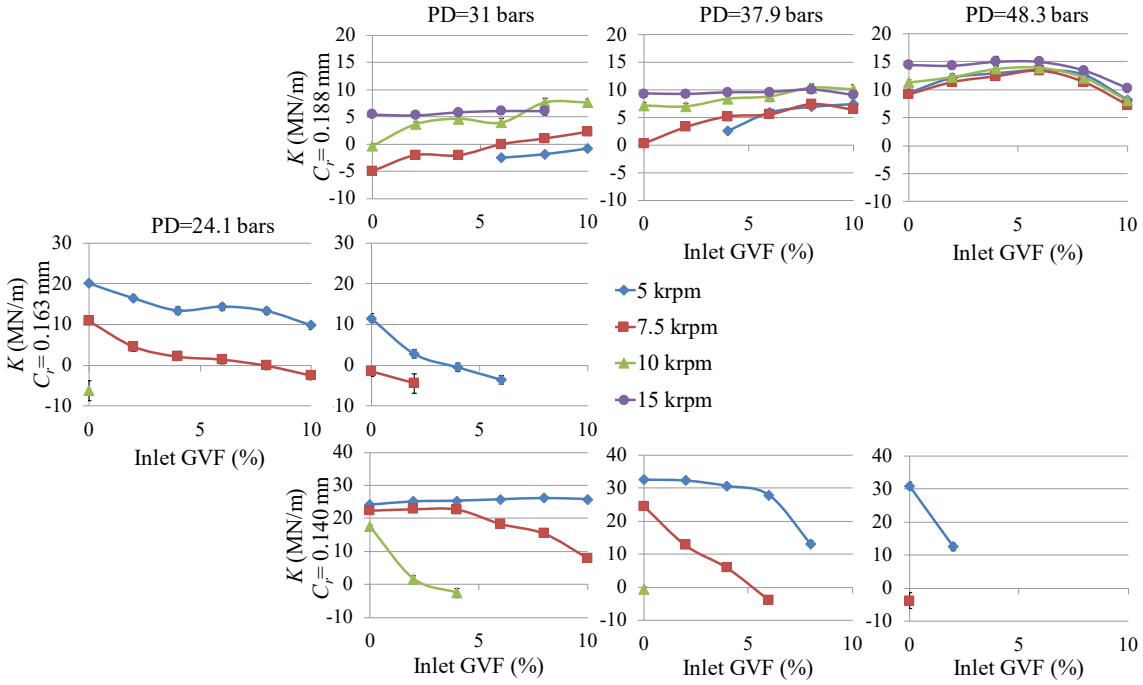

Figure 28. Measured K vs. inlet GVF under pure- or mainly-oil conditions

5.5 Cross-Coupled Stiffness

Increasing k directly decreases the rotordynamic stability. Figure 29 shows k versus inlet GVF for a range of ω, C_r, and PD values. All k values are positive, producing destabilizing forces. As expected, k increases as ω increases because increasing ω increases the fluid's circumferential velocity. The increment of k increases the seal's destabilizing force.

For C_r=0.188 mm (turbulent flow), changing PD has negligible effects on k at pure-oil conditions. This outcome agrees with the test results from Marquette et al. [2]. Adding air into the oil flow does not change this trend. Also, adding air (increasing inlet GVF) has little effect on k, producing negligible effects on the seal's destabilizing force.

When C_r=0.140 and 0.163 mm (laminar flow), adding air strongly impacts k. Increasing inlet GVF generally increases k. For example, when C_r=0.140 mm, PD=37.9 bars, and ω=7.5 krpm, k increases by 70.2% from 12.44 to 21.17 MN/m as inlet GVF increases from zero to 6%. Increasing PD also increases k.

In short, adding air or increasing PD have little effect on k when C_r=0.188 mm (turbulent flow), but generally increase k for C_r=0.140 and 0.163 mm (laminar flow).

PD=31 bars is the only circumstance where only C_r changes. As C_r increases from 0.140 to 0.163 mm, the flow remains laminar, and k increases significantly (by >52.7%) when ω=5 and 7.5 krpm. As C_r further increases to 0.188 mm, the flow transitions to turbulent, and k decreases by about 44% when ω=7.5 krpm and inlet GVF≤2%.

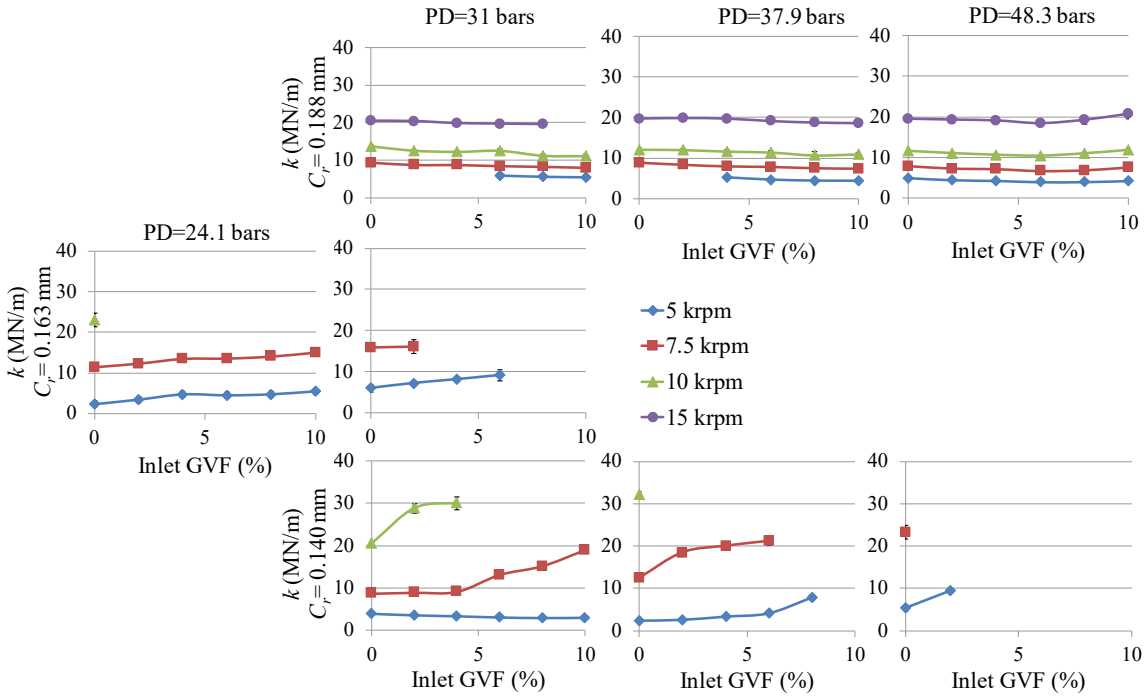

Figure 29. Measured k vs. inlet GVF under pure- or mainly-oil conditions

5.6 Direct Damping

Figure 30 shows C versus inlet GVF for a range of ω, C_r, and PD values. All C values are positive, producing stabilizing forces.

For C_r=0.188 mm (turbulent flow), at pure-oil conditions, increasing PD from 31 to 48.3 bars increases C by about 15%, which generally agrees with test results from Marquette et al. [2]. This trend continues after adding air into the oil flow. The C increment will increase the seal's damping force, making the seal more stabilizing and reducing the peak amplitudes at critical speeds of the pump's rotor. Changing ω has negligible effects on C. This outcome agrees with Marquette et al.'s [2] test data. Adding air into the oil flow (increasing inlet GVF) barely changes C, producing little effect on the seal's damping characteristics.

For C_r=0.140 and 0.163 mm (laminar flow), C increases as PD increases. This outcome is consistent with test results at C_r=0.188 mm. C generally increases as ω increases. This trend is different from test results at C_r=0.188 mm, but agrees with predictions, which will be discussed

in Appendix A.4. Increasing inlet GVF generally increases C. For example, when C_r=0.140 mm, PD=37.9 bars, and ω=7.5 krpm, C increases by 43.8% as inlet GVF increases from zero to 6%.

In short, changing ω or inlet GVF have significant effects on C when C_r=0.140 and 0.163 mm, but have no discernible effects on C when C_r=0.188 mm. A possible reason for this is that the flow transitions from laminar to turbulent as C_r changes from 0.163 to 0.188 mm.

PD=31 bars is the only circumstance to discuss the effects of changes in C_r since it is the only PD where only C_r changes. For PD=31 bars, as C_r increases from 0.140 to 0.163 mm, the flow remains laminar, and C increases (by 14.7%~42.1%) when ω=5 and 7.5 krpm. As C_r further increases from 0.163 to 0.188 mm, the flow transitions to turbulent, and C decreases by about 26% when ω=7.5 krpm and inlet GVF≤2%.

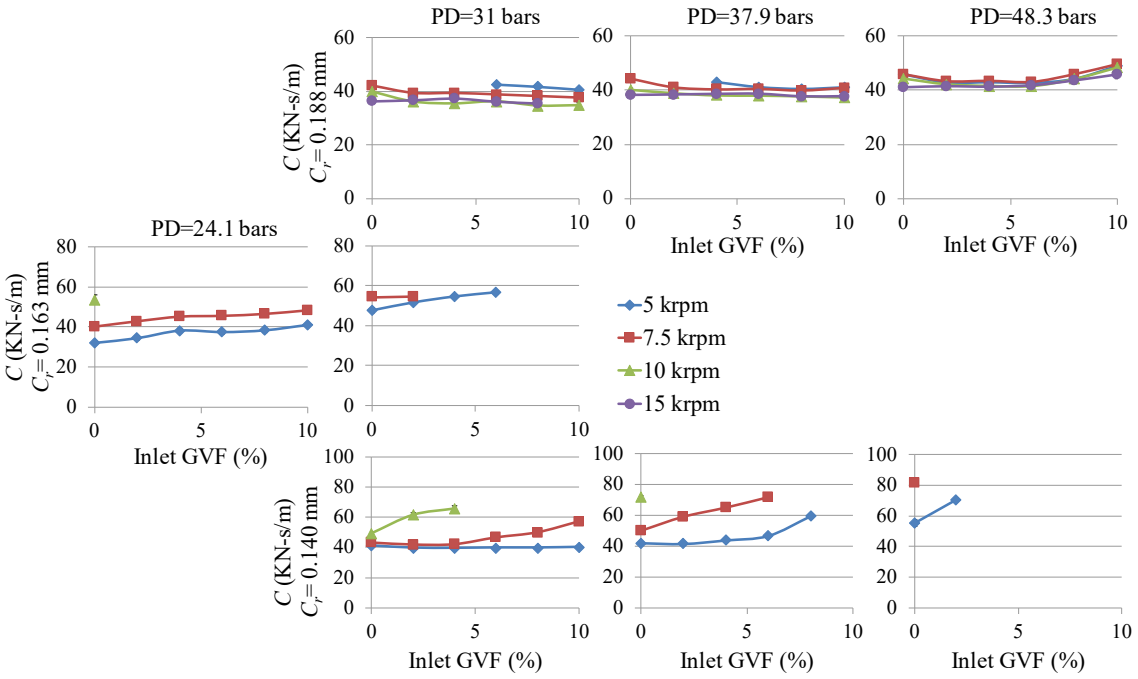

Figure 30. Measured C vs. inlet GVF under pure- or mainly-oil conditions

5.7 Cross-Coupled Damping

Figure 31 shows c versus inlet GVF for a range of ω, C_r, and PD values. All c values are positive except when C_r=0.140 mm, PD=48.3 bars, ω=7.5 krpm, and inlet GVF=0%, where the magnitude of the small negative c is near the same order as the uncertainty. According to Eq. (5), a positive c produces additional centering force on the rotor.

For C_r=0.188 mm (turbulent flow), c increases with increasing ω under pure-oil conditions, which agrees with the test data from Marquette et al. [2]. This outcome is expected because the fluid's circumferential velocity increases as ω increases. And this trend continues after adding air into the oil flow. The increment of c can increase the net centering force of the seal and can then increase the critical speed of the rotor in a centrifugal pump. As with test results from Marquette et al. [2], increasing PD does not significantly change c under pure-oil conditions. This trend generally continues as inlet GVF increases up to 10%. At low ω and PD values, c is insensitive to changes in inlet GVF. As ω or PD increase, c become more dependent on inlet GVF; i.e., c decreases as inlet GVF increases. For example, when PD=48.3 bars and ω=15 krpm, c decreases by 41.7% as inlet GVF increases from zero to 10%. This decrease of c due to increasing inlet GVF is expected because the fluid's effective viscosity decreases as inlet GVF increases. For the same reason, c generally drops as inlet GVF increases for C_r=0.140 and 0.163 mm. Note the rate of decrease varies significantly with operating conditions. For example, when C_r=0.140 mm and PD=31 bars, as inlet GVF increases from zero to 10%, c decreases by 84.8% at ω=7.5 krpm, but decreases by only 12.3% at ω=5 krpm.

For C_r=0.140 and 0.163 mm (laminar flow), increasing PD decreases c. For C_r=0.163 mm, c is invariant with changes in ω. For most cases at C_r=0.140 mm, c decreases as ω increases.

In summary, the observed trends with changes in PD or ω when C_r=0.140 and 0.163 mm are different from test results at C_r=0.188 mm. A possible reason for this is that the flow transitions from laminar to turbulent as C_r increases from 0.163 to 0.188 mm.

Concerning the effects of changes in C_r, PD=31 bars is the only circumstance where only C_r changes. As C_r increases from 0.140 to 0.163 mm, the flow remains laminar, and c drops dramatically (by more than a half) when ω=5 and 7.5 krpm. As C_r further increases from 0.163 to 0.188 mm, the flow transitions to turbulent, and c almost doubles when ω=7.5 krpm and inlet GVF≤2%.

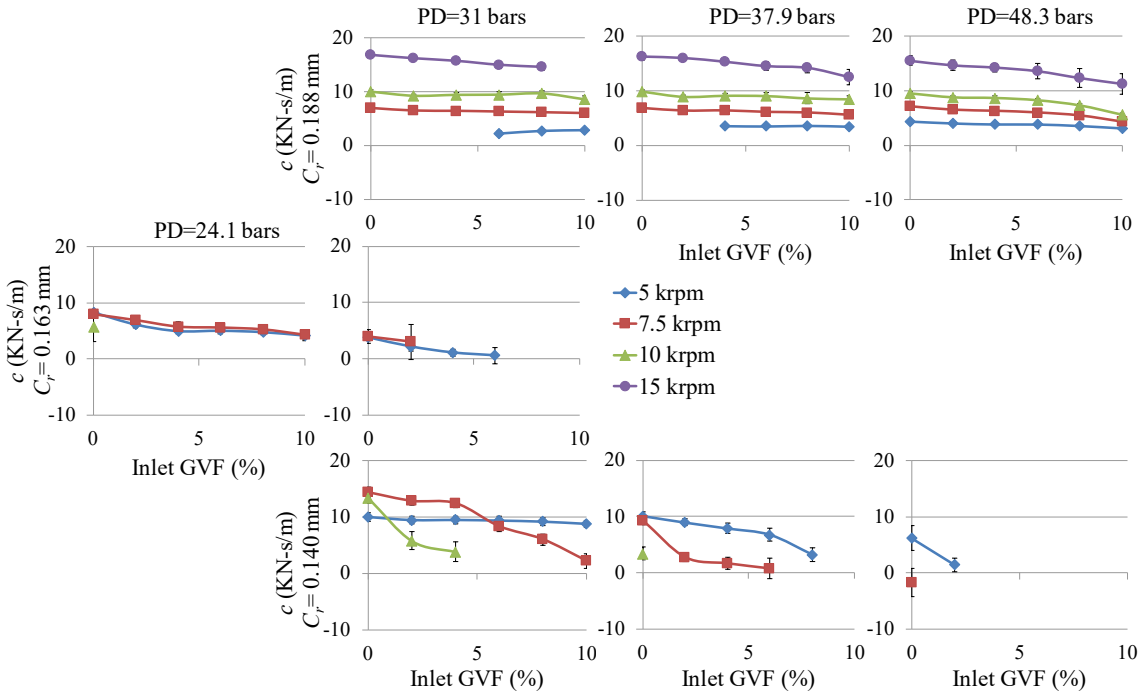

Figure 31. Measured *c* vs. inlet GVF under pure- or mainly-oil conditions

5.8 Direct Virtual-Mass

Figure 32 presents *M* versus inlet GVF for a range of ω, C_r, and PD values. *M* is caused by fluid inertia and can produce comparable dynamic effects in magnitude on the seal's net centering force to the seal's *K*. All *M* values are positive, reducing the net centering force of the seal, according to Eq. (5). Reducing the seal's net centering force can decrease the critical speed of the rotor in a pump.

When C_r=0.188 mm (turbulent flow), *M* generally increases as ω increases. This outcome differs from Marquette et al.'s [2] test results, where *M* is not sensitive to changes in ω. The predictions in Appendix A.6 show good agreement with Marquette et al.'s [2] test trends; i.e., they also differ from measurements. A possible reason for this is that in many C_r=0.188 mm cases, the transitional effects might still be evident, and the flow is not fully turbulent, while the flow is fully turbulent for Marquette et al.'s tests [2] and the predictions in Appendix A.6. In general, *M* is not sensitive to changes in PD. This outcome agree with Marquette et al.'s [2] test results. As expected, at high PD (48.3 bars) or at high ω (15 krpm), *M* drops (by up to 51%) as inlet GVF increases to 10% because increasing inlet GVF decreases the fluid's effective density.

This outcome agrees with predictions in Appendix A.6, where predicted M decreases by about 50% as inlet GVF increases to 10%. However, for ω from 5 to 10 krpm when PD=31 and 37.9 bars, as inlet GVF increases from zero to 10%, M remains generally unchanged, whereas predicted M decreases significantly (by about 50%). This disagreement may also result from the evident transitional effects in those cases while the flow is fully-turbulent in predictions.

For C_r=0.140 and 0.163 mm (laminar flow), M (as expected) drops as inlet GVF increases. M drops as ω increases. This trend is contrary to test results at C_r=0.188 mm, where M generally increases as ω increases. M generally decreases as PD increases. This outcome is different from test data at C_r=0.188 mm, where M remains almost unchanged as PD increases.

In summary, the effects of changes in ω and PD on M change significantly as C_r changes from 0.163 to 0.188 mm. This change may result from the flow status change (from laminar to turbulent) as C_r increases from 0.163 to 0.188 mm.

PD=31 bars is the only circumstance where only C_r changes. As C_r increases from 0.140 to 0.163 mm, the flow remains laminar, and M decreases significantly (by 31.4%~54.0%). Further increasing C_r to 0.188 mm makes the flow transition to turbulent. However, when ω=7.5 krpm and inlet GVF≤2%, increasing C_r from 0.163 to 0.188 mm barely changes M.

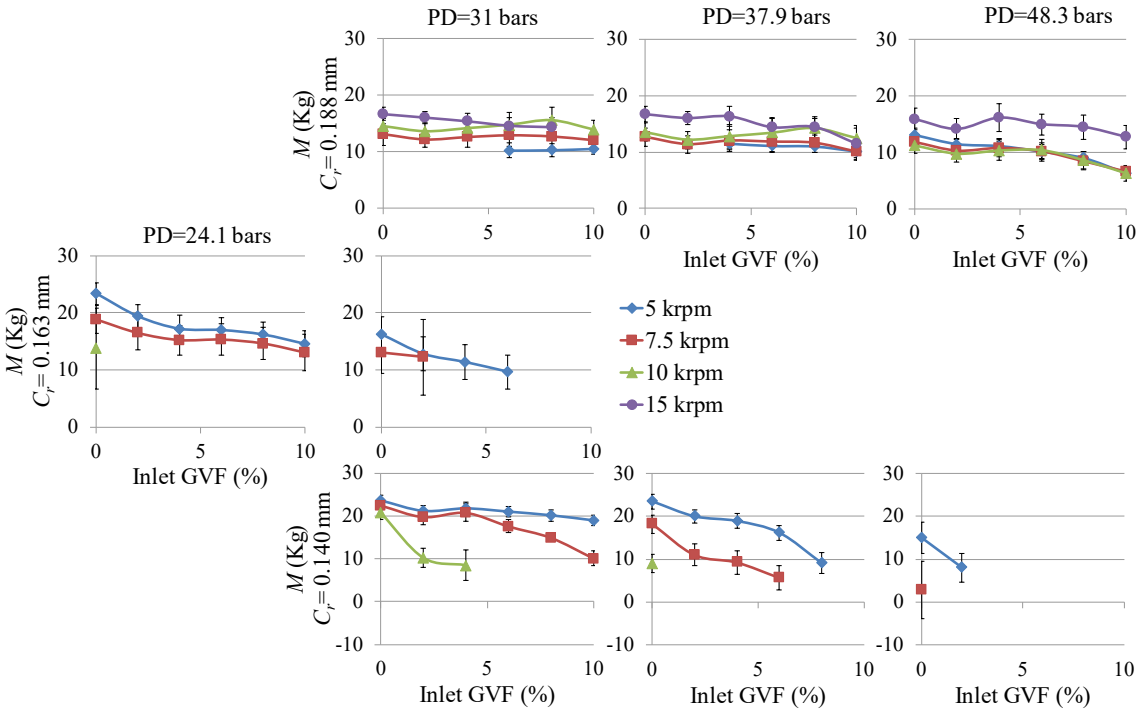

Figure 32. Measured M vs. inlet GVF under pure- or mainly-oil conditions

5.9 Cross-Coupled Virtual-Mass

Figure 33 shows m_q versus inlet GVF for a range of ω, C_r, and PD values. According to Eq. (6), a positive m_q acts as a stabilizing force, and a negative m_q acts as a destabilizing force.

For ω from 5 to 10 krpm, the magnitudes of m_q values are near the same order of the uncertainties and $|m_q\omega/(C\text{-}k/\omega)|$ is less than 13.2%, showing negligible effects on the seal's rotordynamic performance. When C_r=0.188 mm, as ω increases from 10 to 15 krpm, m_q remains negative but significantly increases in magnitude, producing a measurable destabilizing force ($22.2\%<|m_q\omega/(C\text{-}k/\omega)|<50.4\%$). For ω=15 krpm at C_r=0.188 mm, m_q generally decreases (increases in magnitude) as inlet GVF increases from zero to 10%.

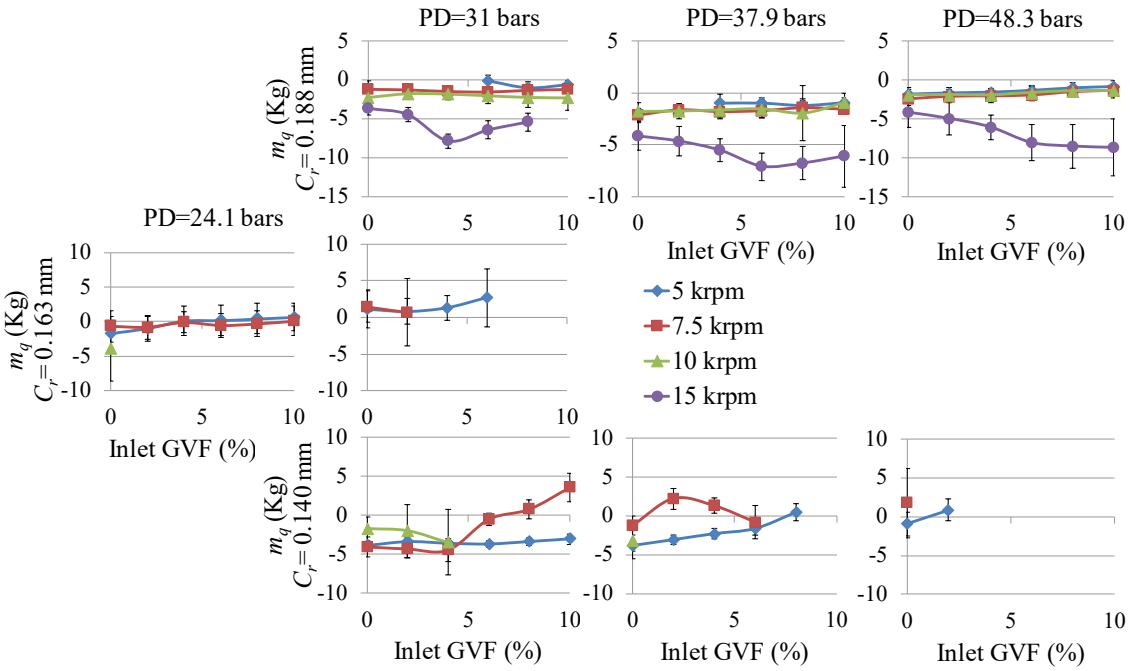

Figure 33. Measured m_q vs. inlet GVF under pure- or mainly-oil conditions

5.10 Effective Damping

Effective damping C_{eff} describes the seal's net damping force and is defined as:

$$C_{eff} = C - k/\omega + m_q\omega \tag{42}$$

Figure 34 shows C_{eff} versus inlet GVF for a range of ω, C_r, and PD. C_{eff} is smaller than the corresponding C (shown in Fig. 30) because the corresponding k (shown in Fig. 29) is positive, and the corresponding m_q (shown in Fig. 33) is either negative (when ω=15 krpm and C_r=0.188 mm) or negligible (for all other cases). For all clearances, increasing PD generally increases C_{eff} because C generally increases as PD increases. The C_{eff} increment increases the seal's effective damping force, making the seal more stabilizing and reducing the rotor's peak amplitudes at critical speeds in a pump.

For C_r=0.188 mm (turbulent flow), increasing inlet GVF from zero to 10% has negligible effects on C_{eff} since increases in inlet GVF generally does not changes C, k, and m_q. As expected, C_{eff} values decrease (by about 40%) as ω increases from 5 to 15 krpm since increasing ω increases k (shown in Fig. 29).

When C_r=0.163 and 0.140 mm (laminar flow), increasing inlet GVF generally increases C_{eff} because the increase in C surpasses the increase in k. Changing ω generally produces negligible effects on C_{eff} because the increase in C offsets the increase in k. This outcome agrees with the predictions in Appendix A.8.

In summary, the effects of changes in inlet GVF and ω on C_{eff} change significantly as C_r changes from 0.163 to 0.188 mm; specifically, increasing inlet GVF does not discernibly change C_{eff} when C_r=0.188 mm but generally increases C_{eff} when C_r=0.163 and 0.140 mm, and increasing ω decreases C_{eff} when C_r=0.188 mm but has little impact on C_{eff} when C_r=0.163 and 0.140 mm. This change may result from the flow status change (from laminar to turbulent) as C_r increases from 0.163 to 0.188 mm.

PD=31 bars is the only circumstance where only C_r changes. When ω=5 and 7.5 krpm, as C_r increases from 0.140 to 0.163 mm, the flow remains laminar, and C_{eff} increases by about 20%, making the seal more stabilizing. When ω=7.5 krpm and inlet GVF≤2%, further increasing C_r to 0.188 mm changes the flow to turbulent and decreases C_{eff} by about 20%.

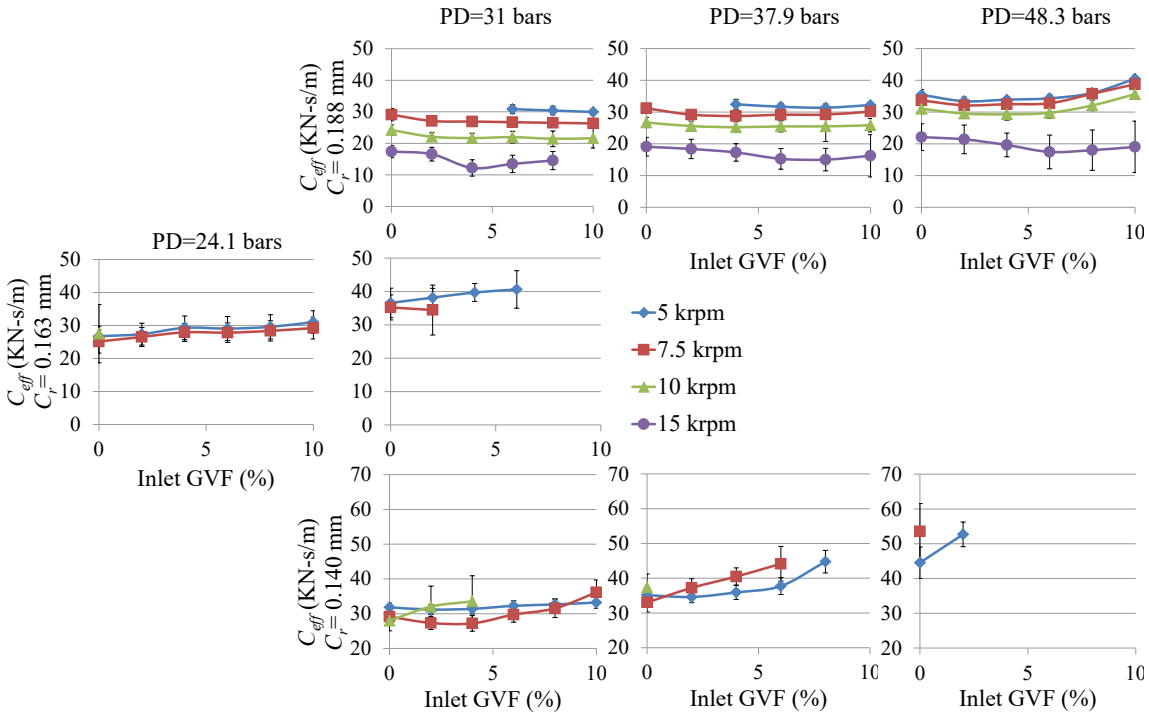

Figure 34. Measured C_{eff} vs. inlet GVF under pure- or mainly-oil conditions

6. EXPERIMENTAL RESULTS FOR PURE- AND MAINLY-AIR TESTING*

Figure 35 shows the real and imaginary parts of $\boldsymbol{H}_{ij}$ for a typical mainly-air test (after subtracting baseline data) when PR=0.57, C_r=0.188 mm, inlet GVF=95%, and ω=15 krpm. Figure 35(a) shows that the quadratic function shown in Eq. (20) does a poor job of fitting Re($\boldsymbol{H}_{ij}$) since the resultant R^2 values are not close to 1.0. Therefore, frequency-independent stiffness K_{ij} and virtual-mass M_{ij} coefficients cannot be extracted from Re($\boldsymbol{H}_{ij}$). This paper uses Re($\boldsymbol{H}_{ij}$) directly to describe the dynamic stiffness of the test seal. Re($\boldsymbol{H}_{ij}$) is frequency-dependent.

Figure 35(b) demonstrates that the linear function of Ω shown in Eq. (20) fits Im($\boldsymbol{H}_{ij}$) well, producing frequency-independent damping coefficients C_{ij}.

|Re($\boldsymbol{H}_{ij}$)| and |C_{ij}| values in Fig. 35 are (as expected) almost identical in X and Y directions. Therefore, the following discussion uses the average values for the rotordynamic coefficients:

$$K_{\Omega} = \frac{\mathrm{Re}(\boldsymbol{H}_{XX}) + \mathrm{Re}(\boldsymbol{H}_{YY})}{2} \tag{43}$$

$$k_{\Omega} = \frac{\mathrm{Re}(\boldsymbol{H}_{XY}) - \mathrm{Re}(\boldsymbol{H}_{YX})}{2} \tag{44}$$

$$C = \frac{C_{XX} + C_{YY}}{2} \tag{45}$$

$$c = \frac{C_{XY} - C_{YX}}{2}, \tag{46}$$

where K_{Ω} is the direct dynamic stiffness, k_{Ω} is the cross-coupled dynamic stiffness, C is the direct damping, and c is the cross-coupled damping.

---

* Portion of this section is reprinted with permission from "Experimental Study of the Static and Dynamic Characteristics of a Long Smooth Seal with Two-Phase, Mainly-Air Mixtures," by Zhang, M., McLean, J., and Childs, D., 2017, *ASME J. Eng. Gas Turbines Power*, 139(12), p. 122504, Copyright 2017 by ASME.

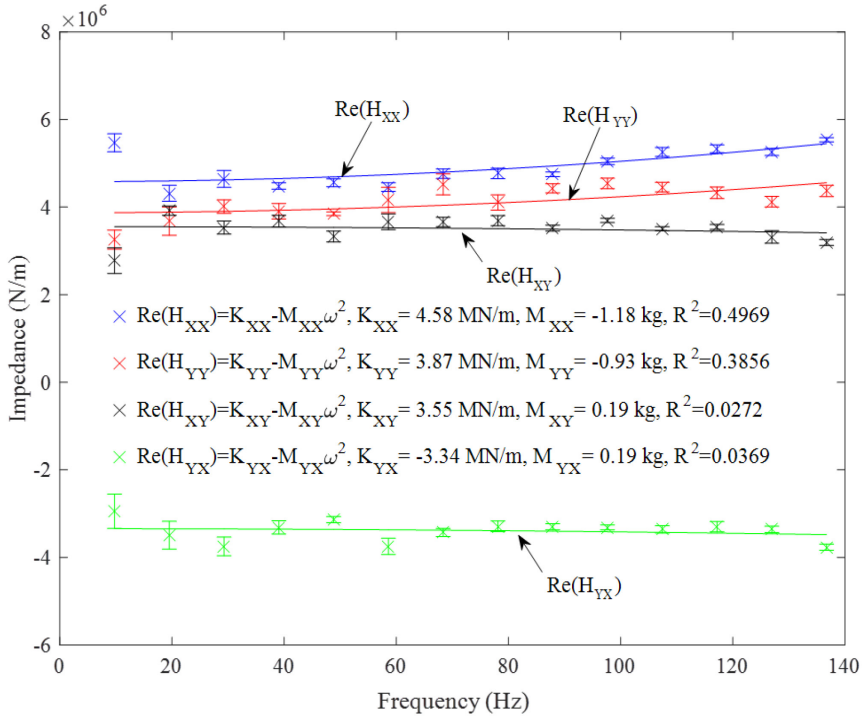

(a) Re($\boldsymbol{H_{ij}}$)

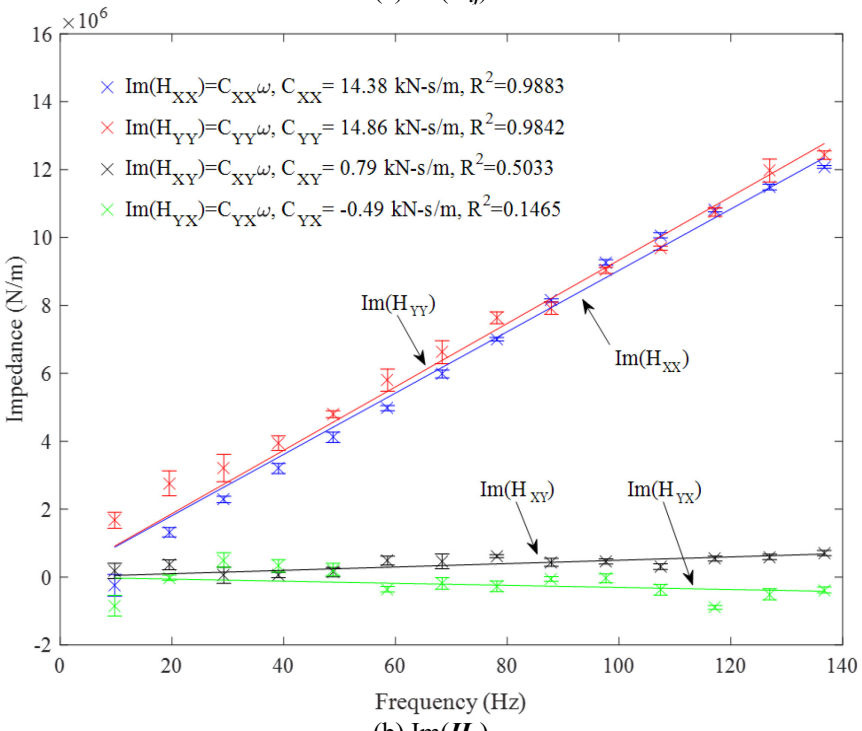

(b) Im($\boldsymbol{H_{ij}}$)

Figure 35. The (a) real and (b) imaginary parts of H_{ij} for a typical mainly-air case (PR=0.57, C_r=0.188 mm, inlet GVF=95%, and ω=15 krpm) after subtracting baseline data [27]

6.1 Sensitivity of Excitation Time on Parameter Identification

As noted in Sec. 4.2, for a mainly-air case, the shaker excites the stator assembly along each direction by steadily repeating a pre-programed waveform 1280 times. Since a waveform lasts 0.1024 seconds, the excitation time t_e along each direction is 131.072 seconds. This section studies the effects of changes in t_e on the seal's identified stiffness coefficients (K_Ω and k_Ω) and their uncertainties.

Figure 36 shows K_Ω versus Ω for three t_e values (32.768 s, 65.536 s, and 131.072 s) when PR=0.57, C_r=0.188 mm, inlet GVF=95%, and ω=15 krpm. The three graphs in Fig. 36 are arranged in increasing t_e from left to right. K_Ω generally increases as Ω increases. However, K_Ω does not steadily increase with increasing Ω; i.e., K_Ω is jittering. This jittering generally decreases as t_e increases.

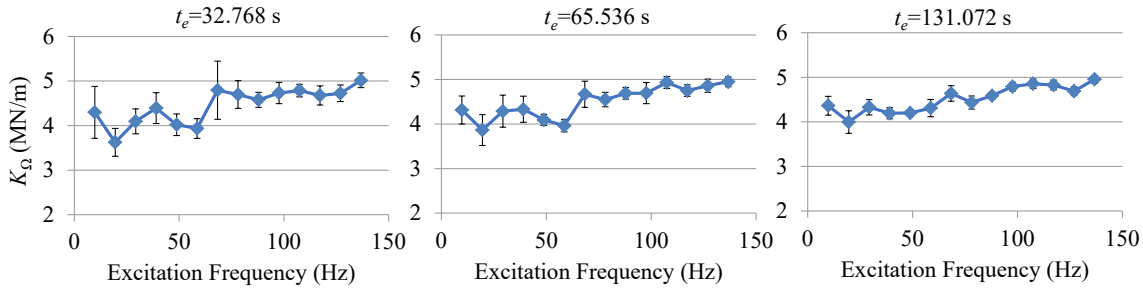

Figure 36. Variation of K_Ω with t_e when PR=0.57, C_r=0.188 mm, inlet GVF=95%, and ω=15 krpm

Figure 37 shows the ratio of the direct dynamic stiffness's uncertainty eK_Ω to K_Ω for three t_e values when PR=0.57, C_r=0.188 mm, inlet GVF=95%, and ω=15 krpm. eK_Ω/K_Ω generally decreases as Ω increases. The decrease of eK_Ω/K_Ω indicates that the repeatability of K_Ω becomes better. Also, as expected, eK_Ω/K_Ω decreases as t_e increases. When t_e=131.072 s, eK_Ω/K_Ω<5% for most Ω values.

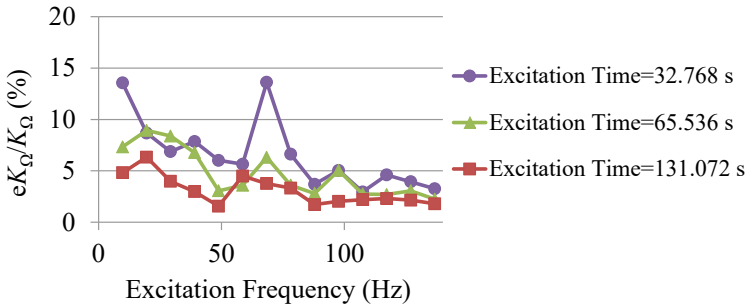

Figure 37. Variation of eK_Ω/K_Ω with t_e when PR=0.57, C_r=0.188 mm, inlet GVF=95%, and ω=15 krpm

Figure 38 shows k_Ω versus Ω for three t_e values when PR=0.57, C_r=0.188 mm, inlet GVF=95%, and ω=15 krpm. The three graphs in Fig. 38 are arranged in increasing t_e from left to right. Similar to K_Ω in Fig. 36, k_Ω is also jittering, and the jittering decreases as t_e increases.

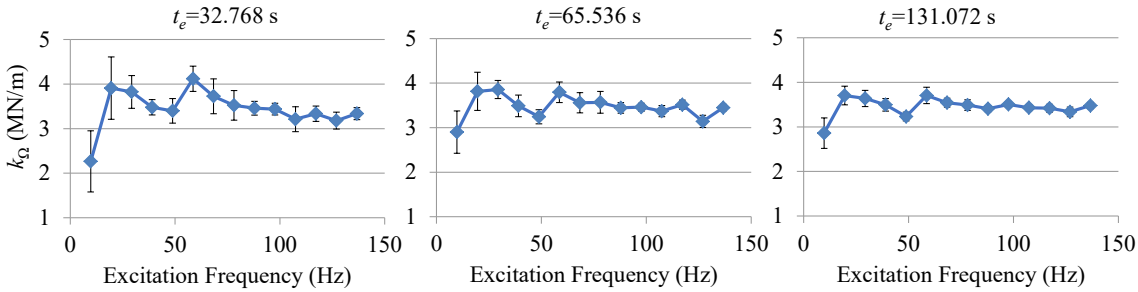

Figure 38. Variation of k_Ω with t_e when PR=0.57, C_r=0.188 mm, inlet GVF=95%, and ω=15 krpm

Figure 39 shows the ratio of the cross-coupled dynamic stiffness's uncertainty ek_Ω to k_Ω for three t_e values when PR=0.57, C_r=0.188 mm, inlet GVF=95%, and ω=15 krpm. As with eK_Ω/K_Ω in Fig. 37, ek_Ω/k_Ω generally decreases as Ω increases, showing that the repeatability of k_Ω becomes better. As expected, ek_Ω/k_Ω decreases as t_e increases. When t_e=131.072 s, ek_Ω/k_Ω<5% for Ω>20 Hz.

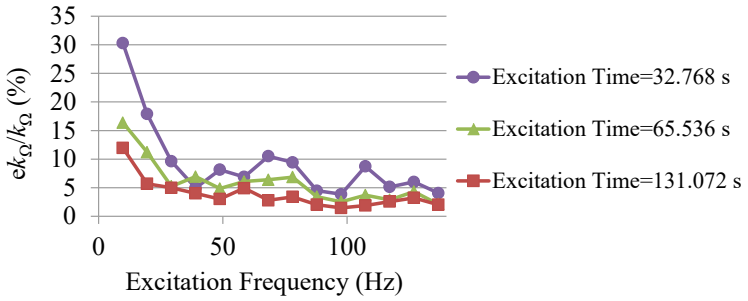

Figure 39. Variation of ek_Q/k_Q with t_e when PR=0.57, C_r=0.188 mm, inlet GVF=95%, and ω=15 krpm

6.2 Test Matrix

For tests under pure- and mainly-air conditions, the test seal is centered, the seal inlet pressure P_i is 62 bars, and no intentional fluid pre-rotation is provided. The targeted test matrix covers:

a) 4 inlet GVFs: 100%, 98%, 95%, and 92%,

b) 3 rotor speeds: 10, 15, and 20 krpm,

c) 3 pressure ratios (PRs): 0.57, 0.5, and 0.43,

d) 3 radial clearances (C_r): 0.140, 0.163, and 0.188 mm.

Since the back-pressure labyrinth seals shown in Fig. 17 did not provide enough resistance to generate the required seal exit pressure P_e, the targeted 0.57 PR was not achieved for all cases at C_r=0.140 mm and all mainly-air cases at C_r=0.163 mm.

For C_r=0.140 mm, when PR=0.5 and 0.43, many mainly-air test cases were not accomplished due to unstable stator motions. In the omitted cases, the stator became unstable immediately when excited by hydraulic shakers. Table 9 shows the resultant test matrix.

Recall from Sec. 3.1.5 that the zero pre-swirl-guide insert injects the test fluid radially inwards to produce a flow with minimum circumferential velocity at the seal inlet. Table 10 shows measured pre-swirl ratio $u_0(0)$ values for all test cases under pure- and mainly-air conditions. Measured $u_0(0)$ values are close to zero, and they are between -0.07 and 0.08.

The uncertainty of the pitot tube differential pressure (shown in Table 4) produces the uncertainty of $u_0(0)$. Since the effective density of the fluid varies with inlet GVF, the uncertainty of $u_0(0)$ varies with inlet GVF. Table 11 shows the uncertainties of measured $u_0(0)$ values.

PR (-)	Inlet GVF (%)	C_r=0.188 mm			C_r=0.163 mm			C_r=0.140 mm		
		ω (krpm)			ω (krpm)			ω (krpm)		
0.57	100	10	15	20	10	15	20	PR cannot be achieved		
	98	10	15	20	PR cannot be achieved					
	95	10	15	20						
	92	10	15	20						
0.5	100	10	15	20	10	15	20	10	15	20
	98	10	15	20	10	15	20	10	15	20
	95	10	15	20	10	15	20	Unstable to test		
	92	10	15	20	10	15	20			
0.43	100	10	15	20	10	15	20	10	15	20
	98	10	15	20	10	15	20	Unstable to test		
	95	10	15	20	10	15	20			
	92	10	15	20	10	15	20			

Table 9. Resultant test matrix under pure- and mainly-air conditions

PR (-)	Inlet GVF (%)	C_r=0.188 mm			C_r=0.163 mm			C_r=0.140 mm		
		10 krpm	15 krpm	20 krpm	10 krpm	15 krpm	20 krpm	10 krpm	15 krpm	20 krpm
0.57	100	0.05	0.05	0.05	0.02	0.04	0.03	PR cannot be achieved		
	98	-0.02	-0.01	-0.01	PR cannot be achieved					
	95	-0.02	-0.01	-0.01						
	92	0.02	0.04	0.03						
0.5	100	0.04	0.06	0.05	0.04	0.05	0.04	0.05	0.05	0.05
	98	0.01	0.00	0.01	0.08	0.01	0.00	0.03	-0.02	0.06
	95	0.02	0.01	-0.01	-0.07	-0.05	-0.04	Unstable to test		
	92	0.01	0.00	0.02	-0.07	-0.04	-0.03			
0.43	100	0.03	0.05	0.05	0.05	0.03	0.02	0.06	0.05	0.05
	98	0.02	-0.02	-0.01	0.08	0.04	0.03	Unstable to test		
	95	0.01	0.02	-0.01	-0.05	-0.05	-0.04			
	92	0.02	0.02	0.02	-0.05	-0.03	-0.03			

Table 10. Measured pre-swirl ratios under pure- and mainly-air conditions

Inlet GVF (%)	10 krpm	15 krpm	20 krpm
100	0.06	0.04	0.03
98	0.06	0.04	0.03
95	0.05	0.03	0.03
92	0.05	0.03	0.02

Table 11. Uncertainties of measured pre-swirl ratios under pure- and mainly-air conditions

6.3 Flow Conditions

Under pure- and mainly-air conditions, the minimum calculated Re_a is 4336, and it is at the seal inlet when C_r=0.163 mm, PR=0.5, ω=10 krpm, and inlet GVF=92%. Since the maximum critical axial Reynolds number $Re_{a,c}$ shown in Figs. 26(a) and (b) is 1500, which is only 34.6% of 4336, the flow can be reasonably treated as fully turbulent under pure- and mainly-air conditions.

6.4 Leakage Mass Flow Rate

Figure 40 shows $\dot{m}$ versus inlet GVF for three PRs (rows), three C_r values (columns), and three ω values. For all clearances, $\dot{m}$ decreases slightly (by less than 6%) as inlet GVF decreases from 100% to 98%, but then increases by about 45% with further decreasing inlet GVF to 92%. This outcome indicates that when inlet GVF decreases from 100% to 98%, the increase in effective viscosity dominates $\dot{m}$, but when inlet GVF further drops to 92%, the increase in effective density dominates. Both effective viscosity and effective density increase as inlet GVF drops. Increasing effective viscosity can decrease $\dot{m}$ while increasing effective density can increase $\dot{m}$.

Under pure-air conditions, $\dot{m}$ is not sensitive to changes in either ω nor PR, which agrees with Kerr's [3] test results for smooth gas annular seals. This trend continues after adding oil into the air flow.

As expected, $\dot{m}$ increases by about 57% as C_r increases from 0.140 to 0.188 mm.

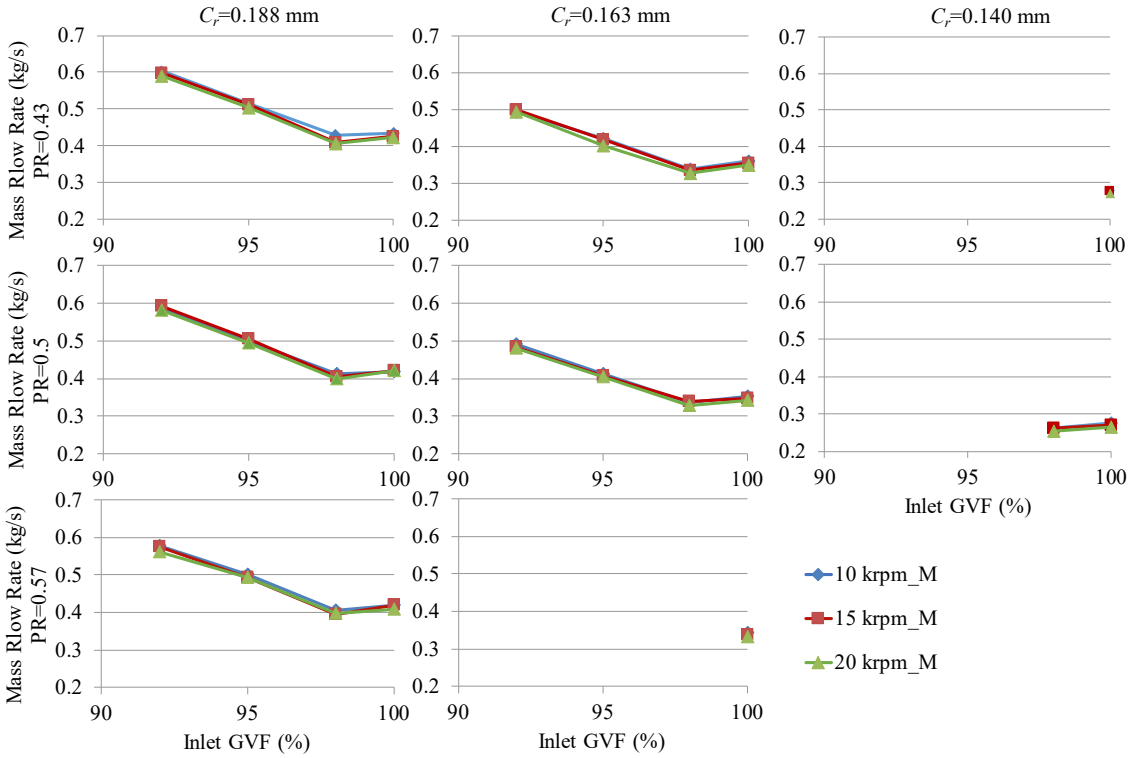

Figure 40. Measured $\dot{m}$ versus inlet GVF under pure- or mainly-air conditions

6.5 Direct Dynamic Stiffness

Figure 41 shows K_Ω versus $\boldsymbol{\Omega}$ at C_r=0.188 mm for three PRs (rows), three ω values (columns), and four inlet GVFs.

For pure-air conditions, as $\boldsymbol{\Omega}$ increases, K_Ω remains constant when PR=0.57 but increases (stiffening effect) when PR=0.5 and 0.43. Decreasing PR (increasing PD) makes K_Ω increase more rapidly with increasing $\boldsymbol{\Omega}$. This outcome agrees with Kerr's test results [3] for smooth gas annular seals. Injecting oil into the air flow makes the stiffening effect more pronounced. Appendix B.2 will discuss more about this stiffening effect.

The effects of changing inlet GVF on K_Ω are best discussed separately for the following two regions:

(1) As inlet GVF decreases from 100% to 98%, K_Ω increases when PR=0.43, but decreases when PR=0.5 and 0.57. The larger that PR becomes, the larger the decrease.

(2) Further decreases in inlet GVF from 98% to 92% decrease K_Ω.

In a centrifugal compressor, the rotor's natural frequency can depend strongly on K_Ω, Kleynhans [44]. For all conditions except decreasing inlet GVF 100% to 98% when PR=0.43, decreasing inlet GVF can act to drop the rotor's natural frequency, and then decrease the rotor's critical speed. Dropping the rotor's natural frequency could also decrease the rotor's stability.

For pure-air conditions, increasing ω does not significantly change K_Ω. This outcome agrees with Kerr's [3] test data, and this trend continues after adding oil into the air flow.

As with Kerr's [3] test results, K_Ω increases (the seal's centering force increases) as PR increases (PD drops) at pure-air conditions. Although K_Ω still generally increases as PR increases (PD drops) after adding oil into the air flow, the increase in K_Ω at mainly-air conditions is significantly less than at pure-air conditions.

Figure 42 shows K_Ω versus Ω at C_r=0.163 mm for three PRs (rows), three ω values (columns), and four inlet GVFs. K_Ω at Ω=30 Hz is quite different from K_Ω values at adjacent excitation frequencies; i.e., compared to K_Ω values at Ω=20 and 40 Hz, K_Ω at Ω=30 Hz is smaller (by about 12%) under pure-air conditions but generally larger (by about 65%) under mainly-air conditions. The unusual test data at Ω=30 Hz are caused by the resonance behavior of the stator at the nominal speed of the pump for hydraulic shakers. The nominal speed of the pump for hydraulic shakers is 1800 rpm (30 Hz), coinciding with the 30 Hz excitation frequency.

As with test data at C_r=0.188 mm, under pure-air conditions, increasing Ω does not change K_Ω when PR=0.57 but increases K_Ω (stiffening effect) when PR=0.5 and 0.43. Decreasing PR (increasing PD) makes K_Ω increase more rapidly with increasing Ω. Also, this stiffening effect becomes more pronounced after adding oil into the air flow.

K_Ω decreases as PR decreases (PD increases) and does not change significantly as ω increases. Therefore, the trends with changes in PR and ω agree with test results at C_r=0.188 mm.

K_Ω generally decreases as inlet GVF decreases from 100% to 95% except increasing as inlet GVF decreases from 100% to 98% when ω=20 krpm and PR=0.43. K_Ω does not change discernibly as inlet GVF decreases from 95% to 92%.

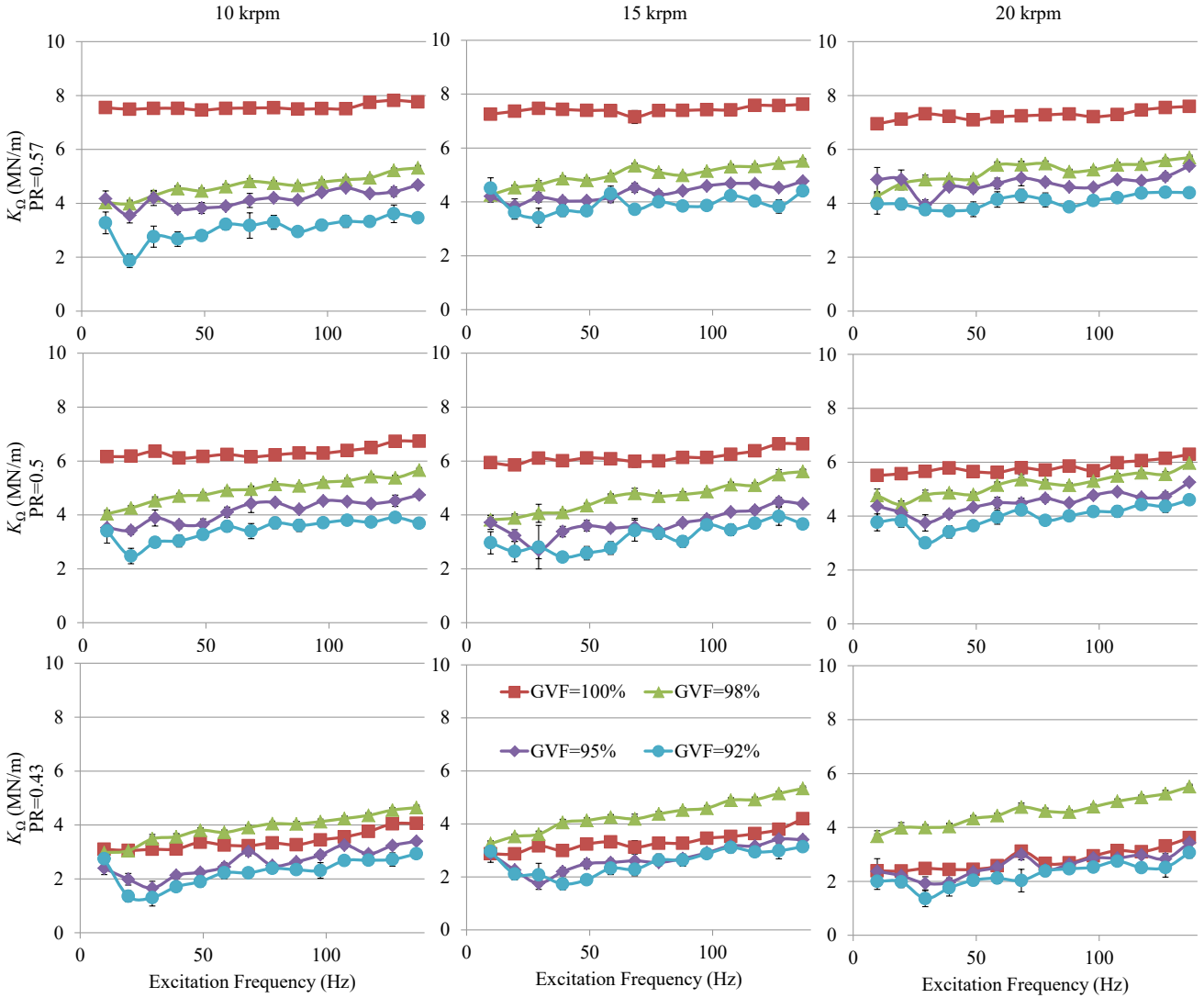

Figure 41. Measured K_Ω under pure- or mainly-air conditions at C_r=0.188 mm. Reproduced from [27]

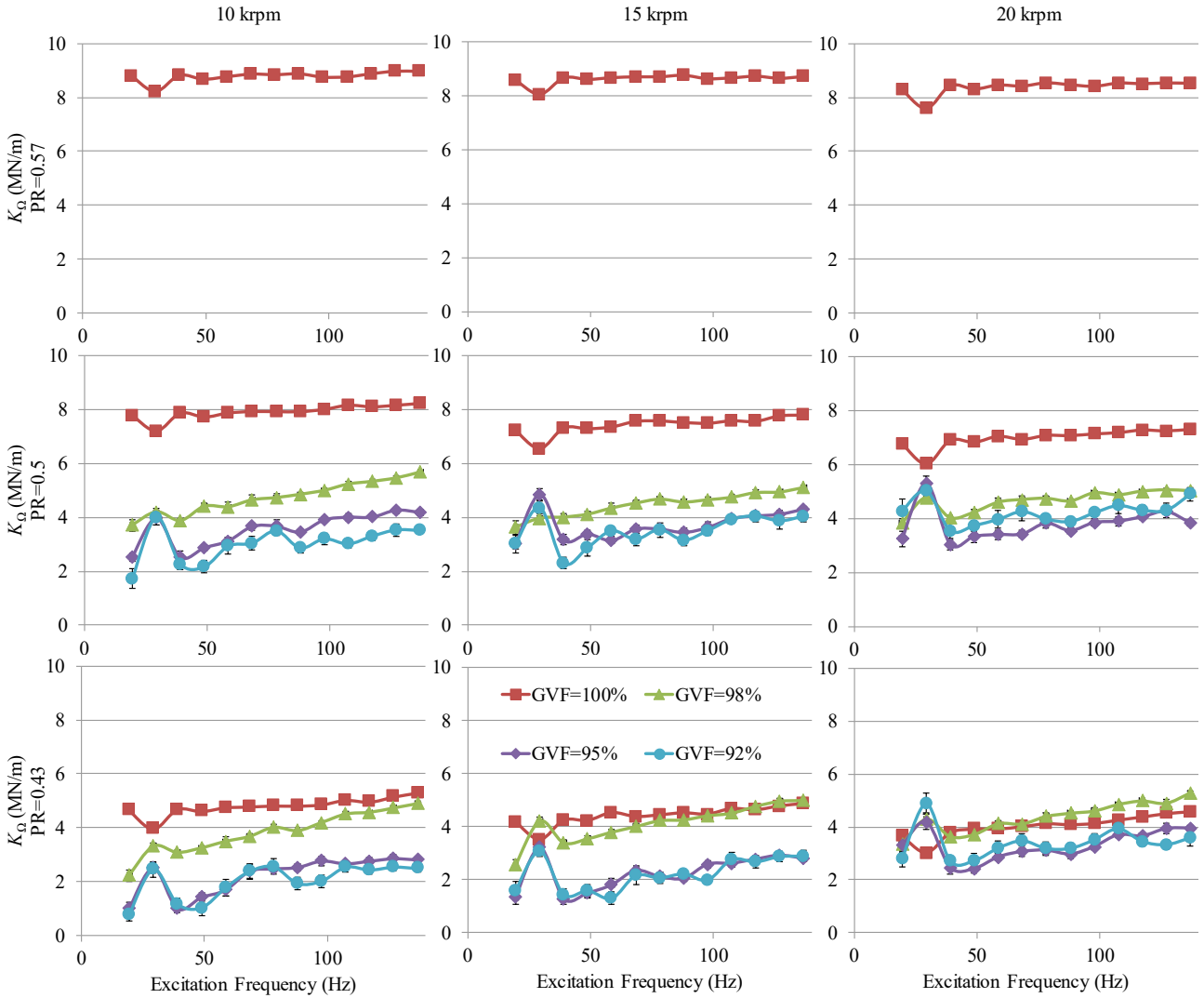

Figure 42. Measured K_Ω under pure- or mainly-air conditions at C_r=0.163 mm

Figure 43(a) shows K_Ω versus Ω for inlet GVF=100% and 98% when PR=0.5 and C_r=0.140 mm. Decreasing inlet GVF from 100% to 98% leads to a significant decrease in K_Ω. Under pure-air conditions, K_Ω increases slightly by about 10% as Ω increases from 10 to 140 Hz. As inlet GVF changes from 100% to 98%, K_Ω increases more rapidly with increasing Ω; i.e., K_Ω increases by about 180% as Ω increases from 10 to 140 Hz.

Figure 43(b) presents K_Ω versus Ω when PR=0.43, C_r=0.140 mm, and inlet GVF=100%. K_Ω increases by about 30% as Ω increases from 10 to 140 Hz.

As shown in Figs. 43(a) and (b), at pure-air conditions, K_Ω increases by about 70% as PR increases from 0.43 to 0.5 (PD decreases). This outcome agrees with the results at C_r=0.188 and 0.163 mm and Kerr's [3] test results.

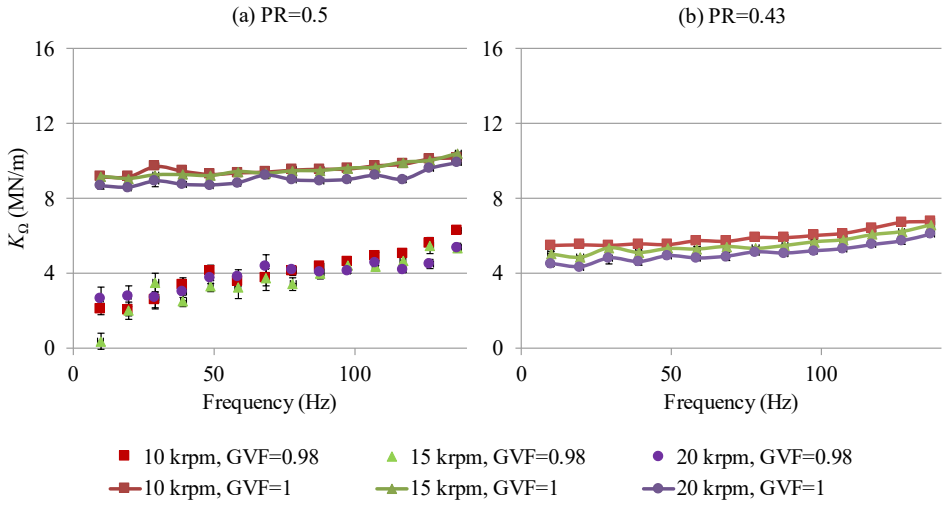

Figure 43. Measured K_Ω at C_r=0.140 mm for (a) PR=0.5 and (b) PR=0.43

Unlike pure- and mainly-oil cases, all K_Ω values at pure- and mainly-air conditions are positive, applying positive centering forces on the rotor. As shown in Fig. 41~43, decreasing inlet GVF from 100% to 92% normally decreases the seal's centering force except that the seal's centering force increases as inlet GVF decreases from 100% to 98% in the following circumstances: (1) cases with PR=0.43 and C_r=0.188 mm, and (2) the case with PR=0.43, ω=20 krpm, and C_r=0.163 mm.

In a centrifugal compressor, dropping the seal's centering force can drop the rotor's natural frequency, and then decrease the rotor's critical speed, Kleynhans [44]. Dropping the rotor's natural frequency could also decrease the rotor's stability.

At pure-air conditions, increasing C_r from 0.140 to 0.188 mm decreases K_Ω and the seal's centering force. This outcome agrees with Kerr's [3] test results. PR=0.5 and inlet GVF=98% is the only mainly-air circumstance where only C_r changes. When PR=0.5 and inlet GVF=98%, increasing C_r from 0.140 to 0.188 mm generally increases K_Ω and increases the seal's centering force. In short, the impact of changes in C_r on K_Ω changes substantially after adding oil into the air flow.

6.6 Cross-Coupled Dynamic Stiffness

Figure 44 shows k_Ω versus Ω at C_r=0.188 mm for three PRs (rows), three ω values (columns), and four inlet GVFs. Under pure-air conditions, k_Ω is frequency independent. This outcome agrees with Kerr's [3] test results. After injecting oil into the air flow, k_Ω remains generally insensitive to changes in Ω. Although not presented, k_Ω is also generally insensitive to changes in Ω at the other two clearances (C_r=0.163 and 0.140 mm). A major finding in Fig. 44 is that when oil is introduced (as inlet GVF decreases from 100% to 98%), k_Ω increases abruptly, and the test seal becomes suddenly more destabilizing.

Recall from Fig. 35 that for a typical mainly-air case, a quadratic fit of $k_\Omega(\Omega)$ would not produce a curve-fit with an R^2 near 1.0. Hence $k_\Omega(\Omega)$ cannot be fitted with frequency independent cross-coupled stiffness k and cross-coupled virtual-mass m_q. However, $k_\Omega(\Omega)$ is just fluctuating around the average value $\bar{k}$ as Ω increases. Although this fluctuation of $k_\Omega(\Omega)$ becomes more pronounced as inlet GVF decreases, the fluctuation level is always small compared to the magnitude of $\bar{k}$. Therefore, in the balance of this section, $\bar{k}$ is used to describe the test seal's cross-coupled stiffness.

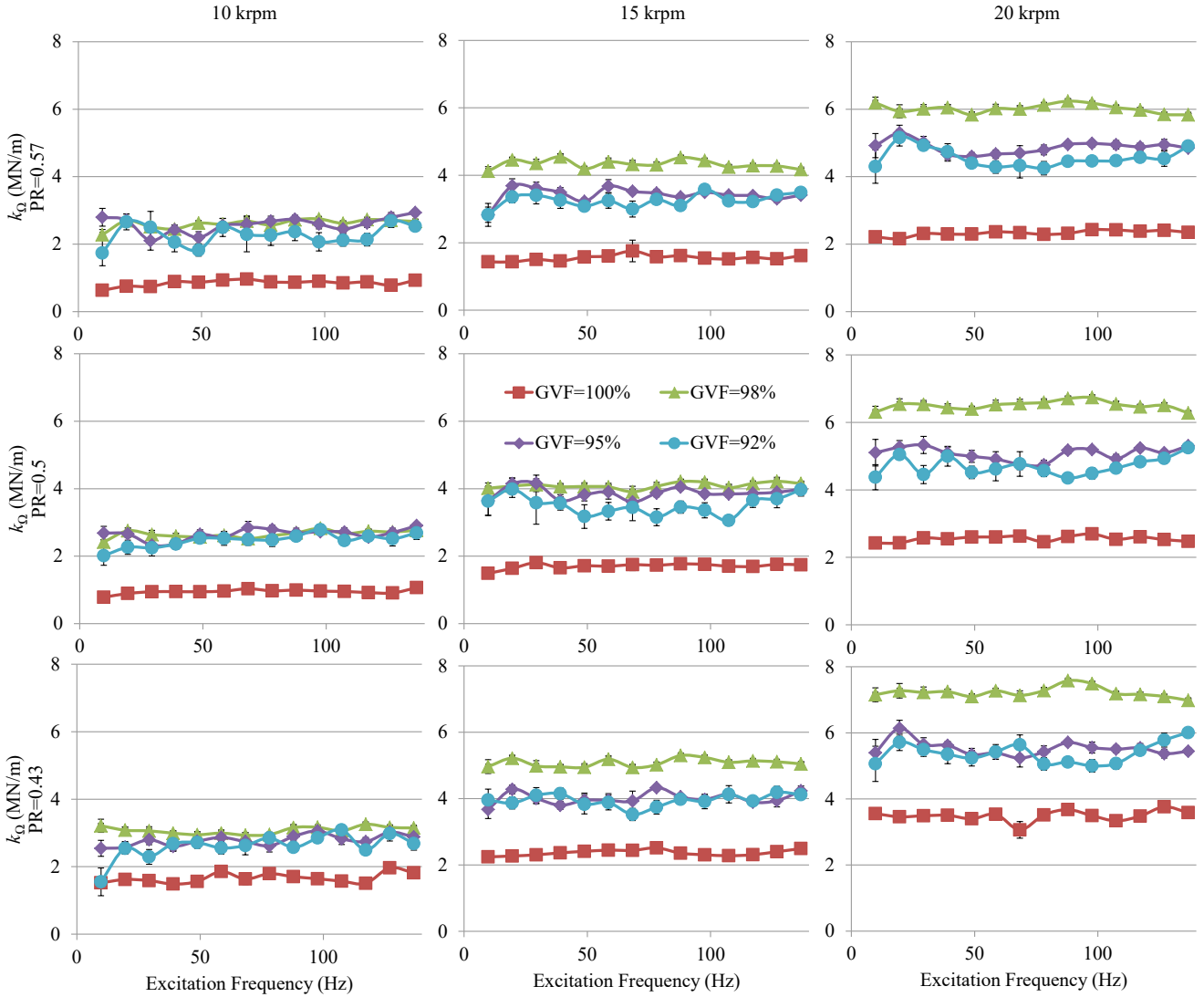

Figure 44. Measured k_Ω under pure- or mainly-air conditions at C_r=0.188 mm. Reproduced from [27]

Figure 45 shows $\bar{k}$ versus inlet GVF for three PRs (rows), three C_r values (columns), and three ω values. All $\bar{k}$ values are positive, producing destabilizing forces. As expected, $\bar{k}$ increases as ω increases since increasing ω increases the fluid's circumferential velocity. $\bar{k}$ is almost invariant with changes in PR, which agrees with Kerr's [3] test results under pure-air conditions. Hence decreasing PR (increasing PD) shows negligible effects on the seal's destabilizing force.

$\bar{k}$ increases significantly (by a factor of about 2) as inlet GVF drops from 100% to 98%. Therefore, the initial increase of injected oil significantly increases the seal's destabilizing force. With further decreasing inlet GVF to 92%, $\bar{k}$ decreases (by less than 35.8%), reducing the seal's destabilizing force. However, $\bar{k}$ from any inlet GVF=92% case is still larger than the value of $\bar{k}$ from the corresponding pure-air case. Therefore, the seal under mainly-air conditions is more destabilizing than at the corresponding pure-air conditions. The increase in $\bar{k}$ as inlet GVF decreases from 100% to 98% is expected since the fluid's viscosity increases, and this outcome is consistent with predictions in Appendix B.3. The decreases in $\bar{k}$ as inlet GVF decreases from 98% to 92% are contrary to predictions in Appendix B.3, where predicted $\bar{k}$ increases steadily as inlet GVF decreases from 100% to 92%. The author has no explanation for these decreases in $\bar{k}$.

Increasing C_r from 0.140 to 0.188 mm decreases $\bar{k}$, decreases the seal's destabilizing force, and makes the rotor more stable in a centrifugal compressor. This outcome agrees with Kerr's [3] test results for smooth gas seals.

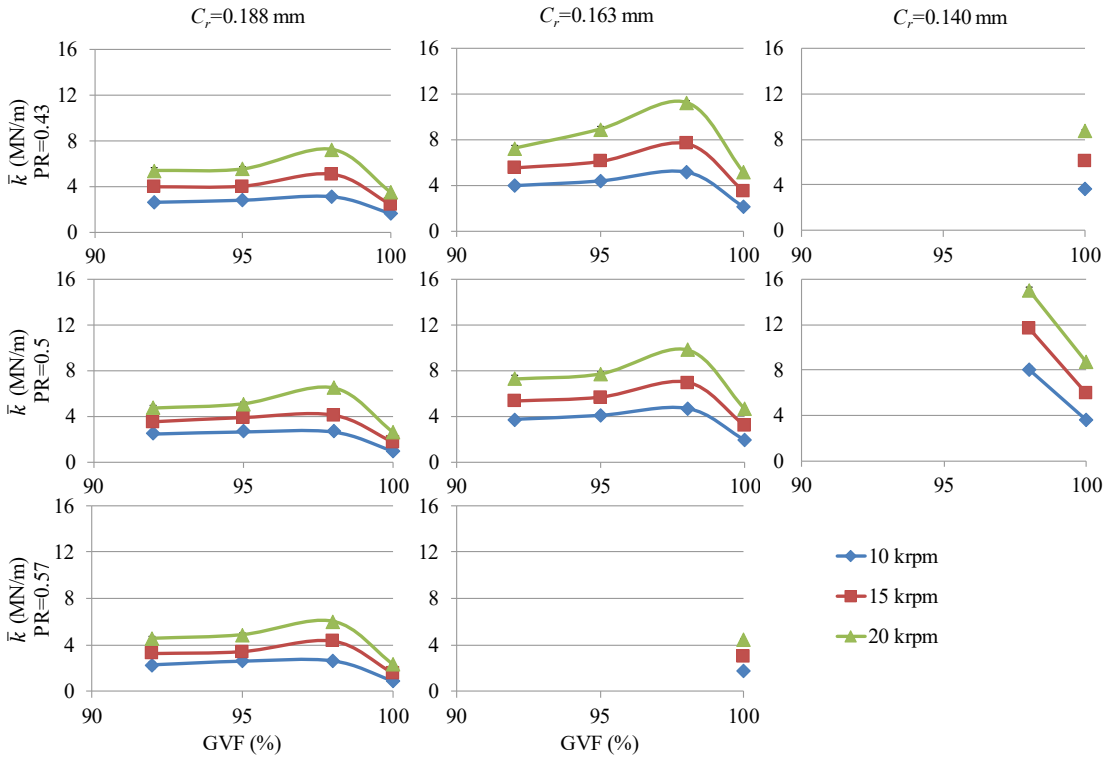

Figure 45. Measured $\overline{k}$ versus inlet GVF under pure- or mainly-air conditions

6.7 Direct Damping

Figure 46 illustrates C versus inlet GVF for three PRs (rows), three C_r values (columns), and three ω values. As with Kerr's [3] test results, under pure-air conditions, C is insensitive to changes in ω. This trend continues after adding oil into the air flow. C increases by 15%~41% as inlet GVF drops from 100% to 98%, and then remains almost unchanged with further decreases in inlet GVF. Therefore, the initial increment of injected oil (decreasing inlet GVF to 98%) significantly increases the seal's damping (stabilizing) force, while further increments of injected oil have negligible effects on the seal's damping force. Increasing PR (decreasing PD) decreases C. Also, increasing C_r decreases C and the seal's damping force. The trends of C with changes in PR and C_r agree with Kerr's [3] test results for smooth gas seals.

Recall from Sec. 6.6 that k_Ω increases significantly (by a factor of about 2) as inlet GVF drops from 100% to 98%. Since increasing k_Ω and increasing C produce opposite effects on the seal's stabilizing capacity, effective damping C_{eff}, which combines the stabilizing impact of C

with the destabilizing impact of k_Ω, will be analyzed to investigate the effects of oil injections (decreasing inlet GVF) on the seal's net damping force. C_{eff} is the topic of the next section.

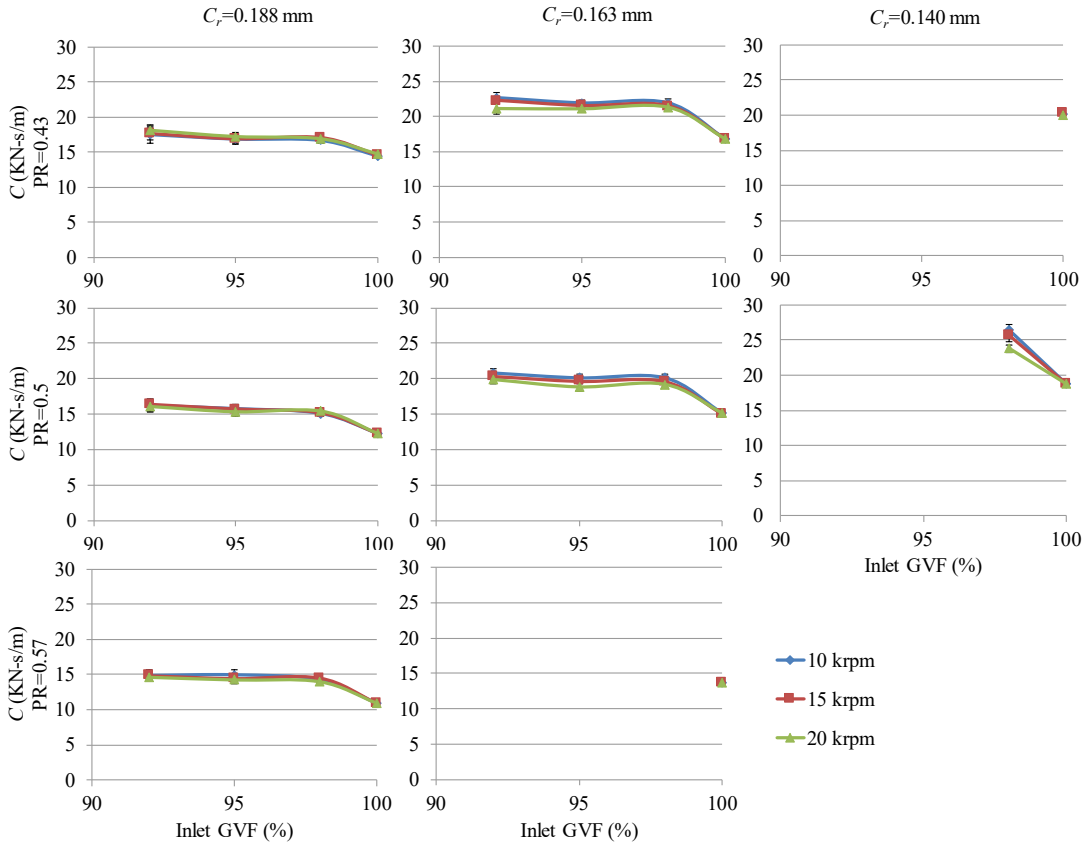

Figure 46. Measured C versus inlet GVF under pure- or mainly-air conditions

6.8 Effective Damping

Effective damping C_{eff} combines the stabilizing impact of C with the destabilizing impact of k_Ω

$$C_{eff} = C - k_\Omega / \Omega . \tag{47}$$

Note that m_q in Eq. (6) has been dropped and its effect (if any) is absorbed by the frequency-dependent nature of k_Ω. A positive C_{eff} value ensures the system stability. A negative value of C_{eff}

indicates that the destabilizing component k_Ω dominates and will create a destabilizing force from the seal. Note that $C_{eff} \rightarrow C$ as $\Omega \rightarrow \infty$.

Figure 47 shows C_{eff} versus Ω at C_r=0.188 mm. For low Ω values, k_Ω dominates Eq. (47) , and C_{eff} values are negative (destabilizing). As Ω increases, C_{eff} changes from negative to positive at Ω_c (the cross-over frequency). Therefore, for Ω values below Ω_c, the seal's net damping forces are destabilizing, and for Ω values above Ω_c, the net damping forces are positive (stabilizing).

Table 12 shows Ω_c values for C_r=0.188 mm. Table 12 shows that injecting oil into the air flow highly influences the seal's effective damping. The initial increment of injected oil (decreasing inlet GVF to 98%) increases Ω_c, indicating a drop in stability. Further increments of injected oil (decreasing inlet GVF further to 92%) decrease Ω_c, showing the seal as less destabilizing. Also, Ω_c in a mainly-air case is always larger than the corresponding value of Ω_c at inlet GVF=100%. This outcome for smooth seals is consistent with the observations from Vannini et al. [10] that injecting liquid directly into the labyrinth seals of a centrifugal compressor could cause sub-synchronous vibrations.

As ω increases, Ω_c increases (become more destabilizing). This outcome is expected because increasing ω increases the fluid's circumferential velocity, thereby increasing the destabilizing component k_Ω.

In general, changing PR does not significantly change Ω_c, showing little impact on the seal's effective stabilizing force. This outcome agrees with Kerr's pure-air test results [3].

PR (-)	Rotor Speed ω (krpm)	Cross-over Frequency Ω_c (Hz)			
		Inlet GVF=100%	Inlet GVF=98%	Inlet GVF=95%	Inlet GVF=92%
0.57	10	8.7	28.6	25.4	27.7
	15	21.4	48.7	38.4	35.1
	20	31.6	68.7	52.3	48.4
0.5	10	10.4	28.0	24.8	22.2
	15	22.1	42.6	38.6	33.8
	20	31.7	68.2	53.4	46.0
0.43	10	18.3	27.8	24.7	22.9
	15	24.7	46.7	36.3	34.8
	20	36.1	68.7	50.0	47.0

Table 12. Ω_c values for pure- and mainly-air cases at C_r=0.188 mm

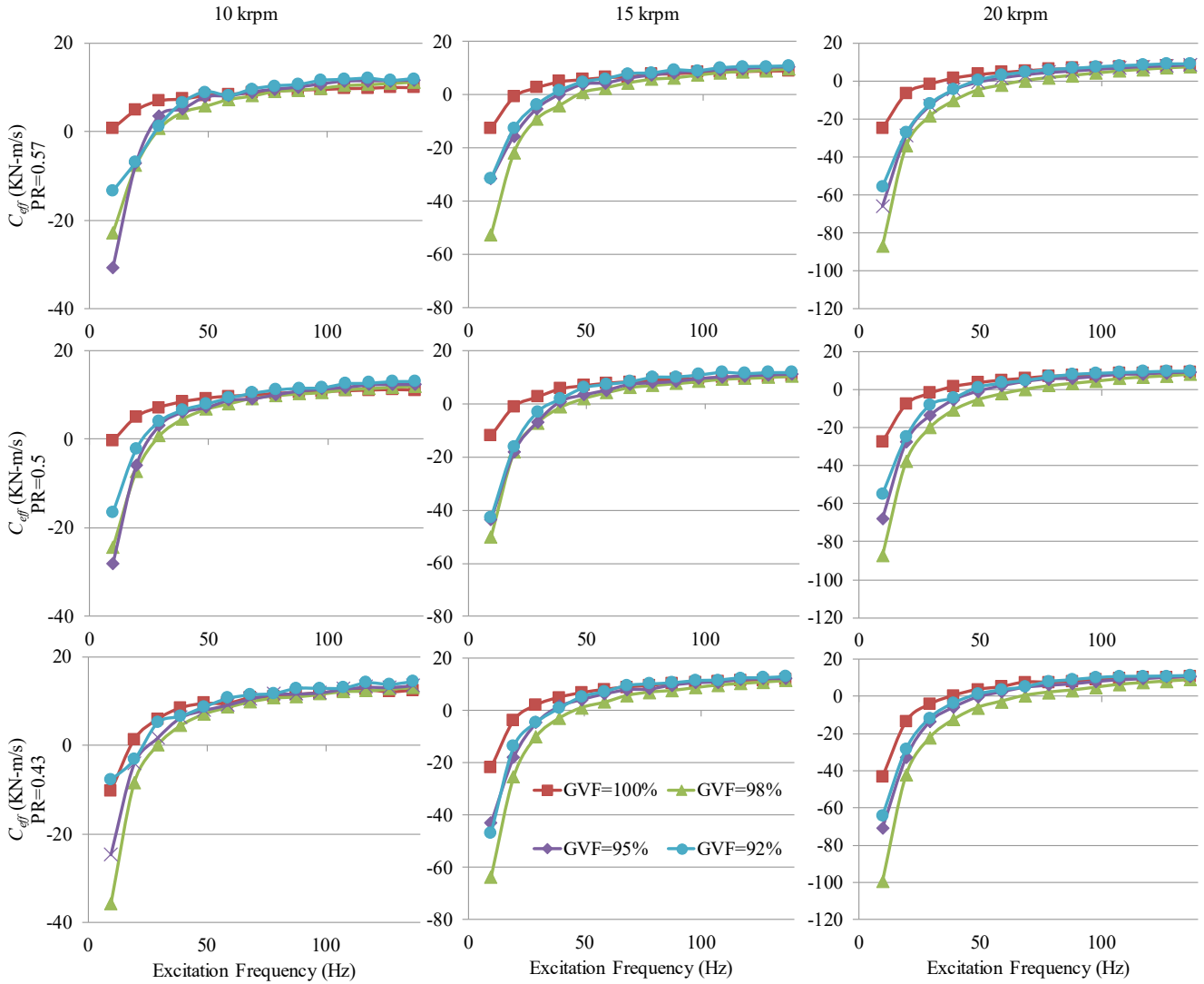

Figure 47. Measured C_{eff} under pure- or mainly-oil conditions at C_r=0.188 mm

Figure 48 shows C_{eff} versus Ω at C_r=0.163 mm. As with test results in Fig. 47 for C_r=0.188 mm, C_{eff} values are negative (destabilizing) when $\Omega<\Omega_c$, and positive (stabilizing) when $\Omega>\Omega_c$. Ω_c has a considerable impact on the system stability.

Table 13 shows Ω_c values at C_r=0.163 mm. Table 13 shows that Ω_c increases (become more destabilizing) as inlet GVF drops from 100% to 98%, and then decreases (become less destabilizing) with further decreasing inlet GVF to 92%. As expected, increasing ω increases Ω_c, making the seal more destabilizing. Changing PR barely changes Ω_c and has negligible effects on the seal's effective stabilizing force. In general, the effects of changes in inlet GVF, ω, and PR on Ω_c largely coincide with the test results in Table 12 for C_r=0.188 mm.

PR (-)	Rotor Speed ω (krpm)	Cross-over Frequency Ω_c (Hz)			
		Inlet GVF=100%	Inlet GVF=98%	Inlet GVF=95%	Inlet GVF=92%
0.57	10	19.9	-		
	15	33.8			
	20	54.8			
0.5	10	19.4	35.4	30.8	27.0
	15	32.3	58.1	44.2	43.5
	20	52.0	76.9	65.6	59.0
0.43	10	19.4	36.7	29.3	28.0
	15	31.9	60.3	44.9	39.1
	20	50.9	80.9	66.9	55.9

Table 13. Ω_c values for pure- and mainly-air cases at C_r=0.163 mm

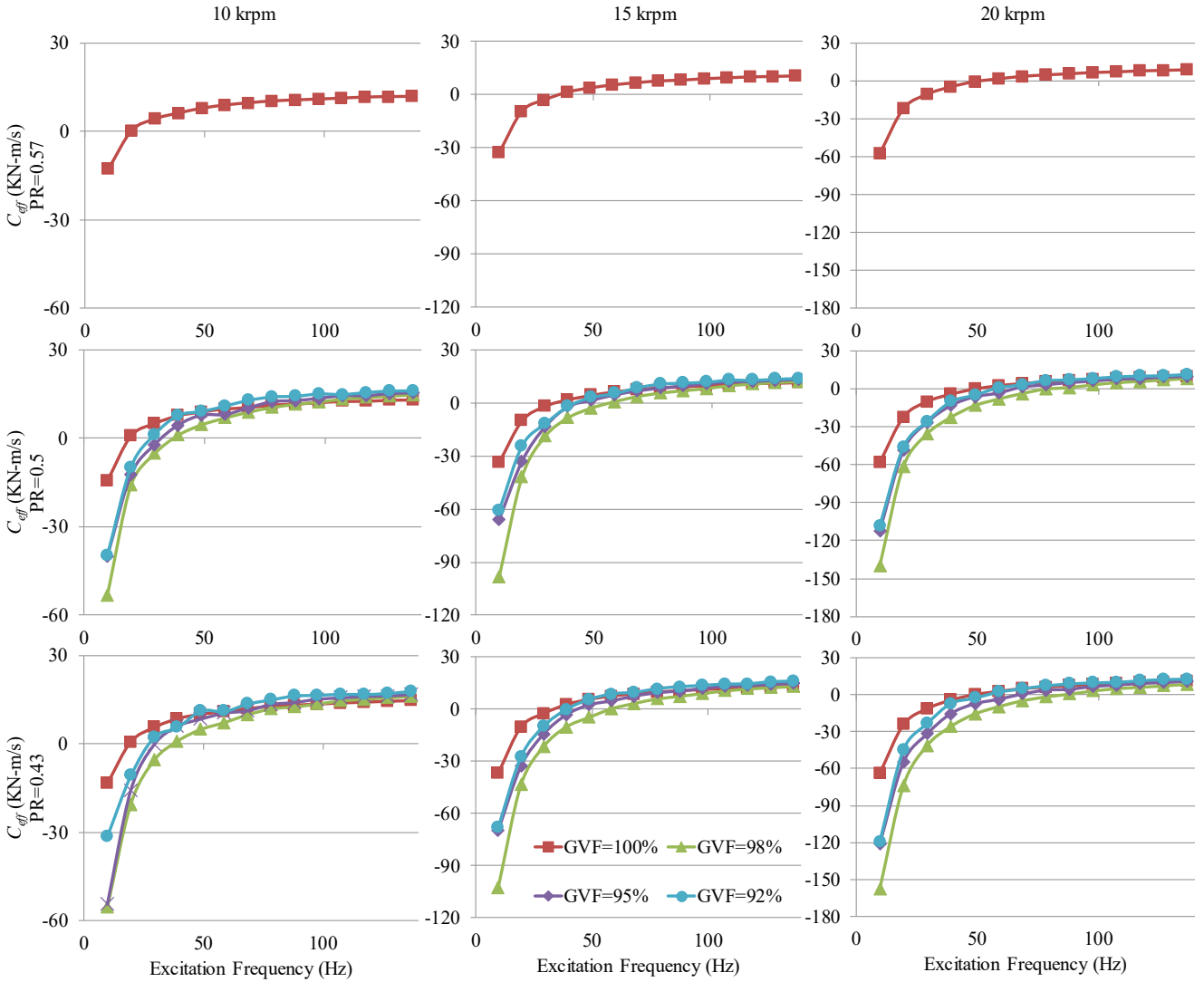

Figure 48. Measured C_{eff} under pure- or mainly-oil conditions at C_r=0.163 mm

Figure 49(a) shows C_{eff} at PR=0.5 and C_r=0.140 mm for inlet GVF=100% and 98%. Table 14 shows the corresponding Ω_c values. As shown in Fig. 49(a) and Table 14, decreasing inlet GVF from 100% to 98% increases Ω_c values (by more than 32%) and increases the magnitudes of negative C_{eff}, making the seal more destabilizing. As expected, increasing ω decreases C_{eff} and increases Ω_c, reducing the seal's effective damping force and making the seal less stabilizing.

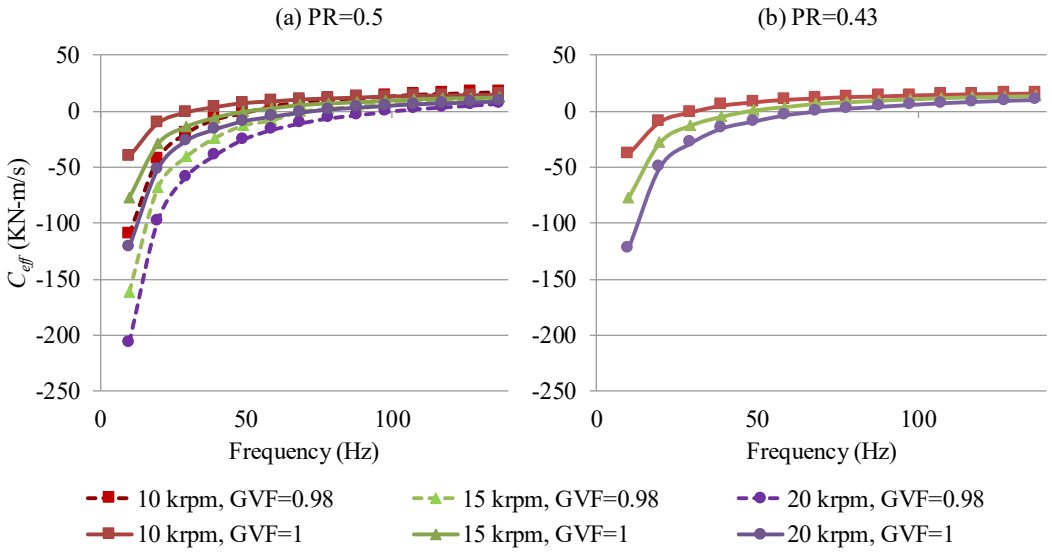

Figure 49. Measured C_{eff} at C_r=0.140 mm for (a) PR=0.5 and (b) PR=0.43

Rotor Speed ω (krpm)	Cross-over Frequency Ω_c (Hz)	
	Inlet GVF=100%	Inlet GVF=98%
10	29.7	51.6
15	53.8	71.0
20	73.0	107.6

Table 14. Ω_c values for pure- and mainly-air cases at PR=0.5 and C_r=0.140 mm

Figure 49 (b) shows C_{eff} at PR=0.43, C_r=0.140 mm, and inlet GVF=100%. Table 15 shows the corresponding Ω_c values. As expected, increasing ω decreases C_{eff} and increases Ω_c, making the seal less stabilizing.

Rotor Speed ω (krpm)	Cross-over Frequency Ω_c (Hz)
10	28.5
15	50.3
20	69.5

Table 15. Ω_c values for pure-air cases at PR=0.43 and C_r=0.140 mm

As shown in Tables 14 and 15, at pure-air conditions, changing PR from 0.5 to 0.43 barely changes Ω_c, producing negligible additional effects on rotor's stability in a centrifugal compressor.

As shown in Tables 12~15, increasing C_r from 0.140 to 0.188 mm decreases Ω_c values, making the rotor in a centrifugal compressor more stable. This outcome agrees with Kerr's [3] test results.

6.9 Cross-Coupled Damping

Figure 50 shows c versus inlet GVF for three PRs (rows), three C_r values (columns), and three ω values. Cross-coupled damping coefficients are close to zero, producing insignificant centering forces compared to K_Ω (the magnitude of $c\Omega/K_\Omega$ is about 6.9%). Note that as inlet GVF changes from 100% to 92%, c generally has its minimum value at inlet GVF=98%. This pattern is similar to the test results of Fig. 46, where $\bar{k}$ has its maximum value at inlet GVF=98%. A possible explanation for this similarity is that both $\bar{k}$ and c values are induced by the fluid's rotation within the seal annulus.

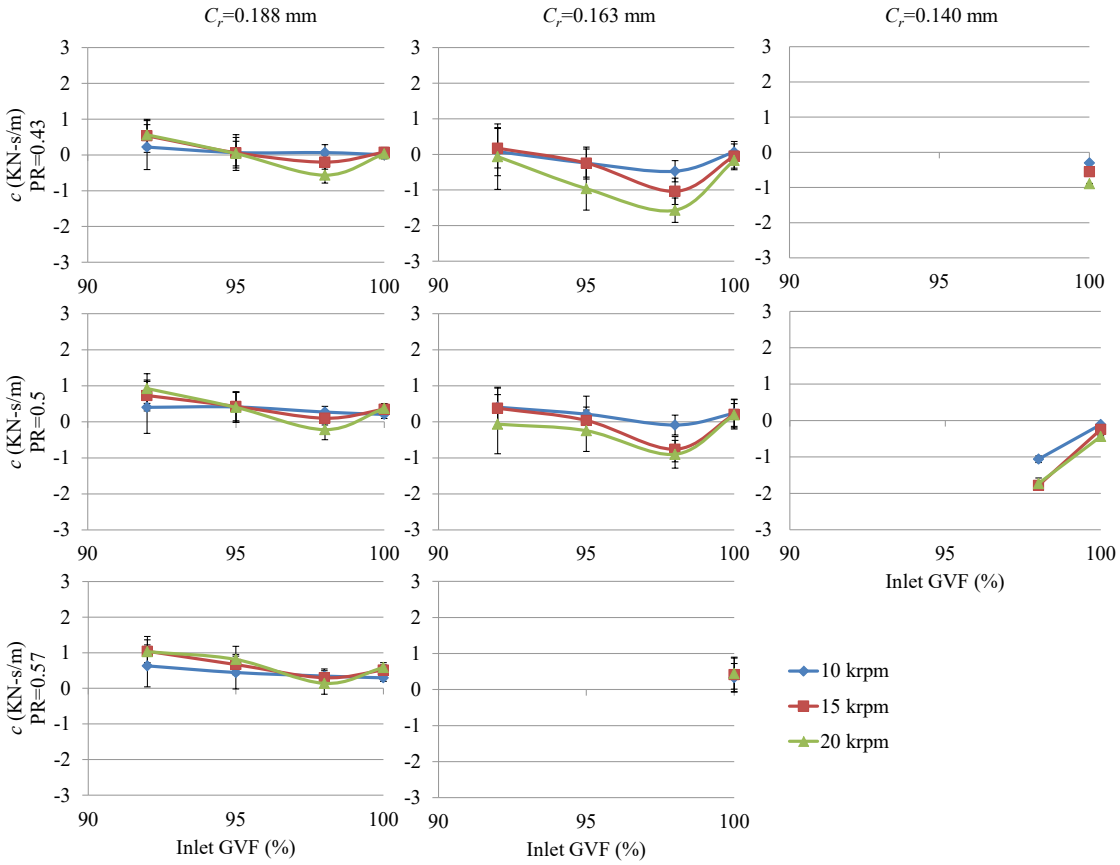

Figure 50. Measured *c* versus inlet GVF under pure- or mainly-air conditions

7. SUMMARY

This dissertation documents the development of a 2-phase annular-seal stand (2PASS) and presents test results for a set of long (length L=57.785 mm and length-to-diameter ratio L/D=0.65) smooth annular seals under 2-phase flow conditions using a mixture of air and silicone oil (PSF-5cSt). The effects of changes in inlet GVF, radial clearance (C_r), pressure drop/ratio (PD/PR), and rotor speed (ω) on the test seal's leakage mass flow rate $\dot{m}$ and rotordynamic coefficients are investigated. A model developed by San Andrés [6] produces predictions to compare with test results. Appendixes A and B show the comparison between measurements and predictions.

Due to the difficulties in making 2-phase homogeneous mixtures with a GVF between 10% and 92% and stator instabilities in some targeted test conditions, the resultant test matrix is divided into two sections: (1) pure- and mainly-oil conditions (inlet GVF≤10%) and (2) pure- and mainly-air conditions (92%≤inlet GVF≤100%). The summary for each section follows.

7.1 Pure- and Mainly-Oil Conditions

For tests under mainly-oil conditions, the flow within the seal annulus is predicted to transition from laminar to turbulent as C_r increases from 0.163 to 0.188 mm; i.e., the flow is predicted to be laminar when C_r=0.140 and 0.163 mm, and is predicted to become turbulent when C_r=0.188 mm. Note, in some C_r=0.188 mm cases, the transitional effects may still be evident; i.e., the flow may not be fully turbulent.

Test results show that the presence of the gas phase in the oil does not significantly change $\dot{m}$, but remarkably impacts the seal's rotordynamic performance. As inlet GVF increases from zero to 10%, $\dot{m}$ remains generally unchanged when C_r=0.188 mm, but slightly increases (by less than 8%) when C_r=0.163 and 0.140 mm.

The targeted test matrix was not completed due to stator instabilities. In the omitted cases, the stator experiences pronounced sub-synchronous vibrations. One possible explanation is that the seal's direct stiffness K becomes negative and lowers the stator's 1st natural frequency. This hypothesis suggests the sub-synchronous vibration occurs at the stator's 1st (rigid body) damped natural frequency. This hypothesis was not proved directly by measurements because

the seal's K cannot be measured in the omitted cases. However, the variation of K with changes in inlet GVF suggests that K should be negative in the omitted cases.

When C_r=0.188 mm, increasing inlet GVF from zero to 10% increases direct stiffness K for PD=31 and 37.9 bars. For PD=48.3 bars, K first increases as inlet GVF increases from zero to 6% and then drops when further increasing the inlet GVF to 10%. A possible explanation is that the transitional effects disappear (the flow becomes fully turbulent) when PD=48.3 bars and inlet GVF=6%, and this flow-status transition significantly affects the impact of changes in inlet GVF on K. In a centrifugal pump, the stiffness increment will increase the natural frequency of the pump's rotor and will increase the rotor's critical speed. Increasing the natural frequency of the rotor would also increase the onset speed of instability (OSI) and enhance the rotor's stability.

Effective damping C_{eff} is a measure of the seal's stabilizing capacity. When C_r=0.188 mm, increasing inlet GVF from zero to 10% barely changes C_{eff}, showing negligible effects on the seal's stabilizing force.

When C_r=0.140 and 0.163 mm, the trends of K and C_{eff} with changes in inlet GVF are different from and even contrary to the trends observed at C_r=0.188 mm; specifically, increasing inlet GVF generally decreases K, but increases C_{eff}. A possible reason for this difference is that the flow transitions from laminar to turbulent as C_r increases from 0.163 to 0.188 mm.

In regard to predictions, predicted $\dot{m}$ values are close to test results. However, the predicted and measured trends of $\dot{m}$ with changes in inlet GVF does not agree. As inlet GVF increases from zero to 10%, predicted $\dot{m}$ decreases (by up to 15%) for all three clearances, while measured $\dot{m}$ remains unchanged when C_r=0.188 mm and increases slightly (by less than 8%) when C_r=0.140 and 0.163 mm.

For most cases, predicted and measured K values are not close. All predicted K values are positive; measured K values are negative at some test conditions. This discrepancy would mean that the critical speed of the rotor in a pump would be lower than predicted. When C_r=0.188 mm, predicted K always decreases with increasing inlet GVF for all PDs. This predicted trend only agrees with test results when PD=48.3 bars and 6%≤inlet GVF≤10%. For all other C_r=0.188 mm cases, increasing inlet GVF increases measured K. A possible explanation for this discrepancy is that for all C_r=0.188 mm cases, except the cases with PD=48.3 bars and 6%≤inlet GVF≤10%, the transitional effects might still be evident; i.e., the flow is not fully turbulent. When C_r=0.163 or 0.140 mm, increasing inlet GVF decreases predicted K, which agrees with measurements.

C_{eff} predictions are reasonably close to test results. For all three clearances, changing inlet GVF has little effect on predicted C_{eff}. This predicted trend agrees with test results when C_r=0.188 mm, but not for C_r=0.163 or 0.140 mm, where increasing inlet GVF generally increases measured C_{eff}.

Since the flow may not be fully turbulent in some C_r=0.188 mm cases, further tests of smooth seals with larger clearances, lower oil viscosity, or higher rotating speeds are needed to have a better understanding of the rotordynamic characteristics of smooth annulus seals under fully-turbulent mainly-oil conditions. Further tests of smooth seals with shorter lengths are also recommended.

7.2 Pure- and Mainly-Air Conditions

For tests under pure- and mainly-air conditions, the inlet GVF changes from 100% to 92%, which covers the expected range for wet-gas compression.

Test results show a remarkable impact of the oil presence in the air flow. $\dot{m}$ decreases slightly (by less than 6%) as inlet GVF drops from 100% to 98%, and then increases (by about 45%) as inlet GVF further decreases to 92%. This outcome indicates that as inlet GVF decreases to 98%, the increase in the fluid's effective viscosity dominates $\dot{m}$, but as inlet GVF further drops to 92%, the increase in the fluid's effective density dominates. Increasing the fluid's effective viscosity can decrease $\dot{m}$, while increasing the fluid's effective density can increase $\dot{m}$. Predicted $\dot{m}$ values correlate well with test results.

For the present smooth seal with pure-air and mainly-air mixtures, frequency-dependent behavior forced the usage of frequency-dependent direct K_Ω and cross-coupled k_Ω stiffness coefficients. The imaginary components of the dynamic-stiffness coefficients could be fitted with frequency-independent direct C and cross-coupled c damping coefficients.

K_Ω is identical to the seal's effective centering force since c produces insignificant centering force compared to K_Ω (the magnitude of $c\Omega/K_\Omega$ is about 6.9%). All K_Ω values are positive, applying positive centering forces on the rotor. Under pure-air conditions, increasing excitation frequency Ω does not change K_Ω when PR=0.57 but increases K_Ω when PR=0.5 and 0.43. This outcome agrees with Kerr's [3] measurements, where K_Ω increases as Ω increases (stiffening effect), and the stiffening effect becomes more pronounced as PR decreases. Adding oil into the air flow makes K_Ω increase more rapidly with increasing Ω. Also, decreasing inlet

GVF from 100% to 92% generally decreases K_Ω except that K_Ω increases as inlet GVF decreases from 100% to 98% in the following circumstances: (1) cases with PR=0.43 and C_r=0.188 mm, and (2) the case with PR=0.43, ω=20 krpm, and C_r=0.163 mm. In a centrifugal compressor, decreasing the seal's K_Ω would decrease the rotor's natural frequency and decrease the rotor's critical speed. Dropping the rotor's natural frequency would also decrease the rotor's stability.

$k_\Omega(\Omega)$ is fluctuating around the average value $\bar{k}$. Since the fluctuation level is small compared to $\bar{k}$'s magnitude, $\bar{k}$ is used to describe the test seal's cross-coupled stiffness. $\bar{k}$ increases significantly (by a factor of about 2) as inlet GVF drops from 100% to 98%, but decreases (by less than 35.8%) with further drops in inlet GVF to 92%. Therefore, the initial increment of injected oil (decreasing inlet GVF to 98%) significantly increases the seal's destabilizing force, but further increments of injected oil (decreasing inlet GVF further to 92%) reduces the seal's destabilizing force.

As with Kerr's test data [3] for a smooth seal tested in air, C is insensitive to changes in ω at pure-air conditions. This tendency continues after adding oil into the air flow. C increases by 15%~41% as inlet GVF decreases from 100% to 98% and then remains generally unchanged with further decreases in inlet GVF. Therefore, decreasing inlet GVF from 100% to 98% increases the seal's damping force, but further decreases in inlet GVF to 92% have negligible effects on the seal's damping characteristics.

C_{eff} combines the destabilizing effect of k_Ω and the stabilizing effect of C. At low Ω values, k_Ω dominates C_{eff}, and C_{eff} values are negative (destabilizing). As Ω increases, C_{eff} changes from negative to positive at Ω_c (the cross-over frequency). Ω_c has a considerable impact on the system stability. Decreasing inlet GVF from 100% to 98% increases Ω_c values (become more destabilizing), but further decreases of inlet GVF to 92% decrease Ω_c values (become less destabilizing). In general, as oil enters the air stream, Ω_c increases and the seal becomes more destabilizing. This outcome explains the observation from Vannini et al. [10] that injecting liquid directly into the labyrinth seals of a centrifugal compressor could cause sub-synchronous vibrations. Also, as C_r increases from 0.140 to 0.188 mm, Ω_c decreases, and the seal become more stabilizing.

In regard to preidcitons, predicted K_Ω values are close to test results only under pure-air conditions when PR=0.5 and 0.57. For all other test conditions, K_Ω predictions are larger than measured, and the discrepancy decreases as Ω increases due to the frequency dependence of measured K_Ω. In a centrifugal compressor, this discrepancy would mean that the rotor's critical

speed would be lower than predicted. Predicted K_Ω decreases slightly (by less than 7.1%) as Ω increases from 10 to 140 Hz while measured K_Ω generally increases. For all clearances, predicted K_Ω decreases as inlet GVF drops from 100% to 92%. This predicted trend generally agrees with measurements.

Average cross-coupled stiffness $\bar{k}$ predictions are close to test results when inlet GVF=100% and 95%, are about 34% smaller than measurements when inlet GVF=98%, and are around 40% larger than measured results when inlet GVF=92%. Therefore, in regard to $\bar{k}$, the seal is more destabilizing than predicted when inlet GVF=98%, but less destabilizing when inlet GVF=92%. Both predicted and measured $\bar{k}$ values increase significantly as inlet GVF decreases from 100% to 98%. As inlet GVF further decreases to 92%, predicted $\bar{k}$ continues increasing while measured $\bar{k}$ decreases. Therefore, as inlet GVF decreases from 98% to 92%, although predictions show that the seal's destabilizing force increases, the seal's actual destabilizing force decreases.

Predicted cross-over frequency Ω_c values are close to measurements when inlet GVF=100% and 98%. When inlet GVF=95% and 92%, Ω_c predictions are larger than measurements by more than 37.1%. Therefore, when inlet GVF=95% and 92%, the seal is more stabilizing than predicted. Predicted Ω_c increases as inlet GVF decreases from 100% to 92%, while measured Ω_c first increases as inlet GVF decreases from 100% to 98%, and then decreases as inlet GVF drops further to 92%. As with test results, increasing C_r from 0.140 to 0.188 mm decreases predicted Ω_c and makes the seal more stabilizing.

Measurements and predictions under pure- and mainly-air conditions lead to the following major conclusions:

(1) Injecting oil into the air flow increases Ω_c, making the seal more destabilizing.

(2) Increasing C_r from 0.140 to 0.188 mm decreases Ω_c and makes the seal more stabilizing. However, an immediate disadvantage is that $\dot{m}$ increases significantly (by about 58%) as C_r increases from 0.140 to 0.188 mm.

(3) The seal's centering force as generated by the effective-stiffness coefficient generally decreases with decreasing inlet GVF from 100% to 92% except that it increases as inlet GVF decreases from 100% to 98% in the following circumstances: (1) cases with PR=0.43 and C_r=0.188 mm, and (2) the case with PR=0.43, ω=20 krpm, and C_r=0.163 mm. For a centrifugal compressor, decreasing the seal's

centering force would decrease the rotor's critical speed, reduce the onset speed of instability, and decrease the rotor's stability.

As previously noted, smooth seals are never used in centrifugal compressors, the test data presented here are sorely needed to examine the correctness of the predictive model [6], and the test of smooth seals is a just a starting place. Further testing of different seal types, such as labyrinth seals, hole-pattern seals, and honeycomb seals, is recommended to fully understand their behavior under mainly-gas conditions and to help the design of centrifugal compressors.

REFERENCES

[1] Childs, D., 1983, "Finite-Length Solutions for Rotordynamic Coefficients of Turbulent Annular Seals," ASME J. Tribol., **105**(3), pp. 437-444.

[2] Marquette, O. R., Childs, D. W., and San Andres, L., 1997, "Eccentricity Effects on the Rotordynamic Coefficients of Plain Annular Seals: Theory Versus Experiment," ASME J. Tribol., **119**(3), pp. 443-447.

[3] Kerr, B., 2004, "Experimental and Theoretical Rotordynamic Coefficients and Leakage of Straight Smooth Annular Gas Seals," Master thesis, Texas A&M University, College Station, TX.

[4] Ransom, D., Podesta, L., Camatti, M., Wilcox, M., Bertoneri, M., and Bigi, M., 2011, "Mechanical Performance of a Two Stage Centrifugal Compressor under Wet Gas Conditions," Proc. 40th Turbomachinery Symposium, Houston, TX.

[5] Brenne, L., Bjørge, T., Gilarranz, J. L., Koch, J., and Miller, H., 2005, "Performance Evaluation of a Centrifugal Compressor Operating under Wet-Gas Conditions," Proc. 34th Turbomachinery Symposium, Houston, TX, pp. 111-120.

[6] San Andrés, L., 2011, "Rotordynamic Force Coefficients of Bubbly Mixture Annular Pressure Seals," ASME J. Eng. Gas Turbines Power, **134**(2), p. 022503.

[7] Vannini, G., Bertoneri, M., Del Vescovo, G., and Wilcox, M., 2014, "Centrifugal Compressor Rotordynamics in Wet Gas Conditions," Proc. 43rd Turbomachinery Symposium, Houston, TX.

[8] Griffin, T., and Maier, W., 2011, "Demonstration of the Rotordynamic Effects of Centrifugal Liquid Separation and Gas Compression in an Oil-Free Integrated Motor-Compressor," Proc. 40th Turbomachinery Symposium, Houston, TX.

[9] Bertoneri, M., Wilcox, M., Toni, L., and Beck, G., 2014, "Development of Test Stand for Measuring Aerodynamic, Erosion, and Rotordynamic Performance of a Centrifugal Compressor Under Wet Gas Conditions," Proc. ASME Turbo Expo 2014, American Society of Mechanical Engineers, Düsseldorf, Germany.

[10] Vannini, G., Bertoneri, M., Nielsen, K. K., Iudiciani, P., and Stronach, R., 2015, "Experimental Results and CFD Simulations of Labyrinth and Pocket Damper Seals for Wet Gas Compression," Proc. ASME Turbo Expo 2015, American Society of Mechanical Engineers, Montreal, Quebec, Canada.

[11] Bibet, P. J., Klepsvik, K. H., Lumpkin, V. A., and Grimstad, H., 2013, "Design and Verification Testing of a New Balance Piston for High Boost Multiphase Pumps," Proc. 29th International Pump User Symposium, Houston, TX.

[12] Beatty, P., and Hughes, W., 1987, "Turbulent Two-Phase Flow in Annular Seals," ASLE Trans., **30**(1), pp. 11-18.

[13] Hughes, W. F., and Beeler, R. M., 1981, "Turbulent Two-Phase Flow in Ring and Face Seals," Proc. 9th International Conference on Fluid Sealing, Noordwijkerhout, Netherlands, pp. 185-202.

[14] Beatty, P., and Hughes, W., 1990, "Stratified Two-Phase Flow in Annular Seals," ASME J. Tribol., **112**(2), pp. 372-381.

[15] Hendricks, R. C., 1987, "Straight Cylindrical Seal for High-Performance Turbomachines," No. NASA-TP-1850, NASA Lewis Research Center, Cleveland, OH.

[16] Arauz, G. L., and San Andrés, L., 1998, "Analysis of Two-Phase Flow in Cryogenic Damper Seals—Part I: Theoretical Model," ASME J. Tribol., **120**(2), pp. 221-227.

[17] Arauz, G. L., and San Andrés, L., 1998, "Analysis of Two-Phase Flow in Cryogenic Damper Seals—Part II: Model Validation and Predictions," ASME J. Tribol., **120**(2), pp. 228-233.

[18] Oike, M., Nosaka, M., Kikuchi, M., and Hasegawa, S., 1999, "Two-Phase Flow in Floating-Ring Seals for Cryogenic Turbopumps," Tribol. Trans., **42**(2), pp. 273-281.

[19] Hassini, M. A., and Arghir, M., 2013, "Phase Change and Choked Flow Effects on Rotordynamic Coefficients of Cryogenic Annular Seals," ASME J. Tribol., **135**(4), p. 042201.

[20] Salhi, A., Rey, C., and Rosant, J. M., 1992, "Pressure Drop in Single-Phase and Two-Phase Couette-Poiseuille Flow," ASME J. Fluids Eng., **114**(1), pp. 80-84.

[21] Iwatsubo, T., and Nishino, T., 1994, "An Experimental Study on the Static and Dynamic Characteristics of Pump Annular Seals with Two Phase Flow," Proc. Rotordynamic Instability Problems in High-Performance Turbomachinery, pp. 49-64.

[22] Arghir, M., Zerarka, A., and Pineau, G., 2011, "Rotordynamic Analysis of Textured Annular Seals With Multiphase (Bubbly) Flow," Incas Bulletin, **3**(3), pp. 3-13.

[23] Kleynhans, G., and Childs, D., 1997, "The Acoustic Influence of Cell Depth on the Rotordynamic Characteristics of Smooth-Rotor/Honeycomb-Stator Annular Gas Seals," ASME J. Eng. Gas Turbines Power, **119**(4), pp. 949-956.

[24] San Andrés, L., Lu, X., and Liu, Q., 2015, "Measurements of Flowrate and Force Coefficients in a Short Length Annular Seal Supplied with a Liquid/Gas Mixture (Stationary Journal)," Tribol. Trans., **59**(4), pp. 758-767.

[25] San Andrés, L., and Lu, X., 2017, "Leakage, Drag Power, and Rotordynamic Force Coefficients of an Air in Oil (Wet) Annular Seal," ASME J. Eng. Gas Turbines Power, **140**(1), p. 012505.

[26] Childs, D., McLean, J., Zhang, M., and Arthur, S., 2015, "Rotordynamic Performance of a Negative-Swirl Brake for a Tooth-on-Stator Labyrinth Seal," ASME J. Eng. Gas Turbines Power, **138**(6), p. 062505.

[27] Zhang, M., McLean, J., and Childs, D., 2017, "Experimental Study of the Static and Dynamic Characteristics of a Long Smooth Seal with Two-Phase, Mainly-Air Mixtures," ASME J. Eng. Gas Turbines Power, **139**(12), p. 122504.

[28] Bracco, F., 1985, "Modeling of Engine Sprays," No. 850394, SAE Technical Paper, Warrendale, PA.

[29] Picardo, A., and Childs, D., 2004, "Rotordynamic Coefficients for a Tooth-on-Stator Labyrinth Seal at 70 Bar Supply Pressures: Measurements Versus Theory and Comparisons to a Hole-Pattern Stator Seal," ASME J. Eng. Gas Turbines Power, **127**(4), pp. 843-855.

[30] Mehta, N., and Childs, D., 2013, "Measured Comparison of Leakage and Rotordynamic Characteristics for a Slanted-Tooth and a Straight-Tooth Labyrinth Seal," ASME J. Eng. Gas Turbines Power, **136**(1), p. 012501.

[31] Kurtin, K. A., Childs, D., San Andres, L., and Hale, K., 1993, "Experimental Versus Theoretical Characteristics of a High-Speed Hybrid (Combination Hydrostatic and Hydrodynamic) Bearing," ASME J. Tribol., **115**(1), pp. 160-168.

[32] Clearco Products Co., "Low Viscosity Pure Silicone Fluids," http://www.clearcoproducts.com/pure-silicone-low-viscosity.html (accessed May 20, 2017).

[33] Clearco Products Co., "Rheological Behavior of Silicone Fluids under Shear," http://www.clearcoproducts.com/pdf/library/Shear-Rhealogical.pdf (accessed May 20, 2017).

[34] Clearco Products Co., "PSF-5cSt Pure Silicone Fluid," http://www.clearcoproducts.com/pdf/low-viscosity/NP-PSF-5cSt.pdf (accessed May 20, 2017).

[35] Tao, L., Diaz, S., San Andrés, L., and Rajagopal, K. R., 1999, "Analysis of Squeeze Film Dampers Operating With Bubbly Lubricants," ASME J. Tribol., **122**(1), pp. 205-210.

[36] Diaz, S., 1999, "The Effect of Air Entrapment on the Performance of Squeeze Film Dampers: Experiments and Analysis," Ph.D dissertation, Texas A&M University, College Station, TX.

[37] Fourar, M., and Bories, S., 1995, "Experimental study of air-water two-phase flow through a fracture (narrow channel)," Int. J. Multiphase Flow, **21**(4), pp. 621-637.

[38] Stanway, R., Burrows, C., and Holmes, R., 1979, "Pseudo-Random Binary Sequence Forcing in Journal and Squeeze-Film Bearings," ASLE Trans., **22**(4), pp. 315-322.

[39] Cornish, R. J., 1933, "Flow of Water through Fine Clearances with Relative Motion of the Boundaries," Proceedings of the Royal Society of London. Series A, Containing Papers of a Mathematical and Physical Character, **140**(840), pp. 227-240.

[40] Yamada, Y., 1962, "Resistance of a Flow Through an Annulus with an Inner Rotating Cylinder," Bulletin of JSME, **5**(18), pp. 302-310.

[41] Jolly, P., Hassini, A., Arghir, M., and Bonneau, O., 2014, "Experimental and Theoretical Rotordynamic Coefficients of Smooth and Round-Hole Pattern Water Fed Annular Seals," Proc. ASME Turbo Expo 2014, American Society of Mechanical Engineers, Düsseldorf, Germany.

[42] Soulas, T., and Andres, L. S., 2007, "A Bulk Flow Model for Off-Centered Honeycomb Gas Seals," ASME J. Eng. Gas Turbines Power, **129**(1), pp. 185-194.

[43] San Andres, L., 2010, "Notes 12(a). Annular Pressure Seals," Modern Lubrication Theory, Texas A&M University Digital Libraries, College Station, TX.

[44] Kleynhans, G., 1991, "A Comparison of Experimental Results and Theoretical Predictions for the Rotordynamic and Leakage Characteristics of Short (L/D=1/6) Honeycomb and Smooth Annular Pressure Seals," Master thesis, Texas A&M University, College Station, TX.

[45] Zirkelback, N., and San Andres, L., 1996, "Bulk-Flow Model for the Transition to Turbulence Regime in Annular Pressure Seals," Tribol. Trans., **39**(4), pp. 835-842.

[46] Childs, D. W., Rodriguez, L. E., Cullotta, V., Al-Ghasem, A., and Graviss, M., 2005, "Rotordynamic-Coefficients and Static (Equilibrium Loci and Leakage) Characteristics for Short, Laminar-Flow Annular Seals," ASME J. Tribol., **128**(2), pp. 378-387.

[47] Delgado-Marquez, A., 2008, "A Linear Fluid Inertia Model for Improved Prediction of Force Coefficients in Grooved Squeeze Film Dampers and Grooved Oil Seal Rings," Ph.D dissertation, Texas A&M University, College Station, TX.

[48] Kleynhans, G. F., 1996, "A Two-Control-Volume Bulk-Flow Rotordynamic Analysis for Smooth-Rotor/Honeycomb-Stator Gas Annular Seals," Ph.D dissertation, Texas A&M University, College Station, TX.

APPENDIX A

This section compares the test results previously presented and discussed in Sec. 5 to predictions from a program developed by San Andrés [6] based on a bulk-flow model and the Moody friction model, assuming the fluid within the seal annulus is a homogeneous mixture with a constant temperature. Besides the operating conditions (inlet GVF, ω, PD, and C_r values) shown in Table 6 and $u_0(0)$ values shown in Table 7, Table 16 shows other input variables needed for predictions.

Variable	Value	Unit
Diameter, D	88.9	mm
Axial Length, L	57.8	mm
Entrance Pressure Loss Factor	0.2	-
Exit pressure Recovery Factor	0	-
Seal Inlet Temperature	39.4	°C
Seal Exit Pressure, P_e	6.9	bars
Liquid Properties		
Viscosity, μ_l	3.83	cP
Density, ρ_l	899.4	kg/m^3
Bulk-Modulus	9987	bars
Surface Tension/Length	0.0197	N/m
Liquid Vapor Pressure	0.001	bars
Gas Properties		
Gas Constant	286.90	J/kg-C
Compressibility	1.00	-
Gas Viscosity, μ_g	1.82E-02	cP
Ratio of the Specific Heat	1.40	-

Table 16. Input variables needed for predictions at pure- and mainly-oil conditions

Before presenting comparisons between predictions and measurements for pure- and mainly-oil conditions, the following differences between the predictive model and experiment need to be noted:

(1) The model assumes that the fluid's temperature remains constant in the seal clearance; however, the fluid's actual/measured temperature increases as the fluid flows through the seal due to power dissipation. The temperature increment decreases as inlet GVF increases from zero to 10%. Table 19 in Appendix C shows the fluid's measured temperatures at the seal inlet and seal exit.

(2) The model assumes that the mixture is homogeneous in the seal clearance while the reality may be different. Although the mixture was visually inspected through a sight-glass view port shortly upstream of the inlet ports of the stator, the mixture might not remain homogeneous in the seal clearance due to the bubble coalescence and centrifugal-inertia effects. The coalescence of fine bubbles could make larger bubbles with diameters larger than the seal clearance. The centrifugal-inertia effect could drive the oil phase outward to the seal surface, with the air phase staying close to the shaft; i.e., the centrifugal inertia effect could lead to a stratified-flow.

(3) As noted in Sec. 5.2, the flow is judged to be laminar when C_r=0.140 and 0.163 mm and turbulent when C_r=0.188 mm. For most C_r=0.188 mm cases, the transitional effects might still be evident. Different from the method described in Sec. 5.2, the model [6] uses another way to determine the flow status. The model treats the flow as laminar when Re_r (or Re_s)<1000, as transitional when 1000<Re_r (or Re_s)<3000, and as fully turbulent when Re_r (or Re_s)>3000 [45]. Since the flow transitions from laminar to turbulent as C_r increases, the code may not predict the flow status correctly.

A.1 Leakage Mass Flow Rate

Figure 51 compares predicted and measured $\dot{m}$ versus inlet GVF for a range of ω, C_r, and PD values. As expected, both predicted and measured $\dot{m}$ values increase as PD or C_r increase for all clearances.

When C_r=0.188 mm, predicted $\dot{m}$ values are larger (by up to 28%) than test results at pure-oil conditions. Since predicted $\dot{m}$ drops as inlet GVF increases while measured $\dot{m}$ is

invariant with changes in inlet GVF, predicted $\dot{m}$ becomes close to measured and even become smaller than measured as inlet GVF increases. Increasing ω from 5 to 15 krpm decreases predicted $\dot{m}$. This predicted pattern agrees with test results.

For C_r=0.140 and 0.163 mm, $\dot{m}$ predictions agree with measurements at pure-oil conditions. Prediction become worse as inlet GVF increases because, as inlet GVF increases, predicted $\dot{m}$ drops slightly (by less than 12%) versus measured $\dot{m}$ that increases slightly (by less than 8%). Under mainly-oil conditions, predicted $\dot{m}$ values are smaller (by up to 19%) than measured. Changing ω has little effect on predicted $\dot{m}$. This predicted trend agrees with measurements.

As inlet GVF increases from zero to 10%, predicted $\dot{m}$ decreases (by up to 15%) for all three clearances, while measured $\dot{m}$ remains generally unchanged when C_r=0.188 mm and increases slightly (by less than 8%) when C_r=0.140 and 0.163 mm. Both effective viscosity and effective density decrease as inlet GVF increases. Decreasing effective viscosity can increase $\dot{m}$, while decreasing effective density can decrease $\dot{m}$. Therefore, the decreases in predicted $\dot{m}$ for all clearances as inlet GVF increases indicate that the decrease in effective density has more impact than the decrease in effective viscosity, while the negligible changes in measured $\dot{m}$ when C_r=0.188 mm indicate that the decrease in effective viscosity and the decrease in effective density have close but opposite effects. The increases in measured $\dot{m}$ when C_r=0.140 and 0.163 mm imply that the decrease in effective viscosity has slightly more impact than the decrease in effective density.

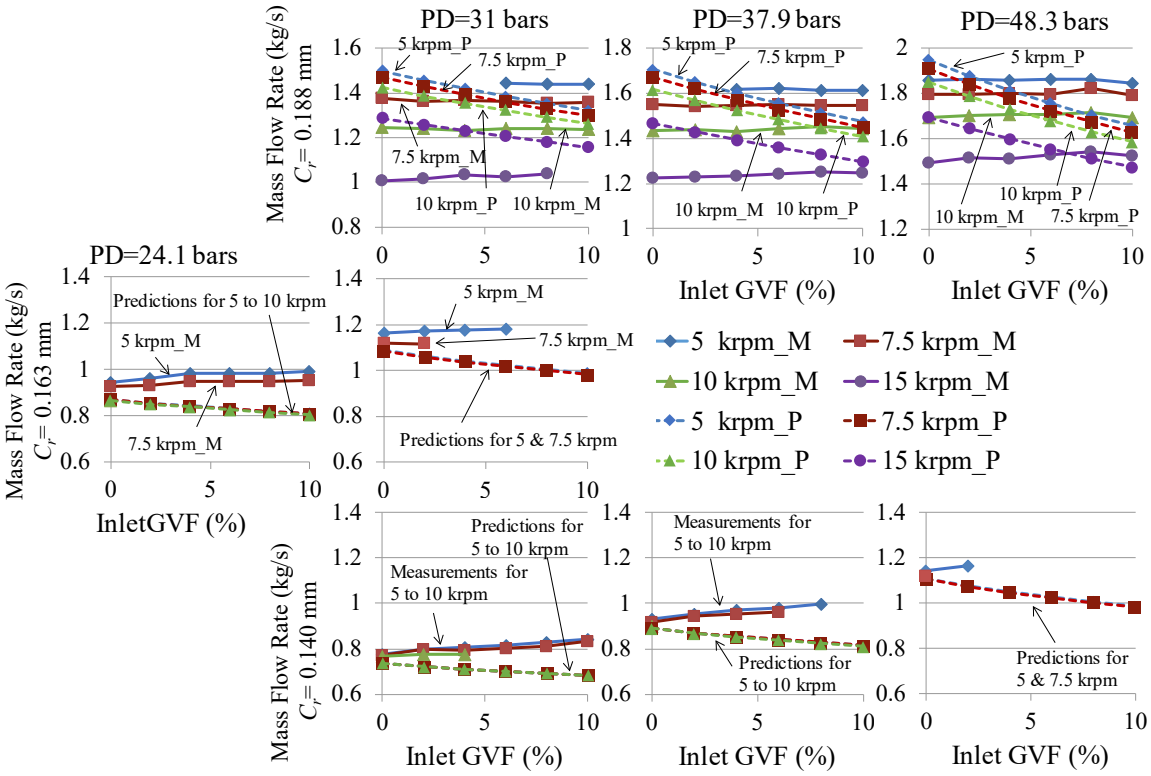

Figure 51. Predictions and measurements of $\dot{m}$ under pure- and mainly-oil conditions

A.2 Direct Stiffness

Figure 52 compares predicted and measured K versus inlet GVF for a range of ω, C_r, and PD values.

When C_r=0.188 mm, predicted K decreases with increasing inlet GVF. This trend only agrees with test results when PD=48.3 bars and 6%≤inlet GVF≤10%. For other conditions, the predicted effects of changes in inlet GVF are contrary to measurements because measured K increases with increasing inlet GVF. Predicted K generally decreases as ω increases, especially at low inlet GVFs. This predicted trend is contrary to measurements since measured K generally increases with increasing ω.

In summary, for most C_r=0.188 mm cases, the predicted effects of changes in inlet GVF and ω on K are contrary to measurements. A possible explanation for this (as previously noted in Sec. 5.4) is that the transitional effects might still be evident in these cases.

When C_r=0.163 and 0.140 mm, predicted K decreases as inlet GVF increases. This predicted trend agrees with measurements. As with measurements, predicted K decreases as ω increases but at a much slower rate.

Concerning the effects of increasing C_r from 0.140 to 0.163 mm, when PD=31 bars and ω=5 and 7.5 krpm, predicted K does not change discernibly, but the actual K decreases significantly.

For most cases, predicted and measured K values are not close. All predicted K values are positive; measured K values are negative at some test conditions. In a centrifugal pump, the prediction accuracy of the seal's K can affect the prediction accuracy of the rotor's natural frequency. If predicted K is smaller (or larger) than the seal's actual K, the rotor's actual natural frequency will be larger (or smaller) than the predicted natural frequency. A poorly predicted natural frequency means OSI and critical speeds are also poorly predicted.

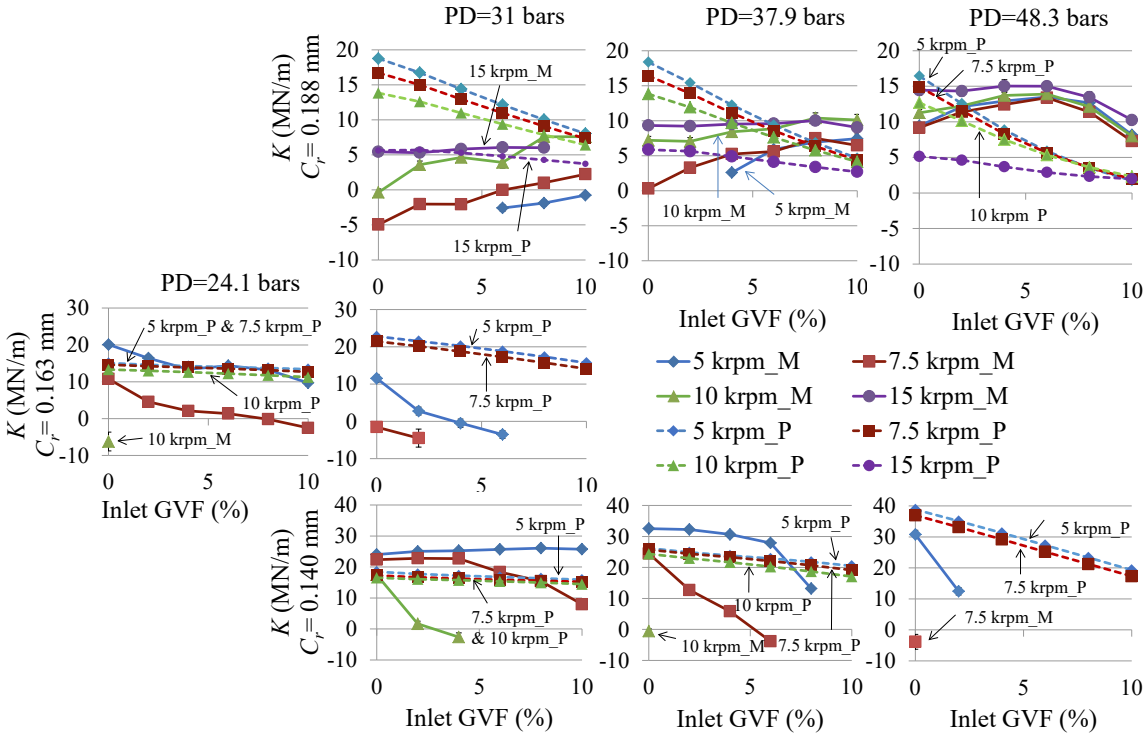

Figure 52. Predictions and measurements of K under pure- and mainly-oil conditions

A.3 Cross-Coupled Stiffness

Figure 53 compares measured and predicted k versus inlet GVF for a range of ω, C_r, and PD values. As expected, both predicted and measured k values increase as ω increases.

In regard to the effects of changes in inlet GVF, when C_r=0.188 mm, increasing inlet GVF from zero to 10% has little effect on predicted k. This predicted trend agrees with measurements. For C_r=0.163 and 0.140 mm, as inlet GVF increases, predicted k remains almost unchanged while measured k generally increases. Hence at C_r=0.163 and 0.140 mm, although predictions show that increasing inlet GVF has negligible effects on the seal's destabilizing force, the seal's actual destabilizing force increases as inlet GVF increases.

When C_r=0.188 mm, predicted k values are close to test results when PD=31 and 37.9 bars and ω=5 and 7.5 krpm. At higher PD (48.3 bars) or higher ω values (10 and 15 krpm), predicted k values are larger than measured, and the discrepancy increases as PD increases because predicted k increases while measured k remains unchanged. For example, when PD=48.3 bars and ω=10 krpm, predicted k values are about 2.2 times as large as measured k values. When the predicted k is larger than the actual k, the seal's actual destabilizing force is smaller than predicted.

When C_r=0.163 and 0.140 mm, predicted k is invariant to changes in PD, which differs from measurements because measured k generally increases as PD increases. For C_r=0.163 mm, k predictions are reasonably close to test results at PD=24.1 bars and ω=5 krpm. For all other cases at C_r=0.163 mm, predicted k values are about 50% of test results. For most cases at C_r=0.140 mm, k predictions are not close to test results.

Also, predictions do not show the significant increases in k (by at least 52.7%) as C_r increases from 0.140 to 0.163 mm when PD=31 bars and ω=5 and 7.5 krpm. Instead, the corresponding predicted value of k decreases by about 50%. When PD=31 bars, ω=7.5 krpm, and inlet GVF≤2%, as C_r increases from 0.163 to 0.188 mm, predicted k increases slightly by 7.8% while measured k decreases by about 44%.

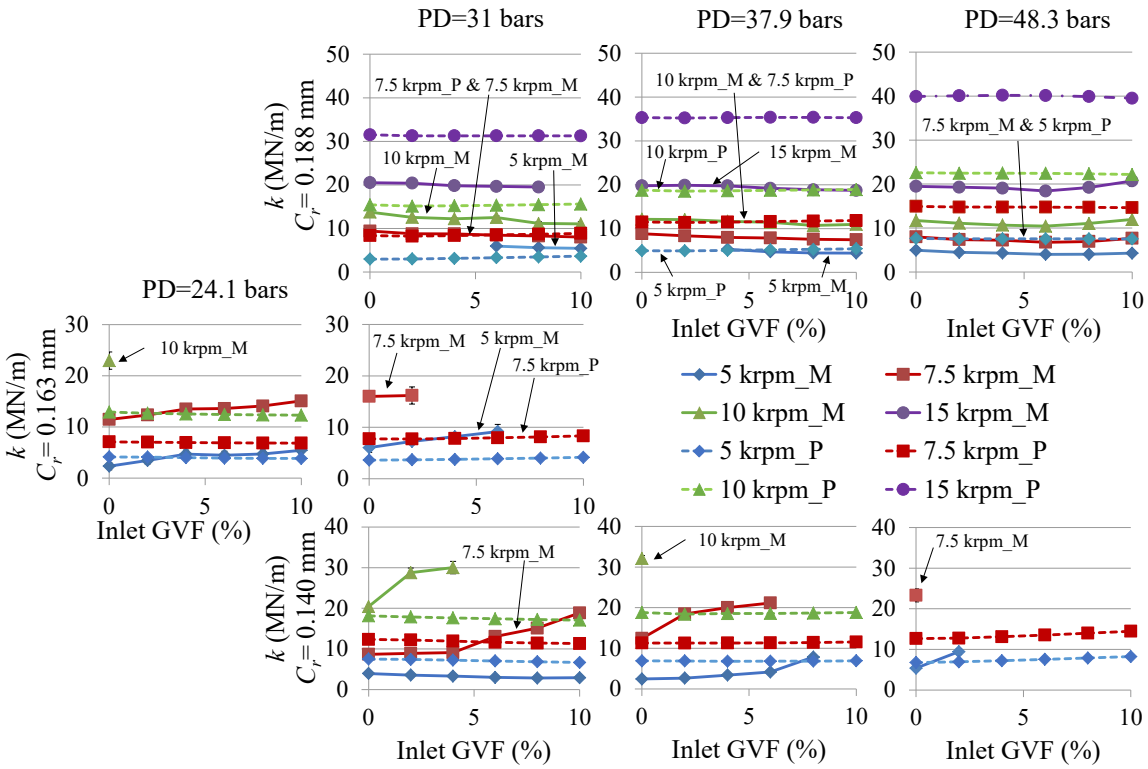

Figure 53. Predictions and measurements of *k* under pure- and mainly-oil conditions

A.4 Direct Damping

Figure 54 compares measured and predicted *C* versus inlet GVF for a range of ω, C_r, and PD values. For all clearances, *C* predictions reasonably correlate with test results, and they are 61.6%~134.4% of measured results. Predictions generally become better as PD decreases.

The code predicts the trends with changes in PD and ω; specifically, both predicted and measured *C* values increase as PD increases for all clearances, remain almost unchanged as ω increases when C_r=0.188 mm, and generally increase with increasing ω when C_r=0.163 and 0.140 mm.

Concerning the effects of changes in inlet GVF, increasing inlet GVF barely changes predicted *C* when C_r=0.188 mm. This predicted trend agrees with test results. When C_r=0.163 and 0.140 mm, predicted *C* remains insensitive to changes in inlet GVF, whereas, measured *C* generally increases as inlet GVF increases. Due to this disagreement, when C_r=0.163 and 0.140 mm, predictions generally become worse as inlet GVF increases.

When ω=5 and 7.5 krpm and PD=31 bars, predicted C decreases by about 15% as C_r increases from 0.140 to 0.163 mm, while the seal's measured C increases (by 14.7%~42.1%). When 7.5 krpm and PD=31 bars, as C_r increases further to 0.188 mm, predicted C remains almost unchanged while the seal's measured C decreases by about 26%.

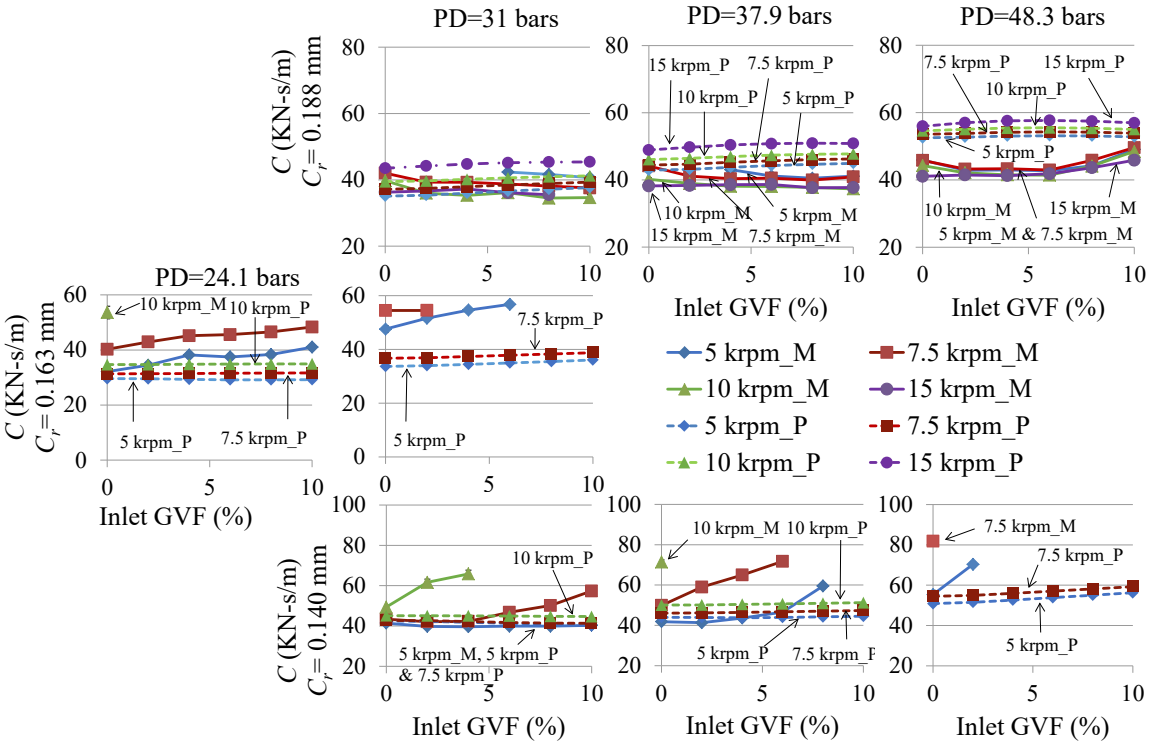

Figure 54. Predictions and measurements of C under pure- and mainly-oil conditions

A.5 Cross-Coupled Damping

Figure 55 compares measured and predicted c versus inlet GVF for a range of ω, C_r, and PD values.

When C_r=0.188 mm, predicted c values are close to measurements at ω=5 krpm. For other speeds at this clearance, predictions agree with test results under pure-oil conditions, but not at mainly-oil conditions, where predictions are generally smaller than test results. For ω>5 krpm, predictions generally become worse as inlet GVF increases because predicted c decreases as inlet GVF increases while measured c decreases at a slower rate at high ω and PD values and

remains unchanged at low ω and PD values. Under pure-oil conditions, predicted c increases as ω increases, which agrees with measurements. As inlet GVF increases, the predicted rate of increase of c with respect to increasing ω decreases significantly and becomes negligible when inlet GVF=10%. This predicted trend is different from measurements because measured c remains strongly dependent on changes in ω as inlet GVF increases from zero to 10%. Predicted c remains generally unchanged as PD increases, which agrees with test results.

When C_r=0.163 mm, c predictions agree with measurements when ω=5 and 7.5 krpm and PD=24.1 bars. For all other cases at this clearance, predicted c values are larger than measured, and the discrepancy increases as PD increases since predicted c is invariant with changes in PD while measured c decreases as PD increases. Predictions generally become worse as ω increases because predicted c increases as ω increases while measured c is not sensitive to changes in ω. When C_r=0.140 mm, there is no clear correlation between predictions and test results, and predicted c could be larger or smaller than measured c. When C_r=0.163 and 0.140 mm, predicted c decreases as inlet GVF increases. This predicted trend agrees with measurements.

Concerning the effects of changes in C_r, as C_r increases from 0.140 to 0.163 mm when PD=31 bars and ω=5 and 7.5 krpm, predicted c barely changes, whereas measured c decreases significantly (by more than 50%). As C_r further increases to 0.188 mm when ω=7.5 krpm and inlet GVF≤2%, predicted c decreases by about 23% while measured c almost doubles.

In general, all predicted and measured c values are positive except at C_r=0.140 mm, PD=48.3 bars, ω=7.5 krpm, and inlet GVF=0%, where the magnitude of the small negative measured c is near the same order as the uncertainty. When c>0, it produces additional centering force on the rotor.

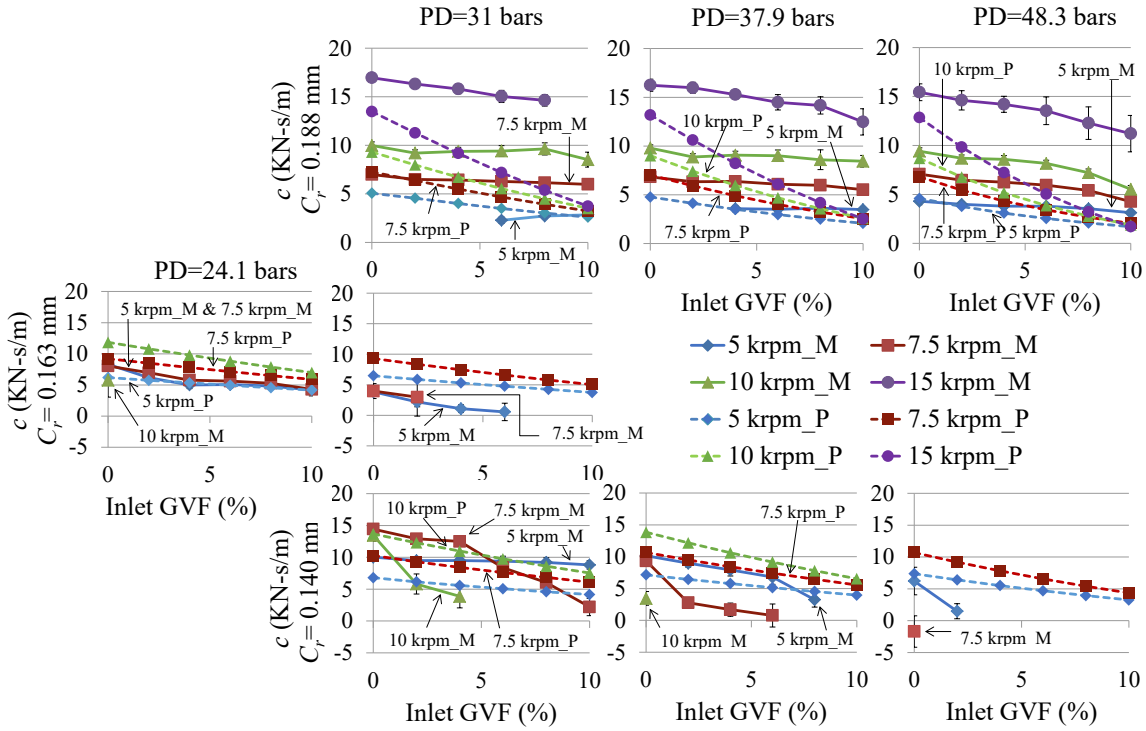

Figure 55. Predictions and measurements of *c* under pure- and mainly-oil conditions

A.6 Direct Virtual-Mass

Figure 57 compares measured and predicted *M* versus inlet GVF over a range of ω, C_r, and PD values.

When C_r=0.188 mm, predicted *M* values are close to test results at pure-oil conditions. Predictions become worse after adding air into the oil flow: as inlet GVF increases, predicted *M* decreases, while measured *M* remains unchanged (for ω from 5 to 10 krpm when PD=31 and 37.9 bars) or drops at a slower rate (for all other C_r=0.188 mm cases). Under mainly-oil conditions, predicted *M* is smaller than measured *M*. Referring to Eq. (5), in a centrifugal pump, *M* affects the seal's centering force, and consequently affects the rotor's critical speed. For cases with measured *M* larger than predicted *M*, the seal's centering force is smaller than predicted, and the rotor's critical speed is lower than predicted. Increasing PD has little effect on predicted *M*, which agrees with measurements. Predictions do not show the observed increases in *M* with increasing ω. Instead, changing ω has little effect on predicted *M*. A possible explanation for this

discrepancy is that, for most cases at this clearance, the transitional effects (as noted in Sec. 5.8) might still be evident, while the flow is fully turbulent in predictions.

When C_r=0.163 and 0.140 mm, as expected, increasing inlet GVF decreases both predicted and measured M values because the fluid's density decreases as inlet GVF increases. Increasing PD has little effect on predicted M but generally decreases measured M. Predicted M is invariant to changes in ω, whereas measured M generally decreases as ω increases. In general, M predictions are either close to test results or less than measurements by less than 60%. Measured M from the case with C_r=0.140 mm, PD=48.3 bars, and ω=7.5 krpm is excluded from comparison because of its large uncertainty.

The discrepancy between predictions and measurements for C_r=0.163 and 0.140 mm (predictions are either close to or less than measurements) is consistent with Childs et al.'s [46] test results for a short (L/D=0.21) smooth laminar-liquid seal, where M predictions are less than 17% of measurements. Regarding this discrepancy, Delgado [47] suggests that an appropriate model is needed to make better predictions. Figure 56 shows the modelled flow regions for predictions. For ease of viewing, the seal clearances are shown greatly enlarged. The flow region 1 is in the oil supply chamber, and the flow region 2 is the seal clearance. A proper height needs to be selected for the flow region 1 to reproduce measured M values. For the short seal tested by Childs et al. [46], the appropriate height for the flow region 1 is 10 to 15 times of the seal radial clearance.

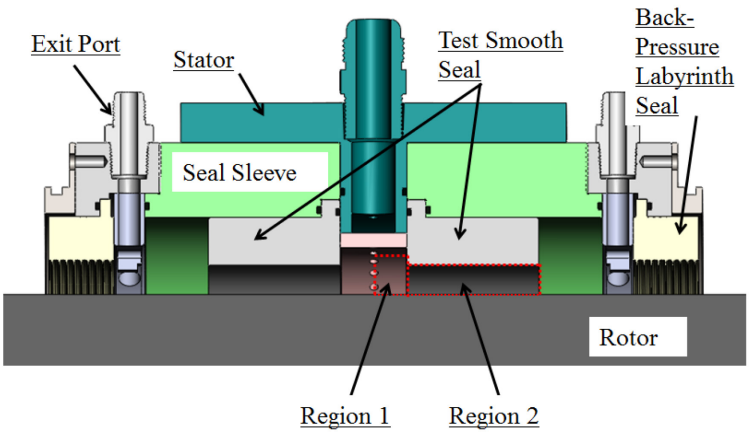

Figure 56. Flow regions for predictions. Reproduced from Delgado [47]

When PD=31 bars and ω=5 and 7.5 krpm, as C_r increases from 0.140 to 0.163 mm, predicted M remains unchanged, whereas measured M decreases significantly (by 31.4%~54.0%). When PD=31 bars, ω=7.5 krpm, and inlet GVF≤2%, increasing C_r further to 0.188 mm decreases predicted M slightly (by about 15%). This generally agrees with test results, where the corresponding measured M remains almost unchanged.

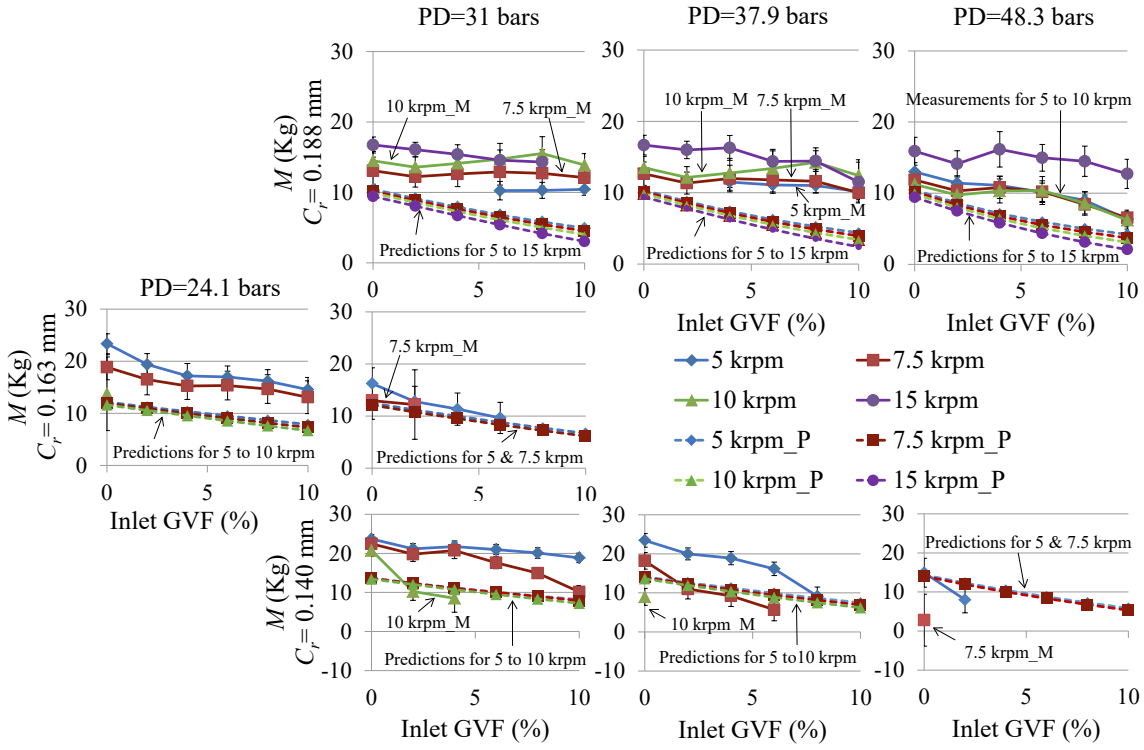

Figure 57. Predictions and measurements of M under pure- and mainly-oil conditions

A.7 Cross-Coupled Virtual-Mass

Figure 58 compares measured and predicted m_q versus inlet GVF over a range of ω, C_r, and PD values. According to Eq. (6), a positive m_q acts as a stabilizing force, and a negative m_q acts as a destabilizing force.

For ω from 5 to 10 krpm at all three clearances, both predicted and measured m_q values are close to zero. Since the predicted and measured magnitudes of $m_q\omega/(C\text{-}k/\omega)$ are less than

13.2%, both predicted and measured m_q values have little effect on the test seal's rotordynamic performance.

Increasing ω from 10 to 15 krpm when C_r=0.188 mm barely changes predicted m_q, but significantly decreases measured m_q (increase in magnitude). When ω=15 krpm and C_r=0.188 mm, both predicted and measured m_q values are negative. However, m_q predictions are close to zero and can be neglected for rotordynamic analysis (the predicted magnitudes of $m_q\omega/(C\text{-}k/\omega)$ are less than 16.1%), while measured m_q values are larger in magnitude and produce considerable destabilizing forces (the measured magnitudes of $m_q\omega/(C\text{-}k/\omega)$ are larger than 22.2% and lower than 50.4%). In regard to m_q, when ω=15 krpm and C_r=0.188 mm, the seal is more destabilizing than predicted.

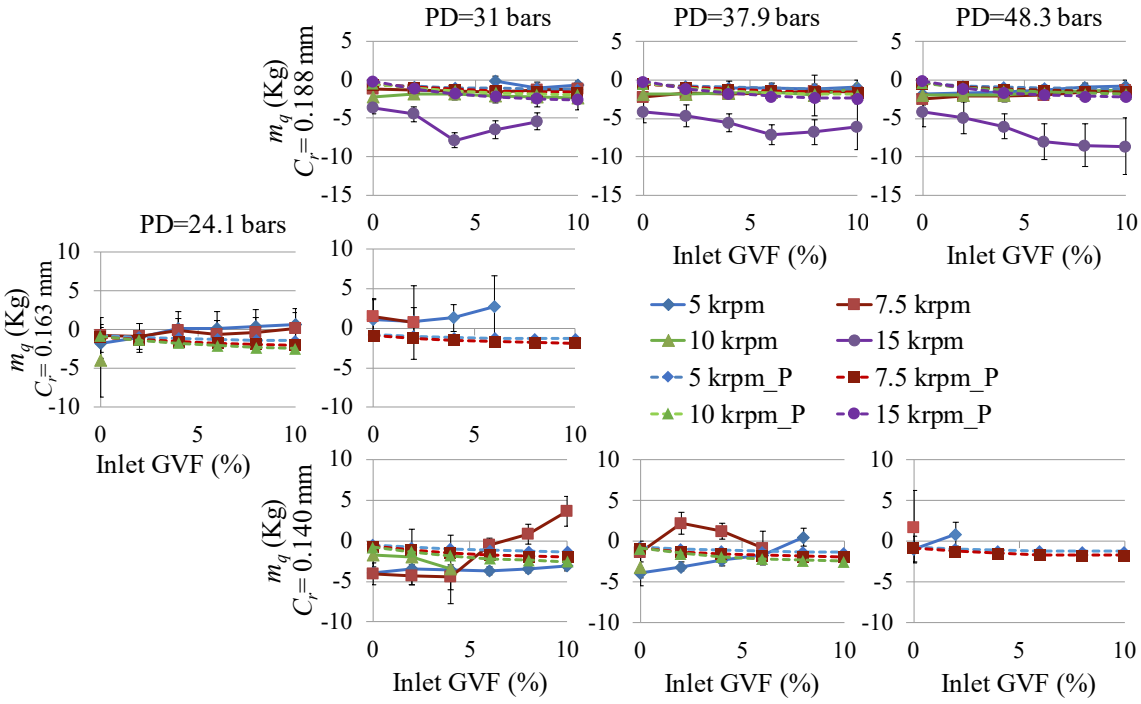

Figure 58. Predictions and measurements of m_q under pure- and mainly-oil conditions

A.8 Effective Damping

Figure 59 compares measured and predicted C_{eff} versus inlet GVF for a range of ω, C_r, and PD values. For all clearances, increasing PD increases predicted C_{eff}. This predicted trend agrees with test results. The C_{eff} increment increases the seal's net damping force and makes the seal more stabilizing.

When C_r=0.188 mm, both predicted and measured C_{eff} values remain generally unchanged as inlet GVF increases from zero to 10%. For C_r=0.163 and 0.140 mm, as inlet GVF increases, predicted C_{eff} remains almost unchanged, while measured C_{eff} generally increases. This discrepancy occurs because when C_r=0.163 and 0.140 mm, increasing inlet GVF has little effect on predicted C and predicted k, but has pronounced effects on measured C and measured k.

As ω increases, both predicted and measured C_{eff} values decrease when C_r=0.188 mm and remain generally unchanged when C_r=0.163 and 0.140 mm.

When PD=31 bars and ω=5 and 7.5 krpm, predictions do not show the increases (by about 20%) in C_{eff} (make the seal more stabilizing) as C_r increases from 0.140 to 0.163 mm. Instead, increasing C_r from 0.140 to 0.163 mm has little effect on predicted C_{eff}. For the same PD, when ω=7.5 krpm and inlet GVF≤2%, as C_r further increases to 0.188 mm, predicted C_{eff} remains unchanged, while measured C_{eff} decreases by about 20%.

In general, for all clearances, C_{eff} predictions are reasonably close to measurements if considering the measurement uncertainties.

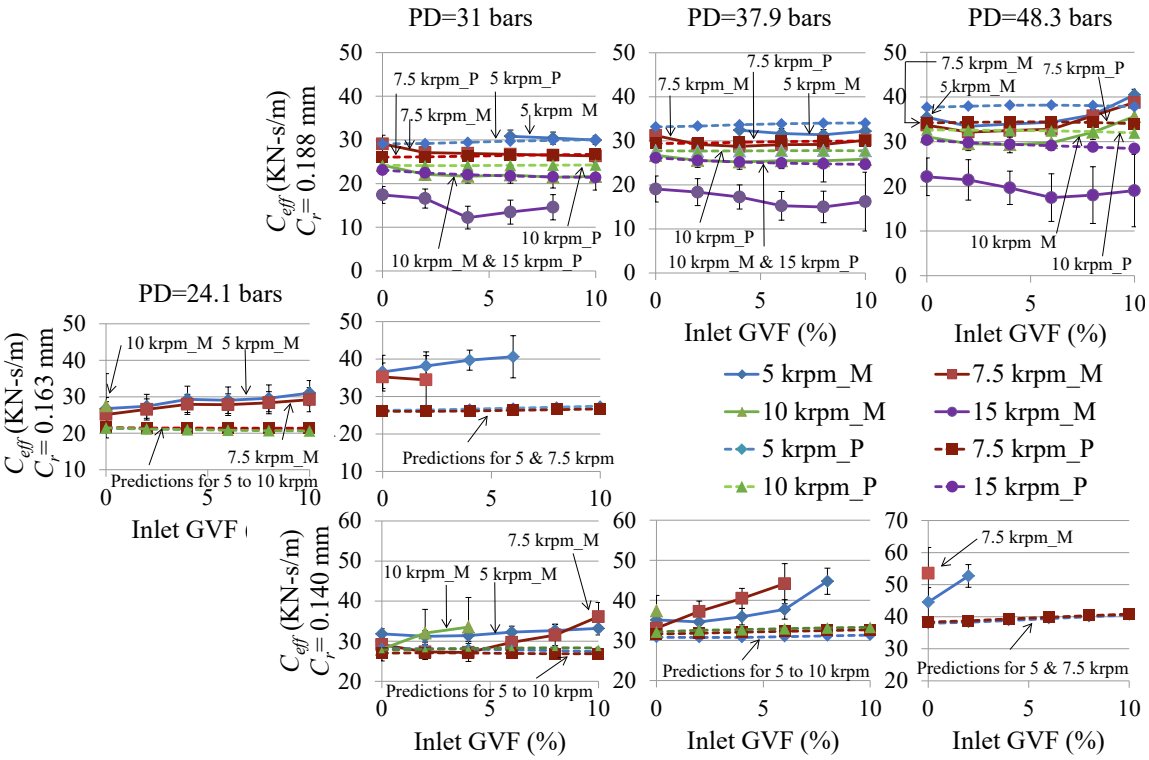

Figure 59. Predictions and measurements of C_{eff} under pure- and mainly-oil conditions

APPENDIX B*

This section compares the test results previously presented and discussed in Sec. 6 to predictions. Besides the operating conditions (inlet GVF, ω, PR, and C_r values) shown in Table 9 and $u_0(0)$ values shown in Table 10, Table 17 shows other input variables needed for predictions.

Variable	Value	Unit
Diameter, D	88.9	mm
Axial Length, L	57.8	mm
Entrance Pressure Loss Factor	0.2	-
Exit pressure Recovery Factor	0	-
Seal Inlet Temperature	See Table 20 in Appendix C	
Seal Inlet Pressure, P_i	62	bars
Liquid Properties		
Viscosity, μ_l	6.28	cP
Density, ρ_l	908.2	kg/m^3
Bulk-Modulus	9987	bars
Surface Tension/Length	0.0197	N/m
Liquid Vapor Pressure	0.001	bars
Gas Properties		
Gas Constant	286.90	J/kg-C
Compressibility	1.00	-
Gas Viscosity, μ_g	1.82E-02	cP
Ratio of the Specific Heat	1.40	-

Table 17. Input variables needed for predictions at pure- and mainly-air conditions

* Portion of this section is reprinted with permission from "Experimental Study of the Static and Dynamic Characteristics of a Long Smooth Seal with Two-Phase, Mainly-Air Mixtures," by Zhang, M., McLean, J., and Childs, D., 2017, *ASME J. Eng. Gas Turbines Power*, 139(12), p. 122504, Copyright 2017 by ASME.

Unlike measured Re($\boldsymbol{H}_{ij}$) shown in Fig. 35, predicted Re($\boldsymbol{H}_{ij}$) can be adequately fitted with frequency-independent direct stiffness K, cross-coupled stiffness k, direct virtual-mass M, and cross-coupled virtual-mass m_q. Hence, the predicted K_Ω and k_Ω are,

$$K_\Omega = \frac{\mathrm{Re}(\boldsymbol{H}_{XX}) + \mathrm{Re}(\boldsymbol{H}_{YY})}{2} = K - M\Omega^2 \tag{48}$$

$$k_\Omega = \frac{\mathrm{Re}(\boldsymbol{H}_{XY}) - \mathrm{Re}(\boldsymbol{H}_{YX})}{2} = k - m_q\Omega^2 \tag{49}$$

Before presenting the comparison between predictions and measurements for pure- and mainly-air conditions, the following differences between the predictive model and experiment need to be noted:

(1) Although the model assumes that the fluid's temperature remains constant in the seal clearance, the fluid's actual/measured temperature throughout the seal may decrease (due to air expansion) or increase (due to power dissipation). Table 20 in Appendix C shows the fluid's measured temperatures at the seal inlet and seal exit.

(2) Although the model assumes the mixture is homogeneous, the actual mixture in the seal clearance might not be homogeneous due to the drop coalescence and centrifugal-inertia effects. During a test, the mixture was visually inspected through a sight-glass view port shortly upstream of the inlet ports of the stator to ensure that the mixture was homogeneous; however, in the seal clearance, the coalescence of fine oil drops can make larger oil drops with diameters larger than the seal clearance. Also, the centrifugal-inertia effect can drive the oil phase outward to the seal surface, with the air phase staying close to the shaft; i.e., the centrifugal inertia effect can lead to a stratified-flow.

B.1 Leakage Mass Flow Rate

Figure 60 compares measured and predicted $\dot{m}$ versus inlet GVF for three PRs (rows), three C_r values (columns), and three ω values. For all clearances, both predicted and measured $\dot{m}$ values decrease slightly (by less than 6%) as inlet GVF decreases from 100% to 98%, and then increase as inlet GVF further decreases to 92%. However, as inlet GVF decreases from 98% to 92%, predicted $\dot{m}$ increases at a slower rate than measured. So, predictions become worse as inlet GVF drops from 98% to 92%; i.e., the discrepancy between predicted and measured $\dot{m}$

values increases with decreasing inlet GVF from 98% to 92%. As expected, both predicted and measured $\dot{m}$ values increase as C_r increases. Neither predicted nor measured $\dot{m}$ values are sensitive to changes in ω.

In general, $\dot{m}$ predictions correlate well with test results. Predicted $\dot{m}$ values are close to measurements when inlet GVF=100% and 98%. When inlet GVF=95% and 92%, predicted $\dot{m}$ values are smaller than measured by less than 28%.

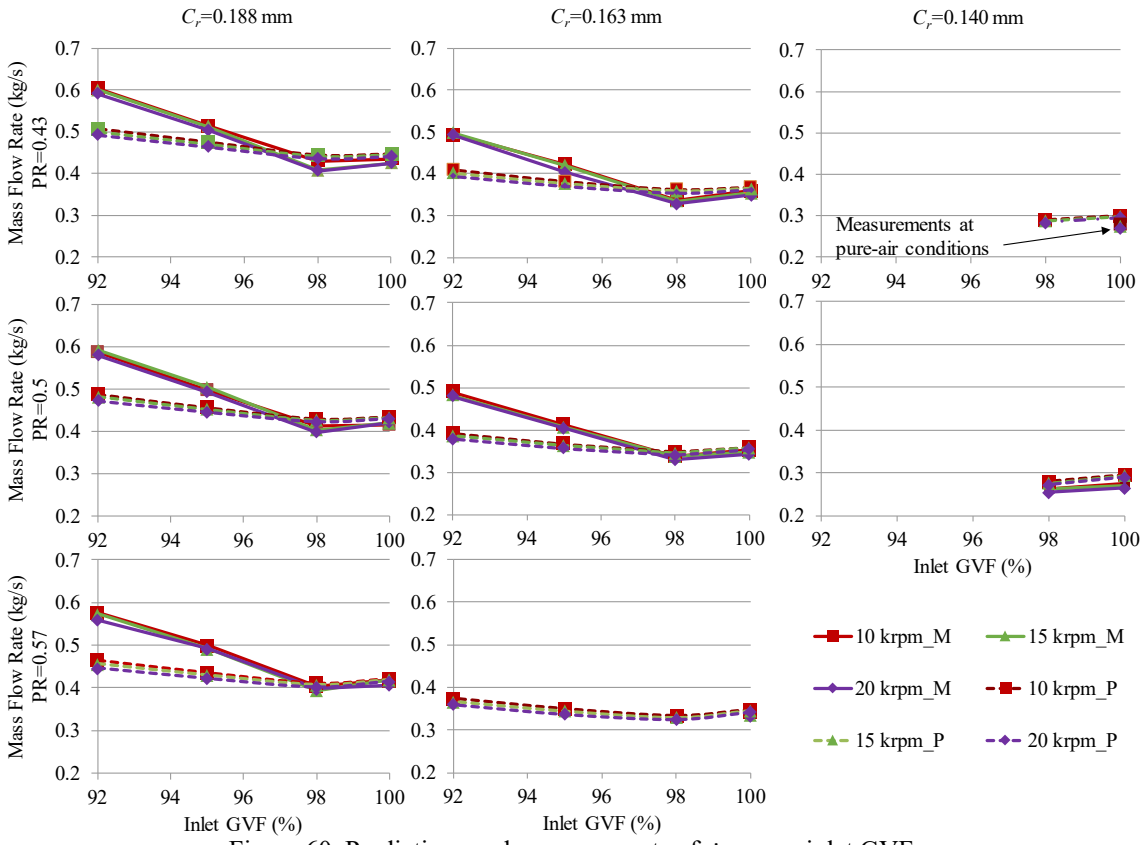

Figure 60. Predictions and measurements of $\dot{m}$ versus inlet GVF

B.2 Direct Dynamic Stiffness

Figure 61 compares measured and predicted K_Ω versus Ω at C_r=0.188 mm for three PRs (rows), three ω values (columns), and four inlet GVFs.

As Ω increases, predicted K_Ω decreases slightly by up to 7.1% while measured K_Ω generally increases. The slight decrease in predicted K_Ω is due to the direct virtual-mass M in Eq. (48). The code assumes that M is induced by fluid inertia. Hence, predicted M is a low positive value because the effective density of the fluid (air or mainly-air mixtures) is low. However, Kerr's [3] test results show that for smooth gas seals, there is a mass-like term causing increases in K_Ω with increasing Ω (stiffening effect). This mass-like term is not induced by fluid inertia and can be incorporated as a negative M. Also, Kerr [3] correctly predicts the stiffening effect for smooth gas seals by using Kleynhans's [48] model.

Injecting oil into the air flow (decreasing inlet GVF from 100% to 92%) decreases predicted K_Ω for all conditions, which agrees with test results except at PR=0.43 and inlet GVF=100% and 98%, where measured K_Ω increases as inlet GVF drops from 100% to 98% while predicted K_Ω decreases. Therefore, when PR=0.43, although predictions show that decreasing inlet GVF from 100% to 98% decreases the seal's centering force, this initial increment of injected oil increases the seal's actual centering force. Increasing/decreasing the seal's centering force can increase/decrease the rotor's critical speed in a centrifugal compressor. Note that for all cases except the pure-air cases when PR=0.43, predicted K_Ω decreases at a significantly slower rate with respect to decreasing inlet GVF than measured.

Increasing ω from 10 to 20 krpm barely changes predicted K_Ω. This predicted trend agrees with test results.

Predicted K_Ω values are close to measurements only under pure-air conditions when PR=0.57 and 0.5. For all other test conditions, K_Ω predictions are larger than measured, and the discrepancy decreases as Ω increases due to the frequency dependence of measured K_Ω. In a centrifugal compressor, this discrepancy would mean that the rotor's critical speed would be lower than predicted.

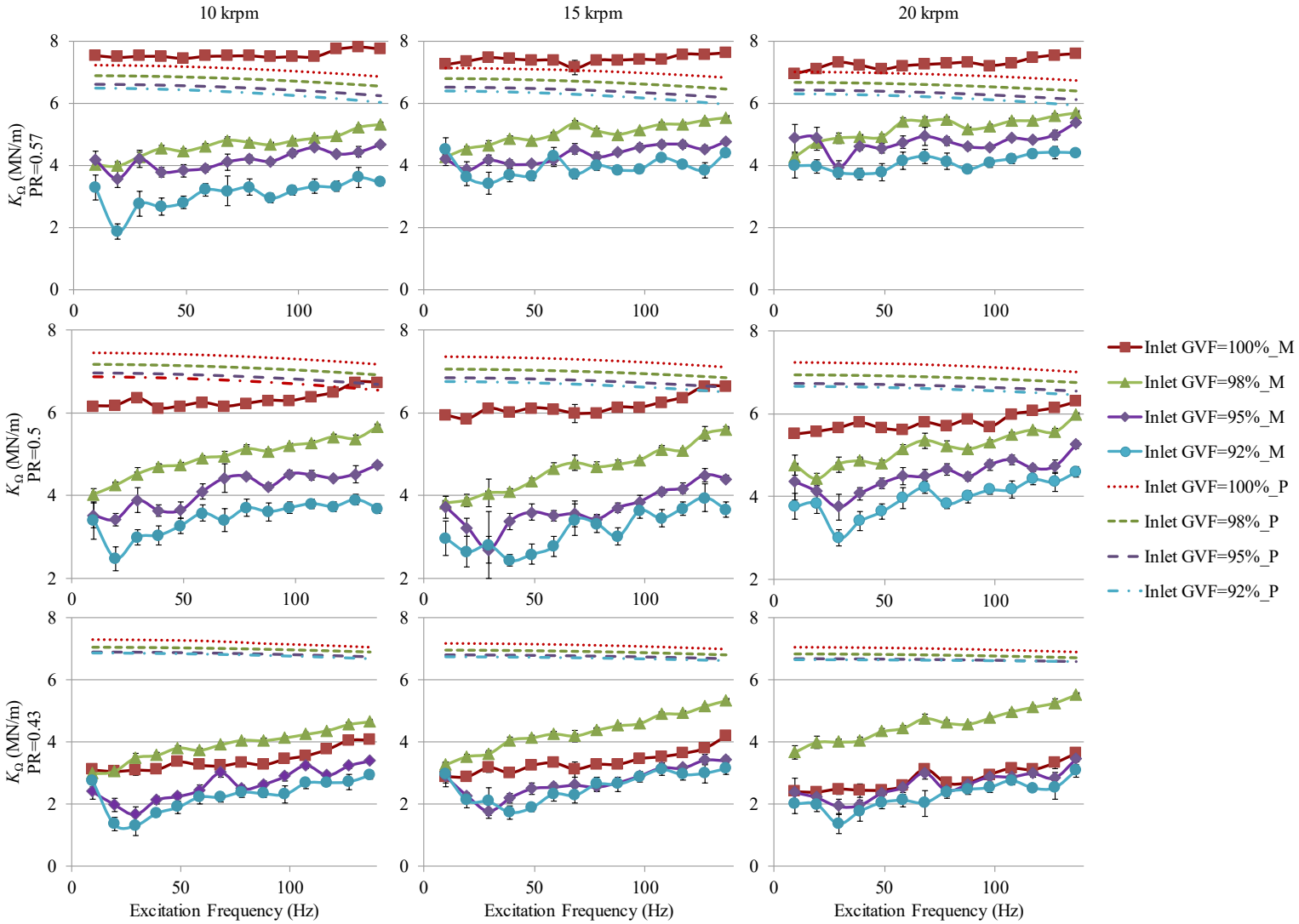

Figure 61. Predictions and measurements of K_Ω at C_r=0.188 mm [27]

Figure 62(a) shows the variation of K_Ω with C_r when PR=0.5, ω=20 krpm, and inlet GVF=100%. Predicted K_Ω decreases as C_r increases from 0.140 to 0.188 mm, which agrees with measurements. Although not presented, for all other pure-air cases, the predicted trend with changes in C_r agrees with test results.

Figure 62(b) shows the variation of K_Ω with C_r at typical mainly-air conditions (PR=0.5, ω=20 krpm, and inlet GVF=98%). As C_r increases from 0.140 to 0.188 mm, predicted K_Ω decreases, while measured K_Ω generally increases.

As shown in Figs. 62(a) and (b), at PR=0.5 and ω=20 krpm, although both predicted and measured K_Ω values decrease as inlet GVF drops from 100% to 98%, the predicted rate of decrease is significantly smaller than measured.

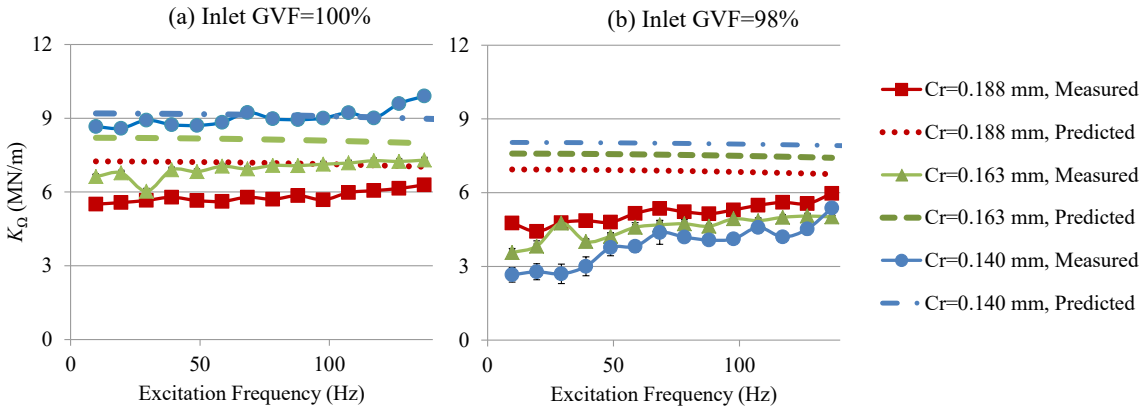

Figure 62. Variation of K_Ω with C_r when PR=0.5 and ω=20 krpm for (a) inlet GVF=100% and (b) inlet GVF=98%

Although not presented, K_Ω predictions for other test cases with C_r=0.163 and 0.140 mm generally agree/disagree with measurements in the same manner as shown in Figs. 61 and 62.

B.3 Cross-Coupled Dynamic Stiffness

Predicted $k_\Omega(\Omega)$ is invariant with changes in Ω; i.e., predicted $k_\Omega(\Omega) \approx$ predicted $\overline{k}$.

Figure 63 compares predicted and measured $\overline{k}$ for three PRs (rows), three C_r values (columns), and three ω values. As expected, both predicted and measured $\overline{k}$ values increase as ω increases since increasing ω increases the fluid's circumferential velocity.

Both predicted and measured $\overline{k}$ values are almost invariant with changes in PR (or PD). This outcome shows that decreasing PR (increasing PD) has negligible effects on the seal's destabilizing force.

Predictions show that increasing C_r decreases $\overline{k}$ and makes the seal more stabilizing. This predicted trend agrees with measurements.

Both predicted and measured $\overline{k}$ values increase significantly as inlet GVF drops from 100% to 98%. As inlet GVF further decreases to 92%, predicted $\overline{k}$ continues increasing while measured $\overline{k}$ decreases. Therefore, as inlet GVF decreases from 98% to 92%, although predictions show that the seal's destabilizing force increases, the seal's actual destabilizing force decreases.

When inlet GVF=100% and 95%, predicted $\overline{k}$ values are close to test results. When inlet GVF=98%, $\overline{k}$ predictions are smaller than measured by about 34%. When inlet GVF=92%, $\overline{k}$ predictions are larger than measured by around 40%. Therefore, the seal is more destabilizing than predicted when inlet GVF=98%, but less destabilizing than predicted when inlet GVF=92%.

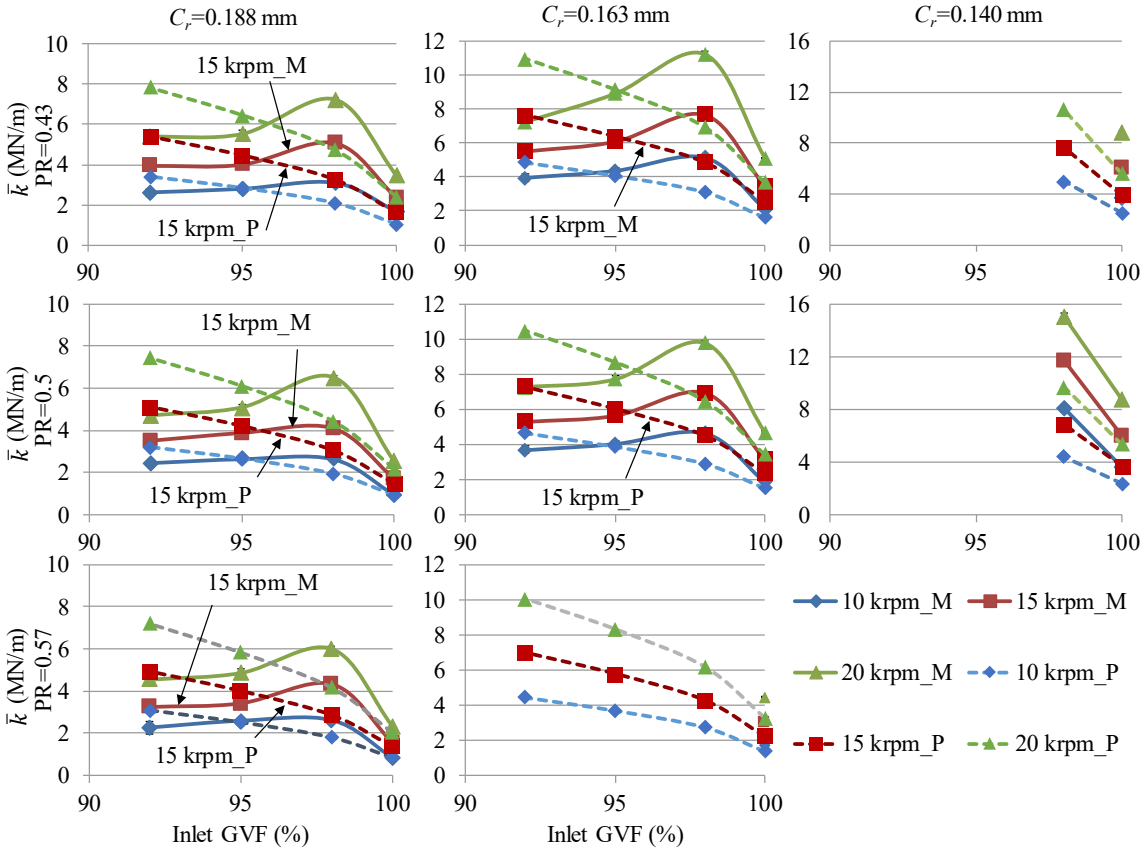

Figure 63. Predictions and measurements of $\bar{k}$

B.4 Direct Damping

Figure 64 compares measured and predicted C versus inlet GVF for three PRs (rows), three C_r values (columns), and three ω values.

For all clearances, both predicted and measured C values increase as inlet GVF decreases from 100% to 98%. As inlet GVF further drops to 92%, predicted C continues increasing versus measured C that remains generally unchanged. Therefore, as inlet GVF decreases from 98% to 92%, although the predicted damping force of the seal increases, the seal's actual damping force remains generally unchanged.

The predicted trends with changes in ω, C_r, and PR agree with test results; specifically, predicted C remains unchanged as ω increases, decreases as C_r increases, and decreases as PR increases (PD decreases).

C predictions are reasonably close to measurements, and are smaller than test results by 14%~48%. Therefore, the test seal has larger damping (stabilizing) force than predicted. Also, predictions become better as C_r increases.

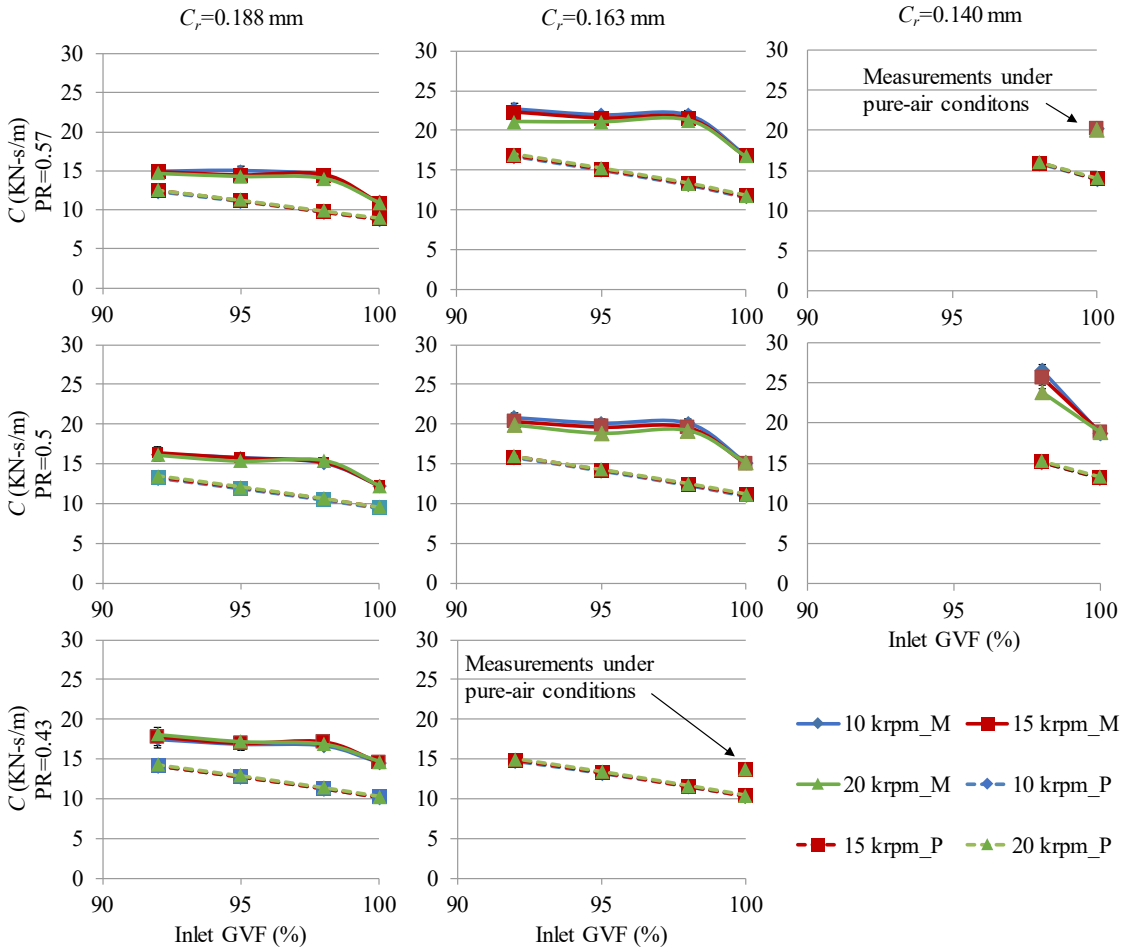

Figure 64. Predictions and measurements of C versus inlet GVF

B.5 Effective Damping

Both measured and predicted C_{eff} values are defined by Eq. (47). Figure 65 compares predicted and measured C_{eff} versus Ω when C_r=0.188 mm, PR=0.5, and ω=15 krpm. As with

measured results, predicted C_{eff} increases from negative to positive at Ω_c. A negative C_{eff} produces a destabilizing force, and a positive C_{eff} acts as a stabilizing force.

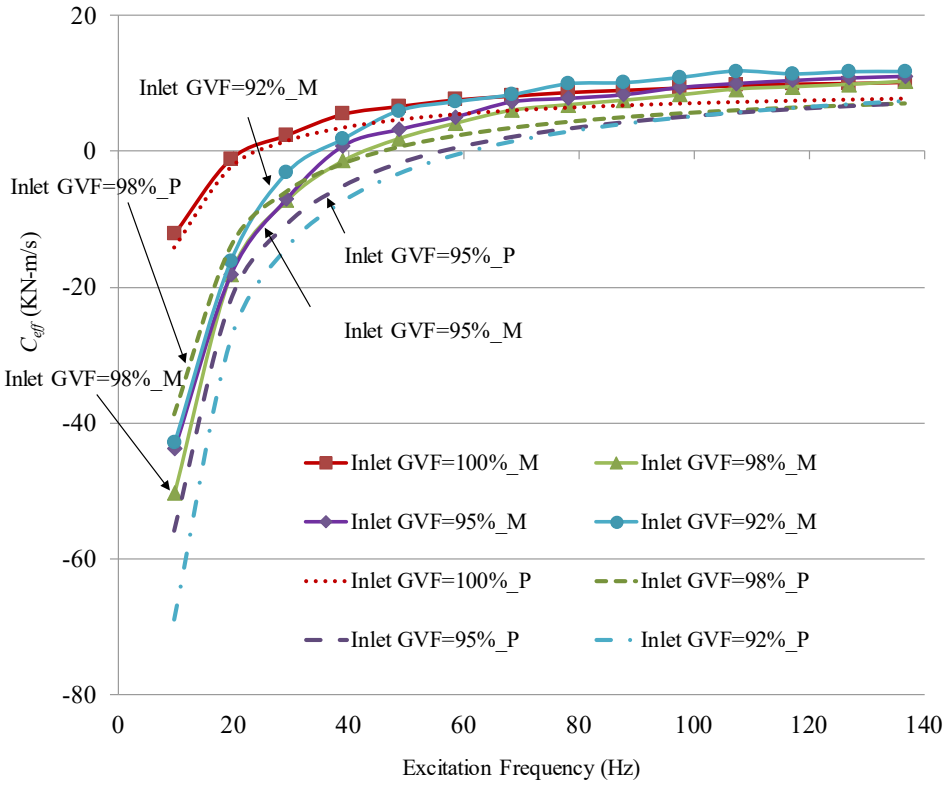

Figure 65. Predictions and measurements of C_{eff} when C_r=0.188 mm, PR=0.5, and ω=15 krpm [27]

Ω_c has a considerable impact on the system stability. Table 18 shows predicted and measured Ω_c values for all cases at C_r=0.188 mm. Predicted Ω_c increases as inlet GVF decreases from 100% to 92%, while measured Ω_c first increases as inlet GVF decreases from 100% to 98% and then decreases as inlet GVF drops further to 92%. Therefore, predictions show that decreasing inlet GVF from 98% to 92% makes the seal more destabilizing, whereas test results show that the seal becomes less destabilizing as inlet GVF decreases from 98% to 92%.

When inlet GVF=100% and 98%, predicted Ω_c values are close to test results except at cases with PR=0.57 and 0.5 and ω=10 krpm, where predicted Ω_c values are larger than measurements by at least 58.7%. The author has no explanation for this exception. Also, this exception does not occur for the other two clearances (0.163 and 0.140 mm); i.e., when C_r=0.163

and 0.140 mm, predicted Ω_c values are close to test results for all cases when inlet GVF=100% and 98%. For inlet GVF=95% and 92% at C_r=0.188 mm, predicted Ω_c values are larger than measured by more than 37.1%, showing the seal more stabilizing than predicted. This happens for the following reasons:

(1) When inlet GVF=95% and 92%, measured C values are larger than predicted;

(2) Measured k_Ω values are close to predictions when inlet GVF=95%, and are smaller than predictions when inlet GVF=92%.

Adding oil into the air flow increases both predicted and measured Ω_c values, making the seal more destabilizing. This outcome for smooth seals is consistent with the observations from Vannini et al. [10] that injecting liquid directly into the labyrinth seals of a centrifugal compressor could cause sub-synchronous vibrations.

As expected, increasing ω increases predicted Ω_c, making the seal more destabilizing. This predicted trend agrees with test results.

Increasing PR from 0.43 to 0.57 (decreasing PD) barely changes Ω_c values, showing little impact on the stabilizing capacity of the seal. This predicted trend agrees with measurements.

PR (-)	Rotor Speed ω (krpm)	Ω_c (Hz)							
		Inlet GVF=100%		Inlet GVF=98%		Inlet GVF=95%		Inlet GVF=92%	
		Meas.	Pred.	Meas.	Pred.	Meas.	Pred.	Meas.	Pred.
0.57	10	8.7	16.2	28.6	28.4	25.4	34.7	27.7	38.8
	15	21.4	24.1	48.7	47.8	38.4	59.8	35.1	64.8
	20	31.6	34.4	68.7	67.9	52.3	78.4	48.4	86.1
0.5	10	10.4	16.5	28.0	28.3	24.8	34.0	22.2	37.4
	15	22.1	24.3	42.6	47.2	38.6	58.7	33.8	63.3
	20	31.7	34.4	68.2	67.2	53.4	77.0	46.0	82.9
0.43	10	18.3	17.0	27.8	28.4	24.7	33.9	22.9	37.2
	15	24.7	24.8	46.7	47.3	36.3	58.3	34.8	62.7
	20	36.1	35.2	68.7	67.1	50.0	76.4	47.0	82.0

Table 18. Ω_c values for pure- and mainly-air cases at C_r=0.188 mm

Although not presented, Ω_c predictions for the other two clearances (C_r=0.163 and 0.140 mm) agree/disagree with measurements in the same manner as shown in Table 18.

Figure 66 compares measured and predicted Ω_c versus C_r when inlet GVF=98%, PR=0.5, and ω=10 krpm. Increasing C_r from 0.140 to 0.188 mm decreases predicted Ω_c, making the seal more stabilizing. This predicted trend agrees with test results. Although not presented, predicted Ω_c for all other test conditions decreases as C_r increases, which agrees with measurements.

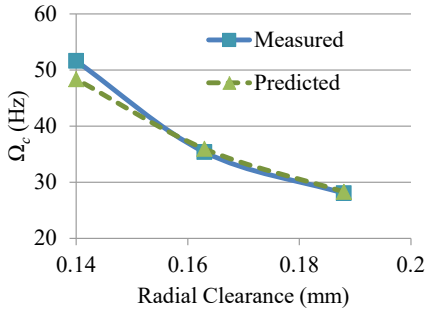

Figure 66. Variation of Ω_c with C_r when PR=0.5, ω=10 krpm, and inlet GVF=98%

B.6 Cross-Coupled Damping

Figure 67 compares predicted and measured c versus inlet GVF. c predictions are close to measurements. Both predicted and measured c values produce insignificant centering forces compared to K_Ω; specifically, the predicted magnitude of $c\Omega/K_\Omega$ is about 3.1%, and the measured magnitude of $c\Omega/K_\Omega$ is about 6.9%. Therefore, both predicted and measured c values has little effect on the seal's rotordynamic characteristics.

As inlet GVF drops from 100% to 92%, measured c generally has its minimum value at inlet GVF=98%. This observed pattern is similar to the measurements of $\bar{k}$ in Fig. 63, where $\bar{k}$ reaches its maximum value at inlet GVF=98%. As noted in in Sec. 6.9, this similarity may result from the fact that both $\bar{k}$ and c coefficients are induced by the fluid's rotation in the seal.

For cases with PR=0.57 and 0.5 at C_r=0.188 mm and cases with PR=0.43 at C_r=0.163 mm, predicted c first decreases as inlet GVF decreases from 100% to 98% and then generally increases with further decreases in inlet GVF to 92%. This predicted trend generally agrees with measurements. For all other test cases, the model predicts the decreases in c as inlet GVF drops from 100% to 98% but does not predict the increases in c with further decreasing inlet GVF to

92%; i.e., as inlet GVF decreases from 98% to 92%, predicted c decreases while measured c generally increases.

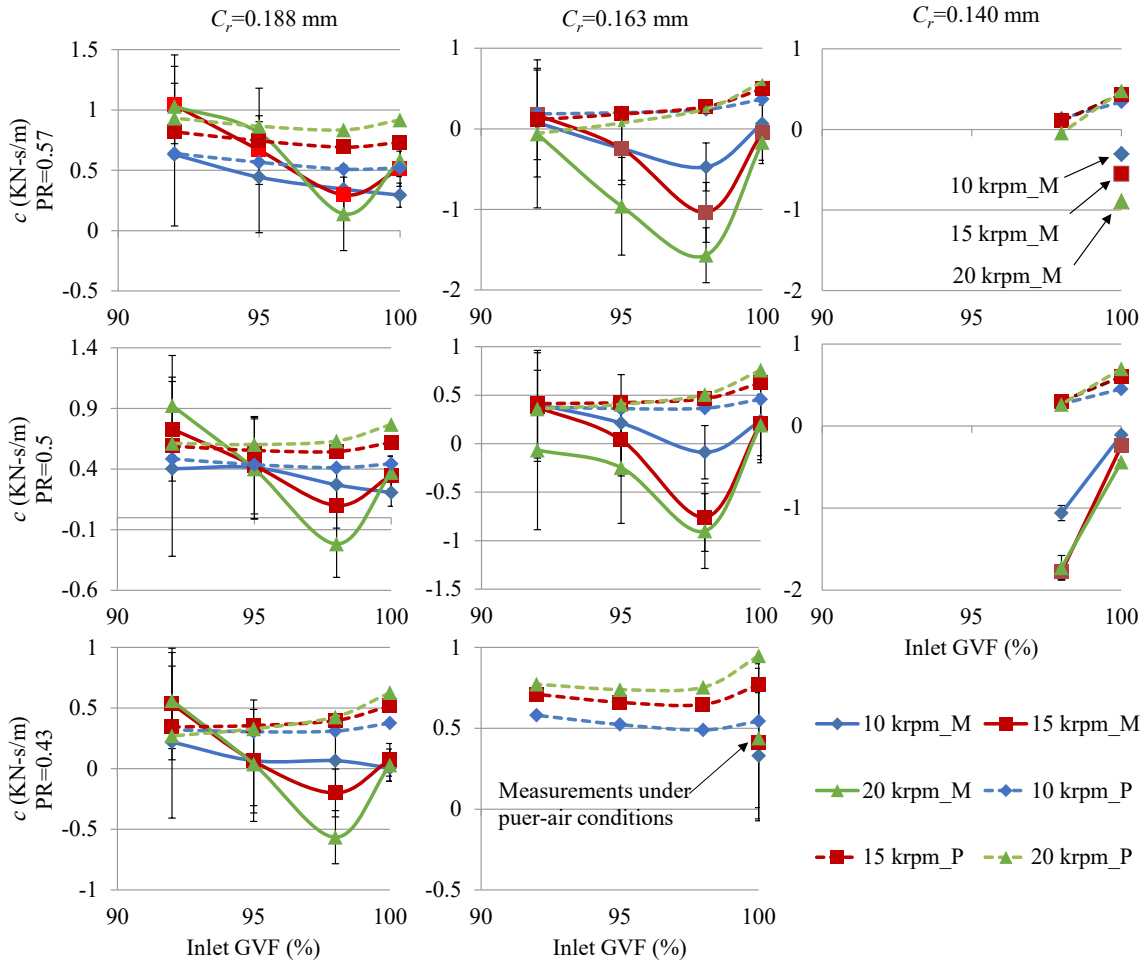

Figure 67. Predictions and measurements of c versus inlet GVF

APPENDIX C

Radial Clearance C_r (mm)	PD (bars)	Inlet GVF (%)	5 krpm		7.5 krpm		10 krpm		15 krpm	
			T_i (°C)	T_e (°C)	T_i (°C)	T_e (°C)	T_i (°C)	T_e (°C)	T_i (°C)	T_e (°C)
0.188	48.3	0	38.5	40.3	38.3	40.5	38.6	41.9	38.4	45.0
		2	38.7	40.2	38.7	41.0	37.3	40.5	39.3	45.7
		4	38.2	39.7	37.9	40.1	38.7	42.0	39.1	45.2
		6	38.3	39.8	38.0	40.2	38.1	41.2	39.3	45.3
		8	38.9	40.5	38.8	41.2	36.3	39.1	38.1	43.9
		10	39.6	41.3	39.1	41.2	38.8	41.8	38.9	44.9
	37.9	0	-		38.0	39.9	41.2	44.0	39.9	47.1
		2			39.2	41.2	38.2	41.2	39.1	46.3
		4	38.9	40.1	39.1	41.2	38.6	41.7	39.2	46.2
		6	39.1	40.4	37.7	39.6	37.6	40.4	37.9	44.3
		8	38.9	40.0	39.2	41.1	39.0	42.0	37.7	43.8
		10	38.9	40.1	38.4	40.2	38.3	41.0	39.1	44.8
	31	0	-		37.9	39.4	38.3	41.2	37.8	45.8
		2			40.1	41.8	38.6	41.5	39.5	47.5
		4			38.1	39.8	38.5	41.4	38.8	46.4
		6	38.6	39.5	39.4	41.1	36.4	39.0	39.3	46.2
		8	38.9	39.7	38.6	40.3	40.0	42.8	38.1	44.4
		10	38.2	38.9	39.3	40.7	38.4	41.1	39.4	45.6
0.163	31	0	38.0	39.1	37.9	39.7	-		-	
		2	38.1	39.2	38.2	40.1				
		4	38.3	39.2	-					
		6	38.3	39.2						
	24.1	0	38.3	39.2	38.2	39.8	38.3	41.4		
		2	38.1	38.9	38.2	39.8	-			
		4	39.1	40.2	38.7	40.4				
		6	37.8	38.6	38.5	40.2				
		8	37.6	38.4	38.4	40.1				
		10	38.0	38.8	38.3	40.0				
0.140	48.3	0	39.1	40.7	39.0	41.3				
		2	39.0	40.5	-					
	37.9	0	38.8	40.3	39.1	41.2	39.1	42.5		
		2	38.9	40.2	39.3	41.3	-			
		4	39.4	40.7	39.2	41.2				
		6	38.8	40.2	39.4	41.4				
		8	39.4	40.8	-					
	31	0	39.5	40.5	39.8	41.6	39.4	42.4		
		2	39.6	40.5	38.4	39.8	39.1	42.2		
		4	39.5	40.5	38.2	39.8	38.9	41.9		
		6	39.3	40.2	39.2	40.8	-			
		8	39.2	40.1	39.2	40.8				
		10	39.3	40.1	39.6	41.1				

Table 19. Measured inlet and exit temperatures for pure- and mainly-oil cases

Radial Clearance C_r (mm)	PR (-)	Inlet GVF (%)	10 krpm		15 krpm		20 krpm	
			T_i (°C)	T_e (°C)	T_i (°C)	T_e (°C)	T_i (°C)	T_e (°C)
0.188	0.43	100	8.6	0.7	6.9	0.4	5.3	0.6
		98	12.3	7.5	8.9	5.5	8.2	7.8
		95	16.0	12.9	16.2	14.7	16.8	17.4
		92	21.4	19.5	20.7	19.9	22.1	22.5
	0.5	100	10.3	4.0	8.2	3.3	7.8	4.6
		98	11.8	7.6	9.9	7.3	10.3	10.8
		95	16.0	13.8	18.5	17.8	17.2	18.2
		92	21.1	19.3	20.0	19.4	21.4	22.4
	0.57	100	5.5	0.3	6.4	2.3	9.1	7.2
		98	12.6	9.6	10.9	9.5	12.3	13.8
		95	20.4	19.0	17.9	17.6	17.5	19.3
		92	20.3	19.2	21.9	21.9	21.8	23.1
0.163	0.43	100	10.6	3.2	11.6	6.1	12.5	9.4
		98	11.4	7.5	12.3	10.5	11.0	12.6
		95	20.0	18.3	22.4	22.3	18.9	21.2
		92	22.8	22.3	25.4	25.9	26.6	28.8
	0.5	100	7.0	0.8	8.7	4.1	9.7	7.5
		98	12.7	9.6	15.4	14.3	15.7	17.8
		95	19.7	18.3	20.9	21.1	23.1	25.6
		92	24.0	23.2	24.9	25.5	25.0	27.5
0.140	0.57	100	5.1	0.1	5.5	2.0	6.4	5.3
	0.43	100	5.2	-0.6	4.9	1.0	5.7	4.6
	0.5	100	12.7	10.1	16.9	20.4	9.4	4.5
		98	15.3	15.1	8.9	2.3	10.2	8.0

Table 20. Measured inlet and exit temperatures for pure- and mainly-air cases

APPENDIX D

Freq.	Re($\boldsymbol{H_{XX}}$)	Re($\boldsymbol{H_{XY}}$)	Re($\boldsymbol{H_{YX}}$)	Re($\boldsymbol{H_{YY}}$)	Im($\boldsymbol{H_{XX}}$)	Im($\boldsymbol{H_{XY}}$)	Im($\boldsymbol{H_{YX}}$)	Im($\boldsymbol{H_{YY}}$)	Re($\boldsymbol{eH_{XX}}$)	Re($\boldsymbol{eH_{XY}}$)	Re($\boldsymbol{eH_{YX}}$)	Re($\boldsymbol{eH_{YY}}$)	Im($\boldsymbol{eH_{XX}}$)	Im($\boldsymbol{eH_{XY}}$)	Im($\boldsymbol{eH_{YX}}$)	Im($\boldsymbol{eH_{YY}}$)
Hz	MN/m	MN/m	MN/m	MN/m	MN/m	MN/m	MN/m	MN/m	MN/m	MN/m	MN/m	MN/m	MN/m	MN/m	MN/m	MN/m
9.8	9.5	6.6	-2.8	8.6	3.2	-0.1	-0.2	4.0	-0.3	-0.2	-0.2	-0.4	-0.2	-0.2	-0.1	-0.1
19.5	9.7	6.8	-3.2	9.1	5.9	0.5	-0.7	5.5	-0.3	-0.3	-0.1	-0.3	-0.1	-0.1	-0.2	-0.1
29.3	9.7	6.7	-3.3	9.7	7.9	1.1	-1.0	7.9	-0.3	-0.1	-0.2	-0.5	-0.1	-0.3	-0.1	-0.2
39.1	8.8	6.9	-3.1	8.6	11.0	0.3	-1.4	11.0	-0.3	-0.2	-0.1	-0.3	-0.1	-0.1	-0.1	-0.1
48.8	8.3	7.2	-3.0	7.5	14.0	1.0	-2.1	14.0	-0.3	-0.2	-0.2	-0.3	-0.2	-0.1	-0.1	-0.1
58.6	8.1	6.6	-3.3	7.6	16.0	1.4	-2.4	16.0	-0.3	-0.2	-0.1	-0.3	-0.1	-0.1	-0.2	-0.2
68.4	7.1	7.6	-3.2	5.7	19.0	1.2	-2.7	20.0	-0.2	-0.2	-0.2	-0.5	0.0	-0.2	-0.2	-0.3
78.1	6.6	7.4	-3.4	5.9	22.0	1.6	-3.7	23.0	-0.2	-0.2	-0.1	-0.3	-0.1	-0.1	-0.1	-0.1
87.9	5.2	7.5	-3.7	4.9	25.0	1.8	-3.6	26.0	-0.2	-0.2	-0.1	-0.3	-0.1	-0.1	-0.1	-0.1
97.7	4.5	7.8	-4.6	4.3	28.0	2.0	-3.6	28.0	-0.2	-0.2	-0.1	-0.2	-0.1	-0.2	0.0	-0.1
107.4	4.0	7.9	-4.4	4.2	31.0	1.3	-3.8	32.0	-0.3	-0.1	-0.1	-0.3	-0.2	-0.1	-0.2	-0.3
117.2	2.8	8.2	-3.9	2.3	33.0	1.8	-4.2	34.0	-0.4	-0.2	-0.2	-0.3	-0.1	-0.1	-0.1	-0.2
127.0	1.3	7.5	-3.9	2.4	36.0	2.2	-4.2	36.0	-0.3	-0.2	-0.1	-0.3	-0.1	-0.2	-0.1	-0.3
136.7	-0.5	8.7	-3.6	-1.4	39.0	1.8	-5.2	41.0	-0.2	-0.2	-0.1	-0.2	-0.2	-0.2	-0.1	-0.2

Table 21. Raw data for the test seal at ω=5 krpm, PD=48.3 bars, C_r=0.188 mm, and inlet GVF=0%

Freq.	Re($\boldsymbol{H_{XX}}$)	Re($\boldsymbol{H_{XY}}$)	Re($\boldsymbol{H_{YX}}$)	Re($\boldsymbol{H_{YY}}$)	Im($\boldsymbol{H_{XX}}$)	Im($\boldsymbol{H_{XY}}$)	Im($\boldsymbol{H_{YX}}$)	Im($\boldsymbol{H_{YY}}$)	Re($\boldsymbol{eH_{XX}}$)	Re($\boldsymbol{eH_{XY}}$)	Re($\boldsymbol{eH_{YX}}$)	Re($\boldsymbol{eH_{YY}}$)	Im($\boldsymbol{eH_{XX}}$)	Im($\boldsymbol{eH_{XY}}$)	Im($\boldsymbol{eH_{YX}}$)	Im($\boldsymbol{eH_{YY}}$)
Hz	MN/m	MN/m	MN/m	MN/m	MN/m	MN/m	MN/m	MN/m	MN/m	MN/m	MN/m	MN/m	MN/m	MN/m	MN/m	MN/m
9.8	12.0	6.3	-2.9	11.0	3.5	0.0	-0.6	4.0	-0.1	-0.2	-0.2	-0.3	-0.1	-0.1	-0.2	-0.1
19.5	12.0	6.1	-2.8	12.0	5.8	0.5	-0.7	5.6	-0.1	-0.3	-0.1	-0.4	-0.1	-0.2	-0.1	-0.1
29.3	12.0	5.8	-3.4	12.0	7.8	1.0	-0.7	8.4	-0.3	-0.1	-0.3	-0.3	-0.1	-0.1	-0.1	-0.1
39.1	12.0	5.9	-3.3	11.0	10.0	0.5	-1.6	11.0	-0.2	-0.2	-0.1	-0.3	-0.1	-0.1	-0.2	-0.1
48.8	11.0	6.0	-3.3	11.0	13.0	0.8	-1.8	13.0	-0.1	-0.2	-0.1	-0.3	-0.1	-0.1	-0.1	-0.2
58.6	11.0	5.9	-3.1	10.0	16.0	1.2	-2.0	16.0	-0.1	-0.2	-0.2	-0.3	-0.1	-0.1	-0.2	-0.1
68.4	11.0	6.3	-3.0	9.6	18.0	1.3	-2.2	19.0	-0.2	-0.1	-0.1	-0.7	-0.1	-0.3	-0.1	-0.3
78.1	9.9	6.0	-3.1	9.0	21.0	1.5	-2.8	21.0	-0.1	-0.1	-0.2	-0.3	-0.1	-0.1	-0.2	-0.1
87.9	9.0	6.8	-3.7	7.9	23.0	1.7	-3.3	24.0	-0.2	-0.2	-0.1	-0.4	-0.1	-0.1	-0.1	-0.2
97.7	8.5	6.6	-4.2	7.7	26.0	1.8	-3.5	27.0	-0.2	-0.2	-0.1	-0.3	-0.1	-0.2	-0.1	-0.1
107.4	7.7	6.7	-4.0	7.1	29.0	1.7	-3.3	29.0	-0.2	-0.1	-0.1	-0.3	-0.1	-0.2	-0.1	-0.2
117.2	6.6	7.0	-4.1	5.6	31.0	1.7	-3.6	32.0	-0.2	-0.2	-0.1	-0.3	-0.1	-0.1	-0.1	-0.2
127.0	5.4	6.6	-4.0	5.4	33.0	2.2	-3.7	34.0	-0.1	-0.2	-0.1	-0.3	-0.1	-0.2	-0.1	-0.2
136.7	3.3	7.5	-3.8	2.2	36.0	2.2	-4.6	38.0	-0.2	-0.2	-0.1	-0.4	-0.1	-0.1	-0.1	-0.2

Table 22. Raw data for the test seal at ω=5 krpm, PD=48.3 bars, C_r=0.188 mm, and inlet GVF=2%

Freq.	Re(H_{XX})	Re(H_{XY})	Re(H_{YX})	Re(H_{YY})	Im(H_{XX})	Im(H_{XY})	Im(H_{YX})	Im(H_{YY})	Re(eH_{XX})	Re(eH_{XY})	Re(eH_{YX})	Re(eH_{YY})	Im(eH_{XX})	Im(eH_{XY})	Im(eH_{YX})	Im(eH_{YY})
Hz	MN/m	MN/m	MN/m	MN/m	MN/m	MN/m	MN/m	MN/m	MN/m	MN/m	MN/m	MN/m	MN/m	MN/m	MN/m	MN/m
9.8	13.0	5.6	-2.6	11.0	3.0	-0.1	-0.2	3.7	-0.1	-0.1	-0.1	-0.2	-0.2	-0.1	-0.2	-0.1
19.5	13.0	5.5	-3.0	12.0	5.6	0.6	-0.9	5.4	-0.2	-0.1	-0.1	-0.2	-0.1	-0.1	-0.1	-0.1
29.3	13.0	6.1	-3.3	12.0	7.7	0.4	-1.1	8.2	-0.1	-0.3	-0.1	0.0	-0.1	-0.3	-0.1	-0.1
39.1	13.0	5.8	-3.3	12.0	10.0	0.3	-1.4	11.0	-0.1	-0.1	-0.1	-0.2	-0.1	-0.1	-0.1	-0.1
48.8	12.0	6.1	-3.4	11.0	13.0	0.6	-1.6	14.0	-0.2	-0.1	-0.2	-0.1	-0.1	0.0	-0.1	-0.1
58.6	12.0	5.5	-3.3	11.0	16.0	0.9	-1.9	16.0	-0.1	-0.1	-0.2	-0.2	-0.2	-0.1	-0.2	-0.1
68.4	12.0	5.7	-3.1	10.0	18.0	1.2	-2.1	19.0	-0.1	-0.3	0.0	-0.2	-0.1	-0.2	-0.1	-0.1
78.1	11.0	6.0	-3.3	9.8	21.0	1.2	-2.7	21.0	-0.1	-0.1	-0.2	-0.2	-0.1	-0.1	-0.1	-0.1
87.9	11.0	5.8	-3.4	9.1	23.0	1.4	-3.1	24.0	-0.1	-0.1	-0.1	-0.2	-0.2	-0.1	-0.1	-0.1
97.7	9.7	6.1	-3.7	8.3	26.0	1.4	-3.2	26.0	-0.1	-0.1	-0.1	-0.2	-0.1	-0.1	-0.1	-0.1
107.4	8.8	6.2	-3.8	7.9	28.0	1.6	-3.6	29.0	-0.2	-0.1	-0.2	-0.3	-0.1	-0.1	-0.1	-0.1
117.2	8.1	6.6	-3.7	6.3	31.0	1.6	-3.8	32.0	-0.1	-0.1	-0.1	-0.1	-0.1	-0.1	-0.1	-0.1
127.0	6.5	6.4	-4.1	5.8	34.0	2.0	-3.9	34.0	-0.1	-0.2	0.0	-0.1	-0.1	-0.3	-0.1	-0.1
136.7	4.6	7.0	-4.2	2.5	37.0	2.1	-4.6	38.0	-0.1	-0.1	-0.1	-0.1	-0.1	-0.1	-0.1	-0.1

Table 23. Raw data for the test seal at ω=5 krpm, PD=48.3 bars, C_r=0.188 mm, and inlet GVF=4%

Freq.	Re(H_{XX})	Re(H_{XY})	Re(H_{YX})	Re(H_{YY})	Im(H_{XX})	Im(H_{XY})	Im(H_{YX})	Im(H_{YY})	Re(eH_{XX})	Re(eH_{XY})	Re(eH_{YX})	Re(eH_{YY})	Im(eH_{XX})	Im(eH_{XY})	Im(eH_{YX})	Im(eH_{YY})
Hz	MN/m	MN/m	MN/m	MN/m	MN/m	MN/m	MN/m	MN/m	MN/m	MN/m	MN/m	MN/m	MN/m	MN/m	MN/m	MN/m
9.8	13.0	4.8	-2.8	13.0	3.4	0.3	0.1	3.3	-0.2	-0.2	-0.2	-0.1	-0.3	-0.3	-0.2	-0.2
19.5	13.0	4.9	-2.6	13.0	5.7	0.5	-0.7	5.7	-0.1	-0.2	-0.2	-0.1	-0.2	-0.2	-0.2	-0.1
29.3	13.0	5.4	-3.4	13.0	8.1	0.4	-1.3	8.4	-0.4	-0.2	-0.1	-0.3	-0.2	-0.1	-0.2	-0.3
39.1	12.0	5.8	-3.4	13.0	10.0	0.5	-1.1	11.0	-0.1	-0.1	-0.2	-0.3	-0.3	-0.1	-0.2	-0.2
48.8	13.0	5.0	-3.1	13.0	13.0	0.8	-1.4	13.0	-0.2	-0.2	-0.1	-0.2	-0.1	-0.1	-0.3	-0.3
58.6	13.0	4.8	-3.6	12.0	16.0	0.8	-1.8	15.0	-0.3	-0.2	-0.2	-0.1	-0.2	-0.2	-0.2	-0.2
68.4	12.0	5.2	-3.1	12.0	18.0	0.9	-1.9	18.0	-0.3	-0.3	-0.3	-0.1	-0.2	-0.2	-0.1	-0.3
78.1	12.0	5.4	-2.9	12.0	21.0	1.5	-2.3	21.0	-0.2	-0.3	-0.2	-0.2	-0.4	-0.1	-0.3	-0.1
87.9	11.0	5.2	-3.3	10.0	23.0	1.3	-2.7	24.0	-0.1	-0.2	-0.1	-0.2	-0.2	-0.3	-0.1	-0.1
97.7	10.0	5.5	-3.8	9.4	26.0	1.9	-3.1	27.0	-0.1	-0.3	-0.2	-0.1	-0.1	-0.2	-0.2	-0.2
107.4	9.2	5.6	-3.6	9.1	28.0	1.6	-3.9	29.0	-0.1	-0.1	-0.2	-0.2	-0.1	-0.1	-0.2	-0.2
117.2	8.7	5.6	-3.7	7.7	31.0	2.1	-3.8	31.0	-0.2	-0.1	-0.2	-0.2	-0.2	-0.1	-0.2	-0.1
127.0	6.7	5.8	-4.1	7.5	34.0	2.2	-3.5	34.0	-0.4	-0.2	-0.2	-0.4	-0.1	-0.2	-0.1	-0.1
136.7	5.5	5.9	-4.1	4.8	37.0	2.5	-4.1	38.0	-0.2	-0.2	-0.2	-0.3	-0.2	-0.2	-0.2	-0.1

Table 24. Raw data for the test seal at ω=5 krpm, PD=48.3 bars, C_r=0.188 mm, and inlet GVF=6%

Freq.	Re($\boldsymbol{H_{XX}}$)	Re($\boldsymbol{H_{XY}}$)	Re($\boldsymbol{H_{YX}}$)	Re($\boldsymbol{H_{YY}}$)	Im($\boldsymbol{H_{XX}}$)	Im($\boldsymbol{H_{XY}}$)	Im($\boldsymbol{H_{YX}}$)	Im($\boldsymbol{H_{YY}}$)	Re($\boldsymbol{eH_{XX}}$)	Re($\boldsymbol{eH_{XY}}$)	Re($\boldsymbol{eH_{YX}}$)	Re($\boldsymbol{eH_{YY}}$)	Im($\boldsymbol{eH_{XX}}$)	Im($\boldsymbol{eH_{XY}}$)	Im($\boldsymbol{eH_{YX}}$)	Im($\boldsymbol{eH_{YY}}$)
Hz	MN/m	MN/m	MN/m	MN/m	MN/m	MN/m	MN/m	MN/m	MN/m	MN/m	MN/m	MN/m	MN/m	MN/m	MN/m	MN/m
9.8	12.0	5.3	-2.7	12.0	3.0	0.1	-0.5	3.5	-0.2	-0.2	-0.4	-0.3	-0.2	-0.2	-0.2	-0.2
19.5	12.0	5.1	-2.9	12.0	5.7	0.3	-1.0	6.2	-0.1	-0.1	-0.2	-0.3	-0.1	-0.1	-0.2	-0.2
29.3	12.0	5.5	-2.8	12.0	8.3	0.8	-1.2	8.8	-0.2	-0.2	-0.2	-0.3	-0.1	-0.1	-0.2	-0.2
39.1	12.0	5.6	-3.2	12.0	11.0	0.4	-1.1	11.0	-0.2	-0.2	-0.2	-0.2	-0.1	-0.2	-0.2	-0.2
48.8	12.0	5.3	-3.2	12.0	14.0	0.6	-1.3	14.0	-0.1	-0.1	-0.2	-0.1	-0.1	-0.2	-0.1	-0.3
58.6	11.0	4.8	-3.3	12.0	17.0	0.2	-1.4	17.0	-0.1	-0.2	-0.2	-0.1	-0.2	-0.1	-0.1	-0.1
68.4	11.0	5.4	-3.3	12.0	19.0	0.8	-1.7	19.0	-0.1	-0.4	-0.3	-0.4	-0.2	-0.3	-0.2	-0.2
78.1	11.0	5.1	-2.9	12.0	21.0	1.1	-2.4	22.0	-0.3	-0.2	-0.1	-0.2	-0.1	-0.2	-0.1	-0.2
87.9	10.0	5.1	-3.4	10.0	24.0	0.7	-2.7	25.0	-0.1	-0.3	-0.1	-0.3	-0.1	-0.2	-0.3	-0.2
97.7	9.2	5.0	-3.3	9.6	27.0	1.6	-2.9	27.0	-0.1	-0.1	-0.2	-0.2	-0.2	-0.2	-0.1	-0.2
107.4	8.6	5.1	-3.6	9.3	30.0	1.9	-3.3	30.0	-0.1	-0.1	-0.3	-0.2	-0.1	-0.2	-0.2	-0.1
117.2	7.5	5.2	-3.6	7.9	32.0	1.7	-3.8	32.0	-0.1	-0.2	-0.1	-0.1	-0.2	-0.1	-0.2	-0.1
127.0	6.5	6.0	-3.8	7.5	34.0	1.9	-3.6	34.0	-0.1	-0.3	-0.2	-0.3	-0.2	-0.3	-0.1	-0.4
136.7	4.7	5.4	-4.3	5.8	38.0	2.1	-4.4	39.0	-0.1	-0.2	-0.2	-0.2	-0.1	-0.2	-0.1	-0.4

Table 25. Raw data for the test seal at ω=5 krpm, PD=48.3 bars, C_r=0.188 mm, and inlet GVF=8%

Freq.	Re($\boldsymbol{H_{XX}}$)	Re($\boldsymbol{H_{XY}}$)	Re($\boldsymbol{H_{YX}}$)	Re($\boldsymbol{H_{YY}}$)	Im($\boldsymbol{H_{XX}}$)	Im($\boldsymbol{H_{XY}}$)	Im($\boldsymbol{H_{YX}}$)	Im($\boldsymbol{H_{YY}}$)	Re($\boldsymbol{eH_{XX}}$)	Re($\boldsymbol{eH_{XY}}$)	Re($\boldsymbol{eH_{YX}}$)	Re($\boldsymbol{eH_{YY}}$)	Im($\boldsymbol{eH_{XX}}$)	Im($\boldsymbol{eH_{XY}}$)	Im($\boldsymbol{eH_{YX}}$)	Im($\boldsymbol{eH_{YY}}$)
Hz	MN/m	MN/m	MN/m	MN/m	MN/m	MN/m	MN/m	MN/m	MN/m	MN/m	MN/m	MN/m	MN/m	MN/m	MN/m	MN/m
9.8	7.9	5.1	-2.6	7.7	3.3	0.0	-0.1	3.7	-0.2	-0.2	-0.2	-0.2	-0.3	-0.1	-0.1	-0.1
19.5	8.1	5.5	-2.9	7.3	6.0	0.2	-0.9	6.7	-0.1	-0.1	-0.1	-0.2	-0.1	-0.3	-0.1	-0.1
29.3	7.9	5.6	-3.2	7.2	9.1	0.6	-0.9	9.7	-0.1	-0.1	-0.2	-0.4	-0.1	-0.3	-0.2	-0.3
39.1	7.6	5.4	-3.8	7.3	12.0	0.6	-1.1	12.0	-0.1	-0.2	-0.1	-0.3	-0.1	-0.2	-0.1	-0.3
48.8	8.0	5.6	-3.5	7.4	15.0	0.5	-1.3	15.0	-0.2	-0.1	-0.1	-0.1	-0.1	-0.1	-0.1	-0.2
58.6	7.7	5.4	-3.8	7.6	18.0	0.6	-1.6	19.0	-0.2	-0.1	-0.2	-0.1	-0.1	-0.1	-0.2	-0.3
68.4	7.1	5.3	-3.4	6.8	21.0	0.0	-1.5	21.0	-0.2	-0.2	-0.1	-0.4	-0.2	-0.4	-0.2	-0.4
78.1	7.3	5.1	-3.5	7.5	24.0	1.0	-2.0	25.0	-0.1	-0.2	-0.1	-0.2	-0.1	-0.1	-0.2	-0.2
87.9	6.6	5.2	-3.7	6.2	27.0	0.8	-2.4	28.0	-0.1	-0.3	-0.1	-0.2	-0.2	-0.3	-0.2	-0.2
97.7	6.3	5.4	-4.3	6.0	30.0	1.0	-2.7	31.0	-0.1	-0.2	-0.1	-0.2	-0.1	-0.3	-0.2	-0.3
107.4	5.7	5.3	-3.7	5.4	32.0	1.0	-2.9	34.0	-0.2	0.0	-0.2	-0.2	-0.1	-0.2	-0.3	-0.2
117.2	4.7	5.4	-3.9	4.5	35.0	1.5	-3.7	37.0	-0.1	-0.1	-0.1	-0.1	-0.2	-0.1	-0.1	-0.1
127.0	3.9	5.5	-3.9	4.4	38.0	1.9	-3.6	39.0	-0.1	-0.4	-0.1	-0.3	-0.1	-0.2	-0.3	-0.4
136.7	2.8	6.0	-3.9	2.7	42.0	1.7	-3.8	43.0	-0.1	-0.2	-0.1	-0.1	-0.1	-0.2	-0.1	-0.2

Table 26. Raw data for the test seal at ω=5 krpm, PD=48.3 bars, C_r=0.188 mm, and inlet GVF=10%

Freq.	Re($\boldsymbol{H_{XX}}$)	Re($\boldsymbol{H_{XY}}$)	Re($\boldsymbol{H_{YX}}$)	Re($\boldsymbol{H_{YY}}$)	Im($\boldsymbol{H_{XX}}$)	Im($\boldsymbol{H_{XY}}$)	Im($\boldsymbol{H_{YX}}$)	Im($\boldsymbol{H_{YY}}$)	Re($\boldsymbol{eH_{XX}}$)	Re($\boldsymbol{eH_{XY}}$)	Re($\boldsymbol{eH_{YX}}$)	Re($\boldsymbol{eH_{YY}}$)	Im($\boldsymbol{eH_{XX}}$)	Im($\boldsymbol{eH_{XY}}$)	Im($\boldsymbol{eH_{YX}}$)	Im($\boldsymbol{eH_{YY}}$)
Hz	MN/m	MN/m	MN/m	MN/m	MN/m	MN/m	MN/m	MN/m	MN/m	MN/m	MN/m	MN/m	MN/m	MN/m	MN/m	MN/m
9.8	9.2	9.2	-7.5	8.6	2.8	0.4	-0.3	3.7	-0.2	-0.3	-0.2	-0.1	-0.1	-0.1	-0.2	-0.2
19.5	9.1	8.9	-7.0	8.7	6.0	0.9	-1.1	5.8	-0.1	-0.1	-0.1	-0.2	-0.1	-0.1	-0.1	-0.1
29.3	9.2	9.2	-6.9	8.7	8.2	1.0	-1.1	8.7	-0.1	-0.1	-0.2	-0.2	-0.2	-0.3	-0.1	-0.2
39.1	8.7	9.1	-7.1	8.5	11.0	1.5	-1.9	11.0	-0.2	-0.1	-0.1	-0.1	-0.2	-0.2	-0.1	-0.1
48.8	8.6	9.2	-6.9	8.0	14.0	2.3	-2.3	14.0	-0.3	-0.2	-0.3	-0.1	-0.2	-0.1	-0.3	-0.2
58.6	7.7	9.2	-7.1	7.1	16.0	2.5	-2.6	17.0	-0.2	-0.3	-0.2	-0.2	-0.3	-0.2	-0.2	-0.1
68.4	7.0	9.2	-6.9	5.8	19.0	2.6	-3.6	20.0	-0.2	-0.3	-0.2	-0.1	-0.3	-0.2	-0.2	-0.2
78.1	6.8	10.0	-7.5	5.6	22.0	3.2	-4.5	23.0	-0.1	-0.2	-0.2	-0.1	-0.1	-0.1	-0.1	-0.1
87.9	6.0	9.9	-7.6	5.1	25.0	3.5	-4.7	26.0	-0.1	-0.1	-0.1	-0.1	-0.1	-0.1	-0.1	-0.1
97.7	5.1	10.0	-8.5	4.6	28.0	3.8	-5.0	29.0	-0.1	-0.1	-0.1	-0.1	-0.1	-0.1	-0.1	-0.1
107.4	4.8	10.0	-8.1	4.1	31.0	3.6	-5.5	31.0	-0.1	-0.1	-0.1	-0.2	-0.2	-0.1	-0.2	-0.1
117.2	3.8	11.0	-7.9	2.7	33.0	4.4	-5.7	34.0	-0.1	-0.1	-0.1	-0.1	-0.1	-0.1	-0.1	-0.1
127.0	4.9	19.0	-13.0	-4.9	30.0	-1.8	-7.2	30.0	-9.1	-5.2	-5.0	-7.3	-5.5	-8.1	-8.3	-5.4
136.7	-0.1	11.0	-7.8	-0.6	38.0	5.1	-6.8	40.0	-0.1	-0.1	-0.1	-0.1	-0.1	-0.1	-0.1	-0.1

Table 27. Raw data for the test seal at ω=7.5 krpm, PD=48.3 bars, C_r=0.188 mm, and inlet GVF=0%

Freq.	Re($\boldsymbol{H_{XX}}$)	Re($\boldsymbol{H_{XY}}$)	Re($\boldsymbol{H_{YX}}$)	Re($\boldsymbol{H_{YY}}$)	Im($\boldsymbol{H_{XX}}$)	Im($\boldsymbol{H_{XY}}$)	Im($\boldsymbol{H_{YX}}$)	Im($\boldsymbol{H_{YY}}$)	Re($\boldsymbol{eH_{XX}}$)	Re($\boldsymbol{eH_{XY}}$)	Re($\boldsymbol{eH_{YX}}$)	Re($\boldsymbol{eH_{YY}}$)	Im($\boldsymbol{eH_{XX}}$)	Im($\boldsymbol{eH_{XY}}$)	Im($\boldsymbol{eH_{YX}}$)	Im($\boldsymbol{eH_{YY}}$)
Hz	MN/m	MN/m	MN/m	MN/m	MN/m	MN/m	MN/m	MN/m	MN/m	MN/m	MN/m	MN/m	MN/m	MN/m	MN/m	MN/m
9.8	11.0	8.4	-6.7	11.0	3.2	0.2	-0.9	3.7	-0.2	-0.1	-0.3	-0.3	-0.2	-0.1	-0.1	-0.1
19.5	11.0	8.3	-6.6	11.0	5.6	0.5	-0.7	5.6	-0.2	-0.2	-0.1	-0.1	-0.2	-0.1	-0.1	-0.1
29.3	11.0	8.5	-6.4	11.0	8.3	1.3	-1.1	8.6	-0.1	-0.2	-0.1	-0.2	-0.1	-0.1	-0.1	-0.2
39.1	11.0	8.5	-6.6	11.0	11.0	1.1	-1.6	11.0	0.0	-0.1	-0.1	-0.2	-0.1	-0.1	-0.1	-0.1
48.8	10.0	8.3	-6.7	10.0	13.0	1.6	-1.9	13.0	-0.2	-0.1	-0.1	-0.2	-0.1	-0.1	-0.1	-0.1
58.6	10.0	8.1	-6.7	10.0	16.0	2.4	-2.2	16.0	-0.1	-0.2	-0.2	-0.2	-0.2	-0.2	-0.2	-0.2
68.4	9.6	8.7	-6.6	8.9	19.0	2.3	-2.9	19.0	-0.3	-0.2	-0.2	-0.2	-0.1	-0.2	-0.1	-0.2
78.1	9.5	9.1	-6.7	9.0	21.0	3.0	-3.7	22.0	-0.1	-0.2	-0.1	-0.1	-0.1	-0.1	-0.1	-0.1
87.9	8.7	9.0	-7.3	8.1	24.0	3.1	-4.2	24.0	-0.1	-0.1	-0.1	-0.2	-0.1	-0.1	-0.2	-0.1
97.7	7.9	9.0	-7.7	7.9	27.0	3.4	-4.6	27.0	-0.1	-0.1	-0.1	-0.2	0.0	-0.1	-0.1	-0.1
107.4	7.3	9.3	-7.5	7.1	29.0	3.5	-4.9	29.0	-0.2	-0.1	-0.1	-0.2	-0.1	-0.1	-0.1	0.0
117.2	6.3	9.6	-7.5	6.0	31.0	4.1	-5.5	32.0	0.0	-0.1	-0.1	-0.1	-0.1	0.0	-0.1	-0.1
127.0	5.2	16.0	-7.9	4.2	33.0	4.1	-5.6	29.0	-2.5	-5.0	-3.3	-6.7	-3.8	-7.3	-2.5	-4.5
136.7	2.9	10.0	-7.6	2.7	36.0	4.8	-6.6	37.0	0.0	-0.1	-0.1	-0.1	-0.1	-0.1	-0.1	-0.1

Table 28. Raw data for the test seal at ω=7.5 krpm, PD=48.3 bars, C_r=0.188 mm, and inlet GVF=2%

Freq.	Re($\boldsymbol{H_{XX}}$)	Re($\boldsymbol{H_{XY}}$)	Re($\boldsymbol{H_{YX}}$)	Re($\boldsymbol{H_{YY}}$)	Im($\boldsymbol{H_{XX}}$)	Im($\boldsymbol{H_{XY}}$)	Im($\boldsymbol{H_{YX}}$)	Im($\boldsymbol{H_{YY}}$)	Re($\boldsymbol{eH_{XX}}$)	Re($\boldsymbol{eH_{XY}}$)	Re($\boldsymbol{eH_{YX}}$)	Re($\boldsymbol{eH_{YY}}$)	Im($\boldsymbol{eH_{XX}}$)	Im($\boldsymbol{eH_{XY}}$)	Im($\boldsymbol{eH_{YX}}$)	Im($\boldsymbol{eH_{YY}}$)
Hz	MN/m	MN/m	MN/m	MN/m	MN/m	MN/m	MN/m	MN/m	MN/m	MN/m	MN/m	MN/m	MN/m	MN/m	MN/m	MN/m
9.8	12.0	8.3	-6.2	11.0	3.4	0.1	-0.4	3.3	-0.1	-0.2	-0.1	-0.2	-0.1	-0.1	-0.1	-0.2
19.5	12.0	8.6	-6.5	11.0	6.0	0.8	-1.2	6.1	-0.1	-0.2	-0.1	-0.1	-0.1	-0.1	-0.2	-0.2
29.3	12.0	8.7	-6.2	12.0	8.1	1.1	-1.3	8.2	-0.1	-0.2	-0.1	-0.2	-0.2	-0.2	-0.1	-0.2
39.1	12.0	8.6	-6.3	11.0	10.0	1.1	-1.8	11.0	-0.2	-0.2	0.0	-0.1	-0.2	-0.1	-0.1	-0.1
48.8	12.0	8.6	-6.4	11.0	13.0	1.5	-1.8	13.0	-0.2	-0.1	-0.1	-0.2	-0.1	-0.2	-0.2	-0.1
58.6	12.0	8.3	-6.2	10.0	16.0	1.9	-2.7	16.0	-0.3	-0.2	-0.2	-0.2	-0.2	-0.2	-0.3	-0.1
68.4	11.0	7.9	-6.0	9.4	19.0	2.2	-3.2	19.0	-0.1	-0.2	-0.2	-0.2	-0.2	-0.2	-0.1	-0.2
78.1	11.0	8.9	-6.4	9.3	21.0	2.6	-3.9	22.0	-0.2	-0.1	-0.2	-0.1	-0.1	-0.1	-0.1	-0.1
87.9	10.0	8.9	-6.8	8.9	24.0	3.0	-4.3	24.0	-0.2	-0.1	-0.1	-0.1	-0.1	-0.1	-0.1	-0.1
97.7	9.5	9.1	-7.4	8.2	26.0	3.1	-4.5	27.0	-0.1	-0.1	-0.1	-0.1	-0.1	-0.1	-0.1	-0.1
107.4	8.7	9.4	-7.0	7.8	29.0	3.1	-5.0	29.0	-0.2	-0.1	-0.1	-0.1	-0.1	-0.1	-0.1	-0.1
117.2	7.2	9.6	-7.1	6.3	31.0	3.7	-5.4	32.0	-0.1	-0.1	-0.1	-0.1	-0.1	-0.1	-0.2	-0.1
127.0	-2.7	26.0	-2.9	-7.7	37.0	-7.9	2.2	21.0	-7.4	-8.5	-4.5	-5.3	-4.5	-5.4	-6.6	-7.8
136.7	3.9	10.0	-7.3	2.8	37.0	4.2	-6.7	37.0	-0.1	-0.1	-0.2	-0.1	-0.1	-0.1	-0.1	-0.1

Table 29. Raw data for the test seal at ω=7.5 krpm, PD=48.3 bars, C_r=0.188 mm, and inlet GVF=4%

Freq.	Re($\boldsymbol{H_{XX}}$)	Re($\boldsymbol{H_{XY}}$)	Re($\boldsymbol{H_{YX}}$)	Re($\boldsymbol{H_{YY}}$)	Im($\boldsymbol{H_{XX}}$)	Im($\boldsymbol{H_{XY}}$)	Im($\boldsymbol{H_{YX}}$)	Im($\boldsymbol{H_{YY}}$)	Re($\boldsymbol{eH_{XX}}$)	Re($\boldsymbol{eH_{XY}}$)	Re($\boldsymbol{eH_{YX}}$)	Re($\boldsymbol{eH_{YY}}$)	Im($\boldsymbol{eH_{XX}}$)	Im($\boldsymbol{eH_{XY}}$)	Im($\boldsymbol{eH_{YX}}$)	Im($\boldsymbol{eH_{YY}}$)
Hz	MN/m	MN/m	MN/m	MN/m	MN/m	MN/m	MN/m	MN/m	MN/m	MN/m	MN/m	MN/m	MN/m	MN/m	MN/m	MN/m
9.8	13.0	8.0	-5.6	12.0	3.4	0.4	-0.6	3.4	-0.2	-0.2	-0.1	-0.2	-0.1	-0.2	-0.1	-0.1
19.5	14.0	7.7	-5.7	13.0	5.7	0.7	-0.9	5.9	-0.1	-0.2	-0.2	-0.2	-0.1	-0.1	-0.1	-0.1
29.3	13.0	8.2	-5.9	13.0	7.7	0.8	-1.1	7.8	-0.1	-0.2	-0.1	-0.2	-0.1	-0.1	-0.1	-0.2
39.1	13.0	8.2	-5.9	12.0	11.0	1.5	-1.9	11.0	-0.1	-0.1	-0.1	-0.2	-0.1	0.0	-0.1	-0.1
48.8	13.0	8.2	-6.0	12.0	13.0	1.5	-2.2	13.0	-0.3	-0.2	-0.2	-0.1	-0.1	-0.1	-0.2	-0.2
58.6	12.0	8.3	-5.9	11.0	16.0	1.3	-2.1	15.0	-0.2	-0.1	-0.2	-0.2	-0.2	-0.2	-0.2	-0.2
68.4	12.0	7.9	-5.5	11.0	18.0	1.6	-3.0	19.0	-0.2	-0.1	-0.1	-0.3	-0.1	-0.3	-0.1	-0.2
78.1	12.0	8.0	-5.8	11.0	21.0	2.5	-4.0	21.0	-0.2	-0.1	-0.1	-0.1	-0.1	-0.2	-0.2	-0.1
87.9	11.0	8.6	-6.2	9.8	23.0	2.7	-4.0	24.0	-0.1	-0.1	-0.1	-0.2	0.0	-0.1	-0.1	-0.1
97.7	11.0	8.5	-6.6	9.5	26.0	2.8	-4.3	27.0	-0.1	-0.1	-0.1	-0.2	-0.1	-0.1	0.0	-0.1
107.4	9.7	8.7	-6.6	9.0	28.0	3.0	-4.8	29.0	-0.1	-0.1	-0.1	-0.1	-0.1	-0.1	-0.1	-0.1
117.2	8.5	8.9	-6.7	7.4	31.0	3.5	-5.4	32.0	-0.1	-0.1	-0.1	-0.1	-0.1	-0.1	-0.1	-0.1
127.0	4.3	15.0	-6.6	-1.8	34.0	-4.3	-3.1	30.0	-4.5	-6.4	-4.8	-7.4	-4.9	-8.0	-3.9	-6.4
136.7	5.4	9.8	-6.9	4.3	37.0	4.2	-6.3	38.0	-0.2	-0.1	-0.2	-0.2	-0.1	-0.1	-0.1	-0.1

Table 30. Raw data for the test seal at ω=7.5 krpm, PD=48.3 bars, C_r=0.188 mm, and inlet GVF=6%

Freq.	Re($\boldsymbol{H_{XX}}$)	Re($\boldsymbol{H_{XY}}$)	Re($\boldsymbol{H_{YX}}$)	Re($\boldsymbol{H_{YY}}$)	Im($\boldsymbol{H_{XX}}$)	Im($\boldsymbol{H_{XY}}$)	Im($\boldsymbol{H_{YX}}$)	Im($\boldsymbol{H_{YY}}$)	Re($\boldsymbol{eH_{XX}}$)	Re($\boldsymbol{eH_{XY}}$)	Re($\boldsymbol{eH_{YX}}$)	Re($\boldsymbol{eH_{YY}}$)	Im($\boldsymbol{eH_{XX}}$)	Im($\boldsymbol{eH_{XY}}$)	Im($\boldsymbol{eH_{YX}}$)	Im($\boldsymbol{eH_{YY}}$)
Hz	MN/m	MN/m	MN/m	MN/m	MN/m	MN/m	MN/m	MN/m	MN/m	MN/m	MN/m	MN/m	MN/m	MN/m	MN/m	MN/m
9.8	11.0	8.0	-5.8	11.0	3.2	0.0	-0.1	3.5	-0.2	-0.3	-0.1	-0.1	-0.2	-0.1	-0.1	-0.2
19.5	11.0	7.9	-5.7	11.0	5.8	0.5	-0.7	5.9	-0.1	-0.2	-0.1	-0.2	-0.1	-0.1	-0.1	-0.2
29.3	10.0	8.1	-6.0	11.0	8.4	0.8	-1.3	8.8	-0.1	-0.2	-0.1	-0.2	-0.1	-0.2	-0.1	-0.2
39.1	11.0	8.2	-5.9	11.0	11.0	0.9	-1.6	12.0	-0.1	-0.1	-0.1	-0.2	-0.1	0.0	-0.1	0.0
48.8	10.0	8.3	-6.4	11.0	14.0	1.1	-1.7	14.0	-0.1	-0.1	-0.2	-0.1	-0.1	0.0	-0.2	-0.1
58.6	10.0	8.0	-6.3	11.0	17.0	1.6	-2.2	17.0	-0.2	-0.1	-0.2	-0.1	-0.1	-0.2	-0.2	-0.2
68.4	9.6	8.5	-6.0	10.0	20.0	1.6	-2.7	20.0	-0.1	-0.1	-0.1	-0.1	-0.2	-0.4	-0.1	-0.2
78.1	10.0	8.2	-6.2	10.0	22.0	2.3	-3.3	23.0	-0.1	-0.1	-0.1	-0.1	-0.1	-0.1	-0.1	-0.1
87.9	9.1	8.5	-6.3	9.2	25.0	2.3	-3.8	26.0	0.0	-0.1	0.0	-0.1	-0.1	-0.1	-0.1	0.0
97.7	8.5	8.3	-6.9	8.8	28.0	2.3	-4.1	28.0	-0.1	-0.1	-0.1	-0.1	-0.1	-0.1	-0.1	-0.1
107.4	7.9	8.4	-6.8	8.3	30.0	2.5	-4.7	31.0	-0.1	-0.1	-0.1	-0.1	-0.1	-0.1	-0.1	-0.1
117.2	6.7	8.6	-6.9	6.8	33.0	3.1	-5.0	34.0	-0.1	-0.1	0.0	-0.2	-0.2	-0.1	-0.1	-0.1
127.0	5.9	10.0	-7.5	-2.7	35.0	-6.6	-4.8	37.0	-4.9	-6.8	-4.6	-6.2	-4.2	-6.6	-4.3	-6.9
136.7	4.0	9.5	-6.6	4.6	39.0	3.8	-5.7	40.0	-0.1	-0.1	-0.1	-0.2	-0.1	-0.1	-0.1	-0.2

Table 31. Raw data for the test seal at ω=7.5 krpm, PD=48.3 bars, C_r=0.188 mm, and inlet GVF=8%

Freq.	Re($\boldsymbol{H_{XX}}$)	Re($\boldsymbol{H_{XY}}$)	Re($\boldsymbol{H_{YX}}$)	Re($\boldsymbol{H_{YY}}$)	Im($\boldsymbol{H_{XX}}$)	Im($\boldsymbol{H_{XY}}$)	Im($\boldsymbol{H_{YX}}$)	Im($\boldsymbol{H_{YY}}$)	Re($\boldsymbol{eH_{XX}}$)	Re($\boldsymbol{eH_{XY}}$)	Re($\boldsymbol{eH_{YX}}$)	Re($\boldsymbol{eH_{YY}}$)	Im($\boldsymbol{eH_{XX}}$)	Im($\boldsymbol{eH_{XY}}$)	Im($\boldsymbol{eH_{YX}}$)	Im($\boldsymbol{eH_{YY}}$)
Hz	MN/m	MN/m	MN/m	MN/m	MN/m	MN/m	MN/m	MN/m	MN/m	MN/m	MN/m	MN/m	MN/m	MN/m	MN/m	MN/m
9.8	7.0	8.6	-6.4	6.5	3.7	-0.3	-0.3	3.6	-0.2	-0.2	-0.1	-0.2	-0.2	-0.2	-0.3	-0.2
19.5	7.3	8.9	-6.3	6.9	6.4	0.3	-0.7	6.5	-0.2	-0.1	-0.1	-0.1	-0.1	-0.1	-0.2	-0.1
29.3	7.3	9.1	-6.4	6.3	9.0	0.9	-1.2	9.4	-0.1	-0.1	-0.2	-0.2	-0.1	-0.1	-0.1	-0.2
39.1	7.1	9.1	-6.7	6.8	12.0	1.0	-1.2	13.0	-0.2	-0.1	-0.2	-0.1	-0.1	-0.1	-0.1	0.0
48.8	6.8	9.0	-7.1	6.3	15.0	0.8	-1.8	15.0	-0.1	-0.1	-0.1	-0.1	-0.1	-0.1	-0.1	-0.1
58.6	7.0	8.8	-6.6	6.3	18.0	1.1	-1.8	18.0	-0.1	-0.1	-0.2	-0.1	-0.2	-0.1	-0.3	-0.1
68.4	6.4	8.6	-6.9	5.4	21.0	1.2	-2.1	22.0	-0.4	-0.3	-0.2	-0.1	-0.2	-0.1	-0.2	-0.2
78.1	6.8	9.0	-7.3	5.6	24.0	1.4	-2.5	25.0	-0.2	-0.1	-0.1	-0.1	-0.1	-0.1	-0.1	-0.1
87.9	6.1	9.2	-7.0	5.1	27.0	1.6	-3.2	28.0	-0.1	-0.1	-0.2	-0.1	-0.1	-0.1	-0.1	-0.1
97.7	5.5	9.1	-7.5	4.6	30.0	1.9	-3.8	31.0	-0.1	-0.1	-0.1	-0.1	-0.1	-0.1	-0.1	-0.1
107.4	4.7	9.1	-7.4	4.6	33.0	1.8	-3.8	34.0	-0.1	-0.1	-0.2	-0.1	-0.3	-0.1	-0.2	-0.1
117.2	4.1	9.2	-7.4	3.4	35.0	2.2	-4.0	37.0	-0.1	-0.1	-0.2	-0.1	-0.1	-0.1	-0.1	-0.1
127.0	1.4	20.0	-10.0	1.0	34.0	1.5	-1.7	30.0	-7.2	-13.0	-8.7	-8.7	-9.2	-9.3	-7.1	-13.0
136.7	2.0	10.0	-7.3	1.7	42.0	2.8	-4.8	44.0	-0.2	-0.1	-0.2	-0.1	-0.3	-0.1	-0.1	-0.1

Table 32. Raw data for the test seal at ω=7.5 krpm, PD=48.3 bars, C_r=0.188 mm, and inlet GVF=10%

Freq.	Re($\boldsymbol{H_{XX}}$)	Re($\boldsymbol{H_{XY}}$)	Re($\boldsymbol{H_{YX}}$)	Re($\boldsymbol{H_{YY}}$)	Im($\boldsymbol{H_{XX}}$)	Im($\boldsymbol{H_{XY}}$)	Im($\boldsymbol{H_{YX}}$)	Im($\boldsymbol{H_{YY}}$)	Re($\boldsymbol{eH_{XX}}$)	Re($\boldsymbol{eH_{XY}}$)	Re($\boldsymbol{eH_{YX}}$)	Re($\boldsymbol{eH_{YY}}$)	Im($\boldsymbol{eH_{XX}}$)	Im($\boldsymbol{eH_{XY}}$)	Im($\boldsymbol{eH_{YX}}$)	Im($\boldsymbol{eH_{YY}}$)
Hz	MN/m	MN/m	MN/m	MN/m	MN/m	MN/m	MN/m	MN/m	MN/m	MN/m	MN/m	MN/m	MN/m	MN/m	MN/m	MN/m
9.8	12.0	13.0	-11.0	9.3	3.2	-0.5	-1.1	3.8	-0.3	-0.3	-0.5	-0.3	-0.2	-0.2	-0.3	-0.2
19.5	12.0	13.0	-10.0	10.0	6.1	1.1	-1.1	5.9	-0.1	-0.2	-0.2	-0.2	-0.2	-0.2	-0.2	-0.2
29.3	11.0	13.0	-10.0	10.0	8.1	1.3	-1.5	7.9	-0.2	-0.2	-0.2	-0.3	-0.2	-0.1	-0.2	-0.2
39.1	11.0	13.0	-10.0	10.0	11.0	2.0	-2.6	11.0	-0.2	-0.1	-0.3	-0.1	-0.1	-0.2	-0.2	-0.2
48.8	11.0	13.0	-10.0	9.8	13.0	2.8	-3.2	13.0	-0.1	-0.1	-0.3	-0.2	-0.2	-0.3	-0.1	-0.1
58.6	10.0	13.0	-11.0	8.8	16.0	3.2	-3.5	16.0	-0.3	-0.3	-0.3	-0.2	-0.3	-0.2	-0.2	-0.2
68.4	9.3	13.0	-11.0	8.6	19.0	4.0	-4.5	20.0	-0.1	-0.4	-0.2	-0.4	-0.3	-0.4	-0.1	-0.3
78.1	9.0	13.0	-11.0	7.9	22.0	4.1	-5.3	22.0	-0.1	-0.2	-0.2	-0.4	-0.3	-0.3	-0.2	-0.1
87.9	8.5	14.0	-11.0	7.4	25.0	4.4	-5.9	26.0	-0.1	-0.1	-0.1	-0.1	-0.2	-0.1	-0.2	-0.2
97.7	7.7	14.0	-11.0	7.1	28.0	4.9	-6.6	28.0	-0.2	-0.1	-0.2	-0.1	-0.1	-0.1	-0.2	-0.1
107.4	7.3	14.0	-11.0	6.8	30.0	5.2	-6.7	30.0	-0.1	-0.1	-0.1	-0.1	-0.2	-0.1	-0.2	-0.1
117.2	6.2	14.0	-11.0	4.9	32.0	6.1	-7.6	32.0	-0.1	-0.1	-0.1	-0.1	-0.1	-0.1	-0.1	-0.1
127.0	4.6	14.0	-11.0	4.0	34.0	6.8	-8.5	35.0	-0.2	-0.1	-0.1	-0.3	-0.1	-0.3	-0.1	-0.2
136.7	2.0	15.0	-11.0	1.7	37.0	7.2	-9.5	38.0	-0.1	-0.1	-0.1	-0.1	-0.1	-0.2	-0.1	-0.1

Table 33. Raw data for the test seal at ω=10 krpm, PD=48.3 bars, C_r=0.188 mm, and inlet GVF=0%

Freq.	Re($\boldsymbol{H_{XX}}$)	Re($\boldsymbol{H_{XY}}$)	Re($\boldsymbol{H_{YX}}$)	Re($\boldsymbol{H_{YY}}$)	Im($\boldsymbol{H_{XX}}$)	Im($\boldsymbol{H_{XY}}$)	Im($\boldsymbol{H_{YX}}$)	Im($\boldsymbol{H_{YY}}$)	Re($\boldsymbol{eH_{XX}}$)	Re($\boldsymbol{eH_{XY}}$)	Re($\boldsymbol{eH_{YX}}$)	Re($\boldsymbol{eH_{YY}}$)	Im($\boldsymbol{eH_{XX}}$)	Im($\boldsymbol{eH_{XY}}$)	Im($\boldsymbol{eH_{YX}}$)	Im($\boldsymbol{eH_{YY}}$)
Hz	MN/m	MN/m	MN/m	MN/m	MN/m	MN/m	MN/m	MN/m	MN/m	MN/m	MN/m	MN/m	MN/m	MN/m	MN/m	MN/m
9.8	12.0	13.0	-10.0	11.0	3.1	-0.2	-0.2	3.3	-0.1	-0.2	-0.2	-0.3	-0.2	-0.3	-0.1	-0.2
19.5	13.0	12.0	-9.8	11.0	5.5	1.1	-1.1	5.9	-0.2	-0.1	-0.1	-0.1	-0.1	-0.2	-0.3	-0.2
29.3	13.0	13.0	-9.7	11.0	8.2	1.0	-1.3	8.3	-0.2	-0.2	-0.2	-0.1	-0.1	-0.1	-0.1	-0.1
39.1	12.0	13.0	-9.4	11.0	10.0	1.4	-2.1	11.0	-0.1	-0.1	-0.1	-0.1	-0.1	-0.1	-0.1	-0.1
48.8	12.0	13.0	-9.8	11.0	13.0	2.1	-2.8	13.0	-0.2	-0.1	-0.2	-0.2	-0.2	-0.1	-0.2	-0.2
58.6	12.0	12.0	-9.7	11.0	15.0	2.9	-3.5	15.0	-0.3	-0.2	-0.1	-0.1	-0.1	-0.1	-0.2	-0.2
68.4	11.0	13.0	-9.8	9.0	18.0	3.4	-4.2	19.0	-0.1	-0.1	-0.1	-0.1	-0.1	-0.3	-0.2	-0.3
78.1	11.0	13.0	-10.0	9.0	21.0	3.6	-4.8	22.0	-0.1	-0.2	-0.1	-0.1	-0.1	-0.2	-0.1	-0.1
87.9	10.0	13.0	-10.0	8.7	23.0	4.0	-5.6	24.0	-0.2	-0.1	-0.1	-0.2	-0.1	-0.1	-0.1	-0.2
97.7	9.9	13.0	-11.0	8.2	26.0	4.5	-6.4	27.0	-0.1	-0.1	-0.2	-0.1	-0.1	-0.1	-0.1	-0.2
107.4	9.4	13.0	-10.0	7.9	28.0	4.5	-6.8	29.0	-0.1	-0.1	-0.1	-0.1	-0.1	-0.1	-0.1	-0.1
117.2	8.0	14.0	-11.0	6.4	30.0	5.4	-7.4	31.0	-0.2	-0.1	-0.1	-0.1	0.0	-0.1	-0.1	-0.1
127.0	6.8	14.0	-11.0	5.9	32.0	5.9	-8.0	33.0	-0.1	-0.1	-0.1	-0.2	-0.1	-0.2	-0.1	-0.2
136.7	4.5	15.0	-10.0	3.1	35.0	6.6	-9.3	36.0	-0.1	-0.1	-0.1	-0.1	-0.1	-0.1	-0.1	-0.1

Table 34. Raw data for the test seal at ω=10 krpm, PD=48.3 bars, C_r=0.188 mm, and inlet GVF=2%

Freq.	Re($\boldsymbol{H_{XX}}$)	Re($\boldsymbol{H_{XY}}$)	Re($\boldsymbol{H_{YX}}$)	Re($\boldsymbol{H_{YY}}$)	Im($\boldsymbol{H_{XX}}$)	Im($\boldsymbol{H_{XY}}$)	Im($\boldsymbol{H_{YX}}$)	Im($\boldsymbol{H_{YY}}$)	Re($\boldsymbol{eH_{XX}}$)	Re($\boldsymbol{eH_{XY}}$)	Re($\boldsymbol{eH_{YX}}$)	Re($\boldsymbol{eH_{YY}}$)	Im($\boldsymbol{eH_{XX}}$)	Im($\boldsymbol{eH_{XY}}$)	Im($\boldsymbol{eH_{YX}}$)	Im($\boldsymbol{eH_{YY}}$)
Hz	MN/m	MN/m	MN/m	MN/m	MN/m	MN/m	MN/m	MN/m	MN/m	MN/m	MN/m	MN/m	MN/m	MN/m	MN/m	MN/m
9.8	13.0	11.0	-11.0	13.0	2.8	0.0	-0.3	3.1	-0.3	-0.2	-0.2	-0.3	-0.2	-0.3	-0.2	-0.1
19.5	13.0	11.0	-10.0	13.0	5.4	0.9	-0.6	5.5	-0.2	-0.2	-0.1	-0.1	-0.1	-0.1	-0.1	-0.2
29.3	13.0	11.0	-9.7	13.0	7.7	1.5	-1.1	8.3	-0.2	-0.2	-0.1	-0.1	-0.1	-0.2	-0.2	-0.1
39.1	13.0	12.0	-9.8	13.0	10.0	1.7	-2.1	11.0	-0.1	-0.1	-0.1	-0.1	-0.1	-0.1	-0.2	-0.1
48.8	13.0	11.0	-10.0	13.0	13.0	2.3	-3.1	13.0	-0.1	-0.2	-0.1	-0.1	-0.1	-0.1	-0.2	-0.2
58.6	12.0	12.0	-10.0	12.0	15.0	2.5	-2.9	15.0	-0.2	-0.3	-0.2	-0.2	-0.2	-0.1	-0.1	-0.1
68.4	12.0	12.0	-10.0	11.0	18.0	3.0	-3.9	18.0	-0.2	-0.1	-0.2	-0.3	-0.2	-0.3	-0.2	-0.3
78.1	12.0	12.0	-10.0	11.0	21.0	3.7	-4.6	22.0	-0.2	-0.1	-0.2	-0.2	-0.1	-0.2	-0.2	-0.1
87.9	11.0	12.0	-11.0	11.0	23.0	4.2	-5.4	24.0	-0.2	-0.1	-0.1	-0.1	-0.1	-0.1	-0.1	-0.1
97.7	10.0	12.0	-11.0	10.0	26.0	4.6	-5.7	26.0	-0.1	-0.2	-0.1	-0.1	-0.1	0.0	-0.2	-0.2
107.4	9.9	13.0	-11.0	10.0	28.0	5.0	-6.2	28.0	-0.1	-0.1	-0.1	-0.1	-0.1	-0.1	-0.1	-0.2
117.2	8.9	13.0	-11.0	8.4	30.0	5.6	-7.1	30.0	-0.1	-0.1	-0.1	-0.1	-0.1	-0.1	-0.1	-0.1
127.0	7.2	12.0	-11.0	7.4	31.0	6.7	-7.0	32.0	-0.2	-0.1	-0.2	-0.3	-0.2	-0.1	-0.1	-0.1
136.7	4.6	13.0	-11.0	4.6	35.0	7.3	-8.8	36.0	-0.1	-0.1	-0.1	-0.1	-0.1	-0.1	-0.1	-0.1

Table 35. Raw data for the test seal at ω=10 krpm, PD=48.3 bars, C_r=0.188 mm, and inlet GVF=4%

Freq.	Re($\boldsymbol{H_{XX}}$)	Re($\boldsymbol{H_{XY}}$)	Re($\boldsymbol{H_{YX}}$)	Re($\boldsymbol{H_{YY}}$)	Im($\boldsymbol{H_{XX}}$)	Im($\boldsymbol{H_{XY}}$)	Im($\boldsymbol{H_{YX}}$)	Im($\boldsymbol{H_{YY}}$)	Re($\boldsymbol{eH_{XX}}$)	Re($\boldsymbol{eH_{XY}}$)	Re($\boldsymbol{eH_{YX}}$)	Re($\boldsymbol{eH_{YY}}$)	Im($\boldsymbol{eH_{XX}}$)	Im($\boldsymbol{eH_{XY}}$)	Im($\boldsymbol{eH_{YX}}$)	Im($\boldsymbol{eH_{YY}}$)
Hz	MN/m	MN/m	MN/m	MN/m	MN/m	MN/m	MN/m	MN/m	MN/m	MN/m	MN/m	MN/m	MN/m	MN/m	MN/m	MN/m
9.8	13.0	11.0	-9.7	13.0	2.8	0.4	-0.7	2.9	-0.2	-0.1	-0.2	-0.1	-0.3	-0.2	-0.1	-0.1
19.5	13.0	11.0	-9.5	13.0	5.5	1.2	-0.8	5.6	-0.2	-0.1	-0.1	-0.1	-0.1	-0.1	-0.1	-0.1
29.3	13.0	11.0	-9.4	13.0	7.9	1.6	-1.3	8.1	-0.1	-0.1	-0.2	-0.2	-0.1	-0.2	-0.1	-0.2
39.1	13.0	11.0	-9.5	13.0	10.0	1.9	-2.4	11.0	-0.1	-0.1	0.0	-0.1	-0.1	-0.1	-0.1	-0.1
48.8	13.0	12.0	-10.0	13.0	13.0	2.3	-2.7	13.0	-0.1	-0.1	-0.1	-0.1	-0.2	-0.2	-0.1	-0.1
58.6	12.0	12.0	-10.0	12.0	16.0	2.6	-2.8	15.0	-0.2	-0.1	-0.2	-0.1	-0.1	-0.2	-0.2	-0.3
68.4	12.0	12.0	-9.2	12.0	19.0	3.1	-3.8	19.0	-0.2	-0.3	-0.2	-0.2	-0.2	-0.3	-0.1	-0.3
78.1	12.0	11.0	-10.0	12.0	21.0	3.8	-4.9	21.0	-0.2	-0.2	-0.2	-0.1	-0.1	-0.1	-0.1	-0.2
87.9	12.0	12.0	-11.0	11.0	23.0	4.2	-4.8	24.0	-0.1	-0.1	-0.1	-0.1	-0.1	-0.1	-0.1	-0.2
97.7	11.0	12.0	-11.0	11.0	25.0	4.5	-5.4	26.0	-0.1	-0.1	-0.1	-0.1	-0.1	-0.2	-0.1	-0.1
107.4	10.0	12.0	-11.0	10.0	28.0	4.7	-5.7	28.0	-0.1	-0.2	-0.2	-0.2	-0.1	-0.1	-0.1	-0.1
117.2	9.1	12.0	-10.0	8.5	30.0	5.0	-6.5	30.0	-0.1	-0.1	-0.1	-0.1	-0.1	-0.2	-0.1	-0.1
127.0	7.9	12.0	-10.0	6.8	31.0	5.6	-7.1	33.0	-0.1	-0.1	-0.2	-0.2	-0.2	-0.3	-0.2	-0.2
136.7	4.4	13.0	-10.0	4.4	34.0	6.8	-8.5	36.0	-0.1	-0.2	-0.2	-0.1	-0.2	-0.2	-0.1	-0.2

Table 36. Raw data for the test seal at ω=10 krpm, PD=48.3 bars, C_r=0.188 mm, and inlet GVF=6%

Freq.	Re($\boldsymbol{H_{XX}}$)	Re($\boldsymbol{H_{XY}}$)	Re($\boldsymbol{H_{YX}}$)	Re($\boldsymbol{H_{YY}}$)	Im($\boldsymbol{H_{XX}}$)	Im($\boldsymbol{H_{XY}}$)	Im($\boldsymbol{H_{YX}}$)	Im($\boldsymbol{H_{YY}}$)	Re($\boldsymbol{eH_{XX}}$)	Re($\boldsymbol{eH_{XY}}$)	Re($\boldsymbol{eH_{YX}}$)	Re($\boldsymbol{eH_{YY}}$)	Im($\boldsymbol{eH_{XX}}$)	Im($\boldsymbol{eH_{XY}}$)	Im($\boldsymbol{eH_{YX}}$)	Im($\boldsymbol{eH_{YY}}$)
Hz	MN/m	MN/m	MN/m	MN/m	MN/m	MN/m	MN/m	MN/m	MN/m	MN/m	MN/m	MN/m	MN/m	MN/m	MN/m	MN/m
9.8	12.0	12.0	-9.6	12.0	2.8	0.3	-0.9	3.2	-0.1	-0.2	-0.3	-0.1	-0.2	-0.2	-0.2	-0.2
19.5	12.0	12.0	-9.6	11.0	5.7	0.8	-1.5	6.0	-0.2	-0.2	-0.2	-0.1	-0.1	-0.1	-0.1	-0.1
29.3	11.0	12.0	-9.8	12.0	8.1	1.6	-2.2	8.9	0.0	-0.1	-0.1	-0.2	-0.1	-0.2	-0.1	-0.3
39.1	11.0	12.0	-10.0	12.0	11.0	2.0	-2.6	12.0	-0.1	-0.2	-0.1	-0.1	-0.1	-0.1	-0.1	-0.1
48.8	11.0	13.0	-10.0	11.0	14.0	2.0	-2.9	14.0	-0.2	-0.2	-0.1	-0.2	-0.1	-0.1	-0.1	-0.1
58.6	11.0	13.0	-10.0	11.0	17.0	1.7	-2.6	16.0	-0.2	-0.2	-0.2	-0.2	-0.2	-0.1	-0.3	-0.2
68.4	10.0	12.0	-9.9	11.0	20.0	2.2	-3.4	20.0	-0.2	-0.1	-0.1	-0.1	-0.2	-0.4	-0.1	-0.2
78.1	11.0	12.0	-10.0	9.9	23.0	2.8	-4.6	22.0	-0.2	-0.2	-0.1	-0.1	-0.1	-0.1	-0.2	-0.2
87.9	10.0	12.0	-11.0	9.5	25.0	3.1	-4.8	25.0	-0.1	0.0	-0.1	-0.2	-0.1	-0.1	-0.1	-0.1
97.7	9.4	13.0	-11.0	10.0	27.0	3.7	-5.2	27.0	-0.1	-0.1	-0.2	-0.2	-0.1	-0.1	-0.2	-0.2
107.4	8.8	13.0	-11.0	9.1	30.0	3.8	-5.7	30.0	-0.2	-0.1	-0.1	-0.2	-0.1	-0.2	-0.1	-0.1
117.2	7.9	13.0	-10.0	7.6	32.0	4.2	-6.7	32.0	-0.2	-0.1	-0.1	-0.1	-0.1	0.0	-0.1	-0.2
127.0	6.4	13.0	-11.0	7.4	34.0	4.7	-6.2	34.0	-0.2	-0.5	-0.1	-0.2	-0.1	-0.2	-0.2	-0.1
136.7	4.3	13.0	-10.0	4.4	37.0	5.0	-7.7	38.0	-0.2	-0.1	-0.2	-0.2	-0.1	-0.2	-0.2	-0.3

Table 37. Raw data for the test seal at ω=10 krpm, PD=48.3 bars, C_r=0.188 mm, and inlet GVF=8%

Freq.	Re($\boldsymbol{H_{XX}}$)	Re($\boldsymbol{H_{XY}}$)	Re($\boldsymbol{H_{YX}}$)	Re($\boldsymbol{H_{YY}}$)	Im($\boldsymbol{H_{XX}}$)	Im($\boldsymbol{H_{XY}}$)	Im($\boldsymbol{H_{YX}}$)	Im($\boldsymbol{H_{YY}}$)	Re($\boldsymbol{eH_{XX}}$)	Re($\boldsymbol{eH_{XY}}$)	Re($\boldsymbol{eH_{YX}}$)	Re($\boldsymbol{eH_{YY}}$)	Im($\boldsymbol{eH_{XX}}$)	Im($\boldsymbol{eH_{XY}}$)	Im($\boldsymbol{eH_{YX}}$)	Im($\boldsymbol{eH_{YY}}$)
Hz	MN/m	MN/m	MN/m	MN/m	MN/m	MN/m	MN/m	MN/m	MN/m	MN/m	MN/m	MN/m	MN/m	MN/m	MN/m	MN/m
9.8	8.4	12.0	-10.0	7.7	2.6	0.3	-0.7	3.3	-0.2	-0.3	-0.1	-0.1	-0.2	-0.1	-0.1	-0.1
19.5	8.0	12.0	-11.0	7.3	6.1	0.9	-1.3	6.1	-0.2	-0.1	-0.2	-0.1	-0.1	-0.1	-0.2	-0.1
29.3	7.9	13.0	-11.0	7.1	8.8	1.6	-1.8	9.0	-0.2	-0.2	-0.2	-0.1	-0.2	-0.1	-0.2	-0.2
39.1	8.0	13.0	-11.0	7.3	11.0	1.6	-2.2	12.0	-0.1	-0.1	-0.2	-0.2	-0.1	-0.1	-0.1	-0.1
48.8	7.3	14.0	-12.0	7.0	14.0	1.6	-2.2	15.0	-0.1	-0.1	-0.2	-0.1	-0.3	-0.2	-0.1	-0.1
58.6	6.7	13.0	-11.0	7.0	18.0	1.7	-2.0	18.0	-0.2	-0.2	-0.2	-0.1	-0.2	-0.1	-0.3	-0.1
68.4	6.6	13.0	-11.0	6.4	22.0	1.5	-2.7	21.0	-0.2	-0.2	-0.2	-0.2	-0.2	-0.2	-0.2	-0.2
78.1	7.4	13.0	-11.0	6.2	24.0	1.9	-3.4	25.0	-0.1	-0.2	-0.2	-0.1	-0.3	-0.1	-0.2	-0.1
87.9	7.1	13.0	-11.0	6.0	27.0	2.1	-3.9	27.0	-0.1	-0.1	-0.1	-0.1	-0.2	-0.2	-0.1	-0.1
97.7	6.5	13.0	-12.0	6.0	29.0	2.6	-4.3	30.0	-0.2	-0.1	-0.2	-0.1	-0.2	-0.2	-0.1	-0.1
107.4	5.8	14.0	-11.0	5.6	33.0	2.8	-5.0	33.0	-0.3	-0.1	-0.1	-0.1	-0.2	-0.1	-0.2	-0.1
117.2	5.4	14.0	-12.0	4.3	35.0	2.9	-5.2	36.0	-0.1	-0.1	-0.1	-0.1	-0.2	-0.1	-0.2	-0.1
127.0	4.7	13.0	-12.0	3.6	37.0	3.0	-5.2	39.0	-0.2	-0.4	-0.1	-0.2	-0.2	-0.3	-0.3	-0.2
136.7	2.6	14.0	-12.0	2.2	41.0	3.8	-5.8	43.0	-0.1	-0.2	0.0	-0.1	-0.2	-0.2	-0.1	-0.1

Table 38. Raw data for the test seal at ω=10 krpm, PD=48.3 bars, C_r=0.188 mm, and inlet GVF=10%

Freq.	Re($\boldsymbol{H_{XX}}$)	Re($\boldsymbol{H_{XY}}$)	Re($\boldsymbol{H_{YX}}$)	Re($\boldsymbol{H_{YY}}$)	Im($\boldsymbol{H_{XX}}$)	Im($\boldsymbol{H_{XY}}$)	Im($\boldsymbol{H_{YX}}$)	Im($\boldsymbol{H_{YY}}$)	Re($\boldsymbol{eH_{XX}}$)	Re($\boldsymbol{eH_{XY}}$)	Re($\boldsymbol{eH_{YX}}$)	Re($\boldsymbol{eH_{YY}}$)	Im($\boldsymbol{eH_{XX}}$)	Im($\boldsymbol{eH_{XY}}$)	Im($\boldsymbol{eH_{YX}}$)	Im($\boldsymbol{eH_{YY}}$)
Hz	MN/m	MN/m	MN/m	MN/m	MN/m	MN/m	MN/m	MN/m	MN/m	MN/m	MN/m	MN/m	MN/m	MN/m	MN/m	MN/m
9.8	14.0	21.0	-19.0	15.0	2.3	1.5	-1.2	1.3	-0.4	-0.4	-0.3	-0.4	-0.3	-0.3	-0.4	-0.3
19.5	14.0	21.0	-19.0	14.0	4.7	1.8	-2.8	5.1	-0.2	-0.3	-0.4	-0.3	-0.5	-0.4	-0.5	-0.4
29.3	14.0	21.0	-19.0	13.0	7.9	1.9	-3.5	7.1	-0.2	-0.3	-0.5	-0.4	-0.6	-0.6	-0.2	-0.4
39.1	13.0	21.0	-19.0	13.0	9.8	3.1	-3.2	9.8	-0.2	-0.3	-0.2	-0.3	-0.4	-0.5	-0.4	-0.3
48.8	13.0	21.0	-19.0	13.0	12.0	3.8	-4.8	12.0	-0.3	-0.4	-0.2	-0.2	-0.3	-0.2	-0.3	-0.3
58.6	12.0	21.0	-19.0	12.0	14.0	5.4	-5.0	15.0	-0.2	-0.2	-0.2	-0.2	-0.3	-0.3	-0.3	-0.2
68.4	11.0	20.0	-19.0	11.0	18.0	6.3	-6.5	18.0	-0.1	-0.1	-0.2	-0.3	-0.3	-0.4	-0.2	-0.3
78.1	11.0	20.0	-19.0	11.0	20.0	7.2	-8.2	21.0	-0.2	-0.2	-0.2	-0.2	-0.1	-0.2	-0.3	-0.2
87.9	11.0	20.0	-19.0	11.0	23.0	9.2	-10.0	24.0	-0.2	-0.2	-0.2	-0.3	-0.1	-0.2	-0.2	-0.2
97.7	11.0	23.0	-20.0	10.0	25.0	11.0	-12.0	25.0	-0.4	-0.3	-0.3	-0.3	-0.3	-0.4	-0.2	-0.3
107.4	7.3	24.0	-22.0	8.2	26.0	10.0	-11.0	27.0	-0.2	-0.2	-0.4	-0.3	-0.2	-0.2	-0.3	-0.3
117.2	5.1	24.0	-21.0	5.7	29.0	11.0	-11.0	30.0	-0.2	-0.2	-0.2	-0.2	-0.3	-0.3	-0.2	-0.1
127.0	3.2	24.0	-21.0	4.3	33.0	11.0	-11.0	33.0	-0.3	-0.4	-0.3	-0.4	-0.3	-0.4	-0.3	-0.3
136.7	1.6	23.0	-21.0	2.3	36.0	12.0	-14.0	37.0	-0.3	-0.1	-0.2	-0.3	-0.1	-0.3	-0.2	-0.2

Table 39. Raw data for the test seal at ω=15 krpm, PD=48.3 bars, C_r=0.188 mm, and inlet GVF=0%

Freq.	Re($\boldsymbol{H_{XX}}$)	Re($\boldsymbol{H_{XY}}$)	Re($\boldsymbol{H_{YX}}$)	Re($\boldsymbol{H_{YY}}$)	Im($\boldsymbol{H_{XX}}$)	Im($\boldsymbol{H_{XY}}$)	Im($\boldsymbol{H_{YX}}$)	Im($\boldsymbol{H_{YY}}$)	Re($\boldsymbol{eH_{XX}}$)	Re($\boldsymbol{eH_{XY}}$)	Re($\boldsymbol{eH_{YX}}$)	Re($\boldsymbol{eH_{YY}}$)	Im($\boldsymbol{eH_{XX}}$)	Im($\boldsymbol{eH_{XY}}$)	Im($\boldsymbol{eH_{YX}}$)	Im($\boldsymbol{eH_{YY}}$)
Hz	MN/m	MN/m	MN/m	MN/m	MN/m	MN/m	MN/m	MN/m	MN/m	MN/m	MN/m	MN/m	MN/m	MN/m	MN/m	MN/m
9.8	15.0	20.0	-19.0	14.0	2.0	0.7	-1.4	2.2	-0.2	-0.2	-0.3	-0.3	-0.2	-0.2	-0.3	-0.3
19.5	15.0	20.0	-19.0	14.0	4.5	1.9	-1.8	5.3	-0.3	-0.3	-0.2	-0.2	-0.2	-0.3	-0.2	-0.2
29.3	13.0	21.0	-19.0	13.0	7.1	3.2	-2.7	7.4	-0.4	-0.5	-0.2	-0.2	-0.3	-0.4	-0.4	-0.5
39.1	13.0	21.0	-19.0	13.0	10.0	3.1	-3.5	10.0	-0.2	-0.3	-0.3	-0.4	-0.2	-0.4	-0.2	-0.3
48.8	12.0	21.0	-19.0	13.0	12.0	3.6	-4.2	13.0	-0.2	-0.3	-0.3	-0.3	-0.2	-0.2	-0.2	-0.3
58.6	12.0	21.0	-19.0	12.0	15.0	4.4	-5.0	15.0	-0.2	-0.2	-0.2	-0.3	-0.2	-0.3	-0.2	-0.1
68.4	11.0	20.0	-19.0	12.0	18.0	5.7	-6.0	18.0	-0.2	-0.2	-0.2	-0.4	-0.2	-0.2	-0.2	-0.4
78.1	11.0	20.0	-19.0	11.0	21.0	6.9	-7.4	21.0	-0.2	-0.2	-0.2	-0.2	-0.1	-0.1	-0.1	-0.2
87.9	11.0	20.0	-19.0	11.0	23.0	8.9	-9.5	24.0	-0.1	-0.1	-0.2	-0.2	-0.2	-0.2	-0.2	-0.2
97.7	11.0	22.0	-21.0	11.0	25.0	11.0	-12.0	25.0	-0.2	-0.2	-0.3	-0.2	-0.3	-0.2	-0.3	-0.3
107.4	8.0	24.0	-22.0	8.4	26.0	9.4	-11.0	27.0	-0.2	-0.2	-0.2	-0.2	-0.1	-0.2	-0.2	-0.2
117.2	6.2	24.0	-22.0	6.6	30.0	9.7	-11.0	30.0	-0.2	-0.2	-0.2	-0.1	-0.1	-0.1	-0.2	-0.2
127.0	4.7	23.0	-22.0	4.7	33.0	9.6	-11.0	34.0	-0.3	-0.3	-0.2	-0.3	-0.2	-0.3	-0.3	-0.5
136.7	2.7	23.0	-21.0	4.0	36.0	11.0	-13.0	37.0	-0.2	-0.2	-0.2	-0.3	-0.2	-0.3	-0.2	-0.2

Table 40. Raw data for the test seal at ω=15 krpm, PD=48.3 bars, C_r=0.188 mm, and inlet GVF=2%

Freq.	Re($\boldsymbol{H_{XX}}$)	Re($\boldsymbol{H_{XY}}$)	Re($\boldsymbol{H_{YX}}$)	Re($\boldsymbol{H_{YY}}$)	Im($\boldsymbol{H_{XX}}$)	Im($\boldsymbol{H_{XY}}$)	Im($\boldsymbol{H_{YX}}$)	Im($\boldsymbol{H_{YY}}$)	Re($\boldsymbol{eH_{XX}}$)	Re($\boldsymbol{eH_{XY}}$)	Re($\boldsymbol{eH_{YX}}$)	Re($\boldsymbol{eH_{YY}}$)	Im($\boldsymbol{eH_{XX}}$)	Im($\boldsymbol{eH_{XY}}$)	Im($\boldsymbol{eH_{YX}}$)	Im($\boldsymbol{eH_{YY}}$)
Hz	MN/m	MN/m	MN/m	MN/m	MN/m	MN/m	MN/m	MN/m	MN/m	MN/m	MN/m	MN/m	MN/m	MN/m	MN/m	MN/m
9.8	15.0	19.0	-18.0	15.0	2.0	0.2	-1.6	2.5	-0.2	-0.3	-0.2	-0.2	-0.2	-0.3	-0.1	-0.2
19.5	14.0	20.0	-19.0	14.0	4.4	2.7	-2.1	4.8	-0.2	-0.2	-0.2	-0.3	-0.3	-0.2	-0.2	-0.2
29.3	15.0	20.0	-19.0	14.0	7.0	2.1	-3.4	7.6	-0.4	-0.5	-0.3	-0.4	-0.1	-0.2	-0.4	-0.5
39.1	14.0	20.0	-19.0	14.0	9.1	3.2	-3.8	9.5	-0.2	-0.2	-0.3	-0.3	-0.2	-0.2	-0.2	-0.1
48.8	13.0	20.0	-19.0	13.0	12.0	4.2	-4.4	13.0	-0.2	-0.1	-0.2	-0.2	-0.2	-0.1	-0.3	-0.3
58.6	12.0	21.0	-19.0	12.0	15.0	5.1	-5.6	15.0	-0.2	-0.3	-0.3	-0.2	-0.2	-0.3	-0.3	-0.3
68.4	12.0	21.0	-19.0	12.0	18.0	5.4	-6.4	18.0	-0.2	-0.4	-0.3	-0.4	-0.3	-0.4	-0.2	-0.3
78.1	12.0	21.0	-19.0	12.0	21.0	6.4	-7.5	20.0	-0.2	-0.2	-0.1	-0.2	-0.1	-0.2	-0.1	-0.1
87.9	12.0	21.0	-20.0	11.0	23.0	8.1	-8.7	23.0	-0.1	-0.2	-0.1	-0.1	-0.2	-0.2	-0.1	-0.1
97.7	11.0	22.0	-21.0	11.0	24.0	9.5	-11.0	25.0	-0.2	-0.2	-0.1	-0.1	-0.2	-0.2	-0.2	-0.1
107.4	8.4	24.0	-22.0	9.2	26.0	9.6	-11.0	27.0	-0.3	-0.2	-0.2	-0.3	-0.2	-0.3	-0.3	-0.3
117.2	5.8	24.0	-22.0	6.5	29.0	9.3	-11.0	30.0	-0.3	-0.2	-0.2	-0.2	-0.1	-0.2	-0.3	-0.2
127.0	3.0	24.0	-22.0	4.2	33.0	9.2	-10.0	33.0	-0.4	-0.5	-0.5	-0.7	-0.5	-0.7	-0.4	-0.5
136.7	2.0	23.0	-21.0	2.0	37.0	11.0	-13.0	37.0	-0.3	-0.3	-0.2	-0.2	-0.2	-0.2	-0.3	-0.3

Table 41. Raw data for the test seal at ω=15 krpm, PD=48.3 bars, C_r=0.188 mm, and inlet GVF=4%

Freq.	Re($\boldsymbol{H_{XX}}$)	Re($\boldsymbol{H_{XY}}$)	Re($\boldsymbol{H_{YX}}$)	Re($\boldsymbol{H_{YY}}$)	Im($\boldsymbol{H_{XX}}$)	Im($\boldsymbol{H_{XY}}$)	Im($\boldsymbol{H_{YX}}$)	Im($\boldsymbol{H_{YY}}$)	Re($\boldsymbol{eH_{XX}}$)	Re($\boldsymbol{eH_{XY}}$)	Re($\boldsymbol{eH_{YX}}$)	Re($\boldsymbol{eH_{YY}}$)	Im($\boldsymbol{eH_{XX}}$)	Im($\boldsymbol{eH_{XY}}$)	Im($\boldsymbol{eH_{YX}}$)	Im($\boldsymbol{eH_{YY}}$)
Hz	MN/m	MN/m	MN/m	MN/m	MN/m	MN/m	MN/m	MN/m	MN/m	MN/m	MN/m	MN/m	MN/m	MN/m	MN/m	MN/m
9.8	16.0	20.0	-17.0	15.0	2.0	1.1	-1.1	2.7	-0.3	-0.3	-0.3	-0.4	-0.3	-0.2	-0.3	-0.4
19.5	14.0	19.0	-17.0	15.0	5.0	1.5	-2.0	4.4	-0.2	-0.3	-0.3	-0.3	-0.4	-0.3	-0.6	-0.4
29.3	14.0	19.0	-18.0	14.0	6.3	3.2	-3.6	7.4	-0.2	-0.3	-0.3	-0.5	-0.4	-0.4	-0.3	-0.6
39.1	13.0	20.0	-19.0	14.0	8.9	3.4	-4.0	9.6	-0.2	-0.2	-0.2	-0.2	-0.2	-0.2	-0.2	-0.3
48.8	13.0	20.0	-18.0	13.0	12.0	4.1	-5.0	12.0	-0.2	-0.2	-0.1	-0.1	-0.3	-0.3	-0.2	-0.2
58.6	12.0	20.0	-19.0	12.0	15.0	5.3	-6.1	15.0	-0.3	-0.3	-0.3	-0.4	-0.2	-0.3	-0.3	-0.3
68.4	12.0	20.0	-19.0	13.0	18.0	5.5	-6.6	18.0	-0.2	-0.2	-0.2	-0.2	-0.3	-0.5	-0.3	-0.4
78.1	12.0	21.0	-19.0	12.0	21.0	6.9	-8.2	21.0	-0.1	-0.1	-0.3	-0.2	-0.2	-0.2	-0.2	-0.2
87.9	11.0	21.0	-20.0	11.0	22.0	9.1	-9.3	23.0	-0.2	-0.2	-0.1	-0.1	-0.2	-0.2	-0.2	-0.2
97.7	11.0	22.0	-21.0	10.0	24.0	10.0	-11.0	25.0	-0.2	-0.2	-0.2	-0.2	-0.2	-0.2	-0.2	-0.3
107.4	9.3	25.0	-22.0	9.7	27.0	9.5	-11.0	27.0	-0.3	-0.3	-0.4	-0.3	-0.3	-0.4	-0.2	-0.3
117.2	6.0	25.0	-24.0	7.0	30.0	8.3	-10.0	30.0	-0.4	-0.3	-0.5	-0.3	-0.2	-0.2	-0.3	-0.4
127.0	4.1	24.0	-24.0	5.4	34.0	7.5	-8.9	34.0	-0.4	-0.7	-0.5	-0.4	-0.3	-0.3	-0.5	-0.9
136.7	3.0	24.0	-21.0	3.9	39.0	8.8	-11.0	39.0	-0.3	-0.4	-0.3	-0.4	-0.3	-0.3	-0.5	-0.4

Table 42. Raw data for the test seal at ω=15 krpm, PD=48.3 bars, C_r=0.188 mm, and inlet GVF=6%

Freq.	Re($\boldsymbol{H_{XX}}$)	Re($\boldsymbol{H_{XY}}$)	Re($\boldsymbol{H_{YX}}$)	Re($\boldsymbol{H_{YY}}$)	Im($\boldsymbol{H_{XX}}$)	Im($\boldsymbol{H_{XY}}$)	Im($\boldsymbol{H_{YX}}$)	Im($\boldsymbol{H_{YY}}$)	Re($\boldsymbol{eH_{XX}}$)	Re($\boldsymbol{eH_{XY}}$)	Re($\boldsymbol{eH_{YX}}$)	Re($\boldsymbol{eH_{YY}}$)	Im($\boldsymbol{eH_{XX}}$)	Im($\boldsymbol{eH_{XY}}$)	Im($\boldsymbol{eH_{YX}}$)	Im($\boldsymbol{eH_{YY}}$)
Hz	MN/m	MN/m	MN/m	MN/m	MN/m	MN/m	MN/m	MN/m	MN/m	MN/m	MN/m	MN/m	MN/m	MN/m	MN/m	MN/m
9.8	14.0	20.0	-19.0	15.0	2.2	0.7	-1.0	3.4	-0.4	-0.4	-0.3	-0.3	-0.3	-0.4	-0.3	-0.3
19.5	13.0	20.0	-19.0	13.0	4.2	1.3	-1.3	4.8	-0.2	-0.3	-0.4	-0.4	-0.5	-0.6	-0.4	-0.3
29.3	13.0	20.0	-18.0	13.0	6.5	3.0	-2.8	7.7	-0.3	-0.3	-0.3	-0.5	-0.3	-0.5	-0.3	-0.5
39.1	12.0	21.0	-19.0	13.0	9.3	3.8	-4.0	9.3	-0.2	-0.1	-0.2	-0.2	-0.2	-0.3	-0.2	-0.3
48.8	11.0	21.0	-19.0	11.0	12.0	3.8	-4.1	12.0	-0.2	-0.1	-0.2	-0.2	-0.2	-0.3	-0.2	-0.2
58.6	10.0	20.0	-19.0	11.0	15.0	5.4	-4.9	16.0	-0.3	-0.2	-0.3	-0.3	-0.2	-0.3	-0.4	-0.4
68.4	11.0	20.0	-19.0	10.0	19.0	6.0	-6.8	19.0	-0.4	-0.5	-0.3	-0.4	-0.2	-0.4	-0.4	-0.4
78.1	11.0	22.0	-20.0	11.0	22.0	7.4	-7.8	21.0	-0.2	-0.2	-0.3	-0.3	-0.3	-0.3	-0.2	-0.2
87.9	9.6	23.0	-21.0	9.7	23.0	8.5	-9.1	24.0	-0.1	-0.2	-0.1	-0.1	-0.1	-0.2	-0.1	-0.2
97.7	9.1	24.0	-22.0	9.2	26.0	8.5	-9.9	26.0	-0.1	-0.2	-0.3	-0.2	-0.3	-0.2	-0.2	-0.2
107.4	8.1	26.0	-24.0	8.0	28.0	8.0	-11.0	28.0	-0.2	-0.3	-0.2	-0.3	-0.3	-0.3	-0.3	-0.2
117.2	5.1	27.0	-25.0	5.4	31.0	6.7	-9.3	31.0	-0.2	-0.2	-0.2	-0.3	-0.3	-0.3	-0.3	-0.2
127.0	4.2	25.0	-23.0	2.4	36.0	4.9	-8.4	36.0	-0.4	-0.6	-0.4	-0.6	-0.3	-0.4	-0.4	-0.4
136.7	1.9	24.0	-23.0	2.9	40.0	8.7	-9.0	41.0	-0.2	-0.2	-0.3	-0.3	-0.2	-0.2	-0.2	-0.3

Table 43. Raw data for the test seal at ω=15 krpm, PD=48.3 bars, C_r=0.188 mm, and inlet GVF=8%

Freq.	Re($\boldsymbol{H_{XX}}$)	Re($\boldsymbol{H_{XY}}$)	Re($\boldsymbol{H_{YX}}$)	Re($\boldsymbol{H_{YY}}$)	Im($\boldsymbol{H_{XX}}$)	Im($\boldsymbol{H_{XY}}$)	Im($\boldsymbol{H_{YX}}$)	Im($\boldsymbol{H_{YY}}$)	Re($\boldsymbol{eH_{XX}}$)	Re($\boldsymbol{eH_{XY}}$)	Re($\boldsymbol{eH_{YX}}$)	Re($\boldsymbol{eH_{YY}}$)	Im($\boldsymbol{eH_{XX}}$)	Im($\boldsymbol{eH_{XY}}$)	Im($\boldsymbol{eH_{YX}}$)	Im($\boldsymbol{eH_{YY}}$)
Hz	MN/m	MN/m	MN/m	MN/m	MN/m	MN/m	MN/m	MN/m	MN/m	MN/m	MN/m	MN/m	MN/m	MN/m	MN/m	MN/m
9.8	11.0	22.0	-20.0	11.0	3.1	0.7	-0.5	0.9	-0.6	-0.6	-0.4	-0.4	-0.3	-0.2	-0.4	-0.3
19.5	11.0	22.0	-20.0	10.0	5.0	1.1	-1.9	4.0	-0.5	-0.4	-0.4	-0.3	-0.3	-0.4	-0.3	-0.2
29.3	10.0	21.0	-20.0	8.9	7.6	1.9	-2.5	8.2	-0.5	-0.5	-0.5	-0.4	-0.4	-0.3	-0.4	-0.4
39.1	9.3	22.0	-21.0	8.9	10.0	2.9	-3.5	9.8	-0.2	-0.2	-0.2	-0.3	-0.3	-0.2	-0.3	-0.2
48.8	8.3	22.0	-21.0	8.7	13.0	3.6	-2.3	14.0	-0.2	-0.2	-0.4	-0.3	-0.3	-0.2	-0.3	-0.3
58.6	7.9	22.0	-20.0	7.9	16.0	4.8	-4.7	17.0	-0.4	-0.3	-0.2	-0.3	-0.3	-0.3	-0.3	-0.2
68.4	7.6	22.0	-21.0	7.3	19.0	5.8	-7.2	21.0	-0.5	-0.4	-0.4	-0.5	-0.3	-0.3	-0.6	-0.6
78.1	7.3	23.0	-21.0	7.5	23.0	7.0	-6.8	23.0	-0.2	-0.3	-0.5	-0.4	-0.3	-0.2	-0.3	-0.4
87.9	7.1	24.0	-23.0	6.1	25.0	7.7	-8.2	25.0	-0.2	-0.2	-0.2	-0.3	-0.3	-0.2	-0.4	-0.3
97.7	7.2	26.0	-24.0	6.3	28.0	8.0	-9.3	28.0	-0.2	-0.3	-0.4	-0.3	-0.3	-0.1	-0.3	-0.3
107.4	5.1	27.0	-27.0	5.5	29.0	7.0	-9.3	30.0	-0.3	-0.5	-0.4	-0.3	-0.8	-0.6	-0.6	-0.6
117.2	2.5	28.0	-26.0	2.6	33.0	4.5	-6.1	32.0	-0.4	-0.5	-0.9	-0.4	-0.5	-0.3	-0.7	-0.8
127.0	0.2	27.0	-24.0	0.7	39.0	5.4	-6.3	38.0	-0.7	-0.6	-0.5	-0.8	-0.6	-0.6	-0.9	-0.6
136.7	0.4	25.0	-24.0	0.4	42.0	7.3	-7.4	43.0	-0.5	-0.5	-0.6	-0.7	-0.2	-0.4	-0.7	-0.5

Table 44. Raw data for the test seal at ω=15 krpm, PD=48.3 bars, C_r=0.188 mm, and inlet GVF=10%

Freq.	Re(H_{XX})	Re(H_{XY})	Re(H_{YX})	Re(H_{YY})	Im(H_{XX})	Im(H_{XY})	Im(H_{YX})	Im(H_{YY})	Re(eH_{XX})	Re(eH_{XY})	Re(eH_{YX})	Re(eH_{YY})	Im(eH_{XX})	Im(eH_{XY})	Im(eH_{YX})	Im(eH_{YY})
Hz	MN/m	MN/m	MN/m	MN/m	MN/m	MN/m	MN/m	MN/m	MN/m	MN/m	MN/m	MN/m	MN/m	MN/m	MN/m	MN/m
9.8	2.9	6.8	-3.6	1.5	3.2	0.5	-0.3	3.5	-0.3	-0.3	-0.1	-0.5	-0.2	-0.1	-0.2	-0.1
19.5	2.9	7.1	-3.4	1.8	5.3	0.4	-0.6	5.6	-0.2	-0.4	-0.1	-0.4	-0.1	0.0	-0.1	-0.1
29.3	2.6	6.9	-3.5	2.3	7.7	0.8	-0.9	7.8	-0.1	-0.3	-0.1	-0.5	-0.1	-0.1	-0.2	-0.1
39.1	2.0	7.2	-3.6	1.0	10.0	0.2	-1.1	11.0	-0.2	-0.3	-0.1	-0.5	-0.1	-0.2	-0.1	-0.2
48.8	2.0	7.1	-3.5	1.0	13.0	0.5	-1.8	14.0	-0.2	-0.2	-0.2	-0.5	-0.1	-0.2	-0.2	-0.1
58.6	1.5	6.8	-3.4	0.8	15.0	1.3	-1.7	16.0	-0.2	-0.3	-0.2	-0.5	-0.1	-0.1	-0.1	-0.2
68.4	1.1	8.2	-3.5	-0.7	18.0	0.5	-2.5	20.0	-0.1	-0.4	-0.1	-0.4	-0.2	-0.3	-0.2	-0.4
78.1	1.1	7.6	-3.9	-0.1	21.0	1.0	-2.6	22.0	-0.2	-0.4	-0.2	-0.5	-0.1	-0.2	-0.2	-0.2
87.9	-0.3	7.4	-3.9	-1.5	23.0	1.4	-3.2	24.0	-0.1	-0.3	-0.2	-0.4	-0.1	-0.3	-0.2	-0.3
97.7	-1.3	7.4	-4.3	-1.7	26.0	1.5	-3.3	27.0	-0.3	-0.2	-0.1	-0.4	-0.2	-0.2	-0.1	-0.2
107.4	-2.1	7.6	-4.2	-2.3	28.0	1.1	-3.5	29.0	-0.2	-0.2	-0.1	-0.3	-0.1	-0.3	-0.2	-0.2
117.2	-3.7	8.1	-3.9	-3.9	31.0	1.4	-3.6	32.0	-0.2	-0.2	-0.1	-0.4	-0.2	-0.2	-0.2	-0.2
127.0	-4.5	6.9	-3.6	-4.0	34.0	2.4	-3.5	34.0	-0.2	-0.3	-0.2	-0.4	-0.2	-0.4	-0.1	-0.4
136.7	-6.6	8.0	-4.2	-6.8	37.0	1.2	-4.3	39.0	-0.2	-0.2	-0.1	-0.3	-0.1	-0.3	-0.1	-0.4

Table 45. Raw data for the test seal at ω=5 krpm, PD=37.9 bars, C_r=0.188 mm, and inlet GVF=4%

Freq.	Re(H_{XX})	Re(H_{XY})	Re(H_{YX})	Re(H_{YY})	Im(H_{XX})	Im(H_{XY})	Im(H_{YX})	Im(H_{YY})	Re(eH_{XX})	Re(eH_{XY})	Re(eH_{YX})	Re(eH_{YY})	Im(eH_{XX})	Im(eH_{XY})	Im(eH_{YX})	Im(eH_{YY})
Hz	MN/m	MN/m	MN/m	MN/m	MN/m	MN/m	MN/m	MN/m	MN/m	MN/m	MN/m	MN/m	MN/m	MN/m	MN/m	MN/m
9.8	5.9	6.0	-3.2	5.2	3.2	0.2	-0.5	3.2	-0.2	-0.2	-0.1	-0.3	-0.2	-0.1	-0.1	-0.1
19.5	5.7	6.1	-3.3	5.5	5.2	0.8	-0.6	5.2	-0.3	-0.3	-0.1	-0.4	-0.1	-0.3	-0.1	-0.1
29.3	5.6	6.0	-3.5	5.3	7.2	0.7	-0.9	7.6	-0.2	-0.3	-0.2	-0.3	-0.1	-0.1	-0.1	-0.1
39.1	5.2	6.5	-3.6	4.8	10.0	0.3	-0.9	11.0	-0.3	-0.2	-0.1	-0.4	-0.1	-0.1	-0.1	-0.1
48.8	5.2	6.1	-3.4	4.5	13.0	0.6	-1.2	13.0	-0.3	-0.2	-0.1	-0.4	-0.2	-0.1	-0.1	-0.1
58.6	5.0	5.7	-3.5	4.2	15.0	1.0	-1.6	15.0	-0.3	-0.2	-0.2	-0.4	-0.1	0.0	-0.2	-0.1
68.4	4.3	6.5	-3.1	3.5	17.0	0.6	-1.8	18.0	-0.2	-0.3	-0.2	-0.6	-0.2	-0.2	-0.1	-0.2
78.1	4.0	6.4	-3.6	3.2	20.0	1.0	-2.5	21.0	-0.2	-0.2	-0.2	-0.3	-0.1	-0.2	-0.2	-0.3
87.9	3.0	6.5	-3.5	2.1	23.0	1.4	-2.8	23.0	-0.4	-0.3	-0.2	-0.5	-0.2	-0.3	-0.1	-0.2
97.7	2.1	6.4	-3.9	1.9	24.0	1.5	-3.0	26.0	-0.4	-0.2	-0.1	-0.4	-0.1	-0.2	-0.1	-0.1
107.4	1.3	6.5	-4.1	1.3	27.0	1.4	-3.3	28.0	-0.3	-0.3	-0.2	-0.4	-0.2	-0.1	-0.2	-0.1
117.2	0.1	6.7	-3.8	0.0	30.0	1.7	-3.5	31.0	-0.4	-0.1	-0.1	-0.4	-0.1	-0.1	-0.1	-0.2
127.0	-1.4	6.8	-3.9	-0.6	32.0	2.3	-3.2	33.0	-0.3	-0.3	-0.1	-0.3	-0.2	-0.2	-0.1	-0.3
136.7	-3.0	6.7	-3.8	-3.3	35.0	2.0	-4.1	37.0	-0.3	-0.1	-0.2	-0.4	-0.2	-0.3	-0.1	-0.2

Table 46. Raw data for the test seal at ω=5 krpm, PD=37.9 bars, C_r=0.188 mm, and inlet GVF=6%

Freq.	Re($\boldsymbol{H_{XX}}$)	Re($\boldsymbol{H_{XY}}$)	Re($\boldsymbol{H_{YX}}$)	Re($\boldsymbol{H_{YY}}$)	Im($\boldsymbol{H_{XX}}$)	Im($\boldsymbol{H_{XY}}$)	Im($\boldsymbol{H_{YX}}$)	Im($\boldsymbol{H_{YY}}$)	Re($\boldsymbol{eH_{XX}}$)	Re($\boldsymbol{eH_{XY}}$)	Re($\boldsymbol{eH_{YX}}$)	Re($\boldsymbol{eH_{YY}}$)	Im($\boldsymbol{eH_{XX}}$)	Im($\boldsymbol{eH_{XY}}$)	Im($\boldsymbol{eH_{YX}}$)	Im($\boldsymbol{eH_{YY}}$)
Hz	MN/m	MN/m	MN/m	MN/m	MN/m	MN/m	MN/m	MN/m	MN/m	MN/m	MN/m	MN/m	MN/m	MN/m	MN/m	MN/m
9.8	6.8	5.7	-2.8	6.1	2.7	-0.1	-0.4	3.4	-0.2	-0.1	-0.1	-0.3	-0.1	-0.1	-0.2	-0.1
19.5	6.7	5.9	-3.0	6.2	5.0	0.8	-0.7	5.2	-0.2	-0.2	-0.2	-0.3	-0.1	-0.1	-0.1	-0.1
29.3	6.3	5.7	-3.6	6.6	7.4	0.5	-0.9	7.5	-0.1	-0.2	-0.2	-0.2	-0.1	-0.2	-0.1	-0.2
39.1	6.3	6.0	-3.5	6.2	9.9	0.5	-1.3	10.0	-0.1	-0.1	-0.2	-0.2	-0.1	-0.1	-0.2	-0.1
48.8	6.2	5.8	-3.4	5.6	13.0	0.4	-1.0	13.0	-0.2	-0.2	-0.2	-0.3	-0.2	-0.2	-0.2	-0.1
58.6	5.6	5.2	-3.4	5.7	15.0	1.1	-1.7	15.0	-0.1	-0.2	-0.2	-0.3	-0.2	-0.1	-0.2	-0.1
68.4	5.0	5.7	-3.2	4.8	17.0	0.8	-1.7	17.0	-0.1	-0.2	-0.1	-0.3	-0.1	-0.3	-0.1	-0.3
78.1	4.8	6.1	-3.6	4.5	20.0	1.2	-2.5	20.0	-0.2	-0.2	-0.2	-0.3	-0.1	-0.1	-0.1	-0.1
87.9	4.0	6.1	-3.6	3.5	22.0	1.6	-2.8	22.0	-0.1	-0.2	-0.2	-0.3	-0.2	-0.1	-0.1	-0.1
97.7	3.0	5.8	-3.8	2.8	24.0	1.8	-3.1	25.0	0.0	-0.1	-0.2	-0.3	-0.1	-0.1	-0.1	-0.1
107.4	2.4	6.3	-4.0	2.3	27.0	1.6	-3.3	28.0	-0.2	-0.2	-0.1	-0.2	-0.2	-0.1	-0.1	-0.2
117.2	1.2	6.5	-4.0	1.0	29.0	2.0	-3.3	30.0	-0.1	-0.2	-0.1	-0.3	-0.1	-0.1	-0.1	-0.1
127.0	-0.2	6.0	-4.2	0.6	32.0	2.6	-3.4	32.0	-0.1	-0.2	-0.1	-0.2	-0.1	-0.2	-0.1	-0.2
136.7	-1.8	6.6	-3.9	-2.4	35.0	2.0	-4.0	36.0	-0.1	-0.2	-0.1	-0.2	-0.1	-0.1	-0.1	-0.3

Table 47. Raw data for the test seal at ω=5 krpm, PD=37.9 bars, C_r=0.188 mm, and inlet GVF=8%

Freq.	Re($\boldsymbol{H_{XX}}$)	Re($\boldsymbol{H_{XY}}$)	Re($\boldsymbol{H_{YX}}$)	Re($\boldsymbol{H_{YY}}$)	Im($\boldsymbol{H_{XX}}$)	Im($\boldsymbol{H_{XY}}$)	Im($\boldsymbol{H_{YX}}$)	Im($\boldsymbol{H_{YY}}$)	Re($\boldsymbol{eH_{XX}}$)	Re($\boldsymbol{eH_{XY}}$)	Re($\boldsymbol{eH_{YX}}$)	Re($\boldsymbol{eH_{YY}}$)	Im($\boldsymbol{eH_{XX}}$)	Im($\boldsymbol{eH_{XY}}$)	Im($\boldsymbol{eH_{YX}}$)	Im($\boldsymbol{eH_{YY}}$)
Hz	MN/m	MN/m	MN/m	MN/m	MN/m	MN/m	MN/m	MN/m	MN/m	MN/m	MN/m	MN/m	MN/m	MN/m	MN/m	MN/m
9.8	7.1	5.5	-2.9	6.6	3.2	0.1	-0.3	3.2	-0.2	-0.1	-0.1	-0.1	-0.1	-0.1	-0.1	-0.1
19.5	7.0	5.8	-3.2	6.9	5.2	0.3	-1.1	5.4	-0.1	-0.1	-0.1	-0.2	-0.1	0.0	-0.1	-0.1
29.3	6.7	5.9	-3.3	6.9	7.4	0.6	-1.1	8.0	-0.2	-0.2	-0.1	-0.2	-0.1	-0.1	-0.1	-0.2
39.1	6.6	5.8	-3.6	6.6	10.0	0.3	-1.1	11.0	-0.2	-0.2	-0.1	-0.1	-0.1	-0.1	-0.1	-0.2
48.8	6.6	5.8	-3.3	6.4	13.0	0.4	-1.0	13.0	-0.1	-0.1	-0.1	-0.2	-0.1	-0.1	-0.1	-0.1
58.6	6.6	5.5	-3.2	6.3	15.0	1.0	-1.6	15.0	-0.1	-0.1	-0.1	-0.2	-0.1	-0.1	-0.1	-0.1
68.4	6.0	5.7	-3.3	5.9	17.0	0.4	-2.0	18.0	-0.1	-0.2	-0.1	-0.3	-0.1	-0.3	-0.1	-0.1
78.1	5.7	5.7	-3.2	5.6	20.0	1.1	-2.3	20.0	-0.2	-0.1	-0.2	-0.2	-0.2	-0.2	-0.2	-0.1
87.9	4.8	5.7	-3.3	4.0	22.0	1.1	-2.9	23.0	-0.1	-0.2	-0.2	-0.2	-0.1	-0.2	-0.2	-0.1
97.7	3.9	5.7	-3.8	3.6	25.0	1.4	-3.3	25.0	-0.1	-0.1	-0.1	-0.1	-0.1	-0.1	-0.1	-0.1
107.4	3.3	5.9	-4.0	3.0	27.0	1.5	-3.5	28.0	-0.1	-0.1	-0.1	-0.1	-0.1	-0.1	-0.1	-0.1
117.2	2.1	6.3	-3.9	1.7	30.0	1.8	-3.6	30.0	-0.2	0.0	-0.1	-0.2	-0.1	-0.1	-0.1	-0.1
127.0	1.1	6.1	-4.1	1.3	32.0	2.0	-3.3	32.0	-0.2	-0.3	-0.1	-0.2	-0.1	-0.2	-0.1	-0.2
136.7	-0.5	6.1	-3.9	-1.3	36.0	1.9	-3.8	37.0	-0.2	-0.2	-0.1	-0.2	-0.1	-0.2	-0.1	-0.1

Table 48. Raw data for the test seal at ω=5 krpm, PD=37.9 bars, C_r=0.188 mm, and inlet GVF=10%

Freq.	Re($\boldsymbol{H_{XX}}$)	Re($\boldsymbol{H_{XY}}$)	Re($\boldsymbol{H_{YX}}$)	Re($\boldsymbol{H_{YY}}$)	Im($\boldsymbol{H_{XX}}$)	Im($\boldsymbol{H_{XY}}$)	Im($\boldsymbol{H_{YX}}$)	Im($\boldsymbol{H_{YY}}$)	Re($\boldsymbol{eH_{XX}}$)	Re($\boldsymbol{eH_{XY}}$)	Re($\boldsymbol{eH_{YX}}$)	Re($\boldsymbol{eH_{YY}}$)	Im($\boldsymbol{eH_{XX}}$)	Im($\boldsymbol{eH_{XY}}$)	Im($\boldsymbol{eH_{YX}}$)	Im($\boldsymbol{eH_{YY}}$)
Hz	MN/m	MN/m	MN/m	MN/m	MN/m	MN/m	MN/m	MN/m	MN/m	MN/m	MN/m	MN/m	MN/m	MN/m	MN/m	MN/m
9.8	0.9	10.0	-7.7	-0.9	3.1	0.0	-0.6	3.4	-0.1	-0.1	-0.1	-0.2	-0.1	-0.1	-0.1	-0.1
19.5	0.8	10.0	-7.7	-0.7	5.3	0.8	-0.8	5.6	-0.1	-0.1	-0.1	-0.2	-0.1	-0.1	-0.1	-0.1
29.3	0.5	10.0	-7.3	-0.9	7.9	1.5	-1.0	7.3	-0.1	-0.1	-0.1	-0.2	-0.1	0.0	-0.1	-0.1
39.1	0.3	10.0	-7.6	-1.1	11.0	1.1	-1.9	11.0	-0.1	-0.1	-0.1	-0.2	-0.1	-0.1	-0.1	-0.1
48.8	-0.3	10.0	-7.6	-1.9	13.0	1.6	-2.5	14.0	-0.1	-0.1	-0.1	-0.2	-0.1	-0.1	-0.1	-0.1
58.6	-0.7	10.0	-7.6	-2.3	16.0	2.5	-2.6	16.0	-0.1	-0.1	-0.2	-0.2	-0.1	-0.1	-0.2	-0.1
68.4	-1.6	11.0	-7.7	-4.1	19.0	2.3	-3.8	20.0	-0.1	-0.2	-0.2	-0.3	-0.1	-0.2	-0.2	-0.1
78.1	-1.3	11.0	-8.2	-3.0	22.0	2.7	-4.3	23.0	-0.1	-0.1	-0.1	-0.2	-0.1	-0.1	-0.1	-0.1
87.9	-2.6	11.0	-8.4	-4.1	24.0	3.3	-4.5	25.0	-0.1	-0.1	-0.1	-0.2	-0.1	-0.1	-0.1	-0.1
97.7	-3.3	11.0	-8.3	-4.6	27.0	3.7	-4.6	27.0	-0.1	-0.1	-0.1	-0.2	-0.1	-0.1	-0.1	-0.1
107.4	-4.1	11.0	-8.5	-5.1	29.0	3.7	-5.4	31.0	-0.1	-0.1	-0.1	-0.2	-0.1	-0.1	-0.1	-0.1
117.2	-5.5	11.0	-8.3	-6.8	31.0	4.1	-6.0	33.0	-0.1	-0.1	-0.1	-0.3	-0.1	-0.1	-0.1	-0.1
127.0	-8.4	19.0	-16.0	-10.0	25.0	2.9	-3.7	29.0	-5.9	-11.0	-7.0	-7.2	-7.8	-6.7	-5.6	-9.4
136.7	-9.6	12.0	-8.5	-11.0	36.0	4.6	-7.0	39.0	-0.1	-0.1	0.0	-0.2	-0.1	-0.2	-0.1	-0.2

Table 49. Raw data for the test seal at ω=7.5 krpm, PD=37.9 bars, C_r=0.188 mm, and inlet GVF=0%

Freq.	Re($\boldsymbol{H_{XX}}$)	Re($\boldsymbol{H_{XY}}$)	Re($\boldsymbol{H_{YX}}$)	Re($\boldsymbol{H_{YY}}$)	Im($\boldsymbol{H_{XX}}$)	Im($\boldsymbol{H_{XY}}$)	Im($\boldsymbol{H_{YX}}$)	Im($\boldsymbol{H_{YY}}$)	Re($\boldsymbol{eH_{XX}}$)	Re($\boldsymbol{eH_{XY}}$)	Re($\boldsymbol{eH_{YX}}$)	Re($\boldsymbol{eH_{YY}}$)	Im($\boldsymbol{eH_{XX}}$)	Im($\boldsymbol{eH_{XY}}$)	Im($\boldsymbol{eH_{YX}}$)	Im($\boldsymbol{eH_{YY}}$)
Hz	MN/m	MN/m	MN/m	MN/m	MN/m	MN/m	MN/m	MN/m	MN/m	MN/m	MN/m	MN/m	MN/m	MN/m	MN/m	MN/m
9.8	3.2	9.5	-7.4	2.4	3.0	0.2	-0.5	3.2	-0.1	-0.1	-0.1	-0.1	-0.1	-0.1	0.0	-0.1
19.5	3.2	9.5	-7.4	2.6	5.4	0.8	-0.8	5.3	-0.1	-0.1	-0.1	-0.1	-0.1	-0.1	0.0	0.0
29.3	3.2	9.7	-7.1	2.5	7.7	1.2	-0.9	7.3	-0.1	-0.1	-0.1	-0.1	-0.1	-0.1	0.0	-0.1
39.1	2.9	9.7	-7.2	2.2	10.0	1.2	-1.6	10.0	-0.1	-0.1	-0.1	-0.1	-0.1	-0.1	0.0	-0.1
48.8	2.6	9.6	-7.4	1.5	13.0	1.5	-2.0	13.0	-0.1	-0.1	-0.1	-0.1	0.0	-0.1	-0.1	-0.1
58.6	2.1	9.4	-7.3	1.2	15.0	2.3	-2.5	15.0	-0.1	-0.1	-0.1	-0.2	-0.1	-0.1	-0.1	-0.1
68.4	1.4	10.0	-7.2	0.3	18.0	2.6	-3.2	18.0	-0.1	-0.1	-0.1	-0.2	-0.1	-0.1	-0.1	-0.1
78.1	1.6	9.9	-7.5	0.6	20.0	2.6	-3.7	21.0	-0.1	-0.1	-0.1	-0.1	0.0	-0.1	-0.1	-0.1
87.9	0.7	10.0	-7.7	-0.3	23.0	2.9	-4.1	23.0	-0.1	-0.1	-0.1	-0.1	0.0	0.0	0.0	-0.1
97.7	0.0	10.0	-7.9	-0.7	25.0	3.4	-4.3	25.0	-0.1	-0.1	-0.1	-0.1	0.0	-0.1	0.0	0.0
107.4	-0.9	10.0	-7.8	-1.4	27.0	3.5	-4.9	28.0	-0.1	-0.1	-0.1	-0.1	-0.1	0.0	-0.1	-0.1
117.2	-2.2	11.0	-7.8	-2.9	29.0	4.0	-5.5	30.0	-0.1	-0.1	0.0	-0.1	-0.1	-0.1	0.0	-0.1
127.0	-5.4	9.5	-9.1	-2.7	30.0	5.5	-3.6	34.0	-1.0	-2.8	-1.2	-2.2	-1.2	-2.5	-0.9	-2.6
136.7	-6.1	12.0	-7.6	-6.5	34.0	4.5	-6.4	36.0	-0.1	-0.1	0.0	-0.1	0.0	-0.1	-0.1	-0.1

Table 50. Raw data for the test seal at ω=7.5 krpm, PD=37.9 bars, C_r=0.188 mm, and inlet GVF=2%

Freq.	Re($\boldsymbol{H_{XX}}$)	Re($\boldsymbol{H_{XY}}$)	Re($\boldsymbol{H_{YX}}$)	Re($\boldsymbol{H_{YY}}$)	Im($\boldsymbol{H_{XX}}$)	Im($\boldsymbol{H_{XY}}$)	Im($\boldsymbol{H_{YX}}$)	Im($\boldsymbol{H_{YY}}$)	Re($\boldsymbol{eH_{XX}}$)	Re($\boldsymbol{eH_{XY}}$)	Re($\boldsymbol{eH_{YX}}$)	Re($\boldsymbol{eH_{YY}}$)	Im($\boldsymbol{eH_{XX}}$)	Im($\boldsymbol{eH_{XY}}$)	Im($\boldsymbol{eH_{YX}}$)	Im($\boldsymbol{eH_{YY}}$)
Hz	MN/m	MN/m	MN/m	MN/m	MN/m	MN/m	MN/m	MN/m	MN/m	MN/m	MN/m	MN/m	MN/m	MN/m	MN/m	MN/m
9.8	5.1	9.0	-7.1	4.0	3.0	0.1	-0.3	3.2	-0.1	0.0	-0.1	-0.1	-0.1	0.0	0.0	-0.1
19.5	5.2	9.2	-6.9	4.2	5.4	0.6	-0.9	5.2	-0.1	0.0	-0.1	-0.1	-0.1	0.0	0.0	-0.1
29.3	5.0	9.5	-6.7	4.1	7.7	1.0	-0.9	7.4	-0.1	0.0	0.0	0.0	0.0	-0.1	0.0	0.0
39.1	4.9	9.2	-7.0	4.1	9.8	1.2	-1.6	10.0	-0.1	0.0	0.0	-0.1	0.0	-0.1	-0.1	0.0
48.8	4.6	9.3	-6.9	3.4	12.0	1.5	-2.0	12.0	-0.1	-0.1	-0.1	-0.1	-0.1	0.0	-0.1	-0.1
58.6	4.3	9.0	-6.9	2.8	15.0	2.0	-2.6	15.0	-0.1	-0.1	-0.1	-0.1	-0.1	-0.1	-0.1	-0.1
68.4	3.5	9.4	-7.0	2.3	17.0	2.3	-3.2	18.0	-0.1	-0.1	-0.1	-0.1	0.0	-0.1	-0.1	-0.1
78.1	3.5	9.6	-7.3	2.3	20.0	2.7	-4.0	21.0	-0.1	-0.1	-0.1	-0.1	-0.1	0.0	0.0	0.0
87.9	2.7	9.8	-7.4	1.3	22.0	3.0	-4.2	23.0	0.0	0.0	0.0	-0.1	0.0	-0.1	0.0	-0.1
97.7	2.0	9.8	-7.8	0.9	25.0	3.2	-4.4	25.0	-0.1	0.0	0.0	-0.1	-0.1	-0.1	0.0	0.0
107.4	1.0	10.0	-7.7	0.3	27.0	3.6	-4.9	28.0	0.0	-0.1	-0.1	-0.1	0.0	-0.1	0.0	-0.1
117.2	-0.3	10.0	-7.6	-1.4	29.0	3.8	-5.5	29.0	0.0	0.0	-0.1	-0.1	0.0	0.0	-0.1	0.0
127.0	-1.6	9.5	-8.2	-3.0	30.0	3.9	-5.8	33.0	-2.8	-4.5	-2.5	-3.2	-2.6	-3.5	-2.6	-4.3
136.7	-4.8	11.0	-7.4	-5.4	34.0	4.8	-6.4	35.0	0.0	0.0	0.0	-0.1	0.0	0.0	-0.1	-0.1

Table 51. Raw data for the test seal at ω=7.5 krpm, PD=37.9 bars, C_r=0.188 mm, and inlet GVF=4%

Freq.	Re($\boldsymbol{H_{XX}}$)	Re($\boldsymbol{H_{XY}}$)	Re($\boldsymbol{H_{YX}}$)	Re($\boldsymbol{H_{YY}}$)	Im($\boldsymbol{H_{XX}}$)	Im($\boldsymbol{H_{XY}}$)	Im($\boldsymbol{H_{YX}}$)	Im($\boldsymbol{H_{YY}}$)	Re($\boldsymbol{eH_{XX}}$)	Re($\boldsymbol{eH_{XY}}$)	Re($\boldsymbol{eH_{YX}}$)	Re($\boldsymbol{eH_{YY}}$)	Im($\boldsymbol{eH_{XX}}$)	Im($\boldsymbol{eH_{XY}}$)	Im($\boldsymbol{eH_{YX}}$)	Im($\boldsymbol{eH_{YY}}$)
Hz	MN/m	MN/m	MN/m	MN/m	MN/m	MN/m	MN/m	MN/m	MN/m	MN/m	MN/m	MN/m	MN/m	MN/m	MN/m	MN/m
9.8	5.2	9.1	-6.7	4.4	2.9	0.2	-0.4	2.9	-0.1	-0.1	-0.1	-0.1	-0.1	-0.1	-0.1	-0.1
19.5	5.6	9.0	-6.8	4.6	5.3	0.7	-1.0	5.2	0.0	-0.1	0.0	0.0	0.0	0.0	0.0	0.0
29.3	5.4	9.4	-6.5	4.5	7.6	1.1	-1.3	7.4	0.0	0.0	-0.1	-0.1	0.0	-0.1	0.0	-0.1
39.1	5.1	9.2	-7.0	4.3	9.8	1.2	-1.7	10.0	-0.1	0.0	-0.1	-0.1	-0.1	-0.1	-0.1	-0.1
48.8	4.7	9.3	-6.9	3.8	13.0	1.3	-1.7	12.0	-0.1	0.0	-0.1	0.0	0.0	0.0	-0.1	-0.1
58.6	4.5	9.0	-6.6	3.5	15.0	2.2	-2.3	15.0	-0.1	-0.1	-0.1	-0.1	-0.1	-0.1	-0.1	-0.1
68.4	4.1	9.0	-6.9	3.1	17.0	2.1	-3.1	18.0	-0.1	-0.1	-0.1	-0.1	-0.1	-0.1	-0.1	-0.2
78.1	3.9	9.6	-7.0	2.8	20.0	2.5	-3.6	20.0	0.0	-0.1	-0.1	-0.1	-0.1	-0.1	0.0	-0.1
87.9	3.2	9.8	-7.3	2.0	22.0	2.9	-4.0	23.0	0.0	-0.1	-0.1	-0.1	-0.1	-0.1	0.0	-0.1
97.7	2.3	9.6	-7.6	1.5	24.0	3.0	-4.2	25.0	-0.1	0.0	-0.1	-0.1	-0.1	0.0	0.0	-0.1
107.4	1.4	9.8	-7.7	0.7	27.0	3.3	-4.9	28.0	-0.1	-0.1	-0.1	-0.1	-0.1	-0.1	0.0	0.0
117.2	0.0	10.0	-7.6	-1.2	29.0	3.7	-5.3	29.0	-0.1	-0.1	-0.1	-0.1	-0.1	0.0	-0.1	0.0
127.0	-0.2	8.2	-9.4	-3.9	29.0	2.7	-6.4	34.0	-0.5	-0.3	-0.2	-0.4	-0.3	-0.4	-0.5	-0.3
136.7	-4.3	11.0	-7.3	-4.9	34.0	4.7	-6.0	35.0	0.0	-0.1	0.0	0.0	-0.1	0.0	-0.1	-0.1

Table 52. Raw data for the test seal at ω=7.5 krpm, PD=37.9 bars, C_r=0.188 mm, and inlet GVF=6%

Freq.	Re($\boldsymbol{H_{XX}}$)	Re($\boldsymbol{H_{XY}}$)	Re($\boldsymbol{H_{YX}}$)	Re($\boldsymbol{H_{YY}}$)	Im($\boldsymbol{H_{XX}}$)	Im($\boldsymbol{H_{XY}}$)	Im($\boldsymbol{H_{YX}}$)	Im($\boldsymbol{H_{YY}}$)	Re($\boldsymbol{eH_{XX}}$)	Re($\boldsymbol{eH_{XY}}$)	Re($\boldsymbol{eH_{YX}}$)	Re($\boldsymbol{eH_{YY}}$)	Im($\boldsymbol{eH_{XX}}$)	Im($\boldsymbol{eH_{XY}}$)	Im($\boldsymbol{eH_{YX}}$)	Im($\boldsymbol{eH_{YY}}$)
Hz	MN/m	MN/m	MN/m	MN/m	MN/m	MN/m	MN/m	MN/m	MN/m	MN/m	MN/m	MN/m	MN/m	MN/m	MN/m	MN/m
9.8	7.1	8.4	-6.6	6.8	2.7	0.3	-0.5	2.8	-0.3	-0.1	-0.1	-0.1	-0.1	-0.1	-0.1	-0.1
19.5	7.2	8.3	-6.6	6.7	5.0	0.8	-1.1	5.2	-0.2	-0.1	-0.1	-0.1	0.0	0.0	-0.1	-0.1
29.3	7.0	8.7	-6.5	6.6	7.4	1.1	-1.2	7.4	-0.2	-0.1	-0.1	-0.1	-0.1	-0.1	0.0	-0.1
39.1	6.7	8.7	-7.1	6.4	9.7	1.4	-1.7	10.0	-0.2	-0.1	-0.1	-0.1	-0.1	0.0	-0.1	-0.1
48.8	6.4	8.7	-6.8	6.2	12.0	1.4	-1.6	12.0	-0.2	-0.1	0.0	-0.1	0.0	0.0	-0.1	0.0
58.6	6.4	8.6	-6.5	5.4	15.0	1.9	-2.4	15.0	-0.2	-0.1	-0.1	-0.1	-0.1	0.0	-0.1	0.0
68.4	5.8	8.6	-6.9	5.2	17.0	2.1	-3.0	18.0	-0.2	-0.1	-0.1	-0.1	-0.1	-0.1	-0.1	-0.1
78.1	5.6	9.0	-7.1	5.0	20.0	2.7	-3.5	20.0	-0.2	-0.1	-0.1	-0.2	0.0	0.0	-0.1	-0.1
87.9	4.7	9.1	-7.1	4.2	22.0	2.8	-4.0	22.0	-0.2	-0.1	-0.1	-0.1	0.0	-0.1	-0.1	-0.1
97.7	3.9	8.9	-7.5	3.5	24.0	3.0	-4.1	25.0	-0.2	-0.1	-0.1	-0.1	-0.1	-0.1	-0.1	0.0
107.4	2.9	9.1	-7.4	2.8	26.0	3.3	-4.5	27.0	-0.2	-0.1	-0.1	-0.1	-0.1	-0.1	-0.1	-0.1
117.2	1.7	9.3	-7.3	1.1	29.0	3.7	-5.0	29.0	-0.2	-0.1	-0.1	-0.1	-0.1	0.0	-0.1	-0.1
127.0	0.1	9.5	-7.9	0.8	31.0	5.3	-4.8	32.0	-3.4	-4.0	-2.5	-4.2	-2.8	-4.6	-3.1	-3.8
136.7	-2.2	10.0	-6.8	-2.5	34.0	4.7	-6.0	35.0	-0.2	-0.1	-0.1	-0.1	-0.1	-0.1	-0.1	0.0

Table 53. Raw data for the test seal at ω=7.5 krpm, PD=37.9 bars, C_r=0.188 mm, and inlet GVF=8%

Freq.	Re($\boldsymbol{H_{XX}}$)	Re($\boldsymbol{H_{XY}}$)	Re($\boldsymbol{H_{YX}}$)	Re($\boldsymbol{H_{YY}}$)	Im($\boldsymbol{H_{XX}}$)	Im($\boldsymbol{H_{XY}}$)	Im($\boldsymbol{H_{YX}}$)	Im($\boldsymbol{H_{YY}}$)	Re($\boldsymbol{eH_{XX}}$)	Re($\boldsymbol{eH_{XY}}$)	Re($\boldsymbol{eH_{YX}}$)	Re($\boldsymbol{eH_{YY}}$)	Im($\boldsymbol{eH_{XX}}$)	Im($\boldsymbol{eH_{XY}}$)	Im($\boldsymbol{eH_{YX}}$)	Im($\boldsymbol{eH_{YY}}$)
Hz	MN/m	MN/m	MN/m	MN/m	MN/m	MN/m	MN/m	MN/m	MN/m	MN/m	MN/m	MN/m	MN/m	MN/m	MN/m	MN/m
9.8	6.0	8.5	-5.7	5.9	2.7	0.4	-0.7	3.2	-0.2	-0.1	0.0	-0.1	-0.1	-0.1	-0.1	-0.1
19.5	6.4	8.6	-6.3	5.9	5.3	0.7	-0.8	5.0	-0.1	-0.1	-0.2	-0.1	-0.1	-0.1	-0.1	-0.1
29.3	5.9	8.8	-6.1	5.9	7.3	1.3	-1.4	7.4	-0.2	-0.1	-0.1	-0.1	-0.1	-0.1	-0.1	-0.2
39.1	5.7	8.9	-6.6	5.6	10.0	1.1	-1.9	10.0	-0.1	-0.1	-0.1	-0.1	-0.1	0.0	-0.1	-0.1
48.8	5.3	9.0	-6.5	5.1	13.0	1.3	-1.9	13.0	-0.2	-0.1	-0.1	-0.1	-0.1	-0.1	-0.1	-0.1
58.6	5.4	9.2	-6.4	5.0	15.0	1.6	-1.8	15.0	-0.1	-0.1	-0.2	-0.1	-0.1	-0.1	-0.2	-0.2
68.4	5.4	9.0	-6.7	4.3	18.0	1.3	-3.0	19.0	-0.1	-0.1	-0.1	-0.1	-0.2	-0.2	-0.1	-0.1
78.1	5.1	9.0	-6.7	4.3	20.0	2.2	-3.4	20.0	-0.2	-0.1	-0.1	-0.1	-0.1	-0.1	-0.2	-0.1
87.9	4.2	9.1	-6.6	3.3	22.0	2.4	-3.8	23.0	-0.1	-0.1	-0.1	-0.1	-0.1	-0.1	-0.1	-0.1
97.7	3.3	9.2	-7.1	2.9	25.0	2.6	-4.3	25.0	-0.2	-0.1	-0.1	-0.1	-0.1	-0.1	-0.1	-0.1
107.4	2.8	9.3	-7.2	2.2	27.0	2.7	-4.6	27.0	-0.2	-0.1	-0.1	-0.1	-0.1	-0.1	-0.3	-0.1
117.2	1.7	9.4	-7.2	0.8	29.0	2.9	-5.1	30.0	-0.2	-0.1	-0.2	-0.1	-0.2	-0.1	-0.1	-0.1
127.0	-0.6	18.0	-6.9	0.6	32.0	5.8	-4.5	24.0	-3.8	-2.6	-2.9	-5.7	-3.1	-6.4	-3.4	-2.8
136.7	-1.4	9.6	-7.4	-2.5	35.0	3.9	-6.0	36.0	-0.1	-0.2	-0.2	-0.1	-0.2	-0.2	-0.1	-0.1

Table 54. Raw data for the test seal at ω=7.5 krpm, PD=37.9 bars, C_r=0.188 mm, and inlet GVF=10%

Freq.	Re($\boldsymbol{H_{XX}}$)	Re($\boldsymbol{H_{XY}}$)	Re($\boldsymbol{H_{YX}}$)	Re($\boldsymbol{H_{YY}}$)	Im($\boldsymbol{H_{XX}}$)	Im($\boldsymbol{H_{XY}}$)	Im($\boldsymbol{H_{YX}}$)	Im($\boldsymbol{H_{YY}}$)	Re($\boldsymbol{eH_{XX}}$)	Re($\boldsymbol{eH_{XY}}$)	Re($\boldsymbol{eH_{YX}}$)	Re($\boldsymbol{eH_{YY}}$)	Im($\boldsymbol{eH_{XX}}$)	Im($\boldsymbol{eH_{XY}}$)	Im($\boldsymbol{eH_{YX}}$)	Im($\boldsymbol{eH_{YY}}$)
Hz	MN/m	MN/m	MN/m	MN/m	MN/m	MN/m	MN/m	MN/m	MN/m	MN/m	MN/m	MN/m	MN/m	MN/m	MN/m	MN/m
9.8	7.3	13.0	-12.0	5.7	2.6	0.0	-0.7	3.3	-0.2	-0.3	-0.1	-0.2	-0.2	-0.1	-0.2	-0.2
19.5	7.2	13.0	-11.0	6.4	5.1	1.2	-1.1	4.9	-0.2	-0.2	-0.2	-0.1	-0.1	-0.1	-0.1	-0.1
29.3	7.0	13.0	-11.0	6.3	7.5	2.0	-1.5	7.1	-0.2	-0.1	-0.1	-0.2	-0.1	-0.2	-0.1	-0.1
39.1	7.0	13.0	-11.0	5.8	9.8	1.8	-2.8	9.9	-0.1	-0.1	-0.1	-0.2	-0.1	-0.1	-0.1	-0.2
48.8	6.1	13.0	-11.0	5.4	12.0	2.8	-3.4	13.0	-0.1	-0.1	-0.1	-0.1	-0.1	-0.1	-0.1	-0.1
58.6	5.6	13.0	-11.0	4.5	15.0	3.1	-3.6	15.0	-0.1	-0.2	-0.2	-0.2	-0.1	-0.1	-0.2	-0.1
68.4	4.9	14.0	-11.0	4.2	17.0	4.1	-4.4	18.0	-0.2	-0.2	-0.3	-0.3	-0.1	-0.2	-0.1	-0.2
78.1	4.8	14.0	-12.0	4.2	20.0	4.0	-4.8	21.0	-0.1	-0.1	-0.1	-0.2	-0.2	-0.2	-0.1	-0.1
87.9	3.9	14.0	-11.0	3.4	22.0	4.6	-5.7	23.0	-0.1	-0.1	-0.1	-0.1	-0.1	-0.1	-0.1	-0.1
97.7	3.3	14.0	-12.0	2.5	25.0	5.4	-6.2	25.0	-0.2	-0.1	-0.1	-0.1	-0.1	-0.1	-0.1	-0.1
107.4	2.1	14.0	-12.0	1.6	26.0	6.0	-6.9	28.0	-0.1	-0.2	-0.1	-0.1	-0.1	-0.1	-0.1	-0.1
117.2	0.6	14.0	-12.0	-0.1	29.0	6.9	-7.9	30.0	-0.1	-0.1	-0.1	-0.2	-0.1	-0.1	-0.1	-0.1
127.0	-1.1	15.0	-12.0	-1.6	30.0	7.2	-8.6	32.0	-0.1	-0.2	-0.1	-0.1	-0.1	-0.1	-0.2	-0.1
136.7	-4.4	16.0	-11.0	-4.1	34.0	8.2	-9.7	35.0	-0.1	-0.1	-0.1	-0.2	-0.1	-0.1	-0.1	-0.1

Table 55. Raw data for the test seal at ω=10 krpm, PD=37.9 bars, C_r=0.188 mm, and inlet GVF=0%

Freq.	Re($\boldsymbol{H_{XX}}$)	Re($\boldsymbol{H_{XY}}$)	Re($\boldsymbol{H_{YX}}$)	Re($\boldsymbol{H_{YY}}$)	Im($\boldsymbol{H_{XX}}$)	Im($\boldsymbol{H_{XY}}$)	Im($\boldsymbol{H_{YX}}$)	Im($\boldsymbol{H_{YY}}$)	Re($\boldsymbol{eH_{XX}}$)	Re($\boldsymbol{eH_{XY}}$)	Re($\boldsymbol{eH_{YX}}$)	Re($\boldsymbol{eH_{YY}}$)	Im($\boldsymbol{eH_{XX}}$)	Im($\boldsymbol{eH_{XY}}$)	Im($\boldsymbol{eH_{YX}}$)	Im($\boldsymbol{eH_{YY}}$)
Hz	MN/m	MN/m	MN/m	MN/m	MN/m	MN/m	MN/m	MN/m	MN/m	MN/m	MN/m	MN/m	MN/m	MN/m	MN/m	MN/m
9.8	7.2	14.0	-11.0	6.1	3.3	0.0	-0.3	3.0	-0.1	-0.1	-0.1	-0.1	-0.1	-0.1	-0.1	-0.1
19.5	7.1	13.0	-11.0	6.0	5.2	0.9	-0.7	5.3	-0.2	-0.1	-0.1	-0.1	-0.1	-0.1	-0.1	-0.1
29.3	7.1	14.0	-10.0	5.6	7.5	1.3	-1.3	7.0	-0.1	-0.1	-0.1	-0.1	0.0	-0.1	-0.1	-0.1
39.1	7.1	14.0	-10.0	5.4	9.9	1.4	-2.3	9.7	-0.1	-0.1	-0.1	-0.1	-0.1	-0.1	-0.1	-0.1
48.8	6.6	14.0	-11.0	4.9	12.0	2.2	-3.2	12.0	-0.1	-0.1	-0.1	-0.1	-0.1	-0.1	-0.1	-0.1
58.6	6.0	14.0	-11.0	4.5	14.0	2.9	-3.6	15.0	-0.1	-0.1	-0.1	-0.1	-0.1	-0.1	-0.1	-0.1
68.4	5.3	14.0	-11.0	3.6	17.0	2.9	-4.2	18.0	-0.1	-0.1	-0.1	-0.2	-0.1	-0.1	-0.2	-0.2
78.1	5.4	14.0	-11.0	3.9	20.0	3.3	-4.8	20.0	-0.1	-0.1	-0.1	-0.1	-0.1	-0.1	-0.1	-0.1
87.9	4.7	14.0	-11.0	3.0	22.0	3.9	-5.5	22.0	-0.1	-0.1	0.0	-0.1	0.0	-0.1	-0.1	-0.1
97.7	3.9	14.0	-11.0	2.5	24.0	4.5	-5.9	24.0	-0.1	-0.1	-0.1	-0.1	0.0	-0.1	0.0	0.0
107.4	3.0	14.0	-11.0	1.8	26.0	5.1	-6.8	27.0	-0.1	-0.1	0.0	-0.1	0.0	-0.1	-0.1	-0.1
117.2	1.6	15.0	-11.0	0.1	28.0	5.9	-7.6	28.0	-0.1	-0.1	0.0	0.0	-0.1	0.0	0.0	0.0
127.0	0.0	15.0	-11.0	-1.5	30.0	6.1	-8.3	31.0	0.0	-0.1	-0.1	-0.1	-0.1	-0.1	-0.1	-0.1
136.7	-2.9	16.0	-11.0	-3.8	33.0	7.0	-9.3	34.0	-0.1	-0.1	0.0	-0.1	0.0	-0.1	-0.1	0.0

Table 56. Raw data for the test seal at ω=10 krpm, PD=37.9 bars, C_r=0.188 mm, and inlet GVF=2%

Freq.	Re($\boldsymbol{H_{XX}}$)	Re($\boldsymbol{H_{XY}}$)	Re($\boldsymbol{H_{YX}}$)	Re($\boldsymbol{H_{YY}}$)	Im($\boldsymbol{H_{XX}}$)	Im($\boldsymbol{H_{XY}}$)	Im($\boldsymbol{H_{YX}}$)	Im($\boldsymbol{H_{YY}}$)	Re($\boldsymbol{eH_{XX}}$)	Re($\boldsymbol{eH_{XY}}$)	Re($\boldsymbol{eH_{YX}}$)	Re($\boldsymbol{eH_{YY}}$)	Im($\boldsymbol{eH_{XX}}$)	Im($\boldsymbol{eH_{XY}}$)	Im($\boldsymbol{eH_{YX}}$)	Im($\boldsymbol{eH_{YY}}$)
Hz	MN/m	MN/m	MN/m	MN/m	MN/m	MN/m	MN/m	MN/m	MN/m	MN/m	MN/m	MN/m	MN/m	MN/m	MN/m	MN/m
9.8	8.3	13.0	-11.0	7.2	3.0	0.2	-0.4	3.1	-0.2	-0.2	-0.2	-0.2	-0.1	-0.2	-0.1	-0.2
19.5	8.4	13.0	-10.0	7.3	4.9	0.9	-0.6	4.9	-0.1	-0.1	-0.1	-0.1	-0.1	-0.1	-0.1	-0.1
29.3	8.3	13.0	-9.9	6.8	7.3	1.4	-1.4	7.0	-0.1	-0.1	-0.1	-0.1	-0.1	-0.1	-0.1	-0.1
39.1	8.2	13.0	-10.0	7.1	9.5	1.7	-2.4	9.7	-0.1	0.0	-0.1	-0.1	0.0	0.0	0.0	0.0
48.8	7.7	13.0	-10.0	6.5	12.0	2.3	-3.0	12.0	-0.1	-0.1	-0.1	-0.1	-0.1	-0.1	-0.1	-0.1
58.6	7.2	13.0	-10.0	5.7	14.0	2.9	-3.4	14.0	-0.2	-0.1	-0.1	-0.1	-0.1	-0.1	-0.1	-0.1
68.4	6.6	14.0	-10.0	4.6	17.0	3.1	-4.4	17.0	-0.1	-0.1	-0.1	-0.2	-0.1	-0.1	-0.1	-0.2
78.1	6.9	13.0	-11.0	5.4	19.0	3.5	-5.1	20.0	-0.1	-0.1	-0.1	-0.1	-0.1	-0.1	-0.1	0.0
87.9	5.9	14.0	-11.0	4.7	21.0	4.0	-5.5	21.0	0.0	-0.1	0.0	-0.1	0.0	-0.1	-0.1	0.0
97.7	5.3	13.0	-11.0	3.8	23.0	4.6	-5.9	24.0	0.0	-0.1	0.0	-0.1	0.0	-0.1	-0.1	0.0
107.4	4.3	14.0	-11.0	3.1	25.0	5.0	-6.6	26.0	-0.1	-0.1	-0.1	-0.1	-0.1	-0.1	-0.1	-0.1
117.2	2.9	14.0	-11.0	1.1	27.0	6.0	-7.6	28.0	-0.1	-0.1	-0.1	-0.1	-0.1	0.0	-0.1	-0.1
127.0	0.7	14.0	-11.0	-0.5	29.0	6.7	-8.5	30.0	-0.1	-0.1	-0.1	-0.1	-0.1	-0.1	-0.1	-0.1
136.7	-2.2	16.0	-11.0	-3.5	32.0	7.1	-9.9	33.0	-0.1	-0.1	0.0	-0.1	0.0	-0.1	-0.1	-0.1

Table 57. Raw data for the test seal at ω=10 krpm, PD=37.9 bars, C_r=0.188 mm, and inlet GVF=4%

Freq.	Re($\boldsymbol{H_{XX}}$)	Re($\boldsymbol{H_{XY}}$)	Re($\boldsymbol{H_{YX}}$)	Re($\boldsymbol{H_{YY}}$)	Im($\boldsymbol{H_{XX}}$)	Im($\boldsymbol{H_{XY}}$)	Im($\boldsymbol{H_{YX}}$)	Im($\boldsymbol{H_{YY}}$)	Re($\boldsymbol{eH_{XX}}$)	Re($\boldsymbol{eH_{XY}}$)	Re($\boldsymbol{eH_{YX}}$)	Re($\boldsymbol{eH_{YY}}$)	Im($\boldsymbol{eH_{XX}}$)	Im($\boldsymbol{eH_{XY}}$)	Im($\boldsymbol{eH_{YX}}$)	Im($\boldsymbol{eH_{YY}}$)
Hz	MN/m	MN/m	MN/m	MN/m	MN/m	MN/m	MN/m	MN/m	MN/m	MN/m	MN/m	MN/m	MN/m	MN/m	MN/m	MN/m
9.8	8.4	13.0	-10.0	7.9	2.9	0.4	-0.9	2.8	-0.1	-0.1	-0.4	-0.2	-0.2	-0.2	-0.2	-0.1
19.5	8.2	12.0	-11.0	7.8	5.0	0.9	-0.7	5.0	-0.1	-0.1	-0.1	-0.1	-0.1	-0.1	-0.1	-0.1
29.3	8.2	13.0	-10.0	7.3	7.2	1.5	-1.3	7.1	-0.1	-0.1	-0.1	-0.1	-0.1	-0.1	-0.1	-0.1
39.1	8.3	13.0	-10.0	7.6	9.8	1.8	-2.5	9.8	-0.1	-0.1	0.0	-0.1	-0.1	0.0	0.0	-0.1
48.8	7.7	13.0	-11.0	7.0	12.0	2.3	-2.9	12.0	-0.1	-0.1	-0.1	-0.1	0.0	-0.1	-0.1	-0.1
58.6	7.2	13.0	-10.0	6.3	14.0	2.6	-2.8	14.0	-0.1	-0.1	-0.1	-0.1	-0.1	-0.1	-0.1	-0.1
68.4	6.9	13.0	-10.0	5.7	17.0	3.1	-4.1	17.0	-0.1	-0.2	-0.1	-0.2	-0.1	-0.1	-0.1	-0.1
78.1	7.0	13.0	-11.0	6.0	19.0	3.3	-4.8	20.0	-0.1	-0.1	-0.1	-0.1	-0.1	-0.1	-0.1	-0.1
87.9	6.1	13.0	-11.0	5.3	21.0	4.0	-5.1	22.0	-0.1	-0.1	-0.1	-0.1	-0.1	-0.1	-0.1	-0.1
97.7	5.5	13.0	-11.0	4.5	23.0	4.4	-5.5	23.0	-0.1	-0.1	0.0	-0.1	0.0	-0.1	-0.1	-0.1
107.4	4.5	13.0	-11.0	3.6	25.0	4.9	-6.3	26.0	-0.1	-0.1	-0.1	-0.1	-0.1	-0.1	-0.1	-0.1
117.2	2.9	13.0	-11.0	1.4	27.0	6.0	-7.5	28.0	-0.1	-0.1	-0.1	-0.1	0.0	0.0	-0.1	-0.1
127.0	0.6	14.0	-11.0	-0.4	29.0	7.1	-8.2	30.0	-0.1	-0.1	-0.1	-0.1	-0.1	-0.1	-0.1	-0.1
136.7	-3.2	15.0	-11.0	-3.5	32.0	8.2	-9.8	34.0	-0.1	-0.1	-0.1	-0.1	-0.1	-0.1	-0.1	-0.1

Table 58. Raw data for the test seal at ω=10 krpm, PD=37.9 bars, C_r=0.188 mm, and inlet GVF=6%

Freq.	Re($\boldsymbol{H_{XX}}$)	Re($\boldsymbol{H_{XY}}$)	Re($\boldsymbol{H_{YX}}$)	Re($\boldsymbol{H_{YY}}$)	Im($\boldsymbol{H_{XX}}$)	Im($\boldsymbol{H_{XY}}$)	Im($\boldsymbol{H_{YX}}$)	Im($\boldsymbol{H_{YY}}$)	Re($\boldsymbol{eH_{XX}}$)	Re($\boldsymbol{eH_{XY}}$)	Re($\boldsymbol{eH_{YX}}$)	Re($\boldsymbol{eH_{YY}}$)	Im($\boldsymbol{eH_{XX}}$)	Im($\boldsymbol{eH_{XY}}$)	Im($\boldsymbol{eH_{YX}}$)	Im($\boldsymbol{eH_{YY}}$)
Hz	MN/m	MN/m	MN/m	MN/m	MN/m	MN/m	MN/m	MN/m	MN/m	MN/m	MN/m	MN/m	MN/m	MN/m	MN/m	MN/m
9.8	11.0	12.0	-9.4	10.0	1.4	0.0	-0.4	2.0	-0.1	-0.1	-0.1	-0.1	0.0	-0.1	-0.2	-0.2
19.5	9.9	11.0	-9.6	9.9	3.5	0.5	-0.6	4.1	-0.2	-0.2	-0.1	-0.1	-0.1	-0.1	-0.1	-0.2
29.3	9.3	11.0	-8.8	9.1	6.3	1.3	-1.4	6.1	-0.1	-0.1	-0.1	-0.1	-0.1	-0.1	0.0	0.0
39.1	9.1	11.0	-8.9	9.1	9.1	1.9	-2.6	9.0	-0.1	-0.1	-0.2	-0.1	-0.1	-0.1	-0.1	-0.1
48.8	9.1	11.0	-9.1	8.8	12.0	2.9	-3.5	12.0	-0.1	-0.1	-0.1	-0.2	-0.1	-0.2	-0.1	-0.1
58.6	9.7	12.0	-9.3	9.0	14.0	4.5	-5.0	14.0	-0.1	-0.1	-0.2	-0.1	-0.2	-0.1	-0.1	-0.1
68.4	9.4	13.0	-11.0	9.1	15.0	5.1	-5.9	16.0	-0.1	-0.1	-0.1	-0.1	-0.1	-0.2	-0.1	-0.1
78.1	7.4	15.0	-13.0	6.8	16.0	3.8	-5.4	16.0	-0.1	-0.1	-0.1	-0.1	-0.1	-0.2	-0.1	-0.1
87.9	4.4	13.0	-11.0	4.3	21.0	2.3	-3.8	21.0	-0.1	-0.1	-0.2	-0.2	-0.1	-0.1	-0.1	-0.2
97.7	4.4	12.0	-11.0	4.4	24.0	3.9	-5.0	24.0	-0.1	-0.1	-0.1	-0.1	-0.1	-0.1	-0.1	-0.1
107.4	4.6	12.0	-11.0	4.4	26.0	4.5	-5.9	26.0	-0.2	-0.1	-0.1	-0.1	-0.1	-0.1	-0.1	-0.1
117.2	3.6	12.0	-10.0	2.7	28.0	5.5	-7.0	28.0	-0.1	-0.1	0.0	-0.1	-0.1	-0.1	-0.1	-0.1
127.0	1.8	13.0	-10.0	1.4	30.0	6.2	-7.3	31.0	-0.1	-0.2	-0.2	-0.2	-0.1	-0.1	-0.1	-0.2
136.7	-0.6	14.0	-9.5	-0.6	33.0	6.7	-8.8	34.0	-0.1	-0.2	-0.2	-0.1	-0.1	-0.1	-0.2	-0.1

Table 59. Raw data for the test seal at ω=10 krpm, PD=37.9 bars, C_r=0.188 mm, and inlet GVF=8%

Freq.	Re($\boldsymbol{H_{XX}}$)	Re($\boldsymbol{H_{XY}}$)	Re($\boldsymbol{H_{YX}}$)	Re($\boldsymbol{H_{YY}}$)	Im($\boldsymbol{H_{XX}}$)	Im($\boldsymbol{H_{XY}}$)	Im($\boldsymbol{H_{YX}}$)	Im($\boldsymbol{H_{YY}}$)	Re($\boldsymbol{eH_{XX}}$)	Re($\boldsymbol{eH_{XY}}$)	Re($\boldsymbol{eH_{YX}}$)	Re($\boldsymbol{eH_{YY}}$)	Im($\boldsymbol{eH_{XX}}$)	Im($\boldsymbol{eH_{XY}}$)	Im($\boldsymbol{eH_{YX}}$)	Im($\boldsymbol{eH_{YY}}$)
Hz	MN/m	MN/m	MN/m	MN/m	MN/m	MN/m	MN/m	MN/m	MN/m	MN/m	MN/m	MN/m	MN/m	MN/m	MN/m	MN/m
9.8	9.3	12.0	-9.8	8.8	2.5	0.9	-0.7	2.5	-0.1	-0.3	-0.1	-0.2	-0.2	-0.3	-0.2	-0.2
19.5	9.5	12.0	-10.0	9.2	5.2	1.1	-0.9	5.4	-0.2	-0.3	-0.2	-0.1	-0.2	-0.1	-0.2	-0.3
29.3	9.1	11.0	-10.0	9.1	7.1	2.3	-2.0	8.0	-0.2	-0.2	-0.3	-0.4	-0.2	-0.3	-0.2	-0.5
39.1	9.3	12.0	-11.0	10.0	9.3	2.4	-2.1	9.5	-0.2	-0.4	-0.3	-0.3	-0.2	-0.3	-0.2	-0.4
48.8	8.6	13.0	-11.0	8.6	12.0	1.6	-2.9	12.0	-0.2	-0.2	-0.3	-0.4	-0.2	-0.2	-0.2	-0.5
58.6	8.5	12.0	-10.0	7.8	15.0	2.4	-3.2	14.0	-0.4	-0.2	-0.3	-0.4	-0.2	-0.1	-0.4	-0.3
68.4	8.1	12.0	-10.0	8.1	17.0	3.2	-2.9	17.0	-0.4	-0.5	-0.4	-0.4	-0.3	-0.4	-0.3	-0.3
78.1	8.4	11.0	-10.0	8.0	19.0	3.4	-4.2	20.0	-0.2	-0.2	-0.2	-0.3	-0.2	-0.2	-0.2	-0.3
87.9	7.4	12.0	-10.0	6.9	21.0	3.5	-4.5	21.0	-0.1	-0.3	-0.1	-0.1	-0.2	-0.3	-0.1	-0.3
97.7	7.2	12.0	-11.0	6.1	23.0	4.0	-5.5	23.0	-0.2	-0.3	-0.3	-0.4	-0.2	-0.3	-0.2	-0.3
107.4	5.8	12.0	-11.0	4.8	25.0	5.0	-6.0	25.0	-0.2	-0.3	-0.2	-0.3	-0.3	-0.4	-0.3	-0.2
117.2	4.0	12.0	-11.0	3.1	26.0	5.7	-7.1	27.0	-0.2	-0.3	-0.2	-0.2	-0.2	-0.2	-0.2	-0.2
127.0	1.6	12.0	-11.0	1.7	28.0	6.6	-7.3	29.0	-0.2	-0.4	-0.5	-0.8	-0.3	-0.4	-0.3	-0.3
136.7	-1.1	13.0	-12.0	0.1	32.0	8.2	-8.5	33.0	-0.2	-0.4	-0.3	-0.4	-0.2	-0.2	-0.2	-0.4

Table 60. Raw data for the test seal at ω=10 krpm, PD=37.9 bars, C_r=0.188 mm, and inlet GVF=10%

Freq.	Re($\boldsymbol{H_{XX}}$)	Re($\boldsymbol{H_{XY}}$)	Re($\boldsymbol{H_{YX}}$)	Re($\boldsymbol{H_{YY}}$)	Im($\boldsymbol{H_{XX}}$)	Im($\boldsymbol{H_{XY}}$)	Im($\boldsymbol{H_{YX}}$)	Im($\boldsymbol{H_{YY}}$)	Re($\boldsymbol{eH_{XX}}$)	Re($\boldsymbol{eH_{XY}}$)	Re($\boldsymbol{eH_{YX}}$)	Re($\boldsymbol{eH_{YY}}$)	Im($\boldsymbol{eH_{XX}}$)	Im($\boldsymbol{eH_{XY}}$)	Im($\boldsymbol{eH_{YX}}$)	Im($\boldsymbol{eH_{YY}}$)
Hz	MN/m	MN/m	MN/m	MN/m	MN/m	MN/m	MN/m	MN/m	MN/m	MN/m	MN/m	MN/m	MN/m	MN/m	MN/m	MN/m
9.8	9.1	20.0	-19.0	9.3	2.9	1.3	-1.1	2.8	-0.4	-0.4	-0.4	-0.6	-0.3	-0.3	-0.4	-0.3
19.5	8.6	21.0	-19.0	8.9	4.5	2.0	-2.3	4.7	-0.3	-0.3	-0.3	-0.2	-0.2	-0.2	-0.1	-0.2
29.3	8.4	22.0	-19.0	8.0	7.1	2.9	-2.7	6.2	-0.2	-0.2	-0.2	-0.3	-0.2	-0.2	-0.2	-0.2
39.1	8.7	21.0	-20.0	8.6	8.8	3.5	-4.3	9.4	-0.2	-0.3	-0.2	-0.3	-0.3	-0.3	-0.3	-0.3
48.8	7.1	21.0	-20.0	7.7	12.0	4.0	-4.8	11.0	-0.2	-0.3	-0.2	-0.2	-0.2	-0.2	-0.2	-0.3
58.6	6.5	21.0	-19.0	6.8	14.0	5.4	-5.0	14.0	-0.2	-0.2	-0.2	-0.2	-0.2	-0.1	-0.2	-0.2
68.4	6.0	21.0	-19.0	6.3	16.0	5.8	-7.0	17.0	-0.1	-0.1	-0.2	-0.2	-0.2	-0.2	-0.2	-0.2
78.1	5.8	21.0	-19.0	5.7	19.0	7.7	-8.2	19.0	-0.1	-0.1	-0.2	-0.2	-0.2	-0.2	-0.2	-0.2
87.9	5.1	22.0	-19.0	4.8	21.0	9.2	-10.0	21.0	-0.1	-0.1	-0.1	-0.1	-0.1	-0.1	-0.1	-0.1
97.7	4.1	22.0	-20.0	3.8	23.0	11.0	-11.0	23.0	-0.1	-0.1	-0.1	-0.1	-0.2	-0.1	-0.2	-0.1
107.4	2.2	23.0	-21.0	2.3	25.0	11.0	-12.0	25.0	-0.2	-0.2	-0.2	-0.2	-0.2	-0.2	-0.2	-0.2
117.2	0.3	24.0	-22.0	0.2	28.0	11.0	-12.0	28.0	-0.2	-0.1	-0.1	-0.1	-0.2	-0.2	-0.2	-0.2
127.0	-1.5	24.0	-21.0	-1.5	30.0	12.0	-13.0	31.0	-0.2	-0.2	-0.2	-0.4	-0.2	-0.1	-0.3	-0.2
136.7	-4.0	24.0	-20.0	-3.7	33.0	13.0	-15.0	34.0	-0.2	-0.3	-0.1	-0.2	-0.2	-0.3	-0.2	-0.2

Table 61. Raw data for the test seal at ω=15 krpm, PD=37.9 bars, C_r=0.188 mm, and inlet GVF=0%

Freq.	Re($\boldsymbol{H_{XX}}$)	Re($\boldsymbol{H_{XY}}$)	Re($\boldsymbol{H_{YX}}$)	Re($\boldsymbol{H_{YY}}$)	Im($\boldsymbol{H_{XX}}$)	Im($\boldsymbol{H_{XY}}$)	Im($\boldsymbol{H_{YX}}$)	Im($\boldsymbol{H_{YY}}$)	Re($\boldsymbol{eH_{XX}}$)	Re($\boldsymbol{eH_{XY}}$)	Re($\boldsymbol{eH_{YX}}$)	Re($\boldsymbol{eH_{YY}}$)	Im($\boldsymbol{eH_{XX}}$)	Im($\boldsymbol{eH_{XY}}$)	Im($\boldsymbol{eH_{YX}}$)	Im($\boldsymbol{eH_{YY}}$)
Hz	MN/m	MN/m	MN/m	MN/m	MN/m	MN/m	MN/m	MN/m	MN/m	MN/m	MN/m	MN/m	MN/m	MN/m	MN/m	MN/m
9.8	9.2	21.0	-18.0	8.7	2.5	0.7	-1.4	2.4	-0.2	-0.2	-0.3	-0.3	-0.1	-0.2	-0.1	-0.1
19.5	8.8	21.0	-19.0	8.4	4.6	2.3	-2.6	4.8	-0.2	-0.2	-0.2	-0.2	-0.2	-0.2	-0.2	-0.2
29.3	8.4	22.0	-19.0	8.4	7.0	3.3	-3.1	6.7	-0.1	-0.1	-0.2	-0.2	-0.2	-0.2	-0.2	-0.2
39.1	8.3	22.0	-20.0	8.3	9.1	3.8	-4.3	9.1	-0.1	-0.1	-0.2	-0.2	-0.2	-0.2	-0.1	-0.1
48.8	7.6	22.0	-20.0	7.5	11.0	4.1	-4.8	11.0	-0.2	-0.2	-0.1	-0.2	-0.1	-0.1	-0.2	-0.1
58.6	6.9	21.0	-20.0	6.6	14.0	5.1	-5.4	14.0	-0.2	-0.1	-0.1	-0.1	-0.1	-0.1	-0.2	-0.2
68.4	6.0	21.0	-19.0	6.3	17.0	6.0	-6.4	17.0	-0.1	-0.2	-0.1	-0.1	-0.1	-0.1	-0.1	-0.1
78.1	6.0	21.0	-19.0	5.7	19.0	7.4	-8.4	19.0	0.0	0.0	-0.1	-0.1	-0.1	-0.1	0.0	-0.1
87.9	5.2	22.0	-20.0	4.8	21.0	9.2	-10.0	21.0	-0.1	-0.1	-0.1	-0.1	-0.1	-0.1	-0.1	-0.2
97.7	4.2	23.0	-21.0	3.7	23.0	10.0	-11.0	24.0	-0.1	-0.1	-0.1	-0.1	-0.1	-0.1	-0.1	-0.1
107.4	2.3	24.0	-22.0	2.6	25.0	11.0	-11.0	26.0	-0.1	-0.2	-0.1	-0.1	-0.2	-0.1	-0.1	-0.1
117.2	0.7	24.0	-22.0	0.3	28.0	11.0	-12.0	28.0	-0.1	-0.2	-0.1	-0.1	-0.1	-0.1	0.0	-0.1
127.0	-1.4	24.0	-22.0	-1.2	30.0	12.0	-13.0	31.0	-0.2	-0.3	-0.2	-0.1	-0.2	-0.2	-0.2	-0.2
136.7	-3.8	24.0	-21.0	-2.8	33.0	13.0	-14.0	34.0	-0.2	-0.1	-0.2	-0.2	-0.1	-0.2	-0.2	-0.2

Table 62. Raw data for the test seal at ω=15 krpm, PD=37.9 bars, C_r=0.188 mm, and inlet GVF=2%

Freq.	Re($\boldsymbol{H_{XX}}$)	Re($\boldsymbol{H_{XY}}$)	Re($\boldsymbol{H_{YX}}$)	Re($\boldsymbol{H_{YY}}$)	Im($\boldsymbol{H_{XX}}$)	Im($\boldsymbol{H_{XY}}$)	Im($\boldsymbol{H_{YX}}$)	Im($\boldsymbol{H_{YY}}$)	Re($\boldsymbol{eH_{XX}}$)	Re($\boldsymbol{eH_{XY}}$)	Re($\boldsymbol{eH_{YX}}$)	Re($\boldsymbol{eH_{YY}}$)	Im($\boldsymbol{eH_{XX}}$)	Im($\boldsymbol{eH_{XY}}$)	Im($\boldsymbol{eH_{YX}}$)	Im($\boldsymbol{eH_{YY}}$)
Hz	MN/m	MN/m	MN/m	MN/m	MN/m	MN/m	MN/m	MN/m	MN/m	MN/m	MN/m	MN/m	MN/m	MN/m	MN/m	MN/m
9.8	9.2	20.0	-18.0	9.0	2.5	1.2	-1.1	2.4	-0.1	-0.1	-0.2	-0.2	-0.2	-0.2	-0.1	-0.2
19.5	8.9	21.0	-19.0	9.2	4.1	2.1	-2.4	4.3	-0.2	-0.1	-0.1	-0.1	-0.2	-0.3	-0.1	-0.2
29.3	8.6	21.0	-19.0	8.5	6.9	2.6	-2.8	6.5	-0.2	-0.2	-0.1	-0.1	-0.1	-0.1	-0.1	-0.1
39.1	8.0	21.0	-20.0	8.1	8.7	3.8	-4.1	9.1	-0.1	-0.1	-0.1	-0.1	-0.1	-0.1	-0.2	-0.2
48.8	7.5	21.0	-20.0	7.5	11.0	4.2	-4.8	12.0	-0.1	-0.1	-0.1	-0.1	-0.1	-0.1	0.0	-0.1
58.6	7.2	21.0	-20.0	6.9	14.0	5.4	-5.7	14.0	-0.1	-0.1	-0.1	-0.1	-0.1	-0.1	-0.1	-0.1
68.4	6.8	21.0	-20.0	6.8	17.0	6.1	-6.5	17.0	-0.1	-0.1	-0.1	-0.1	-0.1	-0.1	-0.1	-0.1
78.1	6.4	22.0	-20.0	6.4	19.0	7.5	-7.9	19.0	-0.1	-0.1	-0.1	-0.1	-0.1	-0.1	-0.1	-0.1
87.9	5.7	22.0	-20.0	5.4	21.0	8.5	-9.2	21.0	-0.1	-0.1	-0.1	-0.1	-0.1	-0.2	-0.1	-0.1
97.7	4.2	23.0	-21.0	4.2	23.0	9.7	-10.0	23.0	-0.1	-0.1	-0.1	-0.1	-0.1	-0.1	-0.1	-0.1
107.4	2.8	24.0	-22.0	3.0	25.0	9.9	-11.0	26.0	-0.1	-0.1	-0.2	-0.1	-0.1	-0.1	-0.1	-0.2
117.2	0.5	24.0	-22.0	0.9	28.0	10.0	-12.0	28.0	-0.1	-0.2	-0.1	-0.1	-0.2	-0.1	-0.1	-0.1
127.0	-1.0	24.0	-22.0	-1.6	31.0	11.0	-12.0	31.0	-0.2	-0.3	-0.2	-0.2	-0.3	-0.3	-0.2	-0.3
136.7	-4.1	25.0	-22.0	-3.1	35.0	12.0	-14.0	36.0	-0.1	-0.2	-0.1	-0.2	-0.1	-0.1	-0.1	-0.1

Table 63. Raw data for the test seal at ω=15 krpm, PD=37.9 bars, C_r=0.188 mm, and inlet GVF=4%

Freq.	Re($\boldsymbol{H_{XX}}$)	Re($\boldsymbol{H_{XY}}$)	Re($\boldsymbol{H_{YX}}$)	Re($\boldsymbol{H_{YY}}$)	Im($\boldsymbol{H_{XX}}$)	Im($\boldsymbol{H_{XY}}$)	Im($\boldsymbol{H_{YX}}$)	Im($\boldsymbol{H_{YY}}$)	Re($\boldsymbol{eH_{XX}}$)	Re($\boldsymbol{eH_{XY}}$)	Re($\boldsymbol{eH_{YX}}$)	Re($\boldsymbol{eH_{YY}}$)	Im($\boldsymbol{eH_{XX}}$)	Im($\boldsymbol{eH_{XY}}$)	Im($\boldsymbol{eH_{YX}}$)	Im($\boldsymbol{eH_{YY}}$)
Hz	MN/m	MN/m	MN/m	MN/m	MN/m	MN/m	MN/m	MN/m	MN/m	MN/m	MN/m	MN/m	MN/m	MN/m	MN/m	MN/m
9.8	9.9	21.0	-18.0	10.0	1.9	1.6	-1.6	1.5	-0.3	-0.3	-0.2	-0.2	-0.2	-0.3	-0.2	-0.2
19.5	8.8	20.0	-19.0	8.8	3.7	1.9	-1.7	4.4	-0.2	-0.1	-0.1	-0.1	-0.1	-0.2	-0.2	-0.2
29.3	8.9	20.0	-18.0	8.3	6.4	2.9	-3.0	6.5	-0.1	-0.1	-0.1	-0.1	-0.2	-0.2	-0.2	-0.3
39.1	8.7	20.0	-18.0	8.8	8.5	3.7	-4.1	8.7	-0.1	-0.1	-0.2	-0.2	-0.2	-0.1	-0.1	-0.1
48.8	7.8	21.0	-19.0	7.3	11.0	4.9	-5.3	11.0	-0.2	-0.2	-0.1	-0.1	-0.1	-0.2	-0.2	-0.2
58.6	7.5	21.0	-19.0	6.9	14.0	6.2	-6.3	14.0	-0.2	-0.2	-0.2	-0.2	-0.1	-0.1	-0.2	-0.2
68.4	6.8	21.0	-19.0	6.9	17.0	6.3	-6.9	17.0	-0.2	-0.2	-0.2	-0.2	-0.1	-0.1	-0.1	-0.2
78.1	6.4	22.0	-20.0	7.1	19.0	7.8	-8.1	19.0	-0.1	-0.1	-0.2	-0.2	-0.1	-0.2	-0.2	-0.2
87.9	5.8	22.0	-21.0	5.9	21.0	8.2	-9.7	21.0	-0.1	-0.1	-0.1	-0.1	-0.1	-0.1	-0.1	-0.1
97.7	5.0	24.0	-22.0	5.2	24.0	9.0	-9.8	23.0	-0.1	-0.1	-0.1	-0.2	-0.1	-0.2	-0.2	-0.1
107.4	3.4	24.0	-22.0	3.4	25.0	8.8	-10.0	25.0	-0.1	-0.1	-0.2	-0.1	-0.1	-0.1	-0.2	-0.2
117.2	2.4	24.0	-22.0	1.2	28.0	9.2	-11.0	28.0	-0.1	-0.1	-0.2	-0.1	-0.1	-0.1	-0.1	-0.2
127.0	0.2	24.0	-23.0	0.8	31.0	9.9	-11.0	32.0	-0.2	-0.2	-0.3	-0.2	-0.2	-0.3	-0.2	-0.4
136.7	-2.6	25.0	-22.0	-1.6	35.0	11.0	-13.0	35.0	-0.1	-0.1	-0.2	-0.2	-0.1	-0.2	-0.2	-0.2

Table 64. Raw data for the test seal at ω=15 krpm, PD=37.9 bars, C_r=0.188 mm, and inlet GVF=6%

Freq.	Re($\boldsymbol{H_{XX}}$)	Re($\boldsymbol{H_{XY}}$)	Re($\boldsymbol{H_{YX}}$)	Re($\boldsymbol{H_{YY}}$)	Im($\boldsymbol{H_{XX}}$)	Im($\boldsymbol{H_{XY}}$)	Im($\boldsymbol{H_{YX}}$)	Im($\boldsymbol{H_{YY}}$)	Re($\boldsymbol{eH_{XX}}$)	Re($\boldsymbol{eH_{XY}}$)	Re($\boldsymbol{eH_{YX}}$)	Re($\boldsymbol{eH_{YY}}$)	Im($\boldsymbol{eH_{XX}}$)	Im($\boldsymbol{eH_{XY}}$)	Im($\boldsymbol{eH_{YX}}$)	Im($\boldsymbol{eH_{YY}}$)
Hz	MN/m	MN/m	MN/m	MN/m	MN/m	MN/m	MN/m	MN/m	MN/m	MN/m	MN/m	MN/m	MN/m	MN/m	MN/m	MN/m
9.8	10.0	20.0	-18.0	11.0	1.7	1.7	-0.6	0.8	-0.3	-0.3	-0.3	-0.3	-0.3	-0.3	-0.4	-0.4
19.5	9.4	20.0	-18.0	9.0	3.9	1.3	-1.2	3.7	-0.2	-0.2	-0.2	-0.2	-0.2	-0.2	-0.1	-0.2
29.3	8.8	19.0	-18.0	8.5	6.2	2.4	-2.0	6.4	-0.2	-0.2	-0.2	-0.2	-0.2	-0.2	-0.1	-0.2
39.1	9.0	20.0	-18.0	9.2	8.9	3.7	-4.0	8.9	-0.2	-0.3	-0.2	-0.2	-0.2	-0.1	-0.2	-0.2
48.8	8.3	20.0	-18.0	8.6	11.0	4.5	-5.4	11.0	-0.2	-0.2	-0.1	-0.1	-0.1	-0.1	-0.1	-0.1
58.6	8.3	20.0	-19.0	8.2	13.0	6.2	-6.3	13.0	-0.1	-0.2	-0.3	-0.4	-0.2	-0.3	-0.2	-0.4
68.4	7.1	21.0	-19.0	7.1	16.0	6.6	-7.5	17.0	-0.3	-0.3	-0.2	-0.2	-0.2	-0.3	-0.3	-0.3
78.1	7.3	22.0	-20.0	7.0	18.0	7.3	-8.5	19.0	-0.2	-0.2	-0.2	-0.2	-0.2	-0.2	-0.2	-0.2
87.9	5.8	23.0	-21.0	6.2	21.0	8.2	-9.7	20.0	-0.1	-0.1	-0.2	-0.2	-0.1	-0.2	-0.1	-0.1
97.7	5.3	23.0	-22.0	5.2	23.0	8.2	-9.4	23.0	-0.2	-0.1	-0.1	-0.2	-0.1	-0.2	-0.2	-0.2
107.4	3.7	24.0	-21.0	3.7	25.0	8.9	-9.9	25.0	-0.1	-0.2	-0.3	-0.2	-0.2	-0.2	-0.1	-0.2
117.2	2.4	24.0	-22.0	2.2	28.0	9.8	-11.0	28.0	-0.1	-0.1	-0.2	-0.1	-0.1	-0.1	-0.2	-0.2
127.0	1.2	24.0	-22.0	0.9	29.0	9.3	-11.0	30.0	-0.2	-0.1	-0.1	-0.1	-0.2	-0.3	-0.1	-0.2
136.7	-2.1	25.0	-21.0	-1.2	33.0	10.0	-12.0	34.0	-0.2	-0.2	-0.2	-0.3	-0.2	-0.3	-0.2	-0.3

Table 65. Raw data for the test seal at ω=15 krpm, PD=37.9 bars, C_r=0.188 mm, and inlet GVF=8%

Freq.	Re($\boldsymbol{H_{XX}}$)	Re($\boldsymbol{H_{XY}}$)	Re($\boldsymbol{H_{YX}}$)	Re($\boldsymbol{H_{YY}}$)	Im($\boldsymbol{H_{XX}}$)	Im($\boldsymbol{H_{XY}}$)	Im($\boldsymbol{H_{YX}}$)	Im($\boldsymbol{H_{YY}}$)	Re($\boldsymbol{eH_{XX}}$)	Re($\boldsymbol{eH_{XY}}$)	Re($\boldsymbol{eH_{YX}}$)	Re($\boldsymbol{eH_{YY}}$)	Im($\boldsymbol{eH_{XX}}$)	Im($\boldsymbol{eH_{XY}}$)	Im($\boldsymbol{eH_{YX}}$)	Im($\boldsymbol{eH_{YY}}$)
Hz	MN/m	MN/m	MN/m	MN/m	MN/m	MN/m	MN/m	MN/m	MN/m	MN/m	MN/m	MN/m	MN/m	MN/m	MN/m	MN/m
9.8	10.0	20.0	-19.0	9.4	0.9	1.2	-0.9	1.9	-0.4	-0.5	-1.0	-0.9	-0.9	-1.0	-0.7	-0.7
19.5	8.5	20.0	-19.0	7.4	2.9	1.2	-1.6	4.0	-0.7	-0.6	-0.5	-0.6	-0.6	-0.8	-0.8	-0.8
29.3	7.7	19.0	-18.0	7.6	7.4	0.7	-1.5	7.3	-0.7	-1.0	-0.9	-1.4	-0.5	-0.7	-0.7	-0.7
39.1	10.0	18.0	-18.0	6.3	9.6	1.8	-3.5	8.2	-0.8	-1.3	-0.6	-0.7	-0.8	-1.1	-0.7	-1.1
48.8	8.3	18.0	-18.0	7.7	12.0	4.4	-5.4	12.0	-0.5	-0.7	-0.7	-0.9	-0.6	-0.8	-0.5	-0.5
58.6	7.1	21.0	-20.0	7.3	14.0	5.9	-4.6	12.0	-0.7	-0.8	-0.8	-1.0	-0.4	-0.6	-0.7	-0.7
68.4	8.9	19.0	-18.0	7.2	18.0	1.7	-4.8	13.0	-1.0	-1.4	-1.4	-1.8	-1.3	-1.9	-1.1	-1.6
78.1	7.3	21.0	-18.0	5.5	18.0	7.2	-8.0	18.0	-0.5	-0.5	-0.7	-1.0	-0.4	-0.5	-0.4	-0.4
87.9	5.3	23.0	-21.0	6.1	21.0	7.8	-8.4	20.0	-0.6	-0.6	-0.6	-0.7	-0.2	-0.5	-0.8	-1.0
97.7	5.3	22.0	-22.0	4.2	23.0	6.6	-8.6	22.0	-0.5	-0.8	-0.7	-0.8	-0.6	-0.7	-0.7	-0.9
107.4	4.4	23.0	-21.0	3.8	25.0	8.0	-9.0	27.0	-0.7	-0.7	-1.1	-1.4	-0.6	-0.6	-1.0	-1.4
117.2	3.3	22.0	-20.0	4.5	27.0	9.2	-9.8	28.0	-0.5	-0.8	-0.4	-0.9	-0.6	-0.7	-0.9	-1.1
127.0	-1.4	26.0	-20.0	-1.6	31.0	9.7	-12.0	29.0	-1.3	-1.1	-0.7	-0.8	-0.4	-1.3	-0.9	-1.0
136.7	-0.6	24.0	-22.0	-0.9	34.0	7.9	-11.0	34.0	-0.8	-2.0	-0.7	-1.0	-1.2	-0.6	-0.4	-0.5

Table 66. Raw data for the test seal at ω=15 krpm, PD=37.9 bars, C_r=0.188 mm, and inlet GVF=10%

Freq.	Re(H_{XX})	Re(H_{XY})	Re(H_{YX})	Re(H_{YY})	Im(H_{XX})	Im(H_{XY})	Im(H_{YX})	Im(H_{YY})	Re(eH_{XX})	Re(eH_{XY})	Re(eH_{YX})	Re(eH_{YY})	Im(eH_{XX})	Im(eH_{XY})	Im(eH_{YX})	Im(eH_{YY})
Hz	MN/m	MN/m	MN/m	MN/m	MN/m	MN/m	MN/m	MN/m	MN/m	MN/m	MN/m	MN/m	MN/m	MN/m	MN/m	MN/m
9.8	-1.2	8.0	-3.7	-4.0	3.3	-0.3	-0.4	2.6	-0.2	-0.2	-0.1	-0.2	-0.1	-0.2	-0.1	-0.1
19.5	-1.7	8.2	-3.9	-4.3	5.3	0.4	-0.7	5.0	-0.3	-0.2	-0.1	-0.2	-0.1	-0.2	-0.1	-0.1
29.3	-1.8	8.6	-3.5	-5.8	7.6	0.1	-1.0	8.0	-0.3	-0.2	-0.1	-0.2	-0.1	-0.1	-0.1	-0.2
39.1	-2.1	8.1	-4.3	-4.5	10.0	-0.6	-1.1	10.0	-0.3	-0.2	-0.2	-0.2	-0.1	-0.2	-0.1	-0.1
48.8	-2.0	7.4	-4.1	-4.9	13.0	-0.7	-1.5	13.0	-0.3	-0.1	-0.1	-0.2	-0.2	-0.2	-0.1	-0.1
58.6	-2.6	8.0	-4.0	-5.3	15.0	-0.2	-1.9	16.0	-0.3	-0.2	-0.1	-0.3	-0.1	-0.2	-0.1	-0.1
68.4	-3.3	7.8	-4.3	-4.9	17.0	-0.3	-2.0	19.0	-0.4	-0.3	-0.2	-0.3	-0.1	-0.2	-0.1	-0.3
78.1	-2.5	7.7	-4.2	-6.1	20.0	-0.5	-2.4	21.0	-0.3	-0.2	-0.2	-0.3	-0.2	-0.3	-0.1	-0.1
87.9	-4.1	7.1	-4.2	-6.9	22.0	-0.3	-3.3	24.0	-0.3	-0.1	-0.2	-0.2	-0.3	-0.2	-0.1	-0.2
97.7	-4.9	7.3	-5.0	-7.5	24.0	-0.4	-3.2	27.0	-0.3	-0.1	-0.1	-0.2	-0.2	-0.2	-0.1	-0.2
107.4	-5.9	7.5	-4.7	-8.1	28.0	-0.4	-3.5	29.0	-0.3	-0.1	-0.2	-0.3	-0.2	-0.3	-0.1	-0.1
117.2	-7.3	7.5	-4.8	-9.3	30.0	-0.1	-3.6	32.0	-0.4	-0.1	-0.1	-0.3	-0.1	-0.2	-0.1	-0.1
127.0	-7.2	7.7	-5.2	-11.0	33.0	-0.3	-3.7	37.0	-0.2	-0.3	-0.1	-0.2	-0.1	-0.4	-0.1	-0.4
136.7	-9.4	6.8	-4.8	-12.0	35.0	0.5	-3.9	38.0	-0.4	-0.2	-0.1	-0.3	-0.2	-0.2	-0.2	-0.3

Table 67. Raw data for the test seal at ω=5 krpm, PD=31 bars, C_r=0.188 mm, and inlet GVF=6%

Freq.	Re(H_{XX})	Re(H_{XY})	Re(H_{YX})	Re(H_{YY})	Im(H_{XX})	Im(H_{XY})	Im(H_{YX})	Im(H_{YY})	Re(eH_{XX})	Re(eH_{XY})	Re(eH_{YX})	Re(eH_{YY})	Im(eH_{XX})	Im(eH_{XY})	Im(eH_{YX})	Im(eH_{YY})
Hz	MN/m	MN/m	MN/m	MN/m	MN/m	MN/m	MN/m	MN/m	MN/m	MN/m	MN/m	MN/m	MN/m	MN/m	MN/m	MN/m
9.8	-1.2	7.6	-3.6	-3.1	3.1	0.3	-0.3	2.8	-0.6	-0.3	-0.2	-0.1	-0.1	-0.1	0.0	-0.1
19.5	-1.2	7.5	-3.7	-3.1	5.0	0.4	-0.8	5.3	-0.6	-0.2	-0.2	-0.1	-0.1	-0.1	-0.1	-0.1
29.3	-1.9	8.1	-3.7	-3.6	7.5	0.2	-1.1	7.9	-0.7	-0.3	-0.2	-0.2	-0.1	-0.3	-0.1	-0.1
39.1	-2.0	8.0	-3.9	-3.4	10.0	-0.2	-1.1	11.0	-0.6	-0.2	-0.2	-0.2	-0.1	-0.2	-0.1	-0.1
48.8	-2.1	7.3	-3.7	-3.8	13.0	0.1	-1.4	13.0	-0.6	-0.1	-0.2	-0.1	-0.2	-0.2	0.0	-0.1
58.6	-2.2	7.0	-3.8	-3.9	14.0	0.3	-1.9	15.0	-0.6	-0.1	-0.2	-0.2	-0.2	-0.2	-0.2	-0.2
68.4	-3.0	7.0	-4.1	-4.0	17.0	0.0	-2.3	19.0	-0.6	-0.1	-0.2	-0.1	-0.1	-0.2	-0.1	-0.2
78.1	-2.0	7.8	-3.7	-4.8	20.0	0.0	-2.7	20.0	-0.4	-0.1	-0.1	-0.1	-0.2	-0.2	-0.1	-0.1
87.9	-4.0	7.6	-4.2	-5.7	22.0	0.5	-3.1	23.0	-0.7	-0.1	-0.2	-0.2	-0.2	-0.3	-0.1	-0.1
97.7	-4.9	7.4	-4.7	-6.7	25.0	0.4	-3.6	26.0	-0.6	-0.1	-0.2	-0.2	-0.3	-0.2	-0.2	-0.2
107.4	-6.1	7.9	-4.6	-7.2	28.0	0.3	-3.3	29.0	-0.6	-0.2	-0.2	-0.2	-0.4	-0.2	-0.3	-0.1
117.2	-7.2	7.9	-4.5	-8.5	29.0	0.2	-3.6	31.0	-0.7	-0.1	-0.2	-0.2	-0.3	-0.2	-0.1	-0.1
127.0	-7.2	8.4	-4.2	-8.9	32.0	0.6	-3.2	34.0	-0.5	-0.1	-0.1	-0.2	-0.5	-0.2	-0.1	-0.2
136.7	-9.5	7.7	-4.7	-10.0	35.0	0.5	-4.1	38.0	-0.8	-0.2	-0.1	-0.1	-0.4	-0.3	-0.1	-0.3

Table 68. Raw data for the test seal at ω=5 krpm, PD=31 bars, C_r=0.188 mm, and inlet GVF=8%

Freq.	Re(H_{XX})	Re(H_{XY})	Re(H_{YX})	Re(H_{YY})	Im(H_{XX})	Im(H_{XY})	Im(H_{YX})	Im(H_{YY})	Re(eH_{XX})	Re(eH_{XY})	Re(eH_{YX})	Re(eH_{YY})	Im(eH_{XX})	Im(eH_{XY})	Im(eH_{YX})	Im(eH_{YY})
Hz	MN/m	MN/m	MN/m	MN/m	MN/m	MN/m	MN/m	MN/m	MN/m	MN/m	MN/m	MN/m	MN/m	MN/m	MN/m	MN/m
9.8	0.2	7.6	-3.2	-2.3	3.0	0.3	-0.4	2.8	-0.3	-0.1	0.0	-0.1	-0.1	-0.1	-0.1	0.0
19.5	0.2	7.4	-3.4	-2.2	4.9	0.2	-0.8	5.3	-0.2	-0.1	-0.1	-0.1	0.0	-0.1	0.0	-0.1
29.3	-0.2	7.7	-3.4	-2.4	7.1	0.4	-1.0	7.5	-0.3	-0.2	-0.1	-0.2	-0.1	-0.2	-0.1	-0.2
39.1	-0.4	7.6	-3.6	-2.5	9.8	0.1	-1.1	10.0	-0.3	-0.2	-0.1	-0.2	-0.1	-0.1	-0.1	-0.1
48.8	-0.6	7.4	-3.3	-2.9	13.0	0.1	-1.6	13.0	-0.3	-0.1	-0.1	-0.2	-0.1	-0.1	-0.1	-0.1
58.6	-0.9	7.1	-3.4	-3.3	14.0	0.4	-1.8	15.0	-0.4	-0.1	-0.2	-0.1	-0.2	-0.2	-0.1	-0.1
68.4	-1.6	7.7	-3.6	-3.7	16.0	0.0	-2.4	18.0	-0.3	-0.2	-0.1	-0.1	-0.1	-0.2	-0.1	-0.2
78.1	-1.0	7.7	-3.5	-3.9	19.0	0.2	-2.6	20.0	-0.2	-0.1	-0.1	-0.2	-0.2	-0.1	-0.2	-0.1
87.9	-2.5	7.4	-3.5	-5.3	22.0	0.2	-3.1	23.0	-0.2	-0.2	-0.1	-0.2	-0.2	-0.2	-0.1	-0.1
97.7	-3.7	7.6	-3.9	-6.0	24.0	0.3	-3.4	25.0	-0.4	-0.2	-0.2	-0.2	-0.1	-0.2	-0.1	-0.1
107.4	-4.5	7.7	-4.2	-6.4	27.0	0.4	-3.6	28.0	-0.3	-0.1	-0.2	-0.1	-0.2	-0.1	-0.2	-0.1
117.2	-5.6	7.9	-4.2	-7.9	29.0	0.4	-3.7	31.0	-0.2	-0.1	-0.1	-0.1	-0.1	-0.1	-0.1	-0.1
127.0	-5.8	7.7	-4.0	-8.4	31.0	0.6	-3.3	33.0	-0.4	-0.4	-0.2	-0.1	-0.2	-0.4	-0.1	-0.1
136.7	-7.9	7.0	-4.2	-9.6	34.0	0.7	-4.4	37.0	-0.3	-0.2	-0.2	-0.3	-0.2	-0.2	-0.2	-0.2

Table 69. Raw data for the test seal at ω=5 krpm, PD=31 bars, C_r=0.188 mm, and inlet GVF=10%

Freq.	Re(H_{XX})	Re(H_{XY})	Re(H_{YX})	Re(H_{YY})	Im(H_{XX})	Im(H_{XY})	Im(H_{YX})	Im(H_{YY})	Re(eH_{XX})	Re(eH_{XY})	Re(eH_{YX})	Re(eH_{YY})	Im(eH_{XX})	Im(eH_{XY})	Im(eH_{YX})	Im(eH_{YY})
Hz	MN/m	MN/m	MN/m	MN/m	MN/m	MN/m	MN/m	MN/m	MN/m	MN/m	MN/m	MN/m	MN/m	MN/m	MN/m	MN/m
9.8	-4.6	11.0	-8.0	-5.3	3.4	0.1	-0.3	2.1	-0.1	-0.1	-0.1	-0.1	-0.1	-0.2	-0.1	-0.1
19.5	-4.4	11.0	-8.3	-5.7	5.3	0.2	-1.0	5.4	-0.1	-0.1	-0.1	-0.1	-0.1	-0.1	-0.1	-0.1
29.3	-5.3	11.0	-7.3	-7.5	7.9	1.0	-1.7	7.5	-0.1	-0.2	-0.1	-0.2	-0.1	-0.1	-0.1	-0.1
39.1	-5.1	11.0	-8.1	-6.3	10.0	1.4	-2.0	9.9	-0.2	-0.1	-0.1	-0.1	-0.1	-0.1	-0.1	-0.1
48.8	-6.0	10.0	-8.3	-7.1	13.0	1.7	-2.7	13.0	-0.2	-0.1	-0.2	-0.2	-0.2	-0.1	-0.2	-0.2
58.6	-6.6	11.0	-8.5	-8.3	15.0	1.8	-3.6	17.0	-0.2	-0.2	-0.3	-0.2	-0.2	-0.3	-0.3	-0.3
68.4	-6.7	9.8	-8.8	-6.3	18.0	2.2	-3.0	18.0	-0.3	-0.7	-0.2	-0.6	-0.3	-0.2	-0.2	-0.2
78.1	-6.7	11.0	-8.6	-8.2	21.0	2.0	-4.5	21.0	-0.1	-0.1	-0.1	-0.1	-0.1	-0.1	-0.1	-0.1
87.9	-7.9	11.0	-9.0	-9.2	23.0	2.6	-4.8	24.0	-0.1	-0.2	-0.1	-0.1	-0.1	-0.1	-0.1	-0.2
97.7	-8.9	11.0	-9.1	-11.0	26.0	3.1	-5.7	27.0	-0.1	-0.1	-0.2	-0.1	-0.1	-0.2	-0.1	-0.2
107.4	-9.7	11.0	-8.6	-11.0	28.0	3.0	-5.9	28.0	-0.1	-0.2	-0.1	-0.2	-0.2	-0.2	-0.1	-0.1
117.2	-12.0	11.0	-9.3	-12.0	30.0	3.8	-6.7	31.0	-0.1	-0.1	-0.2	-0.2	-0.1	-0.1	-0.2	-0.2
127.0	-20.0	21.0	-16.0	-9.5	25.0	12.0	-0.5	25.0	-0.4	-1.1	-1.0	-0.7	-1.1	-0.6	-0.5	-1.0
136.7	-16.0	11.0	-9.5	-15.0	35.0	5.8	-7.0	36.0	-0.2	-0.2	-0.2	-0.2	-0.1	-0.2	-0.1	-0.3

Table 70. Raw data for the test seal at ω=7.5 krpm, PD=31 bars, C_r=0.188 mm, and inlet GVF=0%

Freq.	Re(H_{XX})	Re(H_{XY})	Re(H_{YX})	Re(H_{YY})	Im(H_{XX})	Im(H_{XY})	Im(H_{YX})	Im(H_{YY})	Re(eH_{XX})	Re(eH_{XY})	Re(eH_{YX})	Re(eH_{YY})	Im(eH_{XX})	Im(eH_{XY})	Im(eH_{YX})	Im(eH_{YY})
Hz	MN/m	MN/m	MN/m	MN/m	MN/m	MN/m	MN/m	MN/m	MN/m	MN/m	MN/m	MN/m	MN/m	MN/m	MN/m	MN/m
9.8	-2.3	8.6	-8.8	-2.6	1.9	0.4	0.2	3.4	-0.2	-0.2	-0.1	-0.2	-0.2	0.0	-0.2	-0.1
19.5	-2.2	9.0	-8.8	-2.7	4.7	0.9	-0.5	5.5	-0.2	-0.1	-0.1	-0.2	-0.1	-0.1	-0.1	-0.1
29.3	-2.4	9.1	-8.5	-2.7	7.0	1.3	-0.9	7.6	-0.2	-0.1	-0.1	-0.1	-0.1	-0.1	-0.1	-0.1
39.1	-2.6	9.4	-8.6	-3.0	9.5	1.2	-1.3	10.0	-0.2	-0.2	-0.1	-0.2	-0.1	-0.1	-0.1	-0.1
48.8	-3.3	9.2	-8.8	-3.7	12.0	1.8	-1.6	12.0	-0.3	-0.2	-0.1	-0.1	-0.1	-0.1	-0.1	-0.1
58.6	-3.8	9.0	-8.7	-3.8	14.0	2.5	-2.0	15.0	-0.2	-0.3	-0.2	-0.3	-0.2	-0.2	-0.2	-0.2
68.4	-4.5	9.3	-8.7	-4.8	17.0	2.7	-2.9	19.0	-0.3	-0.3	-0.2	-0.2	-0.2	-0.3	-0.1	-0.2
78.1	-4.4	9.3	-9.0	-4.1	19.0	2.6	-3.2	21.0	-0.2	-0.1	-0.1	-0.1	-0.1	-0.1	-0.1	-0.1
87.9	-5.3	9.5	-8.7	-5.2	21.0	3.4	-3.6	22.0	-0.2	-0.1	-0.1	-0.2	-0.1	-0.1	-0.1	-0.1
97.7	-6.3	9.6	-8.9	-5.8	23.0	4.0	-4.0	25.0	-0.3	-0.1	-0.1	-0.1	-0.1	-0.1	-0.1	-0.1
107.4	-7.6	9.8	-8.9	-6.5	26.0	4.2	-4.6	27.0	-0.3	-0.1	-0.1	-0.2	-0.1	-0.1	-0.1	-0.1
117.2	-8.9	10.0	-8.8	-8.5	28.0	4.7	-5.1	29.0	-0.3	-0.1	-0.1	-0.2	-0.1	-0.1	-0.1	-0.1
127.0	-15.0	29.0	-5.1	-9.6	34.0	9.2	-1.8	16.0	-5.6	-6.6	-5.8	-5.1	-6.7	-7.3	-3.8	-5.7
136.7	-13.0	10.0	-9.0	-11.0	33.0	6.3	-5.6	35.0	-0.3	-0.1	-0.1	-0.2	-0.1	-0.1	-0.1	-0.1

Table 71. Raw data for the test seal at ω=7.5 krpm, PD=31 bars, C_r=0.188 mm, and inlet GVF=2%

Freq.	Re(H_{XX})	Re(H_{XY})	Re(H_{YX})	Re(H_{YY})	Im(H_{XX})	Im(H_{XY})	Im(H_{YX})	Im(H_{YY})	Re(eH_{XX})	Re(eH_{XY})	Re(eH_{YX})	Re(eH_{YY})	Im(eH_{XX})	Im(eH_{XY})	Im(eH_{YX})	Im(eH_{YY})
Hz	MN/m	MN/m	MN/m	MN/m	MN/m	MN/m	MN/m	MN/m	MN/m	MN/m	MN/m	MN/m	MN/m	MN/m	MN/m	MN/m
9.8	-1.7	10.0	-7.7	-3.5	2.6	0.2	-0.5	2.7	-0.1	-0.1	-0.1	-0.1	0.0	-0.1	-0.1	0.0
19.5	-1.7	9.9	-7.7	-3.3	4.9	0.4	-0.8	5.2	0.0	0.0	0.0	-0.1	0.0	0.0	-0.1	-0.1
29.3	-2.1	9.8	-7.5	-3.3	7.3	1.1	-1.0	7.6	-0.1	-0.1	-0.1	-0.1	-0.1	-0.1	-0.1	-0.1
39.1	-2.1	10.0	-7.7	-3.6	9.6	1.0	-1.9	10.0	-0.1	-0.1	-0.1	-0.1	-0.1	-0.1	-0.1	-0.1
48.8	-2.6	10.0	-7.7	-4.6	12.0	1.1	-2.4	12.0	-0.2	-0.2	-0.1	-0.1	-0.2	-0.1	-0.1	-0.1
58.6	-3.1	9.7	-7.5	-4.7	14.0	2.1	-2.6	15.0	-0.1	-0.1	-0.2	-0.2	-0.1	-0.2	-0.2	-0.1
68.4	-3.5	10.0	-7.9	-5.4	17.0	1.7	-3.5	18.0	-0.1	-0.2	-0.1	-0.2	-0.1	-0.1	-0.1	-0.1
78.1	-3.4	10.0	-8.4	-5.3	20.0	2.1	-4.0	20.0	-0.1	-0.1	-0.1	-0.1	-0.1	-0.1	-0.1	-0.1
87.9	-4.5	10.0	-8.0	-6.3	22.0	2.8	-4.3	22.0	-0.1	0.0	-0.1	-0.1	0.0	-0.1	0.0	-0.1
97.7	-5.4	10.0	-8.4	-7.0	24.0	3.3	-4.8	24.0	-0.1	-0.1	-0.1	-0.1	-0.1	-0.1	-0.1	-0.1
107.4	-6.4	10.0	-8.4	-7.5	26.0	3.5	-5.1	27.0	-0.1	-0.1	-0.1	-0.1	-0.1	-0.1	-0.1	-0.1
117.2	-7.8	11.0	-8.5	-9.4	28.0	3.9	-5.6	29.0	-0.1	0.0	-0.1	-0.1	0.0	-0.1	-0.1	-0.1
127.0	-16.0	32.0	-3.4	-11.0	35.0	7.8	-0.9	13.0	-4.5	-5.1	-3.6	-3.4	-4.0	-4.4	-3.6	-4.6
136.7	-12.0	11.0	-8.6	-13.0	32.0	5.0	-6.6	34.0	-0.1	-0.1	-0.1	-0.1	-0.1	-0.1	-0.1	-0.1

Table 72. Raw data for the test seal at ω=7.5 krpm, PD=31 bars, C_r=0.188 mm, and inlet GVF=4%

Freq.	Re(H_{XX})	Re(H_{XY})	Re(H_{YX})	Re(H_{YY})	Im(H_{XX})	Im(H_{XY})	Im(H_{YX})	Im(H_{YY})	Re(eH_{XX})	Re(eH_{XY})	Re(eH_{YX})	Re(eH_{YY})	Im(eH_{XX})	Im(eH_{XY})	Im(eH_{YX})	Im(eH_{YY})
Hz	MN/m	MN/m	MN/m	MN/m	MN/m	MN/m	MN/m	MN/m	MN/m	MN/m	MN/m	MN/m	MN/m	MN/m	MN/m	MN/m
9.8	-0.3	8.7	-8.4	-1.1	2.3	0.2	-0.1	3.2	-0.1	-0.1	-0.1	-0.2	-0.1	-0.1	-0.1	-0.1
19.5	-0.4	8.9	-8.0	-0.6	4.9	0.9	-0.6	5.5	-0.1	-0.1	-0.1	-0.2	-0.1	-0.1	-0.1	0.0
29.3	-0.7	9.2	-7.9	-0.9	7.2	1.1	-1.0	7.4	-0.1	-0.1	-0.1	-0.2	-0.1	-0.1	-0.1	-0.1
39.1	-0.9	9.3	-8.3	-0.9	9.3	1.2	-1.4	9.9	-0.1	-0.1	-0.1	-0.2	-0.1	-0.1	-0.1	-0.1
48.8	-1.6	9.1	-8.0	-1.6	12.0	1.6	-1.7	12.0	-0.1	-0.2	-0.1	-0.2	-0.1	-0.1	-0.1	-0.1
58.6	-1.6	9.0	-7.8	-2.0	14.0	2.2	-2.2	15.0	-0.1	-0.1	-0.1	-0.1	-0.1	-0.1	-0.1	-0.2
68.4	-2.1	9.7	-8.0	-2.4	17.0	2.3	-2.9	17.0	-0.1	-0.4	-0.2	-0.4	-0.1	-0.1	-0.1	-0.2
78.1	-2.4	9.5	-8.5	-2.5	19.0	2.7	-3.3	20.0	-0.1	-0.2	-0.1	-0.2	-0.1	-0.1	-0.1	-0.2
87.9	-3.1	9.6	-8.3	-3.4	21.0	3.1	-3.5	22.0	-0.1	-0.1	-0.1	-0.2	-0.1	-0.1	-0.1	-0.1
97.7	-4.0	9.4	-8.6	-4.1	23.0	3.6	-4.1	24.0	-0.1	-0.2	-0.1	-0.2	-0.1	-0.1	-0.1	-0.1
107.4	-5.4	9.7	-8.6	-5.1	25.0	4.0	-4.5	26.0	-0.1	-0.2	-0.1	-0.2	-0.1	-0.1	-0.1	0.0
117.2	-7.1	10.0	-8.5	-6.7	28.0	4.7	-4.9	28.0	-0.1	-0.1	-0.1	-0.2	-0.1	-0.1	-0.1	-0.1
127.0	-10.0	24.0	-9.4	-11.0	29.0	5.1	-3.6	20.0	-4.9	-7.7	-5.4	-4.0	-6.6	-5.2	-3.6	-6.2
136.7	-11.0	11.0	-8.7	-11.0	33.0	5.7	-5.9	34.0	-0.1	-0.1	-0.1	-0.2	0.0	-0.1	-0.1	-0.1

Table 73. Raw data for the test seal at ω=7.5 krpm, PD=31 bars, C_r=0.188 mm, and inlet GVF=6%

Freq.	Re(H_{XX})	Re(H_{XY})	Re(H_{YX})	Re(H_{YY})	Im(H_{XX})	Im(H_{XY})	Im(H_{YX})	Im(H_{YY})	Re(eH_{XX})	Re(eH_{XY})	Re(eH_{YX})	Re(eH_{YY})	Im(eH_{XX})	Im(eH_{XY})	Im(eH_{YX})	Im(eH_{YY})
Hz	MN/m	MN/m	MN/m	MN/m	MN/m	MN/m	MN/m	MN/m	MN/m	MN/m	MN/m	MN/m	MN/m	MN/m	MN/m	MN/m
9.8	1.2	9.8	-6.8	-0.6	2.6	0.3	-0.6	2.4	-0.2	-0.1	-0.1	-0.1	-0.1	-0.1	-0.1	-0.1
19.5	1.4	9.8	-6.8	-0.3	5.1	0.6	-0.9	4.8	-0.2	-0.1	-0.1	-0.1	-0.1	-0.1	-0.1	-0.1
29.3	1.1	9.7	-6.7	-0.5	7.0	0.9	-1.3	7.0	-0.2	-0.1	-0.1	-0.1	-0.1	-0.2	-0.1	-0.1
39.1	0.8	10.0	-7.2	-0.6	9.3	0.8	-2.0	9.6	-0.2	-0.1	-0.1	-0.1	0.0	-0.1	-0.1	-0.2
48.8	0.6	9.9	-6.8	-1.5	12.0	1.0	-1.9	12.0	-0.2	-0.1	-0.1	-0.2	-0.1	-0.1	-0.2	-0.1
58.6	0.5	9.7	-6.9	-1.7	14.0	2.0	-2.6	14.0	-0.1	-0.2	-0.2	-0.2	-0.1	-0.1	-0.1	-0.1
68.4	-0.4	11.0	-6.9	-2.2	17.0	1.4	-3.2	17.0	-0.3	-0.4	-0.1	-0.3	-0.2	-0.3	-0.1	-0.2
78.1	-0.2	10.0	-7.2	-2.1	19.0	2.1	-3.8	19.0	-0.2	-0.1	-0.1	-0.1	-0.1	-0.2	-0.1	-0.1
87.9	-1.0	10.0	-7.2	-3.4	21.0	2.5	-4.2	21.0	-0.1	-0.1	-0.1	-0.2	-0.1	-0.2	-0.1	-0.1
97.7	-2.0	10.0	-7.7	-4.1	23.0	2.9	-4.5	23.0	-0.1	-0.1	-0.1	-0.2	-0.1	-0.1	-0.1	-0.1
107.4	-3.3	9.8	-7.7	-5.1	25.0	3.1	-5.0	26.0	-0.1	-0.1	-0.1	-0.1	-0.1	-0.2	-0.1	-0.1
117.2	-4.6	10.0	-7.5	-7.1	27.0	3.7	-5.7	28.0	-0.2	-0.1	-0.1	-0.1	-0.1	-0.1	-0.1	-0.1
127.0	-4.3	28.0	-3.8	-17.0	34.0	-4.6	-7.5	16.0	-10.0	-7.7	-9.4	-11.0	-12.0	-12.0	-9.0	-6.0
136.7	-8.8	11.0	-7.9	-11.0	33.0	5.0	-6.5	34.0	-0.2	-0.2	-0.1	-0.2	-0.1	-0.2	-0.1	-0.1

Table 74. Raw data for the test seal at ω=7.5 krpm, PD=31 bars, C_r=0.188 mm, and inlet GVF=8%

Freq.	Re($\boldsymbol{H_{XX}}$)	Re($\boldsymbol{H_{XY}}$)	Re($\boldsymbol{H_{YX}}$)	Re($\boldsymbol{H_{YY}}$)	Im($\boldsymbol{H_{XX}}$)	Im($\boldsymbol{H_{XY}}$)	Im($\boldsymbol{H_{YX}}$)	Im($\boldsymbol{H_{YY}}$)	Re($\boldsymbol{eH_{XX}}$)	Re($\boldsymbol{eH_{XY}}$)	Re($\boldsymbol{eH_{YX}}$)	Re($\boldsymbol{eH_{YY}}$)	Im($\boldsymbol{eH_{XX}}$)	Im($\boldsymbol{eH_{XY}}$)	Im($\boldsymbol{eH_{YX}}$)	Im($\boldsymbol{eH_{YY}}$)
Hz	MN/m	MN/m	MN/m	MN/m	MN/m	MN/m	MN/m	MN/m	MN/m	MN/m	MN/m	MN/m	MN/m	MN/m	MN/m	MN/m
9.8	1.8	8.3	-7.3	1.4	2.3	0.5	-0.4	2.6	-0.1	-0.1	-0.1	-0.2	-0.1	-0.1	-0.1	-0.1
19.5	1.9	8.5	-7.5	1.8	4.8	0.8	-0.7	5.2	-0.1	-0.1	-0.1	-0.2	0.0	-0.1	-0.1	-0.1
29.3	1.6	8.9	-7.4	1.4	6.9	1.1	-1.0	7.2	-0.1	-0.1	-0.2	-0.4	-0.1	-0.1	-0.1	-0.1
39.1	1.2	8.9	-7.9	1.4	9.1	1.3	-1.5	9.5	-0.1	-0.2	-0.1	-0.2	-0.1	-0.1	-0.1	-0.2
48.8	0.8	8.6	-7.6	1.0	12.0	1.6	-1.5	12.0	-0.1	-0.1	-0.1	-0.2	-0.1	-0.1	-0.1	-0.1
58.6	0.8	8.7	-7.4	0.6	14.0	2.1	-2.1	14.0	-0.1	-0.1	-0.1	-0.2	-0.1	-0.1	-0.2	-0.2
68.4	0.2	9.1	-7.5	-0.1	16.0	2.3	-2.6	16.0	-0.2	-0.2	-0.1	-0.3	0.0	-0.1	-0.2	-0.3
78.1	0.1	9.0	-7.8	0.3	18.0	2.6	-3.1	19.0	-0.1	-0.1	-0.1	-0.2	-0.1	-0.1	-0.1	-0.1
87.9	-0.8	9.1	-7.7	-0.9	20.0	2.9	-3.6	21.0	-0.1	-0.1	-0.1	-0.2	-0.1	-0.1	-0.1	0.0
97.7	-1.8	9.1	-8.0	-1.6	22.0	3.1	-4.0	23.0	-0.1	-0.1	-0.1	-0.3	-0.1	0.0	-0.1	-0.1
107.4	-3.1	8.9	-8.1	-2.6	24.0	3.6	-4.0	25.0	-0.1	-0.1	-0.1	-0.3	-0.1	-0.1	-0.2	-0.1
117.2	-4.7	9.3	-8.1	-4.1	27.0	4.4	-4.6	28.0	-0.1	-0.2	-0.1	-0.1	-0.1	-0.1	-0.1	-0.1
127.0	-9.0	24.0	-6.0	-8.2	31.0	4.7	-2.9	18.0	-4.0	-3.7	-2.3	-4.4	-2.3	-6.1	-3.1	-3.9
136.7	-8.2	9.6	-8.3	-7.3	32.0	5.4	-5.8	33.0	-0.1	-0.1	-0.1	-0.3	-0.1	-0.2	-0.1	-0.1

Table 75. Raw data for the test seal at ω=7.5 krpm, PD=31 bars, C_r=0.188 mm, and inlet GVF=10%

Freq.	Re($\boldsymbol{H_{XX}}$)	Re($\boldsymbol{H_{XY}}$)	Re($\boldsymbol{H_{YX}}$)	Re($\boldsymbol{H_{YY}}$)	Im($\boldsymbol{H_{XX}}$)	Im($\boldsymbol{H_{XY}}$)	Im($\boldsymbol{H_{YX}}$)	Im($\boldsymbol{H_{YY}}$)	Re($\boldsymbol{eH_{XX}}$)	Re($\boldsymbol{eH_{XY}}$)	Re($\boldsymbol{eH_{YX}}$)	Re($\boldsymbol{eH_{YY}}$)	Im($\boldsymbol{eH_{XX}}$)	Im($\boldsymbol{eH_{XY}}$)	Im($\boldsymbol{eH_{YX}}$)	Im($\boldsymbol{eH_{YY}}$)
Hz	MN/m	MN/m	MN/m	MN/m	MN/m	MN/m	MN/m	MN/m	MN/m	MN/m	MN/m	MN/m	MN/m	MN/m	MN/m	MN/m
9.8	0.3	15.0	-13.0	-1.8	3.2	0.5	-0.3	3.2	-0.1	-0.2	-0.3	-0.3	-0.3	-0.3	-0.2	-0.2
19.5	0.1	15.0	-12.0	-1.5	5.2	1.1	-1.1	5.1	-0.1	-0.2	-0.1	-0.2	-0.1	-0.1	-0.1	-0.1
29.3	-0.2	15.0	-12.0	-2.1	7.4	1.7	-1.9	7.2	-0.2	-0.1	-0.1	-0.1	-0.1	-0.2	-0.1	-0.1
39.1	-0.7	15.0	-13.0	-2.1	9.8	2.3	-2.6	10.0	-0.1	-0.2	-0.2	-0.2	-0.1	-0.1	-0.1	-0.1
48.8	-1.4	15.0	-13.0	-2.6	12.0	2.9	-2.9	13.0	-0.1	-0.2	-0.2	-0.2	-0.1	-0.1	-0.2	-0.1
58.6	-1.6	15.0	-13.0	-3.4	14.0	3.1	-3.7	15.0	-0.2	-0.2	-0.2	-0.2	-0.1	-0.1	-0.2	-0.1
68.4	-2.1	16.0	-13.0	-3.7	17.0	3.1	-4.2	18.0	-0.1	-0.5	-0.3	-0.5	-0.3	-0.3	-0.2	-0.2
78.1	-2.2	15.0	-12.0	-4.1	20.0	3.8	-5.1	20.0	-0.2	-0.2	-0.1	-0.1	-0.1	-0.1	-0.2	-0.1
87.9	-3.7	16.0	-13.0	-5.1	22.0	4.8	-5.9	22.0	-0.1	-0.2	-0.1	-0.2	-0.1	-0.1	-0.1	-0.1
97.7	-4.8	16.0	-13.0	-5.8	24.0	5.9	-6.3	25.0	-0.1	-0.1	-0.1	-0.2	-0.1	-0.1	-0.1	-0.1
107.4	-5.8	16.0	-13.0	-6.9	27.0	6.2	-7.3	27.0	-0.1	-0.2	-0.2	-0.2	-0.2	-0.1	-0.2	-0.1
117.2	-7.2	16.0	-13.0	-8.9	28.0	6.9	-8.6	29.0	-0.2	-0.1	-0.1	-0.3	-0.1	-0.2	-0.2	-0.1
127.0	-8.9	17.0	-14.0	-9.9	31.0	7.6	-8.5	32.0	-0.1	-0.1	-0.1	-0.1	-0.1	-0.1	-0.1	-0.2
136.7	-12.0	18.0	-14.0	-13.0	33.0	8.2	-9.8	35.0	-0.2	-0.2	-0.1	-0.3	-0.2	-0.3	-0.1	-0.2

Table 76. Raw data for the test seal at ω=10 krpm, PD=31 bars, C_r=0.188 mm, and inlet GVF=0%

Freq.	Re($\boldsymbol{H_{XX}}$)	Re($\boldsymbol{H_{XY}}$)	Re($\boldsymbol{H_{YX}}$)	Re($\boldsymbol{H_{YY}}$)	Im($\boldsymbol{H_{XX}}$)	Im($\boldsymbol{H_{XY}}$)	Im($\boldsymbol{H_{YX}}$)	Im($\boldsymbol{H_{YY}}$)	Re($\boldsymbol{eH_{XX}}$)	Re($\boldsymbol{eH_{XY}}$)	Re($\boldsymbol{eH_{YX}}$)	Re($\boldsymbol{eH_{YY}}$)	Im($\boldsymbol{eH_{XX}}$)	Im($\boldsymbol{eH_{XY}}$)	Im($\boldsymbol{eH_{YX}}$)	Im($\boldsymbol{eH_{YY}}$)
Hz	MN/m	MN/m	MN/m	MN/m	MN/m	MN/m	MN/m	MN/m	MN/m	MN/m	MN/m	MN/m	MN/m	MN/m	MN/m	MN/m
9.8	3.9	15.0	-11.0	2.1	2.9	0.4	-0.4	2.5	-0.2	-0.2	-0.1	-0.2	-0.1	-0.1	-0.1	-0.1
19.5	4.0	14.0	-11.0	2.2	4.7	0.6	-1.0	4.8	-0.1	-0.2	-0.1	-0.1	-0.1	-0.1	-0.1	-0.1
29.3	3.8	15.0	-10.0	1.6	6.9	1.1	-1.6	6.6	-0.1	-0.1	-0.1	-0.1	0.0	0.0	-0.1	-0.1
39.1	3.6	15.0	-11.0	1.5	9.0	1.6	-2.4	9.1	-0.1	-0.1	-0.1	-0.1	-0.1	-0.1	-0.1	-0.1
48.8	3.0	15.0	-11.0	1.2	11.0	2.5	-2.9	11.0	-0.1	-0.1	-0.1	-0.1	-0.1	-0.1	-0.1	-0.1
58.6	2.5	15.0	-11.0	0.6	13.0	2.8	-3.6	14.0	-0.2	-0.1	-0.2	-0.2	-0.1	-0.1	-0.2	-0.2
68.4	2.4	15.0	-11.0	0.2	16.0	2.8	-4.2	16.0	-0.1	-0.2	-0.1	-0.2	-0.1	-0.1	-0.1	-0.2
78.1	2.3	15.0	-11.0	0.0	18.0	3.4	-5.0	18.0	-0.1	-0.1	-0.1	-0.1	-0.1	-0.1	0.0	-0.1
87.9	1.0	15.0	-11.0	-1.0	20.0	4.0	-5.8	20.0	-0.1	-0.1	-0.1	-0.2	-0.1	-0.1	-0.1	-0.1
97.7	0.2	15.0	-11.0	-1.8	22.0	4.8	-6.5	22.0	-0.1	-0.1	-0.1	-0.1	-0.1	-0.1	-0.1	-0.1
107.4	-1.0	15.0	-11.0	-3.1	24.0	5.3	-7.4	24.0	-0.1	-0.1	-0.1	-0.1	-0.1	-0.1	-0.1	-0.1
117.2	-2.4	16.0	-11.0	-4.7	26.0	5.9	-8.3	26.0	-0.1	-0.1	-0.1	-0.1	-0.1	-0.1	-0.1	-0.1
127.0	-4.0	16.0	-12.0	-6.4	28.0	6.4	-8.7	29.0	-0.1	-0.1	-0.1	-0.2	-0.1	-0.1	-0.1	-0.1
136.7	-6.7	17.0	-11.0	-8.5	30.0	6.7	-9.7	31.0	-0.1	-0.1	-0.1	-0.1	-0.1	-0.1	-0.1	-0.1

Table 77. Raw data for the test seal at ω=10 krpm, PD=31 bars, C_r=0.188 mm, and inlet GVF=2%

Freq.	Re($\boldsymbol{H_{XX}}$)	Re($\boldsymbol{H_{XY}}$)	Re($\boldsymbol{H_{YX}}$)	Re($\boldsymbol{H_{YY}}$)	Im($\boldsymbol{H_{XX}}$)	Im($\boldsymbol{H_{XY}}$)	Im($\boldsymbol{H_{YX}}$)	Im($\boldsymbol{H_{YY}}$)	Re($\boldsymbol{eH_{XX}}$)	Re($\boldsymbol{eH_{XY}}$)	Re($\boldsymbol{eH_{YX}}$)	Re($\boldsymbol{eH_{YY}}$)	Im($\boldsymbol{eH_{XX}}$)	Im($\boldsymbol{eH_{XY}}$)	Im($\boldsymbol{eH_{YX}}$)	Im($\boldsymbol{eH_{YY}}$)
Hz	MN/m	MN/m	MN/m	MN/m	MN/m	MN/m	MN/m	MN/m	MN/m	MN/m	MN/m	MN/m	MN/m	MN/m	MN/m	MN/m
9.8	4.8	14.0	-11.0	3.1	2.7	0.3	-0.6	2.6	-0.2	-0.2	-0.1	-0.1	-0.1	-0.2	-0.2	-0.2
19.5	4.8	14.0	-11.0	3.2	4.8	0.9	-1.0	4.6	-0.1	-0.1	-0.1	-0.1	-0.1	-0.1	-0.1	-0.1
29.3	4.7	14.0	-10.0	2.9	6.8	1.3	-1.4	6.4	0.0	0.0	-0.1	-0.1	0.0	-0.1	0.0	0.0
39.1	4.4	14.0	-11.0	2.9	8.8	1.7	-2.4	9.1	-0.1	-0.1	-0.1	-0.1	-0.1	0.0	-0.1	0.0
48.8	3.9	14.0	-11.0	2.1	11.0	2.2	-3.0	11.0	-0.1	-0.1	-0.1	0.0	0.0	-0.1	-0.1	0.0
58.6	3.5	14.0	-11.0	1.7	13.0	2.8	-3.4	13.0	-0.1	-0.1	-0.1	-0.2	-0.1	-0.1	-0.1	-0.1
68.4	3.2	14.0	-11.0	1.0	16.0	2.6	-4.3	17.0	-0.1	-0.1	-0.1	-0.2	-0.1	-0.2	-0.1	-0.1
78.1	3.1	14.0	-11.0	1.2	18.0	3.6	-4.9	18.0	-0.1	-0.1	-0.1	-0.1	-0.1	0.0	-0.1	0.0
87.9	2.1	14.0	-11.0	0.0	19.0	4.1	-5.7	20.0	-0.1	-0.1	0.0	-0.1	-0.1	-0.1	0.0	0.0
97.7	1.0	14.0	-11.0	-0.6	21.0	4.9	-6.2	22.0	-0.1	-0.1	-0.1	-0.1	0.0	-0.1	-0.1	0.0
107.4	-0.3	15.0	-11.0	-1.7	23.0	5.5	-7.2	24.0	-0.1	0.0	-0.1	-0.1	0.0	-0.1	-0.1	0.0
117.2	-1.8	15.0	-11.0	-3.7	25.0	6.2	-8.2	26.0	0.0	-0.1	0.0	-0.1	-0.1	-0.1	0.0	0.0
127.0	-3.5	16.0	-12.0	-5.4	27.0	6.7	-8.9	28.0	-0.1	-0.1	-0.1	-0.1	0.0	-0.1	-0.1	-0.1
136.7	-6.8	16.0	-11.0	-8.1	30.0	7.4	-10.0	31.0	-0.1	-0.1	0.0	-0.1	0.0	-0.1	-0.1	0.0

Table 78. Raw data for the test seal at ω=10 krpm, PD=31 bars, C_r=0.188 mm, and inlet GVF=4%

Freq.	Re($\boldsymbol{H_{XX}}$)	Re($\boldsymbol{H_{XY}}$)	Re($\boldsymbol{H_{YX}}$)	Re($\boldsymbol{H_{YY}}$)	Im($\boldsymbol{H_{XX}}$)	Im($\boldsymbol{H_{XY}}$)	Im($\boldsymbol{H_{YX}}$)	Im($\boldsymbol{H_{YY}}$)	Re($\boldsymbol{eH_{XX}}$)	Re($\boldsymbol{eH_{XY}}$)	Re($\boldsymbol{eH_{YX}}$)	Re($\boldsymbol{eH_{YY}}$)	Im($\boldsymbol{eH_{XX}}$)	Im($\boldsymbol{eH_{XY}}$)	Im($\boldsymbol{eH_{YX}}$)	Im($\boldsymbol{eH_{YY}}$)
Hz	MN/m	MN/m	MN/m	MN/m	MN/m	MN/m	MN/m	MN/m	MN/m	MN/m	MN/m	MN/m	MN/m	MN/m	MN/m	MN/m
9.8	3.9	14.0	-12.0	2.3	2.6	0.9	-0.4	2.8	-0.1	-0.1	-0.1	-0.1	-0.1	-0.1	-0.2	-0.1
19.5	3.7	14.0	-11.0	2.4	5.0	1.0	-0.8	5.0	-0.1	-0.1	-0.1	0.0	-0.1	-0.1	0.0	0.0
29.3	3.6	14.0	-11.0	2.1	6.9	1.4	-1.3	6.9	-0.1	-0.1	-0.1	-0.1	0.0	-0.1	0.0	0.0
39.1	3.4	14.0	-11.0	2.1	9.1	1.8	-2.2	9.3	-0.1	-0.1	-0.1	0.0	0.0	0.0	-0.1	-0.1
48.8	3.0	14.0	-12.0	1.7	11.0	2.4	-2.8	11.0	0.0	-0.1	-0.1	0.0	-0.1	0.0	-0.1	-0.1
58.6	2.2	14.0	-11.0	1.0	14.0	2.5	-3.2	14.0	-0.1	-0.1	-0.1	-0.1	-0.1	-0.1	-0.1	-0.1
68.4	2.8	14.0	-12.0	0.6	16.0	2.7	-4.4	17.0	-0.1	-0.1	-0.1	-0.1	-0.1	-0.1	-0.1	-0.1
78.1	2.4	14.0	-11.0	1.0	18.0	3.6	-4.8	18.0	0.0	0.0	-0.1	-0.1	-0.1	-0.1	-0.1	-0.1
87.9	1.1	14.0	-12.0	-0.3	20.0	4.0	-5.3	20.0	0.0	0.0	0.0	-0.1	0.0	0.0	0.0	-0.1
97.7	0.1	14.0	-12.0	-1.2	21.0	4.8	-5.8	22.0	-0.1	-0.1	0.0	0.0	0.0	0.0	-0.1	-0.1
107.4	-1.3	14.0	-12.0	-2.6	24.0	5.7	-7.0	24.0	-0.1	-0.1	0.0	-0.1	-0.1	-0.1	-0.1	0.0
117.2	-3.2	15.0	-12.0	-4.5	26.0	6.8	-8.2	26.0	-0.1	-0.1	0.0	0.0	0.0	0.0	-0.1	-0.1
127.0	-5.3	16.0	-12.0	-6.4	28.0	7.5	-8.6	29.0	-0.1	-0.2	-0.1	-0.1	-0.1	-0.1	0.0	-0.1
136.7	-8.4	17.0	-12.0	-8.9	31.0	8.1	-9.7	32.0	-0.1	-0.1	-0.1	-0.1	-0.1	-0.1	0.0	-0.1

Table 79. Raw data for the test seal at ω=10 krpm, PD=31 bars, C_r=0.188 mm, and inlet GVF=6%

Freq.	Re($\boldsymbol{H_{XX}}$)	Re($\boldsymbol{H_{XY}}$)	Re($\boldsymbol{H_{YX}}$)	Re($\boldsymbol{H_{YY}}$)	Im($\boldsymbol{H_{XX}}$)	Im($\boldsymbol{H_{XY}}$)	Im($\boldsymbol{H_{YX}}$)	Im($\boldsymbol{H_{YY}}$)	Re($\boldsymbol{eH_{XX}}$)	Re($\boldsymbol{eH_{XY}}$)	Re($\boldsymbol{eH_{YX}}$)	Re($\boldsymbol{eH_{YY}}$)	Im($\boldsymbol{eH_{XX}}$)	Im($\boldsymbol{eH_{XY}}$)	Im($\boldsymbol{eH_{YX}}$)	Im($\boldsymbol{eH_{YY}}$)
Hz	MN/m	MN/m	MN/m	MN/m	MN/m	MN/m	MN/m	MN/m	MN/m	MN/m	MN/m	MN/m	MN/m	MN/m	MN/m	MN/m
9.8	7.2	12.0	-11.0	6.2	2.2	0.4	-1.1	2.9	-0.1	-0.1	-0.1	-0.2	-0.1	-0.1	-0.1	-0.1
19.5	6.8	12.0	-10.0	6.1	4.6	1.1	-0.9	4.5	-0.1	0.0	-0.1	-0.1	-0.1	-0.1	-0.1	0.0
29.3	6.6	13.0	-10.0	5.9	6.5	1.9	-1.5	6.4	-0.1	-0.1	-0.1	-0.1	-0.1	-0.1	0.0	0.0
39.1	6.9	13.0	-10.0	6.1	8.6	1.8	-2.5	8.8	0.0	-0.1	-0.1	-0.1	-0.1	-0.1	-0.1	-0.1
48.8	6.2	13.0	-11.0	5.4	10.0	2.1	-2.9	11.0	-0.1	-0.1	-0.1	-0.1	-0.1	-0.1	-0.1	-0.1
58.6	6.0	12.0	-10.0	5.0	13.0	2.5	-3.2	13.0	-0.1	-0.1	-0.1	-0.1	-0.1	-0.1	-0.1	-0.1
68.4	6.1	13.0	-10.0	4.4	15.0	2.4	-4.7	16.0	-0.1	-0.2	-0.1	-0.1	-0.1	-0.1	-0.1	-0.2
78.1	5.6	12.0	-11.0	4.6	17.0	3.6	-4.7	17.0	-0.1	-0.1	-0.2	-0.1	-0.1	-0.1	-0.1	-0.1
87.9	4.5	13.0	-10.0	3.6	19.0	4.1	-5.3	19.0	-0.1	-0.1	-0.1	-0.1	-0.1	-0.1	-0.1	0.0
97.7	3.4	12.0	-10.0	2.3	20.0	4.9	-6.0	20.0	-0.1	-0.1	-0.1	-0.1	-0.1	-0.1	-0.1	0.0
107.4	1.8	12.0	-11.0	0.9	22.0	5.9	-7.4	23.0	-0.1	-0.1	-0.1	-0.1	0.0	-0.1	-0.1	-0.1
117.2	-0.3	13.0	-11.0	-1.2	24.0	7.0	-8.2	25.0	-0.1	-0.1	-0.1	-0.1	-0.1	0.0	-0.1	-0.1
127.0	-2.5	14.0	-12.0	-2.9	27.0	7.6	-8.9	28.0	-0.1	-0.1	-0.1	-0.1	-0.1	-0.1	-0.1	-0.1
136.7	-5.8	16.0	-12.0	-5.6	31.0	8.2	-10.0	32.0	-0.1	-0.1	-0.1	-0.1	-0.1	-0.1	-0.1	-0.1

Table 80. Raw data for the test seal at ω=10 krpm, PD=31 bars, C_r=0.188 mm, and inlet GVF=8%

Freq.	Re($\boldsymbol{H_{XX}}$)	Re($\boldsymbol{H_{XY}}$)	Re($\boldsymbol{H_{YX}}$)	Re($\boldsymbol{H_{YY}}$)	Im($\boldsymbol{H_{XX}}$)	Im($\boldsymbol{H_{XY}}$)	Im($\boldsymbol{H_{YX}}$)	Im($\boldsymbol{H_{YY}}$)	Re($\boldsymbol{eH_{XX}}$)	Re($\boldsymbol{eH_{XY}}$)	Re($\boldsymbol{eH_{YX}}$)	Re($\boldsymbol{eH_{YY}}$)	Im($\boldsymbol{eH_{XX}}$)	Im($\boldsymbol{eH_{XY}}$)	Im($\boldsymbol{eH_{YX}}$)	Im($\boldsymbol{eH_{YY}}$)
Hz	MN/m	MN/m	MN/m	MN/m	MN/m	MN/m	MN/m	MN/m	MN/m	MN/m	MN/m	MN/m	MN/m	MN/m	MN/m	MN/m
9.8	8.1	12.0	-9.8	7.8	2.0	0.4	-0.7	1.8	-0.1	-0.1	0.0	0.0	-0.1	-0.1	-0.1	-0.1
19.5	7.6	12.0	-10.0	7.2	3.8	1.0	-0.9	3.9	-0.1	-0.1	-0.1	-0.1	-0.1	-0.2	-0.1	-0.1
29.3	6.7	12.0	-9.7	5.9	6.0	1.0	-1.7	6.0	-0.1	-0.2	-0.2	-0.2	-0.2	-0.5	-0.2	-0.2
39.1	6.6	12.0	-9.8	6.7	8.2	1.7	-2.4	8.2	-0.1	-0.2	-0.1	-0.2	-0.1	-0.3	-0.1	-0.2
48.8	6.6	12.0	-9.9	5.9	10.0	2.7	-3.4	10.0	-0.2	-0.2	-0.2	-0.3	-0.2	-0.2	-0.1	-0.1
58.6	6.5	12.0	-10.0	6.6	12.0	3.3	-4.6	12.0	-0.1	-0.1	-0.1	-0.2	-0.2	-0.2	-0.1	-0.2
68.4	5.9	13.0	-11.0	4.7	14.0	5.0	-5.4	14.0	-0.2	-0.4	-0.2	-0.3	-0.2	-0.2	-0.3	-0.6
78.1	4.7	14.0	-12.0	4.6	15.0	4.3	-5.2	15.0	-0.1	-0.2	-0.1	-0.1	-0.2	-0.3	-0.2	-0.2
87.9	2.3	13.0	-12.0	2.0	18.0	2.9	-4.2	18.0	-0.2	-0.3	-0.2	-0.4	-0.2	-0.2	-0.2	-0.1
97.7	1.8	13.0	-11.0	1.7	22.0	3.9	-5.3	22.0	-0.2	-0.2	-0.2	-0.4	-0.2	-0.3	-0.2	-0.3
107.4	2.1	13.0	-12.0	1.8	24.0	4.5	-5.9	24.0	-0.2	-0.3	-0.1	-0.3	-0.2	-0.2	-0.2	-0.2
117.2	0.2	13.0	-11.0	-0.8	26.0	6.0	-7.5	26.0	-0.1	-0.2	-0.1	-0.2	-0.1	-0.2	-0.3	-0.3
127.0	-0.1	13.0	-11.0	-1.0	28.0	5.2	-7.3	28.0	-0.2	-0.5	-0.3	-0.8	-0.2	-0.3	-0.4	-0.5
136.7	-2.4	14.0	-11.0	-3.3	31.0	6.5	-8.7	31.0	-0.3	-0.3	-0.2	-0.2	-0.2	-0.3	-0.2	-0.3

Table 81. Raw data for the test seal at ω=10 krpm, PD=31 bars, C_r=0.188 mm, and inlet GVF=10%

Freq.	Re($\boldsymbol{H_{XX}}$)	Re($\boldsymbol{H_{XY}}$)	Re($\boldsymbol{H_{YX}}$)	Re($\boldsymbol{H_{YY}}$)	Im($\boldsymbol{H_{XX}}$)	Im($\boldsymbol{H_{XY}}$)	Im($\boldsymbol{H_{YX}}$)	Im($\boldsymbol{H_{YY}}$)	Re($\boldsymbol{eH_{XX}}$)	Re($\boldsymbol{eH_{XY}}$)	Re($\boldsymbol{eH_{YX}}$)	Re($\boldsymbol{eH_{YY}}$)	Im($\boldsymbol{eH_{XX}}$)	Im($\boldsymbol{eH_{XY}}$)	Im($\boldsymbol{eH_{YX}}$)	Im($\boldsymbol{eH_{YY}}$)
Hz	MN/m	MN/m	MN/m	MN/m	MN/m	MN/m	MN/m	MN/m	MN/m	MN/m	MN/m	MN/m	MN/m	MN/m	MN/m	MN/m
9.8	5.2	21.0	-20.0	4.5	2.3	1.2	-1.5	2.8	-0.3	-0.3	-0.2	-0.2	-0.2	-0.2	-0.3	-0.3
19.5	5.0	21.0	-19.0	4.9	4.8	2.1	-2.5	4.3	-0.1	-0.1	-0.3	-0.3	-0.2	-0.2	-0.2	-0.1
29.3	4.4	22.0	-20.0	4.1	6.7	3.2	-3.2	6.6	-0.3	-0.3	-0.2	-0.1	-0.2	-0.2	-0.2	-0.2
39.1	4.9	22.0	-20.0	4.4	8.8	4.0	-4.6	8.8	-0.2	-0.2	-0.2	-0.2	-0.1	-0.1	-0.2	-0.2
48.8	4.5	22.0	-21.0	3.9	10.0	5.1	-6.0	11.0	-0.2	-0.2	-0.2	-0.2	-0.1	-0.1	-0.2	-0.2
58.6	3.2	22.0	-21.0	2.9	13.0	5.7	-6.5	14.0	-0.2	-0.1	-0.2	-0.1	-0.1	-0.1	-0.1	-0.1
68.4	2.6	22.0	-20.0	2.4	16.0	6.9	-7.3	15.0	-0.2	-0.3	-0.2	-0.2	-0.2	-0.2	-0.2	-0.1
78.1	2.4	22.0	-21.0	1.9	18.0	7.6	-8.6	18.0	-0.3	-0.2	-0.2	-0.2	-0.2	-0.2	-0.2	-0.2
87.9	0.6	23.0	-21.0	0.6	20.0	9.3	-9.7	20.0	-0.2	-0.2	-0.2	-0.2	-0.2	-0.2	-0.1	-0.1
97.7	-0.3	23.0	-21.0	-1.0	22.0	10.0	-11.0	22.0	-0.1	-0.1	-0.1	-0.1	-0.2	-0.1	-0.2	-0.2
107.4	-1.6	23.0	-21.0	-1.8	24.0	11.0	-12.0	24.0	-0.2	-0.2	-0.2	-0.2	-0.2	-0.2	-0.1	-0.2
117.2	-3.3	24.0	-21.0	-4.1	27.0	12.0	-13.0	26.0	-0.2	-0.2	-0.2	-0.1	-0.2	-0.1	-0.1	-0.2
127.0	-5.3	24.0	-22.0	-5.5	28.0	13.0	-14.0	30.0	-0.2	-0.1	-0.1	-0.2	-0.1	-0.2	-0.3	-0.2
136.7	-7.7	24.0	-21.0	-7.3	32.0	14.0	-16.0	32.0	-0.2	-0.1	-0.2	-0.3	-0.1	-0.1	-0.2	-0.2

Table 82. Raw data for the test seal at ω=15 krpm, PD=31 bars, C_r=0.188 mm, and inlet GVF=0%

Freq.	Re($\boldsymbol{H_{XX}}$)	Re($\boldsymbol{H_{XY}}$)	Re($\boldsymbol{H_{YX}}$)	Re($\boldsymbol{H_{YY}}$)	Im($\boldsymbol{H_{XX}}$)	Im($\boldsymbol{H_{XY}}$)	Im($\boldsymbol{H_{YX}}$)	Im($\boldsymbol{H_{YY}}$)	Re($\boldsymbol{eH_{XX}}$)	Re($\boldsymbol{eH_{XY}}$)	Re($\boldsymbol{eH_{YX}}$)	Re($\boldsymbol{eH_{YY}}$)	Im($\boldsymbol{eH_{XX}}$)	Im($\boldsymbol{eH_{XY}}$)	Im($\boldsymbol{eH_{YX}}$)	Im($\boldsymbol{eH_{YY}}$)
Hz	MN/m	MN/m	MN/m	MN/m	MN/m	MN/m	MN/m	MN/m	MN/m	MN/m	MN/m	MN/m	MN/m	MN/m	MN/m	MN/m
9.8	4.8	21.0	-19.0	4.9	2.3	0.8	-1.3	2.9	-0.2	-0.1	-0.1	-0.1	-0.2	-0.2	-0.2	-0.2
19.5	5.2	21.0	-19.0	4.8	4.6	2.2	-2.0	4.7	-0.2	-0.2	-0.1	-0.1	-0.1	-0.1	-0.1	-0.1
29.3	4.8	22.0	-20.0	4.1	6.5	3.4	-3.2	6.8	-0.1	-0.1	-0.1	-0.1	-0.1	-0.1	-0.1	-0.1
39.1	4.7	22.0	-20.0	4.3	9.0	3.9	-4.4	9.0	-0.1	-0.1	-0.1	-0.1	-0.1	-0.1	-0.1	-0.1
48.8	4.0	22.0	-20.0	3.7	10.0	4.5	-5.1	11.0	-0.1	-0.1	-0.1	-0.1	-0.1	-0.1	-0.1	-0.1
58.6	2.8	22.0	-20.0	2.4	13.0	5.1	-5.3	13.0	-0.1	-0.1	-0.1	-0.1	-0.1	-0.1	-0.2	-0.2
68.4	2.5	22.0	-20.0	2.1	16.0	6.2	-7.1	16.0	-0.1	-0.1	-0.1	-0.2	-0.1	-0.1	-0.1	-0.1
78.1	2.1	22.0	-20.0	1.8	18.0	7.8	-8.5	18.0	-0.1	-0.1	0.0	0.0	-0.1	-0.1	-0.1	-0.1
87.9	1.1	22.0	-21.0	0.7	20.0	8.8	-9.8	20.0	-0.1	-0.1	-0.1	-0.1	-0.1	-0.1	-0.1	0.0
97.7	-0.2	23.0	-22.0	-0.4	22.0	10.0	-11.0	23.0	-0.1	-0.1	-0.1	-0.1	-0.1	-0.1	-0.1	-0.1
107.4	-1.4	24.0	-22.0	-1.7	24.0	11.0	-12.0	24.0	-0.1	-0.1	-0.2	-0.2	-0.1	-0.1	-0.1	-0.1
117.2	-3.4	24.0	-22.0	-3.7	27.0	11.0	-13.0	27.0	-0.1	-0.1	-0.1	-0.1	-0.1	-0.1	-0.1	-0.1
127.0	-5.0	25.0	-22.0	-5.2	29.0	12.0	-13.0	30.0	-0.2	-0.2	-0.2	-0.3	-0.2	-0.3	-0.2	-0.1
136.7	-7.6	25.0	-22.0	-6.8	32.0	13.0	-15.0	33.0	-0.1	-0.1	-0.1	-0.1	-0.1	-0.2	-0.1	-0.1

Table 83. Raw data for the test seal at ω=15 krpm, PD=31 bars, C_r=0.188 mm, and inlet GVF=2%

Freq.	Re($\boldsymbol{H_{XX}}$)	Re($\boldsymbol{H_{XY}}$)	Re($\boldsymbol{H_{YX}}$)	Re($\boldsymbol{H_{YY}}$)	Im($\boldsymbol{H_{XX}}$)	Im($\boldsymbol{H_{XY}}$)	Im($\boldsymbol{H_{YX}}$)	Im($\boldsymbol{H_{YY}}$)	Re($\boldsymbol{eH_{XX}}$)	Re($\boldsymbol{eH_{XY}}$)	Re($\boldsymbol{eH_{YX}}$)	Re($\boldsymbol{eH_{YY}}$)	Im($\boldsymbol{eH_{XX}}$)	Im($\boldsymbol{eH_{XY}}$)	Im($\boldsymbol{eH_{YX}}$)	Im($\boldsymbol{eH_{YY}}$)
Hz	MN/m	MN/m	MN/m	MN/m	MN/m	MN/m	MN/m	MN/m	MN/m	MN/m	MN/m	MN/m	MN/m	MN/m	MN/m	MN/m
9.8	6.2	21.0	-19.0	5.7	2.3	0.9	-1.1	2.6	-0.2	-0.2	-0.1	-0.1	-0.1	-0.2	-0.1	-0.1
19.5	5.7	21.0	-19.0	5.7	3.7	2.4	-2.1	3.5	-0.2	-0.2	-0.1	-0.1	-0.1	-0.1	-0.1	-0.1
29.3	5.3	21.0	-19.0	4.9	6.3	2.9	-2.8	6.1	-0.1	-0.1	-0.1	-0.1	-0.1	-0.1	-0.1	-0.1
39.1	4.8	22.0	-20.0	4.9	8.1	4.0	-4.3	8.2	-0.1	-0.1	-0.1	-0.1	-0.1	-0.1	-0.1	-0.1
48.8	4.3	21.0	-20.0	3.9	10.0	4.8	-5.5	11.0	-0.1	-0.1	-0.1	-0.1	-0.1	-0.1	-0.1	-0.1
58.6	3.4	22.0	-21.0	2.4	12.0	5.6	-6.1	13.0	-0.1	-0.1	-0.1	-0.2	-0.2	-0.2	-0.1	-0.1
68.4	2.6	22.0	-20.0	2.7	16.0	6.7	-7.2	16.0	-0.1	-0.1	-0.2	-0.2	-0.1	-0.1	-0.1	-0.2
78.1	2.6	22.0	-20.0	2.3	18.0	7.9	-8.6	18.0	-0.1	-0.1	-0.1	-0.1	-0.1	-0.1	-0.1	-0.1
87.9	1.8	23.0	-21.0	1.4	20.0	8.8	-9.7	20.0	-0.1	-0.1	-0.1	-0.1	-0.1	-0.1	-0.1	-0.1
97.7	0.6	23.0	-22.0	0.4	23.0	9.8	-11.0	23.0	-0.1	-0.2	-0.1	-0.1	-0.2	-0.2	-0.1	-0.1
107.4	-0.3	24.0	-22.0	-0.6	25.0	10.0	-12.0	25.0	-0.1	-0.1	-0.3	-0.2	-0.2	-0.2	-0.1	-0.2
117.2	-1.8	26.0	-23.0	-2.4	27.0	11.0	-12.0	27.0	-0.2	-0.2	-0.2	-0.1	-0.1	-0.2	-0.1	-0.1
127.0	-4.2	26.0	-24.0	-4.1	30.0	11.0	-13.0	31.0	-0.2	-0.2	-0.2	-0.2	-0.2	-0.3	-0.2	-0.2
136.7	-6.9	27.0	-24.0	-6.0	33.0	12.0	-13.0	34.0	-0.2	-0.1	-0.1	-0.2	-0.2	-0.2	-0.2	-0.2

Table 84. Raw data for the test seal at ω=15 krpm, PD=31 bars, C_r=0.188 mm, and inlet GVF=4%

Freq.	Re(H_{XX})	Re(H_{XY})	Re(H_{YX})	Re(H_{YY})	Im(H_{XX})	Im(H_{XY})	Im(H_{YX})	Im(H_{YY})	Re(eH_{XX})	Re(eH_{XY})	Re(eH_{YX})	Re(eH_{YY})	Im(eH_{XX})	Im(eH_{XY})	Im(eH_{YX})	Im(eH_{YY})
Hz	MN/m	MN/m	MN/m	MN/m	MN/m	MN/m	MN/m	MN/m	MN/m	MN/m	MN/m	MN/m	MN/m	MN/m	MN/m	MN/m
9.8	6.4	21.0	-19.0	6.2	2.0	1.2	-1.0	1.8	-0.3	-0.3	-0.3	-0.3	-0.3	-0.3	-0.3	-0.3
19.5	5.3	21.0	-19.0	4.8	4.0	1.5	-1.6	3.5	-0.3	-0.4	-0.2	-0.2	-0.3	-0.3	-0.2	-0.2
29.3	5.1	21.0	-18.0	4.3	6.7	2.0	-2.4	6.9	-0.2	-0.2	-0.1	-0.2	-0.1	-0.2	-0.1	-0.2
39.1	5.6	21.0	-18.0	5.1	8.6	3.5	-4.1	9.1	-0.1	-0.1	-0.1	-0.1	-0.1	-0.1	-0.1	-0.1
48.8	5.4	21.0	-19.0	5.1	11.0	4.7	-5.4	11.0	-0.2	-0.2	-0.1	-0.1	-0.1	-0.1	-0.1	-0.1
58.6	4.9	21.0	-20.0	4.0	12.0	5.7	-6.4	12.0	-0.2	-0.2	-0.2	-0.2	-0.1	-0.1	-0.1	-0.1
68.4	3.2	21.0	-19.0	2.5	15.0	6.3	-7.2	15.0	-0.2	-0.3	-0.2	-0.2	-0.2	-0.2	-0.2	-0.2
78.1	2.9	22.0	-20.0	2.7	18.0	7.8	-8.4	17.0	-0.2	-0.2	-0.1	-0.1	-0.1	-0.1	-0.1	-0.1
87.9	2.2	23.0	-21.0	1.5	20.0	8.4	-9.8	20.0	-0.2	-0.2	-0.1	-0.1	-0.1	-0.2	-0.2	-0.2
97.7	1.4	23.0	-22.0	0.4	22.0	8.9	-10.0	22.0	-0.1	-0.1	-0.1	-0.1	-0.1	-0.1	-0.2	-0.2
107.4	0.1	24.0	-22.0	-0.1	24.0	9.9	-11.0	25.0	-0.2	-0.1	-0.2	-0.2	-0.1	-0.1	-0.1	-0.2
117.2	-1.3	25.0	-22.0	-1.7	26.0	11.0	-11.0	26.0	-0.1	-0.1	-0.2	-0.1	-0.1	-0.1	-0.1	-0.2
127.0	-3.1	25.0	-23.0	-3.4	28.0	11.0	-12.0	29.0	-0.2	-0.3	-0.3	-0.1	-0.2	-0.2	-0.2	-0.4
136.7	-6.1	26.0	-22.0	-5.0	32.0	11.0	-13.0	33.0	-0.2	-0.2	-0.1	-0.2	-0.1	-0.2	-0.1	-0.1

Table 85. Raw data for the test seal at ω=15 krpm, PD=31 bars, C_r=0.188 mm, and inlet GVF=6%

Freq.	Re(H_{XX})	Re(H_{XY})	Re(H_{YX})	Re(H_{YY})	Im(H_{XX})	Im(H_{XY})	Im(H_{YX})	Im(H_{YY})	Re(eH_{XX})	Re(eH_{XY})	Re(eH_{YX})	Re(eH_{YY})	Im(eH_{XX})	Im(eH_{XY})	Im(eH_{YX})	Im(eH_{YY})
Hz	MN/m	MN/m	MN/m	MN/m	MN/m	MN/m	MN/m	MN/m	MN/m	MN/m	MN/m	MN/m	MN/m	MN/m	MN/m	MN/m
9.8	6.3	21.0	-19.0	6.4	1.1	1.2	-1.2	1.1	-0.5	-0.5	-0.2	-0.2	-0.3	-0.2	-0.3	-0.4
19.5	4.5	21.0	-19.0	4.3	3.5	0.6	-1.2	3.4	-0.2	-0.2	-0.2	-0.2	-0.1	-0.2	-0.2	-0.2
29.3	4.7	20.0	-18.0	4.7	7.0	2.5	-2.5	7.5	-0.2	-0.3	-0.2	-0.2	-0.2	-0.1	-0.1	-0.1
39.1	5.5	20.0	-19.0	5.7	9.2	3.7	-4.3	9.5	-0.1	-0.1	-0.2	-0.2	-0.1	-0.1	-0.2	-0.2
48.8	5.9	21.0	-19.0	5.7	11.0	4.0	-5.2	10.0	-0.2	-0.2	-0.2	-0.2	-0.1	-0.2	-0.1	-0.1
58.6	5.0	21.0	-19.0	3.8	12.0	5.3	-6.4	12.0	-0.1	-0.2	-0.2	-0.1	-0.2	-0.2	-0.2	-0.2
68.4	3.2	21.0	-19.0	3.1	15.0	6.3	-6.8	15.0	-0.2	-0.2	-0.2	-0.2	-0.1	-0.1	-0.2	-0.2
78.1	2.8	22.0	-20.0	2.7	17.0	7.9	-8.3	17.0	-0.2	-0.2	-0.1	-0.1	-0.1	-0.1	-0.2	-0.2
87.9	2.0	23.0	-21.0	1.8	19.0	8.3	-9.0	19.0	-0.2	-0.2	-0.2	-0.2	-0.2	-0.2	-0.1	-0.1
97.7	0.9	23.0	-21.0	0.5	22.0	8.8	-9.6	21.0	-0.1	-0.1	-0.2	-0.1	-0.1	-0.1	-0.2	-0.2
107.4	0.1	23.0	-21.0	-0.5	24.0	9.3	-10.0	24.0	-0.2	-0.2	-0.2	-0.2	-0.2	-0.2	-0.2	-0.2
117.2	-1.4	24.0	-21.0	-1.8	26.0	10.0	-11.0	27.0	-0.2	-0.1	-0.1	-0.1	-0.2	-0.2	-0.2	-0.2
127.0	-2.9	25.0	-22.0	-3.1	29.0	10.0	-12.0	29.0	-0.2	-0.2	-0.2	-0.2	-0.2	-0.2	-0.2	-0.2
136.7	-5.8	24.0	-21.0	-4.5	32.0	11.0	-13.0	32.0	-0.1	-0.1	-0.2	-0.2	-0.1	-0.1	-0.1	-0.2

Table 86. Raw data for the test seal at ω=15 krpm, PD=31 bars, C_r=0.188 mm, and inlet GVF=8%

Freq.	Re(H_{XX})	Re(H_{XY})	Re(H_{YX})	Re(H_{YY})	Im(H_{XX})	Im(H_{XY})	Im(H_{YX})	Im(H_{YY})	Re(eH_{XX})	Re(eH_{XY})	Re(eH_{YX})	Re(eH_{YY})	Im(eH_{XX})	Im(eH_{XY})	Im(eH_{YX})	Im(eH_{YY})
Hz	MN/m	MN/m	MN/m	MN/m	MN/m	MN/m	MN/m	MN/m	MN/m	MN/m	MN/m	MN/m	MN/m	MN/m	MN/m	MN/m
9.8	5.4	26.0	-24.0	7.5	1.4	1.7	-0.6	2.3	-1.4	-1.4	-1.1	-1.2	-0.5	-0.9	-1.4	-1.5
19.5	3.3	25.0	-23.0	4.9	4.4	0.5	-0.9	3.4	-0.8	-0.8	-0.6	-0.8	-0.5	-0.6	-0.6	-0.5
29.3	3.8	25.0	-22.0	5.4	7.6	1.1	-0.2	2.9	-0.7	-0.6	-1.0	-1.2	-0.8	-1.0	-0.8	-0.7
39.1	2.5	28.0	-21.0	1.8	8.5	3.5	-4.2	8.9	-1.1	-1.0	-1.3	-1.4	-0.6	-0.9	-1.0	-1.1
48.8	1.7	26.0	-24.0	3.6	12.0	1.9	-2.8	9.7	-0.9	-0.9	-0.6	-0.6	-0.4	-0.5	-0.6	-0.7
58.6	2.1	26.0	-24.0	2.2	12.0	2.4	-2.5	12.0	-1.3	-1.5	-0.9	-1.0	-1.2	-1.0	-0.9	-0.8
68.4	-1.6	29.0	-23.0	0.9	18.0	3.7	-2.1	13.0	-0.8	-1.1	-1.0	-0.9	-1.1	-0.9	-1.2	-1.3
78.1	0.4	27.0	-25.0	1.0	18.0	3.2	-4.2	15.0	-0.5	-0.6	-1.3	-0.8	-0.6	-0.5	-0.6	-1.2
87.9	-1.6	29.0	-24.0	-0.5	21.0	3.9	-4.0	17.0	-0.4	-0.5	-1.0	-0.9	-0.7	-0.7	-0.6	-0.8
97.7	-5.0	30.0	-23.0	-2.9	24.0	2.3	-1.2	18.0	-1.0	-1.3	-1.9	-1.2	-1.5	-1.4	-0.8	-1.9
107.4	-4.9	31.0	-16.0	-7.4	33.0	-1.2	-1.6	20.0	-2.2	-1.7	-1.7	-1.7	-1.6	-1.8	-1.6	-1.5
117.2	0.2	22.0	-17.0	-8.9	31.0	-2.0	-8.6	30.0	-2.0	-1.0	-0.6	-1.6	-1.0	-2.0	-2.1	-0.7
127.0	-2.2	23.0	-23.0	-6.0	34.0	3.5	-10.0	36.0	-1.6	-0.9	-1.0	-2.6	-0.6	-1.7	-2.3	-1.0
136.7	-4.2	23.0	-24.0	-7.2	36.0	5.8	-13.0	40.0	-0.7	-1.2	-0.8	-1.6	-1.0	-1.0	-1.5	-1.0

Table 87. Raw data for the test seal at ω=15 krpm, PD=31 bars, C_r=0.188 mm, and inlet GVF=10%

Freq.	Re(H_{XX})	Re(H_{XY})	Re(H_{YX})	Re(H_{YY})	Im(H_{XX})	Im(H_{XY})	Im(H_{YX})	Im(H_{YY})	Re(eH_{XX})	Re(eH_{XY})	Re(eH_{YX})	Re(eH_{YY})	Im(eH_{XX})	Im(eH_{XY})	Im(eH_{YX})	Im(eH_{YY})
Hz	MN/m	MN/m	MN/m	MN/m	MN/m	MN/m	MN/m	MN/m	MN/m	MN/m	MN/m	MN/m	MN/m	MN/m	MN/m	MN/m
9.8	9.2	7.9	-6.9	14.0	3.1	1.7	-1.8	7.5	-0.1	-0.1	-0.4	-0.3	-0.2	-0.2	-0.2	-0.2
19.5	9.5	7.2	-6.2	12.0	5.6	0.6	-0.6	4.7	-0.2	-0.2	-0.2	-0.1	-0.1	-0.1	-0.2	-0.1
29.3	11.0	4.0	-7.4	13.0	7.7	1.4	0.7	4.7	-0.2	-0.1	-0.2	-0.2	-0.1	-0.1	-0.2	-0.1
39.1	9.1	6.3	-5.3	11.0	11.0	1.5	-1.3	13.0	-0.1	-0.1	-0.1	-0.1	-0.1	-0.1	-0.1	-0.1
48.8	8.9	4.3	-5.3	8.2	15.0	1.4	-2.0	15.0	-0.2	-0.1	-0.1	-0.2	-0.1	-0.1	-0.1	0.0
58.6	8.6	4.8	-5.3	12.0	17.0	1.9	-1.7	17.0	-0.1	-0.1	-0.2	-0.2	-0.1	-0.1	-0.1	-0.1
68.4	7.9	7.1	-5.6	7.0	21.0	0.8	-2.0	21.0	-0.2	-0.2	-0.1	-0.3	-0.2	-0.1	-0.3	-0.2
78.1	6.8	5.3	-6.9	8.6	23.0	1.2	-2.0	24.0	-0.2	-0.1	-0.2	-0.2	-0.2	-0.2	-0.2	-0.1
87.9	6.5	5.3	-4.9	7.7	26.0	1.8	-2.3	26.0	-0.1	-0.1	-0.1	-0.2	-0.1	-0.1	-0.1	-0.1
97.7	5.5	6.0	-4.8	6.7	29.0	1.7	-2.8	28.0	-0.2	-0.1	-0.1	-0.2	-0.1	0.0	-0.1	0.0
107.4	3.9	5.7	-5.5	6.3	32.0	1.7	-3.8	33.0	-0.1	-0.1	-0.1	-0.2	-0.1	-0.1	-0.2	-0.1
117.2	2.3	5.8	-4.6	4.3	34.0	2.4	-3.0	34.0	-0.1	-0.1	-0.1	-0.1	-0.2	-0.1	-0.1	-0.2
127.0	0.2	6.1	-5.3	3.8	37.0	2.3	-3.5	39.0	-0.2	-0.1	-0.1	-0.2	-0.2	0.0	-0.2	-0.2
136.7	-2.2	8.1	-2.9	-2.5	41.0	2.5	-4.1	43.0	-0.2	-0.1	-0.2	-0.1	-0.1	-0.1	-0.1	-0.1

Table 88. Raw data for the test seal at ω=5 krpm, PD=31 bars, C_r=0.163 mm, and inlet GVF=0%

Freq.	Re($\boldsymbol{H_{XX}}$)	Re($\boldsymbol{H_{XY}}$)	Re($\boldsymbol{H_{YX}}$)	Re($\boldsymbol{H_{YY}}$)	Im($\boldsymbol{H_{XX}}$)	Im($\boldsymbol{H_{XY}}$)	Im($\boldsymbol{H_{YX}}$)	Im($\boldsymbol{H_{YY}}$)	Re($\boldsymbol{eH_{XX}}$)	Re($\boldsymbol{eH_{XY}}$)	Re($\boldsymbol{eH_{YX}}$)	Re($\boldsymbol{eH_{YY}}$)	Im($\boldsymbol{eH_{XX}}$)	Im($\boldsymbol{eH_{XY}}$)	Im($\boldsymbol{eH_{YX}}$)	Im($\boldsymbol{eH_{YY}}$)
Hz	MN/m	MN/m	MN/m	MN/m	MN/m	MN/m	MN/m	MN/m	MN/m	MN/m	MN/m	MN/m	MN/m	MN/m	MN/m	MN/m
9.8	0.2	6.4	-8.4	1.9	2.5	1.5	-1.2	4.0	-0.2	-0.1	-0.1	-0.1	-0.1	-0.1	-0.2	-0.1
19.5	1.2	6.8	-8.7	1.7	6.2	1.3	0.0	7.4	-0.2	-0.2	-0.3	-0.1	-0.1	0.0	-0.2	-0.3
29.3	4.3	5.3	-9.8	4.7	9.5	0.3	0.9	8.2	-0.2	-0.1	-0.2	-0.2	-0.2	-0.2	-0.2	-0.1
39.1	2.2	6.7	-7.2	1.8	13.0	0.6	-0.6	14.0	-0.1	-0.1	-0.2	-0.1	-0.2	-0.1	-0.1	-0.1
48.8	1.5	5.5	-7.4	0.9	15.0	0.5	-1.6	16.0	-0.3	-0.1	-0.2	-0.1	-0.2	-0.1	-0.2	-0.1
58.6	1.8	6.5	-7.4	1.1	19.0	0.1	-1.3	19.0	-0.2	-0.1	-0.2	-0.1	-0.2	-0.3	-0.1	-0.2
68.4	1.0	6.9	-7.7	-0.3	23.0	0.8	-0.9	22.0	-0.2	-0.1	-0.2	-0.3	-0.2	-0.2	-0.2	-0.2
78.1	-1.7	5.8	-8.8	-0.9	25.0	0.6	-1.4	26.0	-0.2	-0.1	-0.3	-0.3	-0.3	-0.1	-0.2	-0.2
87.9	-0.1	5.9	-7.2	-0.6	28.0	0.7	-1.4	28.0	-0.1	-0.1	-0.1	-0.1	-0.2	-0.1	-0.1	-0.1
97.7	-0.8	6.9	-7.1	-0.7	31.0	0.2	-1.6	31.0	-0.1	-0.1	-0.1	-0.1	-0.2	-0.1	-0.2	-0.1
107.4	-2.4	6.5	-7.0	-2.6	34.0	0.9	-2.3	35.0	-0.3	-0.1	-0.2	-0.1	-0.1	-0.1	-0.3	-0.1
117.2	-3.0	6.5	-6.8	-4.2	38.0	1.2	-1.1	38.0	-0.1	-0.1	-0.2	-0.1	-0.1	-0.1	-0.3	-0.1
127.0	-6.9	6.5	-7.9	-5.5	41.0	1.3	-2.5	42.0	-0.2	-0.1	-0.1	-0.2	-0.4	-0.2	-0.2	-0.2
136.7	-7.3	7.7	-5.5	-7.7	45.0	3.3	-1.5	45.0	-0.1	-0.1	-0.2	-0.1	-0.2	-0.2	-0.2	-0.2

Table 89. Raw data for the test seal at ω=5 krpm, PD=31 bars, C_r=0.163 mm, and inlet GVF=2%

Freq.	Re($\boldsymbol{H_{XX}}$)	Re($\boldsymbol{H_{XY}}$)	Re($\boldsymbol{H_{YX}}$)	Re($\boldsymbol{H_{YY}}$)	Im($\boldsymbol{H_{XX}}$)	Im($\boldsymbol{H_{XY}}$)	Im($\boldsymbol{H_{YX}}$)	Im($\boldsymbol{H_{YY}}$)	Re($\boldsymbol{eH_{XX}}$)	Re($\boldsymbol{eH_{XY}}$)	Re($\boldsymbol{eH_{YX}}$)	Re($\boldsymbol{eH_{YY}}$)	Im($\boldsymbol{eH_{XX}}$)	Im($\boldsymbol{eH_{XY}}$)	Im($\boldsymbol{eH_{YX}}$)	Im($\boldsymbol{eH_{YY}}$)
Hz	MN/m	MN/m	MN/m	MN/m	MN/m	MN/m	MN/m	MN/m	MN/m	MN/m	MN/m	MN/m	MN/m	MN/m	MN/m	MN/m
9.8	-2.7	6.7	-8.7	-1.4	3.2	0.5	0.2	3.0	-0.2	-0.1	-0.2	-0.1	-0.1	-0.1	-0.1	-0.2
19.5	-0.8	6.9	-9.4	-2.7	6.4	0.0	-0.2	7.2	-0.2	-0.1	-0.2	-0.2	-0.1	-0.1	-0.2	-0.2
29.3	1.8	6.1	-11.0	0.3	9.8	1.1	0.8	10.0	-0.2	-0.1	-0.2	-0.2	-0.1	0.0	-0.2	-0.2
39.1	-0.8	7.3	-9.0	-1.5	13.0	0.2	0.0	14.0	-0.1	-0.1	-0.1	-0.1	-0.1	-0.1	-0.2	-0.1
48.8	-1.3	6.8	-8.5	-1.5	16.0	0.3	-0.3	17.0	-0.1	-0.1	-0.2	-0.1	-0.3	-0.2	-0.2	-0.1
58.6	-1.3	8.5	-8.8	-2.4	21.0	-0.6	-0.6	20.0	-0.2	-0.4	-0.3	-0.2	-0.3	-0.4	-0.2	-0.3
68.4	-1.5	6.6	-9.5	-2.6	24.0	0.2	0.5	23.0	-0.1	-0.2	-0.3	-0.1	-0.3	-0.1	-0.3	-0.3
78.1	-6.3	6.8	-8.8	-4.0	26.0	1.1	-1.1	27.0	-0.3	-0.2	-0.3	-0.2	-0.2	-0.2	-0.5	-0.3
87.9	-3.1	6.6	-8.3	-3.3	30.0	0.0	-0.4	30.0	-0.3	-0.2	-0.2	-0.3	-0.2	-0.1	-0.1	-0.1
97.7	-3.3	6.7	-8.1	-3.5	33.0	-0.4	-0.1	34.0	-0.3	-0.3	-0.1	-0.2	-0.2	-0.2	-0.2	-0.2
107.4	-4.5	6.8	-7.1	-5.8	36.0	0.5	-1.3	37.0	-0.2	-0.1	-0.3	-0.1	-0.4	-0.1	-0.4	-0.1
117.2	-5.6	7.0	-8.1	-6.4	40.0	1.1	-0.7	40.0	-0.2	-0.2	-0.2	-0.2	-0.1	-0.2	-0.2	-0.1
127.0	-9.0	7.4	-8.1	-8.4	43.0	1.0	-1.7	45.0	-0.3	-0.2	-0.2	-0.5	-0.3	-0.2	-0.3	-0.1
136.7	-8.9	7.9	-6.7	-9.8	47.0	1.6	-1.1	47.0	-0.2	-0.3	-0.2	-0.2	-0.4	-0.2	-0.2	-0.4

Table 90. Raw data for the test seal at ω=5 krpm, PD=31 bars, C_r=0.163 mm, and inlet GVF=4%

Freq.	Re(H_{XX})	Re(H_{XY})	Re(H_{YX})	Re(H_{YY})	Im(H_{XX})	Im(H_{XY})	Im(H_{YX})	Im(H_{YY})	Re(eH_{XX})	Re(eH_{XY})	Re(eH_{YX})	Re(eH_{YY})	Im(eH_{XX})	Im(eH_{XY})	Im(eH_{YX})	Im(eH_{YY})
Hz	MN/m	MN/m	MN/m	MN/m	MN/m	MN/m	MN/m	MN/m	MN/m	MN/m	MN/m	MN/m	MN/m	MN/m	MN/m	MN/m
9.8	-5.8	6.9	-8.2	-3.4	3.2	0.5	0.0	2.8	-0.1	-0.1	-0.3	-0.1	-0.2	-0.1	-0.1	-0.2
19.5	-4.8	6.9	-12.0	-6.2	5.9	-0.1	-3.5	6.8	-0.1	-0.1	-0.3	-0.2	-0.1	0.0	-0.2	-0.2
29.3	-3.0	6.1	-17.0	-2.0	10.0	1.6	3.0	12.0	-0.2	-0.2	-0.2	-0.3	-0.2	-0.2	-0.4	-0.2
39.1	-4.5	7.7	-10.0	-3.6	14.0	0.0	1.6	15.0	-0.2	-0.1	-0.1	-0.1	-0.3	-0.1	-0.3	-0.1
48.8	-4.3	7.7	-8.2	-2.8	18.0	0.0	2.0	17.0	-0.3	-0.1	-0.2	-0.1	-0.3	-0.1	-0.2	-0.1
58.6	-4.5	8.9	-9.7	-5.9	22.0	-1.0	-0.4	22.0	-0.2	-0.4	-0.2	-0.4	-0.4	-0.1	-0.3	-0.2
68.4	-4.6	7.6	-12.0	-3.9	26.0	-0.1	0.1	24.0	-0.5	-0.2	-0.4	-0.2	-0.4	-0.2	-0.4	-0.4
78.1	-8.0	7.3	-6.0	-5.6	27.0	0.6	-3.8	26.0	-0.3	-0.2	-0.4	-0.2	-0.5	-0.4	-0.2	-0.4
87.9	-6.6	7.0	-8.5	-5.2	31.0	0.3	0.0	31.0	-0.3	-0.2	-0.3	-0.1	-0.3	-0.2	-0.3	-0.2
97.7	-7.1	7.0	-9.2	-5.9	35.0	-0.3	0.6	35.0	-0.2	-0.2	-0.3	-0.3	-0.3	-0.2	-0.2	-0.2
107.4	-8.3	7.8	-7.5	-7.3	38.0	0.1	1.1	38.0	-0.1	-0.2	-0.4	-0.2	-0.3	-0.2	-0.4	-0.3
117.2	-7.5	7.2	-9.7	-7.7	43.0	0.3	0.1	42.0	-0.1	-0.3	-0.4	-0.3	-0.3	-0.1	-0.2	-0.2
127.0	-11.0	7.6	-6.8	-11.0	46.0	1.4	-2.1	46.0	-0.6	-0.2	-0.5	-0.3	-0.3	-0.4	-0.4	-0.4
136.7	-12.0	8.0	-7.2	-10.0	49.0	1.4	0.0	47.0	-0.3	-0.3	-0.2	-0.3	-0.4	-0.3	-0.5	-0.2

Table 91. Raw data for the test seal at ω=5 krpm, PD=31 bars, C_r=0.163 mm, and inlet GVF=6%

Freq.	Re(H_{XX})	Re(H_{XY})	Re(H_{YX})	Re(H_{YY})	Im(H_{XX})	Im(H_{XY})	Im(H_{YX})	Im(H_{YY})	Re(eH_{XX})	Re(eH_{XY})	Re(eH_{YX})	Re(eH_{YY})	Im(eH_{XX})	Im(eH_{XY})	Im(eH_{YX})	Im(eH_{YY})
Hz	MN/m	MN/m	MN/m	MN/m	MN/m	MN/m	MN/m	MN/m	MN/m	MN/m	MN/m	MN/m	MN/m	MN/m	MN/m	MN/m
9.8	-5.2	13.0	-16.0	-1.1	1.7	0.8	3.1	5.6	-0.2	-0.1	-0.2	-0.2	-0.2	-0.1	-0.3	-0.2
19.5	-2.6	15.0	-17.0	-2.0	7.7	0.2	0.7	8.2	-0.1	-0.1	-0.1	-0.1	-0.1	0.0	-0.1	-0.1
29.3	0.2	14.0	-20.0	-0.2	10.0	1.0	1.5	9.8	-0.1	-0.1	-0.2	-0.1	-0.1	-0.1	-0.1	-0.2
39.1	-3.3	16.0	-17.0	-3.1	14.0	1.9	-1.1	15.0	-0.1	-0.1	-0.1	-0.1	-0.1	-0.1	-0.1	-0.1
48.8	-2.6	14.0	-17.0	-4.4	17.0	0.8	-0.9	18.0	-0.1	-0.1	-0.1	-0.1	-0.2	-0.1	-0.2	-0.1
58.6	-3.1	15.0	-17.0	-5.6	21.0	1.3	-3.0	21.0	-0.2	-0.1	-0.3	-0.2	-0.1	-0.1	-0.3	-0.1
68.4	-2.9	15.0	-18.0	-2.7	24.0	1.3	-0.9	23.0	-0.1	-0.1	-0.2	-0.1	-0.1	-0.1	-0.1	-0.1
78.1	-4.0	15.0	-15.0	-4.8	27.0	1.7	-2.7	27.0	-0.1	-0.1	-0.1	0.0	-0.1	-0.1	-0.1	-0.1
87.9	-4.0	14.0	-17.0	-4.8	30.0	1.2	-1.3	31.0	-0.1	-0.1	-0.1	-0.1	-0.1	-0.1	-0.1	-0.1
97.7	-4.8	15.0	-16.0	-4.5	33.0	1.0	-1.8	34.0	-0.2	-0.1	-0.1	-0.1	-0.2	-0.1	-0.1	-0.1
107.4	-6.8	15.0	-16.0	-6.5	36.0	3.1	-1.3	37.0	-0.2	-0.1	-0.1	-0.1	-0.1	-0.1	-0.2	-0.1
117.2	-8.0	15.0	-16.0	-8.7	40.0	3.6	-2.7	40.0	-0.1	-0.1	-0.1	-0.1	-0.1	-0.1	-0.2	-0.1
127.0	-12.0	16.0	-14.0	-10.0	43.0	5.1	-3.7	42.0	-1.8	-1.1	-2.1	-0.7	-1.9	-0.8	-1.8	-1.2
136.7	-12.0	16.0	-14.0	-12.0	47.0	4.7	-3.4	45.0	-0.1	-0.1	-0.1	-0.1	-0.1	-0.1	-0.1	-0.1

Table 92. Raw data for the test seal at ω=7.5 krpm, PD=31 bars, C_r=0.163 mm, and inlet GVF=0%

Freq.	Re($\boldsymbol{H_{XX}}$)	Re($\boldsymbol{H_{XY}}$)	Re($\boldsymbol{H_{YX}}$)	Re($\boldsymbol{H_{YY}}$)	Im($\boldsymbol{H_{XX}}$)	Im($\boldsymbol{H_{XY}}$)	Im($\boldsymbol{H_{YX}}$)	Im($\boldsymbol{H_{YY}}$)	Re($\boldsymbol{eH_{XX}}$)	Re($\boldsymbol{eH_{XY}}$)	Re($\boldsymbol{eH_{YX}}$)	Re($\boldsymbol{eH_{YY}}$)	Im($\boldsymbol{eH_{XX}}$)	Im($\boldsymbol{eH_{XY}}$)	Im($\boldsymbol{eH_{YX}}$)	Im($\boldsymbol{eH_{YY}}$)
Hz	MN/m	MN/m	MN/m	MN/m	MN/m	MN/m	MN/m	MN/m	MN/m	MN/m	MN/m	MN/m	MN/m	MN/m	MN/m	MN/m
9.8	-9.5	19.0	-13.0	6.0	8.0	2.1	15.0	4.6	-0.3	-0.3	-0.5	-0.5	-0.4	-0.2	-0.7	-0.3
19.5	-6.6	16.0	-16.0	-5.4	7.8	0.9	0.6	8.2	-0.1	-0.1	-0.1	-0.1	-0.1	-0.1	-0.2	-0.1
29.3	-3.2	15.0	-19.0	-2.7	11.0	1.4	1.9	10.0	-0.1	-0.1	-0.1	-0.1	-0.1	-0.1	-0.1	-0.1
39.1	-4.9	16.0	-15.0	-7.1	13.0	-0.2	-3.1	13.0	-0.1	0.0	-0.1	-0.1	-0.1	-0.1	-0.1	-0.1
48.8	-7.3	14.0	-18.0	-7.6	16.0	0.6	-0.8	18.0	-0.1	-0.1	-0.1	-0.1	-0.1	-0.1	-0.2	-0.1
58.6	-7.4	15.0	-18.0	-11.0	19.0	0.6	-6.0	20.0	-0.2	-0.1	-0.2	-0.2	-0.1	-0.2	-0.3	-0.2
68.4	-7.5	15.0	-19.0	-5.6	22.0	1.2	-1.1	24.0	-0.1	-0.1	-0.1	-0.1	-0.1	-0.1	-0.1	-0.1
78.1	-5.4	16.0	-12.0	-7.9	28.0	0.5	-3.3	26.0	-0.2	-0.1	-0.1	-0.1	-0.1	-0.1	-0.1	-0.1
87.9	-8.8	15.0	-19.0	-7.3	30.0	1.5	-0.2	33.0	-0.2	-0.1	-0.3	-0.1	-0.1	-0.1	-0.1	-0.2
97.7	-8.0	16.0	-15.0	-6.9	34.0	0.8	-1.5	35.0	-0.1	-0.1	-0.1	-0.1	-0.2	-0.1	-0.1	-0.1
107.4	-11.0	16.0	-18.0	-8.3	38.0	2.6	0.7	37.0	-0.2	-0.1	-0.2	-0.2	-0.2	-0.1	-0.2	-0.1
117.2	-12.0	15.0	-18.0	-10.0	40.0	2.7	-1.9	40.0	-0.1	-0.1	-0.1	-0.1	-0.2	-0.1	-0.1	-0.1
127.0	-13.0	16.0	-13.0	-12.0	43.0	2.9	-3.4	40.0	-1.2	-1.3	-2.9	-2.2	-2.6	-1.9	-1.5	-1.6
136.7	-15.0	17.0	-14.0	-12.0	48.0	3.8	-2.2	45.0	-0.1	-0.1	-0.1	-0.2	-0.2	-0.1	-0.1	-0.1

Table 93. Raw data for the test seal at ω=7.5 krpm, PD=31 bars, C_r=0.163 mm, and inlet GVF=2%

Freq.	Re($\boldsymbol{H_{XX}}$)	Re($\boldsymbol{H_{XY}}$)	Re($\boldsymbol{H_{YX}}$)	Re($\boldsymbol{H_{YY}}$)	Im($\boldsymbol{H_{XX}}$)	Im($\boldsymbol{H_{XY}}$)	Im($\boldsymbol{H_{YX}}$)	Im($\boldsymbol{H_{YY}}$)	Re($\boldsymbol{eH_{XX}}$)	Re($\boldsymbol{eH_{XY}}$)	Re($\boldsymbol{eH_{YX}}$)	Re($\boldsymbol{eH_{YY}}$)	Im($\boldsymbol{eH_{XX}}$)	Im($\boldsymbol{eH_{XY}}$)	Im($\boldsymbol{eH_{YX}}$)	Im($\boldsymbol{eH_{YY}}$)
Hz	MN/m	MN/m	MN/m	MN/m	MN/m	MN/m	MN/m	MN/m	MN/m	MN/m	MN/m	MN/m	MN/m	MN/m	MN/m	MN/m
9.8	19.0	4.1	-2.0	20.0	2.4	-0.1	-0.5	2.8	-0.1	-0.1	-0.1	-0.1	-0.1	-0.1	-0.1	-0.1
19.5	18.0	2.8	-1.8	20.0	4.0	1.9	-1.1	4.4	-0.1	-0.1	-0.1	-0.1	-0.1	-0.1	-0.1	-0.1
29.3	20.0	0.7	-4.6	22.0	5.2	2.3	-1.0	4.2	-0.1	-0.1	-0.1	-0.1	-0.1	-0.1	-0.1	-0.1
39.1	18.0	2.7	-1.6	18.0	8.0	1.9	-2.4	7.8	-0.1	-0.1	-0.1	-0.1	-0.1	-0.1	-0.1	-0.1
48.8	17.0	2.5	-2.0	17.0	10.0	2.6	-3.4	10.0	-0.1	-0.1	-0.1	-0.1	-0.1	0.0	-0.1	-0.1
58.6	17.0	2.2	-2.2	17.0	12.0	2.8	-3.7	12.0	-0.1	0.0	-0.1	-0.1	-0.1	-0.1	-0.1	-0.1
68.4	16.0	3.6	-2.3	16.0	14.0	3.0	-4.1	14.0	0.0	-0.1	-0.1	0.0	0.0	0.0	0.0	-0.1
78.1	15.0	2.9	-2.3	15.0	16.0	3.5	-4.6	15.0	0.0	0.0	-0.1	-0.1	-0.1	-0.1	-0.1	0.0
87.9	13.0	3.0	-2.4	14.0	17.0	4.1	-5.5	17.0	-0.1	-0.1	-0.1	-0.1	0.0	0.0	-0.1	-0.1
97.7	11.0	3.5	-2.5	12.0	19.0	4.4	-5.8	19.0	0.0	0.0	0.0	0.0	0.0	0.0	-0.1	0.0
107.4	9.4	3.7	-2.6	10.0	22.0	4.7	-6.1	21.0	0.0	0.0	0.0	0.0	-0.1	0.0	0.0	0.0
117.2	7.3	4.1	-2.3	7.5	24.0	5.3	-6.7	23.0	0.0	0.0	0.0	0.0	0.0	0.0	0.0	0.0
127.0	5.2	4.4	-2.5	5.3	26.0	5.6	-7.5	26.0	0.0	0.0	-0.1	0.0	0.0	0.0	0.0	-0.1
136.7	2.4	6.0	-1.7	2.1	29.0	5.9	-8.2	29.0	0.0	0.0	0.0	0.0	0.0	0.0	0.0	0.0

Table 94. Raw data for the test seal at ω=5 krpm, PD=24.1 bars, C_r=0.163 mm, and inlet GVF=0%

Freq.	Re($\boldsymbol{H_{XX}}$)	Re($\boldsymbol{H_{XY}}$)	Re($\boldsymbol{H_{YX}}$)	Re($\boldsymbol{H_{YY}}$)	Im($\boldsymbol{H_{XX}}$)	Im($\boldsymbol{H_{XY}}$)	Im($\boldsymbol{H_{YX}}$)	Im($\boldsymbol{H_{YY}}$)	Re($\boldsymbol{eH_{XX}}$)	Re($\boldsymbol{eH_{XY}}$)	Re($\boldsymbol{eH_{YX}}$)	Re($\boldsymbol{eH_{YY}}$)	Im($\boldsymbol{eH_{XX}}$)	Im($\boldsymbol{eH_{XY}}$)	Im($\boldsymbol{eH_{YX}}$)	Im($\boldsymbol{eH_{YY}}$)
Hz	MN/m	MN/m	MN/m	MN/m	MN/m	MN/m	MN/m	MN/m	MN/m	MN/m	MN/m	MN/m	MN/m	MN/m	MN/m	MN/m
9.8	15.0	4.1	-3.0	16.0	1.9	1.2	-1.3	4.7	-0.1	-0.1	-0.1	-0.1	-0.1	-0.1	-0.1	-0.2
19.5	15.0	4.1	-2.9	16.0	4.1	1.5	-0.9	4.5	0.0	0.0	-0.1	-0.1	-0.1	-0.1	-0.1	-0.1
29.3	17.0	1.6	-5.2	18.0	5.9	1.3	-0.4	2.8	-0.1	0.0	0.0	-0.1	-0.1	-0.1	-0.1	-0.1
39.1	15.0	4.6	-2.5	15.0	8.5	0.7	-2.0	8.7	-0.1	-0.1	-0.1	-0.1	0.0	0.0	-0.2	-0.1
48.8	14.0	4.0	-3.0	14.0	11.0	1.9	-3.2	11.0	-0.1	-0.1	-0.1	0.0	-0.1	-0.1	-0.1	0.0
58.6	14.0	3.9	-3.1	14.0	13.0	1.7	-3.0	12.0	-0.1	-0.1	-0.1	-0.1	-0.1	0.0	-0.1	0.0
68.4	13.0	4.3	-2.9	12.0	15.0	0.7	-3.0	15.0	-0.1	-0.1	-0.1	-0.1	-0.1	-0.1	0.0	-0.1
78.1	12.0	4.2	-3.4	12.0	16.0	2.2	-3.6	17.0	-0.1	0.0	0.0	0.0	-0.1	0.0	-0.1	-0.1
87.9	11.0	4.3	-2.9	11.0	18.0	2.6	-4.3	19.0	-0.1	-0.1	-0.1	0.0	0.0	0.0	-0.1	0.0
97.7	9.2	4.3	-3.0	9.4	21.0	2.8	-4.8	20.0	0.0	0.0	0.0	-0.1	0.0	0.0	-0.1	-0.1
107.4	7.5	4.6	-3.3	8.4	23.0	2.9	-5.1	23.0	-0.1	0.0	0.0	0.0	-0.1	-0.1	-0.1	0.0
117.2	5.7	5.0	-2.6	6.4	25.0	3.5	-5.5	25.0	0.0	0.0	0.0	0.0	0.0	0.0	-0.1	0.0
127.0	3.9	5.1	-2.9	5.0	28.0	3.8	-6.2	28.0	-0.1	0.0	0.0	0.0	-0.1	0.0	-0.1	-0.1
136.7	1.4	7.1	-1.7	0.7	31.0	3.7	-7.3	31.0	0.0	-0.1	0.0	-0.1	-0.1	0.0	0.0	0.0

Table 95. Raw data for the test seal at ω=5 krpm, PD=24.1 bars, C_r=0.163 mm, and inlet GVF=2%

Freq.	Re($\boldsymbol{H_{XX}}$)	Re($\boldsymbol{H_{XY}}$)	Re($\boldsymbol{H_{YX}}$)	Re($\boldsymbol{H_{YY}}$)	Im($\boldsymbol{H_{XX}}$)	Im($\boldsymbol{H_{XY}}$)	Im($\boldsymbol{H_{YX}}$)	Im($\boldsymbol{H_{YY}}$)	Re($\boldsymbol{eH_{XX}}$)	Re($\boldsymbol{eH_{XY}}$)	Re($\boldsymbol{eH_{YX}}$)	Re($\boldsymbol{eH_{YY}}$)	Im($\boldsymbol{eH_{XX}}$)	Im($\boldsymbol{eH_{XY}}$)	Im($\boldsymbol{eH_{YX}}$)	Im($\boldsymbol{eH_{YY}}$)
Hz	MN/m	MN/m	MN/m	MN/m	MN/m	MN/m	MN/m	MN/m	MN/m	MN/m	MN/m	MN/m	MN/m	MN/m	MN/m	MN/m
9.8	12.0	6.8	-4.2	13.0	2.8	1.2	-1.3	4.9	-0.1	-0.1	-0.2	-0.1	-0.1	-0.1	-0.1	-0.1
19.5	13.0	6.0	-3.8	12.0	4.6	1.2	-0.9	4.5	-0.1	0.0	-0.1	-0.1	-0.1	-0.1	-0.1	0.0
29.3	15.0	3.8	-6.3	15.0	6.5	1.8	0.0	4.3	-0.1	0.0	-0.2	0.0	-0.1	-0.1	-0.2	-0.1
39.1	12.0	5.4	-3.1	12.0	9.4	0.6	-1.7	9.9	-0.1	-0.1	-0.1	-0.1	0.0	-0.1	-0.1	-0.1
48.8	12.0	5.1	-3.5	11.0	12.0	1.1	-2.8	12.0	-0.1	0.0	-0.1	-0.1	-0.1	0.0	-0.1	0.0
58.6	11.0	4.3	-3.6	11.0	14.0	1.2	-2.4	13.0	-0.1	-0.1	-0.1	-0.1	-0.1	-0.1	-0.2	-0.1
68.4	10.0	6.6	-3.6	8.6	16.0	0.8	-2.7	17.0	-0.1	0.0	-0.2	-0.1	0.0	-0.1	-0.1	0.0
78.1	9.9	5.1	-4.5	9.3	18.0	1.3	-3.2	19.0	-0.2	-0.1	0.0	-0.1	-0.1	-0.1	-0.1	-0.1
87.9	8.6	4.8	-3.5	8.1	20.0	1.8	-3.6	21.0	-0.1	-0.1	-0.1	-0.1	-0.1	0.0	-0.1	-0.1
97.7	7.1	5.4	-3.5	6.8	23.0	2.0	-4.1	23.0	-0.1	-0.1	-0.1	-0.1	0.0	-0.1	-0.1	-0.1
107.4	5.9	5.3	-3.9	6.3	25.0	2.0	-4.4	26.0	-0.1	-0.1	-0.1	-0.1	-0.1	-0.1	-0.1	-0.1
117.2	4.2	5.6	-3.2	4.3	28.0	2.7	-4.5	28.0	-0.1	0.0	-0.1	-0.1	-0.1	0.0	-0.1	-0.1
127.0	2.4	5.8	-3.6	3.5	31.0	2.7	-5.4	31.0	-0.1	-0.1	-0.1	-0.1	-0.1	-0.1	-0.1	-0.1
136.7	0.4	7.6	-2.6	-0.9	34.0	3.0	-6.1	35.0	-0.1	-0.1	-0.1	-0.2	-0.1	-0.1	-0.1	0.0

Table 96. Raw data for the test seal at ω=5 krpm, PD=24.1 bars, C_r=0.163 mm, and inlet GVF=4%

Freq.	Re($\boldsymbol{H_{XX}}$)	Re($\boldsymbol{H_{XY}}$)	Re($\boldsymbol{H_{YX}}$)	Re($\boldsymbol{H_{YY}}$)	Im($\boldsymbol{H_{XX}}$)	Im($\boldsymbol{H_{XY}}$)	Im($\boldsymbol{H_{YX}}$)	Im($\boldsymbol{H_{YY}}$)	Re($\boldsymbol{eH_{XX}}$)	Re($\boldsymbol{eH_{XY}}$)	Re($\boldsymbol{eH_{YX}}$)	Re($\boldsymbol{eH_{YY}}$)	Im($\boldsymbol{eH_{XX}}$)	Im($\boldsymbol{eH_{XY}}$)	Im($\boldsymbol{eH_{YX}}$)	Im($\boldsymbol{eH_{YY}}$)
Hz	MN/m	MN/m	MN/m	MN/m	MN/m	MN/m	MN/m	MN/m	MN/m	MN/m	MN/m	MN/m	MN/m	MN/m	MN/m	MN/m
9.8	13.0	6.5	-4.1	15.0	2.6	1.1	-1.1	5.0	-0.1	-0.1	-0.1	-0.1	-0.1	0.0	-0.1	-0.2
19.5	13.0	5.8	-3.8	14.0	4.7	1.3	-1.1	4.5	-0.1	-0.1	-0.1	-0.1	-0.1	-0.1	-0.1	0.0
29.3	15.0	3.0	-6.3	17.0	6.5	1.3	-0.1	4.0	-0.1	-0.1	-0.1	-0.1	-0.1	-0.1	-0.1	-0.2
39.1	13.0	5.2	-3.1	13.0	9.7	0.7	-1.6	9.4	-0.1	-0.1	-0.1	-0.1	-0.1	0.0	-0.2	0.0
48.8	12.0	4.7	-3.4	12.0	12.0	1.0	-2.8	12.0	-0.1	-0.1	-0.1	-0.1	-0.1	-0.1	-0.1	0.0
58.6	12.0	4.0	-3.4	12.0	14.0	1.6	-2.6	13.0	-0.1	0.0	-0.1	0.0	-0.1	-0.1	-0.1	-0.1
68.4	11.0	5.9	-3.5	10.0	16.0	0.8	-2.8	16.0	-0.1	-0.1	-0.1	-0.1	-0.1	-0.1	-0.1	-0.1
78.1	11.0	4.5	-4.2	11.0	18.0	1.5	-3.0	18.0	-0.2	0.0	-0.1	-0.1	-0.1	-0.1	-0.1	-0.1
87.9	9.2	4.7	-3.4	9.5	20.0	1.9	-3.7	20.0	-0.1	0.0	0.0	-0.1	-0.1	-0.1	-0.1	0.0
97.7	7.9	5.0	-3.5	8.2	22.0	2.2	-3.9	22.0	0.0	-0.1	-0.1	-0.1	-0.1	0.0	-0.1	-0.1
107.4	6.6	5.0	-3.8	7.5	25.0	2.1	-4.2	25.0	-0.1	-0.1	-0.1	-0.1	-0.1	-0.1	-0.1	-0.1
117.2	5.0	5.2	-3.0	5.6	27.0	2.8	-4.4	27.0	0.0	0.0	-0.1	-0.1	0.0	-0.1	-0.1	-0.1
127.0	3.4	5.4	-3.5	4.7	30.0	3.0	-5.2	30.0	-0.1	-0.1	-0.1	-0.1	-0.1	0.0	-0.1	-0.1
136.7	1.4	7.0	-2.5	0.6	33.0	3.0	-6.2	34.0	0.0	0.0	-0.1	-0.1	-0.1	-0.1	0.0	0.0

Table 97. Raw data for the test seal at ω=5 krpm, PD=24.1 bars, C_r=0.163 mm, and inlet GVF=6%

Freq.	Re($\boldsymbol{H_{XX}}$)	Re($\boldsymbol{H_{XY}}$)	Re($\boldsymbol{H_{YX}}$)	Re($\boldsymbol{H_{YY}}$)	Im($\boldsymbol{H_{XX}}$)	Im($\boldsymbol{H_{XY}}$)	Im($\boldsymbol{H_{YX}}$)	Im($\boldsymbol{H_{YY}}$)	Re($\boldsymbol{eH_{XX}}$)	Re($\boldsymbol{eH_{XY}}$)	Re($\boldsymbol{eH_{YX}}$)	Re($\boldsymbol{eH_{YY}}$)	Im($\boldsymbol{eH_{XX}}$)	Im($\boldsymbol{eH_{XY}}$)	Im($\boldsymbol{eH_{YX}}$)	Im($\boldsymbol{eH_{YY}}$)
Hz	MN/m	MN/m	MN/m	MN/m	MN/m	MN/m	MN/m	MN/m	MN/m	MN/m	MN/m	MN/m	MN/m	MN/m	MN/m	MN/m
9.8	12.0	6.6	-4.3	13.0	2.9	1.1	-1.1	4.9	-0.1	-0.1	-0.1	-0.1	-0.1	-0.1	-0.1	-0.1
19.5	12.0	6.0	-4.1	13.0	4.6	1.3	-0.8	4.5	-0.1	-0.1	-0.1	-0.1	0.0	0.0	-0.1	-0.1
29.3	14.0	3.5	-6.7	16.0	6.6	1.5	0.1	4.0	-0.1	-0.1	-0.2	-0.1	-0.1	-0.1	-0.1	-0.1
39.1	12.0	5.4	-3.4	12.0	9.7	0.6	-1.3	9.6	-0.2	0.0	-0.1	-0.1	0.0	-0.1	-0.1	-0.1
48.8	11.0	4.9	-3.4	11.0	12.0	1.2	-2.5	12.0	-0.1	-0.1	-0.1	-0.1	-0.1	0.0	-0.2	-0.1
58.6	11.0	4.2	-3.5	12.0	14.0	1.4	-2.3	13.0	-0.1	0.0	-0.1	-0.1	-0.1	-0.1	-0.2	-0.2
68.4	10.0	6.2	-3.5	9.2	16.0	0.8	-2.5	16.0	-0.1	-0.1	-0.1	-0.1	-0.1	-0.1	-0.1	0.0
78.1	9.8	4.9	-4.4	9.6	18.0	1.4	-3.1	19.0	-0.1	0.0	-0.1	-0.1	-0.2	-0.1	-0.1	-0.1
87.9	8.3	4.9	-3.5	8.8	21.0	2.0	-3.6	21.0	0.0	-0.1	-0.1	-0.1	-0.1	-0.1	-0.1	-0.1
97.7	7.1	5.2	-3.4	7.3	23.0	2.0	-3.8	22.0	0.0	-0.1	-0.1	0.0	0.0	0.0	-0.1	0.0
107.4	6.0	5.2	-4.1	6.8	26.0	2.0	-4.3	26.0	-0.1	-0.1	-0.1	-0.1	-0.1	-0.1	-0.1	0.0
117.2	4.1	5.6	-3.1	5.0	28.0	2.7	-4.1	28.0	-0.1	0.0	-0.1	-0.1	-0.1	-0.1	-0.1	0.0
127.0	2.6	5.6	-3.5	4.2	31.0	2.5	-5.0	31.0	-0.1	-0.1	-0.1	-0.1	-0.1	-0.1	-0.1	-0.1
136.7	0.8	7.2	-2.3	0.2	34.0	3.0	-6.0	35.0	0.0	-0.1	-0.1	-0.1	-0.1	-0.1	-0.1	-0.1

Table 98. Raw data for the test seal at ω=5 krpm, PD=24.1 bars, C_r=0.163 mm, and inlet GVF=8%

Freq.	Re($\boldsymbol{H_{XX}}$)	Re($\boldsymbol{H_{XY}}$)	Re($\boldsymbol{H_{YX}}$)	Re($\boldsymbol{H_{YY}}$)	Im($\boldsymbol{H_{XX}}$)	Im($\boldsymbol{H_{XY}}$)	Im($\boldsymbol{H_{YX}}$)	Im($\boldsymbol{H_{YY}}$)	Re($\boldsymbol{eH_{XX}}$)	Re($\boldsymbol{eH_{XY}}$)	Re($\boldsymbol{eH_{YX}}$)	Re($\boldsymbol{eH_{YY}}$)	Im($\boldsymbol{eH_{XX}}$)	Im($\boldsymbol{eH_{XY}}$)	Im($\boldsymbol{eH_{YX}}$)	Im($\boldsymbol{eH_{YY}}$)
Hz	MN/m	MN/m	MN/m	MN/m	MN/m	MN/m	MN/m	MN/m	MN/m	MN/m	MN/m	MN/m	MN/m	MN/m	MN/m	MN/m
9.8	8.2	7.4	-5.2	9.3	2.4	1.1	-1.1	4.8	-0.1	-0.1	-0.2	-0.3	-0.1	-0.1	-0.1	-0.1
19.5	8.6	6.6	-4.6	8.9	4.6	1.2	-0.7	5.2	0.0	0.0	-0.2	-0.1	-0.1	0.0	-0.1	-0.2
29.3	11.0	4.6	-7.1	12.0	7.0	1.2	0.6	4.4	-0.2	-0.1	-0.1	-0.1	-0.2	-0.1	-0.2	-0.1
39.1	8.6	6.3	-3.8	8.9	10.0	0.6	-0.9	11.0	-0.1	-0.1	-0.1	-0.1	-0.1	-0.1	-0.1	-0.1
48.8	7.9	5.7	-4.0	7.4	12.0	0.7	-2.4	13.0	-0.1	-0.1	-0.1	-0.1	-0.1	-0.1	-0.1	-0.1
58.6	7.5	5.2	-4.1	8.4	15.0	0.9	-2.3	15.0	-0.1	0.0	-0.1	-0.2	-0.1	-0.1	-0.1	-0.1
68.4	6.8	7.0	-3.7	5.6	17.0	1.0	-2.8	18.0	-0.1	0.0	-0.1	-0.2	-0.1	-0.1	-0.1	-0.2
78.1	6.5	5.8	-4.7	6.4	20.0	1.0	-2.9	20.0	-0.1	0.0	-0.1	-0.1	-0.1	0.0	-0.1	-0.1
87.9	5.6	5.8	-4.0	5.6	22.0	1.4	-3.2	22.0	0.0	-0.1	-0.1	-0.1	-0.1	-0.1	-0.1	-0.1
97.7	4.3	6.0	-3.9	4.7	24.0	1.3	-3.6	24.0	-0.1	-0.1	-0.1	-0.1	0.0	-0.1	-0.1	-0.1
107.4	3.1	6.2	-4.4	4.0	27.0	1.5	-4.0	28.0	-0.2	-0.1	-0.1	-0.1	-0.1	-0.1	-0.2	-0.1
117.2	1.4	6.3	-3.5	2.4	30.0	1.9	-3.8	30.0	-0.1	0.0	-0.1	-0.1	-0.1	-0.1	-0.1	-0.1
127.0	-0.2	6.6	-3.8	2.0	33.0	1.8	-4.7	34.0	0.0	-0.1	0.0	-0.1	-0.1	-0.1	-0.2	-0.1
136.7	-1.6	7.7	-2.6	-2.4	36.0	2.4	-5.7	38.0	-0.1	-0.1	-0.1	-0.1	-0.1	-0.1	-0.1	-0.1

Table 99. Raw data for the test seal at ω=5 krpm, PD=24.1 bars, C_r=0.163 mm, and inlet GVF=10%

Freq.	Re($\boldsymbol{H_{XX}}$)	Re($\boldsymbol{H_{XY}}$)	Re($\boldsymbol{H_{YX}}$)	Re($\boldsymbol{H_{YY}}$)	Im($\boldsymbol{H_{XX}}$)	Im($\boldsymbol{H_{XY}}$)	Im($\boldsymbol{H_{YX}}$)	Im($\boldsymbol{H_{YY}}$)	Re($\boldsymbol{eH_{XX}}$)	Re($\boldsymbol{eH_{XY}}$)	Re($\boldsymbol{eH_{YX}}$)	Re($\boldsymbol{eH_{YY}}$)	Im($\boldsymbol{eH_{XX}}$)	Im($\boldsymbol{eH_{XY}}$)	Im($\boldsymbol{eH_{YX}}$)	Im($\boldsymbol{eH_{YY}}$)
Hz	MN/m	MN/m	MN/m	MN/m	MN/m	MN/m	MN/m	MN/m	MN/m	MN/m	MN/m	MN/m	MN/m	MN/m	MN/m	MN/m
9.8	8.9	13.0	-13.0	10.0	3.0	0.4	-0.9	3.6	-0.1	-0.1	-0.2	-0.1	-0.2	-0.1	-0.1	-0.1
19.5	9.7	12.0	-11.0	9.4	4.9	1.1	-1.3	5.1	-0.1	-0.1	0.0	-0.1	-0.1	-0.1	-0.1	-0.1
29.3	11.0	10.0	-14.0	13.0	6.9	2.4	-0.4	5.0	-0.1	-0.1	-0.1	-0.1	-0.1	-0.1	-0.1	-0.1
39.1	9.0	12.0	-11.0	9.2	9.9	1.7	-2.0	10.0	-0.1	-0.1	-0.1	-0.1	-0.1	-0.1	-0.1	-0.1
48.8	8.5	11.0	-12.0	7.5	12.0	1.8	-3.2	13.0	-0.2	-0.1	-0.1	-0.1	-0.1	-0.1	-0.1	-0.1
58.6	8.8	11.0	-11.0	8.7	15.0	2.3	-3.0	15.0	-0.1	0.0	-0.2	-0.1	-0.2	-0.1	-0.2	-0.1
68.4	8.0	12.0	-11.0	6.7	18.0	2.9	-3.7	18.0	-0.1	-0.1	-0.1	-0.1	-0.1	-0.1	-0.1	-0.1
78.1	7.1	11.0	-11.0	6.4	20.0	3.2	-4.3	20.0	-0.1	-0.1	-0.1	-0.1	0.0	-0.1	-0.1	-0.1
87.9	6.2	11.0	-11.0	5.6	22.0	3.8	-5.1	22.0	-0.1	-0.1	-0.1	-0.1	-0.1	-0.1	-0.1	-0.1
97.7	4.5	11.0	-11.0	3.9	24.0	4.4	-5.8	24.0	-0.1	-0.1	-0.1	-0.1	-0.1	0.0	-0.1	-0.1
107.4	2.8	12.0	-12.0	2.5	27.0	4.7	-6.6	27.0	-0.1	-0.1	-0.1	-0.1	-0.1	-0.1	-0.1	-0.1
117.2	0.9	12.0	-11.0	0.6	29.0	5.6	-6.4	29.0	-0.1	0.0	-0.1	-0.1	-0.1	0.0	0.0	0.0
127.0	-1.1	14.0	-12.0	-2.3	32.0	4.4	-7.1	32.0	-2.0	-2.1	-2.1	-2.6	-1.9	-2.4	-2.2	-2.2
136.7	-3.3	14.0	-10.0	-4.6	35.0	6.4	-8.4	36.0	-0.1	-0.1	-0.1	-0.1	-0.1	-0.1	-0.1	-0.1

Table 100. Raw data for the test seal at ω=7.5 krpm, PD=24.1 bars, C_r=0.163 mm, and inlet GVF=0%

Freq.	Re($\boldsymbol{H_{XX}}$)	Re($\boldsymbol{H_{XY}}$)	Re($\boldsymbol{H_{YX}}$)	Re($\boldsymbol{H_{YY}}$)	Im($\boldsymbol{H_{XX}}$)	Im($\boldsymbol{H_{XY}}$)	Im($\boldsymbol{H_{YX}}$)	Im($\boldsymbol{H_{YY}}$)	Re($\boldsymbol{eH_{XX}}$)	Re($\boldsymbol{eH_{XY}}$)	Re($\boldsymbol{eH_{YX}}$)	Re($\boldsymbol{eH_{YY}}$)	Im($\boldsymbol{eH_{XX}}$)	Im($\boldsymbol{eH_{XY}}$)	Im($\boldsymbol{eH_{YX}}$)	Im($\boldsymbol{eH_{YY}}$)
Hz	MN/m	MN/m	MN/m	MN/m	MN/m	MN/m	MN/m	MN/m	MN/m	MN/m	MN/m	MN/m	MN/m	MN/m	MN/m	MN/m
9.8	2.7	12.0	-13.0	1.8	1.1	0.8	-1.2	3.2	-0.1	-0.1	-0.2	-0.1	-0.1	-0.1	-0.2	-0.1
19.5	4.1	12.0	-13.0	1.8	5.1	0.6	-1.0	6.0	0.0	-0.1	-0.1	-0.1	-0.1	0.0	-0.1	0.0
29.3	7.1	11.0	-15.0	4.9	7.6	1.2	-0.1	5.9	-0.1	-0.1	-0.1	-0.1	-0.1	-0.1	-0.1	-0.1
39.1	3.8	13.0	-12.0	2.8	11.0	1.2	-1.5	11.0	-0.1	-0.1	-0.1	-0.1	0.0	0.0	-0.1	0.0
48.8	3.6	12.0	-12.0	1.5	12.0	1.6	-2.3	14.0	-0.1	-0.1	-0.1	-0.1	-0.1	-0.1	-0.1	-0.1
58.6	3.6	13.0	-12.0	2.1	16.0	1.4	-2.6	16.0	-0.1	-0.1	-0.1	-0.1	-0.1	-0.1	-0.1	-0.1
68.4	3.9	12.0	-12.0	0.4	18.0	1.6	-2.9	18.0	-0.1	-0.1	-0.1	-0.1	-0.1	-0.1	-0.1	-0.1
78.1	1.8	12.0	-12.0	-0.2	20.0	2.9	-4.0	21.0	0.0	0.0	-0.1	-0.1	-0.1	-0.1	-0.1	-0.1
87.9	1.4	12.0	-12.0	-0.5	23.0	3.2	-4.4	24.0	-0.1	0.0	-0.1	-0.1	0.0	-0.1	-0.1	-0.1
97.7	0.3	13.0	-12.0	-1.5	25.0	3.2	-4.9	26.0	-0.1	0.0	0.0	-0.1	0.0	-0.1	-0.1	-0.1
107.4	-1.8	13.0	-12.0	-3.6	28.0	4.1	-5.6	29.0	-0.1	-0.1	-0.1	-0.1	-0.1	-0.1	-0.1	-0.1
117.2	-3.3	14.0	-12.0	-5.0	31.0	4.9	-5.6	32.0	0.0	-0.1	-0.1	-0.1	-0.1	-0.1	-0.1	-0.1
127.0	-5.6	15.0	-12.0	-7.1	34.0	4.7	-6.7	35.0	-0.6	-0.6	-0.6	-0.6	-0.6	-0.6	-0.6	-0.6
136.7	-7.9	15.0	-11.0	-9.9	37.0	6.1	-7.4	38.0	-0.1	-0.1	0.0	0.0	-0.1	0.0	0.0	-0.1

Table 101. Raw data for the test seal at ω=7.5 krpm, PD=24.1 bars, C_r=0.163 mm, and inlet GVF=2%

Freq.	Re($\boldsymbol{H_{XX}}$)	Re($\boldsymbol{H_{XY}}$)	Re($\boldsymbol{H_{YX}}$)	Re($\boldsymbol{H_{YY}}$)	Im($\boldsymbol{H_{XX}}$)	Im($\boldsymbol{H_{XY}}$)	Im($\boldsymbol{H_{YX}}$)	Im($\boldsymbol{H_{YY}}$)	Re($\boldsymbol{eH_{XX}}$)	Re($\boldsymbol{eH_{XY}}$)	Re($\boldsymbol{eH_{YX}}$)	Re($\boldsymbol{eH_{YY}}$)	Im($\boldsymbol{eH_{XX}}$)	Im($\boldsymbol{eH_{XY}}$)	Im($\boldsymbol{eH_{YX}}$)	Im($\boldsymbol{eH_{YY}}$)
Hz	MN/m	MN/m	MN/m	MN/m	MN/m	MN/m	MN/m	MN/m	MN/m	MN/m	MN/m	MN/m	MN/m	MN/m	MN/m	MN/m
9.8	0.5	13.0	-14.0	0.4	0.7	0.5	-0.6	3.3	-0.1	-0.1	-0.2	-0.1	-0.1	-0.1	-0.2	-0.1
19.5	1.1	13.0	-14.0	-0.4	5.1	0.4	-0.4	6.4	-0.1	-0.1	-0.1	-0.1	-0.2	-0.1	-0.1	-0.1
29.3	4.4	12.0	-16.0	2.6	8.0	0.9	0.5	6.9	-0.1	-0.1	-0.1	-0.2	-0.1	0.0	-0.2	-0.1
39.1	1.5	14.0	-13.0	0.4	11.0	1.2	-1.3	12.0	-0.1	-0.1	-0.1	-0.2	-0.1	-0.1	-0.1	-0.1
48.8	1.8	13.0	-13.0	-0.2	13.0	1.4	-1.7	15.0	-0.1	-0.1	-0.1	-0.1	-0.1	0.0	-0.1	-0.1
58.6	0.8	14.0	-14.0	-0.6	16.0	1.4	-2.6	17.0	-0.1	-0.1	-0.2	-0.2	-0.1	-0.1	-0.1	-0.1
68.4	1.1	13.0	-13.0	-1.8	19.0	0.2	-2.2	18.0	-0.2	-0.2	-0.2	-0.2	-0.1	-0.2	-0.2	-0.2
78.1	-1.3	13.0	-12.0	-1.9	22.0	2.0	-3.3	22.0	-0.1	-0.1	-0.1	-0.2	-0.1	-0.1	-0.1	0.0
87.9	-1.1	13.0	-13.0	-2.7	24.0	2.3	-3.5	25.0	-0.1	-0.1	-0.1	-0.2	-0.1	-0.1	-0.1	-0.1
97.7	-2.3	14.0	-13.0	-3.4	27.0	2.1	-4.2	28.0	-0.1	-0.1	-0.1	-0.1	-0.1	-0.1	-0.1	-0.1
107.4	-3.8	14.0	-13.0	-4.6	29.0	3.1	-4.3	31.0	-0.1	-0.1	-0.2	-0.2	-0.1	-0.1	-0.1	-0.1
117.2	-5.4	14.0	-13.0	-6.1	33.0	3.9	-5.1	34.0	-0.1	-0.1	-0.1	-0.2	-0.1	-0.1	-0.1	-0.1
127.0	-8.2	15.0	-13.0	-8.9	36.0	3.9	-5.7	37.0	-0.8	-1.0	-1.0	-1.1	-0.9	-0.7	-1.0	-1.0
136.7	-9.6	15.0	-12.0	-10.0	39.0	5.8	-6.8	40.0	-0.1	-0.1	-0.1	-0.2	-0.1	-0.1	-0.1	-0.2

Table 102. Raw data for the test seal at ω=7.5 krpm, PD=24.1 bars, C_r=0.163 mm, and inlet GVF=4%

Freq.	Re($\boldsymbol{H_{XX}}$)	Re($\boldsymbol{H_{XY}}$)	Re($\boldsymbol{H_{YX}}$)	Re($\boldsymbol{H_{YY}}$)	Im($\boldsymbol{H_{XX}}$)	Im($\boldsymbol{H_{XY}}$)	Im($\boldsymbol{H_{YX}}$)	Im($\boldsymbol{H_{YY}}$)	Re($\boldsymbol{eH_{XX}}$)	Re($\boldsymbol{eH_{XY}}$)	Re($\boldsymbol{eH_{YX}}$)	Re($\boldsymbol{eH_{YY}}$)	Im($\boldsymbol{eH_{XX}}$)	Im($\boldsymbol{eH_{XY}}$)	Im($\boldsymbol{eH_{YX}}$)	Im($\boldsymbol{eH_{YY}}$)
Hz	MN/m	MN/m	MN/m	MN/m	MN/m	MN/m	MN/m	MN/m	MN/m	MN/m	MN/m	MN/m	MN/m	MN/m	MN/m	MN/m
9.8	-0.6	13.0	-14.0	-0.5	1.1	0.2	0.4	3.2	-0.1	-0.1	-0.1	-0.1	-0.2	-0.1	-0.1	-0.1
19.5	0.4	13.0	-14.0	-0.8	5.7	0.6	-0.2	6.7	-0.1	0.0	-0.1	0.0	-0.1	-0.1	0.0	-0.1
29.3	4.1	12.0	-16.0	1.8	8.5	0.6	0.3	7.2	-0.1	-0.1	-0.1	-0.1	-0.1	0.0	-0.1	-0.1
39.1	0.4	14.0	-14.0	-0.8	11.0	1.1	-1.1	12.0	-0.1	0.0	-0.1	-0.1	-0.1	0.0	-0.1	0.0
48.8	0.7	13.0	-13.0	-1.2	14.0	0.8	-1.1	15.0	-0.2	-0.1	-0.1	-0.1	-0.1	-0.1	-0.1	-0.1
58.6	0.3	14.0	-14.0	-1.9	17.0	1.3	-2.6	18.0	-0.1	-0.1	-0.2	-0.1	-0.1	-0.1	-0.1	-0.1
68.4	0.5	13.0	-14.0	-1.3	19.0	1.0	-2.1	19.0	-0.1	-0.1	-0.1	-0.1	-0.1	-0.1	-0.1	-0.1
78.1	-1.3	13.0	-13.0	-2.5	21.0	2.3	-3.4	22.0	0.0	-0.1	-0.1	-0.1	-0.1	0.0	-0.1	-0.1
87.9	-1.5	13.0	-14.0	-3.1	24.0	2.2	-3.1	25.0	-0.1	-0.1	-0.1	-0.1	-0.1	-0.1	-0.1	-0.1
97.7	-3.1	14.0	-14.0	-4.4	27.0	2.3	-3.9	28.0	-0.1	-0.1	0.0	-0.1	-0.1	0.0	-0.1	-0.1
107.4	-5.1	14.0	-13.0	-6.0	29.0	3.4	-4.3	31.0	-0.1	-0.1	-0.1	-0.1	-0.1	-0.1	-0.2	0.0
117.2	-6.4	15.0	-14.0	-7.4	33.0	4.1	-4.9	34.0	-0.1	-0.1	-0.2	-0.1	-0.1	0.0	-0.1	-0.1
127.0	-8.4	16.0	-13.0	-10.0	37.0	3.8	-6.1	37.0	-0.9	-0.9	-1.0	-1.1	-0.9	-0.9	-1.1	-1.1
136.7	-10.0	15.0	-12.0	-11.0	40.0	5.2	-5.8	40.0	-0.1	-0.1	-0.1	-0.1	-0.1	-0.1	-0.1	-0.1

Table 103. Raw data for the test seal at ω=7.5 krpm, PD=24.1 bars, C_r=0.163 mm, and inlet GVF=6%

Freq.	Re($\boldsymbol{H_{XX}}$)	Re($\boldsymbol{H_{XY}}$)	Re($\boldsymbol{H_{YX}}$)	Re($\boldsymbol{H_{YY}}$)	Im($\boldsymbol{H_{XX}}$)	Im($\boldsymbol{H_{XY}}$)	Im($\boldsymbol{H_{YX}}$)	Im($\boldsymbol{H_{YY}}$)	Re($\boldsymbol{eH_{XX}}$)	Re($\boldsymbol{eH_{XY}}$)	Re($\boldsymbol{eH_{YX}}$)	Re($\boldsymbol{eH_{YY}}$)	Im($\boldsymbol{eH_{XX}}$)	Im($\boldsymbol{eH_{XY}}$)	Im($\boldsymbol{eH_{YX}}$)	Im($\boldsymbol{eH_{YY}}$)
Hz	MN/m	MN/m	MN/m	MN/m	MN/m	MN/m	MN/m	MN/m	MN/m	MN/m	MN/m	MN/m	MN/m	MN/m	MN/m	MN/m
9.8	-2.3	13.0	-14.0	-1.1	1.4	0.5	1.0	3.3	-0.2	-0.1	-0.2	-0.1	-0.1	-0.1	-0.2	-0.1
19.5	-1.2	14.0	-15.0	-2.3	5.8	0.7	-0.4	7.0	0.0	-0.1	-0.1	-0.1	-0.1	0.0	-0.1	-0.1
29.3	2.2	13.0	-17.0	0.9	9.1	0.8	0.5	7.8	-0.1	-0.1	-0.1	-0.1	-0.1	-0.1	-0.1	-0.1
39.1	-1.1	15.0	-14.0	-2.1	12.0	1.0	-0.8	12.0	-0.1	-0.1	-0.1	0.0	-0.1	-0.1	-0.1	-0.1
48.8	-1.0	13.0	-14.0	-2.6	14.0	0.8	-1.3	15.0	-0.1	-0.1	-0.1	-0.1	-0.1	-0.1	-0.1	-0.1
58.6	-1.2	14.0	-14.0	-3.5	17.0	1.2	-3.1	18.0	-0.1	-0.1	-0.1	-0.1	-0.1	-0.1	-0.2	-0.1
68.4	-1.2	14.0	-15.0	-2.5	20.0	0.9	-2.1	19.0	-0.1	-0.1	-0.1	-0.1	-0.1	-0.1	-0.1	-0.1
78.1	-3.0	14.0	-13.0	-3.7	22.0	2.1	-3.1	22.0	-0.1	-0.1	-0.1	-0.1	-0.1	-0.1	-0.1	-0.1
87.9	-3.3	14.0	-14.0	-4.6	25.0	2.2	-3.2	26.0	-0.1	-0.1	0.0	-0.1	-0.1	-0.1	-0.1	-0.1
97.7	-4.3	14.0	-14.0	-5.3	28.0	2.0	-3.3	29.0	-0.1	-0.1	-0.1	-0.1	-0.1	-0.1	-0.1	-0.1
107.4	-6.3	14.0	-14.0	-7.0	30.0	3.4	-3.7	31.0	-0.1	-0.1	-0.2	-0.1	-0.2	-0.1	-0.1	-0.1
117.2	-7.7	15.0	-14.0	-8.6	34.0	3.9	-5.1	35.0	-0.1	-0.1	-0.2	-0.1	-0.1	-0.1	-0.1	-0.1
127.0	-9.5	15.0	-14.0	-11.0	37.0	3.4	-5.8	38.0	-1.0	-1.0	-0.9	-1.0	-0.9	-0.8	-1.2	-1.1
136.7	-11.0	15.0	-13.0	-11.0	41.0	4.5	-5.5	40.0	-0.1	-0.1	-0.1	-0.1	-0.1	-0.1	-0.1	-0.2

Table 104. Raw data for the test seal at ω=7.5 krpm, PD=24.1 bars, C_r=0.163 mm, and inlet GVF=8%

Freq.	Re(H_{XX})	Re(H_{XY})	Re(H_{YX})	Re(H_{YY})	Im(H_{XX})	Im(H_{XY})	Im(H_{YX})	Im(H_{YY})	Re(eH_{XX})	Re(eH_{XY})	Re(eH_{YX})	Re(eH_{YY})	Im(eH_{XX})	Im(eH_{XY})	Im(eH_{YX})	Im(eH_{YY})
Hz	MN/m	MN/m	MN/m	MN/m	MN/m	MN/m	MN/m	MN/m	MN/m	MN/m	MN/m	MN/m	MN/m	MN/m	MN/m	MN/m
9.8	-5.1	14.0	-17.0	-2.0	1.5	1.1	3.2	4.6	-0.2	-0.1	-0.2	-0.2	-0.2	-0.1	-0.3	-0.1
19.5	-2.9	15.0	-16.0	-4.9	5.9	0.5	-0.6	6.3	-0.2	-0.2	-0.4	-0.2	-0.3	-0.2	-0.2	-0.3
29.3	-0.2	14.0	-19.0	-1.5	9.2	1.0	1.2	8.5	-0.2	-0.2	-0.3	-0.2	-0.2	-0.1	-0.2	-0.2
39.1	-3.2	15.0	-15.0	-5.0	12.0	0.6	-0.8	12.0	-0.1	-0.1	-0.1	-0.1	-0.1	-0.1	-0.2	-0.1
48.8	-3.1	14.0	-15.0	-5.2	15.0	0.5	-0.6	16.0	-0.1	-0.1	-0.1	-0.1	-0.1	-0.1	-0.2	-0.1
58.6	-3.5	14.0	-15.0	-6.5	18.0	1.0	-2.8	18.0	-0.1	-0.1	-0.2	-0.1	-0.1	-0.1	-0.2	-0.2
68.4	-3.4	14.0	-16.0	-4.2	20.0	1.0	-1.2	20.0	-0.1	-0.1	-0.1	-0.1	-0.1	-0.2	-0.1	-0.2
78.1	-4.3	14.0	-14.0	-6.1	23.0	1.6	-2.6	24.0	-0.1	-0.1	-0.1	-0.1	-0.1	-0.1	-0.2	-0.1
87.9	-5.0	14.0	-16.0	-6.7	26.0	1.7	-2.3	27.0	-0.1	-0.1	-0.1	-0.1	-0.1	-0.1	-0.2	-0.1
97.7	-6.1	14.0	-15.0	-7.1	29.0	1.9	-2.6	30.0	-0.1	-0.1	-0.1	-0.2	-0.1	-0.1	-0.1	-0.1
107.4	-7.8	15.0	-15.0	-8.9	32.0	3.4	-2.9	33.0	-0.1	-0.1	-0.2	-0.1	-0.2	-0.1	-0.2	-0.2
117.2	-9.3	15.0	-15.0	-10.0	35.0	3.5	-4.1	36.0	-0.1	-0.1	-0.2	-0.1	-0.1	-0.1	-0.1	-0.1
127.0	-11.0	16.0	-15.0	-13.0	38.0	2.2	-4.7	39.0	-0.7	-0.8	-0.6	-0.7	-0.6	-0.5	-1.0	-0.9
136.7	-12.0	16.0	-14.0	-12.0	42.0	4.2	-4.5	42.0	-0.2	-0.1	-0.2	-0.2	-0.1	-0.1	-0.1	-0.2

Table 105. Raw data for the test seal at ω=7.5 krpm, PD=24.1 bars, C_r=0.163 mm, and inlet GVF=10%

Freq.	Re(H_{XX})	Re(H_{XY})	Re(H_{YX})	Re(H_{YY})	Im(H_{XX})	Im(H_{XY})	Im(H_{YX})	Im(H_{YY})	Re(eH_{XX})	Re(eH_{XY})	Re(eH_{YX})	Re(eH_{YY})	Im(eH_{XX})	Im(eH_{XY})	Im(eH_{YX})	Im(eH_{YY})
Hz	MN/m	MN/m	MN/m	MN/m	MN/m	MN/m	MN/m	MN/m	MN/m	MN/m	MN/m	MN/m	MN/m	MN/m	MN/m	MN/m
9.8	-9.2	20.0	-23.0	2.3	0.9	-1.6	9.6	9.8	-0.2	-0.1	-0.5	-0.1	-0.1	-0.2	-0.2	-0.4
19.5	-7.9	21.0	-24.0	-4.0	4.8	-0.1	3.1	10.0	-0.2	-0.2	-0.2	-0.2	-0.2	-0.2	-0.2	-0.2
29.3	-3.1	22.0	-28.0	-4.0	8.0	0.5	3.9	11.0	-0.2	-0.1	-0.2	-0.1	-0.1	-0.1	-0.2	-0.2
39.1	-7.1	24.0	-23.0	-9.7	12.0	0.7	-1.0	14.0	-0.1	-0.1	-0.1	-0.1	-0.1	0.0	-0.1	-0.1
48.8	-7.4	22.0	-23.0	-10.0	15.0	0.8	-1.9	17.0	-0.1	-0.1	-0.1	-0.1	-0.1	-0.1	-0.1	-0.1
58.6	-6.8	22.0	-23.0	-11.0	18.0	0.6	-3.7	21.0	-0.1	-0.2	-0.2	-0.2	-0.1	-0.1	-0.2	-0.2
68.4	-8.8	23.0	-22.0	-12.0	20.0	3.2	-4.9	21.0	-0.2	-0.2	-0.1	-0.2	-0.1	-0.2	-0.2	-0.1
78.1	-7.6	26.0	-26.0	-10.0	27.0	2.1	-1.2	30.0	-0.2	-0.1	-0.2	-0.2	-0.1	-0.2	-0.1	-0.2
87.9	-10.0	23.0	-26.0	-17.0	28.0	3.5	-7.6	30.0	-0.2	-0.1	-0.1	-0.1	-0.1	-0.2	-0.1	-0.1
97.7	-11.0	23.0	-28.0	-13.0	31.0	3.4	-3.2	35.0	-0.2	-0.2	-0.2	-0.1	-0.2	-0.2	-0.1	-0.2
107.4	-12.0	24.0	-27.0	-12.0	36.0	4.1	-1.1	38.0	-0.1	-0.2	-0.2	-0.2	-0.2	-0.1	-0.3	-0.2
117.2	-15.0	24.0	-26.0	-18.0	38.0	6.1	-8.3	41.0	-0.1	-0.1	-0.2	-0.1	-0.2	-0.1	-0.1	-0.2
127.0	-13.0	24.0	-20.0	-16.0	42.0	4.6	-5.0	39.0	-0.2	-0.2	-0.2	-0.1	-0.2	-0.2	-0.1	-0.2
136.7	-14.0	26.0	-28.0	-13.0	48.0	4.6	-2.3	48.0	-0.2	-0.2	-0.1	-0.2	-0.2	-0.2	-0.2	-0.1

Table 106. Raw data for the test seal at ω=10 krpm, PD=24.1 bars, C_r=0.163 mm, and inlet GVF=0%

Freq.	Re(H_{XX})	Re(H_{XY})	Re(H_{YX})	Re(H_{YY})	Im(H_{XX})	Im(H_{XY})	Im(H_{YX})	Im(H_{YY})	Re(eH_{XX})	Re(eH_{XY})	Re(eH_{YX})	Re(eH_{YY})	Im(eH_{XX})	Im(eH_{XY})	Im(eH_{YX})	Im(eH_{YY})
Hz	MN/m	MN/m	MN/m	MN/m	MN/m	MN/m	MN/m	MN/m	MN/m	MN/m	MN/m	MN/m	MN/m	MN/m	MN/m	MN/m
9.8	30.0	5.8	-6.7	31.0	0.2	1.8	-3.0	9.8	-0.2	-0.1	-0.3	-0.3	-0.2	-0.1	-0.2	-0.1
19.5	31.0	4.9	-6.2	29.0	7.4	-0.5	0.5	5.9	-0.2	-0.2	-0.4	-0.3	-0.3	-0.1	-0.1	-0.2
29.3	32.0	5.0	-4.4	29.0	9.6	-0.3	-1.3	9.8	-0.2	-0.2	-0.2	-0.2	-0.3	-0.2	-0.2	-0.2
39.1	34.0	5.4	-3.9	27.0	10.0	1.2	-2.6	13.0	-0.2	-0.1	-0.2	-0.2	-0.1	-0.1	-0.1	-0.1
48.8	29.0	5.1	-6.1	26.0	12.0	1.6	-4.4	18.0	-0.2	-0.1	-0.2	-0.2	-0.2	0.0	-0.1	-0.1
58.6	31.0	5.8	-5.7	28.0	20.0	2.1	-3.1	20.0	-0.2	-0.2	-0.1	-0.1	-0.1	-0.1	-0.2	-0.3
68.4	29.0	4.1	-6.5	25.0	25.0	2.9	-1.9	26.0	-0.1	-0.1	-0.1	-0.3	-0.1	-0.1	-0.1	-0.2
78.1	29.0	5.7	-6.3	26.0	26.0	3.2	-3.0	28.0	-0.1	-0.1	-0.1	-0.3	-0.2	-0.2	-0.1	-0.1
87.9	31.0	6.5	-4.3	26.0	28.0	2.9	-4.1	32.0	-0.1	-0.1	-0.2	-0.3	-0.1	-0.2	-0.1	-0.3
97.7	27.0	5.9	-5.4	23.0	31.0	2.8	-4.4	35.0	-0.1	-0.1	-0.1	-0.2	-0.1	-0.1	-0.1	-0.1
107.4	25.0	6.5	-6.1	24.0	37.0	4.2	-3.4	38.0	-0.1	-0.1	-0.2	-0.2	-0.2	-0.2	-0.1	-0.1
117.2	25.0	6.7	-4.7	21.0	41.0	3.8	-3.8	41.0	-0.1	-0.1	-0.1	-0.1	-0.1	-0.1	-0.2	-0.1
127.0	24.0	8.0	-5.1	22.0	42.0	4.9	-5.2	46.0	-0.2	-0.1	-0.1	-0.2	0.0	-0.1	-0.1	-0.3
136.7	20.0	6.8	-4.2	15.0	47.0	6.0	-6.1	52.0	-0.2	-0.1	-0.1	-0.2	-0.1	-0.1	-0.1	-0.3

Table 107. Raw data for the test seal at ω=5 krpm, PD=48.3 bars, C_r=0.140 mm, and inlet GVF=0%

Freq.	Re(H_{XX})	Re(H_{XY})	Re(H_{YX})	Re(H_{YY})	Im(H_{XX})	Im(H_{XY})	Im(H_{YX})	Im(H_{YY})	Re(eH_{XX})	Re(eH_{XY})	Re(eH_{YX})	Re(eH_{YY})	Im(eH_{XX})	Im(eH_{XY})	Im(eH_{YX})	Im(eH_{YY})
Hz	MN/m	MN/m	MN/m	MN/m	MN/m	MN/m	MN/m	MN/m	MN/m	MN/m	MN/m	MN/m	MN/m	MN/m	MN/m	MN/m
9.8	12.0	9.8	-8.8	9.7	2.6	0.4	-2.2	5.9	-1.3	-0.5	-0.6	-0.8	-0.2	-0.2	-0.1	-0.4
19.5	12.0	10.0	-9.3	11.0	7.9	-0.3	0.3	8.1	-1.4	-0.5	-0.7	-0.8	-0.2	-0.2	-0.2	-0.2
29.3	14.0	11.0	-7.3	11.0	12.0	0.2	0.5	13.0	-1.4	-0.4	-0.5	-0.9	-0.2	-0.2	-0.3	-0.3
39.1	15.0	11.0	-6.5	11.0	17.0	0.2	-0.3	17.0	-1.1	-0.4	-0.5	-0.7	-0.4	-0.4	-0.2	-0.1
48.8	13.0	10.0	-7.6	10.0	18.0	0.3	-2.7	21.0	-1.3	-0.4	-0.3	-0.5	-0.3	-0.4	-0.4	-0.2
58.6	13.0	11.0	-8.0	11.0	26.0	0.3	-0.6	26.0	-1.1	-0.3	-0.7	-0.9	-0.4	-0.3	-0.4	-0.4
68.4	13.0	11.0	-8.3	8.8	31.0	0.4	0.1	31.0	-1.3	-0.3	-0.4	-0.7	-0.8	-0.5	-0.3	-0.1
78.1	9.3	11.0	-9.5	9.8	33.0	1.1	-0.8	35.0	-1.6	-0.2	-0.6	-0.7	-0.5	-0.4	-0.2	-0.2
87.9	13.0	12.0	-6.1	9.7	38.0	-0.3	-0.9	39.0	-1.2	-0.3	-0.6	-1.0	-0.7	-0.5	-0.4	-0.2
97.7	12.0	11.0	-6.6	8.9	42.0	-0.4	-1.8	42.0	-1.0	-0.2	-0.4	-0.8	-0.7	-0.5	-0.4	-0.5
107.4	9.8	11.0	-6.8	9.7	46.0	-0.1	-1.2	48.0	-1.1	-0.4	-0.2	-1.2	-0.6	-0.5	-0.5	-0.4
117.2	11.0	12.0	-6.3	6.7	53.0	-0.1	-1.5	51.0	-0.9	-0.2	-0.2	-1.0	-1.0	-0.4	-0.3	-0.4
127.0	7.5	13.0	-7.1	6.5	56.0	1.0	-2.2	59.0	-1.2	-0.3	-0.6	-1.3	-1.0	-0.6	-0.4	-0.6
136.7	8.2	11.0	-5.4	1.8	60.0	1.0	-2.9	62.0	-1.0	-0.2	-0.4	-0.8	-0.9	-0.5	-0.5	-0.3

Table 108. Raw data for the test seal at ω=5 krpm, PD=48.3 bars, C_r=0.140 mm, and inlet GVF=2%

Freq.	Re($\boldsymbol{H_{XX}}$)	Re($\boldsymbol{H_{XY}}$)	Re($\boldsymbol{H_{YX}}$)	Re($\boldsymbol{H_{YY}}$)	Im($\boldsymbol{H_{XX}}$)	Im($\boldsymbol{H_{XY}}$)	Im($\boldsymbol{H_{YX}}$)	Im($\boldsymbol{H_{YY}}$)	Re($\boldsymbol{eH_{XX}}$)	Re($\boldsymbol{eH_{XY}}$)	Re($\boldsymbol{eH_{YX}}$)	Re($\boldsymbol{eH_{YY}}$)	Im($\boldsymbol{eH_{XX}}$)	Im($\boldsymbol{eH_{XY}}$)	Im($\boldsymbol{eH_{YX}}$)	Im($\boldsymbol{eH_{YY}}$)
Hz	MN/m	MN/m	MN/m	MN/m	MN/m	MN/m	MN/m	MN/m	MN/m	MN/m	MN/m	MN/m	MN/m	MN/m	MN/m	MN/m
9.8	-5.1	21.0	-19.0	-3.7	2.7	-1.4	1.1	4.9	-0.6	-1.4	-0.5	-0.2	-0.6	-0.3	-0.3	-0.6
19.5	-4.2	23.0	-22.0	-4.7	7.9	-0.4	0.8	11.0	-0.7	-1.1	-0.7	-0.4	-0.7	-0.2	-0.2	-0.7
29.3	-2.1	24.0	-22.0	-4.1	14.0	-2.4	1.9	17.0	-0.6	-0.9	-0.9	-0.3	-0.8	-0.2	-0.3	-0.9
39.1	-4.1	25.0	-21.0	-5.2	19.0	0.4	0.5	21.0	-0.9	-1.1	-0.8	-0.6	-0.9	-0.4	-0.3	-0.7
48.8	-4.9	26.0	-23.0	-6.3	25.0	1.6	-0.8	27.0	-1.3	-1.0	-1.2	-0.8	-0.6	-0.8	-0.5	-0.9
58.6	-3.7	28.0	-24.0	-6.3	33.0	-0.6	-0.9	34.0	-1.4	-0.8	-1.3	-0.9	-0.6	-1.2	-0.5	-1.0
68.4	-5.2	27.0	-25.0	-4.9	36.0	2.3	0.2	40.0	-1.5	-0.5	-1.1	-0.6	-0.3	-0.9	-0.6	-0.8
78.1	-2.4	26.0	-18.0	-3.9	38.0	-2.5	0.7	42.0	-1.0	-0.5	-0.5	-1.0	-0.5	-0.7	-0.7	-0.4
87.9	-0.7	25.0	-21.0	-4.7	46.0	-1.1	2.4	49.0	-0.9	-0.3	-0.4	-0.8	-0.7	-0.5	-0.8	-0.5
97.7	-0.5	24.0	-20.0	-3.5	48.0	-3.2	1.8	53.0	-0.4	-0.3	-0.4	-0.7	-0.2	-0.3	-0.8	-0.5
107.4	-3.9	24.0	-18.0	-3.4	52.0	-1.6	1.4	54.0	-1.2	-0.3	-0.2	-0.8	-0.3	-0.7	-0.7	-0.3
117.2	-6.3	26.0	-20.0	-5.9	59.0	-0.2	0.5	60.0	-1.2	-0.3	-0.5	-0.5	-0.4	-0.5	-0.6	-0.3
127.0	-0.4	27.0	-17.0	-18.0	66.0	-9.5	-7.2	60.0	-3.8	-6.5	-5.6	-7.2	-4.9	-6.3	-4.6	-8.0
136.7	-5.2	26.0	-17.0	-6.0	71.0	-1.7	1.4	69.0	-0.7	-0.3	-0.1	-0.6	-0.8	-0.3	-0.5	-0.3

Table 109. Raw data for the test seal at ω=7.5 krpm, PD=48.3 bars, C_r=0.140 mm, and inlet GVF=0%

Freq.	Re($\boldsymbol{H_{XX}}$)	Re($\boldsymbol{H_{XY}}$)	Re($\boldsymbol{H_{YX}}$)	Re($\boldsymbol{H_{YY}}$)	Im($\boldsymbol{H_{XX}}$)	Im($\boldsymbol{H_{XY}}$)	Im($\boldsymbol{H_{YX}}$)	Im($\boldsymbol{H_{YY}}$)	Re($\boldsymbol{eH_{XX}}$)	Re($\boldsymbol{eH_{XY}}$)	Re($\boldsymbol{eH_{YX}}$)	Re($\boldsymbol{eH_{YY}}$)	Im($\boldsymbol{eH_{XX}}$)	Im($\boldsymbol{eH_{XY}}$)	Im($\boldsymbol{eH_{YX}}$)	Im($\boldsymbol{eH_{YY}}$)
Hz	MN/m	MN/m	MN/m	MN/m	MN/m	MN/m	MN/m	MN/m	MN/m	MN/m	MN/m	MN/m	MN/m	MN/m	MN/m	MN/m
9.8	32.0	3.7	-1.6	31.0	2.5	0.1	-0.8	3.5	-0.1	-0.1	-0.1	-0.2	-0.1	-0.1	-0.1	-0.1
19.5	32.0	3.6	-1.2	31.0	5.0	1.0	-1.2	5.4	-0.1	-0.2	-0.1	-0.1	-0.1	-0.1	-0.1	-0.1
29.3	31.0	3.5	-0.9	31.0	7.7	1.8	-2.1	7.4	0.0	-0.1	-0.1	-0.1	-0.1	-0.1	-0.2	-0.1
39.1	31.0	3.8	-1.2	31.0	9.7	2.4	-3.0	10.0	-0.1	0.0	-0.1	-0.1	-0.1	-0.1	-0.1	-0.1
48.8	30.0	4.1	-1.5	30.0	13.0	3.1	-4.2	13.0	-0.1	0.0	-0.1	-0.1	0.0	0.0	-0.1	-0.1
58.6	30.0	4.0	-1.9	29.0	16.0	3.8	-4.5	16.0	-0.1	0.0	-0.1	-0.1	-0.1	-0.1	-0.1	-0.1
68.4	29.0	4.4	-2.3	29.0	18.0	4.4	-4.7	18.0	-0.1	0.0	-0.1	-0.1	0.0	0.0	-0.1	-0.1
78.1	28.0	4.8	-2.4	28.0	20.0	4.9	-5.3	20.0	-0.1	-0.1	-0.1	-0.1	-0.1	-0.1	-0.1	-0.1
87.9	27.0	5.1	-2.6	26.0	22.0	5.2	-6.1	23.0	-0.1	-0.1	-0.1	-0.1	-0.1	-0.1	-0.1	-0.1
97.7	24.0	5.3	-3.0	24.0	25.0	5.6	-6.8	25.0	-0.1	0.0	0.0	0.0	0.0	0.0	0.0	0.0
107.4	22.0	5.6	-3.0	22.0	28.0	6.2	-7.0	28.0	-0.1	0.0	-0.1	0.0	0.0	0.0	0.0	0.0
117.2	20.0	5.9	-2.9	20.0	31.0	6.7	-8.0	31.0	0.0	0.0	0.0	0.0	0.0	0.0	0.0	0.0
127.0	18.0	6.7	-3.0	17.0	33.0	7.2	-8.8	34.0	0.0	0.0	0.0	-0.1	0.0	0.0	-0.1	-0.1
136.7	14.0	7.9	-2.4	14.0	37.0	7.4	-9.6	38.0	-0.1	0.0	0.0	-0.1	0.0	0.0	0.0	0.0

Table 110. Raw data for the test seal at ω=5 krpm, PD=37.9 bars, C_r=0.140 mm, and inlet GVF=0%

Freq.	Re($\boldsymbol{H_{XX}}$)	Re($\boldsymbol{H_{XY}}$)	Re($\boldsymbol{H_{YX}}$)	Re($\boldsymbol{H_{YY}}$)	Im($\boldsymbol{H_{XX}}$)	Im($\boldsymbol{H_{XY}}$)	Im($\boldsymbol{H_{YX}}$)	Im($\boldsymbol{H_{YY}}$)	Re($\boldsymbol{eH_{XX}}$)	Re($\boldsymbol{eH_{XY}}$)	Re($\boldsymbol{eH_{YX}}$)	Re($\boldsymbol{eH_{YY}}$)	Im($\boldsymbol{eH_{XX}}$)	Im($\boldsymbol{eH_{XY}}$)	Im($\boldsymbol{eH_{YX}}$)	Im($\boldsymbol{eH_{YY}}$)
Hz	MN/m	MN/m	MN/m	MN/m	MN/m	MN/m	MN/m	MN/m	MN/m	MN/m	MN/m	MN/m	MN/m	MN/m	MN/m	MN/m
9.8	31.0	3.5	-2.0	31.0	2.6	0.4	-1.0	4.0	-0.1	0.0	-0.1	-0.1	-0.2	-0.1	-0.1	-0.1
19.5	31.0	3.6	-2.0	32.0	5.3	0.9	-0.3	5.2	-0.1	-0.2	-0.1	-0.1	0.0	-0.1	-0.2	-0.1
29.3	31.0	3.6	-1.5	31.0	7.3	1.4	-1.8	7.3	-0.1	-0.1	-0.1	-0.1	-0.1	-0.1	-0.1	-0.2
39.1	31.0	4.0	-1.3	31.0	9.9	1.9	-2.7	10.0	-0.1	-0.1	0.0	-0.1	-0.1	-0.1	-0.1	0.0
48.8	30.0	3.7	-1.9	30.0	12.0	2.8	-3.9	13.0	-0.1	-0.1	-0.1	-0.1	-0.1	-0.1	-0.1	-0.1
58.6	30.0	3.8	-2.1	30.0	15.0	3.3	-4.2	15.0	-0.1	0.0	-0.1	-0.1	0.0	-0.1	-0.1	-0.1
68.4	29.0	4.1	-2.6	29.0	18.0	3.9	-4.2	18.0	-0.1	-0.1	-0.1	-0.2	-0.1	-0.2	0.0	-0.1
78.1	28.0	4.5	-2.7	28.0	20.0	4.2	-4.9	20.0	-0.1	-0.1	-0.1	0.0	-0.1	-0.1	-0.1	-0.1
87.9	27.0	5.1	-2.6	27.0	22.0	4.6	-5.7	22.0	-0.1	-0.1	-0.1	-0.2	-0.1	-0.1	-0.1	-0.1
97.7	25.0	5.0	-3.3	25.0	24.0	4.8	-6.1	25.0	0.0	-0.1	0.0	-0.1	0.0	-0.1	0.0	-0.1
107.4	23.0	5.2	-3.2	24.0	28.0	5.4	-6.1	27.0	0.0	0.0	-0.1	-0.1	-0.1	0.0	0.0	-0.1
117.2	22.0	5.4	-3.0	21.0	31.0	5.7	-7.0	30.0	-0.1	0.0	0.0	0.0	-0.1	0.0	0.0	0.0
127.0	20.0	6.0	-3.1	20.0	33.0	6.3	-7.7	33.0	-0.1	0.0	0.0	-0.1	-0.1	0.0	0.0	-0.1
136.7	16.0	7.1	-2.5	17.0	37.0	6.9	-8.6	37.0	-0.1	0.0	-0.1	0.0	0.0	-0.1	0.0	0.0

Table 111. Raw data for the test seal at ω=5 krpm, PD=37.9 bars, C_r=0.140 mm, and inlet GVF=2%

Freq.	Re($\boldsymbol{H_{XX}}$)	Re($\boldsymbol{H_{XY}}$)	Re($\boldsymbol{H_{YX}}$)	Re($\boldsymbol{H_{YY}}$)	Im($\boldsymbol{H_{XX}}$)	Im($\boldsymbol{H_{XY}}$)	Im($\boldsymbol{H_{YX}}$)	Im($\boldsymbol{H_{YY}}$)	Re($\boldsymbol{eH_{XX}}$)	Re($\boldsymbol{eH_{XY}}$)	Re($\boldsymbol{eH_{YX}}$)	Re($\boldsymbol{eH_{YY}}$)	Im($\boldsymbol{eH_{XX}}$)	Im($\boldsymbol{eH_{XY}}$)	Im($\boldsymbol{eH_{YX}}$)	Im($\boldsymbol{eH_{YY}}$)
Hz	MN/m	MN/m	MN/m	MN/m	MN/m	MN/m	MN/m	MN/m	MN/m	MN/m	MN/m	MN/m	MN/m	MN/m	MN/m	MN/m
9.8	29.0	4.1	-3.3	30.0	2.1	0.9	-1.7	4.8	-0.2	-0.1	-0.1	-0.2	-0.1	-0.1	-0.1	-0.1
19.5	29.0	3.9	-2.9	30.0	5.2	0.6	-0.7	5.3	-0.1	-0.1	-0.1	-0.1	-0.1	-0.1	-0.1	-0.1
29.3	29.0	4.4	-2.4	30.0	7.7	1.0	-1.5	7.3	-0.1	-0.1	0.0	-0.2	-0.1	-0.1	-0.1	-0.1
39.1	30.0	4.4	-2.0	30.0	10.0	1.6	-2.4	11.0	-0.1	-0.1	-0.1	-0.1	-0.1	-0.1	-0.1	-0.1
48.8	28.0	4.3	-3.0	29.0	12.0	2.3	-3.7	13.0	-0.1	-0.1	-0.1	-0.1	-0.1	-0.1	0.0	0.0
58.6	28.0	4.6	-3.0	29.0	16.0	2.8	-3.7	15.0	-0.1	-0.1	-0.1	-0.1	0.0	0.0	-0.1	-0.1
68.4	27.0	4.0	-3.5	28.0	19.0	3.2	-3.3	19.0	-0.1	-0.1	-0.1	0.0	-0.1	-0.1	0.0	0.0
78.1	26.0	5.0	-3.2	27.0	21.0	3.6	-4.2	21.0	0.0	-0.1	-0.1	-0.1	0.0	-0.1	-0.1	-0.1
87.9	26.0	5.3	-2.6	26.0	23.0	3.8	-5.1	23.0	-0.1	-0.1	-0.1	-0.1	0.0	-0.1	-0.1	-0.1
97.7	24.0	5.1	-3.6	24.0	26.0	4.2	-5.5	26.0	-0.1	-0.1	-0.1	-0.1	0.0	-0.1	-0.1	0.0
107.4	22.0	5.7	-3.7	23.0	30.0	4.9	-5.3	29.0	-0.1	-0.1	-0.1	-0.1	-0.1	-0.1	-0.1	-0.1
117.2	21.0	5.8	-3.3	20.0	33.0	5.1	-6.0	32.0	-0.1	-0.1	0.0	-0.1	-0.1	-0.1	0.0	-0.1
127.0	19.0	6.7	-3.3	19.0	35.0	5.6	-6.9	35.0	-0.1	-0.1	0.0	0.0	-0.1	-0.1	-0.1	-0.1
136.7	16.0	7.1	-2.8	15.0	39.0	6.2	-7.8	40.0	-0.1	0.0	0.0	0.0	-0.1	-0.1	0.0	-0.1

Table 112. Raw data for the test seal at ω=5 krpm, PD=37.9 bars, C_r=0.140 mm, and inlet GVF=4%

Freq.	Re($\boldsymbol{H_{XX}}$)	Re($\boldsymbol{H_{XY}}$)	Re($\boldsymbol{H_{YX}}$)	Re($\boldsymbol{H_{YY}}$)	Im($\boldsymbol{H_{XX}}$)	Im($\boldsymbol{H_{XY}}$)	Im($\boldsymbol{H_{YX}}$)	Im($\boldsymbol{H_{YY}}$)	Re($\boldsymbol{eH_{XX}}$)	Re($\boldsymbol{eH_{XY}}$)	Re($\boldsymbol{eH_{YX}}$)	Re($\boldsymbol{eH_{YY}}$)	Im($\boldsymbol{eH_{XX}}$)	Im($\boldsymbol{eH_{XY}}$)	Im($\boldsymbol{eH_{YX}}$)	Im($\boldsymbol{eH_{YY}}$)
Hz	MN/m	MN/m	MN/m	MN/m	MN/m	MN/m	MN/m	MN/m	MN/m	MN/m	MN/m	MN/m	MN/m	MN/m	MN/m	MN/m
9.8	26.0	5.2	-3.7	28.0	1.8	1.0	-1.8	5.4	-0.2	-0.1	-0.2	-0.2	-0.1	-0.1	-0.1	-0.1
19.5	27.0	5.2	-3.6	27.0	5.8	0.3	-0.8	5.3	-0.2	-0.1	-0.1	-0.1	-0.1	-0.1	-0.1	-0.1
29.3	27.0	5.4	-3.1	27.0	8.4	0.4	-1.4	8.2	-0.1	-0.1	-0.1	-0.2	-0.1	-0.1	-0.1	-0.2
39.1	28.0	5.4	-2.4	27.0	11.0	1.1	-2.1	11.0	-0.2	-0.1	-0.1	-0.1	-0.1	-0.1	-0.1	-0.1
48.8	25.0	5.0	-3.6	27.0	12.0	1.7	-3.6	14.0	-0.1	0.0	-0.2	-0.1	-0.1	-0.1	-0.1	-0.1
58.6	26.0	5.4	-3.3	26.0	17.0	2.1	-3.0	16.0	-0.1	-0.2	-0.2	-0.1	0.0	-0.1	-0.1	-0.1
68.4	25.0	4.6	-3.8	26.0	20.0	2.9	-2.9	20.0	-0.1	-0.1	-0.2	-0.1	-0.1	0.0	-0.1	-0.1
78.1	24.0	5.7	-3.8	25.0	22.0	3.2	-3.6	22.0	-0.2	-0.1	-0.1	-0.1	-0.1	-0.1	0.0	-0.1
87.9	24.0	5.8	-3.0	24.0	25.0	3.0	-4.7	25.0	-0.1	-0.2	-0.1	-0.1	-0.2	-0.1	-0.1	-0.2
97.7	22.0	5.8	-4.0	22.0	28.0	3.3	-5.0	28.0	-0.1	0.0	-0.1	-0.1	-0.1	-0.1	0.0	-0.1
107.4	20.0	6.4	-4.2	21.0	31.0	4.1	-4.7	31.0	-0.1	-0.1	-0.1	-0.1	-0.1	-0.1	-0.1	0.0
117.2	19.0	6.5	-3.6	19.0	35.0	4.2	-5.3	34.0	-0.1	-0.1	0.0	-0.1	-0.1	-0.1	-0.1	0.0
127.0	18.0	7.2	-3.7	19.0	38.0	4.5	-6.2	38.0	-0.1	0.0	-0.1	-0.1	-0.1	-0.1	-0.1	-0.1
136.7	15.0	7.3	-2.8	15.0	41.0	5.1	-7.0	42.0	-0.1	-0.1	-0.1	-0.1	-0.1	-0.1	-0.1	-0.1

Table 113. Raw data for the test seal at ω=5 krpm, PD=37.9 bars, C_r=0.140 mm, and inlet GVF=6%

Freq.	Re($\boldsymbol{H_{XX}}$)	Re($\boldsymbol{H_{XY}}$)	Re($\boldsymbol{H_{YX}}$)	Re($\boldsymbol{H_{YY}}$)	Im($\boldsymbol{H_{XX}}$)	Im($\boldsymbol{H_{XY}}$)	Im($\boldsymbol{H_{YX}}$)	Im($\boldsymbol{H_{YY}}$)	Re($\boldsymbol{eH_{XX}}$)	Re($\boldsymbol{eH_{XY}}$)	Re($\boldsymbol{eH_{YX}}$)	Re($\boldsymbol{eH_{YY}}$)	Im($\boldsymbol{eH_{XX}}$)	Im($\boldsymbol{eH_{XY}}$)	Im($\boldsymbol{eH_{YX}}$)	Im($\boldsymbol{eH_{YY}}$)
Hz	MN/m	MN/m	MN/m	MN/m	MN/m	MN/m	MN/m	MN/m	MN/m	MN/m	MN/m	MN/m	MN/m	MN/m	MN/m	MN/m
9.8	11.0	8.8	-8.2	13.0	2.1	0.2	-2.1	5.7	-0.2	-0.2	-0.2	-0.4	-0.1	-0.1	-0.2	-0.1
19.5	11.0	9.1	-7.6	13.0	6.8	0.3	0.0	6.8	-0.2	-0.1	-0.2	-0.5	-0.2	-0.1	-0.2	-0.1
29.3	12.0	9.7	-5.9	14.0	11.0	-0.2	0.0	11.0	-0.3	-0.3	-0.1	-0.4	-0.2	-0.1	-0.1	-0.2
39.1	13.0	9.5	-5.2	13.0	14.0	0.1	-0.3	15.0	-0.2	-0.2	-0.2	-0.4	-0.1	-0.1	-0.1	-0.1
48.8	12.0	8.6	-6.0	13.0	16.0	0.3	-2.7	18.0	-0.2	-0.2	-0.1	-0.4	-0.1	0.0	-0.1	-0.1
58.6	12.0	9.7	-5.6	14.0	22.0	0.8	-1.3	21.0	-0.3	-0.3	-0.2	-0.3	-0.2	-0.2	-0.1	-0.2
68.4	11.0	8.8	-5.9	12.0	26.0	1.0	-0.9	26.0	-0.3	-0.3	-0.1	-0.4	-0.1	-0.2	-0.1	-0.1
78.1	8.9	9.0	-7.3	12.0	29.0	1.6	-2.0	29.0	-0.2	-0.1	-0.1	-0.3	-0.2	-0.2	-0.1	-0.2
87.9	11.0	9.5	-5.0	12.0	32.0	1.0	-2.0	32.0	-0.1	-0.1	-0.2	-0.5	-0.1	-0.2	-0.2	-0.2
97.7	9.7	9.5	-5.5	10.0	36.0	1.0	-3.1	35.0	-0.3	-0.1	-0.1	-0.5	-0.1	-0.2	-0.2	-0.2
107.4	8.6	9.7	-5.9	11.0	40.0	1.3	-3.2	39.0	-0.3	-0.1	-0.2	-0.4	-0.1	-0.2	-0.2	-0.2
117.2	8.0	10.0	-5.0	8.4	45.0	1.2	-2.7	43.0	-0.1	0.0	-0.1	-0.4	-0.1	-0.2	-0.2	-0.2
127.0	5.6	11.0	-6.2	9.8	48.0	2.2	-3.3	49.0	-0.3	-0.3	-0.2	-0.5	-0.2	-0.2	-0.3	-0.3
136.7	5.4	9.7	-4.1	5.1	52.0	2.4	-4.3	53.0	-0.2	-0.1	-0.1	-0.5	-0.2	-0.2	-0.1	-0.3

Table 114. Raw data for the test seal at ω=5 krpm, PD=37.9 bars, C_r=0.140 mm, and inlet GVF=8%

Freq.	Re($\boldsymbol{H_{XX}}$)	Re($\boldsymbol{H_{XY}}$)	Re($\boldsymbol{H_{YX}}$)	Re($\boldsymbol{H_{YY}}$)	Im($\boldsymbol{H_{XX}}$)	Im($\boldsymbol{H_{XY}}$)	Im($\boldsymbol{H_{YX}}$)	Im($\boldsymbol{H_{YY}}$)	Re($\boldsymbol{eH_{XX}}$)	Re($\boldsymbol{eH_{XY}}$)	Re($\boldsymbol{eH_{YX}}$)	Re($\boldsymbol{eH_{YY}}$)	Im($\boldsymbol{eH_{XX}}$)	Im($\boldsymbol{eH_{XY}}$)	Im($\boldsymbol{eH_{YX}}$)	Im($\boldsymbol{eH_{YY}}$)
Hz	MN/m	MN/m	MN/m	MN/m	MN/m	MN/m	MN/m	MN/m	MN/m	MN/m	MN/m	MN/m	MN/m	MN/m	MN/m	MN/m
9.8	24.0	14.0	-12.0	23.0	2.2	0.1	-2.7	4.6	-0.3	-0.4	-0.3	-0.3	-0.1	-0.1	-0.2	-0.2
19.5	24.0	14.0	-12.0	23.0	6.4	0.5	-1.1	5.6	-0.3	-0.4	-0.3	-0.4	-0.2	-0.2	-0.1	-0.2
29.3	24.0	14.0	-11.0	23.0	8.9	0.8	-2.0	8.3	-0.2	-0.5	-0.3	-0.3	-0.2	-0.1	-0.2	-0.1
39.1	24.0	14.0	-10.0	23.0	12.0	1.4	-3.0	12.0	-0.3	-0.4	-0.3	-0.5	-0.1	-0.3	-0.1	-0.1
48.8	23.0	14.0	-12.0	21.0	14.0	1.9	-5.1	15.0	-0.2	-0.3	-0.2	-0.4	-0.2	-0.2	-0.1	-0.2
58.6	22.0	14.0	-11.0	22.0	19.0	2.4	-3.5	19.0	-0.2	-0.3	-0.4	-0.5	-0.2	-0.3	-0.1	-0.2
68.4	22.0	13.0	-12.0	21.0	22.0	3.5	-3.7	23.0	-0.1	-0.4	-0.3	-0.4	-0.1	-0.1	-0.1	-0.1
78.1	21.0	13.0	-12.0	21.0	24.0	4.1	-4.7	25.0	-0.2	-0.2	-0.3	-0.4	-0.1	-0.3	-0.2	-0.2
87.9	21.0	14.0	-11.0	20.0	27.0	4.3	-6.2	27.0	-0.2	-0.3	-0.2	-0.3	-0.2	-0.3	-0.2	-0.2
97.7	19.0	14.0	-12.0	18.0	30.0	4.9	-7.2	30.0	-0.1	-0.3	-0.3	-0.4	-0.2	-0.3	-0.2	-0.2
107.4	17.0	14.0	-12.0	17.0	33.0	5.9	-6.7	33.0	-0.2	-0.2	-0.2	-0.3	-0.1	-0.3	-0.2	-0.2
117.2	15.0	15.0	-12.0	14.0	37.0	6.4	-7.2	36.0	-0.1	-0.2	-0.2	-0.3	-0.2	-0.4	-0.2	-0.2
127.0	13.0	16.0	-12.0	13.0	40.0	6.4	-8.2	40.0	-1.4	-2.2	-1.8	-2.5	-1.3	-2.2	-1.6	-2.5
136.7	9.6	16.0	-10.0	9.3	44.0	7.3	-9.4	44.0	-0.2	-0.1	-0.2	-0.3	-0.2	-0.4	-0.2	-0.2

Table 115. Raw data for the test seal at ω=7.5 krpm, PD=37.9 bars, C_r=0.140 mm, and inlet GVF=0%

Freq.	Re($\boldsymbol{H_{XX}}$)	Re($\boldsymbol{H_{XY}}$)	Re($\boldsymbol{H_{YX}}$)	Re($\boldsymbol{H_{YY}}$)	Im($\boldsymbol{H_{XX}}$)	Im($\boldsymbol{H_{XY}}$)	Im($\boldsymbol{H_{YX}}$)	Im($\boldsymbol{H_{YY}}$)	Re($\boldsymbol{eH_{XX}}$)	Re($\boldsymbol{eH_{XY}}$)	Re($\boldsymbol{eH_{YX}}$)	Re($\boldsymbol{eH_{YY}}$)	Im($\boldsymbol{eH_{XX}}$)	Im($\boldsymbol{eH_{XY}}$)	Im($\boldsymbol{eH_{YX}}$)	Im($\boldsymbol{eH_{YY}}$)
Hz	MN/m	MN/m	MN/m	MN/m	MN/m	MN/m	MN/m	MN/m	MN/m	MN/m	MN/m	MN/m	MN/m	MN/m	MN/m	MN/m
9.8	11.0	21.0	-17.0	11.0	2.6	-0.5	-1.3	3.9	-0.3	-0.5	-0.3	-0.4	-0.1	-0.1	-0.2	-0.2
19.5	12.0	21.0	-17.0	12.0	7.6	-0.8	-0.2	6.9	-0.2	-0.4	-0.3	-0.4	-0.2	-0.2	-0.1	-0.2
29.3	12.0	21.0	-16.0	12.0	11.0	-0.8	-0.5	11.0	-0.3	-0.4	-0.3	-0.5	-0.2	-0.2	-0.1	-0.1
39.1	13.0	21.0	-15.0	12.0	15.0	-0.6	-0.8	14.0	-0.3	-0.5	-0.3	-0.5	-0.2	-0.3	-0.1	-0.1
48.8	11.0	20.0	-16.0	11.0	18.0	-0.6	-2.1	19.0	-0.2	-0.4	-0.3	-0.6	-0.2	-0.2	-0.2	-0.1
58.6	12.0	20.0	-15.0	12.0	23.0	-0.3	-1.3	22.0	-0.2	-0.4	-0.3	-0.5	-0.2	-0.2	-0.2	-0.2
68.4	12.0	20.0	-16.0	11.0	26.0	-0.2	-1.9	26.0	-0.2	-0.4	-0.3	-0.7	-0.2	-0.2	-0.3	-0.2
78.1	11.0	20.0	-17.0	9.9	29.0	0.4	-2.2	29.0	-0.2	-0.4	-0.3	-0.6	-0.2	-0.3	-0.2	-0.2
87.9	12.0	20.0	-15.0	9.7	32.0	0.0	-2.7	32.0	-0.3	-0.3	-0.2	-0.7	-0.2	-0.3	-0.2	-0.1
97.7	10.0	20.0	-15.0	8.4	35.0	0.3	-3.3	36.0	-0.2	-0.3	-0.2	-0.7	-0.2	-0.3	-0.3	-0.2
107.4	8.3	20.0	-15.0	7.9	39.0	0.9	-3.6	39.0	-0.2	-0.3	-0.2	-0.5	-0.2	-0.4	-0.2	-0.3
117.2	6.9	20.0	-15.0	5.9	44.0	0.8	-3.6	43.0	-0.3	-0.2	-0.1	-0.6	-0.2	-0.3	-0.3	-0.3
127.0	5.2	23.0	-14.0	3.4	49.0	-0.2	-4.2	45.0	-1.6	-3.0	-2.4	-3.0	-1.8	-2.2	-2.2	-3.9
136.7	3.8	20.0	-13.0	2.9	52.0	1.3	-4.4	51.0	-0.2	-0.2	-0.1	-0.6	-0.2	-0.3	-0.3	-0.4

Table 116. Raw data for the test seal at ω=7.5 krpm, PD=37.9 bars, C_r=0.140 mm, and inlet GVF=2%

Freq.	Re($\boldsymbol{H_{XX}}$)	Re($\boldsymbol{H_{XY}}$)	Re($\boldsymbol{H_{YX}}$)	Re($\boldsymbol{H_{YY}}$)	Im($\boldsymbol{H_{XX}}$)	Im($\boldsymbol{H_{XY}}$)	Im($\boldsymbol{H_{YX}}$)	Im($\boldsymbol{H_{YY}}$)	Re($\boldsymbol{eH_{XX}}$)	Re($\boldsymbol{eH_{XY}}$)	Re($\boldsymbol{eH_{YX}}$)	Re($\boldsymbol{eH_{YY}}$)	Im($\boldsymbol{eH_{XX}}$)	Im($\boldsymbol{eH_{XY}}$)	Im($\boldsymbol{eH_{YX}}$)	Im($\boldsymbol{eH_{YY}}$)
Hz	MN/m	MN/m	MN/m	MN/m	MN/m	MN/m	MN/m	MN/m	MN/m	MN/m	MN/m	MN/m	MN/m	MN/m	MN/m	MN/m
9.8	5.3	21.0	-20.0	3.3	2.0	-0.8	-1.0	4.6	-0.2	-0.2	-0.3	-0.2	-0.1	-0.1	-0.2	-0.3
19.5	5.5	21.0	-20.0	4.2	7.5	-0.8	0.3	8.6	-0.2	-0.2	-0.3	-0.3	-0.2	-0.1	-0.1	-0.2
29.3	5.8	22.0	-19.0	4.4	12.0	-0.8	0.5	13.0	-0.2	-0.2	-0.3	-0.3	-0.1	-0.1	-0.2	-0.2
39.1	5.7	21.0	-19.0	4.8	16.0	-0.1	0.4	17.0	-0.3	-0.2	-0.3	-0.2	-0.1	-0.2	-0.2	-0.2
48.8	5.5	21.0	-18.0	4.3	19.0	-0.3	-0.4	21.0	-0.3	-0.3	-0.2	-0.2	-0.1	-0.2	-0.2	-0.2
58.6	5.5	21.0	-18.0	5.3	24.0	0.2	0.0	25.0	-0.3	-0.2	-0.2	-0.2	-0.1	-0.2	-0.2	-0.2
68.4	5.1	21.0	-18.0	4.2	27.0	0.6	-0.5	29.0	-0.2	-0.2	-0.3	-0.3	-0.1	-0.1	-0.2	-0.2
78.1	4.2	21.0	-19.0	4.4	31.0	0.5	-0.9	33.0	-0.3	-0.1	-0.1	-0.3	-0.1	-0.2	-0.2	-0.2
87.9	4.5	21.0	-17.0	4.0	35.0	0.7	-0.6	36.0	-0.4	-0.1	-0.1	-0.2	-0.2	-0.2	-0.2	-0.1
97.7	3.5	21.0	-17.0	3.0	38.0	0.3	-1.2	40.0	-0.3	-0.1	-0.1	-0.2	-0.1	-0.2	-0.2	-0.2
107.4	2.0	21.0	-17.0	2.6	42.0	1.2	-1.7	43.0	-0.3	-0.1	-0.1	-0.3	-0.2	-0.2	-0.4	-0.1
117.2	0.7	22.0	-18.0	0.5	48.0	1.1	-1.9	48.0	-0.4	-0.1	-0.1	-0.3	-0.1	-0.2	-0.4	-0.1
127.0	-2.7	25.0	-16.0	-0.8	53.0	1.5	-0.9	50.0	-2.6	-4.5	-4.1	-5.2	-3.1	-3.9	-3.6	-5.9
136.7	-2.3	22.0	-17.0	-3.0	57.0	2.0	-2.9	58.0	-0.3	-0.1	-0.1	-0.2	-0.2	-0.2	-0.3	-0.2

Table 117. Raw data for the test seal at ω=7.5 krpm, PD=37.9 bars, C_r=0.140 mm, and inlet GVF=4%

Freq.	Re($\boldsymbol{H_{XX}}$)	Re($\boldsymbol{H_{XY}}$)	Re($\boldsymbol{H_{YX}}$)	Re($\boldsymbol{H_{YY}}$)	Im($\boldsymbol{H_{XX}}$)	Im($\boldsymbol{H_{XY}}$)	Im($\boldsymbol{H_{YX}}$)	Im($\boldsymbol{H_{YY}}$)	Re($\boldsymbol{eH_{XX}}$)	Re($\boldsymbol{eH_{XY}}$)	Re($\boldsymbol{eH_{YX}}$)	Re($\boldsymbol{eH_{YY}}$)	Im($\boldsymbol{eH_{XX}}$)	Im($\boldsymbol{eH_{XY}}$)	Im($\boldsymbol{eH_{YX}}$)	Im($\boldsymbol{eH_{YY}}$)
Hz	MN/m	MN/m	MN/m	MN/m	MN/m	MN/m	MN/m	MN/m	MN/m	MN/m	MN/m	MN/m	MN/m	MN/m	MN/m	MN/m
9.8	-2.9	20.0	-21.0	-5.5	2.6	-2.0	-0.2	6.2	-0.3	-0.5	-0.3	-0.3	-0.4	-0.1	-0.2	-0.4
19.5	-3.9	20.0	-22.0	-5.6	6.7	-0.2	0.8	11.0	-0.3	-0.3	-0.4	-0.3	-0.2	-0.1	-0.1	-0.4
29.3	-3.6	21.0	-22.0	-5.0	11.0	0.5	1.7	15.0	-0.3	-0.4	-0.4	-0.3	-0.3	-0.1	-0.2	-0.3
39.1	-4.0	21.0	-22.0	-4.6	17.0	0.4	0.7	21.0	-0.4	-0.5	-0.5	-0.4	-0.4	-0.1	-0.2	-0.4
48.8	-4.4	21.0	-21.0	-4.8	21.0	1.3	-0.2	25.0	-0.5	-0.5	-0.4	-0.4	-0.3	-0.3	-0.2	-0.3
58.6	-4.4	21.0	-22.0	-3.6	26.0	1.9	-0.3	28.0	-0.6	-0.4	-0.5	-0.6	-0.3	-0.4	-0.3	-0.3
68.4	-6.2	24.0	-22.0	-6.7	31.0	3.0	-2.0	34.0	-0.4	-0.4	-0.6	-0.6	-0.3	-0.4	-0.4	-0.4
78.1	-4.5	21.0	-19.0	-1.8	32.0	0.3	2.3	36.0	-0.4	-0.2	-0.3	-0.6	-0.1	-0.4	-0.6	-0.2
87.9	-5.2	23.0	-20.0	-4.8	39.0	2.6	0.8	39.0	-0.5	-0.3	-0.3	-0.6	-0.3	-0.4	-0.4	-0.2
97.7	-5.3	23.0	-20.0	-5.3	43.0	2.2	0.9	44.0	-0.4	-0.1	-0.3	-0.6	-0.2	-0.3	-0.5	-0.3
107.4	-5.8	23.0	-20.0	-4.0	47.0	1.2	2.0	49.0	-0.4	-0.2	-0.2	-0.5	-0.3	-0.3	-0.3	-0.3
117.2	-7.7	24.0	-21.0	-6.8	53.0	1.7	-0.7	54.0	-0.5	-0.2	-0.4	-0.4	-0.5	-0.3	-0.3	-0.3
127.0	-9.5	26.0	-16.0	-7.8	57.0	0.4	-0.3	54.0	-5.2	-7.7	-4.9	-8.6	-3.6	-6.9	-6.8	-11.0
136.7	-8.8	24.0	-19.0	-8.5	62.0	0.3	-0.2	64.0	-0.4	-0.3	-0.2	-0.3	-0.2	-0.2	-0.3	-0.1

Table 118. Raw data for the test seal at ω=7.5 krpm, PD=37.9 bars, C_r=0.140 mm, and inlet GVF=6%

Freq.	Re($\boldsymbol{H_{XX}}$)	Re($\boldsymbol{H_{XY}}$)	Re($\boldsymbol{H_{YX}}$)	Re($\boldsymbol{H_{YY}}$)	Im($\boldsymbol{H_{XX}}$)	Im($\boldsymbol{H_{XY}}$)	Im($\boldsymbol{H_{YX}}$)	Im($\boldsymbol{H_{YY}}$)	Re($\boldsymbol{eH_{XX}}$)	Re($\boldsymbol{eH_{XY}}$)	Re($\boldsymbol{eH_{YX}}$)	Re($\boldsymbol{eH_{YY}}$)	Im($\boldsymbol{eH_{XX}}$)	Im($\boldsymbol{eH_{XY}}$)	Im($\boldsymbol{eH_{YX}}$)	Im($\boldsymbol{eH_{YY}}$)
Hz	MN/m	MN/m	MN/m	MN/m	MN/m	MN/m	MN/m	MN/m	MN/m	MN/m	MN/m	MN/m	MN/m	MN/m	MN/m	MN/m
9.8	-0.3	34.0	-31.0	-3.6	2.4	-2.7	-1.8	4.6	-0.6	-0.6	-0.4	-0.6	-0.3	-0.3	-0.6	-0.7
19.5	0.6	34.0	-30.0	-2.1	8.0	-2.5	0.3	8.5	-0.3	-0.4	-0.5	-0.7	-0.3	-0.2	-0.3	-0.4
29.3	1.2	34.0	-30.0	-2.4	12.0	-1.7	0.5	13.0	-0.4	-0.6	-0.8	-0.6	-0.4	-0.2	-0.2	-0.8
39.1	1.0	35.0	-30.0	-2.2	17.0	-0.6	-0.9	18.0	-0.4	-0.6	-0.7	-0.7	-0.4	-0.2	-0.1	-0.6
48.8	-0.6	34.0	-30.0	-2.4	20.0	0.5	-1.4	22.0	-0.4	-0.6	-0.7	-0.5	-0.4	-0.2	-0.2	-0.7
58.6	0.6	34.0	-30.0	-2.9	25.0	-0.2	-1.3	26.0	-0.5	-0.8	-0.9	-0.5	-0.7	-0.1	-0.1	-0.8
68.4	-1.4	36.0	-30.0	-4.5	30.0	1.4	-3.0	31.0	-0.7	-0.9	-1.2	-0.6	-0.6	-0.4	-0.4	-1.1
78.1	0.4	37.0	-31.0	-3.3	36.0	0.7	-2.1	36.0	-0.7	-0.8	-1.2	-0.3	-0.6	-0.5	-0.6	-1.1
87.9	-1.5	36.0	-30.0	-5.1	38.0	2.5	-3.0	39.0	-1.2	-0.8	-0.8	-0.4	-0.5	-0.8	-0.6	-0.8
97.7	-2.3	35.0	-30.0	-6.0	41.0	1.9	-4.0	44.0	-1.2	-0.5	-0.8	-0.6	-0.4	-0.9	-0.7	-0.8
107.4	-2.5	37.0	-31.0	-5.1	48.0	0.5	-3.3	49.0	-1.2	-0.2	-0.8	-0.7	-0.4	-1.0	-0.9	-0.7
117.2	-5.5	38.0	-32.0	-7.8	53.0	2.9	-5.0	54.0	-1.2	-0.2	-0.6	-0.7	-0.5	-0.9	-0.8	-0.5
127.0	-3.6	36.0	-31.0	-7.3	55.0	0.2	-3.8	59.0	-1.0	-0.2	-0.3	-0.9	-0.3	-0.7	-1.1	-0.3
136.7	-5.9	38.0	-30.0	-9.6	62.0	0.9	-4.4	64.0	-0.7	-0.4	-0.4	-0.4	-0.7	-0.6	-0.7	-0.5

Table 119. Raw data for the test seal at ω=10 krpm, PD=37.9 bars, C_r=0.140 mm, and inlet GVF=0%

Freq.	Re($\boldsymbol{H_{XX}}$)	Re($\boldsymbol{H_{XY}}$)	Re($\boldsymbol{H_{YX}}$)	Re($\boldsymbol{H_{YY}}$)	Im($\boldsymbol{H_{XX}}$)	Im($\boldsymbol{H_{XY}}$)	Im($\boldsymbol{H_{YX}}$)	Im($\boldsymbol{H_{YY}}$)	Re($\boldsymbol{eH_{XX}}$)	Re($\boldsymbol{eH_{XY}}$)	Re($\boldsymbol{eH_{YX}}$)	Re($\boldsymbol{eH_{YY}}$)	Im($\boldsymbol{eH_{XX}}$)	Im($\boldsymbol{eH_{XY}}$)	Im($\boldsymbol{eH_{YX}}$)	Im($\boldsymbol{eH_{YY}}$)
Hz	MN/m	MN/m	MN/m	MN/m	MN/m	MN/m	MN/m	MN/m	MN/m	MN/m	MN/m	MN/m	MN/m	MN/m	MN/m	MN/m
9.8	24.0	4.8	-3.2	23.0	2.7	0.3	-0.3	3.1	-0.1	-0.1	-0.1	-0.1	-0.1	0.0	0.0	-0.1
19.5	23.0	5.0	-3.0	23.0	4.9	1.1	-1.2	5.0	0.0	0.0	0.0	-0.1	-0.1	0.0	-0.1	-0.1
29.3	23.0	5.1	-2.9	23.0	7.4	1.8	-2.1	7.3	-0.1	0.0	-0.1	-0.1	-0.1	-0.1	-0.1	-0.1
39.1	22.0	5.3	-2.9	22.0	10.0	2.2	-3.0	10.0	-0.1	0.0	-0.1	0.0	-0.1	0.0	0.0	-0.1
48.8	22.0	5.4	-3.5	22.0	13.0	2.9	-3.9	13.0	-0.1	-0.1	-0.1	-0.1	-0.1	-0.1	-0.1	0.0
58.6	22.0	5.4	-3.5	21.0	15.0	3.4	-4.2	15.0	0.0	0.0	-0.1	-0.1	0.0	-0.1	-0.1	0.0
68.4	20.0	5.5	-3.7	20.0	17.0	4.1	-4.7	18.0	-0.1	-0.1	-0.1	-0.1	-0.1	-0.1	0.0	-0.1
78.1	19.0	5.9	-3.8	19.0	19.0	4.5	-5.7	20.0	-0.1	-0.1	-0.1	-0.1	0.0	-0.1	0.0	-0.1
87.9	17.0	6.3	-4.2	17.0	22.0	5.2	-6.3	22.0	-0.1	-0.1	-0.1	-0.1	-0.1	-0.1	-0.1	-0.1
97.7	15.0	6.6	-4.6	15.0	24.0	5.5	-6.9	25.0	-0.1	0.0	-0.1	-0.1	0.0	0.0	0.0	0.0
107.4	13.0	6.9	-4.6	13.0	27.0	6.1	-7.5	28.0	-0.1	0.0	0.0	0.0	0.0	0.0	0.0	0.0
117.2	11.0	7.5	-4.8	11.0	30.0	6.4	-8.3	31.0	-0.1	0.0	0.0	-0.1	0.0	0.0	0.0	0.0
127.0	9.1	8.0	-5.0	8.7	33.0	6.8	-8.8	34.0	0.0	0.0	0.0	-0.1	0.0	0.0	0.0	-0.1
136.7	6.1	8.6	-4.7	6.0	36.0	7.0	-9.6	38.0	0.0	-0.1	0.0	-0.1	0.0	0.0	0.0	0.0

Table 120. Raw data for the test seal at ω=5 krpm, PD=31 bars, C_r=0.140 mm, and inlet GVF=0%

Freq.	Re(H_{XX})	Re(H_{XY})	Re(H_{YX})	Re(H_{YY})	Im(H_{XX})	Im(H_{XY})	Im(H_{YX})	Im(H_{YY})	Re(eH_{XX})	Re(eH_{XY})	Re(eH_{YX})	Re(eH_{YY})	Im(eH_{XX})	Im(eH_{XY})	Im(eH_{YX})	Im(eH_{YY})
Hz	MN/m	MN/m	MN/m	MN/m	MN/m	MN/m	MN/m	MN/m	MN/m	MN/m	MN/m	MN/m	MN/m	MN/m	MN/m	MN/m
9.8	24.0	4.3	-2.7	24.0	2.9	0.3	-0.3	3.3	-0.1	-0.1	-0.1	-0.1	-0.1	-0.1	-0.1	0.0
19.5	24.0	4.4	-2.7	24.0	5.0	1.1	-0.9	5.1	-0.1	-0.1	-0.1	0.0	0.0	-0.1	-0.1	0.0
29.3	24.0	4.8	-2.5	24.0	7.3	1.4	-1.8	7.2	-0.1	-0.1	-0.1	-0.1	0.0	-0.1	0.0	-0.1
39.1	23.0	4.5	-2.6	23.0	9.8	1.9	-2.6	10.0	-0.1	-0.1	-0.1	-0.1	-0.1	-0.1	-0.1	-0.1
48.8	23.0	4.8	-3.0	23.0	12.0	2.8	-3.6	12.0	-0.1	-0.1	0.0	-0.1	-0.1	-0.1	-0.1	0.0
58.6	23.0	4.7	-3.3	23.0	15.0	3.4	-4.0	15.0	-0.1	0.0	-0.1	-0.1	0.0	0.0	-0.1	-0.1
68.4	22.0	5.1	-3.5	22.0	17.0	3.7	-4.5	17.0	-0.1	0.0	0.0	-0.1	0.0	-0.1	0.0	0.0
78.1	21.0	5.5	-3.4	21.0	19.0	4.4	-5.3	19.0	-0.1	-0.1	-0.1	-0.1	0.0	0.0	0.0	0.0
87.9	19.0	5.7	-3.9	19.0	21.0	4.9	-6.0	21.0	-0.1	0.0	0.0	-0.1	0.0	0.0	0.0	0.0
97.7	17.0	5.9	-4.3	17.0	24.0	5.2	-6.4	24.0	-0.1	0.0	-0.1	-0.1	0.0	0.0	0.0	-0.1
107.4	16.0	6.0	-4.3	15.0	27.0	5.5	-6.9	27.0	0.0	0.0	-0.1	-0.1	-0.1	-0.1	0.0	-0.1
117.2	14.0	6.4	-4.4	13.0	29.0	6.2	-7.6	30.0	-0.1	0.0	0.0	-0.1	0.0	0.0	0.0	0.0
127.0	12.0	6.9	-4.3	11.0	32.0	6.6	-8.3	32.0	-0.1	0.0	0.0	-0.1	-0.1	0.0	0.0	-0.1
136.7	8.8	7.8	-4.0	8.7	35.0	7.0	-9.3	36.0	-0.1	0.0	0.0	0.0	0.0	0.0	0.0	0.0

Table 121. Raw data for the test seal at ω=5 krpm, PD=31 bars, C_r=0.140 mm, and inlet GVF=2%

Freq.	Re(H_{XX})	Re(H_{XY})	Re(H_{YX})	Re(H_{YY})	Im(H_{XX})	Im(H_{XY})	Im(H_{YX})	Im(H_{YY})	Re(eH_{XX})	Re(eH_{XY})	Re(eH_{YX})	Re(eH_{YY})	Im(eH_{XX})	Im(eH_{XY})	Im(eH_{YX})	Im(eH_{YY})
Hz	MN/m	MN/m	MN/m	MN/m	MN/m	MN/m	MN/m	MN/m	MN/m	MN/m	MN/m	MN/m	MN/m	MN/m	MN/m	MN/m
9.8	24.0	4.1	-2.5	24.0	2.8	0.5	-0.6	3.3	-0.1	-0.1	-0.2	0.0	-0.1	-0.1	-0.1	-0.1
19.5	24.0	4.2	-2.5	25.0	5.0	1.2	-1.1	4.9	0.0	-0.1	-0.1	0.0	0.0	-0.1	0.0	0.0
29.3	24.0	4.4	-2.4	24.0	7.3	1.5	-1.8	7.1	-0.1	-0.1	-0.1	-0.1	0.0	-0.1	0.0	-0.1
39.1	24.0	4.1	-2.4	24.0	9.7	2.2	-2.6	10.0	-0.1	-0.1	0.0	-0.1	0.0	-0.1	-0.1	-0.1
48.8	23.0	4.4	-2.6	24.0	12.0	2.9	-3.5	12.0	-0.1	-0.1	-0.1	-0.1	0.0	-0.1	-0.1	0.0
58.6	23.0	4.5	-3.1	23.0	15.0	3.3	-4.1	15.0	-0.1	0.0	-0.1	-0.1	0.0	0.0	-0.1	-0.1
68.4	22.0	4.8	-3.4	22.0	17.0	3.8	-4.6	17.0	-0.1	0.0	0.0	-0.1	0.0	-0.1	0.0	0.0
78.1	21.0	5.1	-3.4	21.0	18.0	4.4	-5.3	19.0	-0.1	0.0	0.0	-0.1	0.0	0.0	-0.1	0.0
87.9	19.0	5.4	-3.9	19.0	21.0	5.0	-5.9	21.0	-0.1	0.0	-0.1	0.0	0.0	0.0	0.0	0.0
97.7	17.0	5.6	-4.3	17.0	23.0	5.2	-6.3	24.0	-0.1	0.0	0.0	0.0	0.0	-0.1	0.0	0.0
107.4	15.0	5.9	-4.1	16.0	26.0	5.6	-6.8	26.0	-0.1	0.0	0.0	-0.1	0.0	0.0	0.0	0.0
117.2	13.0	6.3	-4.2	13.0	29.0	6.1	-7.6	29.0	-0.1	0.0	0.0	0.0	0.0	0.0	0.0	0.0
127.0	11.0	6.8	-4.3	11.0	32.0	6.7	-8.3	32.0	-0.1	0.0	-0.1	-0.1	0.0	-0.1	-0.1	0.0
136.7	8.4	7.6	-4.0	8.5	35.0	6.9	-9.2	36.0	-0.1	0.0	0.0	0.0	0.0	0.0	0.0	0.0

Table 122. Raw data for the test seal at ω=5 krpm, PD=31 bars, C_r=0.140 mm, and inlet GVF=4%

Freq.	Re(H_{XX})	Re(H_{XY})	Re(H_{YX})	Re(H_{YY})	Im(H_{XX})	Im(H_{XY})	Im(H_{YX})	Im(H_{YY})	Re(eH_{XX})	Re(eH_{XY})	Re(eH_{YX})	Re(eH_{YY})	Im(eH_{XX})	Im(eH_{XY})	Im(eH_{YX})	Im(eH_{YY})
Hz	MN/m	MN/m	MN/m	MN/m	MN/m	MN/m	MN/m	MN/m	MN/m	MN/m	MN/m	MN/m	MN/m	MN/m	MN/m	MN/m
9.8	25.0	3.8	-1.9	25.0	2.8	0.7	-0.7	3.3	-0.1	-0.1	0.0	-0.1	0.0	0.0	-0.1	-0.1
19.5	25.0	4.2	-2.1	25.0	4.9	0.9	-1.3	5.1	-0.1	-0.1	-0.1	-0.1	0.0	0.0	0.0	-0.1
29.3	24.0	4.2	-2.1	25.0	7.3	1.4	-1.6	7.1	-0.1	-0.1	-0.1	-0.1	0.0	-0.1	-0.1	-0.1
39.1	24.0	4.2	-1.9	24.0	9.8	2.2	-2.4	10.0	-0.1	0.0	-0.1	-0.1	0.0	-0.1	0.0	-0.1
48.8	24.0	4.3	-2.3	24.0	12.0	2.7	-3.6	12.0	-0.1	0.0	-0.1	0.0	-0.1	-0.1	-0.1	0.0
58.6	24.0	4.4	-2.6	23.0	14.0	3.1	-4.0	15.0	-0.1	0.0	-0.1	0.0	0.0	0.0	-0.1	0.0
68.4	23.0	4.5	-3.0	23.0	16.0	3.7	-4.5	17.0	-0.1	-0.1	-0.1	-0.1	0.0	-0.1	0.0	-0.1
78.1	21.0	4.8	-3.1	21.0	18.0	4.3	-5.3	19.0	-0.1	0.0	-0.1	-0.1	0.0	0.0	0.0	-0.1
87.9	20.0	5.2	-3.2	19.0	21.0	4.9	-5.7	21.0	-0.1	0.0	-0.1	0.0	0.0	0.0	0.0	-0.1
97.7	18.0	5.5	-3.6	18.0	24.0	5.2	-6.3	24.0	-0.1	0.0	0.0	-0.1	0.0	0.0	0.0	0.0
107.4	16.0	5.9	-3.7	16.0	26.0	5.6	-7.0	27.0	-0.1	0.0	-0.1	0.0	0.0	0.0	0.0	0.0
117.2	15.0	6.1	-3.8	14.0	29.0	6.1	-7.6	30.0	-0.1	0.0	0.0	0.0	0.0	0.0	0.0	0.0
127.0	13.0	6.6	-4.0	12.0	32.0	6.5	-8.2	33.0	0.0	-0.1	0.0	-0.1	0.0	-0.1	0.0	-0.1
136.7	9.7	7.6	-3.7	9.3	35.0	6.9	-9.1	36.0	-0.1	0.0	0.0	-0.1	0.0	0.0	0.0	0.0

Table 123. Raw data for the test seal at ω=5 krpm, PD=31 bars, C_r=0.140 mm, and inlet GVF=6%

Freq.	Re(H_{XX})	Re(H_{XY})	Re(H_{YX})	Re(H_{YY})	Im(H_{XX})	Im(H_{XY})	Im(H_{YX})	Im(H_{YY})	Re(eH_{XX})	Re(eH_{XY})	Re(eH_{YX})	Re(eH_{YY})	Im(eH_{XX})	Im(eH_{XY})	Im(eH_{YX})	Im(eH_{YY})
Hz	MN/m	MN/m	MN/m	MN/m	MN/m	MN/m	MN/m	MN/m	MN/m	MN/m	MN/m	MN/m	MN/m	MN/m	MN/m	MN/m
9.8	25.0	3.7	-2.0	25.0	2.9	0.7	-0.9	2.9	-0.1	-0.1	-0.1	0.0	0.0	-0.1	0.0	-0.1
19.5	25.0	4.0	-2.0	25.0	4.8	1.0	-1.3	4.9	-0.1	0.0	0.0	-0.1	-0.1	-0.1	-0.1	0.0
29.3	25.0	4.2	-2.1	25.0	7.4	1.2	-1.6	7.4	-0.1	-0.1	-0.1	-0.2	-0.1	0.0	-0.1	-0.1
39.1	25.0	3.9	-1.6	25.0	9.9	1.9	-2.3	9.9	-0.1	-0.1	0.0	-0.1	-0.1	-0.1	-0.1	-0.1
48.8	24.0	3.9	-2.0	24.0	12.0	2.8	-3.5	12.0	-0.1	0.0	0.0	-0.1	-0.1	0.0	-0.1	-0.1
58.6	24.0	4.2	-2.3	24.0	14.0	3.1	-3.9	14.0	-0.1	0.0	-0.1	-0.1	-0.1	0.0	-0.1	-0.1
68.4	23.0	4.1	-2.7	23.0	17.0	3.7	-4.6	16.0	-0.1	0.0	0.0	-0.1	-0.1	-0.1	0.0	-0.1
78.1	22.0	4.5	-2.8	22.0	19.0	4.3	-5.3	19.0	-0.1	-0.1	-0.1	-0.1	0.0	-0.1	0.0	-0.1
87.9	21.0	5.0	-3.2	20.0	21.0	5.0	-5.6	21.0	-0.1	-0.1	-0.1	-0.1	0.0	-0.1	-0.1	-0.1
97.7	19.0	5.2	-3.5	18.0	24.0	5.2	-6.0	24.0	0.0	0.0	0.0	-0.1	0.0	0.0	0.0	-0.1
107.4	17.0	5.7	-3.4	17.0	27.0	5.6	-6.6	26.0	0.0	-0.1	0.0	-0.1	-0.1	0.0	0.0	-0.1
117.2	15.0	6.0	-3.4	15.0	30.0	5.9	-7.3	29.0	0.0	0.0	-0.1	-0.1	0.0	0.0	0.0	0.0
127.0	13.0	6.5	-3.4	13.0	32.0	6.4	-8.0	33.0	0.0	0.0	0.0	-0.1	0.0	-0.1	0.0	-0.1
136.7	11.0	7.2	-3.1	10.0	36.0	6.8	-8.9	36.0	0.0	-0.1	0.0	-0.1	0.0	0.0	0.0	0.0

Table 124. Raw data for the test seal at ω=5 krpm, PD=31 bars, C_r=0.140 mm, and inlet GVF=8%

Freq.	Re($\boldsymbol{H_{XX}}$)	Re($\boldsymbol{H_{XY}}$)	Re($\boldsymbol{H_{YX}}$)	Re($\boldsymbol{H_{YY}}$)	Im($\boldsymbol{H_{XX}}$)	Im($\boldsymbol{H_{XY}}$)	Im($\boldsymbol{H_{YX}}$)	Im($\boldsymbol{H_{YY}}$)	Re($\boldsymbol{eH_{XX}}$)	Re($\boldsymbol{eH_{XY}}$)	Re($\boldsymbol{eH_{YX}}$)	Re($\boldsymbol{eH_{YY}}$)	Im($\boldsymbol{eH_{XX}}$)	Im($\boldsymbol{eH_{XY}}$)	Im($\boldsymbol{eH_{YX}}$)	Im($\boldsymbol{eH_{YY}}$)
Hz	MN/m	MN/m	MN/m	MN/m	MN/m	MN/m	MN/m	MN/m	MN/m	MN/m	MN/m	MN/m	MN/m	MN/m	MN/m	MN/m
9.8	25.0	3.8	-2.0	25.0	2.9	0.7	-0.7	2.9	-0.1	-0.1	-0.1	0.0	-0.1	-0.1	-0.1	-0.1
19.5	25.0	4.4	-2.1	25.0	4.9	1.0	-1.2	4.9	-0.1	-0.1	0.0	-0.1	0.0	-0.1	0.0	-0.1
29.3	24.0	4.1	-2.1	25.0	7.5	1.0	-1.4	7.5	-0.1	-0.1	-0.1	-0.2	-0.1	-0.1	-0.1	-0.1
39.1	24.0	4.0	-1.6	25.0	9.8	1.6	-2.0	10.0	-0.1	-0.1	-0.1	-0.1	-0.1	-0.1	0.0	0.0
48.8	24.0	4.0	-1.8	25.0	12.0	2.5	-3.3	12.0	-0.2	-0.1	-0.1	-0.1	0.0	-0.1	-0.1	-0.1
58.6	23.0	4.3	-2.1	24.0	15.0	2.9	-4.0	15.0	-0.1	-0.1	-0.1	-0.1	-0.1	0.0	-0.1	-0.1
68.4	23.0	3.9	-2.7	23.0	17.0	3.5	-4.5	17.0	-0.1	-0.1	-0.1	0.0	-0.1	-0.1	-0.1	-0.1
78.1	22.0	4.6	-2.7	22.0	19.0	4.2	-5.2	19.0	-0.1	-0.1	0.0	-0.1	0.0	-0.1	-0.1	0.0
87.9	20.0	5.1	-3.2	21.0	22.0	4.4	-5.5	21.0	-0.1	-0.1	-0.1	-0.1	-0.1	0.0	-0.1	-0.1
97.7	19.0	5.2	-3.4	19.0	24.0	4.8	-5.9	24.0	-0.1	0.0	0.0	0.0	0.0	0.0	-0.1	-0.1
107.4	17.0	5.6	-3.3	18.0	27.0	5.2	-6.2	27.0	-0.1	-0.1	-0.1	0.0	-0.1	-0.1	0.0	-0.1
117.2	16.0	5.8	-3.2	15.0	30.0	5.6	-7.1	30.0	0.0	0.0	0.0	-0.1	-0.1	0.0	0.0	0.0
127.0	14.0	6.5	-3.2	14.0	33.0	6.1	-7.8	33.0	-0.1	-0.1	0.0	-0.1	-0.1	-0.1	0.0	0.0
136.7	11.0	6.9	-3.0	11.0	36.0	6.4	-8.7	36.0	0.0	0.0	-0.1	0.0	0.0	0.0	0.0	-0.1

Table 125. Raw data for the test seal at ω=5 krpm, PD=31 bars, C_r=0.140 mm, and inlet GVF=10%

Freq.	Re($\boldsymbol{H_{XX}}$)	Re($\boldsymbol{H_{XY}}$)	Re($\boldsymbol{H_{YX}}$)	Re($\boldsymbol{H_{YY}}$)	Im($\boldsymbol{H_{XX}}$)	Im($\boldsymbol{H_{XY}}$)	Im($\boldsymbol{H_{YX}}$)	Im($\boldsymbol{H_{YY}}$)	Re($\boldsymbol{eH_{XX}}$)	Re($\boldsymbol{eH_{XY}}$)	Re($\boldsymbol{eH_{YX}}$)	Re($\boldsymbol{eH_{YY}}$)	Im($\boldsymbol{eH_{XX}}$)	Im($\boldsymbol{eH_{XY}}$)	Im($\boldsymbol{eH_{YX}}$)	Im($\boldsymbol{eH_{YY}}$)
Hz	MN/m	MN/m	MN/m	MN/m	MN/m	MN/m	MN/m	MN/m	MN/m	MN/m	MN/m	MN/m	MN/m	MN/m	MN/m	MN/m
9.8	22.0	11.0	-7.5	22.0	2.0	0.7	-0.6	2.1	-0.1	-0.2	-0.1	-0.1	-0.1	-0.1	-0.1	-0.1
19.5	21.0	9.9	-7.6	22.0	4.9	0.8	-1.3	5.4	-0.2	-0.2	-0.1	-0.1	-0.1	-0.1	-0.2	-0.1
29.3	21.0	10.0	-7.2	22.0	7.7	1.7	-2.6	7.6	-0.1	-0.1	-0.2	-0.1	-0.1	-0.1	-0.1	-0.1
39.1	21.0	9.6	-7.2	21.0	11.0	3.0	-3.6	11.0	0.0	-0.1	-0.1	0.0	-0.1	-0.1	-0.1	0.0
48.8	21.0	10.0	-7.1	21.0	13.0	5.1	-5.7	13.0	-0.1	-0.1	-0.2	-0.1	-0.1	-0.1	-0.1	-0.1
58.6	19.0	11.0	-9.0	20.0	14.0	4.8	-6.0	15.0	-0.1	-0.1	-0.1	-0.1	-0.1	-0.2	-0.2	-0.1
68.4	18.0	11.0	-8.6	18.0	18.0	5.4	-6.0	17.0	-0.2	-0.1	-0.1	-0.1	-0.1	-0.1	-0.1	-0.1
78.1	17.0	11.0	-8.2	17.0	21.0	5.9	-7.3	21.0	-0.1	-0.1	0.0	-0.1	-0.1	0.0	-0.1	-0.1
87.9	15.0	11.0	-8.4	15.0	24.0	7.0	-8.4	24.0	-0.1	-0.1	-0.1	-0.1	-0.1	-0.1	0.0	-0.1
97.7	14.0	11.0	-8.8	14.0	27.0	7.6	-9.6	27.0	-0.1	0.0	-0.1	-0.1	-0.1	-0.1	-0.1	0.0
107.4	13.0	12.0	-8.9	13.0	29.0	9.0	-11.0	30.0	0.0	-0.1	-0.1	-0.1	-0.1	0.0	-0.1	-0.1
117.2	11.0	12.0	-9.4	10.0	32.0	9.9	-12.0	32.0	-0.1	0.0	-0.1	-0.1	0.0	0.0	-0.1	0.0
127.0	-9.9	25.0	-30.0	-5.8	19.0	-1.4	8.0	22.0	-12.0	-20.0	-10.0	-8.3	-8.5	-6.6	-15.0	-24.0
136.7	5.2	14.0	-9.9	5.8	38.0	12.0	-14.0	39.0	-0.1	-0.1	-0.1	-0.1	-0.1	-0.1	0.0	-0.1

Table 126. Raw data for the test seal at ω=7.5 krpm, PD=31 bars, C_r=0.140 mm, and inlet GVF=0%

Freq.	Re($\boldsymbol{H_{XX}}$)	Re($\boldsymbol{H_{XY}}$)	Re($\boldsymbol{H_{YX}}$)	Re($\boldsymbol{H_{YY}}$)	Im($\boldsymbol{H_{XX}}$)	Im($\boldsymbol{H_{XY}}$)	Im($\boldsymbol{H_{YX}}$)	Im($\boldsymbol{H_{YY}}$)	Re($\boldsymbol{eH_{XX}}$)	Re($\boldsymbol{eH_{XY}}$)	Re($\boldsymbol{eH_{YX}}$)	Re($\boldsymbol{eH_{YY}}$)	Im($\boldsymbol{eH_{XX}}$)	Im($\boldsymbol{eH_{XY}}$)	Im($\boldsymbol{eH_{YX}}$)	Im($\boldsymbol{eH_{YY}}$)
Hz	MN/m	MN/m	MN/m	MN/m	MN/m	MN/m	MN/m	MN/m	MN/m	MN/m	MN/m	MN/m	MN/m	MN/m	MN/m	MN/m
9.8	21.0	10.0	-8.1	22.0	2.6	0.2	-0.4	3.2	-0.2	-0.3	-0.2	-0.1	-0.1	-0.2	-0.1	-0.2
19.5	22.0	10.0	-7.9	22.0	5.7	0.6	-1.4	5.2	-0.1	0.0	-0.2	-0.1	-0.1	-0.1	-0.1	-0.1
29.3	22.0	10.0	-7.7	22.0	7.9	1.7	-2.3	7.3	-0.1	-0.1	-0.1	-0.1	-0.1	-0.1	-0.1	-0.1
39.1	21.0	10.0	-7.9	21.0	10.0	2.7	-3.5	10.0	-0.1	-0.2	-0.1	-0.1	0.0	-0.1	-0.1	-0.2
48.8	21.0	10.0	-8.3	21.0	13.0	3.1	-4.6	13.0	-0.1	-0.2	-0.1	0.0	-0.1	-0.1	-0.1	-0.1
58.6	20.0	11.0	-8.1	21.0	16.0	4.1	-4.7	16.0	-0.1	-0.1	-0.1	0.0	0.0	-0.1	-0.1	-0.1
68.4	20.0	9.9	-9.0	20.0	18.0	5.1	-5.8	18.0	-0.1	-0.1	-0.1	-0.1	-0.1	-0.1	-0.1	-0.1
78.1	19.0	11.0	-8.6	19.0	20.0	6.1	-6.8	20.0	-0.1	-0.1	-0.1	0.0	-0.1	-0.1	0.0	-0.1
87.9	18.0	11.0	-8.6	17.0	23.0	6.6	-8.1	22.0	-0.1	-0.1	0.0	0.0	0.0	-0.1	-0.1	0.0
97.7	15.0	12.0	-9.6	16.0	25.0	7.0	-8.8	25.0	-0.1	-0.1	-0.1	-0.1	0.0	-0.1	0.0	0.0
107.4	14.0	12.0	-9.7	14.0	28.0	7.9	-9.3	28.0	-0.1	-0.1	-0.1	0.0	-0.1	-0.1	-0.1	-0.1
117.2	12.0	13.0	-10.0	12.0	31.0	8.3	-10.0	31.0	-0.1	-0.1	-0.1	-0.1	-0.1	-0.1	-0.1	0.0
127.0	9.9	14.0	-9.5	11.0	34.0	10.0	-11.0	33.0	-0.4	-0.3	-0.3	-0.4	-0.2	-0.2	-0.3	-0.3
136.7	7.1	14.0	-10.0	7.3	37.0	9.9	-12.0	38.0	-0.1	0.0	0.0	-0.1	0.0	-0.1	-0.1	0.0

Table 127. Raw data for the test seal at ω=7.5 krpm, PD=31 bars, C_r=0.140 mm, and inlet GVF=2%

Freq.	Re($\boldsymbol{H_{XX}}$)	Re($\boldsymbol{H_{XY}}$)	Re($\boldsymbol{H_{YX}}$)	Re($\boldsymbol{H_{YY}}$)	Im($\boldsymbol{H_{XX}}$)	Im($\boldsymbol{H_{XY}}$)	Im($\boldsymbol{H_{YX}}$)	Im($\boldsymbol{H_{YY}}$)	Re($\boldsymbol{eH_{XX}}$)	Re($\boldsymbol{eH_{XY}}$)	Re($\boldsymbol{eH_{YX}}$)	Re($\boldsymbol{eH_{YY}}$)	Im($\boldsymbol{eH_{XX}}$)	Im($\boldsymbol{eH_{XY}}$)	Im($\boldsymbol{eH_{YX}}$)	Im($\boldsymbol{eH_{YY}}$)
Hz	MN/m	MN/m	MN/m	MN/m	MN/m	MN/m	MN/m	MN/m	MN/m	MN/m	MN/m	MN/m	MN/m	MN/m	MN/m	MN/m
9.8	22.0	11.0	-8.8	21.0	2.5	0.3	-0.9	3.1	-0.2	-0.2	-0.2	-0.1	-0.1	-0.1	-0.2	-0.2
19.5	22.0	11.0	-8.1	22.0	5.8	0.6	-1.2	5.4	-0.2	-0.1	-0.1	-0.1	-0.1	-0.1	-0.1	-0.1
29.3	21.0	11.0	-8.0	22.0	8.0	1.4	-2.4	7.4	-0.1	-0.1	-0.2	-0.1	-0.1	-0.1	-0.1	-0.1
39.1	21.0	11.0	-8.0	21.0	10.0	2.7	-3.4	11.0	-0.1	-0.1	-0.1	-0.1	0.0	-0.1	-0.1	0.0
48.8	20.0	11.0	-8.1	21.0	14.0	3.0	-4.0	13.0	-0.2	-0.1	-0.2	-0.1	-0.2	-0.1	-0.1	-0.1
58.6	20.0	11.0	-8.1	21.0	16.0	4.1	-4.8	16.0	-0.1	-0.1	-0.2	-0.1	-0.1	-0.1	0.0	0.0
68.4	20.0	10.0	-8.9	20.0	18.0	4.9	-5.7	18.0	-0.1	-0.1	-0.1	-0.1	-0.1	-0.1	-0.1	-0.1
78.1	19.0	11.0	-8.7	19.0	20.0	5.9	-6.6	20.0	-0.1	-0.1	-0.1	-0.1	-0.1	0.0	-0.1	0.0
87.9	17.0	11.0	-8.9	17.0	23.0	6.4	-8.0	22.0	-0.1	-0.1	-0.1	0.0	-0.1	-0.1	-0.1	0.0
97.7	16.0	12.0	-9.7	15.0	25.0	7.1	-8.7	25.0	-0.1	-0.1	-0.1	-0.1	-0.1	-0.1	-0.1	0.0
107.4	13.0	13.0	-9.7	13.0	28.0	7.8	-9.2	28.0	-0.1	-0.1	-0.1	-0.1	-0.1	0.0	-0.1	-0.1
117.2	12.0	13.0	-9.9	11.0	31.0	8.3	-10.0	31.0	-0.1	-0.1	-0.1	-0.1	-0.1	-0.1	-0.1	-0.1
127.0	9.8	15.0	-11.0	7.6	34.0	7.4	-12.0	33.0	-1.7	-2.2	-2.0	-3.0	-1.6	-2.4	-2.1	-2.6
136.7	6.8	14.0	-10.0	6.9	38.0	9.6	-12.0	39.0	-0.1	-0.1	-0.1	0.0	0.0	-0.1	-0.1	-0.1

Table 128. Raw data for the test seal at ω=7.5 krpm, PD=31 bars, C_r=0.140 mm, and inlet GVF=4%

Freq.	Re($\boldsymbol{H_{XX}}$)	Re($\boldsymbol{H_{XY}}$)	Re($\boldsymbol{H_{YX}}$)	Re($\boldsymbol{H_{YY}}$)	Im($\boldsymbol{H_{XX}}$)	Im($\boldsymbol{H_{XY}}$)	Im($\boldsymbol{H_{YX}}$)	Im($\boldsymbol{H_{YY}}$)	Re($\boldsymbol{eH_{XX}}$)	Re($\boldsymbol{eH_{XY}}$)	Re($\boldsymbol{eH_{YX}}$)	Re($\boldsymbol{eH_{YY}}$)	Im($\boldsymbol{eH_{XX}}$)	Im($\boldsymbol{eH_{XY}}$)	Im($\boldsymbol{eH_{YX}}$)	Im($\boldsymbol{eH_{YY}}$)
Hz	MN/m	MN/m	MN/m	MN/m	MN/m	MN/m	MN/m	MN/m	MN/m	MN/m	MN/m	MN/m	MN/m	MN/m	MN/m	MN/m
9.8	18.0	14.0	-13.0	18.0	1.8	0.2	-2.0	3.8	-0.3	-0.3	-0.4	-0.3	-0.1	-0.1	-0.1	-0.1
19.5	18.0	14.0	-12.0	17.0	5.6	0.2	-1.1	4.8	-0.2	-0.4	-0.3	-0.3	-0.1	-0.1	-0.1	-0.1
29.3	18.0	14.0	-12.0	17.0	8.0	0.5	-1.9	7.7	-0.2	-0.3	-0.5	-0.3	-0.1	-0.1	-0.1	-0.2
39.1	18.0	14.0	-11.0	17.0	11.0	1.3	-2.6	11.0	-0.2	-0.4	-0.4	-0.3	-0.1	-0.2	-0.2	-0.1
48.8	18.0	14.0	-12.0	16.0	14.0	2.3	-4.7	14.0	-0.2	-0.3	-0.4	-0.2	-0.1	-0.1	-0.1	-0.1
58.6	17.0	14.0	-12.0	16.0	16.0	2.7	-3.1	17.0	-0.2	-0.3	-0.5	-0.3	-0.1	-0.2	-0.2	-0.1
68.4	15.0	14.0	-13.0	14.0	19.0	2.3	-2.9	20.0	-0.3	-0.3	-0.4	-0.2	-0.1	-0.2	-0.3	-0.2
78.1	14.0	14.0	-13.0	14.0	22.0	3.4	-3.9	23.0	-0.3	-0.3	-0.5	-0.2	-0.2	-0.2	-0.3	-0.2
87.9	14.0	14.0	-12.0	14.0	25.0	3.8	-5.2	25.0	-0.2	-0.2	-0.3	-0.2	-0.2	-0.2	-0.3	-0.2
97.7	12.0	14.0	-12.0	12.0	28.0	4.2	-5.9	28.0	-0.2	-0.3	-0.3	-0.2	-0.2	-0.2	-0.3	-0.2
107.4	11.0	14.0	-12.0	10.0	31.0	4.7	-6.4	32.0	-0.2	-0.1	-0.3	-0.2	-0.2	-0.3	-0.3	-0.1
117.2	9.2	14.0	-12.0	8.6	35.0	5.7	-6.7	35.0	-0.2	-0.2	-0.2	-0.2	-0.2	-0.2	-0.3	-0.2
127.0	8.7	15.0	-12.0	5.2	38.0	4.3	-9.0	39.0	-0.2	-0.2	-0.1	-0.2	-0.4	-0.3	-0.4	-0.4
136.7	4.8	15.0	-12.0	4.8	41.0	6.9	-9.0	42.0	-0.3	-0.2	-0.3	-0.3	-0.3	-0.4	-0.3	-0.3

Table 129. Raw data for the test seal at ω=7.5 krpm, PD=31 bars, C_r=0.140 mm, and inlet GVF=6%

Freq.	Re($\boldsymbol{H_{XX}}$)	Re($\boldsymbol{H_{XY}}$)	Re($\boldsymbol{H_{YX}}$)	Re($\boldsymbol{H_{YY}}$)	Im($\boldsymbol{H_{XX}}$)	Im($\boldsymbol{H_{XY}}$)	Im($\boldsymbol{H_{YX}}$)	Im($\boldsymbol{H_{YY}}$)	Re($\boldsymbol{eH_{XX}}$)	Re($\boldsymbol{eH_{XY}}$)	Re($\boldsymbol{eH_{YX}}$)	Re($\boldsymbol{eH_{YY}}$)	Im($\boldsymbol{eH_{XX}}$)	Im($\boldsymbol{eH_{XY}}$)	Im($\boldsymbol{eH_{YX}}$)	Im($\boldsymbol{eH_{YY}}$)
Hz	MN/m	MN/m	MN/m	MN/m	MN/m	MN/m	MN/m	MN/m	MN/m	MN/m	MN/m	MN/m	MN/m	MN/m	MN/m	MN/m
9.8	15.0	16.0	-16.0	15.0	1.7	-0.2	-1.7	3.7	-0.4	-0.4	-0.6	-0.4	-0.2	-0.1	-0.2	-0.2
19.5	15.0	16.0	-14.0	14.0	5.6	-0.3	-0.9	4.9	-0.4	-0.4	-0.5	-0.4	-0.1	-0.2	-0.1	-0.1
29.3	15.0	16.0	-15.0	14.0	8.7	0.0	-1.2	8.7	-0.3	-0.4	-0.5	-0.4	-0.1	-0.1	-0.2	-0.1
39.1	15.0	16.0	-14.0	14.0	12.0	0.4	-1.6	12.0	-0.4	-0.4	-0.5	-0.4	-0.1	-0.2	-0.2	-0.2
48.8	15.0	15.0	-14.0	14.0	14.0	1.5	-3.8	15.0	-0.5	-0.4	-0.5	-0.4	-0.2	-0.2	-0.2	-0.2
58.6	14.0	16.0	-15.0	14.0	17.0	2.0	-2.1	17.0	-0.4	-0.3	-0.5	-0.4	-0.2	-0.3	-0.3	-0.2
68.4	13.0	15.0	-14.0	12.0	21.0	1.2	-1.4	21.0	-0.4	-0.3	-0.4	-0.4	-0.1	-0.2	-0.3	-0.2
78.1	12.0	15.0	-15.0	12.0	24.0	2.4	-2.4	25.0	-0.4	-0.3	-0.4	-0.4	-0.1	-0.2	-0.3	-0.2
87.9	11.0	15.0	-13.0	11.0	27.0	2.7	-3.3	27.0	-0.4	-0.4	-0.4	-0.4	-0.2	-0.3	-0.4	-0.2
97.7	10.0	15.0	-14.0	9.6	30.0	3.0	-4.3	31.0	-0.4	-0.3	-0.4	-0.4	-0.2	-0.3	-0.4	-0.2
107.4	8.7	16.0	-14.0	8.8	33.0	3.7	-4.8	34.0	-0.4	-0.3	-0.4	-0.4	-0.2	-0.3	-0.3	-0.2
117.2	7.5	16.0	-14.0	7.2	37.0	4.2	-4.8	37.0	-0.4	-0.2	-0.4	-0.4	-0.3	-0.3	-0.4	-0.2
127.0	5.8	17.0	-14.0	6.0	41.0	4.3	-5.4	41.0	-0.5	-0.1	-0.3	-0.4	-0.2	-0.3	-0.5	-0.4
136.7	3.9	17.0	-13.0	4.1	44.0	5.6	-6.8	45.0	-0.4	-0.2	-0.3	-0.4	-0.2	-0.3	-0.4	-0.2

Table 130. Raw data for the test seal at ω=7.5 krpm, PD=31 bars, C_r=0.140 mm, and inlet GVF=8%

Freq.	Re($\boldsymbol{H_{XX}}$)	Re($\boldsymbol{H_{XY}}$)	Re($\boldsymbol{H_{YX}}$)	Re($\boldsymbol{H_{YY}}$)	Im($\boldsymbol{H_{XX}}$)	Im($\boldsymbol{H_{XY}}$)	Im($\boldsymbol{H_{YX}}$)	Im($\boldsymbol{H_{YY}}$)	Re($\boldsymbol{eH_{XX}}$)	Re($\boldsymbol{eH_{XY}}$)	Re($\boldsymbol{eH_{YX}}$)	Re($\boldsymbol{eH_{YY}}$)	Im($\boldsymbol{eH_{XX}}$)	Im($\boldsymbol{eH_{XY}}$)	Im($\boldsymbol{eH_{YX}}$)	Im($\boldsymbol{eH_{YY}}$)
Hz	MN/m	MN/m	MN/m	MN/m	MN/m	MN/m	MN/m	MN/m	MN/m	MN/m	MN/m	MN/m	MN/m	MN/m	MN/m	MN/m
9.8	9.0	20.0	-19.0	8.0	0.7	-0.3	-0.5	2.6	-0.3	-0.4	-0.4	-0.4	-0.1	-0.2	-0.1	-0.3
19.5	9.0	19.0	-18.0	7.1	5.0	-1.3	0.1	5.5	-0.4	-0.5	-0.4	-0.4	-0.2	-0.1	-0.2	-0.3
29.3	8.0	19.0	-18.0	6.4	8.9	-1.2	0.4	9.8	-0.4	-0.5	-0.5	-0.4	-0.2	-0.1	-0.2	-0.3
39.1	8.0	19.0	-17.0	7.0	13.0	-0.1	-0.2	14.0	-0.4	-0.5	-0.5	-0.5	-0.2	-0.2	-0.3	-0.3
48.8	8.0	19.0	-18.0	7.0	16.0	0.6	-1.3	17.0	-0.4	-0.4	-0.4	-0.5	-0.2	-0.2	-0.3	-0.2
58.6	7.5	21.0	-19.0	5.8	19.0	-0.3	-0.8	20.0	-0.4	-0.5	-0.5	-0.5	-0.3	-0.4	-0.4	-0.3
68.4	5.0	19.0	-17.0	3.9	24.0	-2.4	1.0	24.0	-0.5	-0.3	-0.2	-0.6	-0.3	-0.4	-0.4	-0.2
78.1	5.5	18.0	-17.0	4.9	28.0	-0.4	-0.6	29.0	-0.4	-0.4	-0.2	-0.6	-0.3	-0.5	-0.4	-0.3
87.9	6.1	18.0	-16.0	4.6	31.0	0.4	-1.3	32.0	-0.4	-0.2	-0.2	-0.6	-0.2	-0.4	-0.4	-0.3
97.7	5.4	18.0	-16.0	4.0	34.0	0.7	-1.9	35.0	-0.4	-0.2	-0.2	-0.5	-0.2	-0.4	-0.4	-0.4
107.4	3.8	19.0	-16.0	3.3	38.0	1.5	-2.6	39.0	-0.5	-0.2	-0.2	-0.4	-0.2	-0.4	-0.3	-0.3
117.2	2.9	19.0	-16.0	2.3	42.0	1.3	-2.7	43.0	-0.5	-0.1	-0.3	-0.4	-0.3	-0.3	-0.3	-0.4
127.0	2.1	17.0	-17.0	0.2	45.0	0.8	-3.8	49.0	-1.7	-3.0	-2.3	-2.2	-1.7	-1.7	-2.2	-3.9
136.7	0.9	18.0	-15.0	0.5	50.0	3.1	-3.9	50.0	-0.4	-0.1	-0.1	-0.4	-0.3	-0.3	-0.3	-0.3

Table 131. Raw data for the test seal at ω=7.5 krpm, PD=31 bars, C_r=0.140 mm, and inlet GVF=10%

Freq.	Re($\boldsymbol{H_{XX}}$)	Re($\boldsymbol{H_{XY}}$)	Re($\boldsymbol{H_{YX}}$)	Re($\boldsymbol{H_{YY}}$)	Im($\boldsymbol{H_{XX}}$)	Im($\boldsymbol{H_{XY}}$)	Im($\boldsymbol{H_{YX}}$)	Im($\boldsymbol{H_{YY}}$)	Re($\boldsymbol{eH_{XX}}$)	Re($\boldsymbol{eH_{XY}}$)	Re($\boldsymbol{eH_{YX}}$)	Re($\boldsymbol{eH_{YY}}$)	Im($\boldsymbol{eH_{XX}}$)	Im($\boldsymbol{eH_{XY}}$)	Im($\boldsymbol{eH_{YX}}$)	Im($\boldsymbol{eH_{YY}}$)
Hz	MN/m	MN/m	MN/m	MN/m	MN/m	MN/m	MN/m	MN/m	MN/m	MN/m	MN/m	MN/m	MN/m	MN/m	MN/m	MN/m
9.8	16.0	25.0	-16.0	18.0	2.4	1.1	-1.1	1.4	-0.4	-0.8	-0.2	-0.3	-0.2	-0.1	-0.2	-0.2
19.5	16.0	25.0	-17.0	18.0	6.4	0.2	-2.3	6.0	-0.4	-0.8	-0.2	-0.2	-0.1	-0.1	-0.1	-0.2
29.3	16.0	25.0	-17.0	18.0	9.2	0.0	-3.6	8.9	-0.3	-0.8	-0.2	-0.3	-0.2	-0.2	-0.1	-0.2
39.1	15.0	25.0	-16.0	17.0	12.0	1.4	-3.3	11.0	-0.3	-0.7	-0.2	-0.4	-0.2	-0.2	-0.1	-0.1
48.8	14.0	24.0	-16.0	16.0	15.0	2.3	-5.4	14.0	-0.3	-0.7	-0.2	-0.3	-0.1	-0.2	-0.1	-0.1
58.6	14.0	24.0	-16.0	16.0	18.0	3.5	-6.8	18.0	-0.3	-0.7	-0.2	-0.3	-0.2	-0.3	-0.1	-0.1
68.4	14.0	24.0	-18.0	16.0	20.0	5.5	-7.7	19.0	-0.3	-0.7	-0.2	-0.3	-0.2	-0.3	-0.1	-0.2
78.1	12.0	25.0	-18.0	13.0	23.0	4.5	-8.5	22.0	-0.3	-0.7	-0.2	-0.3	-0.3	-0.4	-0.1	-0.1
87.9	10.0	25.0	-17.0	11.0	28.0	4.4	-9.2	26.0	-0.3	-0.7	-0.2	-0.3	-0.3	-0.3	-0.1	-0.1
97.7	8.8	25.0	-18.0	9.8	31.0	4.9	-11.0	30.0	-0.3	-0.6	-0.2	-0.4	-0.3	-0.3	-0.1	-0.1
107.4	7.5	25.0	-17.0	8.4	34.0	6.3	-11.0	32.0	-0.2	-0.6	-0.2	-0.4	-0.3	-0.4	-0.2	-0.1
117.2	6.3	25.0	-18.0	6.6	38.0	6.9	-13.0	36.0	-0.2	-0.7	-0.2	-0.4	-0.3	-0.4	-0.2	-0.2
127.0	3.9	26.0	-17.0	4.3	41.0	8.1	-14.0	39.0	-0.2	-0.7	-0.3	-0.5	-0.4	-0.6	-0.2	-0.1
136.7	1.4	25.0	-18.0	2.9	44.0	9.6	-15.0	42.0	-0.1	-0.5	-0.2	-0.4	-0.4	-0.6	-0.2	-0.1

Table 132. Raw data for the test seal at ω=10 krpm, PD=31 bars, C_r=0.140 mm, and inlet GVF=0%

Freq.	Re($\boldsymbol{H_{XX}}$)	Re($\boldsymbol{H_{XY}}$)	Re($\boldsymbol{H_{YX}}$)	Re($\boldsymbol{H_{YY}}$)	Im($\boldsymbol{H_{XX}}$)	Im($\boldsymbol{H_{XY}}$)	Im($\boldsymbol{H_{YX}}$)	Im($\boldsymbol{H_{YY}}$)	Re($\boldsymbol{eH_{XX}}$)	Re($\boldsymbol{eH_{XY}}$)	Re($\boldsymbol{eH_{YX}}$)	Re($\boldsymbol{eH_{YY}}$)	Im($\boldsymbol{eH_{XX}}$)	Im($\boldsymbol{eH_{XY}}$)	Im($\boldsymbol{eH_{YX}}$)	Im($\boldsymbol{eH_{YY}}$)
Hz	MN/m	MN/m	MN/m	MN/m	MN/m	MN/m	MN/m	MN/m	MN/m	MN/m	MN/m	MN/m	MN/m	MN/m	MN/m	MN/m
9.8	-1.2	31.0	-28.0	-1.1	-1.0	-1.9	-2.8	0.1	-0.4	-0.3	-0.2	-0.3	-0.2	-0.2	-0.3	-0.3
19.5	4.6	31.0	-27.0	-0.7	6.7	-3.9	-1.7	4.6	-0.2	-0.3	-0.4	-0.4	-0.3	-0.2	-0.1	-0.3
29.3	4.3	30.0	-27.0	-1.0	9.5	-3.0	-1.8	9.4	-0.2	-0.3	-0.3	-0.2	-0.2	-0.1	-0.1	-0.2
39.1	2.9	33.0	-25.0	-0.6	15.0	-1.7	-1.1	14.0	-0.3	-0.4	-0.3	-0.2	-0.3	-0.1	-0.1	-0.3
48.8	1.4	29.0	-26.0	-2.2	17.0	-0.3	-3.9	17.0	-0.2	-0.3	-0.3	-0.2	-0.2	-0.1	-0.1	-0.3
58.6	2.8	31.0	-26.0	-1.3	23.0	0.2	-4.0	21.0	-0.3	-0.4	-0.4	-0.2	-0.3	-0.2	-0.1	-0.3
68.4	0.7	33.0	-26.0	-2.2	25.0	2.9	-4.5	25.0	-0.3	-0.4	-0.4	-0.2	-0.3	-0.1	-0.1	-0.3
78.1	3.0	34.0	-28.0	-3.0	32.0	0.6	-3.2	30.0	-0.2	-0.5	-0.5	-0.2	-0.4	-0.3	-0.2	-0.4
87.9	1.4	33.0	-26.0	-4.5	34.0	1.5	-4.6	33.0	-0.4	-0.4	-0.5	-0.2	-0.3	-0.3	-0.2	-0.4
97.7	0.6	32.0	-26.0	-5.8	37.0	1.2	-6.2	37.0	-0.4	-0.3	-0.4	-0.2	-0.2	-0.4	-0.3	-0.3
107.4	-0.7	33.0	-27.0	-6.2	42.0	2.0	-6.5	42.0	-0.4	-0.2	-0.3	-0.3	-0.2	-0.4	-0.3	-0.3
117.2	-1.3	34.0	-28.0	-7.0	48.0	2.8	-6.1	47.0	-0.4	-0.2	-0.3	-0.4	-0.2	-0.4	-0.4	-0.2
127.0	-0.6	34.0	-27.0	-8.6	49.0	2.1	-7.9	51.0	-0.4	-0.1	-0.3	-0.4	-0.2	-0.3	-0.4	-0.3
136.7	-3.6	33.0	-25.0	-7.6	52.0	4.6	-6.2	53.0	-0.3	-0.2	-0.2	-0.3	-0.3	-0.3	-0.4	-0.2

Table 133. Raw data for the test seal at ω=10 krpm, PD=31 bars, C_r=0.140 mm, and inlet GVF=2%

Freq.	Re($\boldsymbol{H_{XX}}$)	Re($\boldsymbol{H_{XY}}$)	Re($\boldsymbol{H_{YX}}$)	Re($\boldsymbol{H_{YY}}$)	Im($\boldsymbol{H_{XX}}$)	Im($\boldsymbol{H_{XY}}$)	Im($\boldsymbol{H_{YX}}$)	Im($\boldsymbol{H_{YY}}$)	Re($\boldsymbol{eH_{XX}}$)	Re($\boldsymbol{eH_{XY}}$)	Re($\boldsymbol{eH_{YX}}$)	Re($\boldsymbol{eH_{YY}}$)	Im($\boldsymbol{eH_{XX}}$)	Im($\boldsymbol{eH_{XY}}$)	Im($\boldsymbol{eH_{YX}}$)	Im($\boldsymbol{eH_{YY}}$)
Hz	MN/m	MN/m	MN/m	MN/m	MN/m	MN/m	MN/m	MN/m	MN/m	MN/m	MN/m	MN/m	MN/m	MN/m	MN/m	MN/m
9.8	-4.2	30.0	-29.0	-4.7	-0.4	-2.9	-0.9	2.1	-0.7	-0.4	-0.1	-0.1	-0.2	-0.2	-0.5	-0.4
19.5	-0.3	31.0	-30.0	-4.7	5.9	-4.1	-0.6	6.7	-0.5	-0.4	-0.4	-0.3	-0.4	-0.1	-0.2	-0.5
29.3	-1.1	31.0	-30.0	-4.5	9.1	-3.1	0.0	11.0	-0.5	-0.5	-0.4	-0.3	-0.4	-0.2	-0.1	-0.4
39.1	-1.6	33.0	-28.0	-4.8	16.0	-1.5	-0.9	16.0	-0.5	-0.7	-0.4	-0.4	-0.5	-0.1	-0.1	-0.4
48.8	-2.6	30.0	-28.0	-5.2	18.0	0.1	-2.4	19.0	-0.4	-0.6	-0.4	-0.2	-0.5	-0.1	-0.2	-0.4
58.6	-1.1	32.0	-28.0	-4.8	23.0	-0.1	-2.9	24.0	-0.4	-0.8	-0.5	-0.2	-0.7	-0.2	-0.2	-0.5
68.4	-4.5	35.0	-28.0	-6.9	27.0	1.7	-4.2	27.0	-0.4	-0.9	-0.7	-0.2	-0.8	-0.3	-0.2	-0.7
78.1	-0.5	36.0	-31.0	-5.2	33.0	-1.5	-1.5	34.0	-0.5	-0.9	-0.7	-0.4	-0.9	-0.6	-0.3	-0.7
87.9	-4.8	33.0	-27.0	-7.9	35.0	2.6	-3.4	35.0	-0.9	-0.6	-0.7	-0.4	-0.5	-0.8	-0.2	-0.7
97.7	-4.8	32.0	-28.0	-9.6	38.0	1.9	-5.5	40.0	-0.8	-0.3	-0.6	-0.6	-0.3	-0.8	-0.4	-0.6
107.4	-4.0	34.0	-30.0	-7.9	44.0	0.6	-4.2	46.0	-0.7	-0.2	-0.6	-0.7	-0.3	-0.7	-0.6	-0.5
117.2	-7.7	36.0	-31.0	-11.0	51.0	4.2	-6.1	51.0	-0.7	-0.2	-0.4	-0.8	-0.3	-0.6	-0.5	-0.3
127.0	-5.7	34.0	-28.0	-10.0	50.0	1.5	-5.5	53.0	-0.6	-0.2	-0.3	-0.7	-0.2	-0.5	-0.6	-0.4
136.7	-6.6	37.0	-29.0	-7.8	58.0	0.8	-2.9	58.0	-0.5	-0.4	-0.3	-0.3	-0.4	-0.6	-0.5	-0.2

Table 134. Raw data for the test seal at ω=10 krpm, PD=31 bars, C_r=0.140 mm, and inlet GVF=4%

Freq.	Re($\boldsymbol{H_{XX}}$)	Re($\boldsymbol{H_{XY}}$)	Re($\boldsymbol{H_{YX}}$)	Re($\boldsymbol{H_{YY}}$)	Im($\boldsymbol{H_{XX}}$)	Im($\boldsymbol{H_{XY}}$)	Im($\boldsymbol{H_{YX}}$)	Im($\boldsymbol{H_{YY}}$)	Re($\boldsymbol{eH_{XX}}$)	Re($\boldsymbol{eH_{XY}}$)	Re($\boldsymbol{eH_{YX}}$)	Re($\boldsymbol{eH_{YY}}$)	Im($\boldsymbol{eH_{XX}}$)	Im($\boldsymbol{eH_{XY}}$)	Im($\boldsymbol{eH_{YX}}$)	Im($\boldsymbol{eH_{YY}}$)
Hz	MN/m	MN/m	MN/m	MN/m	MN/m	MN/m	MN/m	MN/m	MN/m	MN/m	MN/m	MN/m	MN/m	MN/m	MN/m	MN/m
9.8	7.8	0.7	-0.6	7.3	0.5	0.0	0.1	0.7	-0.1	-0.1	-0.1	-0.1	-0.1	-0.1	-0.1	0.0
19.5	7.6	0.8	-0.8	7.4	1.4	0.1	0.0	1.1	-0.1	0.0	-0.1	0.0	-0.1	0.0	0.0	-0.1
29.3	7.7	0.7	-0.8	7.4	2.0	0.2	-0.1	1.9	0.0	-0.1	0.0	-0.1	-0.1	-0.1	-0.1	-0.1
39.1	7.6	0.8	-1.0	7.4	2.6	0.2	0.0	2.6	0.0	-0.1	-0.1	-0.1	-0.1	-0.1	-0.1	-0.1
48.8	7.5	0.9	-0.9	7.4	3.3	0.2	0.0	3.3	-0.1	-0.1	0.0	-0.1	-0.1	-0.1	0.0	-0.1
58.6	7.6	1.0	-0.9	7.5	4.1	0.2	-0.2	4.0	-0.1	-0.1	-0.1	0.0	0.0	-0.1	-0.1	0.0
68.4	7.5	1.1	-0.9	7.6	4.8	0.1	-0.2	4.9	0.0	-0.2	-0.1	-0.1	-0.1	0.0	0.0	-0.1
78.1	7.6	0.9	-0.8	7.5	5.3	0.1	-0.2	5.2	0.0	-0.1	-0.1	0.0	-0.1	-0.1	0.0	-0.1
87.9	7.6	0.9	-0.9	7.4	6.2	0.2	-0.2	6.0	0.0	0.0	0.0	-0.1	0.0	0.0	0.0	0.0
97.7	7.5	0.9	-0.9	7.6	6.8	0.1	-0.1	6.7	0.0	0.0	0.0	-0.1	0.0	0.0	0.0	0.0
107.4	7.6	1.0	-0.7	7.5	7.6	0.2	-0.2	7.3	-0.1	-0.1	-0.1	-0.1	-0.1	0.0	0.0	0.0
117.2	7.9	0.8	-0.9	7.6	8.4	0.1	-0.5	8.0	0.0	0.0	0.0	-0.1	-0.1	0.0	0.0	0.0
127.0	8.0	0.7	-0.9	7.6	8.7	0.2	-0.2	8.8	0.0	0.0	0.0	-0.1	0.0	-0.1	0.0	-0.1
136.7	8.0	0.8	-1.1	7.5	9.2	0.2	-0.2	9.4	0.0	-0.1	0.0	0.0	0.0	0.0	0.0	0.0

Table 135. Raw data for the test seal at ω=10 krpm, PR=0.57, C_r=0.188 mm, and inlet GVF=100%

Freq.	Re($\boldsymbol{H_{XX}}$)	Re($\boldsymbol{H_{XY}}$)	Re($\boldsymbol{H_{YX}}$)	Re($\boldsymbol{H_{YY}}$)	Im($\boldsymbol{H_{XX}}$)	Im($\boldsymbol{H_{XY}}$)	Im($\boldsymbol{H_{YX}}$)	Im($\boldsymbol{H_{YY}}$)	Re($\boldsymbol{eH_{XX}}$)	Re($\boldsymbol{eH_{XY}}$)	Re($\boldsymbol{eH_{YX}}$)	Re($\boldsymbol{eH_{YY}}$)	Im($\boldsymbol{eH_{XX}}$)	Im($\boldsymbol{eH_{XY}}$)	Im($\boldsymbol{eH_{YX}}$)	Im($\boldsymbol{eH_{YY}}$)
Hz	MN/m	MN/m	MN/m	MN/m	MN/m	MN/m	MN/m	MN/m	MN/m	MN/m	MN/m	MN/m	MN/m	MN/m	MN/m	MN/m
9.8	4.1	2.3	-2.3	4.0	0.9	0.2	-0.1	1.3	-0.1	-0.1	-0.2	-0.2	-0.1	-0.2	-0.2	-0.1
19.5	4.1	2.6	-2.8	3.8	2.3	0.1	0.3	2.1	-0.1	-0.1	-0.1	-0.2	-0.1	-0.2	-0.1	-0.2
29.3	4.2	2.5	-2.5	4.3	3.2	0.2	0.4	2.7	-0.1	-0.1	-0.1	-0.2	-0.1	-0.1	-0.2	-0.2
39.1	4.9	2.4	-2.5	4.2	3.8	0.2	-0.1	3.7	-0.1	0.0	-0.1	-0.2	-0.1	-0.1	-0.1	-0.1
48.8	4.6	2.5	-2.8	4.4	4.7	0.4	0.1	4.6	-0.1	-0.1	-0.1	-0.2	-0.1	-0.1	-0.1	-0.1
58.6	4.8	2.6	-2.6	4.4	5.5	0.7	0.2	5.1	0.0	0.0	-0.1	-0.2	-0.1	-0.1	-0.1	-0.1
68.4	4.8	2.7	-2.6	4.8	6.4	0.2	0.0	6.5	-0.1	-0.2	-0.1	-0.1	-0.1	-0.3	-0.2	-0.3
78.1	5.0	2.7	-2.4	4.4	7.2	0.3	0.0	6.7	0.0	-0.1	-0.1	-0.1	-0.1	-0.1	-0.1	-0.1
87.9	4.9	2.6	-2.8	4.4	8.1	0.3	0.1	7.7	-0.1	0.0	-0.1	0.0	0.0	-0.1	0.0	0.0
97.7	5.0	2.7	-2.8	4.6	9.1	0.5	0.2	8.8	-0.1	-0.1	0.0	0.0	0.0	-0.1	0.0	-0.1
107.4	5.0	2.7	-2.6	4.7	10.0	0.3	0.0	9.4	-0.1	-0.1	-0.1	-0.1	-0.1	0.0	-0.1	-0.1
117.2	5.2	2.6	-2.8	4.7	11.0	0.3	-0.4	10.0	0.0	0.0	-0.1	-0.1	0.0	0.0	0.0	-0.1
127.0	5.3	2.5	-2.9	5.2	11.0	0.5	0.0	11.0	0.0	-0.1	0.0	-0.1	0.0	-0.1	-0.1	-0.2
136.7	5.4	2.2	-3.1	5.3	12.0	0.7	0.0	12.0	0.0	-0.1	0.0	-0.1	0.0	-0.1	0.0	-0.1

Table 136. Raw data for the test seal at ω=10 krpm, PR=0.57, C_r=0.188 mm, and inlet GVF=98%

Freq.	Re($\boldsymbol{H_{XX}}$)	Re($\boldsymbol{H_{XY}}$)	Re($\boldsymbol{H_{YX}}$)	Re($\boldsymbol{H_{YY}}$)	Im($\boldsymbol{H_{XX}}$)	Im($\boldsymbol{H_{XY}}$)	Im($\boldsymbol{H_{YX}}$)	Im($\boldsymbol{H_{YY}}$)	Re($\boldsymbol{eH_{XX}}$)	Re($\boldsymbol{eH_{XY}}$)	Re($\boldsymbol{eH_{YX}}$)	Re($\boldsymbol{eH_{YY}}$)	Im($\boldsymbol{eH_{XX}}$)	Im($\boldsymbol{eH_{XY}}$)	Im($\boldsymbol{eH_{YX}}$)	Im($\boldsymbol{eH_{YY}}$)
Hz	MN/m	MN/m	MN/m	MN/m	MN/m	MN/m	MN/m	MN/m	MN/m	MN/m	MN/m	MN/m	MN/m	MN/m	MN/m	MN/m
9.8	4.7	0.8	-2.6	3.4	-0.6	0.5	0.6	1.2	-0.2	-0.3	-0.3	-0.4	-0.3	-0.2	-0.5	-0.2
19.5	3.2	2.0	-2.7	2.9	1.0	0.9	0.3	2.0	-0.1	-0.1	-0.2	-0.1	-0.2	-0.3	-0.3	-0.2
29.3	3.6	1.8	-1.6	3.0	2.3	0.4	0.5	2.9	-0.1	-0.2	-0.2	-0.1	-0.1	-0.2	-0.1	-0.4
39.1	3.4	2.3	-2.1	3.8	3.4	0.8	0.3	4.1	-0.2	-0.2	-0.3	-0.2	-0.2	-0.1	-0.2	-0.1
48.8	3.5	2.3	-1.9	3.8	4.4	0.6	0.0	5.1	-0.1	-0.2	-0.2	-0.2	-0.1	-0.1	-0.1	-0.1
58.6	3.5	2.7	-2.0	3.8	5.5	0.5	0.0	5.4	-0.2	-0.2	-0.2	-0.2	-0.1	-0.2	-0.2	-0.2
68.4	3.7	2.3	-1.8	4.1	6.1	1.0	-0.3	6.4	-0.1	-0.3	-0.2	-0.3	-0.2	-0.3	-0.1	-0.1
78.1	3.9	2.2	-2.0	3.7	7.0	0.8	-0.2	7.2	-0.1	-0.2	-0.2	-0.2	-0.1	-0.2	-0.2	-0.2
87.9	3.7	2.3	-2.2	3.5	8.1	0.6	-0.1	7.9	-0.1	-0.1	-0.1	-0.1	-0.1	0.0	-0.1	-0.2
97.7	3.8	2.4	-2.3	3.8	9.1	0.5	-0.1	8.6	0.0	0.0	-0.1	-0.2	-0.1	-0.1	-0.1	-0.1
107.4	4.2	2.4	-2.2	3.8	9.9	0.5	-0.3	9.6	-0.1	-0.1	-0.1	-0.1	0.0	-0.1	-0.2	-0.1
117.2	4.2	2.4	-2.2	3.8	10.0	0.4	-0.6	10.0	-0.1	0.0	-0.2	-0.1	0.0	-0.1	-0.1	-0.1
127.0	4.3	2.5	-2.2	3.8	11.0	0.7	-0.2	11.0	-0.1	-0.1	-0.1	-0.2	-0.1	-0.2	-0.1	-0.3
136.7	4.3	1.9	-2.7	4.0	12.0	0.8	-0.1	12.0	-0.1	-0.1	-0.1	-0.1	0.0	-0.1	-0.1	-0.2

Table 137. Raw data for the test seal at ω=10 krpm, PR=0.57, C_r=0.188 mm, and inlet GVF=95%

Freq.	Re($\boldsymbol{H_{XX}}$)	Re($\boldsymbol{H_{XY}}$)	Re($\boldsymbol{H_{YX}}$)	Re($\boldsymbol{H_{YY}}$)	Im($\boldsymbol{H_{XX}}$)	Im($\boldsymbol{H_{XY}}$)	Im($\boldsymbol{H_{YX}}$)	Im($\boldsymbol{H_{YY}}$)	Re($\boldsymbol{eH_{XX}}$)	Re($\boldsymbol{eH_{XY}}$)	Re($\boldsymbol{eH_{YX}}$)	Re($\boldsymbol{eH_{YY}}$)	Im($\boldsymbol{eH_{XX}}$)	Im($\boldsymbol{eH_{XY}}$)	Im($\boldsymbol{eH_{YX}}$)	Im($\boldsymbol{eH_{YY}}$)
Hz	MN/m	MN/m	MN/m	MN/m	MN/m	MN/m	MN/m	MN/m	MN/m	MN/m	MN/m	MN/m	MN/m	MN/m	MN/m	MN/m
9.8	4.9	1.4	-2.5	2.8	-1.3	1.7	0.9	0.7	-0.3	-0.2	-0.3	-0.3	-0.4	-0.3	-0.2	-0.2
19.5	3.7	2.8	-1.4	2.7	0.1	1.2	0.8	2.7	-0.2	-0.1	-0.2	-0.2	-0.2	-0.2	-0.1	-0.1
29.3	4.0	2.3	-1.6	3.1	1.7	0.8	0.1	2.9	-0.1	-0.2	-0.3	-0.4	-0.2	-0.1	-0.2	-0.2
39.1	3.7	2.6	-1.4	3.8	3.3	0.3	-0.3	4.5	-0.1	-0.1	-0.2	-0.1	-0.1	-0.1	-0.1	-0.2
48.8	4.0	2.3	-1.4	3.5	4.3	0.7	-0.1	5.1	-0.2	-0.1	-0.2	-0.1	-0.1	-0.1	-0.1	-0.2
58.6	4.1	2.3	-1.4	3.4	5.5	0.7	-0.3	5.5	-0.1	-0.1	-0.2	-0.2	-0.1	-0.1	-0.2	-0.2
68.4	4.1	2.4	-1.6	4.1	6.3	0.6	-0.2	7.3	-0.2	-0.4	-0.1	-0.4	-0.2	-0.1	-0.3	-0.4
78.1	4.2	2.5	-1.5	3.7	7.4	0.0	0.0	6.9	-0.1	-0.1	-0.1	-0.4	-0.1	-0.2	-0.1	-0.1
87.9	4.3	2.7	-2.0	3.8	8.7	0.3	0.2	8.1	-0.1	-0.2	-0.1	-0.1	-0.1	-0.1	-0.2	-0.2
97.7	4.7	2.5	-2.2	3.5	9.2	0.6	-0.5	8.8	-0.1	-0.1	-0.1	-0.2	-0.1	-0.1	-0.2	-0.2
107.4	4.7	2.3	-1.9	3.5	9.9	0.3	-0.7	10.0	-0.2	-0.2	-0.2	-0.2	-0.2	0.0	-0.2	-0.1
117.2	4.7	2.4	-2.0	3.5	11.0	0.4	-0.6	11.0	-0.1	-0.1	-0.1	-0.1	-0.1	-0.1	-0.1	-0.1
127.0	4.4	2.5	-2.1	3.2	11.0	1.1	-0.4	12.0	-0.1	-0.1	0.0	-0.2	-0.1	-0.1	-0.2	-0.2
136.7	4.6	2.0	-2.3	3.8	12.0	0.8	-0.4	13.0	-0.1	-0.1	-0.1	-0.1	-0.1	-0.1	-0.1	-0.1

Table 138. Raw data for the test seal at ω=10 krpm, PR=0.57, C_r=0.188 mm, and inlet GVF=92%

Freq.	Re($\boldsymbol{H_{XX}}$)	Re($\boldsymbol{H_{XY}}$)	Re($\boldsymbol{H_{YX}}$)	Re($\boldsymbol{H_{YY}}$)	Im($\boldsymbol{H_{XX}}$)	Im($\boldsymbol{H_{XY}}$)	Im($\boldsymbol{H_{YX}}$)	Im($\boldsymbol{H_{YY}}$)	Re($\boldsymbol{eH_{XX}}$)	Re($\boldsymbol{eH_{XY}}$)	Re($\boldsymbol{eH_{YX}}$)	Re($\boldsymbol{eH_{YY}}$)	Im($\boldsymbol{eH_{XX}}$)	Im($\boldsymbol{eH_{XY}}$)	Im($\boldsymbol{eH_{YX}}$)	Im($\boldsymbol{eH_{YY}}$)
Hz	MN/m	MN/m	MN/m	MN/m	MN/m	MN/m	MN/m	MN/m	MN/m	MN/m	MN/m	MN/m	MN/m	MN/m	MN/m	MN/m
9.8	7.5	1.6	-1.3	7.0	0.5	0.0	-0.2	0.8	-0.1	-0.1	0.0	0.0	-0.1	-0.1	-0.1	-0.1
19.5	7.5	1.5	-1.4	7.2	1.3	0.1	0.0	1.3	-0.1	0.0	-0.1	0.0	0.0	-0.1	-0.1	-0.1
29.3	7.6	1.2	-1.8	7.4	1.9	0.3	-0.2	2.0	0.0	-0.1	-0.1	-0.1	0.0	-0.1	-0.1	-0.1
39.1	7.6	1.4	-1.5	7.3	2.8	0.2	-0.2	2.7	-0.1	-0.1	-0.1	0.0	0.0	-0.1	0.0	0.0
48.8	7.5	1.5	-1.6	7.3	3.4	0.1	-0.2	3.3	0.0	-0.1	-0.1	-0.1	-0.1	-0.1	0.0	0.0
58.6	7.6	1.6	-1.6	7.2	4.0	0.5	-0.2	3.9	0.0	-0.1	-0.1	0.0	-0.1	0.0	-0.1	-0.1
68.4	7.3	2.0	-1.5	7.0	4.8	0.6	-0.3	4.3	-0.2	-0.5	-0.1	-0.3	-0.2	-0.5	-0.1	-0.3
78.1	7.6	1.5	-1.6	7.2	5.4	0.2	-0.4	5.2	-0.1	-0.1	0.0	-0.1	0.0	-0.1	-0.1	0.0
87.9	7.6	1.5	-1.8	7.2	6.3	0.2	-0.2	5.9	0.0	-0.1	0.0	-0.1	0.0	0.0	0.0	0.0
97.7	7.6	1.4	-1.7	7.2	6.8	0.3	-0.3	6.7	-0.1	0.0	0.0	-0.1	-0.1	-0.1	0.0	-0.1
107.4	7.6	1.5	-1.5	7.2	7.6	0.4	-0.3	7.2	-0.1	0.0	0.0	-0.1	-0.1	0.0	0.0	0.0
117.2	7.9	1.5	-1.6	7.3	8.4	0.2	-0.6	8.1	-0.1	0.0	0.0	-0.1	0.0	0.0	0.0	0.0
127.0	8.0	1.4	-1.7	7.2	8.6	0.2	-0.4	8.7	0.0	-0.1	0.0	-0.1	0.0	-0.1	-0.1	-0.1
136.7	8.0	1.3	-1.9	7.2	9.1	0.4	-0.3	9.4	0.0	0.0	0.0	-0.1	0.0	-0.1	0.0	0.0

Table 139. Raw data for the test seal at ω=15 krpm, PR=0.57, C_r=0.188 mm, and inlet GVF=100%

Freq.	Re($\boldsymbol{H_{XX}}$)	Re($\boldsymbol{H_{XY}}$)	Re($\boldsymbol{H_{YX}}$)	Re($\boldsymbol{H_{YY}}$)	Im($\boldsymbol{H_{XX}}$)	Im($\boldsymbol{H_{XY}}$)	Im($\boldsymbol{H_{YX}}$)	Im($\boldsymbol{H_{YY}}$)	Re($\boldsymbol{eH_{XX}}$)	Re($\boldsymbol{eH_{XY}}$)	Re($\boldsymbol{eH_{YX}}$)	Re($\boldsymbol{eH_{YY}}$)	Im($\boldsymbol{eH_{XX}}$)	Im($\boldsymbol{eH_{XY}}$)	Im($\boldsymbol{eH_{YX}}$)	Im($\boldsymbol{eH_{YY}}$)
Hz	MN/m	MN/m	MN/m	MN/m	MN/m	MN/m	MN/m	MN/m	MN/m	MN/m	MN/m	MN/m	MN/m	MN/m	MN/m	MN/m
9.8	4.4	3.7	-4.6	4.1	0.9	0.0	0.2	1.3	-0.2	-0.1	-0.2	-0.1	-0.1	-0.1	-0.2	-0.2
19.5	4.8	4.2	-4.7	4.3	2.1	0.1	0.1	2.1	-0.1	-0.1	-0.1	-0.1	-0.1	-0.1	-0.2	-0.1
29.3	5.0	4.1	-4.6	4.3	3.1	0.1	0.2	3.1	0.0	-0.1	-0.1	-0.3	-0.1	-0.1	-0.2	-0.2
39.1	5.0	4.2	-4.8	4.7	3.9	0.2	0.1	3.7	0.0	0.0	-0.2	-0.1	0.0	-0.1	-0.1	-0.1
48.8	5.1	3.9	-4.5	4.5	4.8	0.2	0.2	4.6	0.0	-0.1	-0.1	-0.1	0.0	-0.1	-0.1	-0.1
58.6	5.4	4.1	-4.7	4.6	5.7	0.6	0.1	5.7	0.0	-0.1	-0.1	-0.2	0.0	0.0	-0.1	-0.1
68.4	5.4	4.3	-4.3	5.3	6.4	0.3	0.0	6.1	-0.1	-0.1	-0.2	-0.1	-0.1	-0.1	-0.1	-0.2
78.1	5.4	4.3	-4.3	4.8	7.0	0.4	0.1	6.7	-0.1	-0.1	-0.1	-0.1	0.0	-0.1	-0.1	0.0
87.9	5.4	4.3	-4.7	4.6	8.2	0.5	0.3	7.9	0.0	0.0	-0.1	0.0	0.0	0.0	-0.1	-0.1
97.7	5.4	4.3	-4.6	4.9	9.1	0.5	0.4	8.9	0.0	0.0	-0.1	0.0	0.0	0.0	-0.1	0.0
107.4	5.5	4.3	-4.2	5.1	10.0	0.4	0.2	9.7	-0.1	-0.1	-0.1	-0.1	0.0	0.0	0.0	-0.1
117.2	5.7	4.2	-4.3	4.9	11.0	0.3	-0.3	10.0	0.0	0.0	0.0	0.0	0.0	0.0	-0.1	-0.1
127.0	5.7	4.2	-4.4	5.2	11.0	0.4	-0.1	11.0	0.0	0.0	-0.1	-0.1	0.0	-0.1	0.0	-0.1
136.7	5.7	3.8	-4.6	5.3	12.0	0.7	-0.1	12.0	0.0	0.0	0.0	-0.1	0.0	0.0	-0.1	-0.1

Table 140. Raw data for the test seal at ω=15 krpm, PR=0.57, C_r=0.188 mm, and inlet GVF=98%

Freq.	Re(H_{XX})	Re(H_{XY})	Re(H_{YX})	Re(H_{YY})	Im(H_{XX})	Im(H_{XY})	Im(H_{YX})	Im(H_{YY})	Re(eH_{XX})	Re(eH_{XY})	Re(eH_{YX})	Re(eH_{YY})	Im(eH_{XX})	Im(eH_{XY})	Im(eH_{YX})	Im(eH_{YY})
Hz	MN/m	MN/m	MN/m	MN/m	MN/m	MN/m	MN/m	MN/m	MN/m	MN/m	MN/m	MN/m	MN/m	MN/m	MN/m	MN/m
9.8	5.3	2.8	-2.8	3.1	-0.2	0.2	-0.8	1.7	-0.2	-0.3	-0.4	-0.2	-0.3	-0.2	-0.3	-0.2
19.5	4.2	4.0	-3.4	3.6	1.3	0.4	0.0	2.8	-0.2	-0.1	-0.3	-0.3	-0.1	-0.1	-0.1	-0.4
29.3	4.4	3.6	-3.6	3.9	2.3	0.0	0.5	3.2	-0.2	-0.2	-0.2	-0.2	-0.1	-0.2	-0.2	-0.4
39.1	4.3	3.8	-3.2	3.8	3.2	0.1	0.3	3.9	-0.1	-0.1	-0.2	-0.2	-0.2	-0.1	-0.2	-0.2
48.8	4.4	3.4	-3.0	3.7	4.1	0.2	0.2	4.7	-0.1	-0.1	-0.1	0.0	-0.2	-0.1	-0.2	-0.1
58.6	4.3	3.7	-3.6	4.0	4.9	0.5	-0.3	5.7	-0.1	-0.2	-0.2	-0.3	-0.1	-0.1	-0.1	-0.3
68.4	4.6	3.8	-3.3	4.4	5.9	0.5	-0.2	6.5	-0.1	-0.1	-0.1	-0.2	-0.1	-0.2	-0.2	-0.3
78.1	4.6	3.9	-3.1	3.9	6.9	0.6	-0.3	7.5	-0.1	-0.1	-0.1	-0.2	-0.1	0.0	-0.2	-0.2
87.9	4.6	3.6	-3.1	4.2	8.0	0.4	-0.1	7.8	-0.1	-0.1	-0.1	-0.1	0.0	-0.1	-0.1	-0.2
97.7	4.8	3.8	-3.2	4.3	9.1	0.5	-0.1	8.9	-0.1	0.0	-0.1	-0.1	-0.1	-0.1	-0.1	-0.1
107.4	5.1	3.6	-3.2	4.3	9.9	0.3	-0.4	9.6	-0.1	0.0	-0.1	-0.1	-0.1	-0.1	-0.2	-0.1
117.2	5.2	3.7	-3.1	4.2	11.0	0.6	-0.8	11.0	-0.1	-0.1	-0.1	-0.1	-0.1	-0.1	-0.1	-0.1
127.0	5.0	3.5	-3.1	4.0	11.0	0.6	-0.5	12.0	-0.1	-0.1	-0.1	-0.1	-0.1	-0.1	-0.2	-0.3
136.7	5.2	3.2	-3.6	4.3	12.0	0.9	-0.5	12.0	0.0	-0.1	-0.1	-0.1	0.0	-0.1	-0.1	-0.1

Table 141. Raw data for the test seal at ω=15 krpm, PR=0.57, C_r=0.188 mm, and inlet GVF=95%

Freq.	Re(H_{XX})	Re(H_{XY})	Re(H_{YX})	Re(H_{YY})	Im(H_{XX})	Im(H_{XY})	Im(H_{YX})	Im(H_{YY})	Re(eH_{XX})	Re(eH_{XY})	Re(eH_{YX})	Re(eH_{YY})	Im(eH_{XX})	Im(eH_{XY})	Im(eH_{YX})	Im(eH_{YY})
Hz	MN/m	MN/m	MN/m	MN/m	MN/m	MN/m	MN/m	MN/m	MN/m	MN/m	MN/m	MN/m	MN/m	MN/m	MN/m	MN/m
9.8	6.1	2.5	-3.1	2.9	-0.7	0.2	-0.2	1.4	-0.3	-0.2	-0.3	-0.5	-0.3	-0.3	-0.5	-0.4
19.5	4.4	3.7	-3.0	2.8	0.9	0.6	0.2	2.1	-0.2	-0.2	-0.2	-0.3	-0.3	-0.2	-0.3	-0.2
29.3	3.7	4.1	-2.7	3.1	2.0	0.7	-0.1	3.0	-0.3	-0.4	-0.2	-0.4	-0.1	-0.2	-0.3	-0.3
39.1	4.0	3.7	-2.8	3.3	3.0	0.2	0.1	4.0	-0.1	-0.3	-0.2	-0.3	-0.1	-0.1	-0.2	-0.2
48.8	4.0	3.6	-2.6	3.3	4.1	0.3	0.3	5.6	-0.2	-0.1	-0.2	-0.2	-0.1	-0.1	-0.2	-0.4
58.6	4.5	3.7	-2.8	4.2	4.9	0.6	0.1	6.3	-0.2	-0.2	-0.2	-0.4	-0.2	-0.3	-0.3	-0.2
68.4	4.0	3.5	-2.5	3.5	6.1	0.6	-1.0	6.8	-0.1	-0.3	-0.2	-0.2	-0.1	-0.1	-0.2	-0.4
78.1	3.9	3.7	-2.9	4.1	7.2	0.6	-0.7	7.7	-0.1	-0.1	-0.1	-0.2	-0.1	-0.1	-0.2	-0.3
87.9	3.9	3.5	-2.7	3.8	8.2	0.6	-0.1	8.3	-0.1	-0.1	-0.1	-0.2	-0.1	-0.1	-0.2	-0.1
97.7	4.1	3.8	-3.4	3.6	9.1	1.0	-0.3	9.0	-0.1	-0.2	-0.1	-0.2	-0.1	-0.1	-0.1	-0.1
107.4	4.5	3.8	-2.6	3.9	10.0	1.1	-0.5	10.0	-0.1	-0.1	-0.2	-0.1	-0.2	-0.1	-0.1	-0.3
117.2	4.7	3.9	-2.6	3.3	11.0	1.0	-1.1	11.0	-0.1	-0.1	-0.2	-0.1	-0.1	-0.1	-0.1	0.0
127.0	4.8	3.8	-3.0	2.9	11.0	0.7	-0.6	12.0	-0.1	-0.1	-0.1	-0.4	-0.1	-0.2	-0.2	-0.3
136.7	4.8	3.6	-3.4	4.0	13.0	0.8	-0.9	13.0	-0.1	-0.1	-0.1	-0.2	-0.1	-0.1	-0.1	0.0

Table 142. Raw data for the test seal at ω=15 krpm, PR=0.57, C_r=0.188 mm, and inlet GVF=92%

Freq.	Re($\boldsymbol{H_{XX}}$)	Re($\boldsymbol{H_{XY}}$)	Re($\boldsymbol{H_{YX}}$)	Re($\boldsymbol{H_{YY}}$)	Im($\boldsymbol{H_{XX}}$)	Im($\boldsymbol{H_{XY}}$)	Im($\boldsymbol{H_{YX}}$)	Im($\boldsymbol{H_{YY}}$)	Re($\boldsymbol{eH_{XX}}$)	Re($\boldsymbol{eH_{XY}}$)	Re($\boldsymbol{eH_{YX}}$)	Re($\boldsymbol{eH_{YY}}$)	Im($\boldsymbol{eH_{XX}}$)	Im($\boldsymbol{eH_{XY}}$)	Im($\boldsymbol{eH_{YX}}$)	Im($\boldsymbol{eH_{YY}}$)
Hz	MN/m	MN/m	MN/m	MN/m	MN/m	MN/m	MN/m	MN/m	MN/m	MN/m	MN/m	MN/m	MN/m	MN/m	MN/m	MN/m
9.8	7.0	2.0	-2.4	6.9	0.8	0.1	0.0	0.8	0.0	-0.1	0.0	0.0	0.0	-0.1	0.0	-0.1
19.5	7.2	2.1	-2.2	7.0	1.5	0.2	0.0	1.4	0.0	-0.1	0.0	0.0	0.0	0.0	0.0	0.0
29.3	7.5	2.1	-2.5	7.1	2.0	0.2	-0.2	2.3	0.0	-0.1	-0.1	-0.1	-0.1	-0.1	-0.1	-0.1
39.1	7.4	2.2	-2.4	7.0	2.7	0.3	-0.2	2.9	-0.1	-0.1	-0.1	-0.1	-0.1	-0.1	-0.1	0.0
48.8	7.2	2.1	-2.5	7.0	3.4	0.4	-0.1	3.4	0.0	0.0	0.0	-0.1	-0.1	0.0	0.0	0.0
58.6	7.4	2.4	-2.3	7.0	4.1	0.4	-0.2	3.9	-0.1	-0.1	-0.1	0.0	0.0	-0.1	-0.1	-0.1
68.4	7.3	2.3	-2.4	7.1	4.9	0.5	-0.3	4.5	-0.1	-0.1	-0.1	-0.1	-0.1	-0.1	0.0	-0.2
78.1	7.5	2.1	-2.4	7.1	5.3	0.4	-0.3	5.2	-0.1	0.0	0.0	0.0	0.0	0.0	0.0	-0.1
87.9	7.6	2.1	-2.5	7.1	6.3	0.3	-0.4	6.0	0.0	0.0	-0.1	0.0	-0.1	0.0	0.0	0.0
97.7	7.4	2.2	-2.6	7.1	6.8	0.5	-0.3	6.6	0.0	-0.1	-0.1	-0.1	0.0	0.0	0.0	-0.1
107.4	7.5	2.4	-2.4	7.0	7.5	0.4	-0.4	7.2	-0.1	-0.1	-0.1	-0.1	-0.1	0.0	-0.1	-0.1
117.2	7.7	2.2	-2.6	7.2	8.3	0.2	-0.7	8.0	-0.1	0.0	-0.1	-0.1	-0.1	0.0	0.0	0.0
127.0	7.9	2.2	-2.6	7.2	8.6	0.3	-0.5	8.5	-0.1	-0.1	0.0	-0.1	0.0	-0.1	0.0	-0.1
136.7	7.9	1.9	-2.8	7.2	9.1	0.5	-0.3	9.2	-0.1	0.0	-0.1	0.0	0.0	-0.1	0.0	0.0

Table 143. Raw data for the test seal at ω=20 krpm, PR=0.57, C_r=0.188 mm, and inlet GVF=100%

Freq.	Re($\boldsymbol{H_{XX}}$)	Re($\boldsymbol{H_{XY}}$)	Re($\boldsymbol{H_{YX}}$)	Re($\boldsymbol{H_{YY}}$)	Im($\boldsymbol{H_{XX}}$)	Im($\boldsymbol{H_{XY}}$)	Im($\boldsymbol{H_{YX}}$)	Im($\boldsymbol{H_{YY}}$)	Re($\boldsymbol{eH_{XX}}$)	Re($\boldsymbol{eH_{XY}}$)	Re($\boldsymbol{eH_{YX}}$)	Re($\boldsymbol{eH_{YY}}$)	Im($\boldsymbol{eH_{XX}}$)	Im($\boldsymbol{eH_{XY}}$)	Im($\boldsymbol{eH_{YX}}$)	Im($\boldsymbol{eH_{YY}}$)
Hz	MN/m	MN/m	MN/m	MN/m	MN/m	MN/m	MN/m	MN/m	MN/m	MN/m	MN/m	MN/m	MN/m	MN/m	MN/m	MN/m
9.8	5.2	5.7	-6.7	3.4	0.7	-0.1	-0.1	0.8	-0.1	-0.1	-0.2	-0.2	-0.1	-0.2	-0.2	-0.1
19.5	5.1	5.2	-6.6	4.3	1.8	0.0	-0.1	2.5	-0.1	-0.1	-0.3	-0.4	-0.1	-0.2	-0.1	-0.2
29.3	5.2	5.7	-6.3	4.6	2.8	0.1	0.6	2.8	-0.1	-0.1	-0.1	-0.3	-0.1	-0.1	-0.1	-0.2
39.1	5.2	5.4	-6.7	4.6	3.6	0.3	0.1	3.7	0.0	0.0	-0.1	-0.1	-0.1	0.0	-0.2	-0.1
48.8	5.2	5.4	-6.3	4.6	4.6	0.5	0.7	4.4	-0.1	-0.1	-0.1	-0.1	-0.1	-0.1	-0.1	-0.2
58.6	5.7	5.6	-6.5	5.2	5.4	0.7	0.3	5.2	-0.1	-0.1	-0.2	-0.2	-0.1	-0.1	-0.2	-0.2
68.4	5.8	5.5	-6.5	5.1	6.0	0.6	0.1	5.9	-0.1	-0.1	-0.1	-0.2	-0.1	-0.2	-0.1	-0.1
78.1	5.7	5.9	-6.3	5.2	6.9	0.5	0.2	6.8	0.0	0.0	-0.1	-0.2	-0.1	-0.1	-0.1	-0.2
87.9	5.7	5.9	-6.6	4.6	7.8	0.5	0.2	7.7	0.0	0.0	-0.1	-0.1	0.0	-0.1	-0.1	-0.1
97.7	5.8	6.0	-6.3	4.7	8.8	0.4	0.4	8.5	0.0	0.0	-0.1	-0.1	0.0	0.0	-0.1	-0.1
107.4	5.8	6.0	-6.1	5.0	9.7	0.2	0.3	9.4	0.0	0.0	-0.1	0.0	-0.1	0.0	0.0	-0.1
117.2	5.9	5.9	-6.1	5.0	11.0	0.2	-0.1	10.0	0.0	-0.1	-0.1	-0.1	0.0	0.0	-0.1	0.0
127.0	5.9	5.6	-6.1	5.2	11.0	0.0	0.2	11.0	-0.1	-0.1	0.0	-0.1	0.0	0.0	-0.1	0.0
136.7	5.8	5.3	-6.3	5.5	12.0	0.7	0.1	12.0	0.0	0.0	0.0	0.0	0.0	0.0	0.0	0.0

Table 144. Raw data for the test seal at ω=20 krpm, PR=0.57, C_r=0.188 mm, and inlet GVF=98%

Freq.	Re($\boldsymbol{H_{XX}}$)	Re($\boldsymbol{H_{XY}}$)	Re($\boldsymbol{H_{YX}}$)	Re($\boldsymbol{H_{YY}}$)	Im($\boldsymbol{H_{XX}}$)	Im($\boldsymbol{H_{XY}}$)	Im($\boldsymbol{H_{YX}}$)	Im($\boldsymbol{H_{YY}}$)	Re($\boldsymbol{eH_{XX}}$)	Re($\boldsymbol{eH_{XY}}$)	Re($\boldsymbol{eH_{YX}}$)	Re($\boldsymbol{eH_{YY}}$)	Im($\boldsymbol{eH_{XX}}$)	Im($\boldsymbol{eH_{XY}}$)	Im($\boldsymbol{eH_{YX}}$)	Im($\boldsymbol{eH_{YY}}$)
Hz	MN/m	MN/m	MN/m	MN/m	MN/m	MN/m	MN/m	MN/m	MN/m	MN/m	MN/m	MN/m	MN/m	MN/m	MN/m	MN/m
9.8	6.4	4.6	-5.2	3.4	-1.0	-1.0	-0.5	1.2	-0.6	-0.2	-0.5	-0.3	-0.3	-0.3	-0.3	-0.5
19.5	5.3	5.3	-5.3	4.5	1.0	0.0	0.4	2.1	-0.2	-0.2	-0.3	-0.5	-0.1	-0.2	-0.2	-0.5
29.3	4.8	5.3	-4.7	3.1	2.1	0.0	0.6	3.1	-0.1	-0.2	-0.1	-0.3	-0.1	-0.2	-0.1	-0.5
39.1	5.3	4.9	-4.4	3.9	3.2	0.1	-0.2	3.9	0.0	-0.1	-0.3	-0.2	-0.1	-0.1	-0.3	-0.2
48.8	5.3	4.8	-4.4	3.9	4.2	0.4	0.2	5.1	-0.1	-0.1	-0.1	-0.2	-0.1	-0.1	-0.3	-0.1
58.6	5.2	5.0	-4.4	4.3	5.0	0.3	-0.1	5.0	-0.1	-0.1	-0.2	-0.3	-0.1	-0.1	-0.2	-0.2
68.4	5.0	4.9	-4.5	4.8	5.9	0.5	0.2	5.9	-0.1	-0.2	-0.2	-0.5	-0.1	-0.3	-0.3	-0.7
78.1	5.1	5.2	-4.4	4.5	6.5	0.6	-0.5	7.2	-0.1	-0.1	-0.2	-0.2	-0.1	-0.1	-0.2	-0.3
87.9	4.9	5.1	-4.8	4.3	7.8	0.6	-0.3	8.0	-0.1	0.0	-0.1	-0.1	-0.1	-0.1	-0.1	-0.2
97.7	4.9	5.4	-4.6	4.3	8.8	0.7	-0.4	9.1	-0.1	-0.1	-0.1	-0.1	-0.1	-0.1	-0.1	-0.1
107.4	5.2	5.4	-4.5	4.5	9.9	0.7	-1.0	9.8	-0.1	-0.1	-0.2	-0.1	-0.1	-0.1	-0.1	-0.1
117.2	5.4	5.3	-4.5	4.2	11.0	0.6	-0.7	11.0	-0.1	-0.1	-0.1	-0.1	-0.1	-0.1	-0.2	-0.1
127.0	5.5	5.1	-4.8	4.5	11.0	0.7	-0.6	12.0	-0.1	-0.2	-0.1	-0.2	-0.1	-0.2	-0.1	-0.2
136.7	5.8	4.8	-4.9	5.0	12.0	0.9	-0.5	12.0	0.0	-0.1	-0.1	-0.2	0.0	-0.1	-0.1	-0.1

Table 145. Raw data for the test seal at ω=20 krpm, PR=0.57, C_r=0.188 mm, and inlet GVF=95%

Freq.	Re($\boldsymbol{H_{XX}}$)	Re($\boldsymbol{H_{XY}}$)	Re($\boldsymbol{H_{YX}}$)	Re($\boldsymbol{H_{YY}}$)	Im($\boldsymbol{H_{XX}}$)	Im($\boldsymbol{H_{XY}}$)	Im($\boldsymbol{H_{YX}}$)	Im($\boldsymbol{H_{YY}}$)	Re($\boldsymbol{eH_{XX}}$)	Re($\boldsymbol{eH_{XY}}$)	Re($\boldsymbol{eH_{YX}}$)	Re($\boldsymbol{eH_{YY}}$)	Im($\boldsymbol{eH_{XX}}$)	Im($\boldsymbol{eH_{XY}}$)	Im($\boldsymbol{eH_{YX}}$)	Im($\boldsymbol{eH_{YY}}$)
Hz	MN/m	MN/m	MN/m	MN/m	MN/m	MN/m	MN/m	MN/m	MN/m	MN/m	MN/m	MN/m	MN/m	MN/m	MN/m	MN/m
9.8	5.4	3.7	-4.9	2.6	0.2	0.0	-0.6	1.8	-0.4	-0.4	-0.6	-0.4	-0.4	-0.4	-0.3	-0.6
19.5	5.4	5.4	-4.9	2.6	0.9	0.1	-0.3	2.2	-0.2	-0.1	-0.4	-0.2	-0.2	-0.2	-0.3	-0.2
29.3	4.2	5.1	-4.7	3.3	1.9	0.5	1.0	3.0	-0.1	-0.2	-0.1	-0.3	-0.1	-0.1	-0.2	-0.4
39.1	4.8	5.0	-4.5	2.6	3.3	0.1	1.0	4.1	-0.2	-0.1	-0.3	-0.2	-0.1	-0.2	-0.2	-0.1
48.8	4.7	5.0	-3.8	2.8	4.4	0.3	0.5	4.9	-0.3	-0.1	-0.1	-0.3	-0.1	-0.1	-0.3	-0.3
58.6	5.0	5.0	-3.6	3.2	5.2	0.1	-0.3	5.9	-0.1	-0.2	-0.2	-0.5	-0.3	-0.2	-0.3	-0.1
68.4	4.6	4.5	-4.2	3.9	5.8	0.4	-0.2	7.0	-0.2	-0.5	-0.2	-0.3	-0.1	-0.1	-0.1	-0.2
78.1	4.6	4.5	-4.0	3.7	6.6	0.5	-0.4	7.6	-0.3	-0.2	-0.2	-0.3	-0.1	-0.1	-0.2	-0.1
87.9	4.5	4.6	-4.3	3.3	7.8	0.8	-0.5	8.3	-0.1	-0.1	-0.1	-0.1	-0.1	-0.1	-0.1	-0.2
97.7	4.6	4.6	-4.4	3.6	8.8	1.1	-0.3	9.4	-0.1	-0.1	-0.1	-0.2	-0.1	-0.1	-0.2	-0.1
107.4	4.7	4.9	-4.0	3.7	9.8	0.6	-1.1	10.0	-0.1	-0.1	-0.1	-0.2	-0.2	-0.1	-0.1	-0.2
117.2	5.3	4.9	-4.2	3.5	11.0	0.8	-1.1	11.0	-0.2	0.0	-0.1	-0.1	0.0	-0.1	-0.2	-0.1
127.0	5.2	5.0	-4.0	3.6	11.0	1.2	-0.6	11.0	-0.1	-0.3	-0.1	-0.3	-0.2	-0.2	-0.2	-0.2
136.7	5.1	4.9	-4.9	3.7	12.0	1.0	-1.1	13.0	-0.1	-0.1	-0.1	-0.1	-0.1	-0.2	-0.2	-0.2

Table 146. Raw data for the test seal at ω=20 krpm, PR=0.57, C_r=0.188 mm, and inlet GVF=92%

Freq.	Re(H_{XX})	Re(H_{XY})	Re(H_{YX})	Re(H_{YY})	Im(H_{XX})	Im(H_{XY})	Im(H_{YX})	Im(H_{YY})	Re(eH_{XX})	Re(eH_{XY})	Re(eH_{YX})	Re(eH_{YY})	Im(eH_{XX})	Im(eH_{XY})	Im(eH_{YX})	Im(eH_{YY})
Hz	MN/m	MN/m	MN/m	MN/m	MN/m	MN/m	MN/m	MN/m	MN/m	MN/m	MN/m	MN/m	MN/m	MN/m	MN/m	MN/m
9.8	6.4	1.0	-0.5	5.9	0.7	0.0	-0.1	0.6	-0.1	0.0	-0.1	-0.1	0.0	-0.1	-0.1	0.0
19.5	6.5	1.1	-0.7	5.9	1.4	0.1	-0.2	1.3	-0.1	0.0	-0.1	0.0	-0.1	0.0	0.0	-0.1
29.3	6.4	1.0	-0.9	6.3	2.1	-0.2	-0.1	2.2	0.0	-0.1	-0.1	-0.1	-0.1	-0.1	0.0	-0.1
39.1	6.3	1.2	-0.7	5.9	2.9	0.2	-0.1	3.2	0.0	-0.1	0.0	-0.1	-0.1	0.0	0.0	0.0
48.8	6.3	1.1	-0.8	6.0	3.5	0.0	0.1	3.8	0.0	0.0	-0.1	-0.1	0.0	-0.1	-0.1	-0.1
58.6	6.4	1.2	-0.7	6.1	4.5	0.2	-0.1	4.4	-0.1	-0.2	-0.1	-0.1	0.0	-0.1	-0.1	-0.1
68.4	6.3	1.3	-0.8	6.0	5.3	-0.1	-0.2	5.3	-0.1	-0.1	0.0	-0.1	-0.1	-0.1	0.0	-0.2
78.1	6.4	1.2	-0.8	6.0	6.0	0.0	-0.2	5.8	-0.1	0.0	0.0	-0.1	-0.1	-0.1	0.0	-0.1
87.9	6.5	1.1	-0.9	6.1	7.0	0.1	-0.1	6.8	-0.1	0.0	0.0	0.0	0.0	0.0	0.0	-0.1
97.7	6.4	1.0	-0.9	6.2	7.6	0.1	-0.1	7.5	0.0	-0.1	-0.1	-0.1	-0.1	0.0	0.0	0.0
107.4	6.5	1.2	-0.8	6.3	8.6	0.1	-0.2	8.2	-0.1	0.0	0.0	0.0	0.0	-0.1	0.0	0.0
117.2	6.7	1.0	-0.9	6.3	9.2	0.0	-0.4	9.1	-0.1	0.0	-0.1	0.0	-0.1	0.0	0.0	0.0
127.0	6.9	0.9	-1.0	6.5	9.7	0.1	-0.3	9.8	-0.1	-0.1	-0.1	-0.1	0.0	-0.1	0.0	-0.2
136.7	7.0	0.9	-1.2	6.5	10.0	0.1	-0.2	11.0	0.0	0.0	-0.1	0.0	0.0	0.0	0.0	0.0

Table 147. Raw data for the test seal at ω=10 krpm, PR=0.5, C_r=0.188 mm, and inlet GVF=100%

Freq.	Re(H_{XX})	Re(H_{XY})	Re(H_{YX})	Re(H_{YY})	Im(H_{XX})	Im(H_{XY})	Im(H_{YX})	Im(H_{YY})	Re(eH_{XX})	Re(eH_{XY})	Re(eH_{YX})	Re(eH_{YY})	Im(eH_{XX})	Im(eH_{XY})	Im(eH_{YX})	Im(eH_{YY})
Hz	MN/m	MN/m	MN/m	MN/m	MN/m	MN/m	MN/m	MN/m	MN/m	MN/m	MN/m	MN/m	MN/m	MN/m	MN/m	MN/m
9.8	4.1	2.5	-2.3	4.0	0.4	0.3	0.0	1.1	-0.2	-0.2	-0.2	-0.1	-0.1	-0.1	-0.2	-0.1
19.5	4.2	2.9	-2.6	4.3	2.2	0.1	0.2	2.1	-0.1	0.0	-0.1	-0.1	-0.2	-0.1	-0.1	-0.2
29.3	4.5	2.9	-2.4	4.5	3.4	0.2	0.4	3.1	-0.1	-0.1	-0.2	-0.2	-0.1	-0.1	-0.1	-0.2
39.1	4.7	2.8	-2.4	4.7	4.0	0.1	0.2	4.0	-0.1	0.0	-0.2	-0.1	-0.1	-0.1	-0.1	-0.1
48.8	4.9	2.6	-2.5	4.6	5.1	0.3	0.3	4.9	-0.1	-0.1	-0.1	-0.1	-0.1	-0.1	-0.1	-0.1
58.6	5.1	2.8	-2.4	4.7	5.7	0.5	0.2	5.9	0.0	-0.1	-0.2	0.0	-0.1	-0.1	-0.1	0.0
68.4	5.1	2.8	-2.3	4.8	6.7	0.4	0.0	6.8	-0.1	-0.1	-0.1	-0.2	-0.1	-0.1	-0.1	-0.2
78.1	5.3	3.0	-2.2	5.0	7.4	0.3	0.0	7.3	-0.1	0.0	-0.1	-0.1	0.0	-0.1	-0.1	-0.1
87.9	5.2	2.8	-2.6	4.9	8.5	0.5	0.1	8.4	0.0	0.0	0.0	-0.1	-0.1	0.0	0.0	0.0
97.7	5.4	2.9	-2.8	5.1	9.4	0.6	0.3	9.5	0.0	0.0	-0.1	0.0	0.0	0.0	-0.1	0.0
107.4	5.4	2.9	-2.4	5.2	10.0	0.4	0.1	9.9	0.0	0.0	-0.1	-0.1	-0.1	0.0	-0.1	0.0
117.2	5.5	2.9	-2.5	5.3	11.0	0.5	-0.2	11.0	-0.1	0.0	-0.1	0.0	0.0	0.0	-0.1	-0.1
127.0	5.4	3.0	-2.5	5.4	12.0	0.6	0.2	12.0	-0.1	0.0	-0.1	-0.1	0.0	-0.1	-0.1	-0.1
136.7	5.5	2.9	-2.7	5.8	13.0	0.7	0.3	12.0	0.0	-0.1	0.0	-0.1	0.0	0.0	-0.1	-0.1

Table 148. Raw data for the test seal at ω=10 krpm, PR=0.5, C_r=0.188 mm, and inlet GVF=98%

Freq.	Re($\boldsymbol{H_{XX}}$)	Re($\boldsymbol{H_{XY}}$)	Re($\boldsymbol{H_{YX}}$)	Re($\boldsymbol{H_{YY}}$)	Im($\boldsymbol{H_{XX}}$)	Im($\boldsymbol{H_{XY}}$)	Im($\boldsymbol{H_{YX}}$)	Im($\boldsymbol{H_{YY}}$)	Re($\boldsymbol{eH_{XX}}$)	Re($\boldsymbol{eH_{XY}}$)	Re($\boldsymbol{eH_{YX}}$)	Re($\boldsymbol{eH_{YY}}$)	Im($\boldsymbol{eH_{XX}}$)	Im($\boldsymbol{eH_{XY}}$)	Im($\boldsymbol{eH_{YX}}$)	Im($\boldsymbol{eH_{YY}}$)
Hz	MN/m	MN/m	MN/m	MN/m	MN/m	MN/m	MN/m	MN/m	MN/m	MN/m	MN/m	MN/m	MN/m	MN/m	MN/m	MN/m
9.8	4.7	2.4	-2.9	2.4	-0.6	0.9	0.1	1.2	-0.3	-0.1	-0.3	-0.3	-0.2	-0.3	-0.2	-0.2
19.5	3.6	2.7	-2.6	3.2	1.5	0.3	1.2	2.3	-0.1	-0.1	-0.1	-0.2	-0.2	-0.1	-0.1	-0.1
29.3	3.8	2.4	-2.3	3.9	2.8	0.7	0.2	3.7	-0.1	-0.1	-0.2	-0.5	-0.1	-0.1	-0.3	-0.4
39.1	4.1	2.7	-2.0	3.1	3.9	0.6	0.2	4.6	-0.1	-0.1	-0.2	-0.2	0.0	-0.1	-0.2	-0.3
48.8	3.9	2.7	-2.5	3.4	5.0	0.8	0.4	5.5	-0.2	-0.1	-0.2	-0.2	-0.1	-0.2	-0.2	-0.3
58.6	4.4	2.8	-2.3	3.8	5.6	1.0	0.1	6.1	-0.2	-0.1	-0.1	-0.2	-0.1	-0.1	-0.2	-0.1
68.4	4.3	3.2	-2.5	4.5	6.6	0.0	0.0	6.4	-0.2	-0.3	-0.1	-0.5	-0.1	-0.2	-0.1	-0.5
78.1	4.6	3.3	-2.3	4.3	7.7	0.3	-0.2	7.6	-0.1	-0.1	-0.1	-0.1	-0.1	-0.1	-0.1	-0.2
87.9	4.4	2.6	-2.8	4.0	9.2	0.5	0.3	8.7	-0.1	-0.2	-0.1	-0.1	-0.1	-0.1	-0.1	-0.1
97.7	5.0	2.9	-2.6	4.1	10.0	0.6	0.0	9.8	-0.1	-0.1	-0.1	-0.1	-0.1	-0.1	-0.1	-0.1
107.4	4.8	3.1	-2.3	4.2	11.0	0.4	-0.1	10.0	-0.1	-0.1	-0.2	-0.1	-0.1	-0.1	-0.2	-0.1
117.2	5.0	2.8	-2.4	3.8	12.0	0.4	0.0	11.0	-0.1	-0.1	-0.1	-0.1	-0.1	0.0	-0.1	-0.1
127.0	5.0	2.8	-2.7	4.1	12.0	0.7	0.1	12.0	-0.1	-0.2	-0.1	-0.4	-0.1	-0.1	-0.1	-0.2
136.7	5.1	2.7	-3.1	4.4	13.0	0.7	0.0	13.0	-0.1	-0.1	-0.1	-0.1	-0.1	-0.1	-0.1	-0.1

Table 149. Raw data for the test seal at ω=10 krpm, PR=0.5, C_r=0.188 mm, and inlet GVF=95%

Freq.	Re($\boldsymbol{H_{XX}}$)	Re($\boldsymbol{H_{XY}}$)	Re($\boldsymbol{H_{YX}}$)	Re($\boldsymbol{H_{YY}}$)	Im($\boldsymbol{H_{XX}}$)	Im($\boldsymbol{H_{XY}}$)	Im($\boldsymbol{H_{YX}}$)	Im($\boldsymbol{H_{YY}}$)	Re($\boldsymbol{eH_{XX}}$)	Re($\boldsymbol{eH_{XY}}$)	Re($\boldsymbol{eH_{YX}}$)	Re($\boldsymbol{eH_{YY}}$)	Im($\boldsymbol{eH_{XX}}$)	Im($\boldsymbol{eH_{XY}}$)	Im($\boldsymbol{eH_{YX}}$)	Im($\boldsymbol{eH_{YY}}$)
Hz	MN/m	MN/m	MN/m	MN/m	MN/m	MN/m	MN/m	MN/m	MN/m	MN/m	MN/m	MN/m	MN/m	MN/m	MN/m	MN/m
9.8	5.0	0.8	-3.2	1.8	-1.5	1.9	1.3	-0.3	-0.3	-0.2	-0.4	-0.6	-0.3	-0.3	-0.6	-0.2
19.5	3.5	2.2	-2.3	1.5	0.7	1.8	0.6	2.5	-0.2	-0.1	-0.3	-0.3	-0.1	-0.2	-0.3	-0.2
29.3	3.3	2.8	-1.7	2.7	2.1	1.0	0.7	3.7	-0.2	-0.3	-0.2	-0.2	-0.1	-0.2	-0.2	-0.3
39.1	3.5	3.0	-1.7	2.6	3.7	0.7	0.7	4.7	-0.1	-0.1	-0.1	-0.3	-0.1	0.0	-0.3	0.0
48.8	3.9	2.9	-2.2	2.7	5.4	0.6	0.2	5.7	-0.2	-0.2	-0.1	-0.2	-0.2	-0.2	-0.2	-0.2
58.6	4.1	2.8	-2.3	3.0	5.8	0.8	0.7	6.6	-0.2	-0.2	-0.2	-0.3	-0.1	-0.2	-0.2	-0.1
68.4	4.0	3.1	-1.9	2.8	6.7	0.4	0.0	7.5	-0.2	-0.2	-0.2	-0.4	-0.2	-0.2	-0.2	-0.3
78.1	4.3	2.8	-2.2	3.1	7.9	0.6	-0.4	8.3	-0.2	-0.2	-0.2	-0.3	-0.1	-0.3	-0.2	-0.5
87.9	4.2	2.9	-2.3	3.0	8.9	0.6	0.2	8.8	-0.2	-0.2	-0.1	-0.3	-0.1	-0.1	-0.1	-0.1
97.7	4.3	3.0	-2.6	3.1	10.0	0.3	-0.1	9.8	-0.1	-0.1	-0.2	-0.2	-0.2	-0.2	-0.1	-0.2
107.4	4.6	3.0	-2.0	3.0	11.0	0.5	0.0	11.0	-0.1	-0.1	-0.2	-0.1	-0.1	-0.1	-0.2	-0.2
117.2	4.8	2.9	-2.3	2.7	12.0	0.3	-0.1	12.0	-0.1	-0.1	-0.2	-0.2	0.0	-0.1	-0.2	-0.1
127.0	4.7	2.7	-2.3	3.1	12.0	0.3	0.1	13.0	-0.1	-0.2	-0.2	-0.2	-0.1	-0.1	-0.2	-0.3
136.7	4.6	2.4	-3.0	2.8	14.0	0.8	-0.1	15.0	-0.1	-0.2	-0.2	-0.1	0.0	-0.1	-0.1	-0.1

Table 150. Raw data for the test seal at ω=10 krpm, PR=0.5, C_r=0.188 mm, and inlet GVF=92%

Freq.	Re(H_{XX})	Re(H_{XY})	Re(H_{YX})	Re(H_{YY})	Im(H_{XX})	Im(H_{XY})	Im(H_{YX})	Im(H_{YY})	Re(eH_{XX})	Re(eH_{XY})	Re(eH_{YX})	Re(eH_{YY})	Im(eH_{XX})	Im(eH_{XY})	Im(eH_{YX})	Im(eH_{YY})
Hz	MN/m	MN/m	MN/m	MN/m	MN/m	MN/m	MN/m	MN/m	MN/m	MN/m	MN/m	MN/m	MN/m	MN/m	MN/m	MN/m
9.8	6.1	1.6	-1.3	5.7	0.8	0.0	0.0	0.8	0.0	0.0	-0.1	-0.1	0.0	-0.1	-0.1	0.0
19.5	6.1	1.8	-1.5	5.6	1.5	0.2	-0.2	1.5	-0.1	0.0	0.0	0.0	-0.1	-0.1	0.0	-0.1
29.3	6.4	1.9	-1.7	5.8	2.1	0.2	0.0	2.6	0.0	-0.2	-0.1	0.0	-0.1	-0.1	0.0	-0.1
39.1	6.2	1.7	-1.6	5.8	2.9	0.1	-0.2	3.2	0.0	-0.1	-0.1	-0.1	0.0	0.0	0.0	-0.1
48.8	6.4	1.9	-1.6	5.9	3.8	0.1	-0.1	3.7	0.0	0.0	-0.1	-0.1	0.0	-0.1	0.0	-0.1
58.6	6.3	1.9	-1.5	5.9	4.4	0.2	-0.2	4.5	0.0	-0.1	0.0	-0.1	0.0	0.0	-0.1	0.0
68.4	6.1	1.8	-1.7	5.9	5.7	0.4	-0.6	5.0	-0.1	-0.3	-0.1	-0.3	-0.1	-0.4	-0.1	-0.2
78.1	6.3	1.8	-1.7	5.7	6.0	0.2	-0.3	6.0	-0.1	0.0	0.0	0.0	-0.1	0.0	0.0	-0.1
87.9	6.4	1.8	-1.7	5.8	6.9	0.2	-0.2	6.8	0.0	0.0	0.0	0.0	0.0	0.0	0.0	0.0
97.7	6.3	1.8	-1.7	5.9	7.7	0.0	-0.1	7.5	0.0	-0.1	0.0	0.0	-0.1	-0.1	0.0	0.0
107.4	6.6	1.8	-1.6	5.9	8.4	0.1	-0.3	8.1	0.0	-0.1	0.0	-0.1	0.0	0.0	0.0	-0.1
117.2	6.7	1.8	-1.6	6.1	9.3	0.0	-0.6	9.0	0.0	-0.1	-0.1	-0.1	0.0	0.0	0.0	0.0
127.0	6.9	1.7	-1.8	6.4	9.6	0.1	-0.3	9.8	0.0	-0.1	0.0	-0.1	0.0	-0.1	0.0	-0.1
136.7	6.9	1.5	-2.0	6.4	10.0	0.1	-0.2	10.0	0.0	0.0	0.0	-0.1	0.0	-0.1	0.0	0.0

Table 151. Raw data for the test seal at ω=15 krpm, PR=0.5, C_r=0.188 mm, and inlet GVF=100%

Freq.	Re(H_{XX})	Re(H_{XY})	Re(H_{YX})	Re(H_{YY})	Im(H_{XX})	Im(H_{XY})	Im(H_{YX})	Im(H_{YY})	Re(eH_{XX})	Re(eH_{XY})	Re(eH_{YX})	Re(eH_{YY})	Im(eH_{XX})	Im(eH_{XY})	Im(eH_{YX})	Im(eH_{YY})
Hz	MN/m	MN/m	MN/m	MN/m	MN/m	MN/m	MN/m	MN/m	MN/m	MN/m	MN/m	MN/m	MN/m	MN/m	MN/m	MN/m
9.8	4.1	3.9	-4.2	3.5	0.3	0.0	0.0	1.2	-0.1	-0.2	-0.2	-0.2	-0.2	-0.2	-0.3	-0.1
19.5	3.8	4.0	-4.2	3.9	1.6	-0.1	0.0	1.9	-0.2	-0.2	-0.3	-0.1	-0.1	-0.1	-0.1	-0.2
29.3	3.9	3.9	-4.3	4.2	2.8	0.3	0.1	3.4	-0.2	-0.2	-0.2	-0.5	-0.2	-0.4	-0.1	-0.4
39.1	4.4	3.8	-4.3	3.8	4.1	-0.2	0.1	3.6	0.0	-0.1	-0.1	-0.1	-0.1	-0.1	-0.1	-0.2
48.8	4.4	3.7	-4.5	4.3	4.9	0.2	0.3	4.6	-0.1	-0.1	-0.1	-0.1	-0.1	-0.1	-0.2	-0.1
58.6	4.7	4.0	-4.1	4.6	5.7	0.4	0.3	5.6	-0.1	-0.1	-0.1	-0.2	-0.1	-0.1	-0.1	-0.1
68.4	4.9	3.8	-4.0	4.7	6.6	0.2	0.0	6.4	-0.2	-0.3	-0.1	-0.2	-0.1	-0.1	-0.2	-0.3
78.1	4.9	3.9	-4.2	4.5	7.5	0.2	0.0	7.3	-0.1	-0.1	-0.1	-0.2	-0.1	-0.1	-0.2	0.0
87.9	4.9	4.0	-4.4	4.6	8.5	0.4	0.2	8.3	-0.1	-0.1	-0.1	-0.1	-0.1	-0.1	-0.1	-0.1
97.7	5.0	4.1	-4.3	4.7	9.6	0.5	0.5	9.4	0.0	0.0	-0.1	-0.1	-0.1	-0.1	-0.1	-0.1
107.4	5.2	4.2	-3.8	5.0	10.0	0.2	0.5	10.0	-0.1	-0.1	-0.2	-0.1	-0.1	0.0	-0.1	-0.1
117.2	5.2	4.0	-4.3	5.0	11.0	0.3	-0.3	11.0	-0.1	0.0	-0.1	0.0	0.0	0.0	-0.1	0.0
127.0	5.5	4.1	-4.4	5.5	12.0	0.5	0.4	12.0	-0.1	-0.2	-0.1	-0.3	-0.1	-0.1	-0.1	-0.1
136.7	5.7	3.9	-4.4	5.5	13.0	0.5	0.4	13.0	-0.1	-0.1	0.0	0.0	0.0	-0.1	-0.1	-0.1

Table 152. Raw data for the test seal at ω=15 krpm, PR=0.5, C_r=0.188 mm, and inlet GVF=98%

Freq.	Re($\boldsymbol{H_{XX}}$)	Re($\boldsymbol{H_{XY}}$)	Re($\boldsymbol{H_{YX}}$)	Re($\boldsymbol{H_{YY}}$)	Im($\boldsymbol{H_{XX}}$)	Im($\boldsymbol{H_{XY}}$)	Im($\boldsymbol{H_{YX}}$)	Im($\boldsymbol{H_{YY}}$)	Re($\boldsymbol{eH_{XX}}$)	Re($\boldsymbol{eH_{XY}}$)	Re($\boldsymbol{eH_{YX}}$)	Re($\boldsymbol{eH_{YY}}$)	Im($\boldsymbol{eH_{XX}}$)	Im($\boldsymbol{eH_{XY}}$)	Im($\boldsymbol{eH_{YX}}$)	Im($\boldsymbol{eH_{YY}}$)
Hz	MN/m	MN/m	MN/m	MN/m	MN/m	MN/m	MN/m	MN/m	MN/m	MN/m	MN/m	MN/m	MN/m	MN/m	MN/m	MN/m
9.8	4.7	3.6	-3.7	2.7	-0.3	0.4	-0.9	0.8	-0.3	-0.5	-0.4	-0.2	-0.4	-0.1	-0.2	-0.5
19.5	3.8	4.3	-4.0	2.7	1.3	0.1	0.2	1.8	-0.3	-0.2	-0.2	-0.2	-0.1	-0.1	-0.2	-0.2
29.3	3.3	4.3	-4.0	2.1	2.2	0.8	1.0	3.5	-0.2	-0.3	-0.2	-0.4	-0.1	-0.2	-0.2	-0.4
39.1	3.7	4.0	-3.3	3.1	3.5	0.1	-0.1	4.1	-0.2	-0.1	-0.3	-0.2	-0.1	-0.2	-0.1	-0.3
48.8	3.7	4.2	-3.4	3.4	4.6	0.3	0.2	5.1	-0.1	-0.2	-0.2	-0.3	-0.2	-0.2	-0.2	-0.3
58.6	3.5	4.5	-3.3	3.5	5.4	0.3	-0.2	6.3	-0.1	-0.2	-0.3	-0.1	-0.1	-0.1	-0.2	-0.3
68.4	3.7	3.8	-3.4	3.4	6.6	0.3	-0.1	6.9	-0.2	-0.1	-0.2	-0.4	-0.2	-0.2	-0.2	-0.3
78.1	3.6	3.8	-3.9	3.2	7.4	0.5	-0.5	7.9	-0.1	-0.1	-0.1	-0.2	-0.2	-0.1	-0.3	-0.2
87.9	3.8	4.4	-3.7	3.7	8.7	0.1	-0.3	8.6	-0.1	-0.1	-0.1	-0.1	-0.2	-0.1	-0.2	-0.1
97.7	4.1	4.1	-3.6	3.6	9.8	0.6	0.0	10.0	-0.2	-0.1	-0.1	-0.1	-0.1	-0.2	-0.2	-0.1
107.4	4.5	4.2	-3.5	3.7	11.0	0.3	-0.5	10.0	-0.1	-0.1	-0.1	-0.1	-0.1	0.0	-0.1	-0.1
117.2	4.7	4.2	-3.5	3.6	12.0	0.0	-0.6	11.0	-0.2	-0.1	-0.2	-0.1	-0.1	-0.1	-0.2	-0.2
127.0	4.9	3.9	-3.8	4.1	12.0	0.0	0.0	13.0	-0.1	-0.2	-0.2	-0.3	-0.1	-0.1	-0.1	-0.4
136.7	4.9	3.9	-4.0	3.9	13.0	0.4	-0.5	14.0	-0.1	-0.1	-0.1	-0.1	-0.1	-0.1	-0.2	-0.1

Table 153. Raw data for the test seal at ω=15 krpm, PR=0.5, C_r=0.188 mm, and inlet GVF=95%

Freq.	Re($\boldsymbol{H_{XX}}$)	Re($\boldsymbol{H_{XY}}$)	Re($\boldsymbol{H_{YX}}$)	Re($\boldsymbol{H_{YY}}$)	Im($\boldsymbol{H_{XX}}$)	Im($\boldsymbol{H_{XY}}$)	Im($\boldsymbol{H_{YX}}$)	Im($\boldsymbol{H_{YY}}$)	Re($\boldsymbol{eH_{XX}}$)	Re($\boldsymbol{eH_{XY}}$)	Re($\boldsymbol{eH_{YX}}$)	Re($\boldsymbol{eH_{YY}}$)	Im($\boldsymbol{eH_{XX}}$)	Im($\boldsymbol{eH_{XY}}$)	Im($\boldsymbol{eH_{YX}}$)	Im($\boldsymbol{eH_{YY}}$)
Hz	MN/m	MN/m	MN/m	MN/m	MN/m	MN/m	MN/m	MN/m	MN/m	MN/m	MN/m	MN/m	MN/m	MN/m	MN/m	MN/m
9.8	4.2	3.8	-3.4	1.7	0.2	0.3	0.5	1.6	-0.5	-0.4	-0.4	-0.3	-0.6	-0.2	-0.7	-0.7
19.5	3.4	4.1	-3.9	1.9	0.3	1.1	0.4	2.4	-0.2	-0.2	-0.3	-0.6	-0.3	-0.2	-0.2	-0.3
29.3	3.1	3.7	-3.4	2.5	2.0	0.0	0.6	3.2	-0.4	-0.7	-0.5	-1.2	-0.2	-0.2	-0.3	-0.9
39.1	3.0	3.5	-3.7	1.9	3.5	-0.2	0.6	4.9	-0.1	-0.1	-0.3	-0.2	-0.1	-0.1	-0.2	-0.4
48.8	2.9	3.3	-3.0	2.2	4.7	0.2	0.6	5.7	-0.2	-0.3	-0.4	-0.3	-0.2	-0.4	-0.2	-0.3
58.6	2.8	3.7	-2.9	2.7	5.7	0.8	-0.1	7.4	-0.2	-0.2	-0.3	-0.3	-0.3	-0.1	-0.2	-0.3
68.4	3.3	3.8	-3.1	3.5	6.8	0.9	-0.5	6.9	-0.2	-0.5	-0.3	-0.5	-0.3	-0.7	-0.1	-0.3
78.1	3.3	3.7	-2.6	3.3	8.0	0.3	-0.3	8.2	-0.1	-0.3	-0.3	-0.3	-0.2	-0.2	-0.2	-0.4
87.9	3.4	3.6	-3.3	2.6	9.0	0.8	-0.2	9.6	-0.1	-0.2	-0.2	-0.3	-0.1	-0.2	-0.2	-0.2
97.7	4.0	3.6	-3.1	3.3	10.0	0.6	-0.3	9.8	-0.1	-0.2	-0.2	-0.3	-0.2	-0.1	-0.2	-0.2
107.4	4.1	3.7	-2.5	2.8	11.0	0.6	-0.5	11.0	-0.2	-0.1	-0.3	-0.2	-0.2	-0.1	-0.3	-0.2
117.2	4.4	3.9	-3.4	3.0	12.0	0.4	-0.7	12.0	-0.2	-0.2	-0.3	-0.2	-0.1	-0.1	-0.3	-0.2
127.0	4.6	3.9	-3.5	3.3	13.0	0.6	-0.5	13.0	-0.1	-0.4	-0.1	-0.6	-0.1	-0.3	-0.2	-0.3
136.7	4.6	4.1	-3.9	2.7	14.0	0.9	-0.6	15.0	-0.2	-0.2	-0.2	-0.2	-0.1	-0.2	-0.3	-0.3

Table 154. Raw data for the test seal at ω=15 krpm, PR=0.5, C_r=0.188 mm, and inlet GVF=92%

Freq.	Re($\boldsymbol{H_{XX}}$)	Re($\boldsymbol{H_{XY}}$)	Re($\boldsymbol{H_{YX}}$)	Re($\boldsymbol{H_{YY}}$)	Im($\boldsymbol{H_{XX}}$)	Im($\boldsymbol{H_{XY}}$)	Im($\boldsymbol{H_{YX}}$)	Im($\boldsymbol{H_{YY}}$)	Re($\boldsymbol{eH_{XX}}$)	Re($\boldsymbol{eH_{XY}}$)	Re($\boldsymbol{eH_{YX}}$)	Re($\boldsymbol{eH_{YY}}$)	Im($\boldsymbol{eH_{XX}}$)	Im($\boldsymbol{eH_{XY}}$)	Im($\boldsymbol{eH_{YX}}$)	Im($\boldsymbol{eH_{YY}}$)
Hz	MN/m	MN/m	MN/m	MN/m	MN/m	MN/m	MN/m	MN/m	MN/m	MN/m	MN/m	MN/m	MN/m	MN/m	MN/m	MN/m
9.8	5.7	2.5	-2.4	5.3	0.8	0.0	0.0	0.8	0.0	0.0	0.0	-0.1	-0.1	0.0	-0.1	0.0
19.5	5.6	2.6	-2.3	5.5	1.6	0.1	0.0	1.7	-0.1	-0.1	0.0	-0.1	-0.1	0.0	-0.1	0.0
29.3	5.8	2.6	-2.5	5.5	2.1	0.4	0.0	2.2	0.0	-0.1	-0.1	-0.1	0.0	-0.1	0.0	-0.1
39.1	5.9	2.7	-2.4	5.7	3.0	0.0	-0.2	3.1	0.0	-0.1	0.0	-0.1	0.0	-0.1	0.0	-0.1
48.8	5.9	2.7	-2.5	5.4	3.8	0.0	-0.3	3.9	0.0	-0.1	0.0	-0.1	0.0	-0.1	0.0	-0.1
58.6	5.8	2.7	-2.5	5.4	4.4	0.2	-0.3	4.3	-0.1	-0.1	0.0	-0.1	-0.1	-0.1	-0.1	-0.1
68.4	5.9	2.7	-2.6	5.7	5.5	0.2	-0.3	5.1	-0.1	-0.2	0.0	-0.1	-0.1	-0.2	-0.1	-0.1
78.1	5.9	2.5	-2.4	5.5	5.9	0.1	-0.4	5.9	0.0	0.0	0.0	-0.1	0.0	0.0	0.0	0.0
87.9	6.1	2.5	-2.8	5.6	7.0	0.1	-0.3	6.8	-0.1	-0.1	0.0	-0.1	-0.1	-0.1	0.0	-0.1
97.7	5.9	2.7	-2.7	5.4	7.7	0.2	-0.2	7.5	0.0	-0.1	0.0	0.0	-0.1	-0.1	0.0	-0.1
107.4	6.2	2.7	-2.4	5.7	8.5	0.1	-0.3	8.1	0.0	-0.1	-0.1	-0.1	-0.1	0.0	0.0	0.0
117.2	6.4	2.6	-2.6	5.7	9.3	0.1	-0.6	9.0	0.0	0.0	0.0	0.0	-0.1	0.0	0.0	0.0
127.0	6.6	2.4	-2.7	5.7	9.5	0.2	-0.3	9.6	0.0	-0.1	0.0	-0.1	0.0	0.0	0.0	-0.1
136.7	6.6	2.1	-2.9	5.9	10.0	0.2	-0.2	10.0	0.0	0.0	0.0	-0.1	0.0	0.0	0.0	0.0

Table 155. Raw data for the test seal at ω=20 krpm, PR=0.5, C_r=0.188 mm, and inlet GVF=100%

Freq.	Re($\boldsymbol{H_{XX}}$)	Re($\boldsymbol{H_{XY}}$)	Re($\boldsymbol{H_{YX}}$)	Re($\boldsymbol{H_{YY}}$)	Im($\boldsymbol{H_{XX}}$)	Im($\boldsymbol{H_{XY}}$)	Im($\boldsymbol{H_{YX}}$)	Im($\boldsymbol{H_{YY}}$)	Re($\boldsymbol{eH_{XX}}$)	Re($\boldsymbol{eH_{XY}}$)	Re($\boldsymbol{eH_{YX}}$)	Re($\boldsymbol{eH_{YY}}$)	Im($\boldsymbol{eH_{XX}}$)	Im($\boldsymbol{eH_{XY}}$)	Im($\boldsymbol{eH_{YX}}$)	Im($\boldsymbol{eH_{YY}}$)
Hz	MN/m	MN/m	MN/m	MN/m	MN/m	MN/m	MN/m	MN/m	MN/m	MN/m	MN/m	MN/m	MN/m	MN/m	MN/m	MN/m
9.8	5.3	6.3	-6.4	4.3	0.8	-0.4	-0.4	0.7	-0.2	-0.1	-0.2	-0.3	-0.2	-0.1	-0.1	-0.1
19.5	5.1	6.1	-7.0	3.7	1.9	0.0	-0.1	2.1	-0.1	-0.1	-0.2	-0.2	-0.1	-0.1	-0.1	-0.2
29.3	5.0	6.3	-6.8	4.6	3.2	0.0	0.5	2.9	-0.2	-0.1	-0.2	-0.2	-0.1	-0.2	-0.1	-0.3
39.1	5.2	6.0	-6.8	4.5	4.1	0.0	0.4	3.8	-0.1	-0.1	-0.2	-0.1	-0.1	0.0	-0.1	-0.2
48.8	5.1	6.0	-6.7	4.5	5.2	0.3	0.6	4.8	-0.1	-0.1	-0.1	-0.1	-0.1	-0.1	-0.1	-0.1
58.6	5.4	6.3	-6.7	4.9	5.8	0.6	0.3	5.5	-0.1	-0.1	-0.2	-0.2	-0.1	0.0	-0.1	-0.1
68.4	5.6	6.4	-6.7	5.2	6.9	0.4	0.1	7.1	-0.1	-0.1	-0.2	-0.3	-0.1	-0.2	-0.1	-0.2
78.1	5.6	6.6	-6.6	4.8	7.6	0.4	0.3	7.5	-0.1	-0.1	-0.1	-0.2	0.0	0.0	-0.1	-0.1
87.9	5.8	6.4	-7.0	4.5	8.8	0.3	0.6	8.5	-0.1	-0.1	-0.1	0.0	-0.1	-0.1	0.0	-0.1
97.7	5.8	6.4	-7.0	4.8	9.6	0.3	0.7	9.7	0.0	0.0	-0.1	-0.1	0.0	0.0	-0.1	-0.1
107.4	5.9	6.6	-6.4	5.1	11.0	0.0	0.5	10.0	-0.1	-0.1	-0.1	-0.1	-0.1	0.0	-0.1	-0.1
117.2	6.1	6.5	-6.4	5.1	11.0	0.0	0.3	11.0	0.0	0.0	-0.1	0.0	0.0	0.0	-0.1	-0.1
127.0	6.0	6.5	-6.5	5.1	12.0	-0.1	0.5	12.0	0.0	-0.1	-0.1	-0.2	0.0	-0.1	-0.1	-0.1
136.7	6.2	6.0	-6.5	5.8	13.0	0.2	0.5	13.0	0.0	-0.1	0.0	0.0	0.0	0.0	0.0	-0.1

Table 156. Raw data for the test seal at ω=20 krpm, PR=0.5, C_r=0.188 mm, and inlet GVF=98%

Freq.	Re(H_{XX})	Re(H_{XY})	Re(H_{YX})	Re(H_{YY})	Im(H_{XX})	Im(H_{XY})	Im(H_{YX})	Im(H_{YY})	Re(eH_{XX})	Re(eH_{XY})	Re(eH_{YX})	Re(eH_{YY})	Im(eH_{XX})	Im(eH_{XY})	Im(eH_{YX})	Im(eH_{YY})
Hz	MN/m	MN/m	MN/m	MN/m	MN/m	MN/m	MN/m	MN/m	MN/m	MN/m	MN/m	MN/m	MN/m	MN/m	MN/m	MN/m
9.8	5.5	5.2	-5.0	3.2	-0.8	-0.1	-0.7	1.4	-0.3	-0.3	-0.5	-0.5	-0.2	-0.4	-0.4	-0.3
19.5	5.0	5.8	-4.8	3.3	1.2	0.1	0.4	2.3	-0.1	-0.2	-0.2	-0.2	-0.2	-0.2	-0.3	-0.3
29.3	4.6	6.0	-4.6	2.9	2.5	-0.1	0.5	2.6	-0.3	-0.1	-0.4	-0.4	-0.2	-0.4	-0.3	-0.6
39.1	4.6	5.4	-4.8	3.5	3.6	-0.3	1.0	3.8	-0.1	-0.2	-0.2	-0.2	-0.2	0.0	-0.2	-0.2
48.8	4.9	5.4	-4.6	3.8	4.4	0.2	0.6	5.4	-0.1	-0.1	-0.3	-0.2	-0.1	-0.1	-0.1	-0.2
58.6	5.2	5.2	-4.7	3.8	5.5	0.4	-0.1	5.9	-0.2	-0.2	-0.2	-0.2	-0.1	-0.1	-0.2	-0.3
68.4	5.1	5.2	-4.3	3.8	6.1	-0.2	0.0	7.0	-0.1	-0.1	-0.3	-0.2	-0.1	-0.4	-0.2	-0.7
78.1	5.2	5.3	-4.2	4.1	7.4	0.3	-0.4	7.8	-0.1	-0.1	-0.2	-0.2	-0.1	-0.2	-0.2	-0.1
87.9	4.9	5.6	-4.8	4.1	8.4	0.5	0.4	8.9	-0.1	-0.1	-0.1	-0.1	-0.1	-0.1	-0.2	-0.1
97.7	5.1	5.5	-4.9	4.4	9.5	0.5	0.2	9.8	-0.1	-0.1	-0.1	-0.1	-0.1	0.0	-0.2	-0.2
107.4	5.4	5.8	-4.1	4.4	10.0	0.3	-0.6	10.0	-0.1	-0.1	-0.2	-0.1	-0.1	-0.1	-0.1	-0.1
117.2	5.2	5.9	-4.6	4.2	11.0	0.3	-0.7	11.0	-0.1	-0.1	-0.1	-0.1	-0.1	0.0	-0.2	-0.1
127.0	5.4	5.9	-4.3	4.1	12.0	0.3	-0.4	12.0	-0.1	-0.1	-0.1	-0.3	-0.1	-0.2	-0.1	-0.2
136.7	5.8	5.5	-5.1	4.7	13.0	0.6	-0.6	13.0	-0.1	0.0	-0.1	-0.1	0.0	-0.1	-0.1	-0.2

Table 157. Raw data for the test seal at ω=20 krpm, PR=0.5, C_r=0.188 mm, and inlet GVF=95%

Freq.	Re(H_{XX})	Re(H_{XY})	Re(H_{YX})	Re(H_{YY})	Im(H_{XX})	Im(H_{XY})	Im(H_{YX})	Im(H_{YY})	Re(eH_{XX})	Re(eH_{XY})	Re(eH_{YX})	Re(eH_{YY})	Im(eH_{XX})	Im(eH_{XY})	Im(eH_{YX})	Im(eH_{YY})
Hz	MN/m	MN/m	MN/m	MN/m	MN/m	MN/m	MN/m	MN/m	MN/m	MN/m	MN/m	MN/m	MN/m	MN/m	MN/m	MN/m
9.8	5.0	4.3	-4.4	2.6	-0.5	0.1	-0.4	1.1	-0.3	-0.4	-0.4	-0.3	-0.6	-0.4	-0.4	-0.4
19.5	5.1	5.5	-4.6	2.5	0.3	0.1	1.0	2.2	-0.3	-0.1	-0.2	-0.2	-0.4	-0.2	-0.2	-0.4
29.3	4.4	5.4	-3.5	1.7	2.0	0.1	0.2	2.6	-0.1	-0.2	-0.3	-0.3	-0.2	-0.2	-0.3	-0.6
39.1	4.3	5.7	-4.3	2.5	3.6	-0.1	0.4	4.7	-0.2	-0.2	-0.4	-0.3	-0.1	-0.3	-0.2	-0.6
48.8	4.7	5.5	-3.5	2.6	4.8	0.1	0.6	5.3	-0.2	-0.2	-0.2	-0.2	-0.3	-0.2	-0.2	-0.2
58.6	4.6	5.5	-3.8	3.3	5.6	0.3	0.1	6.7	-0.2	-0.3	-0.4	-0.3	-0.1	-0.1	-0.4	-0.3
68.4	5.1	5.4	-4.1	3.4	6.4	-0.2	-0.5	7.1	-0.1	-0.4	-0.3	-0.2	-0.2	-0.2	-0.1	-0.3
78.1	4.6	5.5	-3.7	3.0	7.3	0.5	-0.8	8.4	-0.1	-0.2	-0.2	-0.2	-0.1	-0.1	-0.2	-0.3
87.9	4.5	5.0	-3.7	3.6	8.4	0.3	-0.5	9.2	-0.1	-0.2	-0.1	-0.2	-0.1	-0.1	-0.2	-0.1
97.7	4.9	4.9	-4.1	3.5	10.0	0.5	-0.6	10.0	-0.1	-0.1	-0.2	-0.1	-0.2	-0.1	-0.3	-0.1
107.4	5.0	5.2	-4.1	3.4	11.0	0.5	-0.8	11.0	-0.2	-0.1	-0.2	-0.2	-0.1	-0.1	-0.2	-0.1
117.2	5.2	5.5	-4.1	3.7	12.0	1.0	-0.9	12.0	-0.2	-0.1	-0.2	-0.1	-0.1	-0.1	-0.1	-0.1
127.0	5.1	5.4	-4.5	3.6	12.0	1.3	-0.9	13.0	-0.1	-0.2	-0.2	-0.3	-0.1	-0.2	-0.1	-0.4
136.7	5.5	5.7	-4.8	3.7	14.0	1.1	-0.7	14.0	-0.1	-0.2	-0.1	-0.1	-0.1	-0.2	-0.1	-0.1

Table 158. Raw data for the test seal at ω=20 krpm, PR=0.5, C_r=0.188 mm, and inlet GVF=92%

Freq.	Re($\boldsymbol{H_{XX}}$)	Re($\boldsymbol{H_{XY}}$)	Re($\boldsymbol{H_{YX}}$)	Re($\boldsymbol{H_{YY}}$)	Im($\boldsymbol{H_{XX}}$)	Im($\boldsymbol{H_{XY}}$)	Im($\boldsymbol{H_{YX}}$)	Im($\boldsymbol{H_{YY}}$)	Re($\boldsymbol{eH_{XX}}$)	Re($\boldsymbol{eH_{XY}}$)	Re($\boldsymbol{eH_{YX}}$)	Re($\boldsymbol{eH_{YY}}$)	Im($\boldsymbol{eH_{XX}}$)	Im($\boldsymbol{eH_{XY}}$)	Im($\boldsymbol{eH_{YX}}$)	Im($\boldsymbol{eH_{YY}}$)
Hz	MN/m	MN/m	MN/m	MN/m	MN/m	MN/m	MN/m	MN/m	MN/m	MN/m	MN/m	MN/m	MN/m	MN/m	MN/m	MN/m
9.8	3.4	1.5	-1.5	2.8	0.8	-0.1	0.0	1.0	-0.1	0.0	-0.1	-0.1	-0.1	-0.1	-0.1	-0.1
19.5	3.2	1.7	-1.5	2.9	2.1	0.0	0.1	1.8	-0.1	0.0	-0.1	-0.1	-0.1	-0.1	-0.1	-0.1
29.3	3.3	1.5	-1.7	2.9	2.6	0.2	0.0	2.7	-0.1	0.0	-0.1	-0.2	-0.1	-0.1	0.0	-0.1
39.1	3.4	1.5	-1.5	2.8	3.5	0.0	0.1	3.5	-0.1	-0.2	-0.1	-0.2	-0.1	-0.2	-0.1	-0.1
48.8	3.4	1.5	-1.6	3.3	4.5	0.1	0.0	4.5	-0.1	-0.1	-0.1	-0.1	-0.1	-0.1	-0.1	-0.1
58.6	3.4	2.0	-1.7	3.1	5.4	0.0	0.2	5.7	-0.1	-0.1	-0.1	-0.1	-0.1	-0.1	-0.1	-0.1
68.4	3.5	1.5	-1.7	3.0	6.2	0.1	0.0	6.5	-0.1	-0.2	-0.1	-0.2	-0.1	-0.2	-0.1	-0.1
78.1	3.6	1.9	-1.7	3.1	6.9	-0.1	0.0	7.1	-0.1	-0.1	-0.1	-0.1	-0.1	-0.1	0.0	-0.1
87.9	3.5	1.7	-1.7	3.1	8.0	0.0	0.0	8.2	-0.1	-0.1	0.0	-0.1	0.0	-0.1	0.0	-0.1
97.7	3.7	1.6	-1.7	3.2	8.9	-0.1	0.0	9.0	-0.1	0.0	-0.1	0.0	-0.1	0.0	-0.1	0.0
107.4	3.8	1.7	-1.4	3.4	10.0	0.0	0.2	9.8	-0.1	-0.1	-0.1	-0.1	-0.1	-0.1	0.0	-0.1
117.2	4.0	1.6	-1.5	3.5	11.0	-0.1	-0.2	11.0	0.0	0.0	-0.1	-0.1	-0.1	-0.1	0.0	-0.1
127.0	4.1	1.9	-2.0	4.0	11.0	-0.1	-0.1	12.0	-0.1	-0.1	-0.1	-0.2	-0.1	-0.2	0.0	-0.2
136.7	4.3	1.3	-2.4	3.8	12.0	0.1	-0.2	12.0	0.0	0.0	-0.1	0.0	0.0	0.0	0.0	0.0

Table 159. Raw data for the test seal at ω=10 krpm, PR=0.43, C_r=0.188 mm, and inlet GVF=100%

Freq.	Re($\boldsymbol{H_{XX}}$)	Re($\boldsymbol{H_{XY}}$)	Re($\boldsymbol{H_{YX}}$)	Re($\boldsymbol{H_{YY}}$)	Im($\boldsymbol{H_{XX}}$)	Im($\boldsymbol{H_{XY}}$)	Im($\boldsymbol{H_{YX}}$)	Im($\boldsymbol{H_{YY}}$)	Re($\boldsymbol{eH_{XX}}$)	Re($\boldsymbol{eH_{XY}}$)	Re($\boldsymbol{eH_{YX}}$)	Re($\boldsymbol{eH_{YY}}$)	Im($\boldsymbol{eH_{XX}}$)	Im($\boldsymbol{eH_{XY}}$)	Im($\boldsymbol{eH_{YX}}$)	Im($\boldsymbol{eH_{YY}}$)
Hz	MN/m	MN/m	MN/m	MN/m	MN/m	MN/m	MN/m	MN/m	MN/m	MN/m	MN/m	MN/m	MN/m	MN/m	MN/m	MN/m
9.8	2.9	3.2	-3.2	3.0	0.7	0.5	0.4	1.7	-0.1	-0.2	-0.2	-0.2	-0.2	-0.2	-0.1	-0.1
19.5	3.0	3.0	-3.1	3.1	2.3	0.3	0.4	2.5	-0.1	-0.1	-0.1	-0.2	-0.1	-0.1	-0.1	-0.1
29.3	3.2	3.2	-2.9	3.7	3.3	0.2	0.0	3.7	-0.1	-0.1	-0.2	-0.3	-0.1	-0.2	-0.1	-0.1
39.1	3.6	3.2	-2.8	3.6	4.5	0.1	0.2	4.3	-0.1	0.0	-0.1	-0.2	-0.1	-0.1	-0.1	-0.1
48.8	3.8	3.3	-2.6	3.8	5.6	0.3	0.5	5.2	-0.1	0.0	-0.2	-0.1	-0.1	0.0	-0.1	-0.1
58.6	3.8	3.3	-2.7	3.6	6.4	0.5	0.4	6.2	-0.1	-0.1	-0.1	-0.1	-0.1	-0.1	-0.1	-0.1
68.4	4.0	3.2	-2.7	3.8	7.2	0.3	-0.1	7.3	0.0	-0.1	-0.1	-0.1	0.0	-0.1	-0.1	-0.1
78.1	4.2	3.4	-2.5	3.9	8.1	0.4	-0.1	8.2	0.0	0.0	-0.1	0.0	0.0	-0.1	-0.1	-0.1
87.9	4.2	3.3	-3.0	3.8	9.5	0.4	0.5	9.3	-0.1	-0.1	-0.1	-0.1	0.0	0.0	-0.1	0.0
97.7	4.2	3.3	-3.0	4.0	10.0	0.4	0.2	10.0	0.0	0.0	0.0	0.0	0.0	0.0	-0.1	-0.1
107.4	4.4	3.3	-2.8	4.1	11.0	0.2	0.3	11.0	0.0	0.0	-0.1	0.0	-0.1	0.0	-0.1	-0.1
117.2	4.4	3.5	-3.0	4.3	12.0	0.2	0.1	12.0	-0.1	0.0	0.0	0.0	-0.1	0.0	-0.1	-0.1
127.0	4.4	3.5	-2.8	4.7	13.0	0.4	0.5	13.0	0.0	-0.1	-0.1	-0.1	0.0	-0.1	-0.1	-0.1
136.7	4.6	3.2	-3.1	4.7	14.0	0.6	0.4	14.0	0.0	0.0	0.0	0.0	0.0	0.0	-0.1	-0.1

Table 160. Raw data for the test seal at ω=10 krpm, PR=0.43, C_r=0.188 mm, and inlet GVF=98%

Freq.	Re(H_{XX})	Re(H_{XY})	Re(H_{YX})	Re(H_{YY})	Im(H_{XX})	Im(H_{XY})	Im(H_{YX})	Im(H_{YY})	Re(eH_{XX})	Re(eH_{XY})	Re(eH_{YX})	Re(eH_{YY})	Im(eH_{XX})	Im(eH_{XY})	Im(eH_{YX})	Im(eH_{YY})
Hz	MN/m	MN/m	MN/m	MN/m	MN/m	MN/m	MN/m	MN/m	MN/m	MN/m	MN/m	MN/m	MN/m	MN/m	MN/m	MN/m
9.8	3.0	2.1	-3.0	1.8	-1.2	1.2	0.6	0.9	-0.3	-0.2	-0.3	-0.2	-0.3	-0.3	-0.4	-0.4
19.5	2.2	2.9	-2.3	1.8	1.1	0.7	0.6	2.0	-0.1	-0.1	-0.2	-0.3	-0.1	-0.2	-0.2	-0.3
29.3	1.9	3.5	-2.1	1.5	2.5	1.1	0.8	3.4	-0.1	-0.2	-0.1	-0.4	0.0	-0.2	-0.2	-0.4
39.1	2.4	3.0	-2.2	1.8	3.6	0.5	0.0	4.7	-0.1	-0.1	-0.2	-0.1	-0.1	-0.1	-0.1	-0.2
48.8	2.4	3.3	-2.2	2.1	5.5	0.3	0.0	5.7	-0.1	-0.2	-0.1	-0.1	-0.2	-0.2	-0.1	-0.3
58.6	2.5	3.6	-2.1	2.4	5.9	0.8	0.2	6.7	-0.2	-0.1	-0.2	-0.2	-0.2	-0.1	-0.3	-0.1
68.4	3.0	3.6	-1.9	3.1	7.4	-0.2	0.3	7.0	-0.1	-0.2	-0.2	-0.2	-0.1	-0.1	-0.1	-0.3
78.1	2.8	3.1	-2.1	2.2	8.2	0.3	0.0	8.4	-0.1	-0.1	-0.3	-0.1	-0.1	-0.1	-0.2	-0.3
87.9	2.8	3.4	-2.3	2.5	9.5	0.2	-0.3	9.1	-0.1	-0.1	-0.2	-0.1	-0.1	-0.1	-0.1	-0.1
97.7	3.3	3.7	-2.5	2.5	11.0	0.2	0.1	11.0	-0.2	0.0	-0.1	-0.1	-0.1	-0.1	-0.1	-0.1
107.4	3.8	3.6	-2.0	2.7	12.0	0.0	0.2	11.0	-0.1	-0.1	-0.3	-0.1	-0.1	-0.1	-0.2	-0.1
117.2	3.7	3.3	-2.1	2.2	13.0	0.0	-0.3	12.0	-0.1	-0.1	-0.2	0.0	-0.1	0.0	-0.1	-0.1
127.0	3.8	3.3	-2.7	2.6	13.0	0.0	0.3	14.0	0.0	-0.1	-0.1	-0.2	-0.1	-0.1	-0.1	-0.2
136.7	3.9	3.1	-2.7	2.9	14.0	-0.1	0.1	15.0	0.0	-0.1	-0.2	-0.1	-0.1	-0.1	-0.1	-0.1

Table 161. Raw data for the test seal at ω=10 krpm, PR=0.43, C_r=0.188 mm, and inlet GVF=95%

Freq.	Re(H_{XX})	Re(H_{XY})	Re(H_{YX})	Re(H_{YY})	Im(H_{XX})	Im(H_{XY})	Im(H_{YX})	Im(H_{YY})	Re(eH_{XX})	Re(eH_{XY})	Re(eH_{YX})	Re(eH_{YY})	Im(eH_{XX})	Im(eH_{XY})	Im(eH_{YX})	Im(eH_{YY})
Hz	MN/m	MN/m	MN/m	MN/m	MN/m	MN/m	MN/m	MN/m	MN/m	MN/m	MN/m	MN/m	MN/m	MN/m	MN/m	MN/m
9.8	4.7	1.5	-1.6	0.8	-2.2	0.6	0.9	0.0	-0.2	-0.3	-0.5	-0.2	-0.5	-0.4	-0.1	-0.3
19.5	2.3	2.9	-2.2	0.4	0.5	1.6	1.0	3.1	-0.1	-0.1	-0.2	-0.3	-0.2	-0.3	-0.3	-0.3
29.3	2.0	2.8	-1.8	0.6	2.4	1.2	0.9	3.7	-0.1	-0.3	-0.2	-0.5	-0.2	-0.3	-0.3	-0.4
39.1	2.1	3.3	-2.1	1.3	3.8	0.3	0.7	5.0	-0.1	-0.2	-0.2	-0.1	-0.1	-0.2	-0.2	-0.3
48.8	2.6	3.0	-2.4	1.2	5.0	1.1	0.3	6.5	-0.1	-0.2	-0.2	-0.3	-0.1	-0.1	-0.2	-0.2
58.6	2.7	3.2	-1.9	1.7	6.1	0.5	0.4	7.7	-0.2	-0.2	-0.2	-0.2	-0.2	-0.2	-0.2	-0.3
68.4	2.3	3.2	-2.1	2.1	7.4	0.6	0.4	8.0	-0.1	-0.2	-0.3	-0.2	-0.1	-0.4	-0.2	-0.5
78.1	2.7	3.3	-2.4	2.1	8.7	0.6	0.0	8.9	-0.2	-0.1	-0.1	-0.2	-0.2	-0.2	-0.1	-0.2
87.9	3.0	3.1	-2.0	1.7	10.0	0.4	0.0	9.8	-0.1	-0.1	-0.2	-0.1	-0.1	-0.1	-0.1	-0.2
97.7	2.8	3.1	-2.6	1.8	11.0	0.3	0.3	11.0	-0.2	-0.1	-0.2	-0.4	-0.1	-0.2	-0.1	-0.1
107.4	3.3	3.5	-2.7	2.0	12.0	0.4	0.2	12.0	-0.2	-0.1	-0.2	-0.2	-0.1	-0.1	-0.2	-0.1
117.2	3.7	3.2	-1.7	1.6	13.0	0.2	-0.4	13.0	-0.1	-0.1	-0.2	-0.1	-0.2	-0.1	-0.2	-0.2
127.0	3.5	3.5	-2.5	1.9	13.0	0.5	0.3	14.0	-0.1	-0.3	-0.2	-0.4	-0.1	-0.2	-0.2	-0.3
136.7	3.6	2.6	-2.8	2.2	15.0	0.3	0.3	15.0	-0.1	-0.2	-0.2	-0.2	-0.1	-0.2	-0.3	-0.2

Table 162. Raw data for the test seal at ω=10 krpm, PR=0.43, C_r=0.188 mm, and inlet GVF=92%

Freq.	Re($\boldsymbol{H_{XX}}$)	Re($\boldsymbol{H_{XY}}$)	Re($\boldsymbol{H_{YX}}$)	Re($\boldsymbol{H_{YY}}$)	Im($\boldsymbol{H_{XX}}$)	Im($\boldsymbol{H_{XY}}$)	Im($\boldsymbol{H_{YX}}$)	Im($\boldsymbol{H_{YY}}$)	Re($\boldsymbol{eH_{XX}}$)	Re($\boldsymbol{eH_{XY}}$)	Re($\boldsymbol{eH_{YX}}$)	Re($\boldsymbol{eH_{YY}}$)	Im($\boldsymbol{eH_{XX}}$)	Im($\boldsymbol{eH_{XY}}$)	Im($\boldsymbol{eH_{YX}}$)	Im($\boldsymbol{eH_{YY}}$)
Hz	MN/m	MN/m	MN/m	MN/m	MN/m	MN/m	MN/m	MN/m	MN/m	MN/m	MN/m	MN/m	MN/m	MN/m	MN/m	MN/m
9.8	3.2	2.3	-2.2	2.5	1.0	0.0	-0.1	1.0	-0.1	0.0	-0.1	0.0	-0.1	-0.1	-0.1	0.0
19.5	3.1	2.4	-2.2	2.7	1.7	0.1	-0.1	1.9	-0.1	-0.1	-0.1	-0.1	-0.1	0.0	0.0	-0.1
29.3	3.4	2.2	-2.5	2.9	2.6	0.3	0.0	2.7	-0.2	-0.2	-0.1	-0.1	-0.1	-0.1	-0.1	-0.2
39.1	3.4	2.3	-2.4	2.6	3.8	0.0	0.0	3.7	0.0	-0.2	-0.1	-0.2	0.0	-0.2	-0.1	-0.2
48.8	3.4	2.4	-2.4	3.0	4.3	0.0	0.0	4.7	-0.1	-0.1	0.0	-0.1	-0.1	-0.1	-0.1	-0.1
58.6	3.6	2.6	-2.3	3.1	5.2	-0.1	-0.1	5.6	-0.1	-0.1	-0.1	-0.1	-0.1	-0.1	-0.1	-0.1
68.4	3.6	2.6	-2.3	2.6	6.2	-0.2	-0.1	6.4	-0.2	-0.2	-0.1	-0.3	-0.1	-0.3	-0.1	-0.2
78.1	3.5	2.6	-2.4	3.1	7.0	0.2	-0.2	7.2	-0.1	-0.1	-0.1	-0.1	-0.1	0.0	-0.1	-0.1
87.9	3.5	2.2	-2.5	3.0	8.2	-0.2	-0.1	8.2	0.0	-0.1	0.0	0.0	-0.1	-0.1	-0.1	-0.1
97.7	3.7	2.2	-2.4	3.2	9.0	-0.1	0.0	8.9	-0.1	-0.1	-0.1	0.0	-0.1	-0.1	0.0	-0.1
107.4	3.8	2.2	-2.4	3.2	9.8	0.0	-0.1	10.0	-0.1	0.0	-0.1	-0.1	-0.1	-0.1	0.0	-0.1
117.2	4.0	2.1	-2.5	3.2	11.0	-0.2	-0.4	11.0	-0.1	-0.1	-0.1	-0.1	0.0	-0.1	-0.1	-0.1
127.0	4.2	2.1	-2.7	3.4	11.0	0.0	-0.2	12.0	0.0	0.0	-0.1	-0.2	-0.1	-0.2	-0.1	-0.2
136.7	4.4	1.8	-3.2	4.0	12.0	-0.1	-0.1	12.0	-0.1	0.0	0.0	-0.1	0.0	-0.1	-0.1	-0.1

Table 163. Raw data for the test seal at ω=15 krpm, PR=0.43, C_r=0.188 mm, and inlet GVF=100%

Freq.	Re($\boldsymbol{H_{XX}}$)	Re($\boldsymbol{H_{XY}}$)	Re($\boldsymbol{H_{YX}}$)	Re($\boldsymbol{H_{YY}}$)	Im($\boldsymbol{H_{XX}}$)	Im($\boldsymbol{H_{XY}}$)	Im($\boldsymbol{H_{YX}}$)	Im($\boldsymbol{H_{YY}}$)	Re($\boldsymbol{eH_{XX}}$)	Re($\boldsymbol{eH_{XY}}$)	Re($\boldsymbol{eH_{YX}}$)	Re($\boldsymbol{eH_{YY}}$)	Im($\boldsymbol{eH_{XX}}$)	Im($\boldsymbol{eH_{XY}}$)	Im($\boldsymbol{eH_{YX}}$)	Im($\boldsymbol{eH_{YY}}$)
Hz	MN/m	MN/m	MN/m	MN/m	MN/m	MN/m	MN/m	MN/m	MN/m	MN/m	MN/m	MN/m	MN/m	MN/m	MN/m	MN/m
9.8	3.4	5.3	-4.6	3.1	0.9	0.5	0.0	1.6	-0.1	-0.2	-0.2	-0.1	-0.1	-0.1	-0.2	-0.2
19.5	3.7	5.4	-5.0	3.3	2.4	0.0	0.4	2.4	-0.1	-0.1	-0.1	-0.1	-0.1	-0.1	-0.2	-0.1
29.3	3.9	5.0	-4.9	3.3	3.7	-0.3	0.1	3.8	-0.1	-0.2	-0.2	-0.2	-0.1	-0.1	-0.1	0.0
39.1	4.3	5.1	-4.8	3.8	4.6	-0.2	0.1	4.7	-0.1	-0.1	-0.1	-0.1	0.0	-0.1	-0.1	-0.1
48.8	4.6	5.0	-4.9	3.7	5.8	0.1	0.3	5.4	-0.1	-0.1	-0.1	-0.1	-0.1	0.0	-0.1	-0.1
58.6	4.7	5.3	-5.1	3.8	6.5	0.3	0.1	6.5	-0.1	-0.1	-0.1	-0.1	-0.1	-0.1	-0.1	-0.1
68.4	4.7	5.2	-4.6	3.7	7.6	0.0	-0.1	7.4	0.0	-0.1	-0.1	-0.3	0.0	-0.1	-0.1	-0.1
78.1	4.9	5.3	-4.7	3.8	8.4	0.0	0.0	8.3	0.0	-0.1	-0.1	-0.2	-0.1	-0.1	-0.1	-0.1
87.9	5.0	5.3	-5.3	4.1	9.6	0.0	0.5	9.6	0.0	0.0	-0.1	0.0	0.0	0.0	-0.1	-0.1
97.7	5.0	5.2	-5.3	4.2	11.0	0.1	0.4	11.0	-0.1	0.0	-0.1	-0.1	0.0	-0.1	0.0	-0.1
107.4	5.2	5.3	-4.9	4.6	12.0	-0.1	0.4	12.0	0.0	0.0	-0.1	-0.1	0.0	0.0	-0.1	-0.1
117.2	5.3	5.4	-4.9	4.5	13.0	0.0	0.2	13.0	0.0	0.0	0.0	-0.1	0.0	0.0	0.0	-0.1
127.0	5.3	5.3	-4.9	5.0	13.0	0.2	0.5	13.0	-0.1	-0.1	0.0	-0.1	0.0	-0.1	-0.1	-0.1
136.7	5.6	5.0	-5.1	5.1	14.0	0.2	0.5	14.0	0.0	0.0	-0.1	-0.1	0.0	0.0	-0.1	0.0

Table 164. Raw data for the test seal at ω=15 krpm, PR=0.43, C_r=0.188 mm, and inlet GVF=98%

Freq.	Re($\boldsymbol{H_{XX}}$)	Re($\boldsymbol{H_{XY}}$)	Re($\boldsymbol{H_{YX}}$)	Re($\boldsymbol{H_{YY}}$)	Im($\boldsymbol{H_{XX}}$)	Im($\boldsymbol{H_{XY}}$)	Im($\boldsymbol{H_{YX}}$)	Im($\boldsymbol{H_{YY}}$)	Re($\boldsymbol{eH_{XX}}$)	Re($\boldsymbol{eH_{XY}}$)	Re($\boldsymbol{eH_{YX}}$)	Re($\boldsymbol{eH_{YY}}$)	Im($\boldsymbol{eH_{XX}}$)	Im($\boldsymbol{eH_{XY}}$)	Im($\boldsymbol{eH_{YX}}$)	Im($\boldsymbol{eH_{YY}}$)
Hz	MN/m	MN/m	MN/m	MN/m	MN/m	MN/m	MN/m	MN/m	MN/m	MN/m	MN/m	MN/m	MN/m	MN/m	MN/m	MN/m
9.8	4.1	4.5	-2.9	1.7	-0.7	0.8	0.5	1.8	-0.3	-0.3	-0.3	-0.4	-0.3	-0.3	-0.2	-0.2
19.5	2.9	4.8	-3.8	1.6	1.2	0.2	0.5	2.2	-0.1	-0.1	-0.1	-0.1	-0.2	-0.1	-0.3	-0.2
29.3	2.6	5.0	-3.0	1.0	2.0	0.7	0.8	3.4	-0.1	-0.2	-0.1	-0.4	-0.2	-0.3	-0.2	-0.4
39.1	2.7	4.5	-3.1	1.7	3.7	-0.2	0.6	4.0	-0.1	-0.1	-0.2	-0.2	-0.2	-0.2	-0.4	-0.2
48.8	3.0	4.5	-3.4	2.0	5.0	0.0	0.5	5.2	-0.1	-0.2	-0.2	-0.2	-0.1	-0.3	-0.2	-0.3
58.6	2.8	4.8	-3.1	2.3	6.0	0.5	0.1	7.1	-0.1	-0.2	-0.3	-0.2	-0.1	-0.2	-0.1	-0.1
68.4	2.8	4.4	-3.5	2.4	7.2	-0.2	0.1	7.4	-0.2	-0.3	-0.3	-0.6	-0.1	-0.4	-0.2	-0.3
78.1	2.7	4.8	-3.8	2.4	8.1	0.5	-0.1	8.9	-0.2	-0.1	-0.1	-0.1	-0.1	-0.2	-0.2	-0.1
87.9	3.0	4.8	-3.3	2.3	9.4	-0.1	-0.2	9.3	-0.1	-0.1	-0.1	-0.1	-0.1	-0.1	-0.1	-0.1
97.7	3.3	4.9	-3.0	2.5	11.0	0.0	0.3	10.0	-0.1	-0.2	-0.2	-0.2	-0.1	-0.1	-0.1	-0.1
107.4	3.7	5.0	-3.3	2.6	12.0	0.0	0.0	11.0	-0.1	-0.1	-0.2	-0.2	-0.2	-0.1	-0.2	-0.1
117.2	3.9	4.7	-3.1	2.4	13.0	-0.2	-0.5	12.0	-0.1	0.0	-0.2	-0.1	-0.1	-0.1	-0.1	-0.1
127.0	4.0	4.3	-3.6	2.8	13.0	0.2	-0.1	14.0	-0.1	-0.2	-0.2	-0.3	-0.1	-0.2	-0.1	-0.1
136.7	3.9	4.5	-3.9	2.9	14.0	0.2	-0.2	15.0	-0.1	-0.1	-0.2	-0.1	-0.1	-0.1	-0.1	-0.1

Table 165. Raw data for the test seal at ω=15 krpm, PR=0.43, C_r=0.188 mm, and inlet GVF=95%

Freq.	Re($\boldsymbol{H_{XX}}$)	Re($\boldsymbol{H_{XY}}$)	Re($\boldsymbol{H_{YX}}$)	Re($\boldsymbol{H_{YY}}$)	Im($\boldsymbol{H_{XX}}$)	Im($\boldsymbol{H_{XY}}$)	Im($\boldsymbol{H_{YX}}$)	Im($\boldsymbol{H_{YY}}$)	Re($\boldsymbol{eH_{XX}}$)	Re($\boldsymbol{eH_{XY}}$)	Re($\boldsymbol{eH_{YX}}$)	Re($\boldsymbol{eH_{YY}}$)	Im($\boldsymbol{eH_{XX}}$)	Im($\boldsymbol{eH_{XY}}$)	Im($\boldsymbol{eH_{YX}}$)	Im($\boldsymbol{eH_{YY}}$)
Hz	MN/m	MN/m	MN/m	MN/m	MN/m	MN/m	MN/m	MN/m	MN/m	MN/m	MN/m	MN/m	MN/m	MN/m	MN/m	MN/m
9.8	5.4	3.2	-4.7	0.5	-1.4	1.1	-0.2	2.4	-0.2	-0.2	-0.4	-0.4	-0.8	-0.3	-0.4	-0.2
19.5	3.1	4.7	-3.0	1.1	0.3	0.6	0.4	2.4	-0.2	-0.2	-0.2	-0.3	-0.2	-0.2	-0.1	-0.3
29.3	2.8	4.8	-3.4	1.4	2.4	0.2	1.1	3.6	-0.3	-0.3	-0.2	-0.6	-0.2	-0.1	-0.2	-0.4
39.1	2.5	5.1	-3.2	1.0	3.8	0.1	0.1	5.1	-0.2	-0.2	-0.2	-0.3	-0.1	-0.2	-0.2	-0.1
48.8	2.9	4.7	-3.0	0.8	5.1	0.1	0.4	6.7	-0.1	-0.3	-0.3	-0.2	-0.2	-0.2	-0.2	-0.2
58.6	3.0	4.5	-3.3	1.6	6.1	0.6	0.5	7.6	-0.1	-0.2	-0.2	-0.4	-0.2	-0.2	-0.4	-0.1
68.4	3.2	4.2	-2.8	1.4	7.4	0.4	-0.2	8.2	-0.1	-0.2	-0.2	-0.4	-0.2	-0.2	-0.2	-0.4
78.1	3.2	4.8	-2.7	2.0	8.5	0.9	-0.3	8.9	-0.3	-0.3	-0.1	-0.2	-0.2	-0.2	-0.1	-0.2
87.9	3.2	4.8	-3.2	2.1	10.0	0.3	0.0	10.0	-0.2	-0.1	-0.1	-0.3	-0.1	-0.1	-0.2	-0.1
97.7	3.3	4.7	-3.2	2.5	11.0	0.3	-0.1	11.0	-0.1	-0.1	-0.3	-0.2	-0.2	-0.2	-0.1	-0.2
107.4	4.1	5.0	-3.3	2.1	12.0	0.3	-0.2	12.0	-0.1	-0.2	-0.4	-0.3	-0.1	-0.1	-0.2	-0.1
117.2	4.2	4.7	-3.2	1.7	13.0	0.5	-0.6	13.0	-0.1	-0.1	-0.1	-0.3	0.0	-0.1	-0.2	-0.3
127.0	4.1	5.1	-3.3	1.9	13.0	1.0	-0.3	15.0	-0.2	-0.2	-0.2	-0.4	-0.1	-0.2	-0.1	-0.4
136.7	4.3	4.6	-3.6	1.9	15.0	0.5	-0.6	16.0	-0.1	-0.1	-0.2	-0.3	-0.1	-0.1	-0.1	-0.1

Table 166. Raw data for the test seal at ω=15 krpm, PR=0.43, C_r=0.188 mm, and inlet GVF=92%

Freq.	Re($\boldsymbol{H_{XX}}$)	Re($\boldsymbol{H_{XY}}$)	Re($\boldsymbol{H_{YX}}$)	Re($\boldsymbol{H_{YY}}$)	Im($\boldsymbol{H_{XX}}$)	Im($\boldsymbol{H_{XY}}$)	Im($\boldsymbol{H_{YX}}$)	Im($\boldsymbol{H_{YY}}$)	Re($\boldsymbol{eH_{XX}}$)	Re($\boldsymbol{eH_{XY}}$)	Re($\boldsymbol{eH_{YX}}$)	Re($\boldsymbol{eH_{YY}}$)	Im($\boldsymbol{eH_{XX}}$)	Im($\boldsymbol{eH_{XY}}$)	Im($\boldsymbol{eH_{YX}}$)	Im($\boldsymbol{eH_{YY}}$)
Hz	MN/m	MN/m	MN/m	MN/m	MN/m	MN/m	MN/m	MN/m	MN/m	MN/m	MN/m	MN/m	MN/m	MN/m	MN/m	MN/m
9.8	2.6	3.5	-3.6	2.2	0.9	-0.1	-0.1	0.8	-0.1	-0.1	0.0	0.0	-0.1	-0.1	-0.1	0.0
19.5	2.6	3.3	-3.6	2.2	1.9	-0.2	-0.1	2.1	-0.2	-0.1	0.0	-0.1	-0.2	-0.1	-0.2	-0.1
29.3	2.7	3.5	-3.5	2.2	2.8	0.0	-0.1	2.2	-0.1	-0.1	-0.1	-0.2	-0.1	-0.2	-0.2	-0.1
39.1	2.6	3.5	-3.5	2.2	3.4	0.3	-0.2	3.3	-0.1	-0.2	-0.1	-0.3	-0.1	-0.2	-0.1	-0.2
48.8	2.6	3.2	-3.6	2.3	4.8	-0.1	-0.1	4.5	-0.1	-0.1	-0.1	-0.1	-0.2	-0.2	-0.1	-0.1
58.6	2.9	3.3	-3.8	2.3	5.3	0.0	0.0	5.3	-0.1	-0.1	-0.1	-0.1	-0.1	-0.2	-0.1	-0.2
68.4	3.2	2.5	-3.7	3.1	6.3	-0.3	-0.1	6.7	-0.1	-0.4	-0.1	-0.2	-0.1	-0.2	-0.1	-0.1
78.1	3.1	3.2	-3.9	2.2	7.0	0.1	-0.1	7.3	-0.1	-0.1	-0.1	-0.1	0.0	-0.1	-0.1	-0.1
87.9	3.1	3.4	-3.9	2.3	8.1	0.0	-0.2	8.0	-0.1	-0.1	-0.1	-0.1	-0.1	-0.1	-0.1	-0.1
97.7	3.1	3.1	-3.9	2.7	9.1	-0.1	0.0	9.6	-0.1	-0.1	-0.1	-0.1	-0.1	-0.1	-0.1	-0.1
107.4	3.6	3.0	-3.7	2.6	9.8	-0.2	-0.3	10.0	-0.1	-0.2	-0.1	-0.1	-0.1	-0.1	-0.1	-0.2
117.2	3.5	3.3	-3.7	2.7	11.0	-0.2	-0.2	11.0	-0.1	-0.1	-0.1	-0.1	-0.1	-0.1	-0.1	-0.1
127.0	3.7	3.2	-4.3	3.0	11.0	0.1	0.1	12.0	-0.1	-0.2	-0.1	-0.3	-0.1	-0.1	-0.1	-0.2
136.7	4.0	2.7	-4.5	3.3	12.0	-0.1	-0.1	13.0	-0.1	-0.1	-0.1	-0.1	0.0	-0.1	-0.1	-0.1

Table 167. Raw data for the test seal at ω=20 krpm, PR=0.43, C_r=0.188 mm, and inlet GVF=100%

Freq.	Re($\boldsymbol{H_{XX}}$)	Re($\boldsymbol{H_{XY}}$)	Re($\boldsymbol{H_{YX}}$)	Re($\boldsymbol{H_{YY}}$)	Im($\boldsymbol{H_{XX}}$)	Im($\boldsymbol{H_{XY}}$)	Im($\boldsymbol{H_{YX}}$)	Im($\boldsymbol{H_{YY}}$)	Re($\boldsymbol{eH_{XX}}$)	Re($\boldsymbol{eH_{XY}}$)	Re($\boldsymbol{eH_{YX}}$)	Re($\boldsymbol{eH_{YY}}$)	Im($\boldsymbol{eH_{XX}}$)	Im($\boldsymbol{eH_{XY}}$)	Im($\boldsymbol{eH_{YX}}$)	Im($\boldsymbol{eH_{YY}}$)
Hz	MN/m	MN/m	MN/m	MN/m	MN/m	MN/m	MN/m	MN/m	MN/m	MN/m	MN/m	MN/m	MN/m	MN/m	MN/m	MN/m
9.8	4.3	6.9	-7.5	3.0	1.1	-0.3	-0.5	2.2	-0.3	-0.2	-0.2	-0.2	-0.3	-0.2	-0.6	-0.3
19.5	4.3	6.9	-7.6	3.6	2.1	0.0	-0.1	2.4	-0.1	-0.2	-0.3	-0.3	-0.1	-0.1	-0.2	-0.4
29.3	4.4	6.9	-7.5	3.6	3.0	0.1	0.0	3.9	-0.1	-0.1	-0.2	-0.1	-0.1	-0.1	-0.2	-0.3
39.1	4.2	7.0	-7.5	3.8	4.4	0.0	0.5	4.3	-0.1	-0.1	-0.1	-0.2	0.0	-0.1	-0.1	-0.1
48.8	4.7	6.9	-7.3	3.9	5.5	0.2	0.4	5.5	-0.1	-0.1	-0.1	-0.2	-0.1	-0.1	-0.1	-0.2
58.6	4.8	7.2	-7.4	4.0	6.5	0.4	0.3	6.3	0.0	0.0	-0.1	-0.1	-0.1	-0.1	-0.1	-0.1
68.4	5.0	7.2	-7.0	4.5	7.5	0.1	0.4	7.1	-0.1	-0.1	-0.1	-0.2	-0.1	-0.1	-0.1	-0.1
78.1	4.9	7.5	-7.0	4.3	8.4	0.0	0.5	8.0	-0.1	-0.1	-0.1	-0.1	-0.1	-0.1	-0.1	-0.1
87.9	5.3	7.4	-7.8	3.9	9.4	0.0	0.6	9.5	0.0	0.0	-0.1	-0.1	0.0	0.0	-0.1	-0.1
97.7	5.2	7.4	-7.6	4.4	11.0	-0.1	0.9	11.0	0.0	-0.1	-0.1	-0.1	-0.1	0.0	-0.1	0.0
107.4	5.4	7.4	-6.9	4.6	11.0	-0.2	0.7	11.0	-0.1	-0.1	-0.1	-0.1	0.0	0.0	-0.1	-0.1
117.2	5.6	7.3	-7.0	4.6	12.0	-0.3	0.5	12.0	0.0	0.0	-0.1	-0.1	0.0	0.0	-0.1	-0.1
127.0	5.6	7.2	-7.0	4.9	13.0	-0.3	0.8	13.0	-0.1	0.0	-0.1	-0.2	0.0	-0.1	-0.1	-0.1
136.7	5.8	6.9	-7.1	5.2	14.0	-0.1	0.8	14.0	0.0	0.0	-0.1	-0.1	0.0	0.0	-0.1	-0.1

Table 168. Raw data for the test seal at ω=20 krpm, PR=0.43, C_r=0.188 mm, and inlet GVF=98%

Freq.	Re($\boldsymbol{H_{XX}}$)	Re($\boldsymbol{H_{XY}}$)	Re($\boldsymbol{H_{YX}}$)	Re($\boldsymbol{H_{YY}}$)	Im($\boldsymbol{H_{XX}}$)	Im($\boldsymbol{H_{XY}}$)	Im($\boldsymbol{H_{YX}}$)	Im($\boldsymbol{H_{YY}}$)	Re($\boldsymbol{eH_{XX}}$)	Re($\boldsymbol{eH_{XY}}$)	Re($\boldsymbol{eH_{YX}}$)	Re($\boldsymbol{eH_{YY}}$)	Im($\boldsymbol{eH_{XX}}$)	Im($\boldsymbol{eH_{XY}}$)	Im($\boldsymbol{eH_{YX}}$)	Im($\boldsymbol{eH_{YY}}$)
Hz	MN/m	MN/m	MN/m	MN/m	MN/m	MN/m	MN/m	MN/m	MN/m	MN/m	MN/m	MN/m	MN/m	MN/m	MN/m	MN/m
9.8	3.5	6.1	-4.7	1.3	0.1	0.4	0.0	1.4	-0.4	-0.3	-0.5	-0.6	-0.4	-0.4	-0.8	-0.7
19.5	3.2	6.4	-5.9	1.2	1.0	0.2	0.7	2.7	-0.3	-0.1	-0.4	-0.3	-0.1	-0.2	-0.4	-0.4
29.3	2.8	6.5	-4.8	1.0	2.2	-0.1	0.7	2.5	-0.2	-0.1	-0.3	-0.3	-0.1	-0.2	-0.2	-0.3
39.1	2.9	6.4	-4.9	1.0	3.6	-0.2	0.6	4.7	-0.1	-0.1	-0.1	-0.2	-0.1	-0.2	-0.2	-0.2
48.8	2.9	5.9	-4.8	1.8	4.9	-0.5	0.5	5.9	-0.2	-0.1	-0.3	-0.2	-0.2	-0.1	-0.2	-0.2
58.6	3.0	6.3	-4.5	2.1	6.0	-0.2	0.1	7.4	-0.2	-0.1	-0.3	-0.2	-0.1	-0.1	-0.2	-0.3
68.4	3.4	5.8	-4.7	2.6	6.8	0.2	-0.5	8.3	-0.1	-0.3	-0.3	-0.3	-0.1	-0.2	-0.2	-0.2
78.1	2.9	6.1	-4.8	2.0	8.1	0.0	0.1	8.7	-0.1	-0.2	-0.2	-0.3	-0.1	-0.2	-0.2	-0.3
87.9	3.3	6.2	-5.2	2.0	9.4	0.2	-0.1	9.8	-0.1	-0.1	-0.1	-0.1	-0.1	-0.1	-0.1	-0.1
97.7	3.6	6.5	-4.6	2.2	11.0	0.0	-0.2	11.0	-0.1	-0.2	-0.2	-0.2	-0.1	-0.2	-0.1	-0.1
107.4	3.5	6.4	-4.6	2.2	12.0	0.0	0.0	11.0	-0.1	-0.1	-0.2	-0.1	-0.1	-0.1	-0.1	-0.1
117.2	3.8	6.4	-4.7	2.1	12.0	-0.2	-0.5	13.0	-0.1	-0.1	-0.2	-0.1	-0.1	-0.1	-0.2	-0.1
127.0	3.8	6.1	-4.6	1.8	13.0	0.1	-0.4	14.0	-0.1	-0.1	-0.2	-0.3	-0.1	-0.2	-0.1	-0.4
136.7	4.2	6.1	-4.8	2.7	14.0	-0.1	-0.1	15.0	-0.1	-0.1	-0.1	-0.1	-0.1	-0.1	-0.2	-0.1

Table 169. Raw data for the test seal at ω=20 krpm, PR=0.43, C_r=0.188 mm, and inlet GVF=95%

Freq.	Re($\boldsymbol{H_{XX}}$)	Re($\boldsymbol{H_{XY}}$)	Re($\boldsymbol{H_{YX}}$)	Re($\boldsymbol{H_{YY}}$)	Im($\boldsymbol{H_{XX}}$)	Im($\boldsymbol{H_{XY}}$)	Im($\boldsymbol{H_{YX}}$)	Im($\boldsymbol{H_{YY}}$)	Re($\boldsymbol{eH_{XX}}$)	Re($\boldsymbol{eH_{XY}}$)	Re($\boldsymbol{eH_{YX}}$)	Re($\boldsymbol{eH_{YY}}$)	Im($\boldsymbol{eH_{XX}}$)	Im($\boldsymbol{eH_{XY}}$)	Im($\boldsymbol{eH_{YX}}$)	Im($\boldsymbol{eH_{YY}}$)
Hz	MN/m	MN/m	MN/m	MN/m	MN/m	MN/m	MN/m	MN/m	MN/m	MN/m	MN/m	MN/m	MN/m	MN/m	MN/m	MN/m
9.8	3.2	5.6	-4.5	0.8	-0.4	-0.2	-0.7	1.0	-0.3	-0.6	-0.5	-0.4	-0.6	-0.2	-0.3	-0.6
19.5	3.0	6.2	-5.2	0.9	0.5	0.4	0.2	2.3	-0.1	-0.2	-0.3	-0.3	-0.4	-0.3	-0.2	-0.3
29.3	2.3	6.7	-4.3	0.4	2.2	0.3	0.5	3.3	-0.2	-0.2	-0.2	-0.5	-0.1	-0.4	-0.3	-0.6
39.1	3.0	5.9	-4.8	0.6	3.7	-0.2	0.2	4.6	-0.3	-0.2	-0.4	-0.3	-0.2	-0.2	-0.1	-0.3
48.8	3.4	5.8	-4.6	0.6	4.9	-0.3	0.1	6.4	-0.1	-0.1	-0.3	-0.3	-0.2	-0.2	-0.2	-0.2
58.6	2.9	5.9	-5.0	1.3	6.0	-0.2	-0.5	8.1	-0.1	-0.3	-0.2	-0.3	-0.2	-0.3	-0.3	-0.3
68.4	3.0	7.0	-4.3	1.1	7.2	0.0	-1.1	8.7	-0.2	-0.3	-0.3	-0.6	-0.2	-0.4	-0.3	-0.2
78.1	3.5	6.1	-4.0	1.3	8.1	0.0	-0.1	9.2	-0.2	-0.2	-0.2	-0.2	-0.1	-0.2	-0.1	-0.1
87.9	3.0	5.8	-4.4	2.0	9.7	-0.1	0.1	10.0	-0.2	-0.1	-0.2	-0.1	-0.1	-0.1	-0.2	-0.2
97.7	3.1	5.8	-4.2	2.0	11.0	0.6	0.0	11.0	-0.2	-0.1	-0.2	-0.2	-0.1	-0.1	-0.1	-0.1
107.4	3.2	5.9	-4.2	2.3	12.0	0.4	-0.4	13.0	-0.1	-0.2	-0.2	-0.2	-0.1	-0.1	-0.4	-0.3
117.2	3.3	6.2	-4.7	1.7	13.0	0.3	-1.3	13.0	-0.1	0.0	-0.1	-0.1	-0.1	-0.1	-0.2	-0.2
127.0	3.8	6.9	-4.7	1.2	14.0	0.6	-0.9	16.0	-0.1	-0.2	-0.2	-0.6	-0.2	-0.5	-0.2	-0.3
136.7	4.1	6.7	-5.3	2.0	15.0	0.3	-0.5	16.0	-0.1	-0.1	-0.1	-0.3	-0.2	-0.2	-0.1	-0.1

Table 170. Raw data for the test seal at ω=20 krpm, PR=0.43, C_r=0.188 mm, and inlet GVF=92%

Freq.	Re($\boldsymbol{H_{XX}}$)	Re($\boldsymbol{H_{XY}}$)	Re($\boldsymbol{H_{YX}}$)	Re($\boldsymbol{H_{YY}}$)	Im($\boldsymbol{H_{XX}}$)	Im($\boldsymbol{H_{XY}}$)	Im($\boldsymbol{H_{YX}}$)	Im($\boldsymbol{H_{YY}}$)	Re($\boldsymbol{eH_{XX}}$)	Re($\boldsymbol{eH_{XY}}$)	Re($\boldsymbol{eH_{YX}}$)	Re($\boldsymbol{eH_{YY}}$)	Im($\boldsymbol{eH_{XX}}$)	Im($\boldsymbol{eH_{XY}}$)	Im($\boldsymbol{eH_{YX}}$)	Im($\boldsymbol{eH_{YY}}$)
Hz	MN/m	MN/m	MN/m	MN/m	MN/m	MN/m	MN/m	MN/m	MN/m	MN/m	MN/m	MN/m	MN/m	MN/m	MN/m	MN/m
9.8	9.4	2.2	-1.0	8.2	0.7	0.0	0.0	0.7	-0.1	-0.1	-0.1	0.0	0.0	0.0	-0.1	-0.1
19.5	9.2	2.2	-1.2	8.4	1.6	0.1	-0.1	1.7	0.0	0.0	-0.1	0.0	-0.1	0.0	-0.1	-0.1
29.3	8.9	2.9	-0.6	7.5	1.4	1.4	1.1	0.8	-0.1	0.0	-0.1	0.0	-0.1	0.0	0.0	0.0
39.1	9.3	2.5	-1.3	8.4	3.2	0.1	-0.2	3.3	-0.1	0.0	-0.1	0.0	0.0	0.0	-0.1	0.0
48.8	9.1	2.2	-1.4	8.3	4.0	0.2	-0.1	4.2	-0.1	0.0	-0.1	0.0	0.0	-0.1	0.0	-0.1
58.6	9.2	2.4	-1.3	8.4	5.1	0.2	-0.1	4.9	-0.1	-0.1	-0.1	-0.1	0.0	-0.1	-0.1	-0.1
68.4	9.3	2.3	-1.3	8.4	5.9	0.2	-0.1	5.8	-0.1	-0.1	-0.1	-0.1	-0.1	-0.1	-0.1	-0.1
78.1	9.4	2.3	-1.2	8.3	7.0	0.0	-0.1	6.7	-0.1	-0.1	-0.1	-0.1	-0.1	-0.1	0.0	0.0
87.9	9.3	2.1	-1.4	8.5	7.6	0.1	-0.2	7.6	0.0	-0.1	0.0	0.0	0.0	0.0	0.0	-0.1
97.7	9.1	2.2	-1.3	8.4	8.5	0.2	-0.2	8.3	0.0	0.0	0.0	0.0	0.0	-0.1	0.0	0.0
107.4	9.2	2.3	-1.2	8.4	9.5	0.1	-0.1	9.2	0.0	0.0	-0.1	0.0	-0.1	0.0	-0.1	0.0
117.2	9.3	2.2	-1.1	8.5	10.0	0.4	-0.3	10.0	0.0	-0.1	-0.1	0.0	-0.1	-0.1	-0.1	0.0
127.0	9.4	2.1	-1.2	8.5	11.0	0.3	-0.4	11.0	0.0	0.0	-0.1	-0.1	-0.1	0.0	-0.1	0.0
136.7	9.3	2.2	-1.3	8.6	12.0	0.3	-0.3	12.0	0.0	0.0	0.0	0.0	0.0	0.0	0.0	0.0

Table 171. Raw data for the test seal at ω=10 krpm, PR=0.57, C_r=0.163 mm, and inlet GVF=100%

Freq.	Re($\boldsymbol{H_{XX}}$)	Re($\boldsymbol{H_{XY}}$)	Re($\boldsymbol{H_{YX}}$)	Re($\boldsymbol{H_{YY}}$)	Im($\boldsymbol{H_{XX}}$)	Im($\boldsymbol{H_{XY}}$)	Im($\boldsymbol{H_{YX}}$)	Im($\boldsymbol{H_{YY}}$)	Re($\boldsymbol{eH_{XX}}$)	Re($\boldsymbol{eH_{XY}}$)	Re($\boldsymbol{eH_{YX}}$)	Re($\boldsymbol{eH_{YY}}$)	Im($\boldsymbol{eH_{XX}}$)	Im($\boldsymbol{eH_{XY}}$)	Im($\boldsymbol{eH_{YX}}$)	Im($\boldsymbol{eH_{YY}}$)
Hz	MN/m	MN/m	MN/m	MN/m	MN/m	MN/m	MN/m	MN/m	MN/m	MN/m	MN/m	MN/m	MN/m	MN/m	MN/m	MN/m
9.8	9.2	3.4	-2.2	7.8	0.8	0.2	0.0	0.7	-0.1	-0.1	-0.1	-0.1	0.0	-0.1	-0.1	0.0
19.5	9.3	3.3	-2.4	7.9	1.7	0.3	-0.2	1.7	-0.1	0.0	-0.1	0.0	-0.1	0.0	-0.1	-0.1
29.3	9.0	4.2	-2.0	7.2	1.1	1.8	1.3	0.8	-0.1	0.0	-0.1	0.0	-0.1	0.0	-0.1	-0.1
39.1	9.4	3.5	-2.6	8.0	3.3	0.2	-0.1	3.4	-0.1	0.0	-0.1	0.0	-0.1	0.0	0.0	0.0
48.8	9.3	3.5	-2.7	8.0	4.1	0.2	-0.2	4.2	0.0	-0.1	-0.1	-0.1	-0.1	-0.1	0.0	-0.1
58.6	9.4	3.7	-2.5	7.9	5.1	0.3	0.0	5.1	-0.1	-0.1	-0.1	-0.1	-0.1	-0.1	-0.1	-0.1
68.4	9.3	3.7	-2.5	8.1	5.9	0.2	-0.2	5.9	-0.1	-0.1	-0.1	-0.1	-0.1	0.0	-0.1	-0.1
78.1	9.3	3.5	-2.6	8.1	6.7	0.2	-0.1	6.7	-0.1	0.0	-0.1	-0.1	-0.1	-0.1	-0.1	0.0
87.9	9.5	3.6	-2.8	8.1	7.7	0.3	-0.3	7.4	0.0	-0.1	0.0	-0.1	-0.1	0.0	0.0	-0.1
97.7	9.2	3.4	-2.7	8.0	8.4	0.1	-0.1	8.2	-0.1	0.0	0.0	0.0	-0.1	0.0	-0.1	0.0
107.4	9.4	3.6	-2.4	8.0	9.4	0.2	0.0	9.2	-0.1	0.0	-0.1	0.0	-0.1	0.0	-0.1	0.0
117.2	9.3	3.3	-2.5	8.2	10.0	0.3	-0.3	10.0	-0.1	0.0	-0.1	0.0	-0.1	-0.1	-0.1	0.0
127.0	9.3	3.3	-2.5	8.0	11.0	0.4	-0.4	11.0	0.0	0.0	0.0	0.0	0.0	0.0	0.0	0.0
136.7	9.3	3.3	-2.5	8.2	12.0	0.4	-0.4	12.0	0.0	0.0	0.0	0.0	0.0	0.0	0.0	0.0

Table 172. Raw data for the test seal at ω=15 krpm, PR=0.57, C_r=0.163 mm, and inlet GVF=100%

Freq.	Re($\boldsymbol{H_{XX}}$)	Re($\boldsymbol{H_{XY}}$)	Re($\boldsymbol{H_{YX}}$)	Re($\boldsymbol{H_{YY}}$)	Im($\boldsymbol{H_{XX}}$)	Im($\boldsymbol{H_{XY}}$)	Im($\boldsymbol{H_{YX}}$)	Im($\boldsymbol{H_{YY}}$)	Re($\boldsymbol{eH_{XX}}$)	Re($\boldsymbol{eH_{XY}}$)	Re($\boldsymbol{eH_{YX}}$)	Re($\boldsymbol{eH_{YY}}$)	Im($\boldsymbol{eH_{XX}}$)	Im($\boldsymbol{eH_{XY}}$)	Im($\boldsymbol{eH_{YX}}$)	Im($\boldsymbol{eH_{YY}}$)
Hz	MN/m	MN/m	MN/m	MN/m	MN/m	MN/m	MN/m	MN/m	MN/m	MN/m	MN/m	MN/m	MN/m	MN/m	MN/m	MN/m
9.8	9.0	4.9	-3.9	7.5	0.8	0.2	0.0	0.8	-0.1	0.0	-0.2	-0.1	-0.1	-0.2	-0.1	-0.1
19.5	9.0	4.9	-3.9	7.5	1.6	0.2	-0.1	1.7	-0.1	0.0	-0.1	-0.1	-0.1	-0.1	-0.1	-0.1
29.3	8.6	5.6	-3.5	6.6	1.5	1.6	1.1	0.9	-0.1	-0.1	-0.1	0.0	-0.1	-0.1	-0.1	-0.1
39.1	9.3	5.0	-4.2	7.5	3.3	0.1	-0.1	3.4	-0.1	-0.1	-0.1	0.0	-0.1	-0.1	-0.1	0.0
48.8	9.1	4.8	-4.1	7.5	4.2	0.1	-0.2	4.2	-0.1	-0.1	0.0	-0.1	-0.1	-0.1	-0.1	-0.1
58.6	9.3	5.0	-4.0	7.6	5.2	0.1	-0.2	5.2	-0.1	-0.1	-0.1	-0.1	-0.1	-0.1	-0.1	0.0
68.4	9.2	4.8	-4.1	7.6	6.0	0.2	-0.4	5.9	0.0	-0.1	-0.1	-0.1	-0.1	-0.1	-0.1	-0.1
78.1	9.3	5.0	-4.0	7.7	6.8	0.1	-0.4	6.6	-0.1	-0.1	-0.1	-0.1	-0.1	-0.1	-0.1	-0.1
87.9	9.2	4.8	-4.3	7.7	7.5	0.2	-0.3	7.4	-0.1	0.0	-0.1	-0.1	0.0	0.0	0.0	-0.1
97.7	9.2	4.7	-4.2	7.6	8.5	0.2	-0.2	8.2	-0.1	0.0	-0.1	-0.1	-0.1	0.0	0.0	-0.1
107.4	9.2	5.1	-4.0	7.8	9.5	0.2	0.1	9.5	-0.1	-0.1	-0.1	-0.1	-0.1	0.0	-0.1	-0.1
117.2	9.2	4.8	-4.0	7.8	11.0	0.2	-0.5	9.9	-0.1	-0.1	0.0	-0.1	0.0	-0.1	-0.1	0.0
127.0	9.4	4.7	-4.1	7.7	11.0	0.2	-0.6	11.0	-0.1	-0.1	0.0	-0.1	-0.1	-0.1	0.0	0.0
136.7	9.2	4.6	-4.0	7.8	12.0	0.4	-0.5	12.0	0.0	0.0	0.0	0.0	0.0	0.0	0.0	0.0

Table 173. Raw data for the test seal at ω=20 krpm, PR=0.57, C_r=0.163 mm, and inlet GVF=100%

Freq.	Re($\boldsymbol{H_{XX}}$)	Re($\boldsymbol{H_{XY}}$)	Re($\boldsymbol{H_{YX}}$)	Re($\boldsymbol{H_{YY}}$)	Im($\boldsymbol{H_{XX}}$)	Im($\boldsymbol{H_{XY}}$)	Im($\boldsymbol{H_{YX}}$)	Im($\boldsymbol{H_{YY}}$)	Re($\boldsymbol{eH_{XX}}$)	Re($\boldsymbol{eH_{XY}}$)	Re($\boldsymbol{eH_{YX}}$)	Re($\boldsymbol{eH_{YY}}$)	Im($\boldsymbol{eH_{XX}}$)	Im($\boldsymbol{eH_{XY}}$)	Im($\boldsymbol{eH_{YX}}$)	Im($\boldsymbol{eH_{YY}}$)
Hz	MN/m	MN/m	MN/m	MN/m	MN/m	MN/m	MN/m	MN/m	MN/m	MN/m	MN/m	MN/m	MN/m	MN/m	MN/m	MN/m
9.8	8.2	2.6	-1.0	7.2	0.8	0.1	-0.1	0.8	-0.1	-0.1	-0.1	0.0	-0.1	-0.1	-0.1	0.0
19.5	8.3	2.5	-1.0	7.3	1.8	0.1	0.0	1.8	-0.1	0.0	-0.1	-0.1	-0.1	-0.1	-0.1	-0.1
29.3	8.0	3.3	-0.5	6.4	1.8	1.4	1.1	1.1	-0.1	-0.1	-0.1	-0.1	-0.1	0.0	-0.1	0.0
39.1	8.5	2.7	-1.0	7.2	3.7	0.2	0.0	3.6	-0.1	0.0	-0.1	0.0	-0.1	0.0	-0.1	0.0
48.8	8.2	2.6	-1.2	7.2	4.7	0.2	-0.1	4.6	-0.1	0.0	0.0	0.0	-0.1	0.0	-0.1	0.0
58.6	8.4	2.8	-1.1	7.3	5.7	0.2	-0.2	5.7	-0.1	-0.1	-0.1	-0.1	0.0	-0.1	-0.1	-0.1
68.4	8.5	2.8	-1.3	7.3	6.7	-0.1	-0.1	6.5	-0.1	0.0	0.0	0.0	0.0	-0.1	-0.1	0.0
78.1	8.5	2.6	-1.2	7.4	7.5	0.0	-0.2	7.3	-0.1	-0.1	-0.1	0.0	-0.1	0.0	-0.1	-0.1
87.9	8.4	2.6	-1.3	7.4	8.3	0.0	-0.2	8.3	-0.1	-0.1	0.0	-0.1	0.0	-0.1	0.0	0.0
97.7	8.6	2.5	-1.3	7.4	9.4	0.0	-0.1	9.2	-0.1	0.0	0.0	-0.1	-0.1	0.0	0.0	0.0
107.4	8.7	2.7	-1.0	7.6	10.0	0.2	0.0	10.0	-0.1	0.0	-0.1	0.0	-0.1	0.0	-0.1	0.0
117.2	8.6	2.6	-1.3	7.6	11.0	0.2	-0.2	11.0	0.0	0.0	-0.1	0.0	-0.1	0.0	0.0	0.0
127.0	8.7	2.5	-1.2	7.6	12.0	0.2	-0.3	12.0	-0.1	0.0	0.0	0.0	0.0	0.0	0.0	0.0
136.7	8.7	2.5	-1.2	7.7	13.0	0.1	-0.2	13.0	0.0	0.0	0.0	0.0	0.0	0.0	0.0	0.0

Table 174. Raw data for the test seal at ω=10 krpm, PR=0.5, C_r=0.163 mm, and inlet GVF=100%

Freq.	Re($\boldsymbol{H_{XX}}$)	Re($\boldsymbol{H_{XY}}$)	Re($\boldsymbol{H_{YX}}$)	Re($\boldsymbol{H_{YY}}$)	Im($\boldsymbol{H_{XX}}$)	Im($\boldsymbol{H_{XY}}$)	Im($\boldsymbol{H_{YX}}$)	Im($\boldsymbol{H_{YY}}$)	Re($\boldsymbol{eH_{XX}}$)	Re($\boldsymbol{eH_{XY}}$)	Re($\boldsymbol{eH_{YX}}$)	Re($\boldsymbol{eH_{YY}}$)	Im($\boldsymbol{eH_{XX}}$)	Im($\boldsymbol{eH_{XY}}$)	Im($\boldsymbol{eH_{YX}}$)	Im($\boldsymbol{eH_{YY}}$)
Hz	MN/m	MN/m	MN/m	MN/m	MN/m	MN/m	MN/m	MN/m	MN/m	MN/m	MN/m	MN/m	MN/m	MN/m	MN/m	MN/m
9.8	3.9	4.5	-4.5	2.5	0.4	0.4	0.2	1.3	-0.2	-0.1	-0.3	-0.1	-0.1	-0.1	-0.3	-0.3
19.5	4.1	5.0	-3.8	3.3	3.3	0.5	0.4	2.9	-0.2	0.0	-0.2	-0.3	-0.1	-0.1	-0.1	-0.3
29.3	5.0	4.8	-4.6	3.4	4.7	0.4	-0.3	4.0	-0.1	-0.1	-0.1	-0.1	-0.1	-0.1	-0.2	-0.2
39.1	4.6	5.1	-4.2	3.2	5.6	0.2	0.3	4.9	-0.1	-0.1	-0.1	-0.1	-0.2	-0.1	-0.2	-0.2
48.8	5.1	5.4	-4.2	3.7	6.9	0.3	0.5	6.3	-0.1	-0.1	-0.2	-0.2	-0.1	-0.1	-0.1	0.0
58.6	5.1	5.6	-4.1	3.6	7.8	0.2	0.2	7.8	-0.1	0.0	-0.2	-0.3	-0.1	-0.1	-0.2	-0.1
68.4	5.3	5.4	-4.3	4.0	9.1	0.0	0.4	8.9	-0.1	-0.2	-0.2	-0.3	-0.1	-0.1	-0.1	-0.2
78.1	5.6	5.4	-4.0	3.8	10.0	0.2	0.4	10.0	-0.2	0.0	-0.1	-0.2	-0.1	-0.1	-0.2	-0.1
87.9	5.6	5.2	-4.2	4.1	11.0	-0.1	0.4	11.0	-0.1	-0.1	-0.1	-0.1	-0.1	-0.1	-0.1	-0.1
97.7	5.6	5.4	-4.1	4.4	12.0	0.0	0.4	12.0	-0.1	0.0	-0.1	-0.1	-0.1	-0.1	-0.1	-0.1
107.4	5.8	5.4	-3.8	4.6	14.0	-0.1	0.1	14.0	-0.1	0.0	-0.1	-0.1	0.0	0.0	-0.2	-0.1
117.2	5.8	5.4	-3.9	4.8	15.0	0.1	0.0	15.0	0.0	0.0	0.0	0.0	-0.1	-0.1	-0.1	-0.1
127.0	6.0	5.3	-3.8	4.9	16.0	0.0	-0.1	16.0	-0.1	0.0	-0.1	-0.1	-0.1	-0.1	0.0	-0.1
136.7	6.1	5.2	-3.9	5.3	17.0	0.0	0.0	16.0	-0.1	0.0	-0.1	-0.1	0.0	0.0	-0.1	-0.1

Table 175. Raw data for the test seal at ω=10 krpm, PR=0.5, C_r=0.163 mm, and inlet GVF=98%

Freq.	Re($\boldsymbol{H_{XX}}$)	Re($\boldsymbol{H_{XY}}$)	Re($\boldsymbol{H_{YX}}$)	Re($\boldsymbol{H_{YY}}$)	Im($\boldsymbol{H_{XX}}$)	Im($\boldsymbol{H_{XY}}$)	Im($\boldsymbol{H_{YX}}$)	Im($\boldsymbol{H_{YY}}$)	Re($\boldsymbol{eH_{XX}}$)	Re($\boldsymbol{eH_{XY}}$)	Re($\boldsymbol{eH_{YX}}$)	Re($\boldsymbol{eH_{YY}}$)	Im($\boldsymbol{eH_{XX}}$)	Im($\boldsymbol{eH_{XY}}$)	Im($\boldsymbol{eH_{YX}}$)	Im($\boldsymbol{eH_{YY}}$)
Hz	MN/m	MN/m	MN/m	MN/m	MN/m	MN/m	MN/m	MN/m	MN/m	MN/m	MN/m	MN/m	MN/m	MN/m	MN/m	MN/m
9.8	3.8	4.2	-3.2	2.0	-0.5	0.5	-1.6	1.6	-0.2	-0.2	-0.4	-0.4	-0.3	-0.2	-0.4	-0.5
19.5	2.9	4.6	-3.5	2.1	2.0	0.4	0.5	2.6	-0.1	-0.1	-0.2	-0.2	-0.2	-0.1	-0.3	-0.2
29.3	4.3	3.3	-4.9	3.7	3.5	0.1	-0.2	3.8	-0.3	-0.2	-0.4	-0.2	-0.2	-0.3	-0.3	-0.4
39.1	3.0	4.6	-3.2	2.0	4.9	0.3	0.6	5.2	-0.2	-0.2	-0.3	-0.3	-0.2	-0.2	-0.2	-0.2
48.8	3.2	4.4	-3.2	2.5	6.4	0.6	0.6	6.7	-0.1	-0.2	-0.2	-0.2	-0.1	-0.2	-0.1	-0.1
58.6	3.1	5.0	-4.0	3.1	7.7	0.7	0.1	8.0	-0.1	-0.3	-0.3	-0.1	-0.1	-0.2	-0.4	-0.3
68.4	4.0	5.2	-3.3	3.3	8.9	0.5	-0.4	8.9	-0.1	-0.1	-0.2	-0.1	-0.1	-0.1	-0.3	-0.3
78.1	4.2	4.7	-2.9	3.1	9.8	0.0	0.1	9.6	-0.2	-0.2	-0.3	-0.3	-0.2	-0.2	-0.2	-0.2
87.9	3.8	4.7	-3.6	3.1	11.0	0.5	-0.1	11.0	-0.1	-0.1	-0.1	-0.1	-0.1	-0.1	0.0	-0.1
97.7	4.4	4.9	-3.3	3.4	12.0	0.4	0.1	13.0	-0.1	-0.1	-0.2	-0.1	-0.1	-0.1	-0.2	-0.2
107.4	4.7	4.9	-2.9	3.3	13.0	0.0	-0.5	14.0	0.0	-0.1	-0.1	-0.2	-0.1	-0.1	-0.3	-0.2
117.2	4.4	5.0	-3.5	3.6	15.0	0.0	-0.1	15.0	-0.1	-0.1	-0.2	-0.1	-0.1	-0.1	-0.3	-0.2
127.0	4.6	4.6	-3.5	3.9	16.0	0.1	-0.1	16.0	-0.1	-0.1	-0.1	-0.2	-0.2	0.0	-0.2	-0.1
136.7	4.6	5.1	-3.3	3.8	17.0	-0.1	0.0	17.0	-0.1	-0.1	-0.1	-0.2	-0.1	-0.1	-0.1	-0.1

Table 176. Raw data for the test seal at ω=10 krpm, PR=0.5, C_r=0.163 mm, and inlet GVF=95%

Freq.	Re($\boldsymbol{H_{XX}}$)	Re($\boldsymbol{H_{XY}}$)	Re($\boldsymbol{H_{YX}}$)	Re($\boldsymbol{H_{YY}}$)	Im($\boldsymbol{H_{XX}}$)	Im($\boldsymbol{H_{XY}}$)	Im($\boldsymbol{H_{YX}}$)	Im($\boldsymbol{H_{YY}}$)	Re($\boldsymbol{eH_{XX}}$)	Re($\boldsymbol{eH_{XY}}$)	Re($\boldsymbol{eH_{YX}}$)	Re($\boldsymbol{eH_{YY}}$)	Im($\boldsymbol{eH_{XX}}$)	Im($\boldsymbol{eH_{XY}}$)	Im($\boldsymbol{eH_{YX}}$)	Im($\boldsymbol{eH_{YY}}$)
Hz	MN/m	MN/m	MN/m	MN/m	MN/m	MN/m	MN/m	MN/m	MN/m	MN/m	MN/m	MN/m	MN/m	MN/m	MN/m	MN/m
9.8	3.9	3.2	-4.2	1.2	-0.7	0.5	0.2	1.7	-0.5	-0.5	-0.5	-0.4	-0.4	-0.3	-0.2	-0.3
19.5	2.1	4.2	-3.3	1.3	1.4	0.8	1.0	2.8	-0.3	-0.2	-0.2	-0.4	-0.1	-0.2	-0.4	-0.2
29.3	4.4	2.8	-4.4	3.6	3.4	1.4	1.0	3.9	-0.2	-0.2	-0.2	-0.4	-0.2	-0.2	-0.5	-0.6
39.1	3.0	4.5	-1.9	1.6	4.9	0.5	0.7	6.0	-0.3	-0.1	-0.4	-0.1	-0.2	-0.1	-0.3	-0.2
48.8	2.5	4.8	-2.5	1.9	6.3	0.6	-0.1	7.7	-0.2	-0.3	-0.3	-0.3	-0.1	-0.3	-0.3	-0.3
58.6	3.1	4.3	-3.1	2.8	7.9	0.4	-0.3	8.3	-0.2	-0.3	-0.3	-0.4	-0.4	-0.2	-0.4	-0.5
68.4	3.3	4.1	-2.8	2.8	8.9	0.1	0.2	9.1	-0.2	-0.2	-0.3	-0.3	-0.4	-0.4	-0.5	-0.4
78.1	4.3	4.3	-2.5	2.7	10.0	-0.1	0.3	9.9	-0.2	-0.3	-0.2	-0.2	-0.1	-0.1	-0.2	-0.4
87.9	3.5	4.6	-2.7	2.3	11.0	0.6	-0.2	11.0	-0.2	-0.1	-0.2	-0.2	-0.1	-0.3	-0.1	-0.2
97.7	3.8	4.8	-2.3	2.6	13.0	0.5	-0.2	12.0	-0.2	-0.1	-0.2	-0.2	-0.1	-0.2	-0.2	-0.3
107.4	3.8	4.5	-3.6	2.2	14.0	0.5	-0.2	15.0	-0.1	-0.1	-0.1	-0.1	-0.2	-0.1	-0.4	-0.2
117.2	4.2	4.9	-3.0	2.4	15.0	0.2	-0.4	16.0	-0.2	-0.2	-0.3	-0.1	-0.1	-0.1	-0.3	-0.1
127.0	4.3	4.8	-2.9	2.7	16.0	0.5	-0.4	17.0	-0.2	-0.1	-0.2	-0.3	-0.1	-0.2	-0.2	-0.2
136.7	3.9	5.4	-2.9	3.1	17.0	-0.2	-0.7	18.0	-0.1	-0.1	-0.2	-0.1	-0.2	0.0	-0.1	-0.2

Table 177. Raw data for the test seal at ω=10 krpm, PR=0.5, C_r=0.163 mm, and inlet GVF=92%

Freq.	Re($\boldsymbol{H_{XX}}$)	Re($\boldsymbol{H_{XY}}$)	Re($\boldsymbol{H_{YX}}$)	Re($\boldsymbol{H_{YY}}$)	Im($\boldsymbol{H_{XX}}$)	Im($\boldsymbol{H_{XY}}$)	Im($\boldsymbol{H_{YX}}$)	Im($\boldsymbol{H_{YY}}$)	Re($\boldsymbol{eH_{XX}}$)	Re($\boldsymbol{eH_{XY}}$)	Re($\boldsymbol{eH_{YX}}$)	Re($\boldsymbol{eH_{YY}}$)	Im($\boldsymbol{eH_{XX}}$)	Im($\boldsymbol{eH_{XY}}$)	Im($\boldsymbol{eH_{YX}}$)	Im($\boldsymbol{eH_{YY}}$)
Hz	MN/m	MN/m	MN/m	MN/m	MN/m	MN/m	MN/m	MN/m	MN/m	MN/m	MN/m	MN/m	MN/m	MN/m	MN/m	MN/m
9.8	7.9	3.7	-2.3	6.6	0.9	0.2	0.0	0.7	-0.1	-0.1	-0.1	0.0	0.0	-0.1	-0.1	0.0
19.5	7.9	3.8	-2.4	6.5	2.0	0.0	-0.3	1.9	-0.1	0.0	0.0	-0.1	-0.1	-0.1	-0.1	-0.1
29.3	7.4	4.5	-1.8	5.7	1.8	1.5	1.0	1.3	-0.1	0.0	-0.1	-0.1	-0.1	-0.1	-0.1	-0.1
39.1	8.0	4.0	-2.5	6.6	3.9	0.1	-0.1	3.8	0.0	-0.1	0.0	0.0	-0.1	0.0	-0.1	-0.1
48.8	8.0	4.0	-2.7	6.6	4.5	0.2	-0.1	4.6	0.0	-0.1	-0.1	-0.1	-0.1	-0.1	0.0	0.0
58.6	8.0	4.0	-2.5	6.7	5.6	0.0	-0.1	5.6	0.0	0.0	-0.1	0.0	-0.1	-0.1	-0.1	-0.1
68.4	8.3	3.9	-2.6	6.8	6.7	0.0	-0.4	6.3	-0.1	-0.1	-0.1	-0.1	-0.1	-0.1	-0.1	-0.1
78.1	8.3	3.9	-2.4	6.8	7.4	0.0	-0.2	7.5	0.0	-0.1	0.0	0.0	-0.1	-0.1	-0.1	0.0
87.9	8.3	3.9	-2.7	6.8	8.3	-0.1	-0.2	8.2	0.0	0.0	0.0	-0.1	-0.1	0.0	0.0	-0.1
97.7	8.1	3.8	-2.5	6.8	9.2	0.0	0.0	9.2	0.0	0.0	0.0	-0.1	0.0	-0.1	0.0	-0.1
107.4	8.3	3.9	-2.4	6.8	10.0	-0.1	-0.1	10.0	-0.1	0.0	0.0	-0.1	-0.1	-0.1	-0.1	0.0
117.2	8.1	3.7	-2.4	7.0	11.0	0.2	-0.2	11.0	-0.1	-0.1	-0.1	0.0	-0.1	-0.1	0.0	0.0
127.0	8.4	3.8	-2.4	7.1	12.0	0.0	-0.4	12.0	0.0	0.0	0.0	-0.1	0.0	0.0	0.0	-0.1
136.7	8.3	3.6	-2.5	7.2	13.0	0.0	-0.3	13.0	0.0	-0.1	-0.1	0.0	0.0	0.0	0.0	0.0

Table 178. Raw data for the test seal at ω=15 krpm, PR=0.5, C_r=0.163 mm, and inlet GVF=100%

Freq.	Re($\boldsymbol{H_{XX}}$)	Re($\boldsymbol{H_{XY}}$)	Re($\boldsymbol{H_{YX}}$)	Re($\boldsymbol{H_{YY}}$)	Im($\boldsymbol{H_{XX}}$)	Im($\boldsymbol{H_{XY}}$)	Im($\boldsymbol{H_{YX}}$)	Im($\boldsymbol{H_{YY}}$)	Re($\boldsymbol{eH_{XX}}$)	Re($\boldsymbol{eH_{XY}}$)	Re($\boldsymbol{eH_{YX}}$)	Re($\boldsymbol{eH_{YY}}$)	Im($\boldsymbol{eH_{XX}}$)	Im($\boldsymbol{eH_{XY}}$)	Im($\boldsymbol{eH_{YX}}$)	Im($\boldsymbol{eH_{YY}}$)
Hz	MN/m	MN/m	MN/m	MN/m	MN/m	MN/m	MN/m	MN/m	MN/m	MN/m	MN/m	MN/m	MN/m	MN/m	MN/m	MN/m
9.8	4.7	7.0	-7.4	2.3	0.3	-0.1	-0.1	1.3	-0.2	-0.1	-0.3	-0.2	-0.2	-0.1	-0.3	-0.2
19.5	3.9	7.6	-7.4	3.3	2.9	0.5	0.8	2.9	-0.2	-0.2	-0.3	-0.3	-0.1	-0.1	-0.2	-0.3
29.3	4.7	7.1	-7.1	3.2	4.5	0.1	0.7	3.9	-0.2	-0.1	-0.2	-0.2	-0.1	-0.2	-0.2	-0.2
39.1	4.8	7.3	-6.4	3.2	5.4	0.1	0.8	5.0	-0.1	0.0	-0.2	-0.2	-0.1	-0.1	-0.3	-0.1
48.8	5.1	7.2	-6.7	3.2	6.5	0.1	0.6	6.3	-0.1	-0.1	-0.2	-0.1	-0.1	0.0	-0.2	-0.2
58.6	5.2	7.6	-6.4	3.5	7.7	0.0	1.1	7.4	-0.1	-0.2	-0.2	-0.2	-0.1	-0.2	-0.2	-0.3
68.4	5.4	7.3	-6.5	3.6	8.7	0.0	0.6	8.6	-0.1	-0.1	-0.2	-0.1	-0.1	-0.1	-0.2	-0.2
78.1	5.5	7.5	-6.4	3.8	9.3	0.0	1.1	9.8	-0.1	-0.1	-0.1	-0.1	-0.1	-0.1	-0.1	-0.2
87.9	5.4	7.6	-6.6	3.7	11.0	-0.2	0.8	11.0	-0.1	0.0	-0.1	-0.2	-0.1	-0.1	-0.2	-0.2
97.7	5.4	7.6	-6.5	3.9	12.0	-0.1	1.2	12.0	-0.1	-0.1	-0.2	-0.2	-0.1	0.0	-0.1	-0.1
107.4	5.6	7.6	-5.9	3.9	13.0	-0.5	0.9	13.0	-0.1	-0.1	-0.1	-0.1	-0.1	-0.1	-0.1	-0.1
117.2	5.7	7.5	-5.8	4.2	14.0	-0.4	0.4	14.0	-0.1	0.0	-0.1	-0.1	-0.1	-0.1	-0.2	-0.1
127.0	5.6	7.3	-5.9	4.3	15.0	-0.3	0.6	16.0	-0.1	-0.1	-0.1	-0.1	-0.1	-0.1	-0.2	-0.1
136.7	5.6	7.3	-5.9	4.7	17.0	-0.2	0.6	17.0	0.0	-0.1	-0.1	-0.1	-0.1	-0.1	-0.1	-0.1

Table 179. Raw data for the test seal at ω=15 krpm, PR=0.5, C_r=0.163 mm, and inlet GVF=98%

Freq.	Re($\boldsymbol{H_{XX}}$)	Re($\boldsymbol{H_{XY}}$)	Re($\boldsymbol{H_{YX}}$)	Re($\boldsymbol{H_{YY}}$)	Im($\boldsymbol{H_{XX}}$)	Im($\boldsymbol{H_{XY}}$)	Im($\boldsymbol{H_{YX}}$)	Im($\boldsymbol{H_{YY}}$)	Re($\boldsymbol{eH_{XX}}$)	Re($\boldsymbol{eH_{XY}}$)	Re($\boldsymbol{eH_{YX}}$)	Re($\boldsymbol{eH_{YY}}$)	Im($\boldsymbol{eH_{XX}}$)	Im($\boldsymbol{eH_{XY}}$)	Im($\boldsymbol{eH_{YX}}$)	Im($\boldsymbol{eH_{YY}}$)
Hz	MN/m	MN/m	MN/m	MN/m	MN/m	MN/m	MN/m	MN/m	MN/m	MN/m	MN/m	MN/m	MN/m	MN/m	MN/m	MN/m
9.8	4.2	6.1	-4.4	2.4	0.4	0.4	-0.5	1.6	-0.4	-0.2	-0.6	-0.2	-0.4	-0.4	-0.6	-0.5
19.5	3.2	6.5	-6.4	2.9	1.3	0.5	0.5	2.4	-0.1	-0.2	-0.3	-0.3	-0.2	-0.1	-0.2	-0.3
29.3	5.6	4.7	-7.6	4.1	3.4	0.2	0.2	4.2	-0.2	-0.2	-0.3	-0.3	-0.2	-0.2	-0.3	-0.4
39.1	3.7	6.2	-4.6	2.6	4.7	0.0	0.3	5.0	-0.2	-0.1	-0.2	-0.2	-0.2	-0.1	-0.2	-0.1
48.8	3.7	6.3	-4.9	3.1	5.7	0.0	0.3	6.4	-0.1	-0.1	-0.2	-0.1	-0.1	-0.1	-0.2	-0.2
58.6	3.8	6.3	-4.9	2.4	7.2	0.0	0.5	7.9	-0.1	-0.2	-0.1	-0.2	-0.2	-0.2	-0.1	-0.1
68.4	3.9	6.2	-5.0	3.2	8.6	0.1	0.7	9.0	-0.2	-0.2	-0.2	-0.2	-0.2	-0.1	-0.2	-0.3
78.1	3.8	6.7	-4.5	3.3	9.2	0.0	0.2	9.9	-0.1	-0.1	-0.2	-0.2	-0.1	-0.2	-0.2	-0.1
87.9	3.7	6.7	-4.5	3.2	10.0	0.2	0.2	11.0	-0.1	-0.1	-0.1	-0.2	-0.1	-0.1	-0.1	-0.2
97.7	3.9	6.7	-4.3	3.3	12.0	0.3	0.3	12.0	-0.2	-0.1	-0.2	-0.3	-0.1	-0.1	-0.2	-0.2
107.4	4.4	6.6	-4.1	3.5	13.0	0.2	0.1	13.0	-0.1	-0.1	-0.2	-0.1	-0.1	-0.1	-0.1	-0.1
117.2	4.6	6.6	-4.7	3.5	14.0	0.0	-0.6	15.0	-0.1	0.0	-0.3	-0.1	-0.1	-0.1	-0.2	-0.2
127.0	4.5	6.7	-4.4	3.7	15.0	0.1	-0.4	16.0	-0.1	-0.1	-0.1	-0.2	-0.1	-0.2	-0.1	-0.2
136.7	4.4	7.1	-4.2	4.2	17.0	-0.5	-0.5	17.0	-0.1	-0.1	-0.2	-0.2	-0.1	-0.1	-0.1	-0.1

Table 180. Raw data for the test seal at ω=15 krpm, PR=0.5, C_r=0.163 mm, and inlet GVF=95%

Freq.	Re($\boldsymbol{H_{XX}}$)	Re($\boldsymbol{H_{XY}}$)	Re($\boldsymbol{H_{YX}}$)	Re($\boldsymbol{H_{YY}}$)	Im($\boldsymbol{H_{XX}}$)	Im($\boldsymbol{H_{XY}}$)	Im($\boldsymbol{H_{YX}}$)	Im($\boldsymbol{H_{YY}}$)	Re($\boldsymbol{eH_{XX}}$)	Re($\boldsymbol{eH_{XY}}$)	Re($\boldsymbol{eH_{YX}}$)	Re($\boldsymbol{eH_{YY}}$)	Im($\boldsymbol{eH_{XX}}$)	Im($\boldsymbol{eH_{XY}}$)	Im($\boldsymbol{eH_{YX}}$)	Im($\boldsymbol{eH_{YY}}$)
Hz	MN/m	MN/m	MN/m	MN/m	MN/m	MN/m	MN/m	MN/m	MN/m	MN/m	MN/m	MN/m	MN/m	MN/m	MN/m	MN/m
9.8	4.5	5.0	-5.0	2.6	-0.6	0.3	-0.8	1.5	-0.6	-0.3	-0.6	-0.6	-0.5	-0.5	-0.5	-0.2
19.5	4.0	6.4	-4.5	2.0	1.0	0.5	-0.4	2.6	-0.3	-0.4	-0.4	-0.3	-0.5	-0.3	-0.6	-0.3
29.3	5.2	5.1	-6.8	3.5	2.9	0.8	1.2	3.7	-0.3	-0.2	-0.4	-0.3	-0.2	-0.3	-0.5	-0.3
39.1	3.0	6.0	-4.9	1.6	4.7	-0.3	0.5	5.9	-0.3	-0.2	-0.2	-0.2	-0.2	-0.1	-0.3	-0.3
48.8	3.6	6.0	-4.5	2.1	5.9	-0.6	0.4	6.7	-0.3	-0.2	-0.1	-0.4	-0.2	-0.1	-0.3	-0.1
58.6	3.7	6.4	-4.6	3.3	7.0	-0.3	0.2	7.7	-0.2	-0.5	-0.3	-0.2	-0.3	-0.2	-0.2	-0.4
68.4	3.7	6.1	-4.0	2.7	7.9	-0.4	-0.1	8.6	-0.3	-0.2	-0.1	-0.2	-0.3	-0.2	-0.4	-0.2
78.1	3.8	5.2	-4.2	3.3	9.4	0.3	0.2	10.0	-0.2	-0.1	-0.2	-0.3	-0.2	-0.3	-0.3	-0.2
87.9	3.3	5.9	-4.2	3.0	11.0	0.6	-0.4	12.0	-0.2	-0.2	-0.2	-0.2	-0.1	-0.2	-0.2	-0.2
97.7	3.6	6.2	-4.2	3.4	12.0	0.4	-0.4	13.0	-0.2	-0.2	-0.1	-0.1	-0.2	-0.1	-0.3	-0.2
107.4	4.5	6.1	-4.0	3.3	14.0	0.2	-0.5	14.0	-0.1	-0.2	-0.3	-0.1	-0.1	-0.2	-0.2	-0.2
117.2	4.6	6.3	-4.8	3.4	14.0	0.2	-0.6	15.0	-0.2	-0.2	-0.2	-0.2	-0.2	-0.1	-0.4	-0.1
127.0	4.4	6.4	-4.6	3.4	16.0	0.5	-1.0	17.0	-0.2	-0.3	-0.2	-0.4	-0.1	-0.1	-0.3	-0.2
136.7	4.5	6.5	-4.6	3.6	17.0	-0.6	-1.0	18.0	-0.1	-0.2	-0.1	-0.3	-0.2	-0.2	-0.2	-0.2

Table 181. Raw data for the test seal at ω=15 krpm, PR=0.5, C_r=0.163 mm, and inlet GVF=92%

Freq.	Re($\boldsymbol{H_{XX}}$)	Re($\boldsymbol{H_{XY}}$)	Re($\boldsymbol{H_{YX}}$)	Re($\boldsymbol{H_{YY}}$)	Im($\boldsymbol{H_{XX}}$)	Im($\boldsymbol{H_{XY}}$)	Im($\boldsymbol{H_{YX}}$)	Im($\boldsymbol{H_{YY}}$)	Re($\boldsymbol{eH_{XX}}$)	Re($\boldsymbol{eH_{XY}}$)	Re($\boldsymbol{eH_{YX}}$)	Re($\boldsymbol{eH_{YY}}$)	Im($\boldsymbol{eH_{XX}}$)	Im($\boldsymbol{eH_{XY}}$)	Im($\boldsymbol{eH_{YX}}$)	Im($\boldsymbol{eH_{YY}}$)
Hz	MN/m	MN/m	MN/m	MN/m	MN/m	MN/m	MN/m	MN/m	MN/m	MN/m	MN/m	MN/m	MN/m	MN/m	MN/m	MN/m
9.8	7.4	5.2	-3.8	5.9	1.0	0.1	-0.1	1.0	-0.1	-0.1	0.0	0.0	-0.1	-0.1	-0.1	0.0
19.5	7.6	5.3	-3.9	6.0	1.9	0.2	-0.1	1.8	-0.1	0.0	-0.1	0.0	0.0	-0.1	-0.1	-0.1
29.3	7.2	5.9	-3.4	4.9	1.8	1.2	0.7	1.6	-0.1	-0.1	-0.1	-0.1	-0.1	0.0	-0.1	-0.1
39.1	7.9	5.4	-4.1	5.9	3.9	0.0	0.0	3.7	-0.1	-0.1	0.0	-0.1	-0.1	-0.1	-0.1	-0.1
48.8	7.7	5.3	-4.1	5.9	4.7	0.0	-0.1	4.8	-0.1	-0.1	0.0	0.0	-0.1	0.0	-0.1	-0.1
58.6	7.8	5.5	-3.8	6.3	5.5	0.0	-0.2	5.5	-0.1	-0.1	-0.1	-0.1	-0.1	-0.2	-0.1	-0.1
68.4	7.7	5.3	-4.1	6.1	6.6	-0.2	-0.3	6.5	-0.1	0.0	-0.1	-0.1	0.0	-0.1	-0.1	-0.1
78.1	7.9	5.5	-4.1	6.2	7.3	0.0	-0.2	7.4	0.0	-0.1	0.0	-0.1	0.0	-0.1	-0.1	-0.1
87.9	7.9	5.4	-4.4	6.3	8.4	0.0	-0.3	8.3	0.0	-0.1	0.0	0.0	0.0	-0.1	0.0	0.0
97.7	8.0	5.2	-4.3	6.2	9.4	0.0	-0.2	9.2	-0.1	-0.1	0.0	-0.1	-0.1	-0.1	0.0	-0.1
107.4	7.9	5.5	-3.9	6.4	10.0	-0.1	0.1	10.0	-0.1	-0.1	0.0	0.0	-0.1	-0.1	-0.1	0.0
117.2	8.1	5.3	-4.0	6.5	11.0	-0.1	-0.4	11.0	-0.1	0.0	-0.1	0.0	0.0	-0.1	-0.1	0.0
127.0	8.1	5.3	-4.0	6.4	12.0	0.0	-0.3	12.0	0.0	-0.1	0.0	0.0	0.0	0.0	-0.1	-0.1
136.7	8.0	5.1	-4.1	6.6	13.0	0.1	-0.3	13.0	0.0	-0.1	-0.1	0.0	0.0	0.0	0.0	0.0

Table 182. Raw data for the test seal at ω=20 krpm, PR=0.5, C_r=0.163 mm, and inlet GVF=100%

Freq.	Re($\boldsymbol{H_{XX}}$)	Re($\boldsymbol{H_{XY}}$)	Re($\boldsymbol{H_{YX}}$)	Re($\boldsymbol{H_{YY}}$)	Im($\boldsymbol{H_{XX}}$)	Im($\boldsymbol{H_{XY}}$)	Im($\boldsymbol{H_{YX}}$)	Im($\boldsymbol{H_{YY}}$)	Re($\boldsymbol{eH_{XX}}$)	Re($\boldsymbol{eH_{XY}}$)	Re($\boldsymbol{eH_{YX}}$)	Re($\boldsymbol{eH_{YY}}$)	Im($\boldsymbol{eH_{XX}}$)	Im($\boldsymbol{eH_{XY}}$)	Im($\boldsymbol{eH_{YX}}$)	Im($\boldsymbol{eH_{YY}}$)
Hz	MN/m	MN/m	MN/m	MN/m	MN/m	MN/m	MN/m	MN/m	MN/m	MN/m	MN/m	MN/m	MN/m	MN/m	MN/m	MN/m
9.8	4.7	9.5	-10.0	2.4	0.3	0.9	-0.2	1.5	-0.5	-0.3	-0.5	-0.3	-0.5	-0.3	-0.6	-0.2
19.5	4.8	9.9	-9.9	2.8	2.1	0.4	0.1	2.8	-0.2	-0.2	-0.3	-0.1	-0.2	-0.2	-0.4	-0.4
29.3	5.8	9.3	-11.0	3.8	4.1	0.4	0.6	4.0	-0.1	-0.1	-0.3	-0.3	-0.1	-0.1	-0.2	-0.2
39.1	5.2	10.0	-10.0	2.9	4.5	0.0	0.7	5.2	0.0	0.0	-0.2	-0.1	-0.1	-0.1	-0.1	-0.1
48.8	5.0	10.0	-9.8	3.4	6.1	0.4	1.1	6.6	-0.1	-0.1	-0.1	-0.2	-0.1	-0.1	-0.2	-0.2
58.6	5.3	10.0	-9.8	3.8	7.3	0.2	1.0	7.9	-0.1	-0.1	-0.2	-0.3	-0.1	0.0	-0.2	-0.1
68.4	5.4	10.0	-9.4	4.0	8.5	0.0	0.7	8.5	-0.1	-0.1	-0.2	-0.2	-0.1	-0.1	-0.2	-0.2
78.1	5.6	10.0	-8.7	3.9	9.4	0.0	1.1	9.3	-0.1	-0.1	-0.2	-0.1	-0.1	-0.1	-0.2	-0.1
87.9	5.4	10.0	-9.6	3.8	10.0	0.0	1.0	10.0	-0.1	-0.1	-0.1	-0.1	0.0	-0.1	-0.1	-0.1
97.7	5.8	10.0	-9.3	4.1	12.0	-0.2	1.3	12.0	-0.1	-0.1	-0.1	-0.1	-0.1	-0.1	-0.1	-0.1
107.4	5.8	10.0	-8.7	3.9	13.0	-0.3	1.3	13.0	-0.1	-0.1	-0.2	-0.1	-0.1	-0.1	-0.1	0.0
117.2	5.9	10.0	-9.0	4.1	14.0	-0.3	0.9	14.0	0.0	0.0	-0.1	-0.1	-0.1	0.0	-0.1	-0.1
127.0	5.7	10.0	-9.0	4.4	15.0	-0.3	1.0	15.0	-0.1	0.0	-0.1	-0.1	-0.1	-0.1	-0.1	-0.1
136.7	5.7	10.0	-8.5	4.3	17.0	-0.4	0.8	16.0	-0.1	0.0	-0.1	-0.1	-0.1	-0.1	-0.1	-0.1

Table 183. Raw data for the test seal at ω=20 krpm, PR=0.5, C_r=0.163 mm, and inlet GVF=98%

Freq.	Re($\boldsymbol{H_{XX}}$)	Re($\boldsymbol{H_{XY}}$)	Re($\boldsymbol{H_{YX}}$)	Re($\boldsymbol{H_{YY}}$)	Im($\boldsymbol{H_{XX}}$)	Im($\boldsymbol{H_{XY}}$)	Im($\boldsymbol{H_{YX}}$)	Im($\boldsymbol{H_{YY}}$)	Re($\boldsymbol{eH_{XX}}$)	Re($\boldsymbol{eH_{XY}}$)	Re($\boldsymbol{eH_{YX}}$)	Re($\boldsymbol{eH_{YY}}$)	Im($\boldsymbol{eH_{XX}}$)	Im($\boldsymbol{eH_{XY}}$)	Im($\boldsymbol{eH_{YX}}$)	Im($\boldsymbol{eH_{YY}}$)
Hz	MN/m	MN/m	MN/m	MN/m	MN/m	MN/m	MN/m	MN/m	MN/m	MN/m	MN/m	MN/m	MN/m	MN/m	MN/m	MN/m
9.8	5.4	7.8	-8.3	4.2	-0.9	0.6	1.1	1.3	-0.6	-0.2	-0.8	-0.4	-0.6	-0.3	-0.6	-0.4
19.5	4.1	8.9	-7.6	2.4	1.2	0.0	0.9	1.6	-0.2	-0.1	-0.3	-0.4	-0.3	-0.3	-0.3	-0.2
29.3	5.8	6.8	-9.8	4.8	2.9	0.4	1.5	3.5	-0.3	-0.2	-0.4	-0.2	-0.2	-0.2	-0.3	-0.3
39.1	3.7	8.6	-7.0	2.4	4.0	0.0	0.4	5.0	-0.1	-0.1	-0.3	-0.2	-0.1	-0.2	-0.3	-0.2
48.8	3.8	8.5	-6.8	2.9	5.2	0.5	1.3	5.9	-0.2	-0.2	-0.2	-0.3	-0.2	-0.1	-0.2	-0.2
58.6	4.2	8.9	-7.2	2.6	6.6	-0.1	0.7	7.7	-0.2	-0.1	-0.3	-0.2	-0.2	-0.2	-0.2	-0.2
68.4	4.2	8.3	-6.4	2.6	7.5	0.2	-0.1	8.3	-0.1	0.0	-0.4	-0.2	-0.1	-0.2	-0.1	-0.2
78.1	4.4	8.9	-6.2	3.2	8.8	0.0	0.7	9.7	-0.1	-0.1	-0.2	-0.2	-0.2	-0.1	-0.2	-0.1
87.9	4.0	8.8	-6.2	3.1	9.9	0.1	0.2	11.0	-0.1	-0.1	-0.1	-0.1	-0.1	-0.1	-0.1	-0.1
97.7	4.4	9.1	-6.2	3.3	12.0	-0.1	0.4	12.0	-0.1	-0.1	-0.1	-0.2	-0.1	-0.1	-0.1	-0.2
107.4	4.5	9.0	-5.7	3.3	13.0	0.0	0.4	13.0	-0.2	-0.1	-0.2	-0.2	-0.1	-0.1	-0.2	-0.1
117.2	4.6	8.9	-6.4	3.5	14.0	-0.3	-0.4	14.0	-0.1	-0.1	-0.2	-0.2	-0.1	-0.1	-0.1	-0.1
127.0	4.6	8.8	-6.0	4.0	15.0	-0.2	0.1	15.0	-0.1	-0.1	-0.1	-0.1	-0.1	-0.1	-0.1	-0.2
136.7	4.2	8.9	-6.1	3.5	16.0	-0.5	-0.6	17.0	-0.1	-0.1	-0.1	-0.1	-0.1	-0.1	-0.2	-0.1

Table 184. Raw data for the test seal at ω=20 krpm, PR=0.5, C_r=0.163 mm, and inlet GVF=95%

Freq.	Re($\boldsymbol{H_{XX}}$)	Re($\boldsymbol{H_{XY}}$)	Re($\boldsymbol{H_{YX}}$)	Re($\boldsymbol{H_{YY}}$)	Im($\boldsymbol{H_{XX}}$)	Im($\boldsymbol{H_{XY}}$)	Im($\boldsymbol{H_{YX}}$)	Im($\boldsymbol{H_{YY}}$)	Re($\boldsymbol{eH_{XX}}$)	Re($\boldsymbol{eH_{XY}}$)	Re($\boldsymbol{eH_{YX}}$)	Re($\boldsymbol{eH_{YY}}$)	Im($\boldsymbol{eH_{XX}}$)	Im($\boldsymbol{eH_{XY}}$)	Im($\boldsymbol{eH_{YX}}$)	Im($\boldsymbol{eH_{YY}}$)
Hz	MN/m	MN/m	MN/m	MN/m	MN/m	MN/m	MN/m	MN/m	MN/m	MN/m	MN/m	MN/m	MN/m	MN/m	MN/m	MN/m
9.8	6.9	8.5	-7.3	2.7	0.1	-0.6	0.7	1.1	-1.0	-0.5	-1.0	-0.7	-0.6	-0.3	-0.8	-0.5
19.5	5.7	8.6	-7.5	2.8	0.6	-0.8	1.2	2.4	-0.6	-0.2	-0.5	-0.3	-0.2	-0.2	-0.9	-0.7
29.3	5.9	7.7	-9.1	4.2	2.2	0.9	1.7	2.9	-0.3	-0.4	-0.4	-0.3	-0.4	-0.3	-0.2	-0.5
39.1	4.2	8.8	-5.9	2.9	4.2	-0.5	0.6	5.3	-0.3	-0.3	-0.5	-0.3	-0.2	-0.1	-0.4	-0.2
48.8	4.6	8.6	-6.5	2.9	5.6	-1.1	1.2	6.6	-0.2	-0.2	-0.4	-0.2	-0.2	-0.3	-0.4	-0.3
58.6	4.9	7.4	-6.5	3.0	6.7	-1.2	-0.2	7.5	-0.4	-0.2	-0.3	-0.3	-0.1	-0.4	-0.3	-0.4
68.4	4.7	7.8	-6.2	3.8	7.9	-0.8	0.2	8.7	-0.4	-0.5	-0.5	-0.4	-0.2	-0.3	-0.2	-0.3
78.1	4.4	7.4	-5.6	3.6	8.9	-0.7	-0.1	11.0	-0.2	-0.4	-0.2	-0.2	-0.4	-0.2	-0.3	-0.1
87.9	3.9	7.5	-6.3	3.9	10.0	0.3	-0.3	11.0	-0.2	-0.1	-0.2	-0.2	-0.1	-0.2	-0.2	-0.2
97.7	4.6	8.0	-6.0	3.8	12.0	0.1	0.3	13.0	-0.1	-0.3	-0.1	-0.1	-0.2	-0.2	-0.2	-0.3
107.4	5.2	8.2	-5.5	3.8	13.0	0.5	0.1	13.0	-0.2	-0.1	-0.3	-0.4	-0.2	-0.2	-0.3	-0.2
117.2	4.6	8.2	-5.8	4.0	15.0	0.4	-0.9	15.0	-0.3	-0.1	-0.3	-0.1	-0.3	-0.2	-0.2	-0.2
127.0	5.1	8.6	-6.0	3.5	16.0	0.2	-0.6	16.0	-0.2	-0.3	-0.2	-0.3	-0.1	-0.2	-0.2	-0.2
136.7	5.1	8.6	-5.4	4.8	17.0	-0.6	-0.6	18.0	-0.2	-0.1	-0.2	-0.3	-0.1	-0.2	-0.2	-0.1

Table 185. Raw data for the test seal at ω=20 krpm, PR=0.5, C_r=0.163 mm, and inlet GVF=92%

Freq.	Re($\boldsymbol{H_{XX}}$)	Re($\boldsymbol{H_{XY}}$)	Re($\boldsymbol{H_{YX}}$)	Re($\boldsymbol{H_{YY}}$)	Im($\boldsymbol{H_{XX}}$)	Im($\boldsymbol{H_{XY}}$)	Im($\boldsymbol{H_{YX}}$)	Im($\boldsymbol{H_{YY}}$)	Re($\boldsymbol{eH_{XX}}$)	Re($\boldsymbol{eH_{XY}}$)	Re($\boldsymbol{eH_{YX}}$)	Re($\boldsymbol{eH_{YY}}$)	Im($\boldsymbol{eH_{XX}}$)	Im($\boldsymbol{eH_{XY}}$)	Im($\boldsymbol{eH_{YX}}$)	Im($\boldsymbol{eH_{YY}}$)
Hz	MN/m	MN/m	MN/m	MN/m	MN/m	MN/m	MN/m	MN/m	MN/m	MN/m	MN/m	MN/m	MN/m	MN/m	MN/m	MN/m
9.8	5.2	2.9	-0.8	4.1	0.8	0.0	-0.1	0.9	-0.1	0.0	-0.1	0.0	-0.1	-0.1	0.0	0.0
19.5	5.2	2.9	-1.1	4.1	2.1	0.1	-0.2	2.0	0.0	-0.1	0.0	0.0	0.0	0.0	-0.1	0.0
29.3	4.7	3.6	-0.6	3.2	2.2	0.9	0.9	1.9	0.0	-0.1	-0.1	-0.1	-0.1	-0.1	-0.1	-0.1
39.1	5.3	3.0	-1.1	4.1	4.0	0.0	-0.1	4.0	0.0	0.0	-0.1	0.0	-0.1	0.0	-0.1	0.0
48.8	5.2	3.1	-1.2	4.0	5.2	0.0	-0.1	5.0	-0.1	0.0	-0.1	-0.1	0.0	-0.1	-0.1	0.0
58.6	5.3	3.2	-1.2	4.3	6.2	-0.1	-0.3	6.1	-0.1	-0.1	-0.1	-0.1	-0.1	-0.1	-0.1	-0.2
68.4	5.4	3.1	-1.2	4.2	7.3	0.0	-0.2	7.3	-0.1	0.0	-0.1	0.0	-0.1	-0.1	-0.1	-0.1
78.1	5.4	3.1	-1.1	4.3	8.1	0.0	-0.2	8.1	0.0	-0.1	-0.1	0.0	-0.1	-0.1	-0.1	0.0
87.9	5.4	2.9	-1.4	4.2	9.2	-0.2	-0.2	9.3	0.0	0.0	0.0	0.0	0.0	-0.1	0.0	0.0
97.7	5.4	2.9	-1.4	4.3	10.0	-0.1	-0.1	10.0	0.0	0.0	-0.1	-0.1	0.0	-0.1	-0.1	0.0
107.4	5.6	3.1	-1.1	4.5	11.0	-0.2	0.0	11.0	-0.1	0.0	0.0	-0.1	-0.1	0.0	-0.1	0.0
117.2	5.5	2.9	-1.3	4.4	13.0	-0.1	-0.3	13.0	-0.1	0.0	-0.1	0.0	0.0	0.0	-0.1	0.0
127.0	5.7	2.8	-1.2	4.6	14.0	-0.1	-0.3	14.0	0.0	0.0	-0.1	-0.1	-0.1	0.0	0.0	0.0
136.7	5.6	2.8	-1.2	5.0	15.0	-0.2	-0.1	15.0	-0.1	-0.1	-0.1	0.0	0.0	0.0	0.0	0.0

Table 186. Raw data for the test seal at ω=10 krpm, PR=0.43, C_r=0.163 mm, and inlet GVF=100%

Freq.	Re($\boldsymbol{H_{XX}}$)	Re($\boldsymbol{H_{XY}}$)	Re($\boldsymbol{H_{YX}}$)	Re($\boldsymbol{H_{YY}}$)	Im($\boldsymbol{H_{XX}}$)	Im($\boldsymbol{H_{XY}}$)	Im($\boldsymbol{H_{YX}}$)	Im($\boldsymbol{H_{YY}}$)	Re($\boldsymbol{eH_{XX}}$)	Re($\boldsymbol{eH_{XY}}$)	Re($\boldsymbol{eH_{YX}}$)	Re($\boldsymbol{eH_{YY}}$)	Im($\boldsymbol{eH_{XX}}$)	Im($\boldsymbol{eH_{XY}}$)	Im($\boldsymbol{eH_{YX}}$)	Im($\boldsymbol{eH_{YY}}$)
Hz	MN/m	MN/m	MN/m	MN/m	MN/m	MN/m	MN/m	MN/m	MN/m	MN/m	MN/m	MN/m	MN/m	MN/m	MN/m	MN/m
9.8	2.0	5.0	-4.5	1.9	0.9	0.2	0.2	1.8	-0.1	-0.1	-0.2	-0.2	-0.2	-0.3	-0.2	-0.1
19.5	2.3	5.5	-4.9	2.2	3.6	0.5	0.4	3.6	-0.1	-0.1	-0.3	-0.3	-0.1	0.0	-0.3	-0.1
29.3	3.9	4.9	-5.2	2.7	5.1	0.4	0.4	4.3	-0.1	-0.1	-0.2	-0.1	-0.1	-0.1	-0.2	-0.1
39.1	3.7	5.7	-4.7	2.4	6.2	0.3	0.2	5.7	-0.1	-0.1	-0.1	-0.1	-0.1	-0.1	-0.2	-0.1
48.8	4.0	5.6	-4.9	2.4	7.5	0.5	0.6	7.3	-0.1	0.0	-0.1	-0.1	-0.1	0.0	-0.1	-0.1
58.6	4.2	6.1	-4.8	2.7	8.7	0.3	0.4	8.5	-0.2	-0.1	-0.2	-0.2	-0.1	-0.1	-0.1	-0.2
68.4	4.4	6.0	-4.4	3.0	10.0	-0.2	0.7	9.2	-0.1	0.0	-0.1	-0.2	-0.1	-0.1	-0.1	-0.2
78.1	4.8	5.8	-4.1	3.2	11.0	-0.1	0.5	11.0	-0.1	-0.1	-0.1	-0.2	-0.1	0.0	-0.1	-0.1
87.9	4.7	5.9	-4.6	3.0	12.0	-0.1	0.5	12.0	-0.1	-0.1	-0.1	-0.1	-0.1	0.0	0.0	-0.1
97.7	4.9	5.9	-4.5	3.5	14.0	-0.2	0.7	13.0	0.0	0.0	0.0	-0.1	0.0	-0.1	-0.1	-0.1
107.4	5.2	5.9	-4.1	3.8	15.0	-0.3	0.8	15.0	-0.1	-0.1	-0.1	-0.1	-0.1	-0.1	-0.1	-0.1
117.2	5.1	5.9	-4.3	4.0	16.0	-0.1	0.4	16.0	-0.1	0.0	0.0	-0.1	0.0	0.0	0.0	-0.1
127.0	5.3	5.9	-4.3	4.1	17.0	-0.3	0.2	17.0	-0.1	-0.1	-0.1	-0.1	0.0	-0.1	-0.1	-0.1
136.7	5.3	5.9	-4.3	4.5	19.0	-0.3	0.4	18.0	0.0	0.0	-0.1	0.0	0.0	-0.1	-0.1	-0.1

Table 187. Raw data for the test seal at ω=10 krpm, PR=0.43, C_r=0.163 mm, and inlet GVF=98%

Freq.	Re($\boldsymbol{H_{XX}}$)	Re($\boldsymbol{H_{XY}}$)	Re($\boldsymbol{H_{YX}}$)	Re($\boldsymbol{H_{YY}}$)	Im($\boldsymbol{H_{XX}}$)	Im($\boldsymbol{H_{XY}}$)	Im($\boldsymbol{H_{YX}}$)	Im($\boldsymbol{H_{YY}}$)	Re($\boldsymbol{eH_{XX}}$)	Re($\boldsymbol{eH_{XY}}$)	Re($\boldsymbol{eH_{YX}}$)	Re($\boldsymbol{eH_{YY}}$)	Im($\boldsymbol{eH_{XX}}$)	Im($\boldsymbol{eH_{XY}}$)	Im($\boldsymbol{eH_{YX}}$)	Im($\boldsymbol{eH_{YY}}$)
Hz	MN/m	MN/m	MN/m	MN/m	MN/m	MN/m	MN/m	MN/m	MN/m	MN/m	MN/m	MN/m	MN/m	MN/m	MN/m	MN/m
9.8	1.8	4.3	-5.1	0.7	0.1	0.6	0.8	1.6	-0.2	-0.1	-0.4	-0.2	-0.1	-0.1	-0.3	-0.2
19.5	0.9	5.1	-4.1	1.2	2.8	0.4	0.9	3.2	-0.2	-0.2	-0.3	-0.3	-0.2	-0.1	-0.3	-0.3
29.3	3.0	3.4	-4.7	2.0	4.0	0.7	0.6	3.7	-0.3	-0.2	-0.2	-0.2	-0.3	-0.2	-0.2	-0.1
39.1	1.3	4.9	-3.0	0.7	5.8	0.0	0.3	5.6	-0.1	-0.1	-0.1	-0.2	-0.2	-0.2	-0.2	-0.2
48.8	1.7	5.0	-3.3	1.1	7.2	0.1	0.5	7.2	-0.1	-0.2	-0.2	-0.2	-0.1	-0.2	-0.2	-0.1
58.6	2.0	5.2	-3.3	1.4	8.4	0.1	0.2	8.6	-0.1	-0.3	-0.2	-0.3	-0.2	-0.2	-0.3	-0.3
68.4	2.4	5.8	-3.5	2.3	10.0	0.3	0.5	9.5	-0.1	-0.1	-0.3	-0.4	-0.1	-0.1	-0.1	-0.1
78.1	2.8	5.4	-3.0	2.2	11.0	-0.1	-0.1	11.0	-0.1	-0.2	-0.3	-0.1	-0.2	-0.1	-0.1	-0.2
87.9	2.5	5.2	-3.6	2.5	12.0	-0.1	0.4	12.0	-0.1	-0.1	-0.1	-0.2	-0.1	-0.1	-0.1	-0.2
97.7	3.0	5.2	-3.2	2.5	13.0	0.1	0.4	14.0	-0.2	-0.1	-0.2	-0.2	-0.1	-0.1	-0.2	-0.1
107.4	3.1	5.2	-3.5	2.2	14.0	0.0	0.2	15.0	-0.1	0.0	-0.2	-0.1	-0.1	-0.1	-0.2	-0.2
117.2	3.1	5.3	-3.4	2.4	16.0	-0.1	0.0	16.0	-0.1	-0.1	-0.1	-0.2	-0.1	0.0	-0.2	-0.1
127.0	3.0	5.6	-3.6	2.7	17.0	0.0	0.4	18.0	-0.1	-0.1	-0.1	-0.2	-0.1	-0.2	-0.2	-0.3
136.7	2.8	5.5	-3.5	2.8	19.0	-0.4	0.1	19.0	-0.1	-0.1	-0.1	-0.1	-0.1	-0.1	-0.1	-0.2

Table 188. Raw data for the test seal at ω=10 krpm, PR=0.43, C_r=0.163 mm, and inlet GVF=95%

Freq.	Re($\boldsymbol{H_{XX}}$)	Re($\boldsymbol{H_{XY}}$)	Re($\boldsymbol{H_{YX}}$)	Re($\boldsymbol{H_{YY}}$)	Im($\boldsymbol{H_{XX}}$)	Im($\boldsymbol{H_{XY}}$)	Im($\boldsymbol{H_{YX}}$)	Im($\boldsymbol{H_{YY}}$)	Re($\boldsymbol{eH_{XX}}$)	Re($\boldsymbol{eH_{XY}}$)	Re($\boldsymbol{eH_{YX}}$)	Re($\boldsymbol{eH_{YY}}$)	Im($\boldsymbol{eH_{XX}}$)	Im($\boldsymbol{eH_{XY}}$)	Im($\boldsymbol{eH_{YX}}$)	Im($\boldsymbol{eH_{YY}}$)
Hz	MN/m	MN/m	MN/m	MN/m	MN/m	MN/m	MN/m	MN/m	MN/m	MN/m	MN/m	MN/m	MN/m	MN/m	MN/m	MN/m
9.8	2.0	3.3	-3.4	-0.2	-1.2	1.6	0.2	2.2	-0.3	-0.2	-0.4	-0.2	-0.3	-0.1	-0.3	-0.3
19.5	1.1	4.8	-3.4	0.4	1.7	-0.1	1.0	3.2	-0.3	-0.2	-0.2	-0.2	-0.2	-0.2	-0.2	-0.2
29.3	2.9	2.9	-4.6	2.0	3.3	1.2	1.3	3.7	-0.2	-0.3	-0.3	-0.3	-0.2	-0.1	-0.3	-0.1
39.1	1.3	5.5	-2.9	1.0	5.7	0.4	0.5	6.7	-0.2	-0.3	-0.3	-0.2	-0.2	-0.1	-0.4	-0.2
48.8	1.4	4.7	-2.3	0.7	7.0	0.3	0.3	8.0	-0.2	-0.2	-0.1	-0.4	-0.2	-0.2	-0.2	-0.3
58.6	1.9	5.1	-3.5	1.7	8.5	0.0	-0.3	8.8	-0.2	-0.2	-0.3	-0.4	-0.2	-0.3	-0.3	-0.4
68.4	2.4	4.3	-3.5	2.4	9.9	-0.5	0.0	10.0	-0.3	-0.1	-0.3	-0.3	-0.1	-0.2	-0.5	-0.3
78.1	2.8	5.2	-2.4	2.3	11.0	0.1	-0.3	11.0	-0.2	-0.2	-0.4	-0.4	-0.2	-0.3	-0.3	-0.4
87.9	2.2	4.4	-2.7	1.7	12.0	0.4	-0.3	12.0	0.0	-0.2	-0.2	-0.4	-0.2	-0.2	-0.3	-0.2
97.7	2.7	4.7	-2.9	1.3	14.0	0.5	0.4	14.0	-0.2	-0.1	-0.2	-0.3	-0.1	-0.1	-0.2	-0.1
107.4	3.5	5.5	-2.3	1.6	15.0	0.2	0.2	15.0	-0.2	-0.1	-0.2	-0.1	-0.1	-0.1	-0.5	-0.2
117.2	3.1	5.3	-3.4	1.8	16.0	0.0	-0.3	17.0	-0.1	-0.2	-0.1	-0.2	-0.1	-0.1	-0.1	-0.1
127.0	3.1	5.5	-3.4	2.0	17.0	-0.3	-0.5	19.0	-0.2	-0.2	-0.4	-0.1	-0.1	-0.1	-0.2	-0.2
136.7	2.9	5.4	-3.0	2.1	19.0	-0.9	-0.6	20.0	-0.1	-0.1	-0.1	-0.2	-0.1	-0.2	-0.1	-0.2

Table 189. Raw data for the test seal at ω=10 krpm, PR=0.43, C_r=0.163 mm, and inlet GVF=92%

Freq.	Re($\boldsymbol{H_{XX}}$)	Re($\boldsymbol{H_{XY}}$)	Re($\boldsymbol{H_{YX}}$)	Re($\boldsymbol{H_{YY}}$)	Im($\boldsymbol{H_{XX}}$)	Im($\boldsymbol{H_{XY}}$)	Im($\boldsymbol{H_{YX}}$)	Im($\boldsymbol{H_{YY}}$)	Re($\boldsymbol{eH_{XX}}$)	Re($\boldsymbol{eH_{XY}}$)	Re($\boldsymbol{eH_{YX}}$)	Re($\boldsymbol{eH_{YY}}$)	Im($\boldsymbol{eH_{XX}}$)	Im($\boldsymbol{eH_{XY}}$)	Im($\boldsymbol{eH_{YX}}$)	Im($\boldsymbol{eH_{YY}}$)
Hz	MN/m	MN/m	MN/m	MN/m	MN/m	MN/m	MN/m	MN/m	MN/m	MN/m	MN/m	MN/m	MN/m	MN/m	MN/m	MN/m
9.8	4.8	4.3	-2.3	3.4	1.0	0.1	0.0	1.0	-0.1	-0.1	0.0	0.0	-0.1	0.0	-0.1	0.0
19.5	4.9	4.3	-2.4	3.4	2.0	0.1	-0.1	2.1	-0.1	-0.1	0.0	0.0	0.0	-0.1	-0.1	-0.1
29.3	4.5	5.1	-2.1	2.6	2.4	1.3	0.8	2.0	0.0	-0.1	-0.1	-0.1	-0.1	0.0	-0.1	-0.2
39.1	5.0	4.5	-2.6	3.4	4.2	-0.1	-0.1	4.2	-0.1	0.0	0.0	0.0	-0.1	0.0	0.0	0.0
48.8	5.0	4.4	-2.6	3.4	5.1	0.0	0.0	5.1	0.0	0.0	0.0	-0.1	-0.1	-0.1	-0.1	-0.1
58.6	5.2	4.5	-2.4	3.9	6.2	-0.1	-0.1	6.2	-0.1	-0.1	-0.1	-0.1	-0.1	-0.1	-0.1	-0.1
68.4	5.1	4.5	-2.6	3.7	7.2	-0.1	-0.2	7.2	-0.1	-0.1	-0.2	-0.1	-0.1	-0.1	-0.1	-0.1
78.1	5.1	4.4	-2.5	3.7	8.1	-0.3	-0.1	8.3	0.0	-0.1	-0.1	-0.1	-0.1	-0.1	0.0	0.0
87.9	5.2	4.4	-2.8	3.8	9.1	-0.2	-0.2	9.3	-0.1	-0.1	0.0	0.0	0.0	-0.1	0.0	0.0
97.7	5.2	4.3	-2.7	3.7	10.0	-0.4	0.0	10.0	0.0	-0.1	0.0	0.0	0.0	0.0	-0.1	-0.1
107.4	5.4	4.4	-2.6	3.9	11.0	-0.3	0.0	11.0	0.0	-0.1	-0.1	-0.1	0.0	0.0	-0.1	0.0
117.2	5.3	4.3	-2.5	3.9	12.0	-0.3	-0.3	12.0	-0.1	0.0	-0.1	0.0	-0.1	0.0	-0.1	0.0
127.0	5.4	4.3	-2.6	4.1	13.0	-0.4	-0.3	14.0	0.0	-0.1	0.0	0.0	-0.1	0.0	0.0	0.0
136.7	5.4	4.0	-2.7	4.3	14.0	-0.3	-0.3	14.0	0.0	0.0	0.0	0.0	0.0	0.0	0.0	0.0

Table 190. Raw data for the test seal at ω=15 krpm, PR=0.43, C_r=0.163 mm, and inlet GVF=100%

Freq.	Re($\boldsymbol{H_{XX}}$)	Re($\boldsymbol{H_{XY}}$)	Re($\boldsymbol{H_{YX}}$)	Re($\boldsymbol{H_{YY}}$)	Im($\boldsymbol{H_{XX}}$)	Im($\boldsymbol{H_{XY}}$)	Im($\boldsymbol{H_{YX}}$)	Im($\boldsymbol{H_{YY}}$)	Re($\boldsymbol{eH_{XX}}$)	Re($\boldsymbol{eH_{XY}}$)	Re($\boldsymbol{eH_{YX}}$)	Re($\boldsymbol{eH_{YY}}$)	Im($\boldsymbol{eH_{XX}}$)	Im($\boldsymbol{eH_{XY}}$)	Im($\boldsymbol{eH_{YX}}$)	Im($\boldsymbol{eH_{YY}}$)
Hz	MN/m	MN/m	MN/m	MN/m	MN/m	MN/m	MN/m	MN/m	MN/m	MN/m	MN/m	MN/m	MN/m	MN/m	MN/m	MN/m
9.8	3.1	7.4	-7.9	1.9	0.6	0.2	-0.2	1.9	-0.3	-0.1	-0.2	-0.2	-0.3	-0.2	-0.4	-0.1
19.5	2.9	8.2	-7.8	2.2	3.2	0.3	0.7	3.0	-0.2	-0.1	-0.1	-0.2	-0.2	-0.2	-0.1	-0.1
29.3	4.6	7.5	-8.4	3.8	4.7	0.6	0.7	3.8	-0.1	-0.1	-0.2	-0.2	-0.2	-0.2	-0.2	-0.2
39.1	4.2	8.1	-7.4	2.6	5.9	0.1	0.9	5.6	-0.1	-0.1	-0.1	-0.1	-0.1	-0.1	-0.1	-0.1
48.8	4.5	8.5	-7.6	2.6	7.2	0.1	0.8	6.8	-0.1	-0.1	-0.3	-0.1	-0.1	-0.1	-0.1	-0.1
58.6	4.5	8.7	-7.0	3.1	8.5	0.0	1.0	8.0	-0.1	-0.1	-0.2	-0.1	-0.1	0.0	-0.1	-0.1
68.4	5.0	8.5	-7.2	3.0	9.5	-0.2	0.7	9.4	-0.1	-0.1	-0.1	-0.1	-0.1	-0.1	-0.1	-0.1
78.1	5.1	8.6	-6.7	3.3	11.0	-0.4	0.9	11.0	-0.1	-0.1	-0.1	-0.1	-0.1	-0.1	-0.1	-0.1
87.9	5.3	8.5	-7.1	3.3	12.0	-0.5	1.1	12.0	-0.1	-0.1	-0.2	-0.1	0.0	0.0	-0.1	-0.1
97.7	5.3	8.5	-6.9	3.5	13.0	-0.5	1.1	13.0	-0.2	-0.1	-0.2	-0.1	-0.1	0.0	-0.1	-0.1
107.4	5.5	8.5	-6.4	3.6	14.0	-0.6	1.0	14.0	-0.1	-0.1	-0.1	-0.1	0.0	-0.1	-0.1	-0.1
117.2	5.7	8.3	-6.3	3.9	16.0	-0.6	0.8	16.0	-0.1	-0.1	-0.1	-0.1	0.0	0.0	-0.1	-0.1
127.0	5.6	8.4	-6.4	4.4	17.0	-0.5	0.9	17.0	-0.1	-0.1	-0.1	-0.1	-0.1	0.0	-0.1	-0.1
136.7	5.6	8.3	-6.1	4.4	18.0	-0.6	0.6	18.0	-0.1	-0.1	-0.1	0.0	0.0	-0.1	-0.1	-0.1

Table 191. Raw data for the test seal at ω=15 krpm, PR=0.43, C_r=0.163 mm, and inlet GVF=98%

Freq.	Re($\boldsymbol{H_{XX}}$)	Re($\boldsymbol{H_{XY}}$)	Re($\boldsymbol{H_{YX}}$)	Re($\boldsymbol{H_{YY}}$)	Im($\boldsymbol{H_{XX}}$)	Im($\boldsymbol{H_{XY}}$)	Im($\boldsymbol{H_{YX}}$)	Im($\boldsymbol{H_{YY}}$)	Re($\boldsymbol{eH_{XX}}$)	Re($\boldsymbol{eH_{XY}}$)	Re($\boldsymbol{eH_{YX}}$)	Re($\boldsymbol{eH_{YY}}$)	Im($\boldsymbol{eH_{XX}}$)	Im($\boldsymbol{eH_{XY}}$)	Im($\boldsymbol{eH_{YX}}$)	Im($\boldsymbol{eH_{YY}}$)
Hz	MN/m	MN/m	MN/m	MN/m	MN/m	MN/m	MN/m	MN/m	MN/m	MN/m	MN/m	MN/m	MN/m	MN/m	MN/m	MN/m
9.8	2.4	6.6	-4.7	1.2	0.5	0.6	0.0	1.7	-0.3	-0.1	-0.5	-0.3	-0.3	-0.2	-0.3	-0.1
19.5	1.9	7.2	-6.2	0.7	2.1	-0.1	0.5	2.7	-0.3	-0.2	-0.3	-0.2	-0.2	-0.2	-0.2	-0.1
29.3	3.8	5.6	-7.7	2.7	3.7	0.6	0.8	3.1	-0.3	-0.3	-0.2	-0.1	-0.2	-0.2	-0.3	-0.2
39.1	2.1	7.0	-5.2	0.4	5.0	-0.3	0.5	5.7	-0.2	-0.2	-0.3	-0.2	-0.3	-0.2	-0.3	-0.1
48.8	2.1	7.1	-4.7	0.9	6.7	0.0	0.7	7.3	-0.2	-0.2	-0.2	-0.2	-0.2	-0.2	-0.1	-0.3
58.6	2.3	7.8	-4.6	1.3	8.3	0.1	0.9	8.4	-0.1	-0.2	-0.2	-0.4	-0.3	-0.1	-0.3	-0.2
68.4	2.8	7.1	-5.1	1.9	9.0	-0.4	0.5	9.3	-0.2	-0.1	-0.4	-0.2	-0.1	-0.2	-0.3	-0.3
78.1	2.9	7.5	-4.6	1.4	10.0	-0.3	0.1	11.0	-0.1	-0.1	-0.1	-0.2	-0.1	-0.2	-0.1	-0.2
87.9	2.6	7.6	-4.8	1.5	12.0	-0.3	0.3	12.0	-0.1	-0.2	-0.2	-0.1	-0.1	-0.2	-0.2	-0.2
97.7	3.1	7.7	-4.3	2.1	13.0	-0.2	0.4	13.0	-0.1	-0.1	-0.2	-0.2	-0.1	-0.2	-0.1	-0.1
107.4	3.2	7.3	-4.4	2.1	14.0	-0.2	-0.2	15.0	-0.1	-0.1	-0.3	-0.1	-0.1	-0.2	-0.1	-0.1
117.2	3.3	7.2	-4.9	2.2	16.0	-0.1	-0.5	16.0	-0.1	0.0	-0.1	-0.1	-0.1	-0.2	-0.2	-0.2
127.0	3.5	7.4	-4.7	2.3	17.0	-0.5	-0.3	17.0	-0.1	-0.2	-0.1	-0.2	-0.1	-0.1	-0.1	-0.2
136.7	3.5	7.6	-4.3	2.1	18.0	-0.6	-0.6	18.0	-0.1	-0.1	-0.1	-0.1	-0.1	-0.1	-0.1	-0.1

Table 192. Raw data for the test seal at ω=15 krpm, PR=0.43, C_r=0.163 mm, and inlet GVF=95%

Freq.	Re($\boldsymbol{H_{XX}}$)	Re($\boldsymbol{H_{XY}}$)	Re($\boldsymbol{H_{YX}}$)	Re($\boldsymbol{H_{YY}}$)	Im($\boldsymbol{H_{XX}}$)	Im($\boldsymbol{H_{XY}}$)	Im($\boldsymbol{H_{YX}}$)	Im($\boldsymbol{H_{YY}}$)	Re($\boldsymbol{eH_{XX}}$)	Re($\boldsymbol{eH_{XY}}$)	Re($\boldsymbol{eH_{YX}}$)	Re($\boldsymbol{eH_{YY}}$)	Im($\boldsymbol{eH_{XX}}$)	Im($\boldsymbol{eH_{XY}}$)	Im($\boldsymbol{eH_{YX}}$)	Im($\boldsymbol{eH_{YY}}$)
Hz	MN/m	MN/m	MN/m	MN/m	MN/m	MN/m	MN/m	MN/m	MN/m	MN/m	MN/m	MN/m	MN/m	MN/m	MN/m	MN/m
9.8	2.8	5.9	-5.2	0.9	0.1	0.7	-0.9	2.2	-0.5	-0.2	-0.7	-0.3	-0.5	-0.2	-0.5	-0.5
19.5	2.1	7.0	-5.2	1.1	1.1	0.6	-0.1	3.2	-0.3	-0.2	-0.3	-0.4	-0.3	-0.2	-0.4	-0.1
29.3	3.8	4.9	-7.0	2.3	2.7	0.6	1.2	3.5	-0.3	-0.3	-0.4	-0.2	-0.4	-0.3	-0.4	-0.3
39.1	2.3	7.0	-4.1	0.6	5.0	-0.4	0.4	5.9	-0.3	-0.2	-0.4	-0.2	-0.3	-0.1	-0.3	-0.2
48.8	2.1	6.5	-3.9	1.1	6.1	-0.3	0.4	7.0	-0.2	-0.2	-0.2	-0.3	-0.3	-0.2	-0.2	-0.3
58.6	1.9	5.8	-4.3	0.7	7.9	-0.3	-0.5	8.4	-0.1	-0.1	-0.3	-0.3	-0.3	-0.1	-0.4	-0.1
68.4	3.1	6.0	-5.0	1.2	8.5	-0.7	-0.3	10.0	-0.4	-0.3	-0.3	-0.3	-0.3	-0.3	-0.2	-0.3
78.1	2.6	6.4	-4.2	1.6	11.0	-0.5	-0.4	11.0	-0.3	-0.2	-0.3	-0.2	-0.2	-0.4	-0.3	-0.5
87.9	2.5	6.4	-4.2	1.9	12.0	0.0	-0.1	13.0	-0.1	-0.2	-0.1	-0.1	-0.2	-0.1	-0.1	-0.2
97.7	2.3	6.8	-4.1	1.6	14.0	0.2	-0.4	14.0	-0.1	-0.2	-0.2	-0.1	-0.2	-0.1	-0.2	-0.2
107.4	3.4	6.7	-4.3	2.2	15.0	0.1	-0.2	15.0	-0.3	-0.1	-0.2	-0.2	-0.2	-0.1	-0.3	-0.2
117.2	3.1	7.0	-4.7	2.3	16.0	-0.2	-0.6	17.0	-0.3	0.0	-0.4	-0.2	-0.2	-0.3	-0.5	-0.3
127.0	3.2	7.0	-3.8	2.5	17.0	-0.3	-0.9	18.0	-0.2	-0.2	-0.3	-0.2	-0.2	-0.2	-0.3	-0.3
136.7	3.2	7.0	-4.2	2.6	18.0	-1.1	-1.4	20.0	-0.1	-0.2	-0.3	-0.3	-0.1	-0.1	-0.2	-0.3

Table 193. Raw data for the test seal at ω=15 krpm, PR=0.43, C_r=0.163 mm, and inlet GVF=92%

Freq.	Re($\boldsymbol{H_{XX}}$)	Re($\boldsymbol{H_{XY}}$)	Re($\boldsymbol{H_{YX}}$)	Re($\boldsymbol{H_{YY}}$)	Im($\boldsymbol{H_{XX}}$)	Im($\boldsymbol{H_{XY}}$)	Im($\boldsymbol{H_{YX}}$)	Im($\boldsymbol{H_{YY}}$)	Re($\boldsymbol{eH_{XX}}$)	Re($\boldsymbol{eH_{XY}}$)	Re($\boldsymbol{eH_{YX}}$)	Re($\boldsymbol{eH_{YY}}$)	Im($\boldsymbol{eH_{XX}}$)	Im($\boldsymbol{eH_{XY}}$)	Im($\boldsymbol{eH_{YX}}$)	Im($\boldsymbol{eH_{YY}}$)
Hz	MN/m	MN/m	MN/m	MN/m	MN/m	MN/m	MN/m	MN/m	MN/m	MN/m	MN/m	MN/m	MN/m	MN/m	MN/m	MN/m
9.8	4.4	5.8	-4.1	2.9	0.9	0.1	0.2	1.0	-0.1	-0.1	0.0	-0.1	-0.1	-0.1	-0.1	0.0
19.5	4.5	5.9	-4.2	2.8	2.0	0.1	0.0	2.2	0.0	0.0	0.0	-0.1	-0.1	-0.1	-0.1	0.0
29.3	4.0	6.6	-3.7	2.0	2.6	0.8	0.6	2.4	0.0	0.0	-0.1	-0.1	-0.1	-0.1	-0.1	0.0
39.1	4.7	6.1	-4.3	2.8	4.3	-0.1	-0.1	4.3	0.0	0.0	-0.1	0.0	-0.1	-0.1	-0.1	-0.1
48.8	4.8	5.9	-4.3	3.1	5.1	-0.1	0.0	5.4	-0.1	0.0	-0.1	0.0	-0.1	0.0	-0.1	-0.1
58.6	4.8	6.0	-4.3	3.1	6.1	-0.4	-0.2	6.1	-0.1	-0.1	-0.1	-0.1	-0.1	0.0	-0.1	-0.1
68.4	4.8	5.8	-4.4	3.2	7.2	-0.2	-0.1	7.2	-0.1	0.0	-0.1	-0.1	-0.1	0.0	-0.1	-0.1
78.1	4.9	6.0	-4.3	3.4	8.1	-0.4	-0.1	8.3	0.0	0.0	-0.1	-0.1	-0.1	0.0	0.0	0.0
87.9	4.8	5.8	-4.5	3.4	9.1	-0.2	-0.1	9.2	0.0	0.0	0.0	0.0	0.0	0.0	0.0	0.0
97.7	4.9	5.9	-4.4	3.3	10.0	-0.3	0.0	10.0	-0.1	0.0	-0.1	-0.1	-0.1	-0.1	-0.1	0.0
107.4	5.2	6.0	-4.3	3.4	11.0	-0.4	0.0	11.0	-0.1	0.0	0.0	-0.1	0.0	-0.1	-0.1	0.0
117.2	5.3	5.9	-4.3	3.5	12.0	-0.5	-0.3	13.0	-0.1	0.0	0.0	0.0	-0.1	0.0	-0.1	0.0
127.0	5.2	5.9	-4.4	3.8	13.0	-0.4	-0.1	13.0	-0.1	0.0	-0.1	-0.1	0.0	0.0	-0.1	-0.1
136.7	5.3	5.5	-4.3	3.9	14.0	-0.4	-0.2	15.0	0.0	0.0	0.0	-0.1	0.0	0.0	0.0	0.0

Table 194. Raw data for the test seal at ω=20 krpm, PR=0.43, C_r=0.163 mm, and inlet GVF=100%

Freq.	Re($\boldsymbol{H_{XX}}$)	Re($\boldsymbol{H_{XY}}$)	Re($\boldsymbol{H_{YX}}$)	Re($\boldsymbol{H_{YY}}$)	Im($\boldsymbol{H_{XX}}$)	Im($\boldsymbol{H_{XY}}$)	Im($\boldsymbol{H_{YX}}$)	Im($\boldsymbol{H_{YY}}$)	Re($\boldsymbol{eH_{XX}}$)	Re($\boldsymbol{eH_{XY}}$)	Re($\boldsymbol{eH_{YX}}$)	Re($\boldsymbol{eH_{YY}}$)	Im($\boldsymbol{eH_{XX}}$)	Im($\boldsymbol{eH_{XY}}$)	Im($\boldsymbol{eH_{YX}}$)	Im($\boldsymbol{eH_{YY}}$)
Hz	MN/m	MN/m	MN/m	MN/m	MN/m	MN/m	MN/m	MN/m	MN/m	MN/m	MN/m	MN/m	MN/m	MN/m	MN/m	MN/m
9.8	4.1	11.0	-11.0	2.6	1.0	0.3	0.1	2.0	-0.3	-0.2	-0.5	-0.4	-0.6	-0.4	-0.6	-0.4
19.5	4.0	11.0	-12.0	2.7	2.5	0.5	0.6	2.5	-0.2	-0.1	-0.4	-0.4	-0.2	-0.2	-0.3	-0.3
29.3	5.3	10.0	-13.0	3.3	4.3	0.2	0.1	4.5	-0.1	-0.2	-0.2	-0.3	-0.2	-0.2	-0.3	-0.2
39.1	4.6	11.0	-12.0	2.7	5.1	0.0	0.6	5.4	-0.1	-0.1	-0.2	-0.2	-0.1	-0.1	-0.1	-0.1
48.8	4.4	12.0	-11.0	3.1	6.6	0.1	1.1	7.0	-0.1	-0.1	-0.2	-0.1	-0.1	-0.1	-0.2	-0.2
58.6	4.7	11.0	-11.0	3.5	7.8	-0.1	0.9	8.4	-0.1	-0.1	-0.2	-0.1	-0.1	-0.1	-0.2	-0.3
68.4	4.9	11.0	-11.0	3.3	9.2	-0.5	1.0	9.4	-0.1	-0.1	-0.2	-0.2	-0.1	-0.1	-0.1	-0.2
78.1	5.0	12.0	-11.0	3.8	10.0	-0.3	1.3	10.0	-0.1	-0.1	-0.2	-0.1	-0.1	-0.1	-0.1	-0.1
87.9	5.1	12.0	-11.0	3.9	12.0	-0.5	1.4	12.0	-0.1	-0.1	-0.1	-0.1	-0.1	-0.1	-0.1	-0.1
97.7	5.3	12.0	-11.0	3.9	13.0	-0.8	1.4	13.0	-0.1	-0.1	-0.1	-0.2	-0.1	-0.1	-0.1	-0.1
107.4	5.4	11.0	-10.0	4.3	14.0	-0.9	1.7	14.0	-0.1	-0.1	-0.1	-0.1	-0.1	-0.1	-0.1	-0.1
117.2	5.5	11.0	-11.0	4.4	16.0	-0.9	1.4	15.0	-0.1	-0.1	-0.1	-0.1	-0.1	0.0	-0.1	-0.1
127.0	5.7	12.0	-11.0	4.1	17.0	-1.1	1.2	17.0	-0.1	-0.1	-0.1	-0.2	-0.1	-0.1	-0.1	-0.1
136.7	5.8	11.0	-10.0	4.8	18.0	-1.1	1.3	18.0	-0.1	0.0	-0.1	-0.1	-0.1	-0.1	-0.1	-0.1

Table 195. Raw data for the test seal at ω=20 krpm, PR=0.43, C_r=0.163 mm, and inlet GVF=98%

Freq.	Re($\boldsymbol{H_{XX}}$)	Re($\boldsymbol{H_{XY}}$)	Re($\boldsymbol{H_{YX}}$)	Re($\boldsymbol{H_{YY}}$)	Im($\boldsymbol{H_{XX}}$)	Im($\boldsymbol{H_{XY}}$)	Im($\boldsymbol{H_{YX}}$)	Im($\boldsymbol{H_{YY}}$)	Re($\boldsymbol{eH_{XX}}$)	Re($\boldsymbol{eH_{XY}}$)	Re($\boldsymbol{eH_{YX}}$)	Re($\boldsymbol{eH_{YY}}$)	Im($\boldsymbol{eH_{XX}}$)	Im($\boldsymbol{eH_{XY}}$)	Im($\boldsymbol{eH_{YX}}$)	Im($\boldsymbol{eH_{YY}}$)
Hz	MN/m	MN/m	MN/m	MN/m	MN/m	MN/m	MN/m	MN/m	MN/m	MN/m	MN/m	MN/m	MN/m	MN/m	MN/m	MN/m
9.8	3.2	9.6	-7.8	2.7	0.3	0.4	2.1	1.0	-0.4	-0.4	-1.0	-1.1	-0.6	-0.4	-1.0	-0.5
19.5	3.8	9.6	-9.0	2.8	1.6	0.0	1.1	3.2	-0.2	-0.2	-0.6	-0.4	-0.3	-0.3	-0.3	-0.6
29.3	4.5	8.3	-11.0	3.9	3.6	0.2	1.0	3.3	-0.3	-0.1	-0.3	-0.3	-0.2	-0.3	-0.4	-0.4
39.1	2.9	9.8	-8.0	2.0	4.6	-0.1	1.1	5.1	-0.3	-0.1	-0.3	-0.2	-0.1	-0.1	-0.3	-0.3
48.8	3.3	9.3	-8.1	1.5	6.0	-0.2	0.7	7.1	-0.1	-0.2	-0.3	-0.2	-0.1	-0.2	-0.2	-0.2
58.6	3.5	9.8	-8.4	2.2	7.5	-0.5	0.5	8.4	-0.1	-0.2	-0.3	-0.2	-0.2	-0.2	-0.3	-0.2
68.4	3.6	9.7	-7.9	2.5	8.4	-0.4	0.7	9.1	-0.2	-0.2	-0.1	-0.2	-0.1	-0.3	-0.3	-0.2
78.1	3.5	9.9	-7.0	2.7	9.7	-0.3	0.8	9.9	-0.1	-0.1	-0.2	-0.2	-0.1	-0.1	-0.2	-0.2
87.9	3.3	10.0	-7.9	2.6	12.0	-0.4	1.0	12.0	-0.1	-0.2	-0.1	-0.2	-0.1	-0.1	-0.2	-0.2
97.7	3.6	9.9	-7.7	2.9	13.0	-0.4	0.8	14.0	-0.1	-0.1	-0.1	-0.1	-0.1	-0.1	-0.2	-0.1
107.4	4.3	10.0	-7.6	3.1	14.0	-0.8	1.1	15.0	-0.1	-0.1	-0.2	-0.1	-0.1	-0.1	-0.2	-0.1
117.2	4.5	10.0	-7.4	2.9	15.0	-1.0	-0.3	16.0	-0.1	-0.1	-0.3	-0.1	-0.1	-0.1	-0.1	-0.2
127.0	4.4	10.0	-7.6	3.5	16.0	-1.0	0.1	17.0	-0.1	-0.2	-0.2	-0.3	-0.2	-0.1	-0.2	-0.3
136.7	4.4	9.7	-7.5	3.5	18.0	-1.2	-0.2	19.0	-0.1	-0.1	-0.2	-0.1	-0.1	-0.1	-0.1	-0.1

Table 196. Raw data for the test seal at ω=20 krpm, PR=0.43, C_r=0.163 mm, and inlet GVF=95%

Freq.	Re($\boldsymbol{H_{XX}}$)	Re($\boldsymbol{H_{XY}}$)	Re($\boldsymbol{H_{YX}}$)	Re($\boldsymbol{H_{YY}}$)	Im($\boldsymbol{H_{XX}}$)	Im($\boldsymbol{H_{XY}}$)	Im($\boldsymbol{H_{YX}}$)	Im($\boldsymbol{H_{YY}}$)	Re($\boldsymbol{eH_{XX}}$)	Re($\boldsymbol{eH_{XY}}$)	Re($\boldsymbol{eH_{YX}}$)	Re($\boldsymbol{eH_{YY}}$)	Im($\boldsymbol{eH_{XX}}$)	Im($\boldsymbol{eH_{XY}}$)	Im($\boldsymbol{eH_{YX}}$)	Im($\boldsymbol{eH_{YY}}$)
Hz	MN/m	MN/m	MN/m	MN/m	MN/m	MN/m	MN/m	MN/m	MN/m	MN/m	MN/m	MN/m	MN/m	MN/m	MN/m	MN/m
9.8	5.3	9.0	-6.7	0.5	-1.2	-0.7	-0.1	0.9	-0.6	-0.3	-0.9	-0.4	-0.6	-0.5	-1.0	-0.7
19.5	4.8	9.5	-7.5	0.9	1.0	-0.5	0.1	3.0	-0.3	-0.4	-0.3	-0.2	-0.6	-0.2	-0.3	-0.4
29.3	5.2	7.1	-9.8	3.9	1.9	0.2	2.4	3.4	-0.3	-0.3	-0.7	-0.4	-0.4	-0.2	-0.3	-0.5
39.1	2.5	9.3	-5.3	0.7	4.7	-0.8	0.8	5.7	-0.3	-0.2	-0.4	-0.2	-0.4	-0.2	-0.4	-0.4
48.8	3.4	8.9	-5.6	1.3	6.1	-1.1	1.4	7.0	-0.2	-0.3	-0.3	-0.3	-0.6	-0.3	-0.2	-0.3
58.6	3.5	8.1	-6.2	1.9	6.7	-1.3	0.5	9.3	-0.2	-0.3	-0.5	-0.5	-0.3	-0.2	-0.4	-0.2
68.4	3.4	7.8	-5.5	1.9	8.6	-1.5	0.3	10.0	-0.3	-0.2	-0.3	-0.2	-0.4	-0.2	-0.5	-0.3
78.1	3.8	7.6	-5.6	2.3	9.2	-1.3	-0.5	11.0	-0.2	-0.4	-0.3	-0.3	-0.3	-0.3	-0.3	-0.3
87.9	2.6	8.3	-5.9	2.5	12.0	-0.4	-0.3	13.0	-0.1	-0.3	-0.3	-0.2	-0.2	-0.2	-0.2	-0.3
97.7	3.1	7.8	-5.2	2.7	13.0	0.2	0.2	14.0	-0.2	-0.3	-0.2	-0.3	-0.5	-0.1	-0.6	-0.2
107.4	3.2	8.3	-5.7	2.3	14.0	0.4	-0.7	15.0	-0.3	-0.2	-0.3	-0.2	-0.3	-0.2	-0.4	-0.3
117.2	3.7	8.5	-5.2	2.9	15.0	0.0	-0.5	16.0	-0.2	-0.2	-0.3	-0.1	-0.3	-0.2	-0.2	-0.1
127.0	3.9	8.8	-5.6	3.0	16.0	-0.5	-1.0	18.0	-0.3	-0.1	-0.2	-0.3	-0.2	-0.1	-0.2	-0.2
136.7	3.9	8.9	-4.9	2.7	18.0	-1.2	-1.2	19.0	-0.1	-0.1	-0.4	-0.2	-0.2	-0.1	-0.3	-0.2

Table 197. Raw data for the test seal at ω=20 krpm, PR=0.43, C_r=0.163 mm, and inlet GVF=92%

Freq.	Re($\boldsymbol{H_{XX}}$)	Re($\boldsymbol{H_{XY}}$)	Re($\boldsymbol{H_{YX}}$)	Re($\boldsymbol{H_{YY}}$)	Im($\boldsymbol{H_{XX}}$)	Im($\boldsymbol{H_{XY}}$)	Im($\boldsymbol{H_{YX}}$)	Im($\boldsymbol{H_{YY}}$)	Re($\boldsymbol{eH_{XX}}$)	Re($\boldsymbol{eH_{XY}}$)	Re($\boldsymbol{eH_{YX}}$)	Re($\boldsymbol{eH_{YY}}$)	Im($\boldsymbol{eH_{XX}}$)	Im($\boldsymbol{eH_{XY}}$)	Im($\boldsymbol{eH_{YX}}$)	Im($\boldsymbol{eH_{YY}}$)
Hz	MN/m	MN/m	MN/m	MN/m	MN/m	MN/m	MN/m	MN/m	MN/m	MN/m	MN/m	MN/m	MN/m	MN/m	MN/m	MN/m
9.8	9.7	3.6	-3.6	8.6	1.2	0.2	0.2	1.2	-0.1	-0.1	0.0	0.0	-0.1	-0.1	0.0	0.0
19.5	9.8	3.7	-3.6	8.5	2.3	0.1	0.0	2.3	-0.1	0.0	-0.1	-0.1	-0.1	-0.1	0.0	-0.1
29.3	10.0	3.3	-4.0	9.2	3.7	-0.3	-0.1	3.9	-0.1	-0.1	-0.1	-0.1	0.0	-0.1	-0.1	-0.1
39.1	10.0	3.8	-3.7	8.8	4.7	0.1	0.2	4.5	-0.1	0.0	-0.1	-0.1	0.0	-0.1	0.0	-0.1
48.8	9.9	3.4	-3.7	8.7	5.9	0.0	0.2	5.6	-0.2	-0.1	0.0	0.0	0.0	-0.1	-0.1	0.0
58.6	10.0	3.6	-3.8	8.7	7.2	0.0	0.3	6.6	0.0	0.0	-0.1	0.0	-0.1	-0.1	-0.1	0.0
68.4	10.0	3.6	-3.7	8.8	8.3	-0.2	0.3	7.7	0.0	-0.1	-0.1	-0.1	-0.1	0.0	0.0	-0.1
78.1	10.0	3.7	-3.7	8.9	9.5	0.0	0.2	8.7	-0.1	0.0	0.0	0.0	-0.1	0.0	0.0	-0.1
87.9	10.0	3.5	-3.9	8.9	11.0	0.2	0.3	10.0	0.0	0.0	0.0	0.0	0.0	0.0	0.0	0.0
97.7	10.0	3.5	-3.7	8.8	12.0	0.2	0.2	11.0	0.0	-0.1	0.0	0.0	0.0	0.0	0.0	0.0
107.4	10.0	3.5	-3.6	9.2	13.0	0.1	0.4	12.0	-0.1	-0.1	0.0	0.0	0.0	-0.1	-0.1	-0.1
117.2	11.0	3.3	-3.7	9.1	15.0	0.0	0.0	13.0	-0.1	0.0	0.0	0.0	-0.1	0.0	0.0	0.0
127.0	11.0	3.3	-4.1	9.3	16.0	0.2	0.1	14.0	0.0	-0.1	0.0	-0.1	-0.1	-0.1	0.0	-0.2
136.7	11.0	3.1	-4.3	9.3	17.0	0.1	0.2	16.0	0.0	0.0	0.0	-0.1	-0.1	0.0	0.0	-0.1

Table 198. Raw data for the test seal at ω=10 krpm, PR=0.5, C_r=0.140 mm, and inlet GVF=100%

Freq.	Re($\boldsymbol{H_{XX}}$)	Re($\boldsymbol{H_{XY}}$)	Re($\boldsymbol{H_{YX}}$)	Re($\boldsymbol{H_{YY}}$)	Im($\boldsymbol{H_{XX}}$)	Im($\boldsymbol{H_{XY}}$)	Im($\boldsymbol{H_{YX}}$)	Im($\boldsymbol{H_{YY}}$)	Re($\boldsymbol{eH_{XX}}$)	Re($\boldsymbol{eH_{XY}}$)	Re($\boldsymbol{eH_{YX}}$)	Re($\boldsymbol{eH_{YY}}$)	Im($\boldsymbol{eH_{XX}}$)	Im($\boldsymbol{eH_{XY}}$)	Im($\boldsymbol{eH_{YX}}$)	Im($\boldsymbol{eH_{YY}}$)
Hz	MN/m	MN/m	MN/m	MN/m	MN/m	MN/m	MN/m	MN/m	MN/m	MN/m	MN/m	MN/m	MN/m	MN/m	MN/m	MN/m
9.8	2.7	8.3	-8.4	1.5	0.6	-0.2	-0.2	1.6	-0.2	-0.4	-0.4	-0.4	-0.4	-0.4	-0.2	-0.2
19.5	2.5	8.2	-8.8	1.6	4.8	-0.5	0.4	3.6	-0.2	-0.1	-0.2	-0.4	-0.2	-0.2	-0.3	-0.2
29.3	3.3	8.3	-8.6	1.8	6.0	-0.1	0.8	4.7	-0.3	-0.5	-0.2	-0.5	-0.4	-0.9	-0.4	-0.6
39.1	4.2	8.3	-8.3	2.6	7.8	0.5	0.6	6.7	-0.2	-0.4	-0.4	-0.5	-0.1	-0.3	-0.4	-0.4
48.8	4.6	8.5	-8.6	3.6	9.6	0.0	1.6	8.3	-0.2	-0.3	-0.3	-0.5	-0.2	-0.3	-0.2	-0.3
58.6	4.5	7.8	-8.3	2.6	10.0	0.3	1.2	10.0	-0.2	-0.2	-0.3	-0.2	-0.2	-0.3	-0.3	-0.4
68.4	5.4	7.4	-8.2	2.1	12.0	-0.3	0.4	13.0	-0.3	-0.7	-0.2	-0.7	-0.3	-0.6	-0.4	-0.8
78.1	5.4	8.0	-7.7	2.8	13.0	-0.5	0.9	13.0	-0.2	-0.1	-0.2	-0.2	-0.2	-0.2	-0.2	-0.3
87.9	5.6	7.8	-8.1	3.2	16.0	-0.4	1.2	14.0	-0.1	-0.1	-0.1	-0.1	-0.1	-0.2	-0.1	-0.1
97.7	5.8	8.2	-7.9	3.4	17.0	-0.4	1.0	16.0	-0.1	-0.1	-0.2	-0.2	-0.1	-0.2	-0.2	-0.2
107.4	6.0	7.7	-7.7	3.8	19.0	-0.3	1.5	17.0	-0.2	-0.2	-0.1	-0.3	-0.2	-0.1	-0.2	-0.1
117.2	6.2	7.7	-7.9	4.0	20.0	-0.2	0.7	18.0	-0.2	-0.1	-0.2	-0.2	-0.1	-0.1	-0.2	-0.2
127.0	7.3	7.7	-7.8	3.9	22.0	-0.2	1.0	19.0	-0.1	-0.2	-0.2	-0.4	-0.1	-0.3	-0.2	-0.3
136.7	7.6	6.9	-8.6	5.0	23.0	-0.4	1.2	21.0	-0.1	-0.1	-0.2	-0.2	-0.1	-0.2	-0.1	-0.3

Table 199. Raw data for the test seal at ω=10 krpm, PR=0.5, C_r=0.140 mm, and inlet GVF=98%

Freq.	Re($\boldsymbol{H_{XX}}$)	Re($\boldsymbol{H_{XY}}$)	Re($\boldsymbol{H_{YX}}$)	Re($\boldsymbol{H_{YY}}$)	Im($\boldsymbol{H_{XX}}$)	Im($\boldsymbol{H_{XY}}$)	Im($\boldsymbol{H_{YX}}$)	Im($\boldsymbol{H_{YY}}$)	Re($\boldsymbol{eH_{XX}}$)	Re($\boldsymbol{eH_{XY}}$)	Re($\boldsymbol{eH_{YX}}$)	Re($\boldsymbol{eH_{YY}}$)	Im($\boldsymbol{eH_{XX}}$)	Im($\boldsymbol{eH_{XY}}$)	Im($\boldsymbol{eH_{YX}}$)	Im($\boldsymbol{eH_{YY}}$)
Hz	MN/m	MN/m	MN/m	MN/m	MN/m	MN/m	MN/m	MN/m	MN/m	MN/m	MN/m	MN/m	MN/m	MN/m	MN/m	MN/m
9.8	10.0	5.6	-6.2	8.1	1.1	0.0	0.3	1.3	-0.1	-0.1	-0.1	0.0	-0.1	-0.1	-0.1	-0.1
19.5	10.0	5.6	-6.2	7.9	2.3	-0.1	0.0	2.5	-0.1	-0.1	0.0	-0.1	-0.1	-0.1	0.0	0.0
29.3	10.0	5.4	-6.7	8.1	3.4	0.1	0.1	3.7	-0.1	-0.2	-0.1	0.0	-0.1	-0.3	0.0	-0.1
39.1	10.0	5.7	-6.5	8.4	4.7	-0.1	0.2	4.7	-0.1	-0.1	0.0	-0.1	0.0	-0.1	0.0	-0.1
48.8	10.0	5.7	-6.3	8.3	5.7	-0.1	0.4	5.8	-0.1	-0.1	0.0	-0.1	0.0	-0.1	-0.1	-0.1
58.6	10.0	5.6	-6.5	8.5	7.2	0.2	0.2	6.6	-0.1	-0.1	-0.1	-0.1	-0.1	-0.1	-0.1	-0.1
68.4	10.0	5.4	-6.5	8.4	8.2	-0.1	0.2	8.1	0.0	-0.1	-0.1	-0.1	-0.1	-0.1	-0.1	-0.1
78.1	10.0	5.5	-6.5	8.6	9.4	-0.2	0.2	9.0	-0.1	-0.1	0.0	-0.1	0.0	0.0	0.0	-0.1
87.9	11.0	5.6	-6.8	8.4	11.0	-0.1	0.2	10.0	0.0	-0.1	0.0	0.0	0.0	0.0	0.0	0.0
97.7	11.0	5.4	-6.8	8.6	12.0	-0.2	0.5	11.0	-0.1	0.0	0.0	0.0	0.0	-0.1	-0.1	0.0
107.4	11.0	5.4	-6.4	8.7	13.0	0.0	0.6	12.0	-0.1	-0.1	-0.1	0.0	0.0	-0.1	-0.1	-0.1
117.2	11.0	5.1	-6.6	8.9	15.0	0.2	0.2	13.0	0.0	-0.1	-0.1	-0.1	-0.1	-0.1	0.0	-0.1
127.0	11.0	4.8	-7.1	8.8	15.0	0.2	0.3	14.0	0.0	0.0	0.0	0.0	-0.1	-0.1	-0.1	-0.1
136.7	12.0	4.5	-7.3	9.2	16.0	0.3	0.6	16.0	-0.1	-0.1	0.0	0.0	0.0	-0.1	0.0	-0.1

Table 200. Raw data for the test seal at ω=15 krpm, PR=0.5, C_r=0.140 mm, and inlet GVF=100%

Freq.	Re($\boldsymbol{H_{XX}}$)	Re($\boldsymbol{H_{XY}}$)	Re($\boldsymbol{H_{YX}}$)	Re($\boldsymbol{H_{YY}}$)	Im($\boldsymbol{H_{XX}}$)	Im($\boldsymbol{H_{XY}}$)	Im($\boldsymbol{H_{YX}}$)	Im($\boldsymbol{H_{YY}}$)	Re($\boldsymbol{eH_{XX}}$)	Re($\boldsymbol{eH_{XY}}$)	Re($\boldsymbol{eH_{YX}}$)	Re($\boldsymbol{eH_{YY}}$)	Im($\boldsymbol{eH_{XX}}$)	Im($\boldsymbol{eH_{XY}}$)	Im($\boldsymbol{eH_{YX}}$)	Im($\boldsymbol{eH_{YY}}$)
Hz	MN/m	MN/m	MN/m	MN/m	MN/m	MN/m	MN/m	MN/m	MN/m	MN/m	MN/m	MN/m	MN/m	MN/m	MN/m	MN/m
9.8	1.3	11.0	-12.0	-0.6	0.9	0.0	-1.3	2.3	-0.6	-0.5	-0.4	-0.3	-0.5	-0.4	-0.6	-0.8
19.5	2.9	11.0	-12.0	1.2	4.9	-0.3	1.0	2.6	-0.4	-0.8	-0.4	-0.5	-0.4	-0.4	-0.3	-0.5
29.3	3.7	11.0	-14.0	3.4	5.1	0.5	0.3	6.9	-0.3	-0.6	-0.5	-0.6	-0.5	-0.7	-0.5	-0.9
39.1	3.5	12.0	-12.0	1.6	7.5	0.1	0.3	6.7	-0.2	-0.3	-0.4	-0.4	-0.2	-0.2	-0.4	-0.7
48.8	3.6	11.0	-12.0	3.0	9.0	0.2	1.7	7.9	-0.3	-0.3	-0.2	-0.4	-0.2	-0.2	-0.3	-0.3
58.6	3.9	12.0	-13.0	2.6	10.0	0.7	0.6	11.0	-0.2	-0.4	-0.6	-0.9	-0.3	-0.5	-0.4	-0.6
68.4	5.1	11.0	-12.0	2.4	12.0	-0.6	0.9	10.0	-0.4	-0.5	-0.4	-0.9	-0.1	-0.5	-0.7	-1.0
78.1	4.7	11.0	-12.0	2.2	13.0	-0.6	1.4	12.0	-0.2	-0.3	-0.3	-0.5	-0.2	-0.2	-0.2	-0.2
87.9	5.0	11.0	-12.0	3.0	15.0	-0.7	1.8	14.0	-0.2	-0.2	-0.2	-0.5	-0.1	-0.2	-0.3	-0.1
97.7	5.3	11.0	-12.0	3.6	17.0	-0.8	2.1	15.0	-0.2	-0.3	-0.3	-0.4	-0.2	-0.2	-0.3	-0.4
107.4	5.7	11.0	-12.0	3.0	18.0	-0.9	1.6	17.0	-0.1	-0.1	-0.2	-0.4	-0.2	-0.1	-0.3	-0.3
117.2	5.9	11.0	-12.0	3.4	20.0	-0.9	1.5	17.0	-0.2	-0.2	-0.1	-0.3	-0.2	-0.2	-0.3	-0.3
127.0	6.5	11.0	-12.0	4.5	21.0	-0.9	2.0	19.0	-0.1	-0.1	-0.4	-0.8	-0.1	-0.2	-0.4	-0.6
136.7	7.0	9.8	-13.0	3.7	22.0	-1.1	1.8	20.0	-0.2	-0.2	-0.2	-0.3	-0.1	-0.2	-0.2	-0.4

Table 201. Raw data for the test seal at ω=15 krpm, PR=0.5, C_r=0.140 mm, and inlet GVF=98%

Freq.	Re($\boldsymbol{H_{XX}}$)	Re($\boldsymbol{H_{XY}}$)	Re($\boldsymbol{H_{YX}}$)	Re($\boldsymbol{H_{YY}}$)	Im($\boldsymbol{H_{XX}}$)	Im($\boldsymbol{H_{XY}}$)	Im($\boldsymbol{H_{YX}}$)	Im($\boldsymbol{H_{YY}}$)	Re($\boldsymbol{eH_{XX}}$)	Re($\boldsymbol{eH_{XY}}$)	Re($\boldsymbol{eH_{YX}}$)	Re($\boldsymbol{eH_{YY}}$)	Im($\boldsymbol{eH_{XX}}$)	Im($\boldsymbol{eH_{XY}}$)	Im($\boldsymbol{eH_{YX}}$)	Im($\boldsymbol{eH_{YY}}$)
Hz	MN/m	MN/m	MN/m	MN/m	MN/m	MN/m	MN/m	MN/m	MN/m	MN/m	MN/m	MN/m	MN/m	MN/m	MN/m	MN/m
9.8	9.8	8.1	-9.2	7.5	1.1	0.1	0.2	1.5	-0.1	-0.2	-0.2	-0.2	-0.1	0.0	-0.1	-0.1
19.5	9.8	8.2	-9.3	7.4	2.4	-0.1	0.2	2.5	-0.1	-0.1	-0.1	-0.1	-0.1	-0.1	-0.1	-0.1
29.3	11.0	7.0	-9.8	7.3	3.4	-0.4	0.1	4.2	-0.2	-0.4	-0.2	-0.4	-0.2	-0.5	-0.1	-0.3
39.1	10.0	7.9	-9.5	7.4	4.6	-0.2	0.3	4.5	-0.1	-0.1	0.0	-0.1	-0.1	-0.1	-0.1	-0.2
48.8	9.8	7.9	-9.4	7.6	5.7	0.0	0.6	5.9	-0.1	-0.2	-0.1	-0.1	-0.1	-0.2	-0.1	-0.1
58.6	10.0	8.2	-9.5	7.6	7.0	-0.1	0.3	6.6	-0.1	-0.1	-0.1	-0.1	-0.1	-0.2	-0.1	-0.2
68.4	9.9	8.1	-9.5	8.5	8.3	-0.1	0.4	7.6	-0.1	-0.1	-0.1	-0.2	-0.1	-0.2	-0.1	-0.3
78.1	10.0	7.8	-9.3	7.7	9.2	-0.3	0.2	8.9	0.0	-0.1	-0.1	-0.1	0.0	0.0	-0.1	-0.1
87.9	10.0	7.9	-9.8	7.6	11.0	-0.2	0.2	10.0	0.0	-0.1	-0.1	-0.1	0.0	-0.1	-0.1	-0.1
97.7	10.0	7.8	-9.8	7.7	12.0	-0.1	0.5	11.0	-0.1	-0.1	0.0	-0.1	-0.1	-0.1	-0.1	-0.1
107.4	10.0	7.9	-9.5	8.0	13.0	-0.3	0.5	12.0	0.0	0.0	-0.1	0.0	-0.1	-0.1	-0.1	0.0
117.2	10.0	7.9	-9.8	7.6	15.0	0.2	-0.1	14.0	-0.2	-0.2	-0.1	-0.1	-0.1	-0.1	-0.2	-0.1
127.0	11.0	8.0	-9.9	8.4	16.0	-0.1	0.6	14.0	-0.1	-0.1	-0.1	-0.1	0.0	-0.1	-0.1	-0.1
136.7	11.0	7.2	-10.0	8.5	16.0	-0.2	0.7	16.0	0.0	-0.1	0.0	-0.1	-0.1	0.0	-0.1	-0.1

Table 202. Raw data for the test seal at ω=20 krpm, PR=0.5, C_r=0.140 mm, and inlet GVF=100%

Freq.	Re($\boldsymbol{H_{XX}}$)	Re($\boldsymbol{H_{XY}}$)	Re($\boldsymbol{H_{YX}}$)	Re($\boldsymbol{H_{YY}}$)	Im($\boldsymbol{H_{XX}}$)	Im($\boldsymbol{H_{XY}}$)	Im($\boldsymbol{H_{YX}}$)	Im($\boldsymbol{H_{YY}}$)	Re($\boldsymbol{eH_{XX}}$)	Re($\boldsymbol{eH_{XY}}$)	Re($\boldsymbol{eH_{YX}}$)	Re($\boldsymbol{eH_{YY}}$)	Im($\boldsymbol{eH_{XX}}$)	Im($\boldsymbol{eH_{XY}}$)	Im($\boldsymbol{eH_{YX}}$)	Im($\boldsymbol{eH_{YY}}$)
Hz	MN/m	MN/m	MN/m	MN/m	MN/m	MN/m	MN/m	MN/m	MN/m	MN/m	MN/m	MN/m	MN/m	MN/m	MN/m	MN/m
9.8	3.9	13.0	-15.0	1.4	1.2	0.3	-1.0	1.5	-0.5	-0.5	-0.6	-0.7	-0.6	-0.6	-0.6	-0.6
19.5	3.7	14.0	-16.0	1.9	3.4	-0.3	-0.9	3.1	-0.5	-0.5	-0.6	-0.6	-0.3	-0.3	-0.6	-0.7
29.3	4.1	14.0	-16.0	1.3	5.4	-0.8	-0.7	5.1	-0.7	-0.8	-0.6	-0.6	-0.5	-0.6	-0.6	-0.8
39.1	4.0	14.0	-17.0	2.0	5.8	-0.2	0.5	6.5	-0.2	-0.1	-0.3	-0.4	-0.2	-0.2	-0.3	-0.3
48.8	4.4	14.0	-17.0	3.2	7.9	-0.4	1.2	7.7	-0.2	-0.4	-0.3	-0.5	-0.3	-0.4	-0.3	-0.2
58.6	5.0	13.0	-17.0	2.7	9.3	-0.7	0.6	9.2	-0.2	-0.3	-0.4	-0.6	-0.2	-0.2	-0.3	-0.4
68.4	5.4	13.0	-17.0	3.4	11.0	-1.3	1.4	10.0	-0.7	-0.8	-0.4	-0.5	-0.6	-1.0	-0.5	-0.7
78.1	5.1	14.0	-16.0	3.3	12.0	-0.4	1.7	11.0	-0.1	-0.1	-0.1	-0.2	-0.1	-0.1	-0.3	-0.3
87.9	5.2	14.0	-17.0	3.0	14.0	-0.4	1.3	13.0	-0.1	-0.1	-0.1	-0.2	-0.1	-0.2	-0.2	-0.2
97.7	5.6	14.0	-16.0	2.7	15.0	-0.4	1.4	14.0	-0.1	-0.1	-0.2	-0.1	-0.1	-0.1	-0.2	-0.3
107.4	5.9	14.0	-16.0	3.2	17.0	-0.7	1.6	15.0	-0.1	-0.1	-0.2	-0.2	-0.1	-0.1	-0.2	-0.3
117.2	5.5	14.0	-17.0	2.9	18.0	-0.4	1.6	17.0	-0.1	-0.1	-0.2	-0.1	-0.1	-0.1	-0.2	-0.2
127.0	5.9	14.0	-17.0	3.1	19.0	-0.4	2.0	18.0	-0.2	-0.1	-0.2	-0.3	-0.1	-0.3	-0.2	-0.2
136.7	6.4	13.0	-17.0	4.4	20.0	-0.7	2.9	20.0	-0.2	-0.2	-0.2	-0.1	-0.2	-0.2	-0.1	-0.2

Table 203. Raw data for the test seal at ω=20 krpm, PR=0.5, C_r=0.140 mm, and inlet GVF=98%

Freq.	Re($\boldsymbol{H_{XX}}$)	Re($\boldsymbol{H_{XY}}$)	Re($\boldsymbol{H_{YX}}$)	Re($\boldsymbol{H_{YY}}$)	Im($\boldsymbol{H_{XX}}$)	Im($\boldsymbol{H_{XY}}$)	Im($\boldsymbol{H_{YX}}$)	Im($\boldsymbol{H_{YY}}$)	Re($\boldsymbol{eH_{XX}}$)	Re($\boldsymbol{eH_{XY}}$)	Re($\boldsymbol{eH_{YX}}$)	Re($\boldsymbol{eH_{YY}}$)	Im($\boldsymbol{eH_{XX}}$)	Im($\boldsymbol{eH_{XY}}$)	Im($\boldsymbol{eH_{YX}}$)	Im($\boldsymbol{eH_{YY}}$)
Hz	MN/m	MN/m	MN/m	MN/m	MN/m	MN/m	MN/m	MN/m	MN/m	MN/m	MN/m	MN/m	MN/m	MN/m	MN/m	MN/m
9.8	6.0	4.0	-3.2	5.0	1.3	0.1	0.1	1.3	0.0	-0.1	0.0	-0.1	-0.1	-0.1	0.0	-0.1
19.5	6.0	4.1	-3.2	5.0	2.4	0.2	0.2	2.5	0.0	-0.1	0.0	0.0	0.0	0.0	-0.1	-0.1
29.3	6.1	4.3	-3.5	4.9	3.8	-0.2	0.2	4.1	-0.1	-0.1	-0.1	-0.2	-0.1	-0.1	-0.1	-0.2
39.1	6.2	4.1	-3.4	4.9	5.1	-0.4	-0.1	4.8	-0.1	-0.1	-0.1	-0.1	-0.1	-0.2	-0.1	-0.1
48.8	6.0	4.0	-3.5	5.1	6.4	-0.2	0.1	6.0	-0.1	-0.1	-0.1	-0.1	-0.1	-0.1	-0.1	-0.1
58.6	6.3	3.9	-3.4	5.2	7.6	-0.1	0.2	7.2	-0.1	-0.2	-0.1	-0.1	-0.1	-0.1	-0.1	-0.1
68.4	6.2	4.2	-3.3	5.2	9.0	-0.3	0.2	8.5	-0.1	-0.2	-0.2	-0.2	-0.1	-0.2	-0.1	-0.2
78.1	6.4	4.0	-3.4	5.4	9.9	-0.1	0.1	9.4	-0.1	-0.1	-0.1	0.0	-0.1	-0.1	-0.1	-0.1
87.9	6.4	4.1	-3.6	5.4	11.0	-0.2	0.2	11.0	-0.1	-0.1	-0.1	-0.1	-0.1	0.0	0.0	-0.1
97.7	6.5	3.9	-3.6	5.5	13.0	-0.2	0.3	12.0	0.0	-0.1	0.0	-0.1	0.0	-0.1	-0.1	-0.1
107.4	6.6	4.1	-3.3	5.6	14.0	-0.5	0.1	13.0	-0.1	-0.1	-0.1	-0.1	-0.1	-0.1	-0.1	0.0
117.2	7.0	3.9	-3.4	5.8	16.0	-0.4	-0.2	15.0	0.0	-0.1	0.0	-0.1	-0.1	0.0	-0.1	-0.1
127.0	7.4	3.8	-3.6	6.0	16.0	-0.3	0.0	16.0	0.0	-0.1	0.0	-0.1	-0.1	-0.1	-0.1	-0.1
136.7	7.4	3.5	-3.9	6.1	18.0	-0.4	0.1	17.0	0.0	0.0	0.0	-0.2	-0.1	-0.1	0.0	-0.1

Table 204. Raw data for the test seal at ω=10 krpm, PR=0.43, C_r=0.140 mm, and inlet GVF=100%

Freq.	Re($\boldsymbol{H_{XX}}$)	Re($\boldsymbol{H_{XY}}$)	Re($\boldsymbol{H_{YX}}$)	Re($\boldsymbol{H_{YY}}$)	Im($\boldsymbol{H_{XX}}$)	Im($\boldsymbol{H_{XY}}$)	Im($\boldsymbol{H_{YX}}$)	Im($\boldsymbol{H_{YY}}$)	Re($\boldsymbol{eH_{XX}}$)	Re($\boldsymbol{eH_{XY}}$)	Re($\boldsymbol{eH_{YX}}$)	Re($\boldsymbol{eH_{YY}}$)	Im($\boldsymbol{eH_{XX}}$)	Im($\boldsymbol{eH_{XY}}$)	Im($\boldsymbol{eH_{YX}}$)	Im($\boldsymbol{eH_{YY}}$)
Hz	MN/m	MN/m	MN/m	MN/m	MN/m	MN/m	MN/m	MN/m	MN/m	MN/m	MN/m	MN/m	MN/m	MN/m	MN/m	MN/m
9.8	5.6	6.2	-5.9	4.5	1.3	0.0	0.1	1.4	-0.1	-0.1	-0.1	-0.1	-0.1	-0.1	-0.1	-0.1
19.5	5.6	6.1	-5.9	4.2	2.8	-0.2	0.1	2.6	0.0	-0.1	-0.1	-0.1	-0.1	-0.1	0.0	-0.1
29.3	6.0	5.9	-6.3	4.8	3.7	-0.2	0.0	4.0	-0.1	-0.1	-0.1	-0.3	-0.1	-0.2	-0.1	-0.2
39.1	5.9	6.3	-6.1	4.4	5.1	-0.3	0.1	5.0	-0.1	-0.1	-0.1	-0.1	-0.1	-0.1	-0.1	-0.2
48.8	6.1	6.1	-6.0	4.5	6.3	-0.2	0.2	6.2	-0.1	-0.1	-0.1	-0.1	-0.1	-0.1	-0.1	-0.1
58.6	6.0	6.3	-6.1	4.6	7.6	-0.3	0.2	7.4	-0.1	-0.1	-0.1	-0.1	-0.1	-0.1	-0.1	-0.1
68.4	5.9	6.0	-6.0	5.0	8.8	-0.2	0.3	8.8	-0.1	-0.2	-0.1	-0.2	-0.1	-0.3	-0.1	-0.4
78.1	6.1	6.2	-6.0	4.6	9.9	-0.5	0.1	9.7	0.0	-0.1	-0.1	0.0	0.0	-0.1	-0.1	-0.1
87.9	6.3	6.1	-6.2	4.7	12.0	-0.3	0.3	11.0	0.0	-0.1	-0.1	0.0	-0.1	-0.1	0.0	0.0
97.7	6.4	5.8	-6.2	5.0	13.0	-0.4	0.4	12.0	0.0	-0.1	0.0	-0.1	-0.1	0.0	0.0	-0.1
107.4	6.4	6.0	-5.9	5.2	14.0	-0.5	0.5	13.0	-0.1	0.0	-0.1	-0.1	-0.1	-0.1	-0.1	-0.1
117.2	6.8	5.7	-6.0	5.3	15.0	-0.5	0.1	15.0	0.0	-0.1	-0.1	0.0	-0.1	-0.1	-0.1	0.0
127.0	7.2	5.9	-6.2	5.3	16.0	-0.2	0.3	16.0	-0.1	-0.1	-0.1	-0.1	-0.1	-0.1	0.0	-0.1
136.7	7.4	5.3	-6.6	5.8	17.0	-0.5	0.4	17.0	-0.1	-0.1	0.0	-0.2	0.0	-0.1	0.0	-0.1

Table 205. Raw data for the test seal at ω=15 krpm, PR=0.43, C_r=0.140 mm, and inlet GVF=100%

Freq.	Re($\boldsymbol{H_{XX}}$)	Re($\boldsymbol{H_{XY}}$)	Re($\boldsymbol{H_{YX}}$)	Re($\boldsymbol{H_{YY}}$)	Im($\boldsymbol{H_{XX}}$)	Im($\boldsymbol{H_{XY}}$)	Im($\boldsymbol{H_{YX}}$)	Im($\boldsymbol{H_{YY}}$)	Re($\boldsymbol{eH_{XX}}$)	Re($\boldsymbol{eH_{XY}}$)	Re($\boldsymbol{eH_{YX}}$)	Re($\boldsymbol{eH_{YY}}$)	Im($\boldsymbol{eH_{XX}}$)	Im($\boldsymbol{eH_{XY}}$)	Im($\boldsymbol{eH_{YX}}$)	Im($\boldsymbol{eH_{YY}}$)
Hz	MN/m	MN/m	MN/m	MN/m	MN/m	MN/m	MN/m	MN/m	MN/m	MN/m	MN/m	MN/m	MN/m	MN/m	MN/m	MN/m
9.8	5.2	8.5	-9.0	3.8	1.4	-0.3	0.4	1.4	-0.1	-0.1	-0.1	-0.1	-0.1	-0.2	-0.1	-0.2
19.5	5.4	8.5	-8.8	3.3	2.4	0.0	0.1	2.9	-0.1	-0.1	-0.1	-0.1	-0.1	-0.1	-0.1	-0.1
29.3	5.7	8.6	-9.3	3.9	3.6	0.2	0.4	3.7	-0.1	-0.3	-0.2	-0.5	-0.1	-0.3	-0.2	-0.3
39.1	5.5	8.3	-9.0	3.7	5.2	-0.4	0.3	5.3	0.0	-0.1	-0.1	-0.3	-0.1	-0.2	-0.1	-0.3
48.8	5.5	8.8	-9.1	4.4	6.3	-0.1	0.4	6.6	-0.1	-0.2	-0.1	-0.1	-0.1	-0.1	-0.1	-0.2
58.6	5.7	8.7	-8.8	3.9	7.3	-0.1	0.4	7.1	-0.1	-0.1	-0.1	-0.2	-0.1	-0.2	-0.1	-0.1
68.4	5.7	8.5	-9.0	4.0	8.8	-0.2	0.4	8.7	-0.1	-0.3	-0.1	-0.3	-0.1	-0.1	-0.1	-0.2
78.1	5.8	8.6	-8.9	4.4	9.8	-0.6	0.4	9.8	-0.1	-0.1	-0.1	-0.1	-0.1	-0.2	-0.1	-0.2
87.9	6.0	8.6	-9.2	4.1	11.0	-0.7	0.5	11.0	0.0	-0.1	0.0	-0.1	-0.1	-0.1	-0.1	-0.1
97.7	6.0	8.6	-9.2	4.3	13.0	-0.5	0.7	12.0	-0.1	-0.2	-0.1	-0.1	-0.1	-0.1	-0.1	-0.2
107.4	6.0	8.7	-8.8	4.5	14.0	-0.7	0.7	13.0	-0.1	-0.1	-0.1	-0.2	-0.1	-0.1	-0.1	0.0
117.2	6.5	8.3	-9.0	4.6	15.0	-0.7	0.3	15.0	-0.1	0.0	-0.1	0.0	0.0	-0.2	-0.1	-0.1
127.0	6.7	8.2	-9.0	4.7	16.0	-0.6	0.6	15.0	-0.1	-0.2	-0.1	-0.2	-0.1	-0.1	-0.1	-0.2
136.7	6.9	7.8	-9.5	5.3	17.0	-0.8	0.8	17.0	0.0	-0.1	0.0	-0.1	-0.1	-0.1	-0.1	-0.1

Table 206. Raw data for the test seal at ω=20 krpm, PR=0.43, C_r=0.140 mm, and inlet GVF=100%